

Arthritis & Rheumatology

An Official Journal of the American College of Rheumatology
www.arthritisrheum.org and wileyonlinelibrary.com

Editor

Daniel H. Solomon, MD, MPH, *Boston*

Deputy Editors

Richard J. Bucala, MD, PhD, *New Haven*

Mariana J. Kaplan, MD, *Bethesda*

Peter A. Nigrovic, MD, *Boston*

Co-Editors

Karen H. Costenbader, MD, MPH, *Boston*

David T. Felson, MD, MPH, *Boston*

Richard F. Loeser Jr., MD, *Chapel Hill*

Social Media Editor

Paul H. Sufka, MD, *St. Paul*

Journal Publications Committee

Amr Sawalha, MD, *Chair, Pittsburgh*

Susan Boackle, MD, *Denver*

Aileen Davis, PhD, *Toronto*

Deborah Feldman, PhD, *Montreal*

Donnamarie Krause, PhD, OTR/L, *Las Vegas*

Wilson Kuswanto, MD, PhD, *Stanford*

Michelle Ormseth, MD, *Nashville*

R. Hal Scofield, MD, *Oklahoma City*

Editorial Staff

Kimberly M. Murphy, *Managing Editor, Atlanta*

Lesley W. Allen, *Assistant Managing Editor, Atlanta*

Ilani S. Lorber, MA, *Assistant Managing Editor, Atlanta*

Rasa G. Hamilton, *Manuscript Editor, Atlanta*

Stefanie L. McKain, *Manuscript Editor, Atlanta*

Sara Omer, *Manuscript Editor, Atlanta*

Christopher Reynolds, MA, *Editorial Coordinator, Atlanta*

Brittany Swett, MPH, *Assistant Editor, Boston*

Associate Editors

Marta Alarcón-Riquelme, MD, PhD, *Granada*

Heather G. Allore, PhD, *New Haven*

Neal Basu, MD, PhD, *Glasgow*

Edward M. Behrens, MD, *Philadelphia*

Bryce Binstadt, MD, PhD, *Minneapolis*

Nunzio Bottini, MD, PhD, *San Diego*

John Carrino, MD, MPH, *New York*

Andrew Cope, MD, PhD, *London*

Adam P. Croft, MBChB, PhD, MRCP,
Birmingham

Nicola Dalbeth, MD, FRACP, *Auckland*

Brian M. Feldman, MD, FRCPC, MSc, *Toronto*

Richard A. Furie, MD, *Great Neck*

J. Michelle Kahlenberg, MD, PhD,
Ann Arbor

Benjamin Leder, MD, *Boston*

Yvonne Lee, MD, MMSc, *Chicago*

Katherine Liao, MD, MPH, *Boston*

Bing Lu, MD, DrPH, *Boston*

Stephen P. Messier, PhD,
Winston-Salem

Rachel E. Miller, PhD, *Chicago*

Janet E. Pope, MD, MPH, *FRCPC,*

London, Ontario

Lisa G. Rider, MD, *Bethesda*

Christopher T. Ritchlin, MD, MPH,
Rochester

William Robinson, MD, PhD, *Stanford*

Carla R. Scanzello, MD, PhD,
Philadelphia

Georg Schett, MD, *Erlangen*

Sakae Tanaka, MD, PhD, *Tokyo*

Maria Trojanowska, PhD, *Boston*

Betty P. Tsao, PhD, *Charleston*

Fredrick M. Wigley, MD, *Baltimore*

Edith M. Williams, PhD, MS, *Charleston*

Advisory Editors

Ayaz Aghayev, MD, *Boston*

Joshua F. Baker, MD, MSCE,
Philadelphia

Bonnie Bermas, MD, *Dallas*

Jamie Collins, PhD, *Boston*

Kristen Demoruelle, MD, PhD, *Denver*

Christopher Denton, PhD, FRCP, *London*

Anisha Dua, MD, MPH, *Chicago*

John FitzGerald, MD, *Los Angeles*

Lauren Henderson, MD, MMSc, *Boston*

Monique Hinchcliff, MD, MS, *New Haven*

Hui-Chen Hsu, PhD, *Birmingham*

Mohit Kapoor, PhD, *Toronto*

Seouyoung Kim, MD, ScD, MSCE, *Boston*

Vasileios Kytтарыs, MD, *Boston*

Carl D. Langefeld, PhD,
Winston-Salem

Dennis McGonagle, FRCPI, PhD, *Leeds*

Julie Paik, MD, MHS, *Baltimore*

Amr Sawalha, MD, *Pittsburgh*

Julie Zikherman, MD, *San Francisco*

AMERICAN COLLEGE OF RHEUMATOLOGY

Kenneth G. Saag, MD, MSc, *Birmingham*, **President**

Douglas White, MD, PhD, *La Crosse*, **President-Elect**

Carol Langford, MD, MHS, *Cleveland*, **Treasurer**

Deborah Desir, MD, *New Haven*, **Secretary**

Steven Echard, IOM, CAE, *Atlanta*, **Executive Vice-President**

© 2022 American College of Rheumatology. All rights reserved. No part of this publication may be reproduced, stored or transmitted in any form or by any means without the prior permission in writing from the copyright holder. Authorization to copy items for internal and personal use is granted by the copyright holder for libraries and other users registered with their local Reproduction Rights Organization (RRO), e.g. Copyright Clearance Center (CCC), 222 Rosewood Drive, Danvers, MA 01923, USA (www.copyright.com), provided the appropriate fee is paid directly to the RRO. This consent does not extend to other kinds of copying such as copying for general distribution, for advertising or promotional purposes, for creating new collective works or for resale. Special requests should be addressed to: permissions@wiley.com.

Access Policy: Subject to restrictions on certain backfiles, access to the online version of this issue is available to all registered Wiley Online Library users 12 months after publication. Subscribers and eligible users at subscribing institutions have immediate access in accordance with the relevant subscription type. Please go to onlinelibrary.wiley.com for details.

The views and recommendations expressed in articles, letters, and other communications published in Arthritis & Rheumatology are those of the authors and do not necessarily reflect the opinions of the editors, publisher, or American College of Rheumatology. The publisher and the American College of Rheumatology do not investigate the information contained in the classified advertisements in this journal and assume no responsibility concerning them. Further, the publisher and the American College of Rheumatology do not guarantee, warrant, or endorse any product or service advertised in this journal.

Cover design: Todd Machen

©This journal is printed on acid-free paper.

Arthritis & Rheumatology

An Official Journal of the American College of Rheumatology
www.arthritisrheum.org and wileyonlinelibrary.com

VOLUME 74 • September 2022 • NO. 9

In This Issue	A13
Journal Club	A14
Clinical Connections	A15
Special Articles	
Notes from the Field: Recognizing Racial Bias and Promoting Diversity in the Rheumatology Workforce <i>Siobhan M. Case, Gail S. Kerr, Mia Chandler, Valerie E. Stone, Irene Blanco, and Candace H. Feldman</i>	1459
2022 American College of Rheumatology/American Association of Hip and Knee Surgeons Guideline for the Perioperative Management of Antirheumatic Medication in Patients With Rheumatic Diseases Undergoing Elective Total Hip or Total Knee Arthroplasty <i>Susan M. Goodman, Bryan D. Springer, Antonia F. Chen, Marshall Davis, David R. Fernandez, Mark Figgie, Heather Finlayson, Michael D. George, Jon T. Giles, Jeremy Gililland, Brian Klatt, Ronald MacKenzie, Kaleb Michaud, Andy Miller, Linda Russell, Alexander Sah, Matthew P. Abdel, Beverly Johnson, Lisa A. Mandl, Peter Sculco, Marat Turgunbaev, Amy S. Turner, Adolph Yates Jr., and Jasvinder A. Singh</i>	1464
Editorial: Sacroiliac Bone Marrow Edema: Innocent Until Proven Guilty? <i>Michael M. Ward and Lawrence Yao</i>	1474
Editorial: Toward Precision Medicine—Is Genetic Risk Prediction Ready for Prime Time in Osteoarthritis? <i>Michelle S. Yau and John Loughlin</i>	1477
Osteoarthritis	
Genomic Risk Score for Advanced Osteoarthritis in Older Adults <i>Paul Lacaze, Yuanyuan Wang, Galina Polekhina, Andrew Bakshi, Moeen Riaz, Alice Owen, Angus Franks, Jawad Abidi, Jane Tiller, John McNeil, and Flavia Cicuttini</i>	1480
Clinical Images	
Clinical Images: Gout of the Spine <i>Guojie Wang</i>	1487
Osteoarthritis	
Risk Assessment for Hip and Knee Osteoarthritis Using Polygenic Risk Scores <i>Bahar Sedaghati-Khayat, Cindy G. Boer, Jos Runhaar, Sita M. A. Bierma-Zeinstra, Linda Broer, M. Arfan Ikram, Eleftheria Zeggini, André G. Uitterlinden, Jeroen G. J. van Rooij, and Joyce B. J. van Meurs</i>	1488
Spondyloarthritis	
Effects of Anti-Tumor Necrosis Factor Therapy on Osteoblastic Activity at Sites of Inflammatory and Structural Lesions in Radiographic Axial Spondyloarthritis: A Prospective Proof-of-Concept Study Using Positron Emission Tomography/Magnetic Resonance Imaging of the Sacroiliac Joints and Spine <i>Nils Martin Bruckmann, Christoph Rischpler, Styliani Tsiami, Julian Kirchner, Daniel B. Abrar, Timo Bartel, Jens Theysohn, Lale Umutlu, Ken Herrmann, Wolfgang P. Fendler, Christian Buchbender, Gerald Antoch, Lino M. Sawicki, Athanasios Tsobanelis, Juergen Braun, and Xenofon Baraliakos</i>	1497
Progressive Increase in Sacroiliac Joint and Spinal Lesions Detected on Magnetic Resonance Imaging in Healthy Individuals in Relation to Age <i>Thomas Renson, Manouk de Hooge, Ann-Sophie De Craemer, Liselotte Deroo, Zuzanna Lukasik, Philippe Carron, Nele Herregods, Lennart Jans, Roos Colman, Filip Van den Bosch, and Dirk Elewaut</i>	1506
Treatment With Tumor Necrosis Factor Inhibitors Is Associated With a Time-Shifted Retardation of Radiographic Sacroiliitis Progression in Patients With Axial Spondyloarthritis: 10-Year Results From the German Spondyloarthritis Inception Cohort <i>Murat Torgutalp, Valeria Rios Rodriguez, Fabian Proft, Mikhail Protopopov, Maryna Verba, Judith Rademacher, Hiltrun Haibel, Joachim Sieper, Martin Rudwaleit, and Denis Poddubnyy</i>	1515
Psoriatic Arthritis	
Peripheral $\gamma\delta$ T Cells Regulate Neutrophil Expansion and Recruitment in Experimental Psoriatic Arthritis <i>Cuong Thach Nguyen, Hiroki Furuya, Dayasagar Das, Alina I. Marusina, Alexander A. Merleev, Resmi Ravindran, Zahra Jalali, Imran H. Khan, Emanuel Maverakis, and Iannis E. Adamopoulos</i>	1524

Comparative Genetic Analysis of Psoriatic Arthritis and Psoriasis for the Discovery of Genetic Risk Factors and Risk Prediction Modeling
Mehreen Soomro, Michael Stadler, Nick Dand, James Bluett, Deepak Jadon, Farideh Jalali-najafabadi, Michael Duckworth, Pauline Ho, Helena Marzo-Ortega, Philip S. Helliwell, Anthony W. Ryan, David Kane, Eleanor Korendowych, Michael A. Simpson, Jonathan Packham, Ross McManus, Cem Gabay, Céline Lamacchia, Michael J. Nissen, Matthew A. Brown, Suzanne M. M. Verstappen, Tjeerd Van Staa, Jonathan N. Barker, Catherine H. Smith, the BADBIR Study Group, the BSTOP Study Group, Oliver FitzGerald, Neil McHugh, Richard B. Warren, John Bowes, and Anne Barton1535

Systemic Lupus Erythematosus

Interleukin-13 Receptor α 1-Mediated Signaling Regulates Age-Associated/Autoimmune B Cell Expansion and Lupus Pathogenesis
Zhu Chen, Danny Flores Castro, Sanjay Gupta, Swati Phalke, Michela Manni, Juan Rivera-Correa, Rolf Jessberger, Habib Zaghouni, Eugenia Giannopoulou, Tania Pannellini, and Alessandra B. Pernis1544

Plasmablast-like Phenotype Among Antigen-Experienced CXCR5-CD19^{low} B Cells in Systemic Lupus Erythematosus
Franziska Szelinski, Ana Luisa Stefanski, Eva Schrezenmeier, Hector Rincon-Arevalo, Annika Wiedemann, Karin Reiter, Jacob Ritter, Marie Lettau, Van Duc Dang, Sebastian Fuchs, Andreas P. Frei, Tobias Alexander, Andrea C. Lino, and Thomas Dörner1556

Sjögren's Syndrome

Symptom-Based Cluster Analysis Categorizes Sjögren's Disease Subtypes: An International Cohort Study Highlighting Disease Severity and Treatment Discordance
Sara S. McCoy, Miguel Woodham, Christie M. Bartels, Ian J. Saldanha, Vatinee Y. Bunya, Noah Maerz, Esen K. Akpek, Matthew A. Makara, and Alan N. Baer1569

Systemic Sclerosis

Development of Pulmonary Hypertension in Over One-Third of Patients With Th/To Antibody-Positive Scleroderma in Long-Term Follow-Up
Shashank Suresh, Devon Charlton, Erin K. Snell, Maureen Laffoon, Thomas A. Medsger Jr, Lei Zhu, and Robyn T. Domsic1580

Dermatomyositis

Brief Report: Performance of the 2017 European Alliance of Associations for Rheumatology/American College of Rheumatology Classification Criteria in Patients With Idiopathic Inflammatory Myopathy and Anti-Melanoma Differentiation-Associated Protein 5 Positivity
Ho So, Jacqueline So, Tommy Tsz-On Lam, Victor Tak-Lung Wong, Roy Ho, Wai Ling Li, Chi Chiu Mok, Chak Sing Lau, and Lai-Shan Tam1588

Gout

Evaluation of the Relationship Between Serum Urate Levels, Clinical Manifestations of Gout, and Death From Cardiovascular Causes in Patients Receiving Febuxostat or Allopurinol in an Outcomes Trial
Kenneth G. Saag, Michael A. Becker, William B. White, Andrew Whelton, Jeffrey S. Borer, Philip B. Gorelick, Barbara Hunt, Majin Castillo, and Lhanoo Gunawardhana, on behalf of the CARES Investigators1593

Letters

Increased Risk of Statin-Associated Autoimmune Myopathy Among American Indians
Jennie Wei, Elizabeth Ketner, and Andrew L. Mammen1602

von Willebrand Factor as an Indicator of Endothelial Injury in COVID-19: Comment on the Article by Shi et al
Darryl E. Palmer-Toy, Timothy M. Cotter, Hedyeh Shafi, Su-Jau T. Yang, and Alexander H. Cotter1603

Reply
Hui Shi, Jason S. Knight, and Yogendra Kanthi1603

Addressing Readability of Online Patient Materials: Comment on the American College of Rheumatology Online Information Pages for Patients and Caregivers
Ahmad AlAbdulkareem1604

Reply
Mohammad A. Ursani1605

Criteria for the Pathogenicity of Anticentromere (Anti-CENP-B) Autoantibodies in Systemic Sclerosis: Comment on the Article by van Leeuwen et al
Jean-Luc Senécal, Martial Koenig, Gabriel Archambault, and Sabrina Hoa1606

Reply
Nina M. van Leeuwen, Sophie I. E. Liem, Hans U. Scherer, and Jeska K. de Vries-Bouwstra1607

Cover image: The figure on the cover (from Bruckmann et al, pages 1497–1505) shows a hybrid ¹⁸F-NaF PET/MRI image of the sacroiliac joint of a 34-year-old patient with clinically active radiographic axial spondyloarthritis. ¹⁸F-NaF is a bone-seeking radio-pharmaceutical that accumulates in sites of increased bone formation. The increased signal on ¹⁸F-NaF PET/MRI on both sides of the sacroiliac joint provides evidence of increased osteoblastic activity.

In this Issue

Highlights from this issue of *A&R* | By Lara C. Pullen, PhD

Deceleration of Radiographic Sacroiliitis Progression in Patients with Axial SpA Treated with TNFi

In patients with axial spondyloarthritis (SpA), the inflammation process in the spine is followed by repair that transforms inflamed tissue in the subchondral bone marrow into fibrous repair tissue. **p. 1515** The process also activates new bone formation. Previous studies have demonstrated that tumor necrosis factor inhibitor (TNFi) therapy can inhibit radiographic spinal progression in patients with SpA, but the effect is only apparent after 4 years of therapy. **In this issue, Torgutalp et al (p. 1515)** confirm that treatment with TNFi was associated with a reduction in radiographic sacroiliitis progression in patients with axial SpA.

They also found that the reduction in radiographic progression was evident 2–4 years after TNFi therapy was initiated.

The investigators used long-term follow-up data from an inception cohort of 301 individuals with axial SpA who had ≥ 2 sets of radiographs. They analyzed data from 10 years of follow-up on 737 radiographic intervals and found that patients who received ≥ 12 months of treatment with TNFi in the previous 2-year radiographic interval were more likely to experience a significant decrease in the sacroiliitis sum score. In contrast, they found no significant change in the sacroiliitis sum score among patients receiving TNFi in the current radiographic interval. Moreover, the

effect of having received ≥ 12 months of treatment with TNFi in the previous 2-year radiographic interval was stronger in patients with non-radiographic axial SpA when compared to patients with radiographic axial SpA.

The authors emphasize that not only is their study limited to TNFi, but their conclusions are further limited by the fact that they did not include magnetic resonance imaging (MRI) data in their analysis. They explain that such data may have been better able to address the link between inflammation and new bone formation in the sacroiliac joints. Likewise, they observe that, had they had MRI data, they may have been able to detect earlier changes in structural damage.

One-Third of Patients with Th/To Antibody–Positive Scleroderma Develop Pulmonary Hypertension

Recent studies have described anti-Th/To antibody frequency in various populations of patients with systemic sclerosis (SSc). Studies have also revealed a higher frequency of interstitial lung disease in anti-Th/To antibody–positive patients as compared to antibody-negative patients. **In this issue, Suresh et al (p. 1580)** report their analysis of data from the largest cohort of anti-Th/To antibody–positive SSc patients with long-term follow-up data. They found a very high rate (38%) of anti-Th/To antibody–positive patients developing pulmonary hypertension (PH) in the follow-up period. In particular, patients with World Health Organization Group 1 pulmonary arterial hypertension (PAH) were most at risk for PH (with 23% developing PH).

The investigators used the gold standard method of RNA immunoprecipitation

to detect anti-Th/To antibodies. They then described the clinical characteristics of 204 SSc patients with anti-Th/To antibody positivity and compared them to the characteristics of 408 temporally matched SSc patients who were negative for this antibody. They found an approximate 5-fold increased risk of Th/To-positive patients developing PAH within 10 years of their first SSc symptom relative to antibody-negative patients. The researchers also found lower rates of skeletal muscle and joint/tendon involvement in anti-Th/To antibody–positive patients compared to other SSc patients. Finally, they found a lower 5-year cumulative survival from the first SSc visit in anti-Th/To antibody–positive patients compared to controls.

The authors note that only 5 anti-Th/To–positive patients (2.5%) developed diffuse skin involvement, and most had a nucleolar antinuclear antibody (ANA) pattern. Anti-Th/

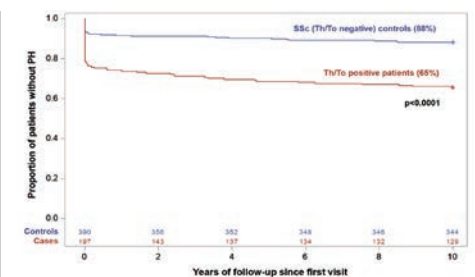


Figure 1. Development of PH over a 10-year follow-up period from the first SSc center visit. The number of patients at risk of developing PH is indicated at the bottom.

To positivity is uncommon, and the investigators note that testing for it has now become possible on some commercial platforms. They conclude that patients presenting with limited skin involvement should be tested for Th/To antibodies and, if they are found to be positive, carefully monitored for PH.

Risk Assessment for Hip and Knee Osteoarthritis Using Polygenic Risk Scores

Sedaghati-Khayat et al, *Arthritis Rheumatol.* 2022;74:1488-1496

The development of osteoarthritis (OA) is influenced by conventional risk factors, such as age and body mass index, but also by genetic factors. Although some risk factors can be modified, many patients do not receive appropriate risk management therapies. A limited number of primary OA prevention programs are available, and many trials have failed to identify structural treatment options because of the heterogeneity of OA patients in the late stage of testing. Therefore, one of the prime opportunities for the prediction of OA exists in the genetic risk factors before conventional risk factors have a chance to occur. Approximately 40–65% of the risk for OA is explained by genetic factors, depending on the affected joint. Existing clinical genetic applications focus on finding carriers of rare Mendelian variants, which are the leading genetic causes of early-onset familial forms of OA. However, genetic risk estimation in the form of polygenic risk scores can identify another significant fraction of the population at sufficiently increased risk for OA to be clinically relevant.

In this issue, Sedaghati-Khayat et al evaluate the ability of polygenic risk score in risk assessment based on the most recent genome-wide association study in a population setting, a clinical setting, and high-risk clinical cohorts. The investigators' findings confirm the association of polygenic risk score with radiographic OA, clinical OA, and total joint replacement. Additionally, their findings demonstrate that the polygenic risk score was most predictive of severe clinical OA, in both cross-sectional as well as longitudinal (incident OA) analyses. Overall, their

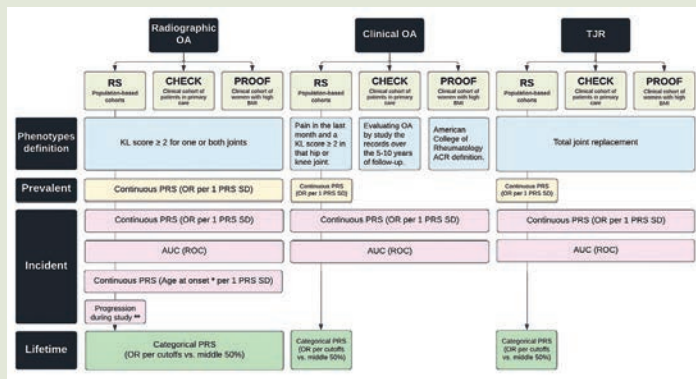


Figure 1. Overview of data availability and performed analysis. * = Age at onset was determined for incident radiographic OA and was calculated as the age at first diagnosis of radiographic OA. ** = Radiographic OA progression was defined as any progression in the Rotterdam Study (RS) with a ≥ 1 -degree increment in K/L score (excluding progression from K/L 0 to K/L 1 or having a total joint replacement [TJR] of one or both joints during the follow-up period). CHECK = Cohort Hip and Cohort Knee; PROOF = Prevention of Knee Osteoarthritis in Overweight Females; BMI = body mass index; PRS = polygenic risk score; ROC = receiving operating characteristic curve; AUC = area under the ROC; OR = odds ratio.

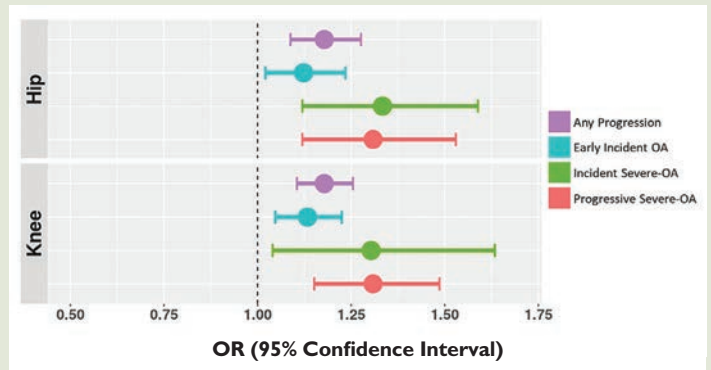


Figure 2. Association between OA polygenic risk scores and risk of OA progression in a meta-analysis of the Rotterdam Study of 3 cohorts. Any progression was defined by a ≥ 1 -degree increment of the K/L score (excluding progression from K/L 0 to K/L 1) or having a TJR of one or both joints during the follow-up period. Early incident OA was defined by a maximum K/L score of 2 for each joint during follow-up (i.e., K/L 0 or K/L 1 to K/L 2). Incident severe OA was defined by a K/L score of ≥ 3 or TJR during follow-up (i.e., K/L 0 or K/L 1 to K/L 3+, or TJR). Progressive severe OA was defined by progression from early OA (K/L 2) to severe OA (K/L 3+) or TJR during follow-up.

research shows a discriminatory ability of the hip OA polygenic risk scores and the knee OA polygenic risk scores across all OA definitions. They also observed a consistently increased risk of OA in the top polygenic risk scores distribution of the study populations. Individuals in the top 10% polygenic risk scores distribution were twice as likely to develop OA than those in the middle 50% of the polygenic risk scores distribution. Therefore, since OA is becoming increasingly frequent in the general population, and primary prevention is not commonly applicable, the researchers propose that a polygenic risk scores-based risk prediction tool could constitute a valuable addition to OA prevention and management in health care systems.

Questions

1. What is currently known about the clinical application of polygenic risk scores in different subjects, such as breast cancer, age-related macular degeneration, or coronary artery disease?
2. Why was the development and assessment of polygenic risk scores appropriate for the study of OA?
3. Given the OA progression susceptibility, when is the best time to test for polygenic risk scores?
4. What are the main limitations and strengths of using polygenic risk scores for population screening or predictive testing in clinics?
5. What is the best clinical setting in which to apply the polygenic risk scores for OA?

In this Issue

Highlights from this issue of *A&R* | By Lara C. Pullen, PhD

Deceleration of Radiographic Sacroiliitis Progression in Patients with Axial SpA Treated with TNFi

In patients with axial spondyloarthritis (SpA), the inflammation process in the spine is followed by repair that transforms inflamed tissue in the subchondral bone marrow into fibrous repair tissue. The process also activates new bone formation. Previous studies have demonstrated that tumor necrosis factor inhibitor (TNFi) therapy can inhibit radiographic spinal progression in patients with SpA, but the effect is only apparent after 4 years of therapy. **In this issue, Torgutalp et al (p. 1515)** confirm that treatment with TNFi was associated with a reduction in radiographic sacroiliitis progression in patients with axial SpA.

They also found that the reduction in radiographic progression was evident 2–4 years after TNFi therapy was initiated.

The investigators used long-term follow-up data from an inception cohort of 301 individuals with axial SpA who had ≥ 2 sets of radiographs. They analyzed data from 10 years of follow-up on 737 radiographic intervals and found that patients who received ≥ 12 months of treatment with TNFi in the previous 2-year radiographic interval were more likely to experience a significant decrease in the sacroiliitis sum score. In contrast, they found no significant change in the sacroiliitis sum score among patients receiving TNFi in the current radiographic interval. Moreover, the

effect of having received ≥ 12 months of treatment with TNFi in the previous 2-year radiographic interval was stronger in patients with non-radiographic axial SpA when compared to patients with radiographic axial SpA.

The authors emphasize that not only is their study limited to TNFi, but their conclusions are further limited by the fact that they did not include magnetic resonance imaging (MRI) data in their analysis. They explain that such data may have been better able to address the link between inflammation and new bone formation in the sacroiliac joints. Likewise, they observe that, had they had MRI data, they may have been able to detect earlier changes in structural damage.

One-Third of Patients with Th/To Antibody–Positive Scleroderma Develop Pulmonary Hypertension

Recent studies have described anti-Th/To antibody frequency in various populations of patients with systemic sclerosis (SSc). Studies have also revealed a higher frequency of interstitial lung disease in anti-Th/To antibody–positive patients as compared to antibody–negative patients. **In this issue, Suresh et al (p. 1580)** report their analysis of data from the largest cohort of anti-Th/To antibody–positive SSc patients with long-term follow-up data. They found a very high rate (38%) of anti-Th/To antibody–positive patients developing pulmonary hypertension (PH) in the follow-up period. In particular, patients with World Health Organization Group 1 pulmonary arterial hypertension (PAH) were most at risk for PH (with 23% developing PH).

The investigators used the gold standard method of RNA immunoprecipitation

to detect anti-Th/To antibodies. They then described the clinical characteristics of 204 SSc patients with anti-Th/To antibody positivity and compared them to the characteristics of 408 temporally matched SSc patients who were negative for this antibody. They found an approximate 5-fold increased risk of Th/To-positive patients developing PAH within 10 years of their first SSc symptom relative to antibody–negative patients. The researchers also found lower rates of skeletal muscle and joint/tendon involvement in anti-Th/To antibody–positive patients compared to other SSc patients. Finally, they found a lower 5-year cumulative survival from the first SSc visit in anti-Th/To antibody–positive patients compared to controls.

The authors note that only 5 anti-Th/To–positive patients (2.5%) developed diffuse skin involvement, and most had a nucleolar antinuclear antibody (ANA) pattern. Anti-Th/

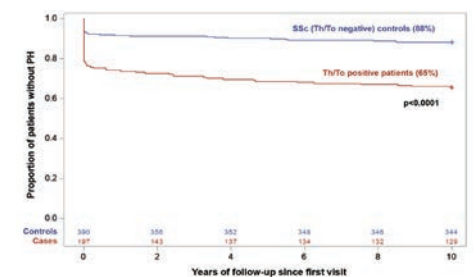


Figure 1. Development of PH over a 10-year follow-up period from the first SSc center visit. The number of patients at risk of developing PH is indicated at the bottom.

To positivity is uncommon, and the investigators note that testing for it has now become possible on some commercial platforms. They conclude that patients presenting with limited skin involvement should be tested for Th/To antibodies and, if they are found to be positive, carefully monitored for PH.

Risk Assessment for Hip and Knee Osteoarthritis Using Polygenic Risk Scores

Sedaghati-Khayat et al, *Arthritis Rheumatol.* 2022;74:1488-1496

The development of osteoarthritis (OA) is influenced by conventional risk factors, such as age and body mass index, but also by genetic factors. Although some risk factors can be modified, many patients do not receive appropriate risk management therapies. A limited number of primary OA prevention programs are available, and many trials have failed to identify structural treatment options because of the heterogeneity of OA patients in the late stage of testing. Therefore, one of the prime opportunities for the prediction of OA exists in the genetic risk factors before conventional risk factors have a chance to occur. Approximately 40–65% of the risk for OA is explained by genetic factors, depending on the affected joint. Existing clinical genetic applications focus on finding carriers of rare Mendelian variants, which are the leading genetic causes of early-onset familial forms of OA. However, genetic risk estimation in the form of polygenic risk scores can identify another significant fraction of the population at sufficiently increased risk for OA to be clinically relevant.

In this issue, Sedaghati-Khayat et al evaluate the ability of polygenic risk score in risk assessment based on the most recent genome-wide association study in a population setting, a clinical setting, and high-risk clinical cohorts. The investigators' findings confirm the association of polygenic risk score with radiographic OA, clinical OA, and total joint replacement. Additionally, their findings demonstrate that the polygenic risk score was most predictive of severe clinical OA, in both cross-sectional as well as longitudinal (incident OA) analyses. Overall, their

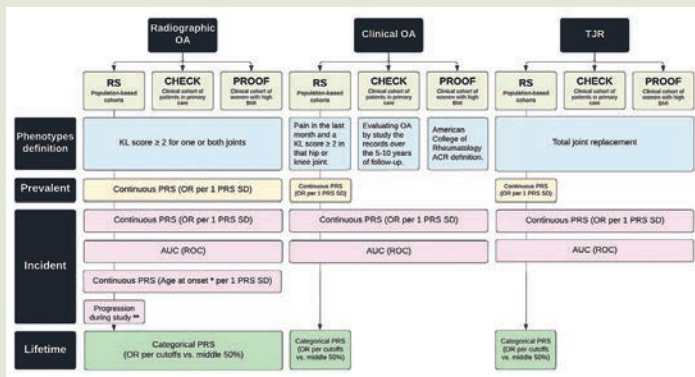


Figure 1. Overview of data availability and performed analysis. * = Age at onset was determined for incident radiographic OA and was calculated as the age at first diagnosis of radiographic OA. ** = Radiographic OA progression was defined as any progression in the Rotterdam Study (RS) with a ≥ 1 -degree increment in K/L score (excluding progression from K/L 0 to K/L 1 or having a total joint replacement [TJR] of one or both joints during the follow-up period). CHECK = Cohort Hip and Cohort Knee; PROOF = Prevention of Knee Osteoarthritis in Overweight Females; BMI = body mass index; PRS = polygenic risk score; ROC = receiving operating characteristic curve; AUC = area under the ROC; OR = odds ratio.

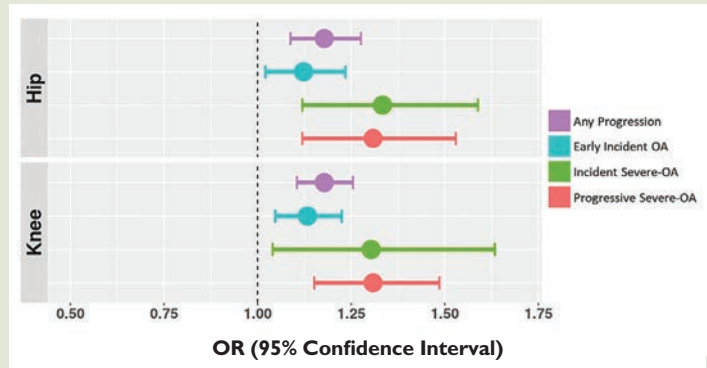


Figure 2. Association between OA polygenic risk scores and risk of OA progression in a meta-analysis of the Rotterdam Study of 3 cohorts. Any progression was defined by a ≥ 1 -degree increment of the K/L score (excluding progression from K/L 0 to K/L 1) or having a TJR of one or both joints during the follow-up period. Early incident OA was defined by a maximum K/L score of 2 for each joint during follow-up (i.e., K/L 0 or K/L 1 to K/L 2). Incident severe OA was defined by a K/L score of ≥ 3 or TJR during follow-up (i.e., K/L 0 or K/L 1 to K/L 3+, or TJR). Progressive severe OA was defined by progression from early OA (K/L 2) to severe OA (K/L 3+) or TJR during follow-up.

research shows a discriminatory ability of the hip OA polygenic risk scores and the knee OA polygenic risk scores across all OA definitions. They also observed a consistently increased risk of OA in the top polygenic risk scores distribution of the study populations. Individuals in the top 10% polygenic risk scores distribution were twice as likely to develop OA than those in the middle 50% of the polygenic risk scores distribution. Therefore, since OA is becoming increasingly frequent in the general population, and primary prevention is not commonly applicable, the researchers propose that a polygenic risk scores-based risk prediction tool could constitute a valuable addition to OA prevention and management in health care systems.

Questions

1. What is currently known about the clinical application of polygenic risk scores in different subjects, such as breast cancer, age-related macular degeneration, or coronary artery disease?
2. Why was the development and assessment of polygenic risk scores appropriate for the study of OA?
3. Given the OA progression susceptibility, when is the best time to test for polygenic risk scores?
4. What are the main limitations and strengths of using polygenic risk scores for population screening or predictive testing in clinics?
5. What is the best clinical setting in which to apply the polygenic risk scores for OA?

Clinical Connections

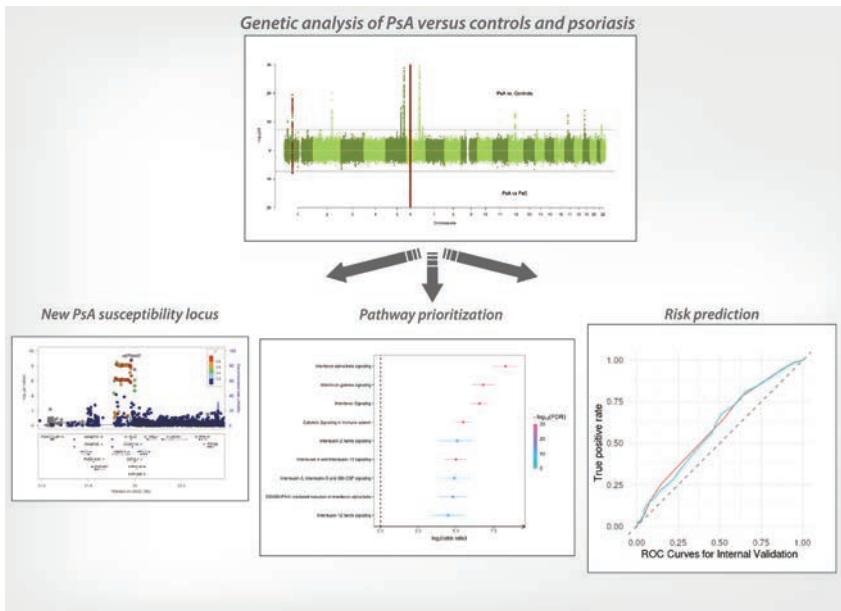
Comparative Genetic Analysis of PsA and Psoriasis for the Discovery of Genetic Risk Factors and Risk Prediction Modeling

Soomro et al, *Arthritis Rheumatol.* 2022;74:1535–1543

CORRESPONDENCE

John Bowes, PhD: j.bowes@manchester.ac.uk

Anne Barton, PhD, FRCP: Anne.Barton@manchester.ac.uk



KEY POINTS

- Key biological pathways for the development of PsA in patients with PsC were identified, highlighting potential therapeutic targets for the translation of genetic discoveries to clinical benefit.
- Risk classification pipelines for the prediction of PsA in patients with psoriasis were developed and existing models were tested, but both approaches show only limited predictive ability in the available datasets.
- Research highlights the need for prospective studies and consideration of the similarity of clinical and demographic features between the training and test datasets (e.g., treatment regimens) in the development of clinical risk prediction models.

SUMMARY

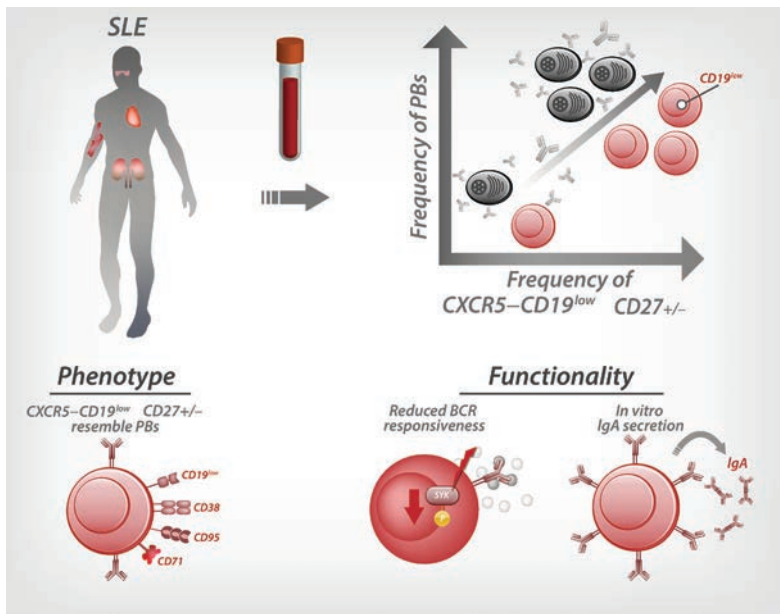
Approximately one-third of patients with psoriasis will develop psoriatic arthritis (PsA), leading to a reduction in their quality of life caused by increasing disability and additional health complications. A key area of research is the identification of risk factors for the development of PsA; this will allow us to understand the underlying cause of disease and ultimately help identify psoriasis patients at high risk of PsA, allowing early treatment to be introduced to reduce the impact of PsA. Soomro et al performed a genome-wide analysis of PsA and psoriasis to identify PsA-specific genetic risk factors and biological pathways that differentiate PsA from psoriasis, identifying the NF- κ B and Wnt signaling pathways as important. The Wnt signaling pathway is of particular interest as it plays a key role in bone formation in normal development and abnormal bone formation in diseases such as axial spondyloarthritis and osteoarthritis and may be of particular interest to PsA. Additionally, the study explores the use of genetics to help classify PsA from psoriasis; however, the currently known PsA-specific genetic risk factors show only modest ability to discriminate PsA from cutaneous-only psoriasis (PsC) in the available data sets presented in the study.

Plasmablast-like Phenotype Among Antigen-Experienced CXCR5-CD19^{low} B Cells in SLE

Szelinski et al, *Arthritis Rheumatol.* 2022;74:1556–1568

CORRESPONDENCE

Thomas Dörner, MD: thomas.doerner@charite.de



KEY POINTS

- Newly identified CXCR5-CD19^{low} B cells are increased in SLE and correlate with PB frequencies.
- Besides bimodal expression of CD27, CXCR5-CD19^{low} B cells show similarities with PBs, e.g., surface marker expression, reduced BCR responsiveness, capacity of antibody secretion, and elevated transcriptional expression of *PRDM1*, *XBPI*, and *IRF4*.
- The finding of CXCR5-CD19^{low} B cells among both CD27⁺ and CD27⁻ cells questions CD27 as marker of B cell differentiation during immune activation, such as in SLE.

SUMMARY

Abnormalities of peripheral B cell subsets have been identified in patients with systemic lupus erythematosus (SLE). Altered distribution of conventional and atypical memory B cells, including IgD-CD27- double-negative B cells, plasmacytosis, and the presence of autoantibodies, are examples of these abnormalities, yet a full encoding of underlying mechanisms remain elusive. However, it would contribute to a better understanding of immunopathogenesis and development of potential selective therapies.

A new peripheral B cell subset enriched in SLE and characterized by low expression of CD19 and absence of CXCR5 has been recently identified by Szelinski et al. CXCR5-CD19^{low} B cells can be found among both IgD-CD27⁺ switched and atypical IgD-CD27⁻ compartments and correlate with peripheral plasmablasts (PBs).

CXCR5-CD19^{low} B cells exhibit activation and proliferation markers CD86 and CD71 and lack immune checkpoint molecule B and T lymphocyte attenuator, characterizing them as activated. The majority of CXCR5-CD19^{low} cells were CD38⁺ and CD95⁺, while early B lineage markers (CD24/CD10) were absent. Expression of class-switched IgG and IgA, in vitro secretion of IgA, PB-like transcriptional activity, and diminished BCR responsiveness mark CXCR5-CD19^{low} B cells as antigen-experienced and precursors of antibody-secreting cells, although without a typical CD27 expression. These cells may represent recent emigrants of extrafollicular induction including a lack of proper immune selection.

Clinically, these cells may be candidates for potential biomarkers in SLE and require consideration to prevent persistent inflammation caused by ongoing induction of antibody-secreting cells and autoantibodies. Therefore, the identification of CXCR5-CD19^{low} precursors of PBs might be candidates for new biomarkers as well as potential co-targets of innovative therapies.

NOTES FROM THE FIELD

Recognizing Racial Bias and Promoting Diversity in the Rheumatology Workforce

Siobhan M. Case,¹  Gail S. Kerr,² Mia Chandler,¹  Valerie E. Stone,³ Irene Blanco,⁴ and Candace H. Feldman³ 

Our rheumatology workforce is facing a moment of reckoning with the stark lack of racial and ethnic diversity. National events have called increasing attention to the multitude of barriers faced by people from groups who are underrepresented in medicine (URiM), defined as “racial and ethnic populations that are underrepresented in the medical profession relative to their numbers in the general population,” including women, people with disabilities, and self-identified Black, Latinx, Native Hawaiian, Pacific Islander, American Indian, and Alaska Native individuals (1).

This article summarizes key concepts from a virtual forum hosted by Brigham and Women’s Hospital with Drs. Kerr, Stone, and Blanco on “Diversity in the Rheumatology Research Workforce.” The forum focused on diversity, equity, and inclusion (DEI) within race and ethnicity, recognizing that these categories are social constructs that do not exist in isolation. Rather, as outlined in the theory of intersectionality, a person’s self-identified race and ethnicity will intersect with other aspects of identity, social position, and processes and policies in complex ways that deserve further dedicated research (2). Herein, we will explore some of the barriers and biases encountered by URiM rheumatology professionals and outline changes that are required to recruit and retain a more diverse workforce.

We must work to diversify the rheumatology workforce not only because it is the only right and equitable approach, but also because it is critical to the patients we serve and to the improvement of our field. URiM physicians have been shown to provide

higher quality care to patients identifying as racial or ethnic minorities, and racial concordance with providers can improve communication and therefore care (3). This makes increasing URiM provider representation an important and necessary component of working toward equity in patient care and health outcomes. However, it is also an independent goal that will bring essential perspectives and experiences, which will impact the quality of the research questions we ask and the clinical care we provide, and thus requires independent attention and strategies (4). While the responsibility to recognize and dismantle structural racism in rheumatology is our shared responsibility, we can only work toward this if URiM voices are heard and valued.

Recognizing these important needs, we will outline 1) the striking shortage of URiM professionals in rheumatology, 2) barriers faced by URiM applicants and professionals, 3) actionable strategies to increase URiM professional recruitment and retention, and 4) methods for teaching bias, structural racism, and structural competency. We will use terminology for race and ethnicity that reflects the cited studies (5).

THE CRITICAL SHORTAGE OF URiM PROFESSIONALS IN RHEUMATOLOGY

The field of medicine struggles with a lack of diversity in many ways, which is reflected in suboptimal care for vulnerable patient

The content of this article is solely the responsibility of the authors and does not necessarily represent the official view of the sources providing funding support to the authors.

The Value and Evidence in Rheumatology using Bioinformatics and Advanced Analytics program was supported by the National Institute of Arthritis and Musculoskeletal and Skin Diseases (NIAMS), NIH (award P30-AR-072577). Dr. Case’s work was supported by the NIH (National Institute of Arthritis and Musculoskeletal and Skin Diseases grant T32-AR-007530). Dr. Chandler’s work was supported by the NIH (5T32-AI-007512-35). Dr. Feldman’s work was supported by the NIAMS, NIH (grant AR0-71500).

¹Siobhan M. Case, MD, MHS, Mia Chandler, MD, MPH: Brigham and Women’s Hospital, Harvard Medical School, and Boston Children’s Hospital, Boston, Massachusetts; ²Gail S. Kerr MD: DC Veterans Affairs Medical Center, Georgetown and Howard University Hospitals, Washington, DC; ³Valerie E. Stone, MD, MPH, Candace H. Feldman, MD, MPH, ScD: Brigham and Women’s Hospital and Harvard Medical School, Boston, Massachusetts; ⁴Irene Blanco, MD, MS: Albert Einstein College of Medicine, New York, New York.

This article summarizes key concepts from a virtual forum hosted on July 9, 2021 by Brigham and Women’s Hospital with Drs. Kerr, Stone, and Blanco on “Diversity in the Rheumatology Research Workforce.” The forum was part of the Value and Evidence in Rheumatology using Bioinformatics and Advanced Analytics (VERITY) program and was presented to an international audience of academic researchers to highlight the lack of diversity in the rheumatology research workforce and consider strategies for resolution. Three speakers presented on the following topics for 20 minutes each, followed by 20 minutes of discussion: Dr. Blanco on “Incorporating DEI into Rheumatology Medical Education,” Dr. Stone on “Increasing Fellow and Faculty Diversity at Academic Medical Institutions,” and Dr. Kerr on “The Role of HBCUs in Rheumatology Workforce Diversity.”

Author disclosures are available at <https://onlinelibrary.wiley.com/action/downloadSupplement?doi=10.1002%2Fart.42151&file=art42151-sup-0001-Disclosureform.pdf>.

Address correspondence to Siobhan M. Case, MD, MHS, 60 Fenwood Road, Boston MA 02115. Email: scase@bwh.harvard.edu.

Submitted for publication December 22, 2021; accepted in revised form April 19, 2022.

populations. People identifying as Black, Hispanic, and Native American are dramatically underrepresented in both health care practice and training (6). A 2019 national survey found that only 5.2% of physicians identified as Black, 6.9% identified as Hispanic, and 0.1% identified as Native American (6), compared to general population US Census estimates of 13.4%, 18.5%, and 1.3%, respectively. Based on current trainee enrollment, it is anticipated that there will be minimal improvement (6), with the percent of physicians and surgeons identifying as Hispanic or Black changing less than a percentage point when comparing 2000–2004 to 2015–2019 (7).

Within rheumatology, the low number of URiM professionals is of immediate concern. In the American College of Rheumatology 2015 workforce report, only 8 of 1,011 adult rheumatologists surveyed identified as Black, 85 identified as Hispanic, and 3 identified as American Indian or Alaska Native (8). In addition, 11% of 530 rheumatology fellows in 2021 identified as URiM (20 identified as Black, 38 identified as Hispanic, and 0 identified as Native Hawaiian/Pacific Islander or American Indian/Alaska Native) (9). In contrast to several other internal medicine subspecialties, there has not been any noticeable improvement over the past 15 years (10). The lack of workforce diversity is compounded by a current workforce shortage that is projected to worsen, with a mismatch between declining numbers of full-time rheumatology professionals and rising demand from the aging and increasingly diverse US population.

BARRIERS FACED BY URiM APPLICANTS AND PROFESSIONALS IN RHEUMATOLOGY

The shortage of URiM persons in rheumatology, and medicine as a whole, stems from systemic racism that runs through our society, health care institutions, and medical practice, with historical inequalities that have grown over time and continue to this day (11). Racism takes many forms and may be implicit, explicit, and/or structural. Accordingly, the multitude of stresses experienced by URiM persons in rheumatology are varied and complex (1). URiM persons can face the aforementioned types of racism throughout higher education and must contend with the “myth of meritocracy” that a person’s academic records and achievements are based on unbiased evaluation on an even playing field (12). Regarding fellowship applications, potential URiM applicants may suffer from a lack of mentorship and lack of exposure to subspecialty areas (1).

In rheumatology practice, URiM professionals must contend with the paternalistic culture of medicine, as well as microaggressions and practices based on assumptions about race that often have no genetic or clinical justification (1,13). Microaggressions and interpersonal racism in medical practice may be perpetuated by individuals in any role, including administrators, other health care professionals, trainees, and patients. The lack of URiM professionals in our workforce perpetuates the cycle of structural

racism, with a paucity of mentors and role models among senior faculty and insufficient representation on leadership teams where critical decisions and priorities are made (1). The “minority tax” also takes a toll, in which URiM faculty are asked to participate in committees and mentoring to improve diversity or address racism but often are not provided necessary tools, compensated, or recognized with promotions (14). Within research, URiM researchers are less likely to receive awards from the National Institutes of Health (NIH) (15) and are often overburdened with clinical workload at academic institutions that primarily see underserved populations (16).

ACTIONABLE STRATEGIES TO INCREASE URiM PROFESSIONAL RECRUITMENT AND RETENTION IN THE RHEUMATOLOGY WORKFORCE

At the institutional level, recruitment and retention of URiM persons must be prioritized with financial resources and support in leadership. This may include performing needs assessments both within the medicine department and rheumatology division to clarify priorities, viewpoints, and potential conflicts across a wide range of stakeholders. There should be clear strategies, achievable benchmarks for success, and enforcement of accountability (Table 1). Sufficient financial resources should be provided to compensate DEI work, execute strategies, and generate competitive offers and retention packages for URiM faculty. There should be regular auditing to ensure that salaries, start-up packages, and laboratory space are equitably allocated to URiM professionals. A robust ombudsperson program should exist for reporting and tracking episodes of racism and institutional responses.

To successfully recruit more URiM providers to rheumatology, there must be exposure to and opportunities within rheumatology to spark interest and engagement. These might include summer research internships or clinical rotations in rheumatology while pursuing undergraduate or medical degrees. To enhance exposure to rheumatology among URiM persons, standardized programs and partnerships should be developed or strengthened with historically Black colleges and universities and student associations that have longstanding pipelines dedicated to supporting and expanding the URiM workforce. Programs can apply for diversity supplements on NIH grants to help create dedicated funding streams. Fellowship directors should develop specific strategies for the recruitment and support of URiM persons and train interviewers in proven techniques to reduce bias (17). Application review can be standardized, for example by blinding reviewers to applicant photos and test scores and using the same structured interview questions for each applicant (17). The process should also be holistic, emphasizing a candidates’ personal qualities and experiences in addition to academic performance (18,19). The interview process should be person-centric and allow for opportunities to foster community and mentoring, such

Table 1. Actionable strategies to increase URiM professional recruitment and retention in the rheumatology workforce*

Goal and strategies	Process	Outcome metrics
Institutional commitment to supporting URiM professionals		
Make DEI a publicly stated priority with clearly communicated strategies and goals	Perform needs assessments for DEI within medicine departments and rheumatology divisions; create benchmarks for success in DEI efforts and consequences for inaction	Publication and dissemination of strategy and goals; incorporation of DEI into mission statements; meeting benchmarks
Create empowered DEI positions with clear leadership and career ladders to develop and execute DEI strategies	Consider creation of a department-wide diversity council and Vice Chairperson for DEI; recognize DEI involvement for career advancement and promotions	Number of DEI positions and percent of efforts toward DEI initiatives; number of promotions and awards related to DEI work
Dedicate financial resources to support DEI strategies	Allocate funding for execution of DEI strategies, DEI positions, and a designated percentage of efforts toward DEI initiatives, URiM professional recruitment efforts, and retention packages and support for URiM faculty	Funding in DEI areas
Create an ombudsperson program		Track reporting of and responses to racism and bias
URiM recruitment to rheumatology		
Create opportunities to expose URiM undergraduate and medical students to rheumatology (“pipeline programs”)	Offer summer research internships and clinical rotations; partner with historically Black colleges and universities and student associations (for example the SNMA, MAPS, and NMA); apply for NIH diversity supplement grants; set specific goals for reaching organizations or individuals through the above pathways	Number of URiM students/residents rotating in rheumatology, attending rheumatology events, and pursuing a rheumatology fellowship
Create strategies to address racial bias during fellowship interviews	Train interviewers on bias and techniques to reduce it; standardize application reviews (e.g., blinded with regard to photos and test scores, same questions for all applicants); adopt holistic review processes (e.g., broad selection criteria emphasizing personal experience and qualities in addition to academic performance); create a mechanism for anonymous feedback from applicants; review metrics and feedback on an annual basis at the divisional and departmental levels	Number of URiM applicants interviewed, ranked, and matched
Facilitate a person-centric interview process	Provide opportunities to identify mentors; host recruitment receptions for URiM persons	Number of URiM applicants interviewed, ranked, and matched
URiM retention in rheumatology		
Create equitable hiring practices in line with DEI strategy	Consider cluster hiring; provide dedicated financial resources for competitive offers; account for the influence of SDOH (e.g., childcare and housing costs)	Number of hiring offers and acceptances; audit offers to ensure equity
Promote retention of URiM faculty	Provide and monitor dedicated financial resources for retention packages and funding support; audit institutional support of URiM faculty, including recognitions and promotions; conduct exit interviews to identify barriers in retention	Amount of dedicated funding; number of URiM faculty retained
Provide dedicated, individualized mentorship for URiM faculty	Offer faculty development programs; facilitate networking opportunities across institutions; employ techniques like training to mentor across cultural differences and group mentoring; develop a hospital directory of URiM professionals to facilitate connections; elicit feedback from URiM faculty to identify successful strategies and areas of need	Track offering of and engagement with mentoring opportunities
Facilitate URiM community engagement	Host social gatherings for affinity groups; host DEI town hall meetings	Number of and attendance at gatherings; track issues raised at town hall meetings and institutional responses

* URiM = underrepresented in medicine; DEI = diversity, equity, and inclusion; SNMA = Student National Medical Association; MAPS = Minority Association of Pre-Medical Students; NMA = National Medical Association; NIH = National Institutes of Health; SDOH = social determinants of health.

as specific URiM applicant recruitment receptions. The number of URiM applicants and the percentages of applicants interviewed, ranked, and matched should be reviewed annually by divisions.

Providing resources to retain URiM faculty is also critical (18). Mentorship is important (1) and given the present lack of diversity in the rheumatology workforce, mentors who identify with different racial groups might benefit from specific training to mentor across cultural differences (20). Mentors can foster motivation for URiM persons to pursue a career in rheumatology by providing community-building experiences through group mentoring, which facilitates peer networking while simultaneously engaging in career coaching (21). Additionally, a hospital directory of URiM residents, fellows, and faculty members can promote relationships and hold collective social gatherings across divisions and departments. Finally, regular town halls and faculty development programs for URiM professionals can likewise create an important space for cross-departmental issues and collaboration and concrete pathways to address matters raised during these meetings. Financial resources for retention packages and awareness of the influences of social determinants of health (SDOH) on URiM professional retention, such as inequitable distribution of wealth and its impact on debt, housing, and childcare costs, are also essential.

METHODS FOR TEACHING ABOUT BIAS, STRUCTURAL RACISM, AND CULTURAL HUMILITY

To support our fellow URiM health care workers and improve patient care, fellows and faculty members should have formal training around structural racism and its downstream effects, as well as the impact of SDOH (22). Implicit bias training is important but should move past traditional models, which have failed to show significant behavior change or reduced bias. Instead, we should focus on evidence-based innovative methods, like individuation (focusing on traits specific to a unique person instead of a group) and reviewing counterstereotypical models (examples that go against usual stereotypes), which provide strategies to actually reduce bias and minimize its impact on patient care (23). We should also shift away from cultural competency toward cultural humility (24), with the acknowledgment that culture is important but fluid, and that an assumption of competency could contribute to bias. Of note, government policies in the US might impede some of these suggested efforts, such as legislation banning the teaching of Critical Race Theory and training on racism. We must advocate for open and honest discussion of the impact of racism on every aspect of our society, including health care.

Now is the moment to leverage our increased consciousness of structural racism and bias to start to achieve real change. Creating pathways and support for URiM persons in the rheumatology workforce will require multilevel interventions, financial resources, accountability, and measurable outcomes. Further

qualitative studies and needs assessments are needed to understand the intersectionality between race, ethnicity, other aspects of identity, social position, processes, and policies that can combine to affect bias for URiM persons. Additional information is required to understand how DEI work can adapt to the nuanced needs of individuals (2). We call on our rheumatology community to critically question our existing systems of medical training, recruitment, and retention and to create actionable strategies backed by institutional and personal commitment to equity.

AUTHOR CONTRIBUTIONS

All authors drafted the article, revised it critically for important intellectual content, and approved the final version to be published.

ACKNOWLEDGMENTS







We would like to thank Ms. Jacklyn Stratton for facilitating the forum and would like to acknowledge her role in organizing and coordinating the forum, which was attended by 38 registered attendees from around the world who were invited through their participation in VERITY.

REFERENCES

1. Ajayi AA, Rodriguez F, de Jesus Perez V. Prioritizing equity and diversity in academic medicine faculty recruitment and retention. *JAMA Health Forum* 2021;2:e212426.
2. Bauer GR. Incorporating intersectionality theory into population health research methodology: challenges and the potential to advance health equity. *Soc Sci Med* 2014;110:10–7.
3. Shen MJ, Peterson EB, Costas-Muniz R, Hernandez MH, Jewell ST, Matsoukas K, et al. The effects of race and racial concordance on patient-physician communication: a systematic review of the literature. *J Racial Ethn Health Disparities* 2018;5:117–40.
4. Crews DC, Collins CA, Cooper LA. Distinguishing workforce diversity from health equity efforts in medicine. *JAMA Health Forum* 2021;2:e214820.
5. Flanagin A, Frey T, Christiansen SL, AMA Manual of Style Committee. Updated guidance on the reporting of race and ethnicity in medical and science journals [editorial]. *JAMA* 2021;326:621–7.
6. Salsberg E, Richwine C, Westergaard S, Martinez MP, Oyeyemi T, Vichare A, et al. Estimation and comparison of current and future racial/ethnic representation in the US health care workforce. *JAMA Netw Open* 2021;4:e213789.
7. Ly DP, Jena AB. Trends in diversity and representativeness of health care workers in the United States, 2000 to 2019. *JAMA Netw Open* 2021;4:e2117086.
8. American College of Rheumatology. The 2015 Workforce Study of Rheumatology Specialists in the United States: survey results. 2015. URL: <https://www.rheumatology.org/portals/0/files/ACR-Workforce-Study-2015.pdf>.
9. Brotherton SE, Etzel SI. Graduate medical education, 2020-2021. *JAMA* 2021;326:1088–110.
10. Santhosh L, Babik JM. Trends in racial and ethnic diversity in internal medicine subspecialty fellowships from 2006 to 2018. *JAMA Netw Open* 2020;3:e1920482.
11. Ortega AN, Roby DH. Ending structural racism in the US health care system to eliminate health care inequities. *JAMA* 2021;326:613–5.
12. Razack S, Risor T, Hodges B, Steinert Y. Beyond the cultural myth of medical meritocracy. *Med Educ* 2020;54:46–53.

13. Olson RM, Feldman CH. A critical look at race-based practices in rheumatology guidelines. *Arthritis Care Res (Hoboken)* 2021. doi: <https://doi.org/10.1002/acr.24645>. E-pub ahead of print.
14. Rodriguez JE, Campbell KM, Pololi LH. Addressing disparities in academic medicine: what of the minority tax? *BMC Med Educ* 2015;15:6.
15. Ginther DK, Haak LL, Schaffer WT, Kington R. Are race, ethnicity, and medical school affiliation associated with NIH R01 type 1 award probability for physician investigators? *Acad Med* 2012;87:1516–24.
16. Xierali IM, Nivet MA. The racial and ethnic composition and distribution of primary care physicians. *J Health Care Poor Underserved* 2018;29:556–70.
17. Fuchs JW, Youmans QR. Mitigating bias in the era of virtual residency and fellowship interviews. *J Grad Med Educ* 2020;12:674–7.
18. Capers Q IV. How clinicians and educators can mitigate implicit bias in patient care and candidate selection in medical education. *ATS Sch* 2020;1:211–7.
19. Association of American Medical Colleges. Holistic review. 2022. URL: <https://www.aamc.org/services/member-capacity-building/holistic-review>.
20. Campbell KM, Rodriguez JE. Mentoring underrepresented minority in medicine (URMM) students across racial, ethnic and institutional differences. *J Natl Med Assoc* 2018;110:421–3.
21. Leyerzapf H, Abma TA, Steenwijk RR, Croiset G, Verdonk P. Standing out and moving up: performance appraisal of cultural minority physicians. *Adv Health Sci Educ Theory Pract* 2015;20:995–1010.
22. Vela MB, Chin MH, Peek ME. Keeping our promise—supporting trainees from groups that are underrepresented in medicine. *N Engl J Med* 2021;385:487–9.
23. FitzGerald C, Martin A, Berner D, Hurst S. Interventions designed to reduce implicit prejudices and implicit stereotypes in real world contexts: a systematic review. *BMC Psychol* 2019;7:29.
24. Tervalon M, Murray-Garcia J. Cultural humility versus cultural competence: a critical distinction in defining physician training outcomes in multicultural education [review]. *J Health Care Poor Underserved* 1998;9:117–25.

2022 American College of Rheumatology/American Association of Hip and Knee Surgeons Guideline for the Perioperative Management of Antirheumatic Medication in Patients With Rheumatic Diseases Undergoing Elective Total Hip or Total Knee Arthroplasty

Susan M. Goodman,¹  Bryan D. Springer,² Antonia F. Chen,³ Marshall Davis,⁴ David R. Fernandez,¹ Mark Figgie,¹ Heather Finlayson,⁵ Michael D. George,⁶  Jon T. Giles,⁷  Jeremy Gililand,⁸ Brian Klatt,⁹ Ronald MacKenzie,¹ Kaleb Michaud,¹⁰ Andy Miller,¹  Linda Russell,¹ Alexander Sah,¹¹ Matthew P. Abdel,¹² Beverly Johnson,¹³ Lisa A. Mandl,¹  Peter Sculco,¹ Marat Turgunbaev,¹⁴ Amy S. Turner,¹⁴  Adolph Yates Jr.,⁹ and Jasvinder A. Singh¹⁵

Guidelines and recommendations developed and/or endorsed by the American College of Rheumatology (ACR) are intended to provide guidance for patterns of practice and not to dictate the care of a particular patient. The ACR considers adherence to the recommendations within this guideline to be voluntary, with the ultimate determination regarding their application to be made by the physician in light of each patient's individual circumstances. Guidelines and recommendations are intended to promote beneficial or desirable outcomes but cannot guarantee any specific outcome. Guidelines and recommendations developed and endorsed by the ACR are subject to periodic revision as warranted by the evolution of medical knowledge, technology, and practice. ACR recommendations are not intended to dictate payment or insurance decisions, and drug formularies or other third-party analyses that cite ACR guidelines should state this. These recommendations cannot adequately convey all uncertainties and nuances of patient care. The ACR is an independent, professional, medical and scientific society that does not guarantee, warrant, or endorse any commercial product or service.

Objective. To develop updated guidelines for the perioperative management of disease-modifying medications for patients with rheumatic diseases, specifically those with inflammatory arthritis (IA) and those with systemic lupus erythematosus (SLE), undergoing elective total hip arthroplasty (THA) or elective total knee arthroplasty (TKA).

Methods. We convened a panel of rheumatologists, orthopedic surgeons, and infectious disease specialists, updated the systematic literature review, and included currently available medications for the clinically relevant population, intervention, comparator, and outcomes (PICO) questions. We used the Grading of Recommendations Assessment, Development and Evaluation (GRADE) methodology to rate the quality of evidence and the strength of recommendations using a group consensus process.

Results. This guideline updates the 2017 recommendations for perioperative use of disease-modifying antirheumatic therapy, including traditional disease-modifying antirheumatic drugs, biologic agents, targeted synthetic small-molecule drugs, and glucocorticoids used for adults with rheumatic diseases, specifically for the treatment of patients with IA, including rheumatoid arthritis and spondyloarthritis, those with juvenile idiopathic arthritis, or those with SLE who are undergoing elective THA or TKA. It updates recommendations regarding when to continue, when to withhold, and when to restart these medications and the optimal perioperative dosing of glucocorticoids.

Conclusion. This updated guideline includes recently introduced immunosuppressive medications to help decision-making by clinicians and patients regarding perioperative disease-modifying medication management for patients with IA and SLE at the time of elective THA or TKA.

INTRODUCTION

Advances in antirheumatic therapy have led to remarkable improvements in treatment and quality of life for people with rheumatic musculoskeletal diseases (RMDs); however, total hip arthroplasty (THA) and total knee arthroplasty (TKA) remain a mainstay of treatment among RMD patients with advanced symptomatic joint damage, most frequently those with inflammatory arthritis (IA), including spondylarthritis (SpA), rheumatoid arthritis (RA), or psoriatic arthritis (PsA), and those with systemic lupus erythematosus (SLE) (1–7). THA and TKA are successful procedures that improve mobility and decrease pain for people with RMD and end-stage arthritis. However, the risk of superficial and deep periprosthetic joint infection (PJI), a devastating complication, is increased after surgery in people with RMD, and avoiding infection is a top priority for them: patients with RA have a 50% increased risk of PJI compared to those with osteoarthritis (8,9). A panel of patients with RA was convened in 2017 prior to the publication of the American College of Rheumatology/American Association of Hip and Knee Surgeons (ACR/AAHKS) perioperative guideline and clearly stated that any risk of infection, while rare, was much more significant to them than the possibility of a postoperative flare, despite flares reported in >60% of patients after surgery (8,10–12). Recommendations regarding perioperative management of antirheumatic medications in the 2017 ACR/AAHKS guideline need updating to include drugs introduced in the interim, as well as review of more recent relevant publications.

The optimal strategy for perioperative medication management remains unknown, but antirheumatic therapy is a readily modifiable risk factor for infection, whereas other risk factors for adverse outcomes, including disease activity or severity or long-term glucocorticoid (GC) use, may not be modifiable (13–15). The ACR systematically updates guidelines every 5 years; therefore, to update the 2017 perioperative medication management guideline, the ACR and AAHKS convened a panel of rheumatologists, orthopedic surgeons, and infectious disease specialists and conducted a systematic review of the new literature published since the last guideline, adding new medications to those

previously available, although direct applicable evidence remains sparse in the literature. This guideline applies to management of antirheumatic medication for adult patients with IA, including those with RA, SpA, PsA, or ankylosing spondylitis (AS), adults with juvenile idiopathic arthritis (JIA), and adult patients with SLE undergoing elective THA or TKA.

Given the increased infection risk seen in patients with IA and patients with SLE undergoing these procedures, the existing evidence base used to guide our recommendations, the time afforded by these elective procedures to manage medications, and the frequent use of these procedures in patients with IA or SLE (4,6,16), we have restricted our recommendations to those undergoing either THA or TKA. A guideline cannot address all clinical situations and scenarios but seeks to provide recommendations for commonly encountered clinical problems.

While the principles surrounding these recommendations may be extrapolated and applied to other surgical procedures, it should be noted that the evidence and consensus used to inform this guideline were drawn primarily from orthopedic literature. As in the prior version, this guideline does not address indications for THA or TKA, medical decisions unrelated to antirheumatic drug therapy, the choice of the implant, the surgical approach, or the perioperative evaluation and management of concurrent disease, such as that affecting the cervical spine of patients with RA. Although routine perioperative care and preoperative optimization for patients with RA, SpA, JIA, or SLE include assessing risk of venous thromboembolism and major acute coronary events (17,18), this guideline does not address cardiac risk assessment or perioperative venous thromboembolism prophylaxis, as both are covered in existing guidelines (19–22). The goal of this updated guideline is to provide optimal support for clinicians and patients making decisions regarding medication management at the time of elective THA or TKA surgery.

METHODS

This guideline was developed following the ACR guideline development process and in accordance with ACR policies guiding

The article is published simultaneously in *Arthritis Care & Research* and *Journal of Arthroplasty*.

Supported by the American College of Rheumatology and the American Association of Hip and Knee Surgeons.

*[Correction added on 18 August 2022, after first online publication: The name of author Jeremy Gilliland has been corrected.]

¹Susan M. Goodman, MD, David R. Fernandez, MD, PhD, Mark Figgie, MD, MBA, Ronald MacKenzie, MD, Andy Miller, MD, Linda Russell, MD, Lisa A. Mandl, MD, MPH, Peter Sculco, MD: Hospital for Special Surgery, Weill Cornell Medicine, New York, New York; ²Bryan D. Springer, MD: OrthoCarolina Hip and Knee Center, Charlotte, North Carolina; ³Antonia F. Chen, MD, MBA: Brigham and Women's Hospital, Boston, Massachusetts; ⁴Marshall Davis: US Department of Defense, Tucson, Arizona; ⁵Heather Finlayson, MS, PA-C: Multispecialty Physician Partners, LLC, Colorado Arthritis Associates, Lakewood, Colorado; ⁶Michael D. George, MD, MSCE: University of Pennsylvania, Philadelphia; ⁷Jon T. Giles, MD, MPH: Columbia University, New York, New York; ⁸Jeremy Gilliland, MD: University of Utah and Veterans Affairs Medical Center, Salt Lake City; ⁹Brian Klatt, MD, Adolph Yates, Jr., MD: University of Pittsburgh

Medical Center, Pittsburgh, Pennsylvania; ¹⁰Kaleb Michaud, PhD: University of Nebraska Medical Center, Omaha, Nebraska, and Forward Databank, Wichita, Kansas; ¹¹Alexander Sah, MD: Sah Orthopaedic Associates, Institute for Joint Restoration, Fremont, California; ¹²Matthew P. Abdel, MD: Mayo Clinic, Rochester, Minnesota; ¹³Beverly Johnson, MD, MSc: Albert Einstein College of Medicine, Bronx, New York; ¹⁴Marat Turgunbaev, MD, MPH, Amy S. Turner: American College of Rheumatology, Atlanta, Georgia; ¹⁵Jasvinder A. Singh, MD, MPH: University of Alabama at Birmingham and Veterans Affairs Medical Center, Birmingham, Alabama.

Drs. Goodman, Springer, Yates, and Singh contributed equally to this work.

Author disclosures are available at <https://onlinelibrary.wiley.com/action/downloadSupplement?doi=10.1002%2Fart.42140&file=art42140-sup-0001-Disclosureform.pdf>.

Address correspondence to Susan M. Goodman, MD, Hospital for Special Surgery, 535 East 70th Street, 5th Floor, New York, NY 10021. Email: goodmans@hss.edu.

Submitted for publication February 9, 2022; accepted in revised form April 7, 2022.

Table 1. Populations included in this guideline*

Adults age ≥ 18 years diagnosed with RA, SpA, including AS and PsA, JIA, or SLE who are deemed to be appropriate surgical candidates, are undergoing elective THA or TKA, and who are receiving antirheumatic drug therapy at the time of surgery
All patients carrying the above diagnoses without restriction to those meeting classification criteria
SLE includes patients with severe or not severe SLE, defined as follows
Severe SLE: currently treated (induction or maintenance) for severe organ manifestations: lupus nephritis, CNS lupus, severe hemolytic anemia (hemoglobin < 9.9 gm/dl), platelets $< 50,000$, vasculitis (other than mild cutaneous vasculitis), including pulmonary hemorrhage, myocarditis, lupus pneumonitis, severe myositis (with muscle weakness, not just high enzymes), lupus enteritis (vasculitis), lupus pancreatitis, cholecystitis, lupus hepatitis, protein-losing enteropathy, malabsorption, orbital inflammation/myositis, severe keratitis, posterior severe uveitis/retinal vasculitis, severe scleritis, optic neuritis, anterior ischemic optic neuropathy (derived from the SELENA-SLEDAI flare index and the BILAG 2004 index)
Not severe SLE: not currently treated for above manifestations

* RA = rheumatoid arthritis; SpA = spondyloarthritis; AS = ankylosing spondylitis; PsA = psoriatic arthritis; JIA = juvenile idiopathic arthritis; SLE = systemic lupus erythematosus; THA = total hip arthroplasty; TKA = total knee arthroplasty; CNS = central nervous system; SELENA-SLEDAI = Safety of Estrogens in Lupus Erythematosus National Assessment version of the Systemic Lupus Erythematosus Disease Activity Index; BILAG = British Isles Lupus Assessment Group.

management of conflicts of interest and disclosures (<https://www.rheumatology.org/Practice-Quality/Clinical-Support/Clinical-Practice-Guidelines>), which includes Grading of Recommendations, Assessment, Development and Evaluations (GRADE) methodology and a framework for developing and presenting evidence (23,24) and adheres to Appraisal of Guidelines for Research and Evaluation (AGREE) criteria (25). The process for updating the 2017 guidelines began in 2021 (26). The populations included in this guideline are defined in Table 1 and are unchanged. Table 2 contains a list of the included drugs, along with their dosing intervals (reflecting the duration of effect), with the drugs newly added for this 2022 update denoted with footnotes. Brand names were used for newer medications that are likely to be unfamiliar to some orthopedists. Supplementary Appendix 1, available on the *Arthritis & Rheumatology* website at <http://onlinelibrary.wiley.com/doi/10.1002/art.42140>, includes a detailed description of the methods. Briefly, 3 teams were formed: a Core Leadership Team, a Literature Review Team, and a Voting Panel. The Core Leadership Team (SMG, BDS, AY, and JAS) confirmed that the population, intervention, comparator, and outcomes (PICO) questions would be the same as the ones used for the 2017 guideline, with updated medication lists to include any therapies approved for use in the US as of August 26, 2021, the stop date of our literature review (see Table 2 for medication list and Supplementary Appendix 2, available on the *Arthritis & Rheumatology* website at <http://onlinelibrary.wiley.com/doi/10.1002/art.42140>, for the PICO list, including outcomes; see Supplementary Appendices 3 and 4,

available at <http://onlinelibrary.wiley.com/doi/10.1002/art.42140>, for the search strategies and study selection process, respectively).

The Literature Review Team performed updates of the systematic literature review for each PICO, graded the quality of evidence (high, moderate, low, very low), and produced the evidence report (see Supplementary Appendix 5, available on the *Arthritis & Rheumatology* website at <http://onlinelibrary.wiley.com/doi/10.1002/art.42140>). The systematic literature review was updated by searching for relevant published literature from March 6, 2016 to August 26, 2021, because the previous systematic literature review for the 2017 guideline was performed from January 1, 1980 through March 6, 2016. Although the updated literature review added to the evidence report, the overall quality of the evidence remained low due to indirect evidence or small numbers of included cases. Because the overall quality of evidence was low, we included a review of the background risk for adverse events associated with THA or TKA in patients with RA, SpA, JIA, or SLE that is independent of use of the medications of interest to give context to our deliberations. Severe SLE is defined in Table 1 and refers to those patients with severe organ manifestations such as nephritis. We did not repeat our search for additional indirect evidence regarding medication risks associated with our drugs of interest; included medications are listed in Table 2.

The Voting Panel included 2 patients who have undergone arthroplasty surgery and who participated in the 2017 guideline's Patient Panel, one of whom participated in the previous Voting Panel. The panel reviewed evidence summaries from both the 2017 project and this update and discussed and voted on recommendation statements. The recommendation regarding anifrolumab and voclosporin was voted on via email. A recommendation could be either in favor of or against the proposed intervention and either strong or conditional. Consensus required $\geq 70\%$ agreement on both direction (for or against) and strength (strong or conditional) for each recommendation. Per GRADE methodology, a recommendation is categorized as strong if the panel is very confident that the benefits of an intervention clearly outweigh the harms (or vice versa); a conditional recommendation denotes uncertainty regarding the balance of benefits and harms, such as when the evidence quality is low or very low, or when the decision is more sensitive to individual patient preferences, or when costs are expected to impact the decision. Thus, conditional recommendations refer to decisions in which incorporation of patient preferences is a particularly essential element of decision-making.

Rosters of the Core Leadership Team, Literature Review Team, and Voting Panel are included in Supplementary Appendix 6, available on the *Arthritis & Rheumatology* website at <http://onlinelibrary.wiley.com/doi/10.1002/art.42140>. This study did not involve human subjects, and therefore, approval from Human Studies Committees was not required.

Table 2. Medications included in this 2022 guideline update*

	Dosing interval	Recommended timing of surgery since last medication dose
Medications to continue through surgery		
DMARDs: continue these medications through surgery (all patients)		
Methotrexate	Weekly	Anytime
Sulfasalazine	Once or twice daily	Anytime
Hydroxychloroquine	Once or twice daily	Anytime
Leflunomide (Arava)	Daily	Anytime
Doxycycline	Daily	Anytime
Apremilast (Otezla)	Twice daily†	Anytime†
Severe SLE-specific medications: continue these medications in the perioperative period in consultation with the treating rheumatologist‡		
Mycophenolate mofetil	Twice daily	Anytime
Azathioprine	Daily or twice daily	Anytime
Cyclosporine	Twice daily	Anytime
Tacrolimus	Twice daily (IV and PO)	Anytime
Rituximab (Rituxan)	IV every 4–6 months†	Month 4–6†
Belimumab SC (Benlysta)	Weekly†	Anytime†
Belimumab IV (Benlysta)	Monthly†	Week 4†
Anifrolumab (Saphnelo)§	IV every 4 weeks†	Week 4†
Voclosporin (Lupkynis)§	Twice daily†	Continue†
Medications to withhold prior to surgery¶		
Biologics: withhold these medications through surgery		
Infliximab (Remicade)	Every 4, 6, or 8 weeks	Week 5, 7, or 9
Adalimumab (Humira)	Every 2 weeks	Week 3
Etanercept (Enbrel)	Every week	Week 2
**Golimumab (Simponi)	Every 4 weeks (SQ) or every 8 weeks (IV)	Week 5; Week 9
Abatacept (Orencia)	Monthly (IV) or weekly (SC)	Week 5; week 2
Certolizumab (Cimzia)	Every 2 or 4 weeks	Week 3 or 5
Rituximab (Rituxan)	2 doses 2 weeks apart every 4–6 months	Month 7
Tocilizumab (Actemra)	Every week (SC) or every 4 weeks (IV)	Week 2; week 5
Anakinra (Kineret)	Daily	Day 2
IL-17 secukinumab (Cosentyx)	Every 4 weeks	Week 5
Ustekinumab (Stelara)	Every 12 weeks	Week 13
Ixekizumab (Taltz)§	Every 4 weeks†	Week 5†
IL-23 guselkumab (Tremfya)§	Every 8 weeks†	Week 9†
JAK inhibitors: withhold this medication 3 days prior to surgery#		
Tofacitinib (Xeljanz)	Daily or twice daily†	Day 4†
Baricitinib (Olumiant)§	Daily†	Day 4†
Upadacitinib (Rinvoq)§	Daily†	Day 4†
Not severe SLE: withhold these medications 1 week prior to surgery		
Mycophenolate mofetil	Twice daily	1 week after last dose†
Azathioprine	Daily or twice daily	1 week after last dose
Cyclosporine	Twice daily	1 week after last dose†
Tacrolimus	Twice daily (IV and PO)	1 week after last dose†
Rituximab (Rituxan)	Every 4–6 months	Month 7
Belimumab IV (Benlysta)	Monthly†	Week 5†
Belimumab SC (Benlysta)	Weekly†	Week 2†

* Dosing intervals obtained from prescribing information provided online by pharmaceutical companies. Adapted from the 2017 American College of Rheumatology/American Association of Hip and Knee Surgeons guideline (26). DMARDs = disease-modifying antirheumatic drugs; SLE = systemic lupus erythematosus; IV = intravenous; PO = by mouth; SC = subcutaneous; IL-17 = interleukin-17.

† Recommendation that has changed since 2017.

‡ Severe SLE indicates organ-threatening disease.

§ Drug added for 2022 update.

¶ For patients with rheumatoid arthritis, ankylosing spondylitis, psoriatic arthritis, or all SLE for whom antirheumatic therapy was withheld prior to undergoing total joint arthroplasty, antirheumatic therapy should be restarted once the wound shows evidence of healing, any sutures/staples are out, there is no significant swelling, erythema, or drainage, and there is no ongoing nonsurgical site infection, which is typically ~14 days.

Recommendation pertains to infection risk and does not account for risk of cardiac events or venous thromboembolism.

** [Correction added on 18 August 2022, after first online publication: One of the biologic medications to withhold prior to surgery was omitted from Table 2. Golimumab (Simponi) and the corresponding dosing/timing have been added.]

RESULTS/RECOMMENDATIONS

How to interpret the recommendations

1. All recommendations in this guideline are conditional due to the quality of the evidence (see bolded statements in Table 3). A

conditional recommendation means that the desirable effects of following the recommendation probably outweigh the undesirable effects, so the course of action would apply to the majority of the patients but may not apply to all patients. Because of this, conditional recommendations are preference sensitive and always warrant a

Table 3. Recommendations for perioperative management of anti-rheumatic drug therapy in patients with inflammatory arthritis and those with systemic lupus erythematosus (SLE) undergoing elective total hip arthroplasty (THA) or total knee arthroplasty (TKA)*

Recommendation/strength of recommendation	Level of evidence
For patients with RA, AS, PsA, JIA, or all SLE undergoing THA or TKA, continuing the usual dosing of the following DMARDs through surgery is conditionally recommended: methotrexate, leflunomide, hydroxychloroquine, sulfasalazine, and/or apremilast.†	Low to moderate
For patients with RA, AS, PsA, or JIA undergoing THA or TKA, withholding all biologics, including rituximab, prior to surgery and planning the surgery after the next dose is due is conditionally recommended.	Low
For patients with RA, AS, PsA, or JIA undergoing THA or TKA, withholding tofacitinib, baricitinib, and upadacitinib for at least 3 days prior to surgery is conditionally recommended.‡	Low
For patients with SLE (not severe) undergoing THA or TKA, withholding the current dose of mycophenolate mofetil, mycophenolic acid, azathioprine, cyclosporine, mizoribine, or tacrolimus 1 week prior to surgery is conditionally recommended.	Low
For patients with SLE (not severe) undergoing THA or TKA, withholding the usual dose of belimumab and rituximab prior to surgery is conditionally recommended.	Low
For patients with severe SLE who have been deemed appropriate to undergo THA or TKA, continuing the usual dose of mycophenolate mofetil, mycophenolic acid (Myfortic), azathioprine, mizoribine, cyclosporine, or tacrolimus, anifrolumab, and voclosporin through surgery is conditionally recommended.‡	Low
For patients with severe SLE undergoing THA or TKA, continuing belimumab and planning surgery in the last month of the dosing cycle of rituximab is conditionally recommended.‡	Low
For patients with RA, AS, PsA, or all SLE for whom antirheumatic therapy was withheld prior to undergoing TJA, antirheumatic therapy should be restarted once the wound shows evidence of healing, any sutures/staples are out, there is no significant swelling, erythema, or drainage, and there is no ongoing nonsurgical site infection, which is typically ~14 days, is conditionally recommended.	Low
For patients with RA, AS, PsA, or all SLE undergoing THA or TKA who are receiving glucocorticoids for their rheumatic condition, continuing their current daily dose of glucocorticoids rather than administering supraphysiologic doses of glucocorticoids on the day of surgery is conditionally recommended.	Low

* RA = rheumatoid arthritis; AS = ankylosing spondylitis; PsA = psoriatic arthritis; JIA = juvenile idiopathic arthritis; DMARDs = disease-modifying antirheumatic drugs; TJA = total joint arthroplasty.

† Apremilast is a change from the prior recommendation.

‡ Indicates a change from the prior recommendation.

shared decision-making approach. No strong recommendations are made in this guideline, although no recommendation achieved <80% of the vote, and 4 of the votes were unanimous.

2. For each recommendation, a summary of the supporting evidence or conditions is provided.

3. Therapies that were approved after the end of the original systematic literature review on March 6, 2016 through August 2021 are included in these updated recommendations. Therapies approved after the end of the updated systematic review (March 6, 2016 to August 26, 2021) are not included in these recommendations.

4. PICO questions were combined in the final recommendations for clarity.

Recommendations

For patients with RA, AS, PsA, JIA, or all SLE undergoing elective THA or TKA, continuing the usual dosing of the following disease-modifying antirheumatic drugs (DMARDs) through surgery is conditionally recommended: methotrexate, leflunomide, hydroxychloroquine, sulfasalazine, and/or apremilast.

This conditional recommendation now includes apremilast, but it is otherwise unchanged from the 2017 guideline. Four observational studies provided additional indirect evidence to the previous systematic literature review and found no relationship between the included drugs and the risk of postoperative infections, although the number of included cases and events were low (11,27–29). Patients with a history of severe or recurrent infections or prior prosthetic joint infection may elect to withhold these medications before surgery.

For patients with RA, AS, PsA, or JIA undergoing elective THA or TKA, withholding all biologics, including rituximab, prior to surgery and planning the surgery after the next dose is due is conditionally recommended.

This recommendation no longer includes patients with SLE, who are addressed separately (see below for rationale) but has not otherwise changed. Table 2 contains the included medications.

This recommendation is conditional because the evidence is indirect and there is a lack of a comparator group in the included studies (27,30). This recommendation was informed by additional new evidence from 2 studies that used administrative claims data to accurately capture the timing of infliximab or abatacept use before THA or TKA and to evaluate associations between biologics timing and outcomes (30,31). In both studies, there was no difference in postoperative outcomes when comparing short medication interruptions of ~1 dosing interval to longer interruptions. Results were similar in an additional study evaluating infliximab or abatacept timing before other types of surgery (32). These studies also showed no difference in outcomes in patients receiving infliximab or abatacept within 1 dosing interval before surgery, although patients receiving intravenous abatacept within 2 weeks of surgery (one-half of a dosing interval) had a

numerically higher rate of adverse events that was not statistically significant (31).

Planning the surgery after the end of the dose interval was favored because active drug levels would be low. For example, for rituximab, dosed every 6 months, surgery should be planned during month 7, and for adalimumab, dosed every 2 weeks, surgery should be planned for week 3 (see Table 2 for drug dosing intervals). Patients and their physicians might elect surgery within the dosing cycle if their symptoms from the operative joint are severe and the anticipated pain relief provided by surgery outweighs the possible risk of infection as may occur with advanced osteonecrosis. In addition, those patients whose disease has been challenging to control may also elect to continue their medications rather than risk loss of disease control, as this may occur when medications are withheld.

For patients with RA, AS, PsA, or JIA undergoing THA or TKA, withholding tofacitinib, baricitinib, and upadacitinib for at least 3 days prior to surgery is conditionally recommended.

This conditional recommendation was changed from the prior guideline. For the previous guideline, while the short serum half-life of tofacitinib was known, concern for a longer duration of the immune effect prompted the recommendation to withhold tofacitinib for 7 days prior to surgery. The new recommendation was informed by trial data demonstrating rapid increases in disease activity after interrupting tofacitinib therapy, suggesting a rapid reversal of the immunosuppressive effects, so the recommendation was changed to withhold tofacitinib for 3 days prior to surgery (33). The serum half-life of the newer JAK inhibitors is similar to that of tofacitinib. However, patients and their physicians might withhold JAK inhibitors for a longer period if a patient has a history of infections or a prior prosthetic joint infection. This recommendation does not pertain to the risk of a cardiac event or a venous thromboembolic event (VTE) potentially associated with JAK inhibitors.

For patients with SLE (not severe) undergoing THA or TKA, withholding the current dose of mycophenolate mofetil, mycophenolic acid, azathioprine, cyclosporine, mizoribine, or tacrolimus 1 week prior to surgery is conditionally recommended.

This recommendation remains unchanged from the prior guideline. Patients with frequent flares or SLE that is difficult to control might continue their medications, but the majority could be followed up closely after surgery to address a flare.

For patients with SLE (not severe) undergoing THA or TKA, withholding the usual dose of belimumab and rituximab prior to surgery is conditionally recommended.

This recommendation is unchanged from the prior guideline. Patients with SLE that is not severe would not be at risk for permanent organ damage should they flare. In addition, nonsevere SLE patients could be followed up closely after surgery, and an intervention could be made to treat a flare as needed. Patients with frequent flares or SLE that is difficult to control might choose

to continue their medications in a shared decision-making approach with their physicians, but the majority could be followed up closely after surgery to address a flare.

For patients with severe SLE (Table 1) who have been deemed appropriate to undergo THA or TKA, continuing the usual dose of mycophenolate mofetil, mycophenolic acid (Myfortic), azathioprine, mizoribine, cyclosporine, or tacrolimus, anifrolumab, and voclosporin through surgery is conditionally recommended.

This recommendation has changed with the addition of anifrolumab and voclosporin, recently introduced medications for severe SLE. These medications should be continued through surgery. There were no new data available to update this recommendation, so the guidance reflects the concern about disease flares and the risk of organ damage in severe SLE that could be precipitated by medication withdrawal; although postoperative adverse events are linked to disease severity, they have not been clearly associated with medication use. As noted in the previous guideline, the patient's rheumatologist should be consulted regarding medication management. A patient with severe SLE who has been stable for >6 months or who has a history of recurrent or severe infections might discontinue the medications in the perioperative period.

For patients with severe SLE undergoing THA or TKA, continuing belimumab and planning surgery in the last month of the dosing cycle of rituximab is conditionally recommended.

In the prior guideline, rituximab was included in the recommendations with other biologics, but increased use for SLE treatment, the long dosing interval for rituximab, and the indication of belimumab as therapy for severe SLE manifestations has informed this change. Surgery should be planned at the end of the dosing cycle, typically during month 5 or 6 for patients receiving rituximab every 6 months, and to avoid disruptions of therapy rather than wait longer, given the long dosing interval for rituximab. The panel noted that rituximab is used in SLE without an indication approved by the US Food and Drug Administration (FDA) but also noted that it has been included in SLE treatment guidelines (34). In addition, there is a risk of disease flares in patients with severe SLE with organ damage if therapy is interrupted. Situations such as prior severe infections and/or SLE that has been stable for >6 months might prompt the clinician to withhold rituximab for a longer period. Recent studies describe an increased risk of adverse events associated with SLE that appears to be more significant for THA than TKA, but there are no strong data to suggest that these outcomes are related to medication management (34–37).

This recommendation has changed since the prior guideline in part because of the additional indication for the use of belimumab in severe SLE including nephritis, as well as increased comfort with belimumab among clinicians and patients given its widespread use, low infection risk described in clinical trials, and

inclusion in SLE treatment guidelines (34,38,39). The panel remained concerned about disruptions of successful treatment regimens in patients with severe SLE given the potential for severe organ damage, although belimumab might be withheld in stable patients with a history of prior infections.

For patients with RA, AS, PsA, or all SLE for whom anti-rheumatic therapy was withheld prior to undergoing total joint arthroplasty, antirheumatic therapy should be restarted once the wound shows evidence of healing, any sutures/staples are out, there is no significant swelling, erythema, or drainage, and there is no ongoing nonsurgical site infection, which is typically ~14 days after surgery, is conditionally recommended.

Drugs should be restarted based on the clinical status of the patient and the status of the healing wound. Although there was additional evidence to support this recommendation from the literature review, it was indirect and of very low quality across the critical outcomes. Patients with nonrheumatic diseases were included, or the study did not include a comparator group. In one study using a large Medicare data set, outcomes were better in patients who restarted infliximab within 4 weeks after surgery compared to those who restarted later, but the authors noted that this was likely because postoperative complications led to delays in restarting therapy (30).

Patients and their physicians might elect longer periods of not taking medication given a history of prior severe infections or a history of a prior prosthetic joint infection.

For patients with RA, AS, PsA, or all SLE undergoing THA or TKA who are receiving GCs for their rheumatic condition, continuing their current daily dose of GCs rather than administering supraphysiologic doses of GCs on the day of surgery is conditionally recommended.

This recommendation is unchanged from the previous guideline, with 2 new studies considered. One study found no significant association of supraphysiologic (“stress dose”) GC doses with adverse events in SLE patients undergoing THA or TKA, but the sizes of the patient groups were small (35). Another study of 432 patients with RA who underwent THA and TKA concluded that patients with higher GC exposure were more likely to have hyperglycemia and other complications and that the risk of short-term complications is increased by 8.4% for every 10-mg increase in GC dose, and a lower cumulative GC dose was not associated with hypotension (40). Exceptions to this recommendation are unchanged. However, wound healing may be affected by use of low-dose (<5 mg/day) GCs when the cumulative dose is high, which may also contribute to perioperative infection risk. This recommendation does not refer to patients with JIA who may have received GCs during childhood developmental stages or to patients receiving GCs to treat primary adrenal insufficiency or primary hypothalamic disease, all of whom may require supraphysiologic doses of GCs to maintain hemodynamic stability.

DISCUSSION

We have updated the 2017 ACR/AAHKS guideline for the perioperative management of DMARDs, biologics, and GCs for adult patients with RA, SpA including AS and PsA, JIA, and SLE undergoing elective THA or TKA. This guideline is intended for use by clinicians and patients and balances the risk of flares of disease when medications are withheld versus infection risk attributed to the medications when they are continued. This update adds new medications introduced and reviews the studies published since the 2017 ACR/AAHKS guideline that have informed our recommendations. The scope of the guideline has not changed and addresses when to withhold and when to restart disease-modifying therapies, as well as perioperative GC management. Although we included patients in our Voting Panel, we did not reinstate the Patient Panel due to the risk associated with the COVID-19 pandemic, and because we thought it was unlikely that patients’ priorities regarding the risk of flare versus the risk of infection would have changed. The updated medication list includes medications introduced to treat RA and SpA, including AS and PsA. We have included perioperative management recommendations for the recently introduced JAK-targeted therapies, baricitinib and upadacitinib, in addition to tofacitinib. We have included new management recommendations for the interleukin-17 (IL-17) blocking agent ixekizumab, the IL-23–blocking drug guselkumab, and the novel synthetic DMARD apremilast. Anifrolumab, approved by the FDA on July 30, 2021, and voclosporin, approved January 22, 2021, were included in this guideline, although there is no information regarding their use in the perioperative period. They increase the risk of infection, and therefore the use of these medications in patients with severe SLE would merit review by the treating rheumatologist in consideration of surgery. The Voting Panel agreed with their inclusion via email voting.

This guideline is informed by cohort studies including pharmacoepidemiologic studies using large administrative databases. To our knowledge, there have been no randomized controlled trials since the publication of the prior ACR/AAHKS guideline in 2017, so much of the data supporting these recommendations remains largely indirect or of low quality. Similar to the last guideline, the major limitation remains the paucity of high-quality direct evidence regarding the added risk of infection from medication use at the time of THA or TKA; therefore, these recommendations continue to rely on indirect studies describing results in patients without rheumatic diseases or on assumptions or conclusions extrapolated from nonsurgical studies. An additional limitation of this guideline is the lack of participation from other orthopedic surgical specialties such as spine or foot and ankle. Moreover, our literature review focused only on THA and TKA, so concerns of other surgical specialists may have not been addressed by our focused assessment of THA and TKA. Therefore, we are unable to generalize our recommendations to rheumatic disease patients undergoing other orthopedic surgical procedures, as well

as non-orthopedic surgery. However, the principles underlying our recommendations may provide a framework to apply in other surgical settings.

A strength of this guideline is the robust collaboration between orthopedic hip and knee surgeons and rheumatologists, as well as the inclusion of patients, epidemiologists, and specialists in infectious diseases who represent other stakeholders for this project. This multidisciplinary collaboration facilitated the uptake and dissemination of the prior guideline, and it is anticipated that these recommendations will be similarly distributed and used to guide busy clinicians and their patients at the time of THA and TKA. GRADE methodology supports consensus-based recommendations that can be reached based on low-quality evidence across the critical outcomes and transparently rates the strength of the recommendation as well as the quality of the evidence supporting the recommendation (24,41). Because most of the evidence informing this guideline is indirect and/or of low quality, all of the recommendations are conditional. Nonetheless, consensus of the Voting Panel was high. Four recommendations received 100% agreement, and none achieved <80% agreement.

This guideline does not address perioperative prophylaxis or treatment of VTEs or perioperative cardiac assessment, as these are addressed in several other focused publications. JAK inhibitors as a class carry an increased risk of VTE, which is a black box warning from the FDA, which more recently issued a warning regarding increased cardiovascular risk (42). Future research should address an assessment of the perioperative cardiac and VTE risks associated with JAK inhibitors and other factors such as disease activity for which there is no direct evidence.

Perioperative management of rituximab has been a challenge given the long dosing interval of 6 months and the recognized risk of severe infection linked to its use (43–46). In this updated guideline, we have separated the perioperative use of rituximab in SLE from the perioperative management of rituximab in other diseases (46). Although rituximab has an FDA indication for RA, but not for SLE, the 2019 European Alliance of Associations for Rheumatology recommendations for the management of SLE include use of rituximab, providing an additional rationale for our change to separate the recommendations for RA and other rheumatic conditions from those for severe SLE (34). Our recommendations are linked to drug dosing intervals given our assumption that the dosing interval reflects the period of immunosuppression; however, infection risk in patients treated with rituximab may be unrelated to the rituximab dosing interval and is increased in those with hypogammaglobulinemia (47,48). Additional research is needed to increase understanding of the factors contributing to infection risk with rituximab therapy, such as duration of therapy or immunoglobulin levels at the time of surgery.

As previously, the recommendations that form this guideline are not treatment mandates. These recommendations will provide the backbone for a shared decision-making process

between patient and physician regarding perioperative medication management around the time of surgery. The previous Patient Panel provided critical insight into the priorities of patients around the time of THA and TKA and the importance of open discussion and consultation between the perioperative physician, the orthopedic surgeon, and the rheumatologist. One patient representative on the current Voting Panel noted the anxiety that patients experience around changes to their medication regimens and urged clinicians to be cognizant of this important issue. Although not all scenarios can be addressed in the scope of a document such as this guideline, the most common scenarios are included, and these recommendations should supplement the usual perioperative clinical assessment, risk benefit discussions, and management for clinical optimization prior to surgery.

We continue to support ongoing research to better inform perioperative management of medications used commonly in rheumatic diseases. While we have added to our information base regarding GC management and the timing of biologic infusion therapy, we still lack high-level data from randomized controlled trials to provide clearer answers to the important questions addressed in the guideline. Data concerning traditional synthetic DMARDs should be updated with randomized controlled trials, and data regarding perioperative management of biologics also needs more definitive study. Patients with rheumatic diseases have higher rates of concomitant metabolic syndrome and cardiac disease and may also be at potentially higher risk of perioperative cardiac and/or thromboembolic events. Therefore, consideration of the role of comorbidities and the interaction with antirheumatic therapy should also be pursued.

In summary, this guideline provides an update to the ACR/AAHKS 2017 guideline to provide clinicians and patients information about risks and benefits regarding management of perioperative antirheumatic medication to inform decisions prior to THA and TKA. We have updated our evidence base through our search of the current literature and assessed that information through the lens of our clinical expertise and the perspectives of the patients who have participated in this process. We acknowledge the gaps in our information base and intend to continue to fill those gaps as more research is available.

ACKNOWLEDGMENTS

We thank the ACR staff, including Regina Parker for assistance in coordinating the administrative aspects of the project and Cindy Force for assistance with manuscript preparation. We thank Janet Waters for her assistance in developing the literature search strategy as well as performing the initial literature search and update searches.

AUTHOR CONTRIBUTIONS

All authors were involved in drafting the article or revising it critically for important intellectual content, and all authors approved the final version to be submitted for publication. Dr. Goodman had full access to all

of the data in the study and takes responsibility for the integrity of the data and the accuracy of the data analysis.

Study conception and design. Goodman, Springer, Klatt, Russell, Sah, Abdel, Johnson, Turner, Yates, Singh.

Acquisition of data. Goodman, Springer, George, Klatt, MacKenzie, Sah, Abdel, Johnson, Mandl, Sculco, Turgunbaev, Yates, Singh.

Analysis and interpretation of data. Goodman, Springer, Chen, Davis, Fernandez, Figgie, Finlayson, George, Giles, Gilliland, Klatt, MacKenzie, Michaud, Miller, Russell, Sah, Abdel, Johnson, Turgunbaev, Yates, Singh.

REFERENCES

- Choi YM, Debbaneh M, Weinberg JM, Yamauchi PS, van Voorhees AS, Armstrong AW, et al. From the medical board of the National Psoriasis Foundation: perioperative management of systemic immunomodulatory agents in patients with psoriasis and psoriatic arthritis. *J Am Acad Dermatol* 2016;75:798–805.e7.
- Strand V, Singh JA. Improved health-related quality of life with effective disease-modifying antirheumatic drugs: evidence from randomized controlled trials. *Am J Manag Care* 2007;13 Suppl 9:237.
- Tung K, Lee Y, Lin C, Lee C, Lin M, Wei JC. Opposing trends in total knee and hip arthroplasties for patients with rheumatoid arthritis vs. the general Population: a 14-year retrospective study in Taiwan. *Front Med* 2021;8:502.
- Mertelsmann-Voss C, Lyman S, Pan TJ, Goodman S, Figgie MP, Mandl LA. Arthroplasty rates are increased among US patients with systemic lupus erythematosus: 1991–2005. *J Rheumatol* 2014;41:867–74.
- Nikiphorou E, Carpenter L, Morris S, Macgregor AJ, Dixey J, Kiely P, et al. Hand and foot surgery rates in rheumatoid arthritis have declined from 1986 to 2011, but large-joint replacement rates remain unchanged: results from two UK inception cohorts. *Arthritis Rheumatol* 2014;66:1081–9.
- Richter MD, Crowson CS, Matteson EL, Makol A. Orthopedic surgery among patients with rheumatoid arthritis: a population-based study to identify risk factors, sex differences, and time trends. *Arthritis Care Res (Hoboken)* 2018;70:1546–50.
- Ward MM. Risk of total knee arthroplasty in young and middle-aged adults with ankylosing spondylitis. *Clin Rheumatol* 2018;37:3431–3.
- Ravi B, Croxford R, Hollands S, Paterson JM, Bogoch E, Kreder H, et al. Increased risk of complications following total joint arthroplasty in patients with rheumatoid arthritis. *Arthritis Rheumatol* 2014;66:254–63.
- Richardson SS, Kahlenberg CA, Goodman SM, Russell LA, Sculco TP, Sculco PK, et al. Inflammatory arthritis is a risk factor for multiple complications after total hip arthroplasty: a population-based comparative study of 68,348 patients. *J Arthroplasty* 2019;34:1150–4.e2.
- Goodman SM, Miller AS, Turgunbaev M, Guyatt G, Yates A, Springer B, et al. Clinical practice guidelines: incorporating input from a patient panel. *Arthritis Care Res (Hoboken)* 2017;69:1125–30.
- Goodman SM, Bykerk VP, DiCarlo E, Cummings RW, Donlin LT, Orange DE, et al. Flares in patients with rheumatoid arthritis after total hip and total knee arthroplasty: rates, characteristics, and risk factors. *J Rheumatol* 2018;45:604–11.
- Goodman SM, Mirza SZ, DiCarlo EF, Pearce-Fisher D, Zhang M, Mehta B, et al. Rheumatoid arthritis flares after total hip and total knee arthroplasty: outcomes at one year. *Arthritis Care Res (Hoboken)* 2020;72:925–32.
- Au K, Reed G, Curtis JR, Kremer JM, Greenberg JD, Strand V, et al. High disease activity is associated with an increased risk of infection in patients with rheumatoid arthritis. *Ann Rheum Dis* 2011;70:785–91.
- Doran MF, Crowson CS, Pond GR, O'Fallon WM, Gabriel SE. Predictors of infection in rheumatoid arthritis. *Arthritis Rheum* 2002;46:2294–300.
- Cordtz RL, Zobbe K, Højgaard P, Kristensen LE, Overgaard S, Odgaard A, et al. Predictors of revision, prosthetic joint infection and mortality following total hip or total knee arthroplasty in patients with rheumatoid arthritis: a nationwide cohort study using Danish health-care registers. *Ann Rheum Dis* 2018;77:281.
- Ward MM. Increased rates of both knee and hip arthroplasties in older patients with ankylosing spondylitis. *J Rheumatol* 2019;46:31–7.
- Salmon JE, Roman MJ. Subclinical atherosclerosis in rheumatoid arthritis and systemic lupus erythematosus. *Am J Med* 2008;121 Suppl 1:3.
- Lin JA, Liao CC, Lee YJ, Wu CH, Huang WQ, Chen TL. Adverse outcomes after major surgery in patients with systemic lupus erythematosus: a nationwide population-based study. *Ann Rheum Dis* 2014;73:1646–51.
- Jacobs JJ, Mont MA, Bozic KJ, Della Valle CJ, Goodman SB, Lewis CG, et al. American Academy of Orthopaedic Surgeons clinical practice guideline on: preventing venous thromboembolic disease in patients undergoing elective hip and knee arthroplasty. *J Bone Joint Surg Am* 2012;94:746–7.
- Falck-Ytter Y, Francis CW, Johanson NA, Curley C, Dahl OE, Schulman S, et al. Prevention of VTE in orthopedic surgery patients: antithrombotic therapy and prevention of thrombosis, 9th ed: American College of Chest Physicians evidence-based clinical practice guidelines. *Chest* 2012;141 Suppl:e278S–e325S.
- Fleisher LA, Beckman JA, Brown KA, Calkins H, Chaikof EL, Fleischmann KE, et al. 2009 ACCF/AHA focused update on perioperative beta blockade incorporated into the ACC/AHA 2007 guidelines on perioperative cardiovascular evaluation and care for noncardiac surgery: a report of the American College of Cardiology Foundation/American Heart Association task force on practice guidelines. *Circulation* 2009;120:e169–276.
- American College of Cardiology Foundation/American Heart Association Task Force on Practice Guidelines, American Society of Echocardiography, American Society of Nuclear Cardiology, Heart Rhythm Society, Society of Cardiovascular Anesthesiologists, Society for Cardiovascular Angiography and Interventions, et al. 2009 ACCF/AHA focused update on perioperative beta blockade incorporated into the ACC/AHA 2007 guidelines on perioperative cardiovascular evaluation and care for noncardiac surgery. *J Am Coll Cardiol* 2009;54:e13–e118.
- Alonso-Coello P, Schünemann HJ, Moberg J, Brignardello-Petersen R, Akl EA, Davoli M, et al. GRADE evidence to decision (EtD) frameworks: a systematic and transparent approach to making well informed health-care choices. 1: Introduction. *BMJ* 2016;353:i2016.
- Andrews JC, Schünemann HJ, Oxman AD, Pottie K, Meerpohl JJ, Coello PA, et al. GRADE guidelines: 15. going from evidence to recommendation—determinants of a recommendation's direction and strength. *J Clin Epidemiol* 2013;66:726–35.
- Brouwers MC, Kho ME, Browman GP, Burgers JS, Cluzeau F, Feder G, et al. AGREE II: advancing guideline development, reporting and evaluation in health care. *CMAJ* 2010;182:E839–42.
- Goodman SM, Springer B, Guyatt G, Abdel MP, Dasa V, George M, et al. 2017 American College of Rheumatology/American Association of Hip and Knee Surgeons guideline for the perioperative management of antirheumatic medication in patients with rheumatic diseases undergoing elective total hip or total knee arthroplasty. *Arthritis Rheumatol* 2017;69:1538–51.
- Hernigou P, Dubory A, Potage D, Roubineau F, Flouzat-Lachaniette CH. Outcome of knee revisions for osteoarthritis and inflammatory arthritis with postero-stabilized arthroplasties: a mean

- ten-year follow-up with 90 knee revisions. *Int Orthop* 2017;41:757–63.
28. Ren Y, Yang Q, Luo T, Lin J, Jin J, Qian W, et al. Better clinical outcome of total knee arthroplasty for rheumatoid arthritis with perioperative glucocorticoids and disease-modifying anti-rheumatic drugs after an average of 11.4-year follow-up. *J Orthop Surg Res* 2021;16:84–9.
29. Borgas Y, Gülfe A, Kindt M, Stefánsdóttir A. Anti-rheumatic treatment and prosthetic joint infection: an observational study in 494 elective hip and knee arthroplasties. *BMC Musculoskelet Disord* 2020;21:410.
30. George MD, Baker JF, Hsu JY, Wu Q, Xie F, Chen L, et al. Perioperative timing of infliximab and the risk of serious infection after elective hip and knee arthroplasty. *Arthritis Care Res (Hoboken)* 2017;69:1845–54.
31. George MD, Baker JF, Winthrop K, Alemao E, Chen L, Connolly S, et al. Timing of abatacept before elective arthroplasty and risk of postoperative outcomes. *Arthritis Care Res (Hoboken)* 2019;71:1224–33.
32. George MD, Baker JF, Winthrop KL, Goldstein SD, Alemao E, Chen L, et al. Immunosuppression and the risk of readmission and mortality in patients with rheumatoid arthritis undergoing hip fracture, abdominopelvic and cardiac surgery. *Ann Rheum Dis* 2020;79:573–80.
33. Kaine J, Tesser J, Takiya L, DeMasi R, Wang L, Snyder M, et al. Re-establishment of efficacy of tofacitinib, an oral JAK inhibitor, after temporary discontinuation in patients with rheumatoid arthritis. *Clin Rheumatol* 2020;39:2127–37.
34. Fanouriakis A, Kostopoulou M, Alunno A, Aringer M, Bajema I, Boletis JN, et al. 2019 update of the EULAR recommendations for the management of systemic lupus erythematosus. *Ann Rheum Dis* 2019;78:736–45.
35. Fein AW, Figgie CA, Dodds TR, Wright-Chisem J, Parks ML, Mandl LA, et al. Systemic lupus erythematosus does not increase risk of adverse events in the first 6 months after total knee arthroplasty. *J Clin Rheumatol* 2016;22:355–9.
36. Merayo-Chalico J, González-Contreras M, Ortíz-Hernández R, Alcocer-Varela J, Marcial D, Gómez-Martín D. Total hip arthroplasty outcomes: an 18-year experience in a single center: is systemic lupus erythematosus a potential risk factor for adverse outcomes? *J Arthroplasty* 2017;32:3462–7.
37. Li Z, Du Y, Xiang S, Feng B, Bian Y, Qian W, et al. Risk factors of perioperative complications and transfusion following total hip arthroplasty in systemic lupus erythematosus patients. *Lupus* 2019;28:1134–40.
38. Navarra SV, Guzmán RM, Gallacher AE, Hall S, Levy RA, Jimenez RE, et al. Efficacy and safety of belimumab in patients with active systemic lupus erythematosus: a randomised, placebo-controlled, phase 3 trial. *Lancet* 2011;377:721–31.
39. Singh JA, Shah NP, Mudano AS. Belimumab for systemic lupus erythematosus. *Cochrane Database Syst Rev* 2021;2:CD010668.
40. Chukir T, Goodman SM, Tornberg H, Do H, Thomas C, Sigmund A, et al. Perioperative glucocorticoids in patients with rheumatoid arthritis having total joint replacements: help or harm? *ACR Open Rheumatol* 2021;3:654–9.
41. Guyatt GH, Oxman AD, Vist GE, Kunz R, Falck-Ytter Y, Alonso-Coello P, et al. GRADE: an emerging consensus on rating quality of evidence and strength of recommendations. *BMJ* 2008;336:924–6.
42. US Food and Drug Administration. FDA requires warnings about increased risk of serious heart-related events, cancer, blood clots, and death for JAK inhibitors that treat certain chronic inflammatory conditions. URL: <https://www.fda.gov/drugs/drug-safety-and-availability/fda-requires-warnings-about-increased-risk-serious-heart-related-events-cancer-blood-clots-and-death>.
43. Lopez-Olivo MA, Urruela MA, McGahan L, Pollono EN, Suarez-Almazor ME. Rituximab for rheumatoid arthritis. *Cochrane Database Syst Rev* 2015;1:CD007356.
44. Singh JA, Christensen R, Wells GA, Suarez-Almazor ME, Buchbinder R, Angeles Lopez-Olivo M, et al. A network meta-analysis of randomized controlled trials of biologics for rheumatoid arthritis: a Cochrane overview. *CMAJ* 2009;181:787–96.
45. Maxwell L, Singh JA. Abatacept for rheumatoid arthritis. *Cochrane Database Syst Rev* 2009:CD007277.
46. Barmettler S, Ong M, Farmer JR, Choi H, Walter J. Association of immunoglobulin levels, infectious risk, and mortality with rituximab and hypogammaglobulinemia. *JAMA Netw Open* 2018;1:e184169.
47. Buch MH, Smolen JS, Betteridge N, Breedveld FC, Burmester G, Dörner T, et al. Updated consensus statement on the use of rituximab in patients with rheumatoid arthritis. *Ann Rheum Dis* 2011;70:909–20.
48. Gottenberg JE, Ravaut P, Bardin T, Cacoub P, Cantagrel A, Combe B, et al. Risk factors for severe infections in patients with rheumatoid arthritis treated with rituximab in the AutoImmunity and Rituximab registry. *Arthritis Rheum* 2010;62:2625–32.

EDITORIAL

Sacroiliac Bone Marrow Edema: Innocent Until Proven Guilty?

Michael M. Ward¹  and Lawrence Yao²

Magnetic resonance imaging (MRI) of the sacroiliac (SI) joints and spine has become an integral part of the evaluation of patients with suspected inflammatory back pain and possible axial spondyloarthritis (SpA). MRI allows for examination of sites of axial skeletal pathology that are not directly assessable by physical examination and can show inflammatory changes despite the frequent absence of elevation of acute phase reactants in these conditions. While MRI can detect synovitis, enthesitis, capsulitis, and structural changes at the SI joints, the MRI-based diagnosis of sacroiliac joints and vertebral inflammation relies on the finding of periarticular bone marrow edema (BME). BME reflects locally increased water content and is characterized by increased signal in the marrow space on short tau inversion recovery (STIR) images, diminished signal on non-fat-suppressed T1 images, and indistinct margins. BME also typically exhibits increased enhancement after gadolinium administration, which may reflect increased cellularity, capillary permeability, and hypervascularity.

Characterization of pathologic SI joint BME gained increased importance in 2009 when MRI abnormalities were designated as part of the imaging pathway to the Assessment of Spondyloarthritis international Society (ASAS) classification of axial SpA (1). SI joint inflammation on MRI was included as an alternative to definite sacroiliitis on plain radiographs and therefore became critical to the identification of patients with early axial SpA. In the ASAS validation cohort, BME typical of sacroiliitis was present in 64.7% of patients with axial SpA and only 2.6% of controls with chronic back pain (1). The ASAS definition of SI joint inflammation includes 3 components: BME, clearly present abnormalities in “typical regions” in subchondral bone, and lesions “highly suggestive of SpA” (2). Although the latter is vague and apparently tautologic, additional interpretive guidance of “two lesions or two slices” was provided. Synovitis, enthesitis, and structural lesions

such as SI joint erosions alone were considered not sufficient to qualify as indicative of axial SpA but could influence the interpretation. Importantly, the ASAS definition was developed by expert opinion, rather than being data-derived and tested for sensitivity and specificity.

Because MRI-detected SI joint inflammation is central to the diagnosis of nonradiographic axial SpA, and therefore provides a gateway to biologic treatment for many patients, it is important to know how accurately axial SpA is identified by MRI criteria. Low specificity could result in misdiagnosis (i.e., overdiagnosis) and potential overtreatment. In this issue of *Arthritis & Rheumatology*, Renson and colleagues report a cross-sectional study that examined the prevalence of MRI abnormalities in the SI joints and spine in 95 healthy individuals (3). Participants comprised a convenience sample of men and women ages 20–49 years, without acute or chronic back pain, who largely had sedentary occupations. Overall, 11.6% of participants had SI joint BME that met the ASAS definition for sacroiliitis. BME was more common among those ages 40–49 years (17.9%) than among those ages 20–29 years (2.8%). According to the Spondyloarthritis Research Consortium of Canada method (4), SI joint BME was present in 24.2% subjects and again increased with age. Only 6.3% of individuals had intense BME, and 4.3% had BME extending far from the joint. Other SI joint changes, including erosions and fat metaplasia, were present in 13.7–20% of subjects and were more common among older individuals, but were typically focal and rarely involved >2 SI joint quadrants. Similar findings were present in the spine, with 20% of individuals having ≥1 vertebral BME lesion, although multiple spine BME lesions were rare. The authors concluded that these findings should temper our reliance on SI joint BME as the primary marker of sacroiliitis in the evaluation of patients with suspected axial SpA.

The views expressed in this article are those of the authors and do not represent those of the US Department of Health and Human Services or the US federal government. Supported by the National Institute of Arthritis and Musculoskeletal and Skin Diseases, NIH (award ZIA-AR-041153).

¹Michael M. Ward, MD, MPH: Intramural Research Program, National Institute of Arthritis and Musculoskeletal and Skin Diseases, NIH, Bethesda, Maryland; ²Lawrence Yao, MD: Radiology and Imaging Sciences, NIH Clinical Center, Bethesda, Maryland.

Author disclosures are available at <https://onlinelibrary.wiley.com/action/downloadSupplement?doi=10.1002%2Fart.42143&file=art42143-sup-0001-Disclosureform.pdf>.

Address correspondence to Michael M. Ward, MD, MPH, NIAMS/NIH, Building 10 CRC, Room 4-1339, 10 Center Drive, Bethesda, MD 20892. Email: wardm1@mail.nih.gov.

Submitted for publication March 18, 2022; accepted in revised form April 12, 2022.

These findings extend those of other recent studies that demonstrated the presence of SI joint BME in 20–40% of athletes and 60% of postpartum women, groups in which mechanical stress has been implicated as a cause (5). Although data on recreational activity were not reported, the current study may suggest that the mechanical demands of everyday life are sufficient to cause apparent BME in some individuals. Other than older age, no subgroups were identified to be at higher risk of SI joint BME, including those with HLA-B27. Three previous smaller studies showed MRI-detected sacroiliitis in 6.8%, 23.4%, and 27.0% of healthy young adults, consistent with the current study (5–7).

In the context of axial SpA, BME has been interpreted to reflect local inflammation. This interpretation is supported by correlations between the degree of gadolinium enhancement or BME on MRI and inflammatory cell infiltrates and increased marrow extracellular fluid in SI joint and zygapophyseal joint biopsies, albeit in small numbers of patients (8,9). Similar findings have been reported in rheumatoid arthritis. Improvement of SI joint BME with tumor necrosis factor inhibitor treatment also suggests an inflammatory origin (10). However, BME is not specific to inflammation or osteitis. It can be seen with fractures, local trauma or stress injury, osteoarthritis, osteonecrosis, and neoplasia, and may also be idiopathic (11). The mechanisms that result in BME are incompletely understood and undoubtedly vary with the underlying cause (11). While ischemia may cause BME in osteonecrosis and sickle cell disease, BME in other settings may be related to hypervascularity, medullary necrosis, fibrosis, or venous stasis. Excess biomechanical stress may result in BME through local hyperperfusion and bone remodeling, with or without microfractures and hemorrhage. Intriguingly, biomechanical stress in the spine tends to be concentrated at the thoracolumbar junction and posterior sacrum, which has been attributed to counterbalancing of the lumbar lordosis (12). Importantly, the mechanisms responsible for BME seen in asymptomatic healthy individuals are not known. SI joint arthrosis can begin at ages 30–39 years and may manifest with BME in some cases (13).

Given the MRI-detected abnormalities in many healthy individuals, the critical diagnostic question becomes whether other MRI features or criteria might increase its specificity for early axial SpA without seriously diminishing sensitivity, compared to analysis of

SI joint BME by the ASAS definition. This is an active area of research. Some features that have been examined, ordered by higher presumed specificity, are listed in Table 1. In the study by Renson et al, SI joint BME lesions that were either intense or deep were less commonly present in healthy individuals, but were still observed in 7–10% of individuals (3). The median number of affected SI joint quadrants was 2, supporting findings from previous studies that a requirement for more diffuse involvement would have higher specificity (6). The pelvic regions most affected by BME were the superior sacrum and inferior ilium. A recent study that used semi-axial slices (perpendicular to the usual semi-coronal slices) to better resolve the 3-dimensional location of incriminating BME lesions in athletes found that lesions in the anterior upper sacrum and posterior lower ilium were attributable to either artifacts from adjacent vessels or ligament insertions in one-third to one-half of individuals (14). These findings highlight how more precise lesion localization may enhance study specificity.

We do not know if the time course of BME lesions would help distinguish innocent lesions from those of axial SpA. However, longitudinal studies would have the additional disadvantage of further delaying a diagnosis. Last, requiring coexisting lesions to be present, either in the SI joint region or spine, could decrease the number of healthy individuals misclassified based on SI joint BME alone (6,15). The frequency of coexistent SI joint BME and structural lesions in the same patient was not reported by Renson et al (3). However, requiring coexisting lesions may compromise test sensitivity, particularly in early disease. For example, Seven et al reported that SI joint BME with adjacent fat metaplasia had a specificity of 0.98 and positive predictive value of 0.88 for axial SpA, but this combination was present in only 7 of 41 patients with axial SpA (sensitivity 0.17) (15).

Supplemental imaging criteria might also be derived from special MRI sequences including diffusion-weighted imaging, which provides an indirect measure of tissue cellularity, and dynamic contrast-enhanced MRI, which estimates marrow perfusion quantitatively. Increased cellularity and hypervascularity may be more specific surrogates of inflammation, although these measures have also been shown to vary with the relative proportion of red and yellow marrow, and consequently by age, sex, and bone

Table 1. Features that describe SI joint inflammatory changes on MRI*

Feature	Characteristic
Presence	Existence of a lesion
Appearance	Intensity of the lesion
Location	Extension away from the joint space, e.g., “deep” lesion
Distribution	Number and location of involved SI regions or quadrants
Persistence	Stable presence and appearance over several months
Response to specific treatment	Improvement with TNFi or IL-17 inhibitor treatment
Adjacent coexisting lesions	Presence of fat metaplasia, SI joint erosions, subchondral sclerosis
Distal coexisting lesions	Vertebral BME, fat metaplasia, erosions, syndesmophytes

* SI = sacroiliac; MRI = magnetic resonance imaging; TNFi = tumor necrosis factor inhibitor; IL-17 = interleukin-17; BME = bone marrow edema.

mineral density. These measures are also more technically challenging to perform and interpret and have lower reliability. In a recent trial of golimumab, diffusion-weighted imaging did not perform better than conventional MRI inflammation scores and did not differentiate clinical responders from nonresponders (16). Higher-resolution MRI techniques may also permit detection of potentially more specific but subtle disease features in the joint space and subchondral bone (17).

The study by Renson et al, and other similar studies, provide important warnings that it is essential to define the range of abnormalities present in unaffected persons before setting standards for what represents disease (3). While we may be somewhat reassured by the low frequency of abnormalities in healthy individuals ages 20–29 years, an age range when many patients first present with inflammatory back pain, larger numbers of individuals need to be studied to confirm these findings. Nonetheless, a substantial proportion of patients present with inflammatory back pain after age 30. For these individuals, as well as for athletes and parous women, having accurate imaging guides that can facilitate early diagnosis while minimizing the risk of overdiagnosis is critical.

AUTHOR CONTRIBUTIONS

Drs. Ward and Yao drafted the article, revised it critically for important intellectual content, and approved the final version to be published.

REFERENCES

- Rudwaleit M, van der Heijde D, Landewé R, Listing J, Akkoc N, Brandt J, et al. The development of Assessment of SpondyloArthritis international Society classification criteria for axial spondyloarthritis (part II): validation and final selection. *Ann Rheum Dis* 2009;68:77–783.
- Lambert RG, Bakker PA, van der Heijde D, Weber U, Rudwaleit M, Hermann KG, et al. Defining active sacroiliitis on MRI for classification of axial spondyloarthritis: update by the ASAS MRI working group. *Ann Rheum Dis* 2016;75:1958–63.
- Renson T, de Hooge M, De Craemer A, Deroo L, Lukasik Z, Carron P, et al. Progressive increase in sacroiliac joint and spinal MRI lesions in healthy individuals in relation to age. *Arthritis Rheumatol* 2022;74:1506–14.
- Maksymowych WP, Inman RD, Salonen D, Dhillon SS, Williams M, Stone M, et al. Spondyloarthritis research Consortium of Canada magnetic resonance imaging index for assessment of sacroiliac joint inflammation in ankylosing spondylitis. *Arthritis Rheum* 2005;53:703–9.
- De Winter J, de Hooge M, van de Sande M, de Jong H, van Hooft L, de Koning A, et al. Magnetic resonance imaging of the sacroiliac joints indicating sacroiliitis according to the Assessment of SpondyloArthritis international society definition in healthy individuals, runners, and women with postpartum back pain. *Arthritis Rheumatol* 2018;70:1042–8.
- Weber U, Lambert RG, Østergaard M, Hodler J, Pedersen SJ, Maksymowych WP. The diagnostic utility of magnetic resonance imaging in spondylarthritis: an international multicenter evaluation of one hundred eighty-seven subjects. *Arthritis Rheum* 2010;62:3048–58.
- Tezcan ME, Temizkan S, Ozal ST, Gul D, Aydin K, Ozderya A, et al. Evaluation of acute and chronic MRI features of sacroiliitis in asymptomatic primary hyperparathyroid patients. *Clin Rheumatol* 2016;35:2777–82.
- Bollow M, Fischer T, Reisschauer H, Backhaus M, Sieper J, Hamm B, et al. Quantitative analyses of sacroiliac biopsies in spondyloarthropathies: T cells and macrophages predominate in early and active sacroiliitis-cellularity correlates with the degree of enhancement detected by magnetic resonance imaging. *Ann Rheum Dis* 2000;59:135–40.
- Appel H, Loddenkemper C, Grozdanovic Z, Ehardt H, Dreimann M, Hempfing A, et al. Correlation of histopathological findings and magnetic resonance imaging in the spine of patients with ankylosing spondylitis. *Arthritis Res Ther* 2006;8:R143.
- Khoury G, Combe B, Morel J, Lukas C. Change in MRI in patients with spondyloarthritis treated with anti-TNF agents: systematic review of the literature and meta-analysis [review]. *Clin Exp Rheumatol* 2021;39:242–52.
- Maraghelli D, Brandi ML, Cerinic MM, Peired AJ, Colagrande S. Edema-like marrow signal intensity: a narrative review with a pictorial essay [review]. *Skeletal Radiol* 2021;50:645–63.
- Nishida N, Ohgi J, Jiang F, Ito S, Imajo Y, Suzuki H, et al. Finite element method analysis of compression fractures on whole-spine models including the rib cage. *Comput Math Methods Med* 2019;8348631.
- Vogler JB III, Brown WH, Helms CA, Genant HK. The normal sacroiliac joint: a CT study of asymptomatic patients. *Radiology* 1984;151:433–7.
- Weber U, Jurik AG, Zejden A, Larsen E, Jørgensen SH, Rufibach K, et al. MRI of the sacroiliac joints in athletes: recognition of non-specific bone marrow oedema by semi-axial added to standard semi-coronal scans. *Rheumatology (Oxford)* 2020;59:1381–90.
- Seven S, Østergaard M, Morsel-Carlson L, Sørensen IJ, Bonde B, Thamsborg G, et al. The utility of magnetic resonance imaging lesion combinations in the sacroiliac joints for diagnosing patients with axial spondyloarthritis. a prospective study of 204 participants including post-partum women, patients with disc herniation, cleaning staff, runners and healthy persons. *Rheumatology (Oxford)* 2020;59:3237–49.
- Møller JM, Østergaard M, Thomsen HS, Krabbe S, Sørensen IJ, Jensen B, et al. Validation of assessment methods for the apparent diffusion coefficient in a clinical trial of axial spondyloarthritis patients treated with golimumab. *Eur J Radiol Open* 2020;7:100285.
- Berkowitz JL, Mandl LA, Burge AJ, Roberts JA IV, Lin B, Schwartzman S, et al. MRI assessment of sacroiliitis with high-resolution protocol. *HSS J* 2022;18:91–7.

EDITORIAL

Toward Precision Medicine—Is Genetic Risk Prediction Ready for Prime Time in Osteoarthritis?

Michelle S. Yau¹  and John Loughlin²

Completion of the Human Genome Project in 2003, an international effort to map all genes in the human genome (1), brought forward the promise of identifying the genetic underpinnings of human disease and ushering in a new era of precision medicine. As genetic technology evolved, genetic studies went from segregation analyses and linkage studies in a limited set of families to large-scale genome-wide association studies (GWAS) in the general population and now whole-genome sequencing. Each step would provide greater resolution to identify genetic variation that explains an ever-growing proportion of disease risk. Recently, a particularly large GWAS of osteoarthritis (OA) has been completed by the Genetics of Osteoarthritis (GO) consortium, involving over 800,000 individuals (2). This effort brought together 13 international cohorts, increasing OA patient numbers by >2-fold to identify 100 OA-associated loci, of which 52 were novel (2). Like other complex diseases with high prevalence and a major public health impact, including cardiovascular disease and type 2 diabetes mellitus, the genetic architecture of OA is highly polygenic. In other words, the genetic contribution to OA comprises many risk variants each with small effects on disease. A logical next step is to combine the identified OA risk variants into a risk score that can be used to predict OA onset and severity, as was done in 2 articles in this issue of *Arthritis & Rheumatology*, by Lacaze et al (3) and Sedaghati-Khayat et al (4), who independently investigated the loci reported by the GO consortium GWAS.

Given the ever-increasing size of GWAS and the ability to robustly identify genetic variants for disease, it is now possible to generate polygenic risk scores (PRS) for many complex traits. A PRS is a weighted sum score of the number of disease risk alleles each person possesses. We carry 2 versions of each autosomal chromosome, and therefore, at each DNA variant location, we

may carry 2 risk-associated variants, 2 protective variants, or 1 of each. The number of risk variants is summed and weighted by its effect size, often taken from the largest GWAS available. Despite the method used for the optimal selection of risk variants and weights (and there are several) (5,6), PRS represents the burden of risk variants for a particular disease, where those who carry a higher burden of risk variants are at increased risk for developing that disease.

While the idea of genetic risk prediction is enticing, its promises have not been borne out in clinical practice. Calculation of PRS from GWAS has become popular in recent years but has generally shown limited predictive ability for many complex traits. Among possible reasons are that genetic factors may constitute only a small fraction of the group of factors that cause a disease. Also, PRS may only capture common variation identified from GWAS and not the entire spectrum of genetic contributions to disease, including rare variants (7). Therefore, we may never achieve perfect prediction with PRS. As Wray et al proposed, “it is important to dispel the dogma that equates a genetic test with high levels of accuracy of current/future diagnosis” (7). As a scientific community, we should heed this warning and adjust our expectations for the role of PRS in clinical practice. While methods are needed to maximize PRS prediction, we also need to understand the greater context of how PRS contributes to other known clinical and behavioral factors. In this sense, Lacaze et al and Sedaghati-Khayat et al have only begun to scratch the surface of whether PRS may play a role in OA clinical care.

Perhaps a good place to start is to take cues from what has been done with PRS in cardiovascular disease. Early PRS studies of coronary heart disease had limited success in identifying PRS useful for clinical risk stratification, only identifying 20% of a

Supported by the National Institute of Arthritis and Musculoskeletal and Skin Diseases, NIH (award R01-AR-075356) and the Medical Research Council and Versus Arthritis Centre for Integrated Research into Musculoskeletal Ageing (CIMA; grants MR/P020941/1 and MR/R502182/1).

¹Michelle S. Yau, PhD: Harvard Medical School, Boston, Massachusetts; ²John Loughlin, PhD: Newcastle University and International Centre for Life, Newcastle-upon-Tyne, UK.

Author disclosures are available at <https://onlinelibrary.wiley.com/action/downloadSupplement?doi=10.1002%2Fart.42155&file=art42155-sup-0001-Disclosureform.pdf>.

Address correspondence to Michelle S. Yau, PhD, Marcus Institute for Aging Research, Hebrew SeniorLife, Harvard Medical School, 1200 Centre Street, Boston, MA 02131 (email: michelle.yau@hsl.harvard.edu); or to John Loughlin, PhD, Newcastle University, Central Parkway, Newcastle-upon-Tyne NE1 3BZ, United Kingdom (email: john.loughlin@ncl.ac.uk).

Submitted for publication March 23, 2022; accepted in revised form April 28, 2022.

population at a 1.4-fold increased risk relative to the rest of the population (8). Odds ratios found by Lacaze et al and Sedaghati-Khayat et al were of the same order of magnitude. In recent years, with the availability of larger data sets and improved PRS methods, the predictive ability of cardiovascular disease PRS has improved and consequently may have some clinical utility.

In 2018, Khera et al developed several predictors based on existing GWAS, selected the PRS that maximized the area under the receiver operating characteristic curve (AUC) in a validation set from UK Biobank Phase 1, then assessed PRS performance in an independent testing set from UK Biobank Phase 2 (9). AUCs in the validation set ranged from 0.79 to 0.81 and performed similarly in the test set with an AUC of 0.81 (9). The PRS for coronary artery disease (CAD) identified 8% of the population as having a >3-fold increased risk for coronary artery disease, which is comparable to the levels of risk prediction provided by known single rare variants that are clinically actionable (9). For example, if an individual carries a rare familial hypercholesterolemia mutation, then aggressive treatment to lower circulating cholesterol levels would be warranted. CAD PRS identifying individuals at a >3-fold increased risk of CAD would warrant the same aggressive treatment. While CAD PRS have not been deployed in clinical practice, several recent studies have shown that adding CAD PRS to existing risk prediction models can reclassify up to 12% of individuals from an intermediate- to high-risk category (10,11). PRS may therefore provide a safe and effective screening strategy to reduce disease burden for high prevalence diseases like CAD. It may be possible to reach similar levels of evidence for OA PRS with larger GWAS and improved methods.

While it is now common to demonstrate highly significant associations between PRS and disease status in other disease areas, the OA community has only begun to do so. The studies by Lacaze et al and Sedaghati-Khayat et al are the first to show that PRS derived from the recent GO consortium GWAS are significantly associated with OA in independent cohorts. Unfortunately, as with earlier cardiovascular studies, these studies present modest odds ratios and limited predictive ability for OA PRS. Further improvement of the OA PRS is needed to yield stronger evidence that OA PRS can identify high-risk subgroups for either incidence or progression. An important component will be to move from disease association in populations to application of PRS to predict disease in an individual. Another aspect is providing a better understanding of how OA PRS contributes to clinical or behavioral risk factors.

Lacaze et al showed an interaction between body mass index and hip OA PRS, but not with knee OA PRS. One would expect to see interactions at both weight-bearing joint sites. Likely, the knee OA PRS was underdeveloped compared to the hip OA PRS and included fewer and less robust risk variants. Sedaghati-Khayat et al showed that OA PRS did not add substantially to clinical risk factors like age, sex, and body mass index, providing little confidence that OA PRS would help improve risk

classification. A limitation of both of these studies is that they, like that of the GO consortium, were conducted in European ancestry cohorts. However, we know that OA PRS developed in one ancestry group may not work as well for populations that were not represented in the OA GWAS (12). Future development of OA PRS will need to consider its application to non-European ancestry groups and ensure that OA PRS does not inadvertently widen existing health disparities. Finally, the value of an OA PRS assumes that there is something we can do for OA if we can identify those individuals who are at a high risk of developing OA or rapidly progressing OA. An OA PRS would be more beneficial if we had a large armamentarium of therapeutics at our disposal or even biomarkers that could be used to monitor disease progression, which currently does not exist for OA.

Our overall feeling is that Lacaze et al and Sedaghati-Khayat et al have taken an important first step toward translating new OA genetic findings to clinical utility but fall short of realizing the promise of OA PRS in improving OA clinical care and treatment. Improved methods and expanded data sets will be needed to better develop a reliable OA PRS that can accurately predict disease status and inform risk stratification in OA. However, given the complexity and heterogeneity of OA, the limitation may be that OA PRS, even if perfected, would never be sufficient to inform clinical care. Genetics cannot afford to stay in its silo and must be appreciated in the context of the wide array of clinical and behavioral factors that influence OA pathogenesis. This must work hand-in-hand with therapeutic and biomarker development so that there are options available for patients if we can identify individuals at increased risk of OA and its progression. The field has come a long way since the completion of the Human Genome Project, but genetic risk prediction and its utility in OA are not ready for prime time. Luckily for some of us, there is more work to do.

AUTHOR CONTRIBUTIONS

Drs. Yau and Loughlin drafted the article, revised it critically for important intellectual content, and approved the final version to be published.

REFERENCES

1. Collins FS, Morgan M, Patrinos A. The Human Genome Project: lessons from large-scale biology. *Science* 2003;300:286–90.
2. Boer CG, Hatzikotoulas K, Southam L, Stefansdottir L, Zhang Y, de Almeida RC, et al. Deciphering osteoarthritis genetics across 826,690 individuals from 9 populations. *Cell* 2021;184:6003–5.
3. Lacaze P, Wang Y, Polekhina G, Bakshi A, Riaz M, Owen A, et al. Genomic risk score for advanced osteoarthritis in older adults. *Arthritis Rheumatol* 2022;74:1480–7.
4. Sedaghati-Khayat B, Boer CG, Runhaar J, Bierma-Zeinstra S, Broer L, Ikram M, et al. Risk assessment for hip and knee osteoarthritis using polygenic risk scores. *Arthritis Rheumatol* 2022;74:1488–96.
5. Euesden J, Lewis CM, O'Reilly PF. PRSice: Polygenic Risk Score software. *Bioinformatics* 2015;31:1466–8.

6. Vilhjalmsson BJ, Yang J, Finucane HK, Gusev A, Lindstrom S, Ripke S, et al. Modeling linkage disequilibrium increases accuracy of polygenic risk scores. *Am J Hum Genet* 2015;97:576–92.
7. Wray NR, Lin T, Austin J, McGrath JJ, Hickie IB, Murray GK, et al. From basic science to clinical application of polygenic risk scores: a primer. *JAMA Psychiatry* 2021;78:101–9.
8. Ripatti S, Tikkanen E, Orho-Melander M, Havulinna AS, Silander K, Sharma A, et al. A multilocus genetic risk score for coronary heart disease: case-control and prospective cohort analyses. *Lancet* 2010; 376:1393–400.
9. Khera AV, Chaffin M, Aragam KG, Haas ME, Roselli C, Choi SH, et al. Genome-wide polygenic scores for common diseases identify individuals with risk equivalent to monogenic mutations. *Nat Genet* 2018;50:1219–24.
10. Sun L, Pennells L, Kaptoge S, Nelson CP, Ritchie SC, Abraham G, et al. Polygenic risk scores in cardiovascular risk prediction: a cohort study and modelling analyses. *PLoS Med* 2021;18:e1003498.
11. Tikkanen E, Havulinna AS, Palotie A, Salomaa V, Ripatti S. Genetic risk prediction and a 2-stage risk screening strategy for coronary heart disease. *Arterioscler Thromb Vasc Biol* 2013;33:2261–6.
12. Martin AR, Kanai M, Kamatani Y, Okada Y, Neale BM, Daly MJ. Clinical use of current polygenic risk scores may exacerbate health disparities. *Nat Genet* 2019;51:584–91.

Genomic Risk Score for Advanced Osteoarthritis in Older Adults

Paul Lacaze,¹ Yuanyuan Wang,¹ Galina Polekhina,¹ Andrew Bakshi,¹ Moeen Riaz,¹ Alice Owen,¹ Angus Franks,¹ Jawad Abidi,² Jane Tiller,¹ John McNeil,¹ and Flavia Cicuttini¹

Objective. Prevention of osteoarthritis (OA) remains important, as there are no disease-modifying treatments. A personalized approach has the potential to better target prevention strategies. In the present study, we used recently identified genetic risk variants from genome-wide association analysis for advanced OA to calculate polygenic risk scores (PRS) for knee and hip OA and assessed PRS performance in an independent population of older community-dwelling adults.

Methods. PRS were calculated in 12,093 individuals of European genetic descent ages ≥ 70 years who were enrolled in the Aspirin in Reducing Events in the Elderly trial. The outcome measure was knee and hip replacement (hospitalizations during the trial and self-reported joint replacements before enrollment). PRS were considered as continuous (per SD) and categorical (low risk [0–20%], medium risk [21–80%], high risk [81–100%]) variables. Logistic regression was used to examine associations between PRS and risk of joint replacement, adjusted for age, sex, body mass index, and socioeconomic status.

Results. Among the participants, 1,422 (11.8%) had knee replacements and 1,297 (10.7%) had hip replacements. PRS (per SD) were associated with a risk of knee replacement (odds ratio [OR] 1.13 [95% confidence interval (95% CI) 1.07–1.20]) and hip replacement (OR 1.23 [95% CI 1.16–1.30]). Participants with high PRS had an increased risk of knee replacement (OR 1.44 [95% CI 1.20–1.73]) and hip replacement (OR 1.88 [95% CI 1.56–2.26]), compared to those with low PRS. Associations were stronger for PRS and hip replacement risk in women than in men. Associations were similar in sensitivity analyses that examined joint replacements before and during the trial separately.

Conclusion. PRS have the potential to improve prevention of severe knee and hip OA by providing a personalized approach and identifying individuals who may benefit from early intervention.

INTRODUCTION

Osteoarthritis (OA), the most common form of arthritis, is estimated to affect 250 million people worldwide, with numbers continuously growing due to aging and increased obesity (1). OA is a chronic disease with no cure, and joint replacement is indicated once conservative management options have been exhausted. The majority of total knee replacement (TKR) and total hip replacement (THR) procedures (98% and 89%, respectively)

are performed for OA (2), resulting in significant healthcare burden. To date, strategies to prevent and treat OA have used a “one-size-fits-all” approach with limited effectiveness, mainly focusing on obesity and physical activity. In general, these strategies do not take into consideration that OA is a heterogeneous disease with distinct phenotypes (3) influenced by genetic and environmental factors (4), with risk factors varying across different joints (5). Current risk prediction models for OA lack the ability to identify with precision those most at risk and include disease

Supported by an ASPREE (Aspirin in Reducing Events in the Elderly) Flagship cluster grant (including the Commonwealth Scientific and Industrial Research Organisation, Monash University, Menzies Research Institute, Australian National University, University of Melbourne), the National Institute on Aging, NIH, and the National Cancer Institute, NIH (grants U01-AG-029824 and U19-AG-062682), the National Health and Medical Research Council of Australia (NHMRC) (grants 334047 and 1127060), and Monash University and the Victorian Cancer Agency. Dr. Lacaze's work was supported by a National Heart Foundation Future Leader Fellowship (ID 102604). Dr. Wang's work was supported by an NHMRC Translating Research into Practice Fellowship (APP1168185). Dr. Cicuttini's work was supported by an NHMRC Investigator Grant (APP1194829).

Drs. Lacaze and Wang contributed equally to this work.

¹Paul Lacaze, PhD, Yuanyuan Wang, PhD, Galina Polekhina, PhD, Andrew Bakshi, MSc, Moeen Riaz, PhD, Alice Owen, PhD, Angus Franks, BMedSc, MD, Jane Tiller, MGenCouns, John McNeil, PhD, Flavia Cicuttini, PhD: Monash University, Melbourne, Australia; ²Jawad Abidi, MBBSHons: Alfred Hospital, Melbourne, Australia.

Author disclosures are available at <https://onlinelibrary.wiley.com/action/downloadSupplement?doi=10.1002%2Fart.42156&file=art42156-sup-0001-Disclosureform.pdf>.

Address correspondence to Flavia Cicuttini, PhD, School of Public Health and Preventive Medicine, Monash University, 553 St. Kilda Road, Melbourne, VIC 3004, Australia. Email: flavia.cicuttini@monash.edu.

Submitted for publication July 23, 2021; accepted in revised form April 28, 2022.

markers, reducing their utility for prevention and treatment of early disease.

Over the last few years, large genetic studies have enabled the discovery of common genetic risk loci associated with OA. In 2019, a large genome-wide association study (GWAS) of advanced OA was undertaken in a population of European ancestry and identified 64 associated genetic loci, 52 of them novel (6). This more than doubled the number of previously identified variants (7). In 2021, a larger multiethnic GWAS meta-analysis of 826,690 individuals from 9 populations (177,517 with OA) identified 100 independent OA-associated variants across 11 OA phenotypes, 52 of which were novel (8).

The discovery of these variants now enables the calculation of polygenic risk scores (PRS), which aggregate the effect of many common disease-associated variants to generate a combined measure of the genetic risk. However, independent validation studies for PRS for advanced OA are challenging and require large genetic studies of older populations independent of the studies used in the original GWAS to derive the PRS, where the majority of OA diagnoses and joint replacements have occurred. PRS validation studies also need to be conducted in a healthcare setting where there is access to procedures such as joint replacement when indicated. Thus, we performed a validation study of newly derived PRS for OA in a well-characterized cohort of older adults in Australia, enrolled into the Aspirin in Reducing Events in the Elderly (ASPREE) trial (9–11), in which detailed information on joint replacements was collected. It was hypothesized that PRS would be associated with the risk of knee and hip replacement in older adults. Our study represents an important step in the assessment of genomic risk scores for prediction of advanced OA in older adults, in which the burden of disease is high.

PATIENTS AND METHODS

Study design and participants. The study population comprised genotyped participants of the ASPREE trial. Study design, participant characteristics, and primary results have been previously published (9–11). Briefly, ASPREE was an international randomized placebo-controlled clinical trial to determine whether daily 100 mg aspirin extended disability-free survival in 19,114 healthy older individuals ages ≥ 70 years (≥ 65 years for US participants). ASPREE participants had no history of diagnosed cardiovascular events, serious illness, dementia, or physical disability at enrollment. The median follow-up period was 4.7 years. Participants provided written informed consent for genetic research, and the study was approved by local Ethics Committees and registered on [ClinicalTrials.gov](https://clinicaltrials.gov) (identifier: NCT01038583). The cohort for the current analysis was drawn from the 16,703 participants from Australia.

Assessment of advanced knee and hip OA. Advanced OA was defined as knee or hip replacement for OA. Australia has a universal healthcare system that includes publicly funded access to joint replacement, so knee and hip replacement can be considered a marker of advanced OA (12). Knee and hip replacements during the ASPREE trial (median follow-up 4.7 years) were identified by review of all hospitalizations for knee and hip surgical procedures, most with the indication recorded as OA. Self-reported history of joint replacements prior to ASPREE enrollment was obtained from the ASPREE Longitudinal Study of Older Persons questionnaire (13). Participants were asked, “Have you had any of the following operations?” and to mark “Hip replacement” and “Knee replacement” as Right, Left, Both, or No. Advanced knee and hip OA were defined as any knee and hip replacement—either hospitalizations or self-reported joint replacements.

Genotyping and PRS. Genotyping was performed on 14,052 DNA samples from ASPREE participants using the Axiom 2.0 Precision Medicine Diversity Research Array (ThermoFisher Scientific) following standard protocols (14). Variant calling used a custom pipeline aligned to human reference genome hg38. We limited our study to participants with European genetic ancestry to mitigate the effect of population stratification bias in polygenic scoring. To define genetic ancestry, principal component analysis was performed using the 1000 Genomes reference population, excluding ASPREE samples that did not overlap with the Non-Finnish European 1000 Genomes cluster (Supplementary Figure 1, available on the *Arthritis & Rheumatology* website at <https://onlinelibrary.wiley.com/doi/10.1002/art.42156>) (15). Samples from 12,093 participants passed the following filters: non-Finnish European genetic descent, unrelated (identity-by-descent to third-degree relative), and minimum age at randomization of 70 years. Imputation was performed using the TOPMed Imputation Panel and Server (16–18). Pre-imputation quality control filtered variants using plink 1.9 for missing genotype rates ($-\text{geno}$, $-\text{mind}$ 0.1) and Hardy-Weinberg equilibrium ($-\text{hwe}$ 10–60). Post-imputation quality control removed variants with low imputation quality scores ($r^2 < 0.3$).

Two different PRS were calculated for knee and hip replacement respectively, based on those reported in the recent GWAS meta-analysis (8). For each PRS, we selected only genome-wide significant single nucleotide polymorphisms (SNPs) specific to the trait reported in the GWAS meta-analysis (8). This can be identified in the paper with the SNPs labeled as TKR and THR, comprising 10 SNPs for TKR and 38 SNPs for THR. In our analysis, 1 THR variant was removed due to poor imputation quality, resulting in SNP counts of 10 for TKR and 37 for THR (Supplementary Table 1, <https://onlinelibrary.wiley.com/doi/10.1002/art.42156>). Plink version 1.9 was used to calculate the weighted sum of the log odds ratios (ORs) reported for the effect alleles for each variant.

Table 1. Baseline characteristics of the study participants based on PRS*

	Low-risk PRS (Q1, 0–20%)	Medium-risk PRS (Q2–4, 21–80%)	High-risk PRS (Q5, 81–100%)
Knee	2,422 (20.0)	7,253 (60.0)	2,418 (20.0)
Age at randomization			
Mean \pm SD years	75.3 \pm 4.3	75.0 \pm 4.2	75. \pm 4.2
Median (range) years	74.1 (70.0–94.8)	73.8 (70.0–95.9)	73.8 (70.1–92.5)
Age category			
<75 years	1,418 (58.6)	4,430 (61.1)	1,472 (60.9)
75–79 years	625 (25.8)	1,842 (25.4)	596 (24.7)
\geq 80 years	379 (15.7)	981 (13.5)	350 (14.5)
Female sex	1,335 (55.1)	3,904 (53.8)	1,314 (54.3)
BMI, mean \pm SD kg/m ²	27.8 \pm 4.5	28.0 \pm 4.5	28.3 \pm 4.6
BMI category			
Underweight	14 (0.6)	42 (0.6)	7 (0.3)
Normal	650 (26.8)	1,811 (25.0)	582 (24.1)
Overweight	1,115 (46.0)	3,312 (45.7)	1,090 (45.1)
Obese	634 (26.2)	2,051 (28.3)	729 (30.2)
Missing	9 (0.4)	37 (0.5)	10 (0.4)
Education >12 years	939 (38.8)	2,885 (39.8)	976 (40.4)
Index of relative socioeconomic advantage and disadvantage score, mean \pm SD	1,006.2 \pm 68.3	1,004.1 \pm 68.4	1,006.0 \pm 69.7
Aspirin group	1,226 (50.6)	3,637 (50.1)	1,171 (48.4)
Hip	2,419 (20.0)	7,256 (60.0)	2,418 (20.0)
Age at randomization			
Mean \pm SD years	75.0 \pm 4.2	75.0 \pm 4.2	75.0 \pm 4.3
Median (range) years	73.8 (70.1–92.7)	73.9 (70.0–95.9)	73.8 (70.0–93.3)
Age category			
<75 years	1,504 (62.2)	4,352 (60.0)	1,464 (60.6)
75–79 years	576 (23.8)	1,876 (25.9)	611 (25.3)
\geq 80 years	339 (14.0)	1,028 (14.2)	343 (14.2)
Female sex	1,292 (53.4)	3,968 (54.7)	1,293 (53.5)
BMI, mean \pm SD kg/m ²	28.0 \pm 4.6	28.0 \pm 4.5	28.0 \pm 4.5
BMI category			
Underweight	15 (0.6)	37 (0.5)	11 (0.5)
Normal	595 (24.6)	1,842 (25.4)	606 (25.1)
Overweight	1,112 (46.4)	3,317 (45.7)	1,078 (44.6)
Obese	675 (27.9)	2,027 (27.9)	712 (29.5)
Missing	12 (0.5)	33 (0.5)	11 (0.5)
Education >12 years	967 (40.0)	2,882 (39.7)	951 (39.3)
Index of relative socioeconomic advantage and disadvantage score, mean \pm SD	1,006.5 \pm 68.3	1,005.2 \pm 68.7	1,002.5 \pm 68.9
Aspirin group	1,235 (51.1)	3,586 (49.4)	1,213 (50.2)

* Except where indicated otherwise, values are the number (%) of participants. PRS = polygenic risk score; Q1 = quintile 1; BMI = body mass index.

Demographic and socioeconomic data. Height and weight were measured using standardized protocols at the ASPREE baseline visit. Body mass index (BMI) was calculated from height and weight, and obesity was defined as a BMI of ≥ 30 kg/m² (19). Age and years of education were self-reported at the baseline ASPREE clinical visit. The index of relative socioeconomic advantage and disadvantage summarizes information about the economic and social conditions of people and households within an area, including both relative advantage and disadvantage measures (20).

Statistical analysis. The PRS were analyzed as continuous variables on the SD scale and were also categorized into 3 groups based on quintiles of the PRS distribution: low-risk

(quintile 1 [Q1], 0–20%), medium-risk (Q2–4, 21–80%) and high-risk (Q5, 81–100%). Multiple logistic regression was used to examine the association between PRS (either as a continuous or as a categorical variable) and risk of knee and hip replacement, with adjustment for age, sex, BMI, education, and index of relative socioeconomic advantage and disadvantage. The area under the receiver operating characteristic curve (AUC) was calculated for the multiple logistic regression analysis before and after PRS was included in the regression models. Additional adjustment for treatment group was performed. We examined the interaction between PRS and treatment group, sex, or obesity for their association with the risk of knee and hip replacement by introducing interaction terms in the regression models. In a sensitivity analysis, incident joint replacements occurring during the trial (reviewed

Table 2. Association of PRS with risk of knee and hip replacement*

	Total participants with joint replacement, no. (%)	Univariable analysis		Multivariable analysis†	
		OR (95% CI)	P	OR (95% CI)	P
Knee replacement	1,422 (11.8)	–	–	–	–
Knee PRS, per SD	–	1.14 (1.08–1.20)	<0.001	1.13 (1.07–1.20)	<0.001
Knee PRS category	–	–	–	–	–
Low-risk PRS (Q1, 0–20%)	231 (9.5)	1.00	–	1.00	–
Medium-risk PRS (Q2–4, 21–80%)	864 (11.9)	1.28 (1.10–1.49)	0.001	1.30 (1.11–1.52)	0.001
High-risk PRS (Q5, 81–100%)	327 (13.5)	1.48 (1.24–1.77)	<0.001	1.44 (1.20–1.73)	<0.001
Hip replacement	1,297 (10.7)	–	–	–	–
Hip PRS, per SD	–	1.23 (1.17–1.31)	<0.001	1.23 (1.16–1.30)	<0.001
Hip PRS category	–	–	–	–	–
Low-risk PRS (Q1, 0–20%)	200 (8.3)	1.00	–	1.00	–
Medium-risk PRS (Q2–4, 21–80%)	745 (10.3)	1.27 (1.08–1.49)	0.004	1.27 (1.08–1.50)	0.004
High-risk PRS (Q5, 81–100%)	352 (14.6)	1.89 (1.57–2.27)	<0.001	1.88 (1.56–2.26)	<0.001

* PRS = polygenic risk score; OR = odds ratio; 95% CI = 95% confidence interval; Q1 = quintile 1.

† Adjusted for age, sex, body mass index, education, and index of relative socioeconomic advantage and disadvantage.

hospitalizations) and prevalent joint replacements occurring before the trial (self-reported) were examined separately, using Cox proportional hazards regression and logistic regression, respectively.

The specificity of PRS was assessed by testing hip PRS against the risk of knee replacement, and knee PRS against the risk of hip replacement. Additional analysis was performed to examine the risk of knee and hip replacement against the middle half of the study population. *P* values less than 0.05 were considered significant. Analyses were performed using R version 3.6.1 (21) and Stata version 16.1.

RESULTS

Characteristics of study participants. The mean age at randomization of the 12,093 participants was 75.0 years, with the majority (86%) ages 70–79 years. The mean ± SD BMI was 28.0 ± 4.5 kg/m², with 3,414 participants (28.2%) classified as obese. Both knee and hip PRS showed a normal distribution (mean ± SD 0.25 ± 0.13 and mean ± SD 0.51 ± 0.34,

respectively). The characteristics of study participants are presented based on PRS categories (Table 1) and joint replacement status (Supplementary Table 2, <https://onlinelibrary.wiley.com/doi/10.1002/art.42156>). In total, 1,422 participants (11.8%) had ≥1 knee replacement and 1,297 participants (10.7%) had ≥1 hip replacement (occurring either during the ASPREE trial or prior to enrollment) (Supplementary Table 3, <https://onlinelibrary.wiley.com/doi/10.1002/art.42156>). Among the participants with knee replacements, 689 had surgeries during the ASPREE trial and 948 had surgeries according to self-reported history. Among the participants with hip replacements, 529 had surgeries during the ASPREE trial and 914 had surgeries according to self-reported history (Supplementary Table 3).

Association between PRS and risk of knee and hip replacement.

The results for the associations between PRS and risk of knee and hip replacement are presented in Table 2 and Figure 1. Higher knee PRS was associated with an increased risk of knee replacement in univariable analysis and after adjustment for age, sex, BMI, education, and index of relative socioeconomic advantage and disadvantage (OR 1.13 [95% confidence interval (95% CI) 1.07–1.20] per SD of PRS). The frequency of participants with knee replacement surgery increased with knee PRS categories: 9.5% in the low-risk group, 11.9% in the medium-risk group, and 13.5% in the high-risk group. Compared to those in the low-risk PRS group (Q1), and after adjustment for confounders, the OR of knee replacement was 1.30 (95% CI 1.11–1.52) in the medium-risk PRS group (Q2–4) and 1.44 (95% CI 1.20–1.73) in the high-risk PRS group (Q5). The AUC was 0.666 (95% CI 0.651–0.680) for the regression model including age, sex, BMI, education, and index of relative socioeconomic advantage and disadvantage, and 0.668 (95% CI 0.654–0.683) when adding PRS to the model.

Higher hip PRS was associated with an increased risk of hip replacement in univariable analysis and after adjustment for

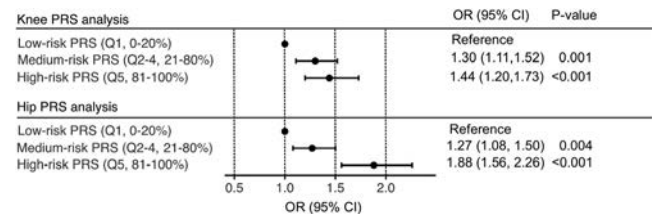


Figure 1. Association between polygenic risk scores (PRS) and risk of knee and hip replacement. Multiple logistic regression models are shown. Odds ratios (ORs) with 95% confidence intervals (95% CIs) were adjusted for age, sex, body mass index, education, and index of relative socioeconomic advantage and disadvantage. PRS were categorized by quintiles into low-risk (quintile 1 [Q1], 0–20%), medium-risk (Q2–4, 21–80%), and high-risk (Q5, 81–100%) groups.

Table 3. Association of PRS with risk of hip replacement, stratified by sex*

	Men		Women	
	OR (95% CI)	<i>P</i>	OR (95% CI)	<i>P</i>
Hip PRS, per SD	1.15 (1.06–1.26)	0.001	1.30 (1.20–1.40)	<0.001
Hip PRS category				
Low-risk PRS (Q1, 0–20%)	1.00		1.00	
Medium-risk PRS (Q2–4, 21–80%)	1.14 (0.90–1.45)	0.26	1.39 (1.11–1.75)	0.005
High-risk PRS (Q5, 81–100%)	1.57 (1.20–2.05)	0.001	2.19 (1.70–2.83)	<0.001

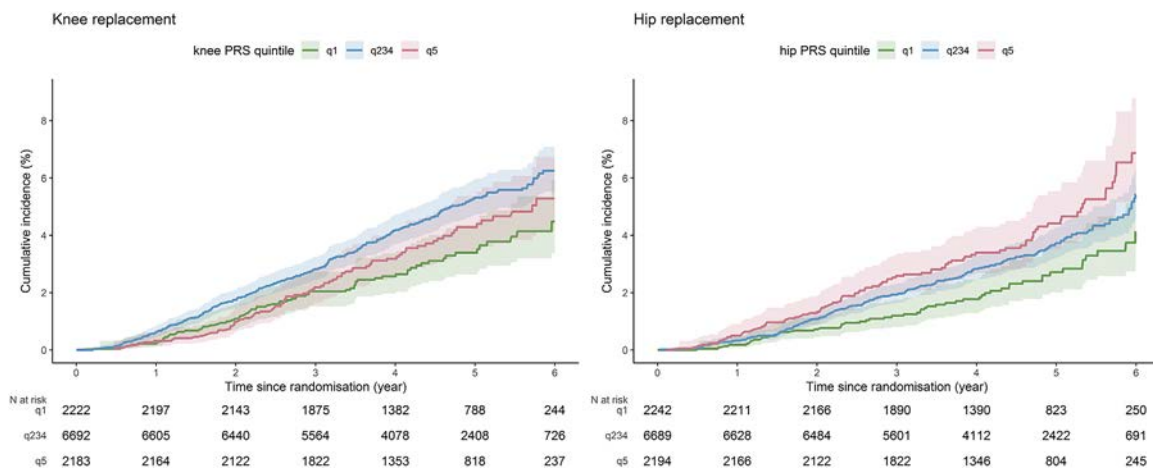
* Adjusted for age, body mass index, education, and index of relative socioeconomic advantage and disadvantage. See Table 2 for definitions.

confounders (OR 1.23 [95% CI 1.16–1.30] per SD of PRS). The frequency of participants with hip replacement surgery increased with hip PRS categories: 8.3% in the low-risk group, 10.3% in the medium-risk group, and 14.6% in the high-risk group. Compared to those in the low-risk PRS group (Q1) and after adjustment for confounders, the OR of hip replacement was 1.27 (95% CI 1.08–1.50) in the medium-risk PRS group (Q2–4), and 1.88 (95% CI 1.56–2.26) in the high-risk PRS group (Q5). The AUC was 0.570 (95% CI 0.554–0.587) for the regression model including age, sex, BMI, education, and index of relative socioeconomic advantage and disadvantage, and 0.589 (95% CI 0.572–0.605) when adding PRS to the model.

Additional adjustment for treatment group did not change the results for the association between PRS and risk of knee and hip replacement. There was no interaction between PRS and treatment group or obesity in the associations with risk of knee and hip replacement ($P > 0.32$ for all). While there was no interaction between PRS and sex in the associations with risk of knee replacement ($P > 0.25$ for all), there was some evidence of an interaction between PRS and sex in the associations with risk of hip replacement ($P = 0.045$ for PRS, $P = 0.25$ for medium-risk PRS category, and $P = 0.08$ for high-risk PRS category). Stronger associations between PRS and the risk of hip replacement were observed in women compared to men (Table 3). The OR of hip replacement in high-risk compared to low-risk PRS group was

2.19 (95% CI 1.70–2.83) in women compared to 1.57 (95% CI 1.20–2.05) in men.

Sensitivity analysis. Associations were similar when intra-articular joint replacement hospitalizations and pretrial self-reported joint replacements were examined separately (Supplementary Tables 4 and 5 and Supplementary Figure 2, <https://onlinelibrary.wiley.com/doi/10.1002/art.42156>). The cumulative incidence of knee and hip replacement in relation to PRS categories is shown in Figure 2, considering only joint replacements occurring prospectively during the ASPREE trial and excluding participants with pretrial self-reported knee or hip replacement. The specificity of PRS was examined (Supplementary Table 6, <https://onlinelibrary.wiley.com/doi/10.1002/art.42156>). Higher hip PRS was associated with an increased risk of knee replacement after adjustment for confounders (OR 1.09 [95% CI 1.03–1.15] per SD of PRS), with knee replacement risk increased in the high-risk hip PRS category compared to the low-risk PRS category (OR 1.27 [95% CI 1.07–1.52]). There was no significant association between knee PRS and risk of hip replacement. The risk of knee and hip replacement against the middle half of the study population was also examined (Supplementary Table 7, <https://onlinelibrary.wiley.com/doi/10.1002/art.42156>). The OR of knee replacement was 0.81 (95% CI 0.70–0.93) in the low-risk PRS group (bottom 25%) and 1.09 (95% CI 0.95–1.24) in the

**Figure 2.** Cumulative incidence of knee and hip replacement in relation to categories of polygenic risk scores (PRS).

high-risk PRS group (top 25%). The OR of hip replacement was 0.80 (95% CI 0.68–0.93) in the low-risk PRS group and 1.40 (95% CI 1.22–1.60) in the high-risk PRS group.

DISCUSSION

We evaluated the performance of newly derived PRS for advanced OA requiring knee or hip replacement in a large genetic study of older community-dwelling individuals who were ambulatory and independently living at baseline. The current study is the first to present independent validation of PRS in relation to the risk of OA and demonstrated an association between specific knee and hip PRS and advanced OA, independent of age, sex, BMI, and socioeconomic status. We found meaningfully different risks of knee and hip replacement among low-risk (Q1), medium-risk (Q2–4), and high-risk (Q5) PRS groups, with stronger associations for hip replacement than knee replacement. Our results suggest that PRS have the potential to better target preventive interventions for severe OA by providing a personalized approach.

We demonstrated that specific genomic risk scores calculated separately for knee and hip OA (8) were associated with advanced OA requiring a knee or hip joint replacement in a well-characterized cohort of community-dwelling, ambulatory older adults, with data suggesting the specificity of knee PRS with less likelihood for hip PRS. We also found that the hip PRS was associated with a stronger risk for hip replacement compared to the knee PRS for knee replacement, independent of age, sex, BMI, and socioeconomic status. This was not unexpected, given that twin studies have suggested that ~70% of the variation in risk of hip OA can be attributed to genetic factors, compared to 45% for knee OA (22). These differences may reflect the stronger association of obesity, physical exertion, and injuries (strongly influenced by lifestyle factors) with knee OA, compared to hip OA (5,23,24).

Our findings are also consistent with evidence suggesting an important role of hip bone shape (strongly influenced by genetic factors) in the pathogenesis of hip OA (25). As there was a lower number of genetic variants for knee PRS compared to hip PRS (10 versus 38), the knee PRS would have lower power with a lower explained variance. The smaller number of variants that have been found for knee OA is probably due to a more heterogeneous etiology of knee OA compared to hip OA. Furthermore, we found stronger associations between hip PRS and risk of hip replacement in women than in men. Sex-specific differences in the anatomy and hip bone shape may alter the predisposition toward hip OA in men and women, and it may be that genetic factors affect the anatomy and hip bone shape or have other heterogeneous effects between sexes. The possible sex-specific association requires further investigation.

Although the overall ORs observed per SD PRS change for knee and hip replacements were modest (<1.3 per SD),

individuals with a high-risk knee PRS had a 44% increased risk of knee replacement, and participants with a high-risk hip PRS had an 88% increased risk of hip replacement compared to those with a low-risk PRS. The magnitude of these associations was comparable to other PRS studies for different diseases and traits, where ORs per SD PRS typically range between 1.1 and 1.8 (e.g., ischemic stroke [26], coronary artery disease [27], and breast cancer [28]). Implementation of targeted therapy based on PRS has commenced for some conditions such as breast cancer and coronary artery disease (29). PRS associations with advanced knee OA and hip OA in our study remained significant when considering only incident joint replacements occurring prospectively during the ASPREE trial.

In the current study, we demonstrate that it is possible to develop a propensity score based on genetic risk, which is an independent risk factor for severe knee and hip OA requiring a joint replacement, independent of age, sex, BMI, and socioeconomic status. As the genotypes used to calculate a PRS do not change over the life course and are not influenced by environmental and lifestyle factors, PRS could act as an independent risk factor versus conventional clinical risk factors for OA. Access to information on genetic risk, prior to the manifestation of clinical symptoms, has the potential to improve compliance with preventive strategies and address risk factors earlier in the disease course. Genetic risk scores for OA therefore have the potential to be incorporated into decision support algorithms earlier in life, to improve targeting of interventions and clinical management. PRS could also potentially be used as part of the algorithm to identify “fast progressors” of OA for inclusion in clinical trials aimed at drug development.

Strengths of our study include the well-characterized, older study population with robust data on knee and hip replacements collected. The median age at recruitment was 75 years in a large community-based population of independently living older adults, allowing for observation of joint replacements in the most clinically relevant population and age group. Knee and hip replacements are valid measures of advanced OA in the context of the Australian healthcare system, as all Australian citizens and permanent residents have access to quality health care services including joint replacement under Australia’s publicly funded universal health insurance system (Medicare). It also identifies an important OA outcome that needs to be prevented.

Limitations of our study include combining incident (hospitalizations during the trial) and prevalent (self-reported, before enrollment) joint replacements as a marker of advanced OA. The median age of TKR and THR is 69 years in Australia, with >85% of total joint replacement procedures performed in people ages >55 years (2). Therefore, including prevalent and incident joint replacements provides a more valid assessment of joint replacement as a marker of severe OA. The observed associations of the PRS were similar for incident versus prevalent joint replacements when analyzed separately, suggesting that there are not

major genetic differences with regard to risk of advanced OA between these groups. It may be that genetic influences are even higher in those who are younger and have a joint replacement. The population we examined, the ASPREE participants ages ≥ 70 years with a median age of 75 years at baseline, represents a significant proportion of all joint replacements, but does not include younger individuals who may be at particularly high genetic risk. Although we found a significant genetic component and validated the PRS for advanced OA in this older population, the genetic influence in younger individuals warrants further investigation.

The use of self-reported data may have overestimated the number of knee and hip replacements. Arthroscopy may have been misidentified for some self-reported joint replacements, but this is still likely to reflect OA, given that arthroscopies in this older population are most likely to have been performed for pathologic conditions such as meniscal pathology due to OA (30). The self-reported joint replacements occurred at a younger age (< 70 years) when hip fracture is very uncommon. Another limitation of our study is limited details on the indication and type (primary or revision) of surgery recorded for hospitalization and/or self-reported joint replacements. However, in Australia, the majority of TKR and THR surgeries (98% and 89%, respectively) are performed in advanced OA, and a minority (10%) of joint replacement procedures are revision surgery for a primary joint replacement (2). Potential misclassifications of knee and hip replacement would most likely have been nondifferential and, if anything, may have underestimated the magnitude of observed PRS associations. Our results may not be generalizable to the general population since only relatively healthy older adults were included in the ASPREE trial, likely free of comorbid disease that is often present in OA patients.

In conclusion, our study demonstrates that genomic risk scores for advanced knee and hip OA are robustly associated with the risk of knee and hip replacement in older community-dwelling individuals, independent of age, sex, BMI, and socioeconomic status. There was a stronger association for the hip PRS than the knee PRS and for hip replacement risk in women. PRS have the potential to improve prevention of severe knee and hip OA by providing a personalized approach and identifying individuals who may benefit from early intervention.

ACKNOWLEDGMENT

Open access publishing was facilitated by Monash University, as part of the Wiley - Monash University agreement via the Council of Australian University Librarians.

AUTHOR CONTRIBUTIONS

All authors were involved in drafting the article or revising it critically for important intellectual content, and all authors approved the final version to be published. Dr. Wang had full access to all of the data in the study and takes responsibility for the integrity of the data and the accuracy of the data analysis.

Study conception and design. Lacaze, Wang, Cicuttini.

Acquisition of data. Lacaze, Franks.

Analysis and interpretation of data. Lacaze, Wang, Polekhina, Bakshi, Riaz, Owen, Abidi, Tiller, McNeil, Cicuttini.

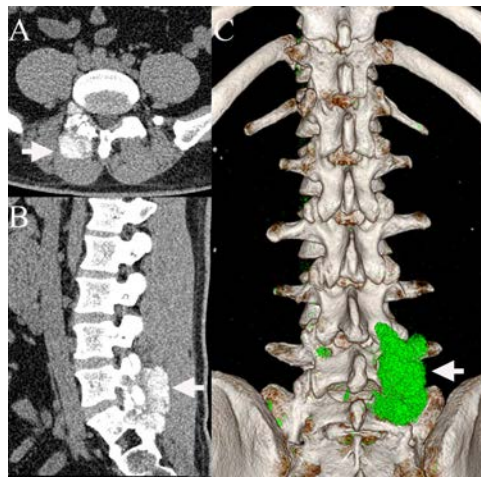
REFERENCES

- Safiri S, Kolahi AA, Smith E, Hill C, Bettampadi D, Mansournia MA, et al. Global, regional and national burden of osteoarthritis 1990-2017: a systematic analysis of the Global Burden of Disease Study 2017. *Ann Rheum Dis* 2020;79:819–28.
- Australian Orthopaedic Association National Joint Replacement Registry (AOANJRR). Hip, Knee & Shoulder Arthroplasty: 2020 Annual Report, Adelaide; AOA, 2020:1–474. URL: <https://aoanjrr.sahmri.com/annual-reports-2020>.
- Deveza LA, Melo L, Yamato TP, Mills K, Ravi V, Hunter DJ. Knee osteoarthritis phenotypes and their relevance for outcomes: a systematic review. *Osteoarthritis Cartilage* 2017;25:1926–41.
- Hunter DJ, Bierma-Zeinstra S. Osteoarthritis. *Lancet* 2019;393:1745–59.
- Chaganti RK, Lane NE. Risk factors for incident osteoarthritis of the hip and knee. *Curr Rev Musculoskelet Med* 2011;4:99–104.
- Tachmazidou I, Hatzikotoulas K, Southam L, Esparza-Gordillo J, Haberland V, Zheng J, et al. Identification of new therapeutic targets for osteoarthritis through genome-wide analyses of UK Biobank data. *Nat Genet* 2019;51:230–6.
- Zengini E, Hatzikotoulas K, Tachmazidou I, Steinberg J, Hartwig FP, Southam L, et al. Genome-wide analyses using UK Biobank data provide insights into the genetic architecture of osteoarthritis. *Nat Genet* 2018;50:549–58.
- Boer CG, Hatzikotoulas K, Southam L, Stefánssdóttir L, Zhang Y, de Almeida RC, et al. Deciphering osteoarthritis genetics across 826,690 individuals from 9 populations. *Cell* 2021;184:4784–818.
- ASPREE Investigator Group. Study design of ASPIrin in Reducing Events in the Elderly (ASPREE): a randomized, controlled trial. *Contemp Clin Trials* 2013;36:555–64.
- McNeil JJ, Woods RL, Nelson MR, Murray AM, Reid CM, Kirpach B, et al. Baseline Characteristics of Participants in the ASPREE (ASPIrin in Reducing Events in the Elderly) Study. *J Gerontol A Biol Sci Med Sci* 2017;72:1586–93.
- McNeil JJ, Woods RL, Nelson MR, Reid CM, Kirpach B, Wolfe R, et al. Effect of Aspirin on disability-free survival in the healthy elderly. *N Engl J Med* 2018;379:1499–508.
- Wang Y, Simpson JA, Wluka AE, Teichtahl AJ, English DR, Giles GG, et al. Relationship between body adiposity measures and risk of primary knee and hip replacement for osteoarthritis: a prospective cohort study. *Arthritis Res Ther* 2009;11:R31.
- McNeil JJ, Woods RL, Ward SA, Britt CJ, Lockery JE, Beilin LJ, et al. Cohort profile: the ASPREE Longitudinal Study of Older Persons (ALSOP). *Int J Epidemiol* 2019;48:1048–9h.
- Lewis JP, Riaz M, Xie S, Polekhina G, Wolfe R, Nelson M, et al. Genetic variation in PEAR1, cardiovascular outcomes and effects of aspirin in a healthy elderly population. *Clin Pharmacol Ther* 2020;108:1289–98.
- Auton A, Brooks LD, Durbin RM, Garrison EP, Kang HM, Korbel JO, et al. A global reference for human genetic variation. *Nature* 2015;526:68–74.
- Taliun D, Harris DN, Kessler MD, Carlson J, Szpiech ZA, Torres R, et al. Sequencing of 53,831 diverse genomes from the NHLBI TOPMed Program. *Nature* 2021;590:290–9.
- Das S, Forer L, Schönerr S, Sidore C, Locke AE, Kwong A, et al. Next-generation genotype imputation service and methods. *Nat Genet* 2016;48:1284–7.
- Fuchsberger C, Abecasis GR, Hinds DA. minimac2: faster genotype imputation. *Bioinformatics*. 2015;31:782–4.

19. World Health Organization. Body mass index – BMI, 2022. URL: <https://www.euro.who.int/en/health-topics/disease-prevention/nutrition/a-healthy-lifestyle/body-mass-index-bmi>.
20. Australian Bureau of Statistics. 2033.0.55.001 - Census of Population and Housing: Socio-Economic Indexes for Areas (SEIFA), Australia, 2011. 2018. URL: [https://www.ausstats.abs.gov.au/ausstats/subscriber.nsf/0/22CEDA8038AF7A0DCA257B3B00116E34/\\$File/2033.0.55.001%20seifa%202011%20technical%20paper.pdf](https://www.ausstats.abs.gov.au/ausstats/subscriber.nsf/0/22CEDA8038AF7A0DCA257B3B00116E34/$File/2033.0.55.001%20seifa%202011%20technical%20paper.pdf).
21. R Core Team. R: a language and environment for statistical computing, 2018. Vienna, Austria.
22. Magnusson K, Scurrah K, Ystrom E, Ørstavik RE, Nilsen T, Steingrimsdóttir ÓA, et al. Genetic factors contribute more to hip than knee surgery due to osteoarthritis - a population-based twin registry study of joint arthroplasty. *Osteoarthritis Cartilage* 2017;25:878–84.
23. Gelber AC, Hochberg MC, Mead LA, Wang NY, Wigley FM, Klag MJ. Body mass index in young men and the risk of subsequent knee and hip osteoarthritis. *Am J Med* 1999;107:542–8.
24. Gelber AC, Hochberg MC, Mead LA, Wang NY, Wigley FM, Klag MJ. Joint injury in young adults and risk for subsequent knee and hip osteoarthritis. *Ann Intern Med* 2000;133:321–8.
25. Ahedi HG, Aspden RM, Blizzard LC, Saunders FR, Cicuttini FM, Aitken DA, et al. Hip shape as a predictor of osteoarthritis progression in a prospective population cohort. *Arthritis Care Res (Hoboken)* 2017;69:1566–73.
26. Abraham G, Malik R, Yonova-Doing E, Salim A, Wang T, Danesh J, et al. Genomic risk score offers predictive performance comparable to clinical risk factors for ischaemic stroke. *Nat Commun* 2019;10:5819.
27. Inouye M, Abraham G, Nelson CP, Wood AM, Sweeting MJ, Dudbridge F, et al. Genomic risk prediction of coronary artery disease in 480,000 adults: implications for primary prevention. *J Am Coll Cardiol* 2018;72:1883–93.
28. Mavaddat N, Michailidou K, Dennis J, Lush M, Fachal L, Lee A, et al. Polygenic risk scores for prediction of breast cancer and breast cancer subtypes. *Am J Hum Genet* 2019;104:21–34.
29. Lambert SA, Abraham G, Inouye M. Towards clinical utility of polygenic risk scores. *Hum Mol Genet* 2019;28:R133–42.
30. Siemieniuk RA, Harris IA, Agoritsas T, Poolman RW, Brignardello-Petersen R, Van de Velde S, et al. Arthroscopic surgery for degenerative knee arthritis and meniscal tears: a clinical practice guideline. *BMJ* 2017;357:j1982.

DOI 10.1002/art.42125

Clinical images: Gout of the spine






The patient, a 34-year-old man with a history of gout for >8 years, presented with symptoms of recurrent joint pain and lower back pain for 3 days. He had been receiving treatment with colchicine and benzbromarone starting in 2013. Laboratory tests revealed marked elevation in serum urate levels to 694 $\mu\text{moles/liter}$ (reference range 180–450 $\mu\text{moles/liter}$). Conventional computed tomography (CT) of the axial (A) and sagittal (B) orientations revealed a hyperdense mass in the L5–S1 facet joint with bone erosion (arrows). Dual-energy CT revealed extensive urate crystal deposition within the lumbosacral facet joint (arrow in C). The findings were consistent with a diagnosis of spinal gout. The patient was started on colchicine, loxoprofen sodium, febuxostat, and sodium bicarbonate; the patient's symptoms were relieved within 1 week, and he was discharged from the hospital. Spinal gout is rarely encountered in clinical practice and therefore early recognition is important to allow timely diagnosis and prompt treatment, potentially averting unnecessary surgeries (1,2). Dual-energy CT may be useful in the diagnosis of spinal gout (1–3).

The author thanks Peixin Qin for contribution of the image in panel C. Author disclosures are available at <https://onlinelibrary.wiley.com/action/downloadSupplement?doi=10.1002%2Fart.42125&file=art42125-sup-0001-Disclosureform.pdf>.

1. Khanna I, Pietro R, Ali Y. What has dual energy CT taught us about gout? *Curr Rheumatol Rep* 2021;23:71.
2. Toprover M, Krasnokutsky S, Pillinger MH. Gout in the spine: imaging, diagnosis, and outcomes. *Curr Rheumatol Rep* 2015;17:70.
3. Gibney B, Murray N. Dual-energy CT of spinal tophaceous gout. *Radiology* 2020;296:276.

Guojie Wang, MD 
wanggj5@mail.sysu.edu.cn
 Fifth Affiliated Hospital of Sun Yat-sen University,
 People's Republic of China

Risk Assessment for Hip and Knee Osteoarthritis Using Polygenic Risk Scores

Bahar Sedaghati-Khayat,¹  Cindy G. Boer,¹ Jos Runhaar,¹  Sita M. A. Bierma-Zeinstra,¹ Linda Broer,¹ M. Arfan Ikram,¹ Eleftheria Zeggini,²  André G. Uitterlinden,¹ Jeroen G. J. van Rooij,¹ and Joyce B. J. van Meurs¹

Objective. Polygenic risk scores (PRS) allow risk stratification using common single-nucleotide polymorphisms (SNPs), and clinical applications are currently explored for several diseases. This study was undertaken to assess the risk of hip and knee osteoarthritis (OA) using PRS.

Methods. We analyzed 12,732 individuals from a population-based cohort from the Rotterdam Study (n = 11,496), a clinical cohort (Cohort Hip and Cohort Knee [CHECK] study; n = 908), and a high-risk cohort of overweight women (Prevention of Knee OA in Overweight Females [PROOF] study; n = 328), for the association of the PRS with prevalence/incidence of radiographic OA, of clinical OA, and of total hip replacement (THR) or total knee replacement (TKR). The hip PRS and knee PRS contained 44 and 24 independent SNPs, respectively, and were derived from a recent genome-wide association study meta-analysis. Standardized PRS (with Z transformation) were used in all analyses.

Results. We found a stronger association of the PRS for clinically defined OA compared to radiographic OA phenotypes, and we observed the highest PRS risk stratification for TKR/THR. The odds ratio (OR) per SD was 1.3 for incident THR (95% confidence interval [95% CI] 1.1–1.5) and 1.6 (95% CI 1.3–1.9) for incident TKR in the Rotterdam Study. The knee PRS was associated with incident clinical knee OA in the CHECK study (OR 1.3 [95% CI 1.1–1.5]), but not for the PROOF study (OR 1.2 [95% CI 0.8–1.7]). The OR for OA increased gradually across the PRS distribution, up to 2.1 (95% CI 1.4–3.2) for individuals with the 10% highest PRS compared to the middle 50% of the PRS distribution.

Conclusion. Our findings validated the association of PRS across OA definitions. Since OA is becoming frequent and primary prevention is not commonly applicable, PRS-based risk assessment could play a role in OA prevention. However, the utility of PRS is dependent on the setting. Further studies are needed to test the integration of genetic risk assessment in diverse health care settings.

INTRODUCTION

Osteoarthritis (OA) is a complex progressive and irreversible degenerative joint disease, causing joint pain and immobility (1). OA is a late-onset disease (>45 years old) and poses a considerable societal burden with over 300 million people affected globally (2,3). Studies show that OA is becoming even more prevalent in the world's aging and increasingly obese population, and will become one of the most common diseases in the coming decades (4,5).

OA can be influenced by conventional risk factors such as age, body mass index (BMI) and/or lifestyle factors (e.g., vigorous physical activity) (6–8). Although some of these risk factors can be modified (9), a limited number of primary OA prevention programs are available, such as a diet and exercise program aimed at reducing body weight (10). In addition, the clinical treatments are aimed at relieving symptoms, and many patients do not receive appropriate OA risk management therapies (11). Many trials have failed to identify structural treatment options, in part because of

Supported by GOALL project. The GOALL project was funded by the internal Koers23 program from the Erasmus Medical Center (project no. 109433). The PROOF study was funded by The Netherlands Organisation for Health Research and Development (ZonMw) and a FP7 Programm Grant (D-BOARD) by the European Committee. The CHECK study was supported by The Dutch Arthritis Society (ReumaNederland).

¹Bahar Sedaghati-Khayat, MSc, Cindy G. Boer, PhD, Jos Runhaar, PhD, Sita M. A. Bierma-Zeinstra, PhD, Linda Broer, PhD, M. Arfan Ikram, PhD, André G. Uitterlinden, PhD, Jeroen G. J. van Rooij, PhD, Joyce B. J. van Meurs, PhD: Erasmus MC University Medical Center Rotterdam, Rotterdam, The Netherlands; ²Eleftheria Zeggini, PhD: Institute of Translational Genomics, Helmholtz Zentrum München, German Research Center for

Environmental Health, Neuherberg, Germany, and Technical University of Munich (TUM) and Klinikum Rechts der Isar, TUM School of Medicine, Munich, Germany.

Author disclosures are available at <https://onlinelibrary.wiley.com/action/downloadSupplement?doi=10.1002%2Fart.42246&file=art42246-sup-0001-Disclosureform.pdf>.

Address correspondence to Joyce B. J. van Meurs, PhD, Professor of Complex Genomics, Department of Internal Medicine, Erasmus Medical Center, room number EE 0559a, Rotterdam, The Netherlands. Email: j.vanmeurs@erasmusmc.nl.

Submitted for publication December 23, 2021; accepted in revised form May 24, 2022.

the patients' heterogeneity in the late stages of OA (12,13). Therefore, it is suggested that the OA burden should be controlled by shifting from the current broad and imprecise approach of OA management to a more precise system of individualized patient care based on the patient's characteristics and specific needs (11). In such a system, the ability to predict OA onset or progression would allow for more efficacious OA-modifying management strategies (1,14,15).

One of the prime opportunities for OA prediction lies in genetic predisposition. Heritability of OA has been estimated at 40–65% by twin studies, depending on the affected joint (15–17). The most extensive genome-wide association study (GWAS) study in OA was conducted by the Genetics of OA (GO) consortium (18), which revealed 100 genetic variants and explained ~6–21% of the total estimated heritability for different types of OA. These ~100 genetic variants are expected to predict individual genetic OA risk through polygenic risk scores (PRS) and could be used as a risk prediction tool in different settings, such as in clinical practice or in screening programs in society (19,20).

In this study, we constructed the PRS for knee and hip OA and examined their performance for radiographic OA, clinical OA, and total hip replacement (THR) or total knee replacement (TKR) in 3 Dutch studies with Caucasian participants: a large population-based cohort, a clinical cohort of patients in primary care, and a cohort of subjects at high risk of developing knee

OA. Additionally, we investigated the optimal PRS cutoffs and the interaction of the OA PRS with conventional risk factors in subsequent sensitivity analyses.

PATIENTS AND METHODS

Study populations. We analyzed samples from 12,732 Dutch Caucasian individuals from 3 population-based cohorts within the Rotterdam Study (RS-I, RS-II, RS-III) and 2 clinical cohorts (the Cohort Hip and Cohort Knee [CHECK] study and the Prevention of Knee OA in Overweight Females [PROOF] study) (Figure 1, Table 1, and Supplementary Figure 1, available on the *Arthritis & Rheumatology* website at <https://onlinelibrary.wiley.com/doi/10.1002/art.42246>). The Rotterdam Study is a large longitudinal population-based cohort study (21). CHECK is a longitudinal cohort of individuals that consulted a general practitioner (GP) for joint complaints for the first time, and the selection of CHECK participants was directed toward early OA cases (22,23). PROOF is a longitudinal study of overweight women ages 50–60 years without clinical OA at baseline (24). More details about each cohort are provided in the Supplementary Methods (<https://onlinelibrary.wiley.com/doi/10.1002/art.42246>).

Outcomes assessment. Radiographic hip and/or knee OA was defined in all 5 cohorts by a Kellgren/Lawrence (K/L)

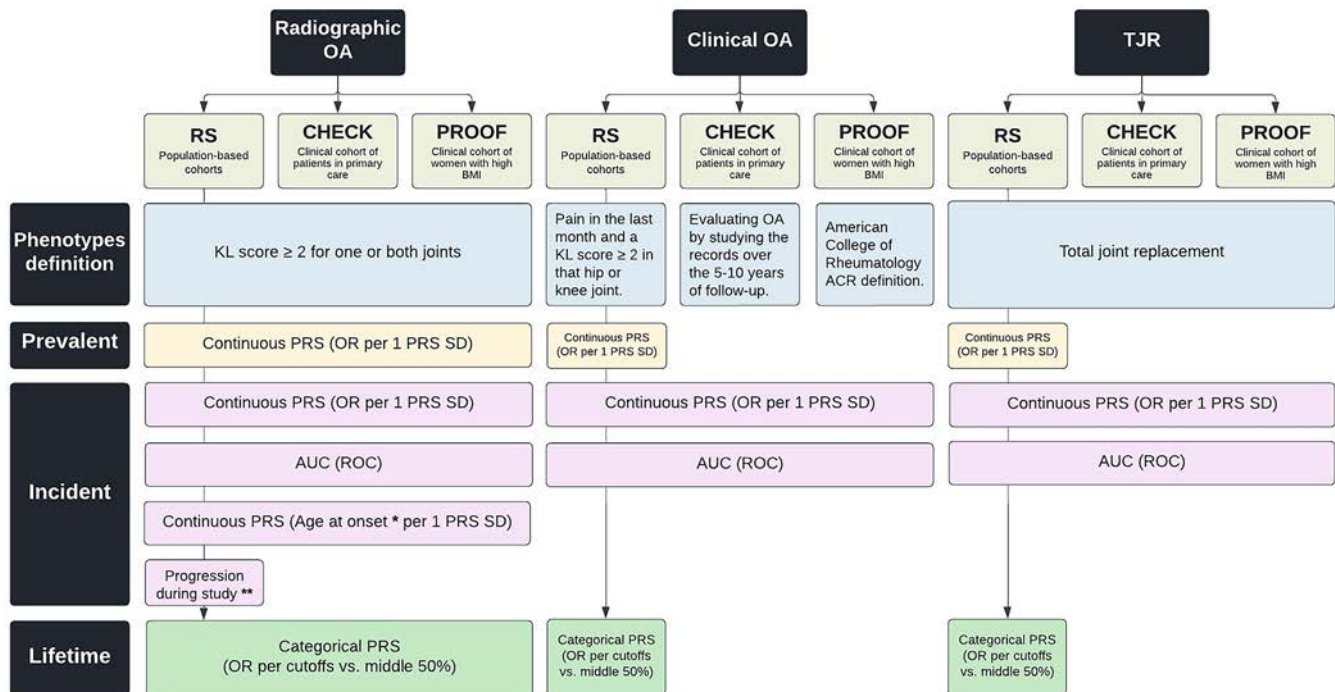


Figure 1. Overview of data availability and performed analysis. * = Age at onset was determined for incident radiographic osteoarthritis (OA) and was calculated as the age at first diagnosis of radiographic OA. ** = Radiographic OA progression was defined as any progression in the Rotterdam Study (RS) with a ≥ 1 -degree increment in Kellgren/Lawrence (K/L) score (excluding progression from K/L 0 to K/L 1 or having a total joint replacement [TJR] of one or both joints during the follow-up period). CHECK = Cohort Hip and Cohort Knee; PROOF = Prevention of Knee Osteoarthritis in Overweight Females; BMI = body mass index; PRS = polygenic risk score; ROC = receiving operating characteristic curve; AUC = area under the ROC; OR = odds ratio. Color figure can be viewed in the online issue, which is available at <http://onlinelibrary.wiley.com/doi/10.1002/art.42246/abstract>.

Table 1. Descriptive statistics of the study populations (n = 16,335 total participants)*

	RS-I (n = 7,983)	RS-II (n = 3,011)	RS-III (n = 3,932)	CHECK study (n = 1,002)	PROOF study (n = 407)
No. of participants with genetic data available (female sex, %)	6,291 (60.1)	2,157 (54.4)	3,048 (56.3)	908 (79)	328 (100)
Baseline age, range/mean \pm SD years	55–99/ 69.5 \pm 9.2	55–95/ 64.8 \pm 8.0	45–97/ 57.1 \pm 6.9	45.1–65.1/ 55.9 \pm 5.2	50.2–61.9/ 55.8 \pm 3.2
Baseline BMI, range/mean \pm SD kg/m ²	14.2–50.7/ 26.3 \pm 3.7	16.7–50.6/ 27.2 \pm 4.0	12.6–56.9/ 27.7 \pm 4.6	18.1–40.1/ 26.2 \pm 4.1	26.1–48.6/ 31.9 \pm 4.1
Hip PRS (original), range/mean \pm SD†	1.33–5.07/ 2.52 \pm 0.29	1.59–4.73/ 2.51 \pm 0.3	1.57–4.86/ 2.52 \pm 0.29	1.74–4.77/ 2.51 \pm 0.29	1.78–3.4/ 2.5 \pm 0.27
Hip PRS (without RS), range/mean \pm SD‡	1.33–5.09/ 2.54 \pm 0.30	1.6–4.76/ 2.54 \pm 0.3	1.6–4.89/ 2.54 \pm 0.3	1.76–4.8/ 2.54 \pm 0.29	1.8–3.44/ 2.53 \pm 0.27
Knee PRS (original), range/mean \pm SD†	0.56–1.96/ 1.26 \pm 0.17	0.8–1.81/ 1.27 \pm 0.16	0.68–1.86/ 1.26 \pm 0.16	0.65–1.68/ 1.25 \pm 0.16	0.84–1.68/ 1.26 \pm 0.16
Knee PRS (without RS), range/mean \pm SD‡	0.55–1.94/ 1.25 \pm 0.17	0.8–1.8/ 1.26 \pm 0.16	0.68–1.85/ 1.26 \pm 0.16	0.64–1.67/ 1.24 \pm 0.16	0.83–1.67/ 1.25 \pm 0.16
Radiographic OA, %					
Prevalent hip	9.7	5.5	2.3	6.0	–
Incident hip	7.8	11.6	5.7	56.9	–
Prevalent knee	19.5	14.2	8.9	6.6	9.5
Incident knee	14.9	14.1	7.5	71.7	16.9
Clinical OA, %					
Prevalent hip	7.8	5.4	2.0	–	–
Incident hip	5.8	6.5	1.6	28.4	–
Prevalent knee	20.7	22.2	14.6	–	–
Incident knee	18.1	9.9	5.5	49.6	10.7
TJR, %					
Prevalent hip	3.3	2.1	1.0	–	–
Incident hip	3.1	3.9	0.8	10.4	–
Prevalent knee	0.7	1.0	0.6	–	–
Incident knee	1.8	3.6	1.2	5.8	–

* RS-I = Rotterdam Study cohort I; CHECK = Cohort Hip and Cohort Knee; PROOF = Prevention of Knee Osteoarthritis in Overweight Females; BMI = body mass index; TJR = total joint replacement.

† Polygenic risk scores (PRS) based on the initially reported effect sizes for osteoarthritis (OA) in 826,690 participants across 13 cohorts worldwide in 10 different OA phenotypes by the Genetics of OA (GO) consortium meta-analysis.

‡ PRS based on the secondary reported effect sizes for only hip OA and knee OA after excluding the Rotterdam Study from the meta-analysis by the GO consortium.

score of ≥ 2 for one or both joints (25). Clinical OA in the Rotterdam Study was defined as reported pain in the last month and a K/L score of ≥ 2 in the same hip or knee joint, and the control group contained all participants who had not been diagnosed as having radiographic OA by the end of the follow-up period. In the CHECK cohort, clinical OA was defined as clinically relevant hip or knee OA by a group of 36 GPs and secondary care physicians by manually evaluating the study records over the 5–10 years of follow-up (23). Finally, clinical OA in the PROOF cohort was defined based on the American College of Rheumatology criteria (26), which includes knee pain on most days of the last month in addition to ≥ 3 of the following clinical findings: age > 50 years, stiffness < 30 minutes, crepitus, bony tenderness, bony enlargement, and no palpable warmth. Prevalent cases were defined at baseline. For incident cases, participants were censored at first diagnosis, death or other loss to follow-up, end of the study period, or after 10 years of follow-up. Age at onset was determined for incident radiographic OA and was calculated as the age at first diagnosis of radiographic OA. A summary of the data availability and performed analysis are shown in Figure 1.

We defined radiographic OA progression in the Rotterdam Study as ≥ 1 -degree increment of the K/L score (excluding progression from K/L 0 to K/L 1) or total joint replacement (TJR) for one or both joints in follow-up time. As a sensitivity analysis, we examined whether the PRS predicts OA progression across the different OA stages by stratifying the progression cases into 3 groups: 1) “early incident OA” includes patients with a maximum K/L score of 2 for each joint during follow-up (K/L 0/1 to K/L 2); 2) “incident severe OA” includes patients with a K/L score of 3 or 4 or joint replacement of each joint during follow-up (from K/L 0/1 at baseline to K/L 3+); 3) “progressive severe OA” includes cases that progressed from early OA (K/L 2) to severe OA (K/L 3+) or joint replacement surgery during follow-up (K/L 2+ to K/L 3+). The control groups for all progression variables were defined separately for hip and knee OA and contained all participants who had not been diagnosed as having radiographic OA (K/L 2+) for either knee or hip by the end of follow-up.

Variant selection and calculating polygenic scores.

In the Rotterdam Study, participants were genotyped using Illumina's 550k or 610k genotyping arrays and imputed to the HRC1.1

reference panel. In CHECK and PROOF, participants were genotyped using Illumina's MEGA and Cytosnp 850K genotyping arrays, respectively, and imputed to the HRC1 reference panel. Sample and variant quality control were performed as described elsewhere (27). We selected all 45 independent variants for hip OA and all 24 independent variants for knee OA that were significantly ($P < 1.3 \times 10^{-8}$) associated, genome-wide, with hip or knee OA in the GO consortium (18). The GO consortium performed a large-scale GWAS meta-analysis for OA in 826,690 participants across 13 cohorts worldwide in 10 different OA phenotypes (Supplementary Table 1, <https://onlinelibrary.wiley.com/doi/10.1002/art.42246>).

Since the Rotterdam Study was part of the original GWAS, which could have impacted the effect estimates, the GO consortium provided us with a meta-analysis for hip OA and knee OA after excluding the Rotterdam Study cohorts. Supplementary Table 2 and Supplementary Figure 2 (<https://onlinelibrary.wiley.com/doi/10.1002/art.42246>) show the reported effect sizes with and without the Rotterdam Study and their correlation, respectively. In Supplementary Table 2, all effect sizes are reported in the positive direction, matching with effect allele and effect allele frequency. In the present study, we used the effect sizes after excluding the Rotterdam Study. For making the PRS, 3 of 45 selected variants for the hip OA PRS were excluded because of low imputation quality ($R^2 > 0.8$) or absence in all 5 data sets, of which 2 could be replaced by proxies with $R^2 > 0.9$ and $D' > 0.9$, and thus the hip OA PRS was constructed based on 44 variants (Supplementary Table 2). For the knee OA PRS, 3 variants were similarly excluded and subsequently replaced by proxies (Supplementary Table 2). We calculated the weighted continuous PRS for hip and knee OA as follows:

$$PRS_i = \sum_j^k (\hat{\beta}_j \times dosage_{ij})$$

where PRS_i is the polygenic score for subject i , $dosage_{ij}$ is the posterior probability of being a heterozygous (probability ~ 1.0) or homozygous (probability ~ 2.0) effect allele carrier after imputations by subject i of a variant j , k is the number of independent variants in the polygenic score for subject i , and $\hat{\beta}_j$ is the weight for variant j obtained from GWAS summary statistics. All PRS were standardized to a mean of 0 and an SD of 1 (with Z transformation) for each of the 5 cohorts.

Statistical analysis. Age- and sex-adjusted binomial generalized linear (GLM) models were used to evaluate the association between the continuous PRS value (expressed as SD) and outcomes. For knee OA risk assessment, the baseline BMI (kg/m^2) was also included in the model. All analyses in the 3 Rotterdam Study subcohorts were followed by a fixed-effect meta-analysis of effects in the Rotterdam Study as a whole. The PRS predictive value was compared to the traditional clinical factors (i.e., age, sex, and BMI) using the area under the receiver operating characteristic curve (AUC). For PRS cutoff analyses, participants were

partitioned into the top and bottom 5%, 10%, 20%, or 25% of the PRS distribution, and each partition was compared to participants in the middle 25–75% as a reference group representing the “average” Dutch Caucasian population. The absolute risks in each partition are based on 10-year incidence and compared to the reference group. Additional gaussian GLM models were used to evaluate PRS association with age at radiographic OA onset for incident radiographic OA. All statistical analyses were performed using R software, version 4.0.0 (R packages: *rmeta*, *MASS*, *survminer*) and SPSS, version 28. A summary of the data availability and performed analysis are shown in Figure 1.

Ethics approval. The Rotterdam Study was approved by the Medical Ethics Committee of the Erasmus MC (registration no. MEC 02.1015) and by the Dutch Ministry of Health, Welfare and Sport (Population Screening Act WBO, license no. 1071272-159521-PG). The Rotterdam Study Personal Registration Data collection is filed with the Erasmus MC Data Protection Officer under registration number EMC1712001. The Rotterdam Study was entered into The Netherlands National Trial Register (www.trialregister.nl) and the World Health Organization International Clinical Trials Registry Platform (<https://apps.who.int/trialsearch/>) under shared catalogue number NL6645/NTR6831. All participants provided written informed consent to participate in the study and to have their information obtained from treating physicians.

The CHECK study was approved by the medical ethics committees of all participating centers, and all participants gave their written informed consent before entering the study. The PROOF study (International Standard Randomised Controlled Trial Number no. 42823086) was approved by the Medical Ethics Committee of Erasmus MC University Medical Centre in 2005.

RESULTS

The mean age, sex, and BMI were different across the 3 study populations (Table 1 and Supplementary Figure 1, <https://onlinelibrary.wiley.com/doi/10.1002/art.42246>). The unstandardized weighted PRS had similar normal distributions in all cohorts (Table 1). The incidence of hip OA and knee OA is noticeably higher in the CHECK cohort than in the other study populations (Table 1), in which $>55\%$ (hip) and $>70\%$ (knee) of the individuals developed radiographic OA. In the PROOF cohort, none of the participants had prevalent clinical knee OA, and no incident TKR was observed (Table 1).

Hip OA PRS. Within the Rotterdam Study, we observed an odds ratio (OR) of 1.2–1.3 per SD of hip PRS in relation to prevalent hip OA phenotypes (Figure 2 and Supplementary Table 3, <https://onlinelibrary.wiley.com/doi/10.1002/art.42246>). The PRS for the clinical OA and THR tended to show larger effect sizes (~ 1.3) compared to radiographic OA (~ 1.2). Similarly, the PRS also discriminated against incident hip OA, with the same trend

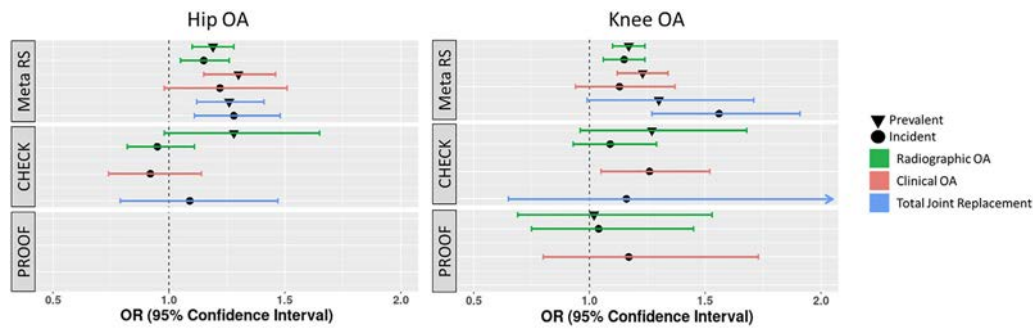


Figure 2. Association between the hip/knee OA PRS and risk of OA according to different definitions in the 3 study populations. The results in the Rotterdam Study are presented as a meta-analysis of the 3 subcohorts. See Figure 1 for definitions.

showing larger effects in clinically defined hip OA (Figure 2 and Supplementary Table 3). In the CHECK cohort, the hip PRS had a similar OR of 1.3 (95% confidence interval [95% CI] 0.98–1.65) for prevalent radiographic hip OA, and no significant OR was observed for incident hip OA (0.95 [95% CI 0.82–1.11]), irrespective of the radiographic or clinical definitions (Figure 2 and Supplementary Table 3). Similarly, we did not observe a significant association between age at onset and the hip PRS within the Rotterdam Study or CHECK cohort (Supplementary Table 4, <https://onlinelibrary.wiley.com/doi/10.1002/art.42246>).

In the Rotterdam Study, the sensitivity analysis showed that the hip PRS was significantly associated with radiographic progression of hip OA (OR 1.18 [95% CI 1.09–1.28]), similar to that observed for incident radiographic OA (OR 1.15 [95% CI 1.05–1.26]). When we stratified the analysis for progressive hip OA patients, we found a higher risk estimate for incident severe OA (OR 1.33 [95% CI 1.12–1.59]) and progressive severe OA (OR 1.31 [95% CI 1.12–1.53]), compared to early incident OA (OR 1.12 [95% CI 1.02–1.23]) (Figure 3 and Supplementary Table 5, <https://onlinelibrary.wiley.com/doi/10.1002/art.42246>).

Knee OA PRS. In the Rotterdam Study, we observed an OR of ~1.2 for radiographic and clinical OA for both prevalent and incident knee OA phenotypes and a slightly higher OR (1.3) for prevalent TKR. However, a larger OR (1.6) was observed for incident TKR. In the CHECK study, the knee PRS showed a trend toward increased risk of prevalent radiographic OA (OR 1.27 [95% CI 0.96–1.68]) and incident clinical knee OA (OR 1.26 [95% CI 1.05–1.52]). For PROOF, we observed a weaker trend of increased risk for the knee PRS with prevalent and incident knee OA, albeit not significant (Figure 2 and Supplementary Table 3). Similarly, we did not observe a significant association in cohorts between age at onset and knee PRS (Supplementary Table 4).

Also in the Rotterdam Study, the sensitivity analysis showed that knee PRS discriminated radiographic progression of knee OA (OR 1.18 [95% CI 1.10–1.25]) similarly to incident radiographic knee OA (OR 1.15 [95% CI 1.06–1.24]) in the Rotterdam Study. After stratifying the analysis for progressive knee OA cases, we found a higher risk estimate for incident severe OA (OR 1.30

[95% CI 1.04–1.63]) and progressive severe OA (OR 1.31 [95% CI 1.15–1.49]) compared to early incident OA (OR 1.13 [95% CI 1.05–1.23]) (Figure 3 and Supplementary Table 5).

Combining PRS with clinical factors to predict incident OA. AUCs were estimated separately for each cohort and combined for the PRS and the clinical risk factors, including age, sex, and BMI, in relation to predicting hip OA or knee OA. For hip OA in the RS, the highest AUC was observed for THR. AUCs for clinical risk factors ($AUC_{THR} = 0.64$) were higher compared to the AUC observed for the PRS alone ($AUC_{THR} = 0.57$) and were slightly increased in the combined model ($AUC_{THR} = 0.66$). Also, a similar trend toward a higher AUC was observed in radiographic and clinical hip OA definitions (Table 2). In the CHECK study, the AUC for clinical risk factors ($AUC_{THR} = 0.64$) was higher than the AUC for the PRS alone ($AUC_{THR} = 0.56$) and did not increase further in the combined models across hip OA definitions. For knee OA in the Rotterdam Study, the AUC for clinical risk factors ($AUC_{THR} = 0.66$) did not improve with the addition of the knee PRS in the combined

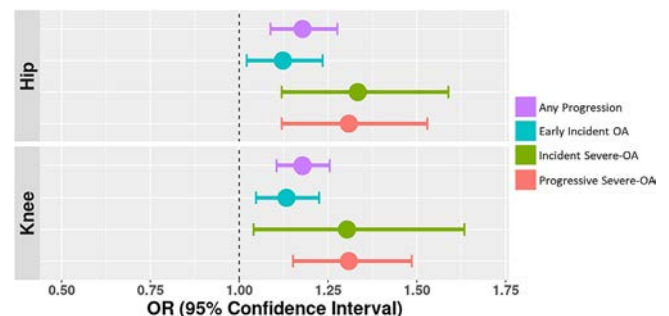


Figure 3. Association between OA PRS and risk of OA progression in a meta-analysis of the Rotterdam Study of 3 cohorts. Any progression was defined by a ≥ 1 -degree increment of the K/L score (excluding progression from K/L 0 to K/L 1) or having a TJR of one or both joints during the follow-up period. Early incident OA was defined by a maximum K/L score of 2 for each joint during follow-up (i.e., K/L 0 or K/L 1 to K/L 2). Incident severe OA was defined by a K/L score of ≥ 3 or TJR during follow-up (i.e., K/L 0 or K/L 1 to K/L 3+, or TJR). Progressive severe OA was defined by progression from early OA (K/L 2) to severe OA (K/L 3+) or TJR during follow-up. See Figure 1 for definitions.

Table 2. Discrimination of OA risk prediction models in the study populations of knee OA and hip OA*

Study and variables	Radiographic OA		Clinical OA		THR	
	AUC (95% CI)	P	AUC (95% CI)	P	AUC (95% CI)	P
Hip OA						
Meta RS†						
PRS	0.54 (0.51–0.56)	<1.0 × 10 ⁻¹⁶	0.56 (0.50–0.63)	<1.0 × 10 ⁻¹⁶	0.57 (0.52–0.61)	<1.0 × 10 ⁻¹⁶
Age and sex	0.57 (0.55–0.60)	<1.0 × 10 ⁻¹⁶	0.58 (0.52–0.64)	<1.0 × 10 ⁻¹⁶	0.64 (0.60–0.68)	<1.0 × 10 ⁻¹⁶
Age, sex, and PRS	0.59 (0.56–0.61)	<1.0 × 10 ⁻¹⁶	0.62 (0.56–0.68)	<1.0 × 10 ⁻¹⁶	0.66 (0.62–0.70)	<1.0 × 10 ⁻¹⁶
CHECK						
PRS	0.51 (0.47–0.55)	7.5 × 10 ⁻¹	0.52 (0.46–0.58)	4.8 × 10 ⁻¹	0.56 (0.46–0.66)	2.2 × 10 ⁻¹
Age and sex	0.62 (0.58–0.65)	2.2 × 10 ⁻⁸	0.53 (0.47–0.59)	3.6 × 10 ⁻¹	0.64 (0.55–0.72)	4.8 × 10 ⁻³
Age, sex, and PRS	0.62 (0.58–0.65)	2.2 × 10 ⁻⁸	0.53 (0.47–0.59)	2.7 × 10 ⁻¹	0.64 (0.55–0.73)	3.8 × 10 ⁻³
Knee OA						
Meta RS†						
PRS	0.51 (0.50–0.53)	<1.0 × 10 ⁻¹⁶	0.53 (0.51–0.57)	<1.0 × 10 ⁻¹⁶	0.53 (0.51–0.56)	<1.0 × 10 ⁻¹⁶
Age, sex, and BMI	0.60 (0.58–0.62)	<1.0 × 10 ⁻¹⁶	0.65 (0.60–0.69)	<1.0 × 10 ⁻¹⁶	0.66 (0.61–0.71)	<1.0 × 10 ⁻¹⁶
Age, sex, BMI, and PRS	0.60 (0.58–0.63)	<1.0 × 10 ⁻¹⁶	0.66 (0.61–0.71)	<1.0 × 10 ⁻¹⁶	0.66 (0.61–0.71)	<1.0 × 10 ⁻¹⁶
CHECK						
PRS	0.55 (0.51–0.60)	2.4 × 10 ⁻²	0.54 (0.49–0.58)	1.5 × 10 ⁻¹	0.58 (0.38–0.77)	3.6 × 10 ⁻¹
Age, sex, and BMI	0.54 (0.49–0.59)	7.5 × 10 ⁻²	0.59 (0.54–0.64)	1.9 × 10 ⁻⁴	0.58 (0.46–0.70)	3.4 × 10 ⁻¹
Age, sex, BMI, and PRS	0.57 (0.53–0.62)	2.7 × 10 ⁻³	0.60 (0.55–0.65)	3.4 × 10 ⁻⁵	0.65 (0.49–0.82)	6.5 × 10 ⁻²
PROOF						
PRS	0.54 (0.45–0.64)	3.7 × 10 ⁻¹	0.51 (0.42–0.61)	8.4 × 10 ⁻¹	–	–
Age and BMI	0.52 (0.44–0.61)	6.0 × 10 ⁻¹	0.52 (0.41–0.64)	6.7 × 10 ⁻¹	–	–
Age, BMI, and PRS	0.53 (0.44–0.63)	4.9 × 10 ⁻¹	0.52 (0.41–0.63)	7.4 × 10 ⁻¹	–	–

* Model performance was classified according to area under the receiver operating characteristic curve (AUC) scores (very poor [scores 0.50–0.60], poor [scores 0.60–0.70], fair [scores 0.70–0.80], good [scores 0.80–0.90], and excellent [scores 0.90–1.0]). 95% CI = 95% confidence interval (see Table 1 for other definitions).

† All analyses in the 3 Rotterdam Study subcohorts were followed by a fixed-effect meta-analysis of effects in the Rotterdam Study as a whole.

model. However, in the CHECK and PROOF studies, the AUCs were slightly increased in the combined model compared to the AUC of clinical risk factors.

Analyses of PRS cutoffs. Since results were very similar for prevalent and incident (hip or knee) OA patients, we combined them for reasons of power and examined various upper and lower

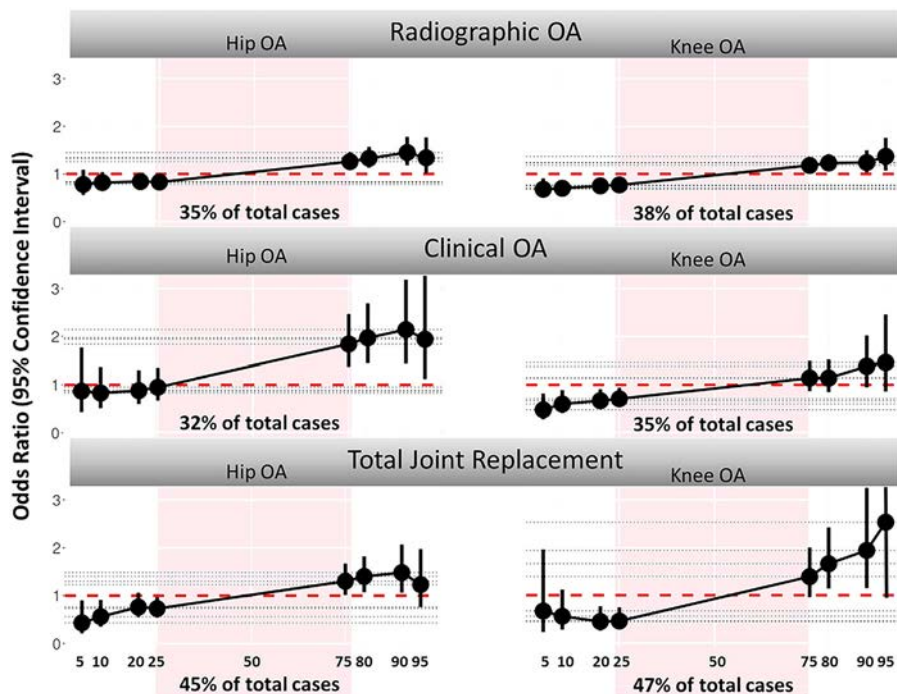


Figure 4. Association between the hip/knee osteoarthritis (OA) polygenic risk score and lifetime presence, prevalence, and incidence of hip/knee OA according to radiographic, clinical, or total joint replacement definitions, as observed in a meta-analysis of the 3 Rotterdam Study cohorts. Color figure can be viewed in the online issue, which is available at <http://onlinelibrary.wiley.com/doi/10.1002/art.42246/abstract>.

PRS cutoffs versus the middle 50% of the PRS distribution. We observed increasing OA risks in the upper tails of the PRS distribution (outermost 25%, 10%, and 5%), as shown in Figure 4. This is most clearly observed at the highest 10% of the PRS distribution in relation to all hip OA definitions used in the Rotterdam Study: OR 1.45 (95% CI 1.18–1.78) for radiographic OA, OR 2.14 (95% CI 1.43–3.19) for clinical OA, and OR 1.48 (1.06–2.07) for THR in the Rotterdam Study. In the Rotterdam Study, these ORs translate to a 10-year absolute risk of 12% for radiographic hip OA, 10% for clinical hip OA, and 4% for THR. This was 2–4 times higher compared to the risk observed for the individuals in the lowest 10% (Supplementary Table 6, <https://onlinelibrary.wiley.com/doi/10.1002/art.42246>). Likewise, the top 10% percentile of patients showed the highest OR (1.39 [95% CI 0.84–2.32]) in the CHECK study, although no significant results were observed across the cutoffs (Supplementary Table 6).

Similar results were observed for the top 10% of the knee PRS distribution in the Rotterdam Study: OR 1.24 (95% CI 1.03–1.50) for radiographic knee OA, OR 1.38 (95% CI 0.95–2.02) for clinical knee OA, and OR 1.94 (95% CI 1.15–3.25) for TKR. The 10-year absolute risks were 15% for both radiographic knee OA and clinical knee OA and 4% for TKR (Figure 4 and Supplementary Table 6). In the Rotterdam Study the risk increased further in higher PRS cutoffs, such as the top 5% of the knee PRS, with OR 2.53 (95% CI 0.88–7.32) for TKR, corresponding with a 10-year absolute risk of 6%. However, no significant results were observed in the CHECK and PROOF studies (Supplementary Table 6).

DISCUSSION

The findings of the present study confirmed the association of PRS with radiographic OA, clinical OA, THR/TKR, and radiographic OA progression across different populations. Also, we observed a modest but significant discriminatory ability of hip PRS and knee PRS across all OA definitions. Overall, prevalent OA, incident OA, and any OA progression of hip OA were associated with a similar OR of 1.2–1.3 per SD in PRS and varied slightly more for knee OA with an OR of 1.1–1.6 per SD in PRS in the population-based setting studies. Our results showed a possible clinically relevant increased risk (1.5–2.2 fold) of OA in the upper 5–25% tails of the PRS distribution compared to the average population in the population-based studies. We also observed a robust association of PRS with progressive severe OA. In the CHECK and PROOF cohorts, results were more scattered, most likely due to power and study setting.

Our results showed a stronger association of clinical OA and TJR compared to radiographic OA. This could be caused by the case definitions used in the discovery of GWAS, in which ~80% of cases were defined by TJR (44% of total) and clinical codes from the International Statistical Classification of Diseases and Related Health Problems, Tenth Revision (unilateral/bilateral primary hip OA or knee OA and primary arthrosis of pelvic region or

thigh or lower leg), which may have yielded higher power for clinical OA and TJR, as observed in our study (18). Similarly, the association with incident severe cases was stronger than early incident OA in our study population, which may be caused by the same case definition bias in the discovery GWAS and was most likely driven by TJR cases. The PRS is therefore valuable in identifying future TJR cases. To identify variants for early detection as one of the main aims of early OA prediction in the clinic (12), we suggest stratifying the discovery GWAS and providing weights or variants per subphenotypes (e.g., for early versus severe OA). This approach is not only relevant for the different OA sites and OA severity, but also for different aspects of OA, such as osteophytosis versus cartilage degradation.

The (large) population-based Rotterdam Study showed stronger PRS associations than the (smaller) CHECK and PROOF clinical cohorts. Although we used the corrected effect sizes for constructing PRS in this study (excluding the Rotterdam Study from the GO consortium meta-analysis), the results based on the original effect size overall showed highly similar performance of PRS across the OA definitions and cohorts (Supplementary Figure 3, <https://onlinelibrary.wiley.com/doi/10.1002/art.42246>). This can be explained by the small contribution of Rotterdam Study sample sizes in the GO consortium, which was only 1.3% of the total study sample.

Aside from power differences, the difference in association results between cohorts might be due to the inclusion criteria for clinical cohorts, which included either participants with early-stage OA-like symptoms (CHECK) or those with high BMI (≥ 27 kg/m²; PROOF). Therefore, the individuals that do not show OA progression in these studies are not like population-based controls, which may diminish the association of the OA PRS within the clinical cohorts. One solution would be to use the controls from the Rotterdam Study for all comparisons, but due to the differences in genotyping platform and processing, this is not straightforward. Methodology for such comparisons or reference population values would aid in comparing PRS directly across studies.

Another concern that could possibly influence the association of the PRS is the underlying biology of the particular variants contained within the genetic score. The most recent GWAS of the GO consortium showed a large genetic correlation between knee OA and BMI (~45%), which could diminish the effect of the OA PRS in high-BMI individuals (18). This explains the poor PRS performance in the PROOF study (all obese women) and the lack of predictive value above clinical risk factors such as BMI.

PRS performance could be improved by looking at a selection of included variants in that PRS based on statistical robustness and/or underlying biology. For example, the GO consortium has demonstrated new associations for 16 of 44 variants in hip PRS and 11 of 24 variants in knee PRS. This increment of associated variants suggests that we may still find more variants

by increasing the sample size. Also, bigger sample size can help for effect sizes accuracy for the variants. Regarding underlying biology, variants for an OA PRS could be evaluated on the particular biologic mechanisms involved (e.g., transforming growth factor β pathway) (18). However, we need to consider that identifying pathways for variants does not have a standard practice (28), and a lack of standardized methodology is observed in this area.

Current clinical applications of genetic information focus on finding (very) rare Mendelian variants in a few families with a segregating OA disease (29–31), causing early-onset familial forms of the disease (31), yet PRS-based risk assessment can identify another and much larger fraction of the population at clinically relevant increased risk (32). However, the added value of using such PRS depends on the setting. In a clinical setting, especially in secondary care, OA disease has progressed too far for efficient intervention (33). It might be more effective to explore genetic OA risk assessment in a prevention setting, such as a GP clinic, such as the risk assessment in PROOF based on the Rotterdam Study results.

Currently, patients that report to the GP with joint complaints, such as pain or stiffness, receive pain relief medication in addition to advice on lifestyle changes, including weight loss and increased physical activity (1). The challenge of these interventions is their long duration, which may increase complaints when they are not successful. Calculating OA PRS in this population could identify the 5% or 10% of individuals whose disease is most likely to progress into OA, who could then be monitored more intensively to identify early OA symptoms and/or receive earlier and/or more severe interventions. In this case, with adequate and timely preventive measures, a patient's referral to secondary care is reduced. However, clinical trials will be needed to evaluate the additive value of the PRS to current procedures.

Similarly, in secondary care, TJR as end-stage OA treatment is examined in the event of a significant reduction in quality of life, such as marked restriction of daily activities during treatment or failure of appropriate conservative options after 6 months (34). Here, if supportive treatments are unsuccessful, the referral time to an orthopedic surgeon could be reduced if the physician is aware of the patient's risk for progression. Combining the OA PRS with clinical risk factors can provide a clearer picture of the need for surgery, e.g., through prediction of disease progression or by including PRS that assess adverse treatment outcomes such as chronic pain. Including more risk-based information such as PRS at this time might distribute the available surgeries to patients most likely to benefit from them and provide care in the most cost-effective manner (35–37).

Our study had several major strengths. The PRS were examined for prevalence, incidence, and any progression of 3 common definitions of OA and provided a great opportunity to compare PRS performance between and within phenotypes. Also, to understand the nature of PRS behavior in different settings, we used 3 different study settings to survey the PRS, the population-based setting, the clinical setting, and the clinical high-risk population. Nevertheless, our study also has some limitations. First, the variants identified by the GO consortium do not explain all of the genetic risks

for OA (i.e., 11% of 44% heritability for knee OA and 21% of 58% heritability for hip OA). Thus, the performance of the PRS will increase when additional variants are uncovered. Also, our current PRS are not powered based on certain subphenotypes or clinical definitions related to OA (e.g., osteophytes versus joint space narrowing or joint pain). We also did not use PRS for particular OA clinical risk factors, such as BMI or pain. Adding such PRS to the genetic profiling for OA could improve high-risk case finding efforts in early preventive settings. Second, the sample size for certain analyses was modest, both in the clinical cohorts and at the tail of the PRS distribution in the population cohort.

More extensive studies are needed to clinically identify the exact cutoffs of PRS risk distributions. In addition, the PRS produced in this study were constructed and validated in European populations. To have an applicable PRS in clinical practice, we need to add validated variants from other ethnicities or adjust the weights of the PRS based on the effect size of the other ethnic groups. Finally, due to the nature of the population study, people with more symptoms are less likely to participate in the studies. In this regard, participants in population studies can be healthier than the general population. This suggests that risk assessment can be underestimated, which may apply to our PRS.

In conclusion, the PRS we analyzed for knee OA and hip OA seem to be robust risk estimators since they were associated with the risk of developing OA across several diverse definitions that we evaluated in this study: incident radiographic OA, incident clinical OA, any OA progression, and TJR. Since OA is becoming increasingly frequent in the general population and primary prevention is not commonly applicable, PRS-based risk assessment could constitute a valuable addition to OA prevention and management in health care systems. Further studies will be required to test the practical applications of polygenic risk information in modifying and updating screening guidelines or guiding lifestyle and medical interventions in the clinical setting.

ACKNOWLEDGMENTS

The Rotterdam Study is funded by Erasmus Medical Center and Erasmus University, Rotterdam, The Netherlands Organization for the Health Research and Development (ZonMw), the Research Institute for Diseases in the Elderly (RIDE), the Ministry of Education, Culture and Science, the Ministry for Health, Welfare and Sports, the European Commission (DG XII), and the Municipality of Rotterdam. The authors are grateful to the study participants, the staff from the Rotterdam Study, and the participating GPs and pharmacists. The authors are thankful to the Human Genotyping Facility of the Genetic Laboratory of the Department of Internal Medicine, Erasmus MC, Rotterdam, The Netherlands for the generation and management of genotype data for the Rotterdam Study (RS-I, RS-II, RS-III), CHECK, and PROOF cohorts.

AUTHOR CONTRIBUTIONS

All authors were involved in drafting the article or revising it critically for important intellectual content, and all authors approved the final version to be published. Ms. Sedaghati-Khayat had full access to all of the data in the study and takes responsibility for the integrity of the data and the accuracy of the data analysis.

Study conception and design. Van Rooij, van Meurs.



Acquisition of data. Sedaghati-Khayat, Boer, Runhaar, Bierma-Zeinstra, Broer, Ikram, Zeggini, van Meurs.

Analysis and interpretation of data. Sedaghati-Khayat, Uitterlinden, van Rooij, van Meurs.

REFERENCES

- Hunter DJ, Bierma-Zeinstra S. Osteoarthritis. *Lancet* 2019;393:1745–59.
- GBD 2017 Disease and Injury Incidence and Prevalence Collaborators. Global, regional, and national incidence, prevalence, and years lived with disability for 354 diseases and injuries for 195 countries and territories, 1990–2017: a systematic analysis for the Global Burden of Disease Study 2017. *Lancet* 2018;392:1789–858.
- Hunter DJ, Schofield D, Callander E. The individual and socioeconomic impact of osteoarthritis [review]. *Nat Rev Rheumatol* 2014;10:437–41.
- Woolf AD, Pfleger B. Burden of major musculoskeletal conditions. *Bull World Health Organ* 2003;81:646–56.
- GBD 2015 Disease and Injury Incidence and Prevalence Collaborators. Global, regional, and national incidence, prevalence, and years lived with disability for 310 diseases and injuries, 1990–2015: a systematic analysis for the Global Burden of Disease Study 2015. *Lancet* 2016;388:1545–602.
- Saberi Hosnijeh F, Kavousi M, Boer CG, Uitterlinden AG, Hofman A, Reijman M, et al. Development of a prediction model for future risk of radiographic hip osteoarthritis. *Osteoarthritis Cartilage* 2018;26:540–6.
- Silverwood V, Blagojevic-Bucknall M, Jinks C, Jordan JL, Protheroe J, Jordan KP. Current evidence on risk factors for knee osteoarthritis in older adults: a systematic review and meta-analysis. *Osteoarthritis Cartilage* 2015;23:507–15.
- Deveza LA, Nelson AE, Loeser RF. Phenotypes of osteoarthritis: current state and future implications. *Clin Exp Rheumatol* 2019;37:64–72.
- Zhang Y, Jordan JM. Epidemiology of osteoarthritis. *Clin Geriatr Med* 2010;26:355–69.
- Runhaar J, van Middelkoop M, Reijman M, Willemsen S, Oei EH, Vroegindewij D, et al. Prevention of knee osteoarthritis in overweight females: the first preventive randomized controlled trial in osteoarthritis. *Am J Med* 2015;128:888–95.
- Hunter DJ, Bowden JL. Therapy: are you managing osteoarthritis appropriately? [review]. *Nat Rev Rheumatol* 2017;13:703–4.
- Runhaar J, Zhang Y. Can we prevent OA? Epidemiology and public health insights and implications. *Rheumatology (Oxford)* 2018;57:iv3–9.
- Previtali D, Andriolo L, Di Laura Frattura G, Boffa A, Candrian C, Zaffagnini S, et al. Pain trajectories in knee osteoarthritis—a systematic review and best evidence synthesis on pain predictors. *J Clin Med* 2020;9:2828.
- Emery CA, Roy TO, Whittaker JL, Nettel-Aguirre A, van Mechelen W. Neuromuscular training injury prevention strategies in youth sport: a systematic review and meta-analysis. *Br J Sports Med* 2015;49:865–70.
- Spector TD, MacGregor AJ. Risk factors for osteoarthritis: genetics. *Osteoarthritis Cartilage* 2004;12:S39–44.
- Styrkarsdottir U, Stefansson OA, Gunnarsdottir K, Thorleifsson G, Lund SH, Stefansson L, et al. GWAS of bone size yields twelve loci that also affect height, BMD, osteoarthritis or fractures. *Nat Commun* 2019;10:2054.
- Boer CG. Osteoarthritis: genetics and phenotypes in all their complexity. Erasmus University Rotterdam 2020;323.
- Boer CG, Hatzikotoulas K, Southam L, Stefánssdóttir L, Zhang Y, de Almeida RC, et al. Deciphering osteoarthritis genetics across 826,690 individuals from 9 populations. *Cell* 2021;184:4784–818.
- Torkamani A, Wineinger NE, Topol EJ. The personal and clinical utility of polygenic risk scores. *Nat Rev Genet* 2018;19:581–90.
- Visscher PM, Wray NR, Zhang Q, Sklar P, McCarthy MI, Brown MA, et al. 10 years of GWAS discovery: biology, function, and translation. *Am J Hum Genet* 2017;101:5–22.
- Hofman A, Brusselle GG, Darwish Murad S, van Duijn CM, Franco OH, Goedegebure A, et al. The Rotterdam Study: 2016 objectives and design update. *Eur J Epidemiol* 2015;30:661–708.
- Wesseling J, Boers M, Viergever MA, Hilberdink WK, Lafeber FP, Dekker J, et al. Cohort profile: Cohort Hip and Cohort Knee (CHECK) study. *Int J Epidemiol* 2016;45:36–44.
- Runhaar J, Kloppenburg M, Boers M, Bijlsma JW, Bierma-Zeinstra SM. Towards developing diagnostic criteria for early knee osteoarthritis: data from the CHECK study. *Rheumatology (Oxford)* 2020;60:2448–55.
- De Vos BC, Landsmeer ML, van Middelkoop M, Oei EH, Krul M, Bierma-Zeinstra SM, et al. Long-term effects of a lifestyle intervention and oral glucosamine sulphate in primary care on incident knee OA in overweight women. *Rheumatology (Oxford)* 2017;56:1326–34.
- Kellgren JH, Lawrence JS. Radiological assessment of osteoarthrosis. *Ann Rheum Dis* 1957;16:494–502.
- Altman R, Asch E, Bloch D, Bole G, Borenstein D, Brandt K, et al. Development of criteria for the classification and reporting of osteoarthritis: Classification of Osteoarthritis of the Knee. *Arthritis Rheum* 1986;29:1039–49.
- Ikram MA, Brusselle G, Ghanbari M, Goedegebure A, Ikram MK, Kavousi M, et al. Objectives, design and main findings until 2020 from the Rotterdam Study. *Eur J Epidemiol* 2020;35:483–517.
- Udler MS, Kim J, von Grotthuss M, Bonàs-Guarch S, Cole JB, Chiou J, et al. Type 2 diabetes genetic loci informed by multi-trait associations point to disease mechanisms and subtypes: a soft clustering analysis. *PLoS Med* 2018;15:e1002654.
- Golan D, Lander ES, Rosset S. Measuring missing heritability: inferring the contribution of common variants. *Proc Natl Acad Sci U S A* 2014;111:E5272–81.
- Fuchsberger C, Flannick J, Teslovich TM, Mahajan A, Agarwala V, Gaulton KJ, et al. The genetic architecture of type 2 diabetes. *Nature* 2016;536:41–7.
- Van Meurs JB. Osteoarthritis year in review 2016: genetics, genomics and epigenetics. *Osteoarthritis Cartilage* 2017;25:181–9.
- Khera AV, Chaffin M, Aragam KG, Haas ME, Roselli C, Choi SH, et al. Genome-wide polygenic scores for common diseases identify individuals with risk equivalent to monogenic mutations. *Nat Genet* 2018;50:1219–24.
- Whittaker JL, Runhaar J, Bierma-Zeinstra S, Roos EM. A lifespan approach to osteoarthritis prevention: narrative review, part of the series "Foundations of OA" for OAC. *Osteoarthritis Cartilage* 2021;29:1638–53.
- Culliford DJ, Maskell J, Kiran A, Judge A, Javaid MK, Cooper C, et al. The lifetime risk of total hip and knee arthroplasty: results from the UK general practice research database. *Osteoarthritis Cartilage* 2012;20:519–24.
- Callender T, Emberton M, Morris S, Eeles R, Kote-Jarai Z, Pharoah PD, et al. Polygenic risk-tailored screening for prostate cancer: a benefit-harm and cost-effectiveness modelling study. *PLoS Med* 2019;16:e1002998.
- Naber SK, Kundu S, Kuntz KM, Dotson WD, Williams MS, Zauber AG, et al. Cost-effectiveness of risk-stratified colorectal cancer screening based on polygenic risk: current status and future potential. *JNCI Cancer Spectr* 2020;4:pkz086.
- Ferket BS, Feldman Z, Zhou J, Oei EH, Bierma-Zeinstra SM, Mazumdar M. Impact of total knee replacement practice: cost effectiveness analysis of data from the Osteoarthritis Initiative. *BMJ* 2017;356:j1131.

Effects of Anti-Tumor Necrosis Factor Therapy on Osteoblastic Activity at Sites of Inflammatory and Structural Lesions in Radiographic Axial Spondyloarthritis: A Prospective Proof-of-Concept Study Using Positron Emission Tomography/Magnetic Resonance Imaging of the Sacroiliac Joints and Spine

Nils Martin Bruckmann,¹  Christoph Rischpler,² Styliani Tsiami,³ Julian Kirchner,¹ Daniel B. Abrar,¹ Timo Bartel,² Jens Theysohn,¹ Lale Umutlu,¹ Ken Herrmann,² Wolfgang P. Fendler,² Christian Buchbender,¹ Gerald Antoch,¹ Lino M. Sawicki,¹ Athanasios Tsobanelis,³ Juergen Braun,³ and Xenofon Baraliakos³ 

Objective. Proof-of-concept trial to determine the effects of tumor necrosis factor inhibitor (TNFi) therapy on osteoblastic activity at sites of inflammatory and structural lesions in patients with radiographic axial spondyloarthritis (SpA), using fluorine 18-labeled NaF (¹⁸F-NaF) positron emission tomography/magnetic resonance imaging (PET/MRI).

Methods. Sixteen patients with clinically active radiographic axial SpA were prospectively enrolled to receive TNFi treatment and undergo ¹⁸F-NaF PET/MRI of the sacroiliac (SI) joints and spine at baseline and at a follow-up visit 3–6 months after treatment initiation. Three readers (1 for PET/MRI and 2 for conventional MRI) evaluated all images, blinded to time point. Bone marrow edema, structural lesions (i.e., fat lesions, sclerosis, erosions, and ankylosis), and ¹⁸F-NaF uptake at SI joint quadrants and vertebral corners (VCs) were recorded.

Results. Overall, 11 male and 5 female patients (mean age ± SD 38.6 ± 12.0 years) were followed up for a mean duration of 4.6 months (range 3–6). ¹⁸F-NaF PET/MRI was conducted on SI joints for 16 patients and the spine for 10; 128 SI joint quadrants and 920 VCs were analyzed at each time point. At baseline, ¹⁸F-NaF uptake was demonstrated in 96.0% of SI joint quadrants with bone marrow edema, 94.2% with sclerosis, and 88.3% with fat lesions. At follow-up, 65.3% of SI joint quadrants with bone marrow edema ($P < 0.001$), 33.8% with sclerosis ($P = 0.23$), and 24.5% with fat lesions ($P = 0.01$) had less ¹⁸F-NaF uptake, compared with baseline. For VCs, ¹⁸F-NaF uptake at baseline was found in 81.5% of edges with sclerosis, 41.9% with fat lesions, and 33.7% with bone marrow edema. At follow-up, 73.5% of VCs with bone marrow edema ($P = 0.01$), 53.3% with fat lesions ($P = 0.03$), and 55.6% with sclerosis ($P = 0.16$) showed less ¹⁸F-NaF uptake, compared with baseline.

Conclusion. Anti-TNF antibody treatment led to a significant decrease in osteoblastic activity within 3–6 months, especially, but not solely, at sites of inflammation. Larger data sets are needed for confirmation of the antiosteoblastic effects of TNFi for the prevention of radiographic progression in axial SpA.

INTRODUCTION

Radiographic axial spondyloarthritis (SpA), also known as ankylosing spondylitis (AS) (1), is a chronic inflammatory rheumatic disease, representing the most advanced form of axial

SpA (2). In its early phase, the disease is characterized by chronic inflammation in the lower back and inflammation in the sacroiliac (SI) joints (3). As the disease progresses, inflammation may extend to the spine, potentially resulting in complete stiffness of the axial skeleton and postural deformation, which are associated

Drs. Bruckmann and Rischpler contributed equally to this study.

Supported by an unrestricted research grant from MSD Germany.

¹Nils Martin Bruckmann, MD, Julian Kirchner, MD, Daniel B. Abrar, MD, Jens Theysohn, MD, Lale Umutlu, MD, Christian Buchbender, MD, Gerald Antoch, MD, Lino M. Sawicki, MD: University Dusseldorf, Dusseldorf, Germany; ²Christoph Rischpler, MD, Timo Bartel, Ken Herrmann, MD, Wolfgang P. Fendler, MD: University of Duisburg-Essen, Essen, Germany; ³Styliani Tsiami, Athanasios Tsobanelis, Juergen Braun, MD, Xenofon Baraliakos, MD: Rheumazentrum Ruhrgebiet, Herne, and Ruhr-University Bochum, Bochum, Germany.

Author disclosures are available at <https://onlinelibrary.wiley.com/action/downloadSupplement?doi=10.1002%2Fart.42149&file=art42149-sup-0001-Disclosureform.pdf>.

Address correspondence to Xenofon Baraliakos, MD, Rheumazentrum Ruhrgebiet, Ruhr-University Bochum, Claudiusstrasse 45, 44649 Herne, Germany. Email: xenofon.baraliakos@elisabethgruppe.de.

Submitted for publication December 5, 2021; accepted in revised form April 19, 2022.

with severe physical disability and reduced quality of life (4,5). Treatment comprises nonpharmacologic and pharmacologic interventions, with the latter involving nonsteroidal antiinflammatory drugs (NSAIDs) as a first step. Among patients who do not respond to NSAID treatment, biologic disease-modifying antirheumatic drugs (bDMARDs), such as antibodies inhibiting tumour necrosis factor (TNFi) or interleukin-17, are efficacious (6).

Imaging plays an essential role in the diagnosis and management of axial SpA and may also be used for assessment of treatment responses, especially in clinical trials (7,8). The current gold standard imaging technique in axial SpA is magnetic resonance imaging (MRI), since it can assess changes in inflammation, such as bone marrow edema, as well as structural damage, such as fat lesions, erosion, sclerosis, and ankylosis (7,9,10). The introduction of hybrid imaging techniques such as positron emission tomography/computed tomography (PET/CT) and PET/MRI has provided additional insights into the pathogenesis and metabolic activity of radiographic axial SpA (11). Therefore, use of the osteoblast-specific radiotracer fluorine 18-labeled NaF (^{18}F -NaF) to visualize local osteoblastic activity in inflammatory and structural lesions due to radiographic axial SpA has recently increased (11–13). These studies confirmed that the level of osteoblastic activity was especially high at sites where bone marrow edema and fat lesions had been detected by MRI and that bone marrow edema and fat lesions are associated with the development of syndesmophytes and new bone formation (14). This is consistent with findings of recent biopsy studies involving patients with radiographic axial SpA (15).

Treatment with TNFi continuously for ≥ 4 years has been shown to result in lower rates of radiographic progression than treatment with non-bDMARDs (7,16–18). This is very likely due to the beneficial effect of bDMARDs on early spinal inflammation as compared to their minimal impact on more advanced disease. However, a direct effect of bDMARDs on osteoblastic activity has not been proven to date. In this prospective, observational, proof-of-concept study, we used ^{18}F -NaF PET/MRI to analyze the effect of TNFi on osteoblastic activity in disease-specific lesions detected by MRI in the SI joints and the spine of patients with active radiographic axial SpA.

PATIENTS AND METHODS

Patients and treatment. This observational proof-of-concept study was approved by the institutional research committee of the University Duisburg-Essen (protocol 17-7709-BO) and accorded with the principles of the 1964 Declaration of Helsinki and its later amendments. Written informed consent was obtained from all individual participants prior to their enrollment in the study.

The main inclusion criteria were 1) diagnosis of radiographic axial SpA by the treating rheumatologist, based on the presence of advanced radiographic changes in the SI joints according to

the modified New York criteria for AS (19), 2) evidence of active disease, based on a Bath AS Disease Activity Index (BASDAI) score of ≥ 4 despite treatment with a full dose of at least 2 NSAIDs for ≥ 4 weeks prior to imaging (20), and 3) presence of at least 1 inflammatory lesion on MRI of the SI joints or spine. Pretreatment with bDMARDs was not allowed. If a decision was made to treat a patient with a compound other than TNFi, the patient was not eligible for study participation. According to the study protocol, treatment had to be initiated within 1 week after the baseline (i.e., initial) MRI. Follow-up imaging was performed at least 3–6 months after treatment initiation, based on the availability of the patient.

Specifications of conventional MRI and PET/MRI. All ^{18}F -NaF PET/MRI examinations were performed on an integrated 3.0T PET/MRI system (Biograph mMR, Siemens Healthineers) in a caudocranial direction. Scanning was performed during the mineralization phase, 40 minutes after intravenous injection of a mean \pm SD ^{18}F -NaF dose of 161 ± 8 MBq. Images were prepared as described by Buchbender et al (11). An attenuation-correction map (μmap) in coronal orientation was generated using a transaxial acquired high-resolution CAIPIRINHA (controlled aliasing in parallel imaging results in higher spatial acceleration), T1-weighted, 3-dimensional Dixon-VIBE (volumetric interpolated breath-hold examination) sequence. In addition, a bone atlas and a truncation correction proposed by Blumhagen et al (21) were used (22–24). The scanning parameters for the sequences used in this study are shown in Table 1.

Analysis of MRI and PET scans. Three experienced readers (1 nuclear medicine specialist [for PET data] and 2 radiologists [for conventional MRI data]) blinded to time point (i.e., baseline versus follow-up) and patient demographic characteristics independently evaluated all MRI and PET scans in paired order.

SI joints. The iliac and sacral parts of each SI joint were subdivided into an upper part (including the first sacral foramen) and a lower part (including the second and third foramen), resulting in 4 SI joint quadrants per side. All SI joint quadrants were evaluated in a binary way for the presence or absence of inflammatory activity (i.e., bone marrow edema, based on the STIR sequence, and chronic structural changes to bone, such as fat lesions, erosion, sclerosis, and ankylosis, based on the T1-weighted turbo spin-echo sequence). Each SI joint quadrant was also assessed for the presence or absence of ^{18}F -NaF uptake.

Spine. All vertebral bodies were divided into 4 vertebral corners (VCs; superior anterior, superior posterior, inferior posterior, and inferior anterior). Similar to the evaluation of SI joints, the presence or absence of bone marrow edema was assessed on the basis of the STIR sequence, and the presence or absence of

Table 1. Scanning parameters of the fluorine 18–labeled NaF positron emission tomography/magnetic resonance imaging sequences used to determine the effect of tumor necrosis factor inhibitor therapy on osteoblastic activity in patients with radiographic axial spondyloarthritis*

Sequence	Orientation(s)	TE/TR, msec	Slice thickness, mm	Matrix size, pixels	Field of view, mm ²
T1-weighted 3D Dixon-VIBE with fat suppression	Semicoronal	2.46/3.97	3.12	192 × 158	492 × 450
T1-weighted TSE	Sagittal for VCs, semicoronal for SI joints	12/650	3.6	448 × 224	715 × 322
T2-weighted STIR with fat suppression	Sagittal for VCs, semicoronal for SI joints	57/6,180	3.0	384 × 230	250 × 250
T1-weighted STIR with fluid suppression	Semicoronal for SI joints	11/2,840	3.0	448 × 314	250 × 250

* TE = echo time; TR = repetition time; 3D = 3-dimensional; VIBE = volumetric interpolated breath-hold examination; TSE = turbo spin-echo; VCs = vertebral corners; SI = sacroiliac.

structural lesions such as fat lesions and sclerosis was assessed using the T1-weighted turbo spin-echo sequence. Each VC was also assessed for the presence or absence of ¹⁸F-NaF uptake on mineralization phase PET (11,14).

Osteoblastic activity. For semiquantitative analysis of osteoblastic activity, maximum standardized uptake values (SUV_{max}) were measured using a volume of interest covering the entire individual lesion at each SI joint quadrant or VC. Focal ¹⁸F-NaF uptake was defined as a visually detectable uptake of ¹⁸F-NaF that was greater than the level in adjacent bone marrow.

Statistical analysis. Only lesions that were identified by the 2 readers of MRIs at each imaging time point were used for analyses. Data are presented as the mean ± SD, the mean (range), or percentage (95% confidence interval [95% CI]). Proportions of SI joint quadrants showing bone marrow edema, fat lesions, erosions, sclerosis, or ankylosis, or any combination of these findings and focal ¹⁸F-NaF uptake were calculated to investigate the relation between MRI-based changes in inflammation before and after initiation of TNFi therapy and local osteoblastic activity visualized by PET/MRI. McNemar's test was performed to compare results between baseline and follow-up examinations. A *P* value of less than 0.05 was considered to indicate statistical significance. Wilcoxon's signed rank test was used to assess differences between SUV_{max} before and SUV_{max} after treatment initiation. Statistical analysis was performed using SPSS, version 24 (IBM).

Data availability. The data sets used and/or analyzed during the current study are available from the corresponding author on reasonable request.

RESULTS

Demographic characteristics and image availability.

Sixteen patients were included. All patients had complete data sets of SI joint images, and 10 had complete data sets of spinal images,

permitting analysis of 128 SI joint quadrants and 920 VCs. The mean ± SD age at baseline was 38.3 ± 12.0 years, 11 patients (68.8%) were male (including 7 of 10 [70%] with spinal images), and 13 patients (81.3%) were HLA-B27 positive. Mean ± SD clinical values at baseline were 6.1 ± 1.6 (range 4.1–7.9) for the BASDAI, 3.4 ± 0.7 (range 2.1–4.9) for the Ankylosing Spondylitis Disease Activity Score (ASDAS) (25), and 1.0 ± 1.3 mg/dl (range 0.0–4.4) for the C-reactive protein level (Table 2). The mean follow-up period was 4.6 months (range 3–6 months).

Analysis of follow-up data showed that all patients improved during treatment. The mean ± SD BASDAI score decreased to 4.1 ± 1.5 (range 2.1–7.4), although 5 patients (31.3%) still reported a BASDAI score of >4, which is indicative of advanced disease on the 10-point index. The mean ± SD ASDAS decreased to 2.1 ± 0.5 (range 1.6–3.2) during treatment, with all 5 patients exhibiting a BASDAI score of >4 also having an ASDAS of >2.1. Finally, the mean ± SD C-reactive protein level decreased to 0.1 ± 0.2 mg/dl (range 0.0–0.5) (Table 2).

Evaluation and quantification of pathologic lesions in SI joints.

Of the 128 SI joint quadrants, 75 (58.6%) showed bone marrow edema, 120 (93.8%) showed fat lesions, 69 (53.9%) showed sclerosis, 99 (77.3%) showed erosions, and 16 (12.5%) showed ankylosis at baseline; focal ¹⁸F-NaF uptake was visible in 111 (86.7%), with a mean ± SD SUV_{max} of 14.637 ± 4.687. Increased ¹⁸F-NaF uptake in SI joint quadrants was most frequently associated with bone marrow edema (72 [96%] of 75 quadrants), but uptake was also in a high percentage of quadrants showing sclerosis (65 [94.2%] of 69), fat lesions (106 [88.3%] of 120), erosions (86 [86.9%] of 99), and ankylosis (14 [87.5%] of 16; all 14 were associated with 5 patients). All SI joint quadrants showing ¹⁸F-NaF uptake also had at least 1 type of lesion detected on conventional MRI at baseline.

At follow-up, 37 SI joint quadrants showed bone marrow edema (including 3 that did not show bone marrow edema at baseline), for a net reduction of 50.7% (95% CI 38.9–62.4;

Table 2. Demographic characteristics, clinical characteristics at baseline and follow-up, and changes between the 2 time points among patients with radiographic axial spondyloarthritis who underwent fluorine 18–labeled NaF (^{18}F -NaF) positron emission tomography/magnetic resonance imaging to determine the effect of tumor necrosis factor inhibitor (TNFi) therapy on osteoblastic activity*

Patient, sex, age, imaging time point†	TNFi duration, week	BASDAI	ASDAS	CRP level, mg/dl	SUV _{max} ‡	
					SI joints	Spine
1, M, 26 years						
Baseline	0	6.4	3.5	0.1	16.254	–
Follow-up	16	5.0	3.0	0.0	11.203	–
Change	–	–1.4	–0.5	–0.1	–5.051	–
2, M, 52 years						
Baseline	0	5.6	3.2	0.5	15.979	–
Follow-up	24	3.6	1.7	0.2	11.696	–
Change	–	–2.0	–1.5	–0.3	–4.283	–
3						
Baseline	0	5.2	3.8	1.5	20.464	–
Follow-up	24	2.4	1.6	0.0	10.000	–
Change	–	–2.8	–2.2	–1.5	–10.464	–
4						
Baseline	0	6.0	3.0	0.3	7.534	–
Follow-up	24	3.8	1.9	0.0	5.354	–
Change	–	–2.2	–1.1	–0.3	–2.180	–
5						
Baseline	0	5.6	3.7	1.6	7.505	–
Follow-up	12	4.0	2.2	0.2	10.102	–
Change	–	–1.6	–1.5	–1.4	2.597	–
6						
Baseline	0	6.5	3.1	0.0	24.154	–
Follow-up	16	5.9	2.6	0.1	11.106	–
Change	–	–0.6	–0.5	0.1	–13.048	–
7						
Baseline	0	6.0	3.2	1.1	14.620	15.695
Follow-up	16	2.2	1.6	0.4	11.225	7.290
Change	–	–3.8	–1.6	–0.7	–3.395	–8.405
8						
Baseline	0	7.9	4.4	1.2	15.332	19.455
Follow-up	12	3.8	1.9	0.0	9.550	13.763
Change	–	–4.1	–2.5	–1.2	–5.782	–5.692
9						
Baseline	0	4.1	2.5	1.2	9.291	5.314
Follow-up	16	2.1	1.7	0.0	11.323	9.797
Change	–	–2.0	–0.8	–1.2	2.032	4.483
10						
Baseline	0	7.5	3.2	0.1	16.534	17.200
Follow-up	20	6.2	2.2	0.1	14.535	13.708
Change	–	–1.3	–1.0	0.0	–1.999	–3.492
11						
Baseline	0	6.9	4.9	4.4	8.312	19.965
Follow-up	20	2.3	2.0	0.2	10.426	10.256
Change	–	–4.6	–2.9	–4.2	2.114	–9.709
12						
Baseline	0	6.4	3.2	0.1	15.662	0.000
Follow-up	16	5.1	2.7	0.3	11.950	0.000
Change	–	–1.3	–0.5	0.2	–3.712	0.000
13						
Baseline	0	4.9	3.8	3.6	16.453	25.159
Follow-up	24	3.6	1.8	0.2	13.375	17.343
Change	–	–1.3	–2.0	–3.4	–3.078	–7.816
14						
Baseline	0	7.5	3.6	0.3	11.930	0.000
Follow-up	20	7.4	3.2	0.5	14.805	0.000
Change	–	–0.1	–0.4	0.2	2.875	0.000

(Continued)

Table 2. (Cont'd)

Patient, sex, age, imaging time point†	TNFi duration, week	BASDAI	ASDAS	CRP level, mg/dl	SUV _{max} ‡	
					SI joints	Spine
15						
Baseline	0	7.6	3.4	0.5	15.858	15.950
Follow-up	12	3.7	1.7	0.1	15.573	0.000
Change	–	–3.9	–1.7	–0.4	–0.285	–15.950
16						
Baseline	0	4.1	2.1	0.1	18.313	0.000
Follow-up	12	3.8	1.9	0.0	11.227	0.000
Change	–	–0.3	–0.2	–0.1	–7.086	0.000

* BASDAI = Bath Ankylosing Spondylitis Disease Activity Index; ASDAS = Ankylosing Spondylitis Disease Activity Score; CRP = C-reactive protein; SI = sacroiliac.

† Imaging was performed before initiation (baseline) and after the specified duration (follow-up) of TNFi therapy.

‡ For semiquantitative analysis of osteoblastic activity, the maximum standardized uptake value (SUV_{max}) for ¹⁸F-NaF in SI joint quadrants and spinal vertebral corners was determined. For patients 1–6, imaging of the spine was not performed.

$P < 0.01$). No significant changes between baseline and follow-up were observed for chronic lesions (Figures 1 and 2).

An improvement in ¹⁸F-NaF uptake was observed for all lesion types. The largest effect was observed for lesions associated with bone marrow edema, with 47 (65.3% [95% CI 53.1–76.1]) fewer SI joint quadrants showing ¹⁸F-NaF uptake at follow-up ($P < 0.01$) (Figures 1 and 2). Of the 3 SI joint quadrants with new onset of bone marrow edema at follow-up, 2 did not show ¹⁸F-NaF uptake at baseline or follow-up, whereas 1 had uptake at baseline and follow-up.

Quantification of osteoblastic activity demonstrated that the mean SUV_{max} for all SI joint quadrants decreased significantly during the study, from 14.637 at baseline to 11.466 at follow-up (change, -3.171 [range $-13.050, 2.875$]; $P < 0.01$). Four patients had a very minor increase in mean SUV_{max} (range 2.031–2.875) without worsening clinical scores. No relation

between changes in mean SUV_{max} and clinical scores was observed (Table 2).

Evaluation and quantification of pathologic lesions in the spine.

Of the 920 VCs, 101 (11.0%) showed bone marrow edema, 62 (6.7%) showed fat lesions, and 11 (1.2%) showed sclerosis at baseline; increased ¹⁸F-NaF uptake was found in 77 VCs (8.4%), with a mean \pm SD SUV_{max} of 11.873 ± 9.140 . Increased ¹⁸F-NaF uptake was most frequently associated with sclerosis (9 [81.8%] of 11 VCs) and less commonly associated with fat lesions (26 [41.9%] of 62 VCs) or bone marrow edema (34 [33.7%] of 101 VCs).

At follow-up, bone marrow edema was still found in 34 VCs (including 6 that did not show bone marrow edema at baseline), for a net reduction of 66.3% (95% CI 57.1–75.6; $P < 0.01$), whereas fat lesions were found in 15 VCs, for a net reduction of

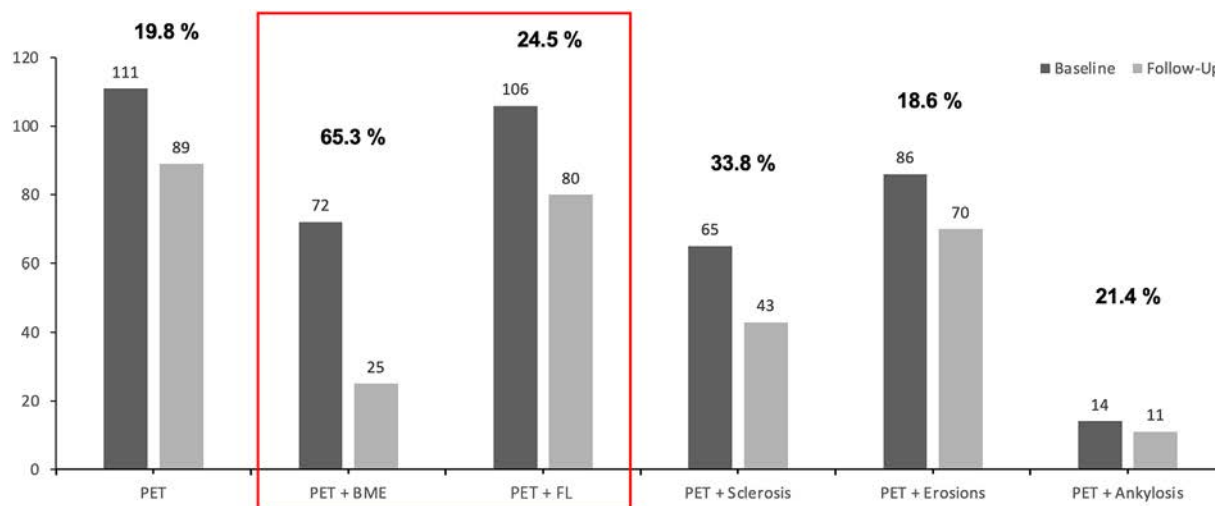


Figure 1. Number of sacroiliac joint quadrants showing lesions on conventional magnetic resonance imaging (MRI) and those showing uptake of fluorine 18–labeled NaF on positron emission tomography (PET)/MRI at baseline (dark gray) and after 4 months of treatment with tumor necrosis factor inhibitors (light gray) among patients with radiographic axial spondyloarthritis. The bold numbers show the percentage decrease between baseline and follow-up. Statistically significant differences are indicated by the red box. BME = bone marrow edema; FL = fat lesions.

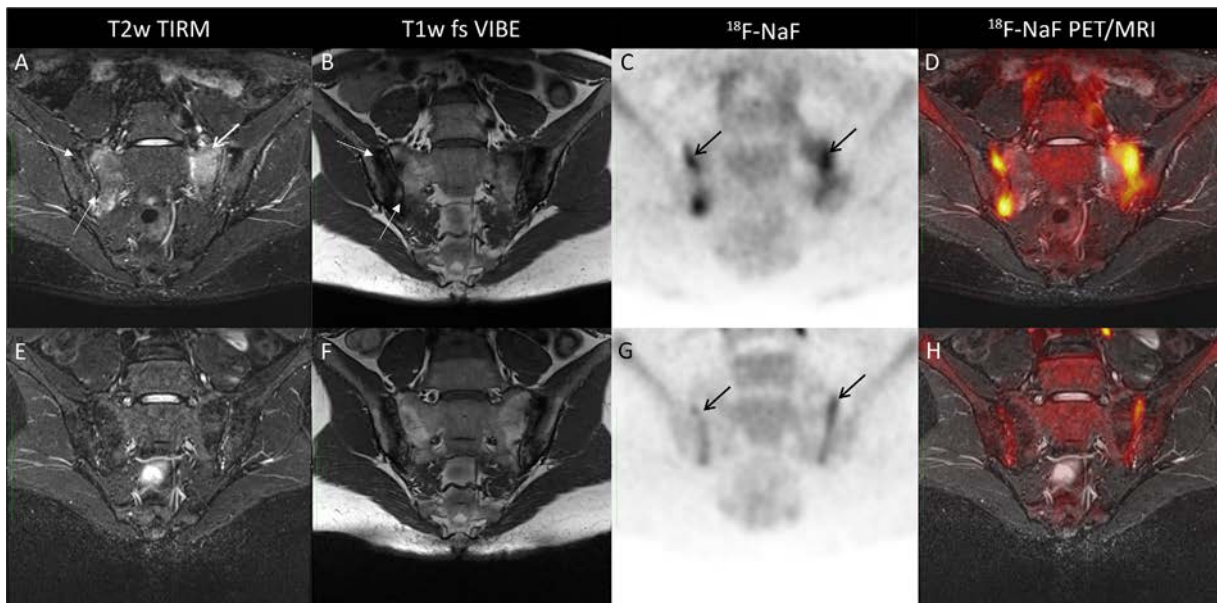


Figure 2. Findings of sacroiliac joint imaging at baseline (A–D) and follow-up (E–H) for a 34-year-old patient with clinically active radiographic axial spondyloarthritis. Shown are areas of sclerosis and erosions (**thin white arrows**) and extensive surrounding bone marrow edema and fatty degeneration (**thick white arrow**) on scans obtained by a T2-weighted turbo inversion recovery magnitude (T2w TIRM) sequence (A) and T1-weighted volumetric interpolated breath-hold examination with fat suppression (T1w fs VIBE) (B), as well as evidence of osteoblastic activity based on increased signal on fluorine 18–labeled NaF (^{18}F -NaF) PET/MRI (C and D; **black arrows**). Follow-up imaging after 4 months of tumor necrosis factor inhibitor treatment showed significant decrease in osteoblastic activity (**black arrows**). See Figure 1 for other definitions.

75.8% (95% CI 62.8–84.8; $P < 0.01$). Sclerosis was found in 43 VCs, which was significantly greater than the number at baseline (Figures 3 and 4).

Similar to the analysis of SI joints, the largest reduction in ^{18}F -NaF uptake was found in lesions associated with bone marrow edema, with 25 (73.5% [95% CI 43.3–71.6]) fewer VCs showing uptake at follow-up ($P = 0.01$). In comparison, 18 (69.2%) fewer VCs associated with fat lesions ($P = 0.03$) and

5 (55.6%) fewer VCs associated with sclerosis ($P = 0.16$) showed ^{18}F -NaF uptake at follow-up (Figures 3 and 4).

Quantification of osteoblastic activity showed that the mean SUV_{max} for all VCs decreased significantly, from 11.873 at baseline to 7.215 at follow-up (change, -4.658 [range -15.950 , 4.483]; $P < 0.025$). Only 1 patient had a slight increase in her mean SUV_{max} . Similar to findings for SI joints, no relation between changes in SUV_{max} and clinical outcomes was observed (Table 2).

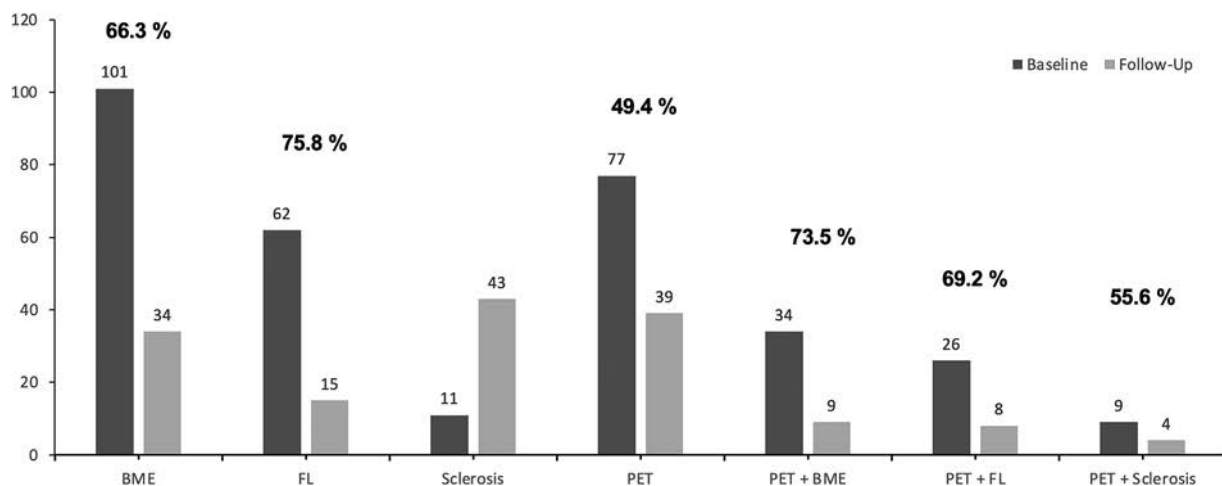


Figure 3. Number of vertebral corners showing lesions on conventional MRI and those showing uptake of fluorine 18–labeled NaF on PET/MRI at baseline (dark gray) and after 4 months of treatment with tumor necrosis factor inhibitors (light gray) among patients with radiographic axial spondyloarthritis. The bold numbers show the percentage decrease between baseline and follow-up. See Figure 1 for definitions.

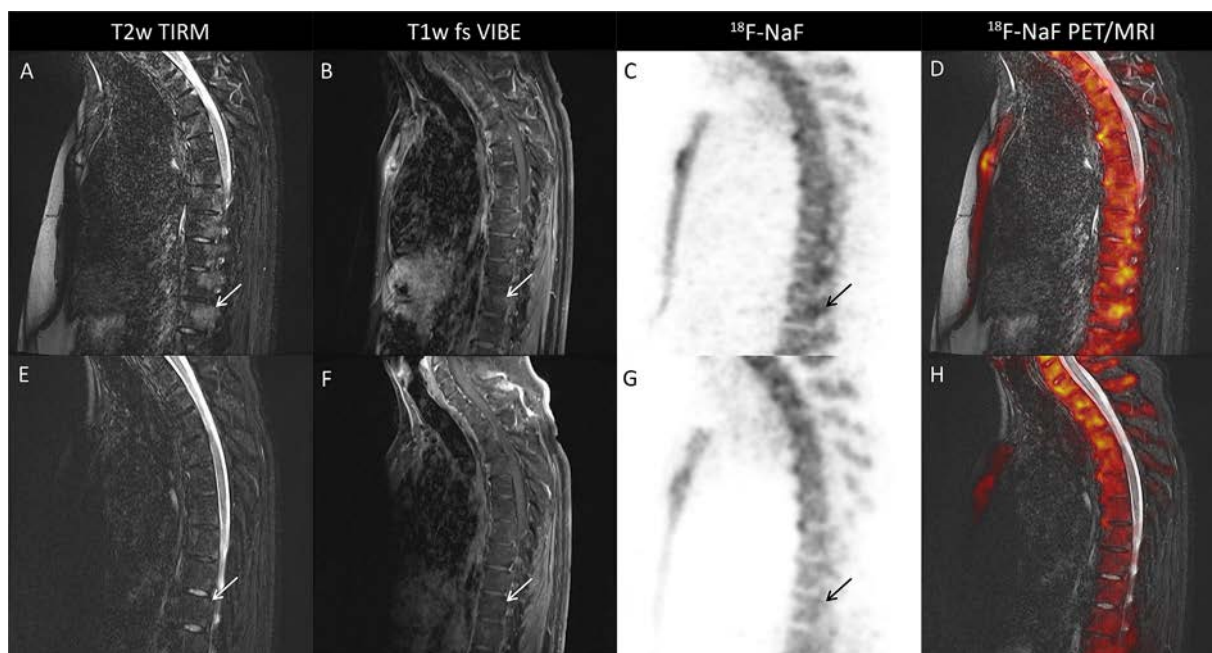


Figure 4. Findings of thoracic spine imaging at baseline (A–D) and follow-up (E–H) for a 40-year-old patient with clinically active radiographic axial spondyloarthritis. At baseline, signs of extensive bone edema are evident in the thoracic vertebral bodies (A and B; white arrows) with evidence of osteoblastic activity based on increased signal on fluorine 18-labeled NaF (^{18}F -NaF) PET/MRI (C and D; black arrow). Follow-up imaging after 4 months of tumor necrosis factor inhibitor treatment (E–H) showed visible decrease of inflammation and osteoblastic activity (white arrows, black arrow). T2w TIRM = T2-weighted turbo inversion recovery magnitude; T1w fs VIBE = T1-weighted volumetric interpolated breath-hold examination with fat suppression (see Figure 1 for other definitions).

DISCUSSION

With this study, we are the first to show that TNFi therapy decreases osteoblastic activity in the SI joints and spine of patients with active radiographic axial SpA within a few months after treatment initiation. As expected, there was clinical improvement at the group level, as assessed by a decrease in BASDAI and ASDAS values, including a significant decrease in C-reactive protein levels. The effect of the treatment on bone metabolism was demonstrated on the basis of a detailed analysis of bone marrow edema, fat lesions, sclerosis, and ankylosis on MRI in comparison to the quantification of osteoblastic activity on PET. Overall, we found a significant reduction of bone marrow edema in both the SI joints and the spine, whereas the beneficial effect on osteoblastic lesions mostly involved those that were present in combination with bone marrow edema prior to treatment initiation. These findings were independent of the anti-TNF compound used (data not shown). In comparison, no changes were observed for chronic lesions of the SI joints, whereas a decrease in fat lesions and an increase in sclerotic lesions were observed in the analysis of spinal VCs at follow-up. Taking into account the short follow-up duration, these data are in line with earlier observations (26) that inflammation and new bone formation are not directly linked but instead represent a reparative process that occurs via erosive, sclerotic, and fat transformation (27) and ends in ankylosis.

Analysis of the lesion types with respect to changes in osteoblastic activity showed a reduction in ^{18}F -NaF uptake at follow-up in both the SI joints and the spine and for both active and chronic lesions. However, the difference in reduction in the SI joints as compared to that in the spine was not statistically significant. This might have been because axial SpA in all patients was in the more advanced, radiographic stage, when the SI joints had likely been affected by the disease for a longer period than the spine, which is generally affected later during the disease course.

On the other hand, no relation was found between the clinical response to TNFi treatment and changes in the quantification of osteoblastic activity as measured by the SUV_{max} . Interestingly, overall and despite disease activity status at follow-up, as assessed by both the BASDAI and the ASDAS, all patients benefited from treatment, but not all of them achieved low disease activity. Still, quantification of osteoblastic activity demonstrated that the SUV_{max} decreased, stayed similar, or, on rare occasion, showed only a minor increase. These data indicate that the magnitude of the treatment effect at the structural level, as assessed by imaging, may not necessarily reflect the magnitude of its effect on treatment outcomes, which might depend on the tool used to assess global disease activity or on the effect of comorbidities, such as concomitant fibromyalgia (28–31). Another explanation for this observation may be that, in some patients, treatment with TNFi but also with other

bDMARDs needs >6 months to reach its full potency with regard to clinical outcomes and structural changes (32,33). However, because the effects of treatment were most visible during the early course of disease, when inflammatory activity was present (i.e., at sites where tissue is just beginning to transform), and less apparent in terms of PET findings and chronic changes, these findings might also be applicable to patients with nonradiographic axial SpA (34).

Some limitations of this study need to be taken into account. Importantly, the sample size in our study was too small to yield strong conclusions about the effect of TNFi on bone metabolism. Furthermore, we did not include bDMARDs other than TNFi in our analysis. We therefore see these results as a proof of concept for future research to understand the expected “disease-modifying” effect of bDMARDs, including TNFi, in patients with radiographic axial SpA (16–18). In an era of broader use of such treatments due to the wide application of biosimilar agents, this information is of great importance for both physicians and patients. Furthermore, as mentioned above, the follow-up period may have been too short to demonstrate the full effect of treatment in all patients. Nevertheless, it is still impressive that, despite this relatively short follow-up period, a clear effect was seen in the imaging analyses. It would be interesting to study these effects over longer follow-up periods and to determine whether the benefit of TNFi therapy becomes even more pronounced. Finally, PET/MRI technology is only available in larger centers and is associated with a high level radiation exposure if performed often, making frequent use of the technology unfeasible.

Together, the results of this observational proof-of-concept study suggest that early initiation of antiinflammatory therapy with TNFi may have a beneficial, antiosteoblastic effect that results in regression of radiographic progression in patients with active radiographic axial SpA. Further research involving larger patient collectives is needed to confirm these results. It will also be interesting to see whether treatment with other bDMARDs, such as interleukin-17 inhibitors, or with small molecules, such as JAK inhibitors, will have similar results.

ACKNOWLEDGMENT

Open Access funding enabled and organized by Projekt DEAL.

AUTHOR CONTRIBUTIONS

All authors were involved in drafting the article or revising it critically for important intellectual content, and all authors approved the final version to be published. Dr. Bruckmann had full access to all of the data in the study and takes responsibility for the integrity of the data and the accuracy of the data analysis.

Study conception and design. Rischpler, Kirchner, Umutlu, Herrmann, Fendler, Buchbender, Antoch, Sawicki, Tsobanelis, Braun, Baraliakos.

Acquisition of data. Bruckmann, Tsiami, Abrar, Bartel, Theysohn.






Analysis and interpretation of data. Bruckmann, Rischpler, Kirchner, Fendler, Baraliakos.

REFERENCES

- Boel A, Molto A, van der Heijde D, Ciurea A, Dougados M, Gensler LS, et al. Do patients with axial spondyloarthritis with radiographic sacroiliitis fulfil both the modified New York criteria and the ASAS axial spondyloarthritis criteria? Results from eight cohorts. *Ann Rheum Dis* 2019;78:1545–9.
- Rudwaleit M, van der Heijde D, Landewé R, Akkoc N, Brandt J, Chou CT, et al. The Assessment of SpondyloArthritis International Society classification criteria for peripheral spondyloarthritis and for spondyloarthritis in general. *Ann Rheum Dis* 2011;70:25–31.
- Sieper J, Rudwaleit M, Baraliakos X, Brandt J, Braun J, Burgos-Vargas R, et al. The Assessment of SpondyloArthritis International Society (ASAS) handbook: a guide to assess spondyloarthritis. *Ann Rheum Dis* 2009;68 Suppl 2:ii1–44.
- Kiltz U, Baraliakos X, Braun J. Ankylosing spondylitis. In: El Miedany Y, ed. *Comorbidity in rheumatic diseases*. Springer; 2017. p. 125–43.
- Kiltz U, Baraliakos X, Regel A, Bühring B, Braun J. Causes of pain in patients with axial spondyloarthritis [review]. *Clin Exp Rheumatol* 2017;35 Suppl 107:102–7.
- Van der Heijde D, Ramiro S, Landewé R, Baraliakos X, Van den Bosch F, Sepriano A, et al. 2016 update of the ASAS-EULAR management recommendations for axial spondyloarthritis. *Ann Rheum Dis* 2017;76:978–91.
- Baraliakos X, Listing J, Rudwaleit M, Sieper J, Braun J. The relationship between inflammation and new bone formation in patients with ankylosing spondylitis. *Arthritis Res Ther* 2008;10:R104.
- Baraliakos X, Fruth M, Kiltz U, Braun J. Inflammatory spinal diseases: axial spondyloarthritis: central importance of imaging. *Z Rheumatol* 2017;76:149–62. In German.
- Krohn M, Braum LS, Sieper J, Song IH, Weiß A, Callhoff J, et al. Erosions and fatty lesions of sacroiliac joints in patients with axial spondyloarthritis: evaluation of different MRI techniques and two scoring methods. *J Rheumatol* 2014;41:473–80.
- Maksymowich WP, Chiowchanwisawakit P, Clare T, Pedersen SJ, Østergaard M, Lambert RG. Inflammatory lesions of the spine on magnetic resonance imaging predict the development of new syndesmophytes in ankylosing spondylitis: evidence of a relationship between inflammation and new bone formation. *Arthritis Rheum* 2009;60:93–102.
- Buchbender C, Ostendorf B, Ruhlmann V, Heusch P, Miese F, Beiderwellen K, et al. Hybrid 18F-labeled fluoride positron emission tomography/magnetic resonance (MR) imaging of the sacroiliac joints and the spine in patients with axial spondyloarthritis: a pilot study exploring the link of MR bone pathologies and increased osteoblastic activity. *J Rheumatol* 2015;42:1631–7.
- Hawkins RA, Choi Y, Huang SC, Hoh CK, Dahlbom M, Schiepers C, et al. Evaluation of the skeletal kinetics of fluorine-18-fluoride ion with PET. *J Nucl Med* 1992;33:633–42.
- Fischer DR, Pfirmann CW, Zubler V, Stumpe KD, Seifert B, Strobel K, et al. High bone turnover assessed by 18E-fluoride PET/CT in the spine and sacroiliac joints of patients with ankylosing spondylitis: comparison with inflammatory lesions detected by whole body MRI. *EJNMMI Res* 2012;2:38.
- Sawicki LM, Lütje S, Baraliakos X, Braun J, Kirchner J, Boos J, et al. Dual-phase hybrid 18F-fluoride positron emission tomography/MRI in ankylosing spondylitis: investigating the link between MRI bone changes, regional hyperaemia and increased osteoblastic activity. *J Med Imaging Radiat Oncol* 2018;62:313–9.
- Baraliakos X, Boehm H, Bahrami R, Samir A, Schett G, Luber M, et al. What constitutes the fat signal detected by MRI in the spine of patients with ankylosing spondylitis? A prospective study based on biopsies obtained during planned spinal osteotomy to correct hyperphosis or spinal stenosis. *Ann Rheum Dis* 2019;78:1220–5.

16. Baraliakos X, Haibel H, Listing J, Sieper J, Braun J. Continuous long-term anti-TNF therapy does not lead to an increase in the rate of new bone formation over 8 years in patients with ankylosing spondylitis. *Ann Rheum Dis* 2014;73:710–5.
17. Haroon N, Inman RD, Learch TJ, Weisman MH, Lee M, Rahbar MH, et al. The impact of tumor necrosis factor α inhibitors on radiographic progression in ankylosing spondylitis. *Arthritis Rheum* 2013;65:2645–4.
18. Molnar C, Scherer A, Baraliakos X, de Hooge M, Micheroli R, Exer P, et al. TNF blockers inhibit spinal radiographic progression in ankylosing spondylitis by reducing disease activity: results from the Swiss Clinical Quality Management cohort. *Ann Rheum Dis* 2018;77:63–9.
19. Van der Linden S, Valkenburg HA, Cats A. Evaluation of diagnostic criteria for ankylosing spondylitis: a proposal for modification of the New York criteria. *Arthritis Rheum* 1984;27:361–8.
20. Garrett S, Jenkinson T, Kennedy LG, Whitelock H, Gaisford P, Calin A. A new approach to defining disease status in ankylosing spondylitis: the Bath Ankylosing Spondylitis Disease Activity Index. *J Rheumatol* 1994;21:2286–91.
21. Blumhagen JO, Ladebeck R, Fenchel M, Scheffler K. MR-based field-of-view extension in MR/PET: B0 homogenization using gradient enhancement (HUGE). *Magn Reson Med* 2013;70:1047–57.
22. Paulus DH, Quick HH, Geppert C, Fenchel M, Zhan Y, Hermosillo G, et al. Whole-body PET/MR imaging: quantitative evaluation of a novel model-based MR attenuation correction method including bone. *J Nucl Med* 2015;56:1061–6.
23. Lindemann ME, Oehmigen M, Blumhagen JO, Gratz M, Quick HH. MR-based truncation and attenuation correction in integrated PET/MR hybrid imaging using HUGE with continuous table motion. *Med Phys* 2017;44:4559–72.
24. Oehmigen M, Lindemann ME, Gratz M, Kirchner J, Ruhlmann V, Umutlu L, et al. Impact of improved attenuation correction featuring a bone atlas and truncation correction on PET quantification in whole-body PET/MR. *Eur J Nucl Med Mol Imaging* 2018;45:642–53.
25. Lukas C, Landewé R, Sieper J, Dougados M, Davis J, Braun J, et al. for the Assessment of SpondyloArthritis international Society. Development of an ASAS-endorsed disease activity score (ASDAS) in patients with ankylosing spondylitis. *Ann Rheum Dis* 2009;68:18–24.
26. Appel H, Sieper J. Spondyloarthritis at the crossroads of imaging, pathology, and structural damage in the era of biologics [review]. *Curr Rheumatol Rep* 2008;10:356–63.
27. Baraliakos X, Heldmann F, Callhoff J, Listing J, Appelboom T, Brandt J, et al. Which spinal lesions are associated with new bone formation in patients with ankylosing spondylitis treated with anti-TNF agents? A long-term observational study using MRI and conventional radiography. *Ann Rheum Dis* 2014;73:1819–25.
28. López-Medina C, Ladehesa-Pineda L, Puche-Larrubia MÁ, Escudero-Contreras A, Font-Ugalde P, Collantes-Estévez E. Which factors explain the patient global assessment in patients with ankylosing spondylitis? A hierarchical cluster analysis on REGISPONSER-AS. *Semin Arthritis Rheum* 2021;51:875–9.
29. Nam B, Koo BS, Lee TH, Shin JH, Kim JJ, Lee S, et al. Low BASDAI score alone is not a good predictor of anti-tumor necrosis factor treatment efficacy in ankylosing spondylitis: a retrospective cohort study. *BMC Musculoskelet Disord* 2021;22:140.
30. Kiltz U, Baraliakos X, Karakostas P, Igelmann M, Kalthoff L, Klink C, et al. The degree of spinal inflammation is similar in patients with axial spondyloarthritis who report high or low levels of disease activity: a cohort study. *Ann Rheum Dis* 2012;71:1207–11.
31. Moltó A, Etcheto A, Gossec L, Boudersa N, Claudepierre P, Roux N, et al. Evaluation of the impact of concomitant fibromyalgia on TNF α blockers' effectiveness in axial spondyloarthritis: results of a prospective, multicentre study. *Ann Rheum Dis* 2018;77:533–40.
32. Kim K, Son SM, Goh TS, Pak K, Kim IJ, Lee JS, et al. Prediction of response to tumor necrosis factor- α blocker is suggested by ^{18}F -NaF SUVmax but not by quantitative pharmacokinetic analysis in patients with ankylosing spondylitis. *Am J Roentgenol* 2020;214:1352–8.
33. Baraliakos X, van den Bosch F, Machado PM, Gensler LS, Marzo-Ortega H, Sherif B, et al. Achievement of remission endpoints with secukinumab over 3 years in active ankylosing spondylitis: pooled analysis of two phase 3 studies. *Rheumatol Ther* 2021;8:273–88.
34. Van der Heijde, Baraliakos X, Hermann KG, Landewé RB, Machado PM, Maksymowych WP, et al. Limited radiographic progression and sustained reductions in MRI inflammation in patients with axial spondyloarthritis: 4-year imaging outcomes from the RAPID-axSpA phase III randomised trial. *Ann Rheum Dis* 2018;77:699–705.

Progressive Increase in Sacroiliac Joint and Spinal Lesions Detected on Magnetic Resonance Imaging in Healthy Individuals in Relation to Age

Thomas Renson,  Manouk de Hooge, Ann-Sophie De Craemer,  Liselotte Deroo,  Zuzanna Lukasik, Philippe Carron,  Nele Herregods, Lennart Jans, Roos Colman, Filip Van den Bosch, and Dirk Elewaut 

Objective. Magnetic resonance imaging (MRI) plays a pivotal role in spondyloarthritis (SpA) diagnosis. However, a detailed description of MRI findings of the sacroiliac (SI) joints and spine in healthy individuals is currently lacking. This study was undertaken to evaluate the occurrence of MRI-detected SI joint and spinal lesions in healthy individuals in relation to age.

Methods. Ninety-five healthy subjects (ages 20–49 years) underwent MRI of the SI joints and spine. Bone marrow edema (BME) and structural lesions of the SI joints were scored using the Spondyloarthritis Research Consortium of Canada (SPARCC) method. Spinal inflammatory and structural lesions were evaluated using the SPARCC MRI spine inflammation index and the Canada-Denmark MRI scoring system, respectively. Fulfillment of the Assessment of SpondyloArthritis international Society definition of a positive MRI for sacroiliitis/spondylitis was reviewed. Findings were compared to MRIs of axial SpA patients from the Belgian Inflammatory Arthritis and Spondylitis cohort.

Results. Of the subjects ≥ 30 years old, 17.2% fulfilled the definition of a positive MRI for sacroiliitis, but this occurred rarely in younger subjects. SI joint erosions (20.0%) and fat metaplasia (13.7%) were detected across all age groups. Erosions were more frequently visualized in subjects ages ≥ 40 years (39.3%). Spinal BME (35.7%) and fat metaplasia (28.6%) were common in subjects older than 40 years. Nonetheless, only 1 subject had ≥ 3 corner inflammatory lesions. SI joint and spinal SPARCC scores and total structural lesions scores increased progressively with age.

Conclusion. Contrary to what is commonly believed, structural MRI-detected SI joint lesions are frequently seen in healthy individuals. Especially in older subjects, the high occurrence of inflammatory and structural MRI-detected lesions impacts their specificity for SpA, which has important implications for the interpretation of MRIs in patients with a clinical suspicion of SpA.

INTRODUCTION

Magnetic resonance imaging (MRI) is the gold standard imaging modality for the detection of sacroiliitis, a hallmark of axial spondyloarthritis (axSpA). Nonetheless, the specificity of MRI in the context of axSpA has been questioned in several studies. A high prevalence of a positive MRI for active sacroiliitis according to the Assessment of SpondyloArthritis international Society (ASAS) definition was found in a non-SpA context (1), such as in postpartum women (60%), elite ice hockey players (41%), recreational runners

(30–35%), and military recruits (23%) (2–5). Surprisingly, extensive data on sacroiliac (SI) joint and spinal MRI of healthy individuals across different age categories are still lacking.

De Winter et al reported the prevalence of bone marrow edema (BME) on MRIs of the SI joints in healthy individuals, runners, and women with postpartum back pain (6). Importantly, the presence of structural lesions was not assessed. A recent article by Baraliakos and colleagues described a high prevalence of BME and fat metaplasia on spinal MRIs in a large population-based cohort (7). Nonetheless, the retrospective study design and the

Supported by an Assessment of SpondyloArthritis international Society (ASAS) research grant (to Dr. de Hooge) and an Innovative Medicines Initiative (IMI) HIPPOCRATES grant.

Thomas Renson, MD, PhD, Manouk de Hooge, PhD, Ann-Sophie De Craemer, MD, Liselotte Deroo, MD, Zuzanna Lukasik, MD, Philippe Carron, MD, PhD, Nele Herregods, MD, PhD, Lennart Jans, MD, PhD, Roos Colman, MSc, Filip Van den Bosch, MD, PhD, Dirk Elewaut, MD, PhD: Ghent University, Ghent, Belgium.

Author disclosures are available at <https://onlinelibrary.wiley.com/action/downloadSupplement?doi=10.1002%2Fart.42145&file=art42145-sup-0001-Disclosureform.pdf>.

Address correspondence to Thomas Renson, MD, PhD, or Dirk Elewaut, MD, PhD, Ghent University Hospital, Department of Internal Medicine and Pediatrics, Corneel Heymanslaan 10, 9000 Gent, Belgium. E-mail: thomas.renson@uzgent.be or filip.vandenbosch@uzgent.be.

Submitted for publication September 8, 2021; accepted in revised form April 12, 2022.

high prevalence of subjects with back pain warrant caution when extrapolating these results. It is obvious to highlight the importance of interpreting imaging results in the appropriate clinical context. In this regard, a detailed reference map of possible SI joint lesions occurring in healthy, asymptomatic individuals in relation to their age may be essential for the correct interpretation of MRI in individuals with a clinical suspicion of SpA. Our working hypothesis was that age-dependent changes may occur, which could play a critical role in this interpretation. We therefore evaluated the occurrence of BME and structural lesions on SI joint and spinal MRI in healthy subjects across different age categories.

SUBJECTS AND METHODS

Subjects. Healthy subjects without symptoms of back pain were recruited from the Ghent University Hospital staff, as well as relatives and acquaintances of the researchers. Subjects were divided into 3 age categories: 20–29 years, 30–39 years, and 40–49 years. Exclusion criteria included a (medical) contraindication for MRI, current or recent chronic back pain, tumor necrosis factor inhibitor (TNFi) treatment, use of nonsteroidal antiinflammatory drugs in the last 2 weeks, and a known diagnosis of SpA. A short questionnaire assessing health status, (family) medical history, and medication use was conducted, and a blood sample was obtained for HLA-B27 status determination. Subsequently, all subjects underwent an MRI of the SI joints and spine. In addition, MRI findings were matched with those of axSpA patients from the Belgian Inflammatory Arthritis and Spondylitis (BeGIANT) cohort, a nationwide observational prospective cohort of newly diagnosed SpA patients (8–10). All axSpA patients who were included were younger than 50 years old at baseline, fulfilled the ASAS classification criteria for axSpA, and were naive to TNFi and interleukin-17 inhibitor treatment prior to inclusion.

MRI. Images of healthy subjects were obtained using a 3T unit (Prisma; Siemens Healthineers). Sequences included 3-mm T1-weighted and turbo inversion recovery magnitude (TIRM) images of the spine, 3-mm semi-coronal T1-weighted turbo spin echo and short tau inversion recovery (STIR) images of the pelvis. SI joint images of axSpA patients were obtained on a 1.5T unit (Avanto; Siemens Healthineers), applying the same sequences. MRIs of the SI joints were evaluated for inflammatory and structural lesions, as defined by the ASAS MRI working group, by 2 trained readers (TR and MdH) with scores calibrated (2).

Unlabeled SI joint MRIs from axSpA patients were mixed with the images from healthy controls to avoid bias. BME was scored using the Spondyloarthritis Research Consortium of Canada (SPARCC) method (11). Deep BME lesions were defined as extending >1 cm from the articular surface, with intense lesions defined as encompassing a high signal intensity as bright or brighter than vascular structures or intervertebral discs. In

addition, fulfillment of the ASAS definition of a positive MRI for sacroiliitis was assessed, defined as the following: ≥ 2 BME lesions on 1 slice, or ≥ 1 lesion on 2 consecutive slices and lesions highly suggestive of SpA (1). Structural lesions were scored using an adjusted SPARCC method (3,5,12,13) as follows: 6 slices, each divided into 4 quadrants, were scored, and in each slice, each quadrant was scored for erosions, fat metaplasia, sclerosis, and (partial) ankylosis. Spinal MRIs were evaluated by the same readers for corner inflammatory lesions (BME) using the SPARCC MRI spinal inflammation index and for corner structural lesions (erosions, fat metaplasia, and new bone formation) using the Canada-Denmark MRI spine scoring system, in which each vertebral unit was divided into quadrants (14,15).

Scores for BME, fat, erosion, and new bone formation at levels with disc degeneration were excluded from the calculation of patient-level sum scores. Unlabeled spinal MRIs from axSpA patients were mixed with the MRIs from healthy controls to avoid bias. Predefined lesion-level cutoffs aiming at high specificity for sacroiliitis and spondylitis were applied (13,16) as follows: fat metaplasia in ≥ 3 SI joint quadrants, erosions in ≥ 3 SI joint quadrants, fat metaplasia and/or erosions in ≥ 5 SI joint quadrants, ≥ 3 corner inflammatory lesions of the spine (positive MRI for the spine according to the ASAS definition), or ≥ 5 spinal fat lesions. Individual reader scores were combined, and for further analyses the mean scores were used. A consensus score was applied in case of dichotomous outputs.

Statistical analysis. All statistical analyses were performed using IBM SPSS Statistics, version 26. Descriptive statistics were used to analyze and report the demographic and clinical characteristics and MRI lesions. MRI scores between subgroups (e.g., HLA-B27-positive versus HLA-B27-negative subjects) were compared using the Mann-Whitney U test. Correlation with demographic and clinical data was assessed by Spearman's rank correlation coefficient in the case of continuous variables. *P* values less than or equal to 0.05 were considered statistically significant.

RESULTS

MRI findings in healthy subjects. Ninety-five healthy subjects were included. Demographic and clinical characteristics are shown in Table 1. None of the subjects had symptoms of back pain. Only 3 subjects (3%) ever had an episode of chronic back pain.

Reliability. In general, two-way intraclass correlation coefficients (ICCs) for both readers were moderate to excellent. Excellent ICC was reached for spinal fat lesions (0.909). Good ICCs were reached for SI joint BME (0.774), SI joint fat lesions (0.849), SI joint partial ankylosis (0.849), and spinal BME (0.765). Moderate ICCs were reached for SI joint erosions (0.691) and spinal erosions (0.675). ICCs for SI joint sclerosis could not be calculated

Table 1. Demographic and clinical characteristics of the healthy subjects (n = 95)*

	Age 20–29 years (n = 36)	Age 30–39 years (n = 31)	Age 40–49 years (n = 28)
Age, median (IQR) years	27 (25–28)	32 (31–36)	43 (40–45)
Male sex	18 (50)	15 (48)	14 (50)
HLA-B27 status, no. positive/no. tested	2/35 (6)	3/30 (10)	2/27 (7)
Psoriasis (current or past)	0 (0)	0 (0)	0 (0)
IBD (current or past)	0 (0)	0 (0)	0 (0)
Uveitis (current or past)	1 (3)	0 (0)	0 (0)

* Except where indicated otherwise, values are the number (%) of subjects. IQR = interquartile range; IBD = inflammatory bowel disease.

because 1 reader never observed sclerosis (whereas the other reader observed sclerosis in 2 subjects). The ICC for spinal syndesmophytes was 0.163 because of the very high number of negative scores by both readers.

BME and structural lesions on SI joint MRI. A summary of the MRI-detected SI joint lesions is shown in Table 2. SI joint lesions were mainly detected in subjects ≥ 30 years old. SI joint BME was observed in 13.9% of subjects ages 20–29 years. However, the extent was limited, as the median SPARCC score in those subjects displaying BME was 1.0 and only 1 subject had a positive MRI for active sacroiliitis according to the ASAS definition. In contrast, 25.8% of the subjects ages 30–39 years and even 35.7% of the subjects ages ≥ 40 years displayed SI joint BME. In addition, SPARCC scores were significantly higher in subjects

≥ 40 years old compared to those 20–29 years old ($P = 0.022$). Consistent with this, sacroiliitis detected by MRI according to the ASAS definition was more frequent in older age categories compared to subjects < 30 years old (16.1% in the 30–39 years group and 17.9% in the 40–49 years group, compared to 2.8%). SI joint SPARCC scores ≥ 5 occurred in 6 of 95 subjects (6%); none of those subjects were younger than 30 years old. Deep and intense BME lesions were rarely detected (Table 2). In Figure 1, heatmaps display the topographic distribution of MRI-detected SI joint lesions in healthy subjects compared to axSpA patients from the Be-GIANT cohort. BME on SI joint MRIs in healthy subjects occurred most frequently in the superior sacrum (both anterior and posterior) followed by the inferior ilium (Supplementary Table 1, available on the *Arthritis & Rheumatology* website at

Table 2. Inflammatory and structural MRI-detected lesions in the SI joints and spine of healthy subjects*

	All age categories (n = 95)		Age 20–29 years (n = 36)		Age 30–39 years (n = 31)		Age 40–49 years (n = 28)	
	No. (%)	Median (IQR)	No. (%)	Median (IQR)	No. (%)	Median (IQR)	No. (%)	Median (IQR)
SI joint								
Sacroiliitis†	11 (11.6)	–	1 (2.8)	–	5 (16.1)	–	5 (17.9)	–
SPARCC score > 0 (BME)	23 (24.2)	2.0 (1.00–4.50)	5 (13.9)	1.0 (0.75–2.00)	8 (25.8)	3.3 (1.13–6.00)	10 (35.7)	2.3 (1.00–5.25)
Deep BME‡	4 (4.2)	1.0 (0.50–2.63)	0 (0.0)	–	2 (6.5)	1.0 (–)	2 (7.1)	1.8 (–)
Intense BME§	6 (6.3)	0.5 (0.50–0.63)	1 (2.8)	1.0 (–)	2 (6.5)	0.5 (0.50–0.50)	3 (10.7)	0.5 (–)
Erosions	19 (20.0)	2.0 (0.50–4.50)	5 (13.9)	0.5 (0.50–0.75)	3 (9.7)	5.5 (–)	11 (39.3)	2.0 (1.50–3.50)
Fat metaplasia	13 (13.7)	2.0 (1.00–3.50)	3 (8.3)	1.0 (–)	6 (19.3)	2.5 (1.00–3.25)	4 (14.3)	3.3 (1.13–10.25)
Sclerosis	2 (2.1)	1.8 (–)	1 (2.8)	3.0 (–)	0 (0.0)	–	1 (3.6)	1.0 (–)
Partial ankylosis	1 (1.1)	9 (–)	0 (0.0)	–	1 (3.2)	9 (–)	0	–
Ankylosis	0 (0.0)	–	0 (0.0)	–	0 (0.0)	–	0 (0.0)	–
Erosions in ≥ 3 quadrants	8 (8.4)	–	0 (0.0)	–	3 (9.7)	–	5 (17.9)	–
Fat in ≥ 3 quadrants	4 (4.2)	–	0 (0.0)	–	2 (6.5)	–	2 (7.1)	–
Erosions and/or fat in ≥ 5 quadrants	7 (7.4)	–	0 (0.0)	–	2 (6.5)	–	5 (17.9)	–
Spine								
SPARCC score > 0 (BME)	19 (20.0)	4.0 (3.00–6.00)	3 (8.3)	4.0 (3.00–8.50)	6 (19.4)	3.0 (2.50–4.00)	10 (35.7)	4.75 (3.00–6.00)
≥ 3 inflammatory lesions (positive spinal MRI)	1 (1.1)	–	0 (0.0)	–	0 (0.0)	–	1 (3.6)	–
Erosions	9 (9.5)	1.0 (1.00–1.50)	5 (13.8)	1.0 (1.00–1.50)	2 (6.5)	1.25 (1.00–1.50)	2 (7.1)	0.75 (0.50–1.00)
Fat metaplasia	12 (12.6)	1.75 (1.00–2.75)	1 (2.8)	1.5 (–)	3 (9.7)	2.5 (1.25–3.50)	8 (28.6)	2.5 (1.25–3.50)
≥ 5 fat lesions	0 (0.0)	–	0 (0.0)	–	0 (0.0)	–	0 (0.0)	–
New bone formation (syndesmophytes)	0 (0.0)	–	0 (0.0)	–	0 (0.0)	–	0 (0.0)	–

* Reported median values are those in subjects displaying ≥ 1 of the respective lesions. MRI = magnetic resonance imaging; IQR = interquartile range; SI = sacroiliac; SPARCC = Spondyloarthritis Research Consortium of Canada.

† Fulfillment of the Assessment of SpondyloArthritis international Society definition of sacroiliitis.

‡ Bone marrow edema (BME) lesions extending > 1 cm from the articular surface.

§ High signal intensity as bright as or brighter than vascular structures or intervertebral discs.

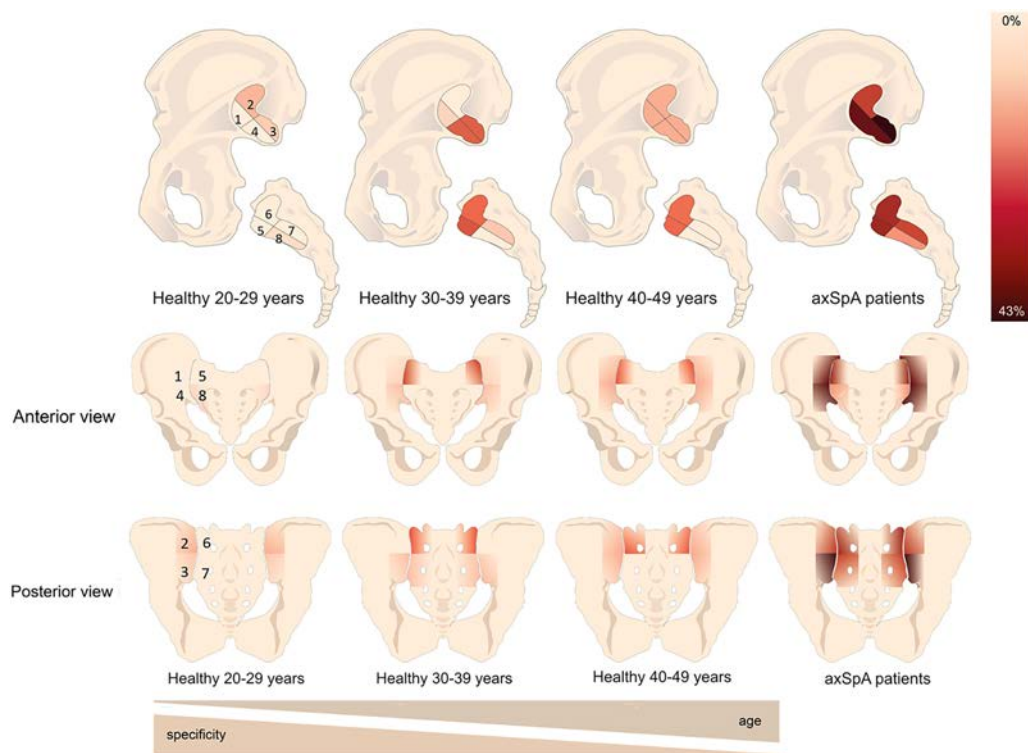


Figure 1. Heatmaps showing bone marrow edema detected by magnetic resonance imaging (sagittal and frontal views) in different quadrants of the sacroiliac joints of healthy, asymptomatic subjects ($n = 95$) compared to patients with axial spondyloarthritis (axSpA) from the Belgian Inflammatory Arthritis and Spondylitis Cohort ($n = 86$). 1 = anterior superior ilium; 2 = posterior superior ilium; 3 = posterior inferior ilium; 4 = anterior inferior ilium; 5 = anterior superior sacrum; 6 = posterior superior sacrum; 7 = posterior inferior sacrum; 8 = anterior inferior sacrum.

<https://onlinelibrary.wiley.com/doi/10.1002/art.42145>). The latter was most frequently affected in axSpA patients.

Erosions and fat metaplasia were the most observed structural lesions on SI joint MRIs, occurring in all age groups. Erosions were distinctly more commonly detected in subjects ≥ 40 years old (39.3%). Applying the cutoff values for erosions and fat metaplasia with $\geq 95\%$ specificity for SpA (13), none of the subjects ages 20–29 years had erosions in ≥ 3 quadrants, fat metaplasia in ≥ 3 quadrants, or erosions and/or fat metaplasia in ≥ 5 quadrants. However, this was increasingly common in older age categories (Table 2). Strikingly, 1 subject had bilateral partial ankylosis of the SI joints.

BME and structural lesions on spinal MRI. A summary of the main findings of MRIs of the spine is presented in Table 2. Notwithstanding the frequent occurrence of BME on MRIs of the spine in subjects ≥ 40 years old (35.7%), median SPARCC scores were low. Importantly, a positive MRI for spondylitis according to the ASAS definition was only observed in 1 subject, a 47-year-old HLA-B27-positive man showing 3 corner inflammatory spine lesions. Structural lesions on spine MRIs were occasionally detected. Fat metaplasia was the most frequently detected structural lesion, occurring mainly in subjects ≥ 40 years old (28.6%). However, none of the subjects had ≥ 5 fat lesions of the spine (maximum number of spinal fat lesions, $n = 2$). New bone formation

(syndesmophytes) was never detected in this study population. In Figure 2, heatmaps display the topographic distribution of MRI-detected spinal lesions in healthy subjects compared to axSpA patients from the Be-GIANT cohort. In general, the lower thoracic spine harbored most lesions in healthy subjects, whereas this was the lower thoracic and lumbar spine in axSpA patients. Overall, BME and fat lesions of the spine were more prevalent in axSpA patients compared to healthy subjects. Examples of MRIs of the SI joints and spines from study subjects are displayed in Figure 3.

Comparison of scores of SI joint MRIs from healthy subjects to those from axSpA patients. SI joint SPARCC scores of 95 healthy subjects were matched with those of 84 axSpA patients from the Be-GIANT cohort who were naive to treatment with biologic disease-modifying antirheumatic drugs, and they were plotted in function of the subject's age in Supplementary Figure 1 (available on the *Arthritis & Rheumatology* website at <https://onlinelibrary.wiley.com/doi/10.1002/art.42145>). In general, a gradual increase in SI joint SPARCC scores of healthy subjects was seen starting around the age of 30. Confidence intervals of the SPARCC scores started overlapping with those of SpA patients around the age of 45 years. Interestingly, SI joint SPARCC scores of SpA patients peaked around the age of 28 years. Dot plots in Figure 4 show the distribution of SI joint scores for BME (SPARCC scores), erosions, fat metaplasia, and total

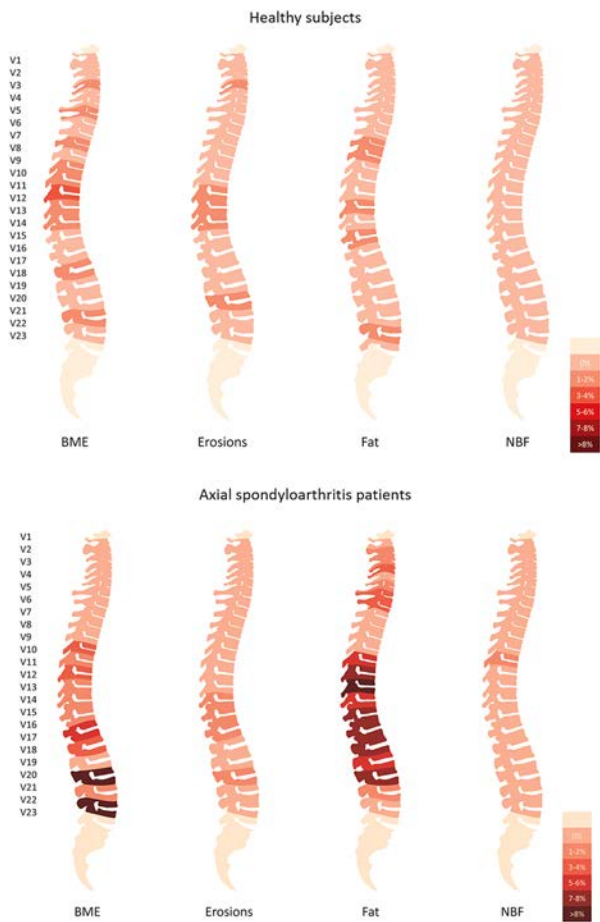


Figure 2. Heatmaps showing spinal lesions detected by magnetic resonance imaging in the different vertebral units of healthy, asymptomatic subjects ($n = 95$) compared to patients with axial spondyloarthritis from the Belgian Inflammatory Arthritis and Spondylitis Cohort ($n = 53$). The presence of lesions per vertebral unit was decided by consensus of the 2 readers. BME = bone marrow edema; NBF = new bone formation; V = vertebral unit.

structural lesions in the different age groups of healthy subjects compared to axSpA patients from the Be-GIANT cohort. All MRI-detected SI joint scores were higher in axSpA patients compared to healthy subjects.

Correlation of MRI findings in healthy subjects with demographic and clinical data.

The correlation of MRI lesions with the demographic and clinical characteristics of healthy subjects is shown in Supplementary Table 2 (available on the *Arthritis & Rheumatology* website at <https://onlinelibrary.wiley.com/doi/10.1002/art.42145>). A subject's age was significantly associated with SI joint SPARCC scores ($\rho = 0.21$, $P = 0.039$), SI joint erosion scores ($\rho = 0.24$, $P = 0.020$), total SI joint structural lesion scores ($\rho = 0.20$, $P = 0.041$), spinal SPARCC scores ($\rho = 0.36$, $P < 0.001$), spinal fat lesion scores ($\rho = 0.34$, $P < 0.001$), and total structural lesion scores of the spine ($\rho = 0.24$, $P = 0.021$). In addition, SI joint erosion scores correlated significantly with body mass index (BMI) ($\rho = 0.24$, $P = 0.018$). Blood samples were available for 92 subjects (97%). Seven subjects (7.6%) were positive for HLA-B27. None of them had inflammatory and/or structural lesions detected on MRI of the SI joints. There were no significant differences in spinal MRI scores between HLA-B27-positive and HLA-B27-negative subjects, except for higher erosion scores in HLA-B27-positive subjects. MRI-detected SI joint and spine lesions were not associated with the occurrence of chronic back pain in the past. Only 3 subjects ever had an episode of chronic back pain (duration ≥ 3 months). Those subjects had SI joint and spinal SPARCC scores of 0. No differences in MRI lesions were found between subjects performing manual compared to non-manual labor (data not shown). Of note, the study population consisted almost exclusively of subjects performing non-manual labor. Therefore, potential differences between both subgroups could not be detected.

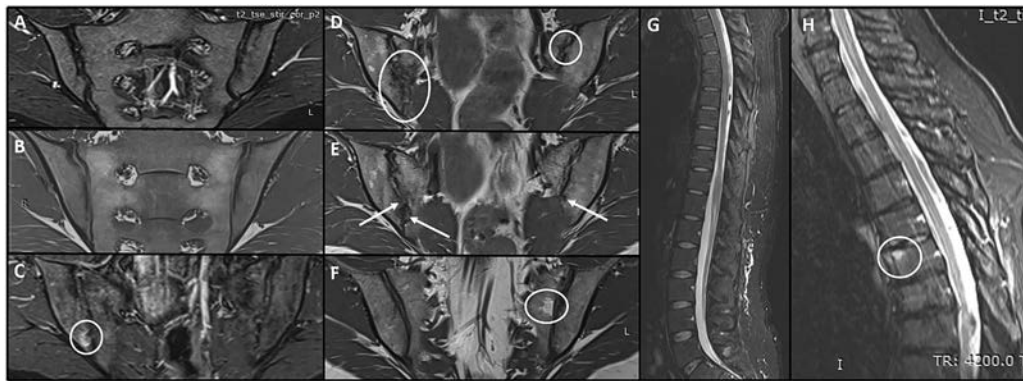


Figure 3. Examples of magnetic resonance images (MRIs) of the sacroiliac (SI) joints and spine in healthy, asymptomatic study subjects. **A**, SI joint MRI (short tau inversion recovery [STIR] sequence) in a 32-year-old female subject showing no bone marrow edema (BME). **B**, SI joint MRI (T1 sequence) in a 26-year-old male subject, displaying no structural lesions. **C**, SI joint MRI (STIR sequence) in a 31-year-old female subject showing limited BME (white circle) in the inferior ilium. **D** and **E**, SI joint MRI (T1 sequence) in a 31-year-old female subject (same as in **C**) displaying bilateral partial ankylosis (white circles in **D**, left arrow in **E**) and erosions (middle and right arrows in **E**). **F**, SI joint MRI (T1 sequence) in a 40-year-old female subject displaying limited sacral fat metaplasia (white circle). **G**, Spinal MRI (TIRM sequence; T4–L5) in a 25-year-old female subject showing no corner inflammatory lesions. **H**, Spinal MRI (TIRM sequence; C6–T9) in a 49-year-old female subject displaying an anterior corner inflammatory lesion (T6) (white circle).

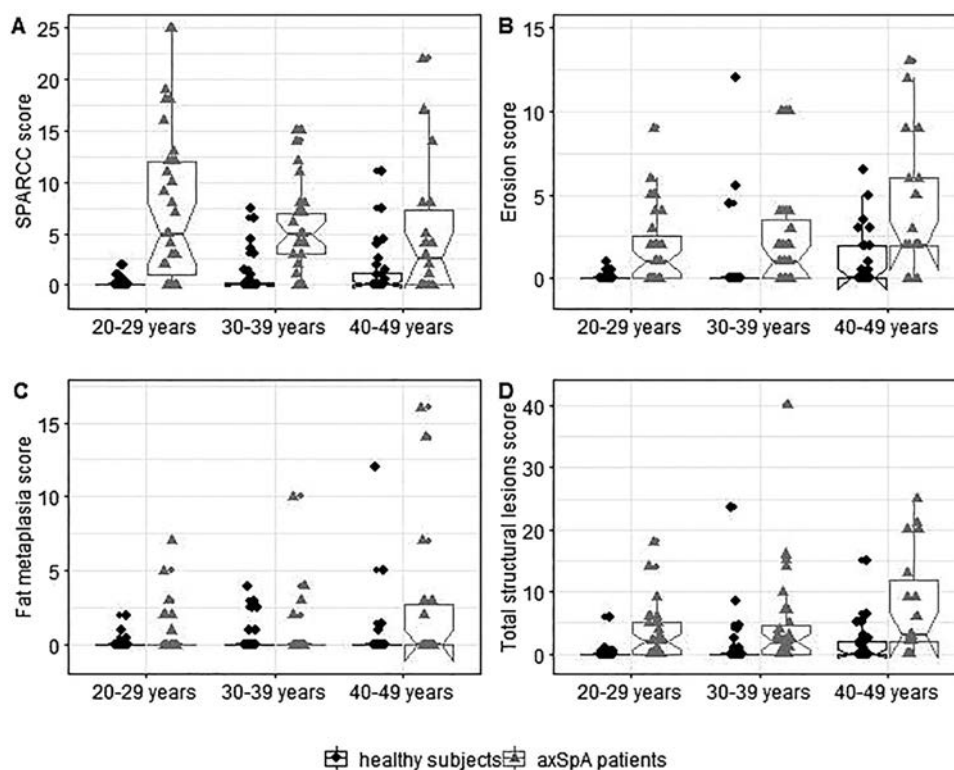


Figure 4. A–D, Sacroiliac joint Spondyloarthritis Research Consortium of Canada (SPARCC) scores, erosion scores, fat metaplasia scores, and total structural lesion scores in the different age categories of the healthy subjects versus axial spondyloarthritis (axSpA) patients from the Belgium Inflammatory Arthritis and Spondylitis Cohort. AxSpA patients display higher SI joint magnetic resonance imaging scores in all categories compared to healthy subjects. Symbols represent individual subjects. Each box represents the 25th to 75th percentiles. Other vertical lines represent the median. The upper whisker extends from the hinge to the largest value no further than 1.5 times the upper and lower interquartile range (IQR) from the hinge. The lower whisker extends from the hinge to the smallest value no further than 1.5 times the upper and lower IQR of the hinge.

DISCUSSION

This is the first study to assess inflammatory and structural lesions of the SI joint and spine on MRI in healthy individuals across different age groups and to correlate these findings with demographic and clinical data. In addition, SI joint SPARCC scores were matched with SI joint involvement as detected on MRI in axSpA patients. We revealed several interesting findings with relevant implications for clinical practice. In general, a marked association of both inflammatory and structural lesions of the SI joint and spine was observed in relation to age. A positive MRI for sacroiliitis occurred relatively frequently in healthy subjects ≥ 30 years old, whereas it was rarely detected in younger subjects. Nonetheless, SI joint SPARCC scores were generally low. Strikingly, we found a high prevalence of erosions and fat metaplasia of the SI joint in all age categories; erosions in particular were especially common in subjects ≥ 40 years old. In the spine, BME was mainly detected in subjects ≥ 40 years old, albeit median scores were low. Importantly, spondylitis on MRI defined by ≥ 3 inflammatory corner lesions was only once detected in our study population. The occurrence of MRI lesions was not associated with the presence of HLA-B27, except for higher spinal erosion scores in HLA-B27-positive subjects.

In 2009, the ASAS group proposed a definition of a positive MRI for active sacroiliitis, requesting the presence of subchondral and periarticular BME suggestive of sacroiliitis (2). Notwithstanding an update in 2016 (1), the definition lacks some level of specificity, as recent studies describe a relatively high prevalence of a positive MRI for active sacroiliitis in a non-SpA context, e.g., in postpartum women and healthy individuals displaying a high level of physical activity (3–6). Although the ASAS definition should only be used in patients with an established SpA diagnosis, MRI of the SI joint is often used in the diagnostic evaluation in patients suffering from (chronic) back pain. As a result, the frequent occurrence of a positive MRI for active sacroiliitis in a non-SpA context raises concern and somehow impacts the prominent role of MRI for diagnostic and classification purposes in SpA.

In 2016, the ASAS MRI working group updated the definition of a positive MRI for sacroiliitis, adding that BME observed on STIR or T2-weighted fat suppression or osteitis on T1-weighted fat suppression post-gadolinium must be clearly present in a typical anatomic location in the subchondral bone marrow, and the appearance should be highly suggestive of SpA (1). In particular, the importance of contextual interpretation of both fat-suppressed and T1-weighted scans was emphasized. This

definition was designated for classification purposes rather than for axSpA diagnosis. Raising the threshold for BME or including particular aspects of MRI-detected SI joint lesions to the ASAS definition of a positive MRI may be of interest in discriminating true active sacroiliitis in the context of axSpA from false positives. However, whereas this would increase the specificity, sensitivity may be dramatically reduced. Besides high cutoff values for BME lesions, the localization of the lesions in the SI joint and detection of highly specific MRI lesions constitute alternative approaches to overcome these limitations for axSpA diagnosis.

De Winter et al described active sacroiliitis in 23.4% of the healthy subjects, albeit with low SPARCC scores (mean 1.7) (6). Of note, only 8.5% of the subjects in the present study had a SPARCC score of ≥ 5 . Interestingly, deep BME on MRIs of the SI joint was not observed in the study by De Winter et al. Deep lesions are occasionally seen in women immediately postpartum, a distinct and easy identifiable group, albeit not during follow-up ≥ 6 months later (3). In contrast, Carron et al found a strong correlation between clear tracer uptake on immunoscintigraphy with radiolabeled certolizumab and deep BME on SI joint MRI in axSpA patients (17). Therefore, deep BME lesions could be considered as highly specific for SpA. This finding is consistent with those of Bennet et al, showing that severe sacroiliitis (defined as $>75\%$ of the quadrant involved) had a high specificity for development of ankylosing spondylitis (AS) in patients with early inflammatory back pain (18). Seven and colleagues confirmed the occurrence of SI joint SPARCC scores ≥ 5 solely in axSpA patients and postpartum women, not in other non-SpA subjects (19). Oliveira et al proposed an SI joint BME cutoff of ≥ 3 , implying the highest sensitivity and specificity (20). In addition, the localization of MRI lesions in the joint may discriminate sacroiliitis in the context of SpA from non-specific BME.

In the aforementioned study by de Winter, SI joint BME in healthy subjects was mainly observed in the inferior ilium and in the posterior joint (6). These results are in agreement with the topographic distribution of BME on MRIs of SI joints in athletes, as lesions were mainly detected in the posterior inferior ilium, followed by the anterior superior sacrum (4). Athletes displayed less fat metaplasia compared to BME, whereas erosions of the SI joint were virtually absent (4). Similarly, structural SI joint lesions on MRI were rarely seen in postpartum women (3). The present study significantly expands on these previous findings. Although SI joint BME was frequently detected in subjects ≥ 30 years old, SPARCC scores were low, and deep or intense BME lesions rarely occurred. Notably, SPARCC scores are generally disregarded in routine clinical practice, where a dichotomous assessment (sacroiliitis or no sacroiliitis) is customary.

According to the current ASAS classification criteria for axSpA, inflammatory back pain should have an onset before the age of 45 years. The importance of this age limit is reflected in Supplementary Figure 1 (available on the *Arthritis & Rheumatology* website at <https://onlinelibrary.wiley.com/doi/10.1002/art.42145>).

Above the age of 45 years, SI joint SPARCC scores in healthy subjects and axSpA patients start overlapping, complicating the interpretation of SI joint MRI in those subjects. Consistent with previous studies (4,6), in the present study, healthy subjects displayed the most SI joint BME in the superior sacrum, followed by inferior ilium. The latter anatomic region was most affected in axSpA patients from the Be-GIANT cohort. However, the superior sacrum was also relatively frequently involved. BME on SI joint MRI in healthy subjects is mainly attributed to biomechanical stress. As biomechanical forces may also play a role in the pathophysiology of SpA (21,22), the anatomic dispersion of SI joint BME may be roughly similar to healthy subjects. Thus, additional research seems necessary to explore whether the topographic distribution of BME on SI joint MRI is of added value in the distinction between axSpA and non-axSpA patients.

Importantly, one of the major novelties of our study is the strikingly high prevalence of SI joint erosions and fat metaplasia detected on MRI, also in subjects ages 20–40 years, challenging the interpretation of SI joint MRI in patients with a clinical suspicion of SpA. Whereas the proposed cutoffs for fat metaplasia and erosions with a high specificity for SpA were rarely positive in subjects <40 years old, they were relatively frequently positive in older subjects. These findings are in contrast with the general belief that structural MRI-detected SI joint lesions are specific for SpA and can contribute to a diagnosis of axSpA, particularly in patients with suggestive symptoms but without BME on SI joint MRI. Interestingly, the occurrence of SI joint erosions was associated with higher BMI. This may be important, considering that higher BMI values are also associated with higher C-reactive protein values, further complicating the distinction of SpA in overweight individuals with chronic back pain. Thus, further studies are needed to better define specific MRI lesions and cutoffs that could be integrated in a new ASAS definition of a positive MRI in SpA, considering the age-related imaging abnormalities of SI joint MRI unveiled here in healthy subjects.

Spinal MRI is regarded as an important imaging tool in axSpA. Spondylitis without active sacroiliitis (i.e., BME detected on SI joint MRI) may particularly occur in AS patients with longstanding disease and in axial psoriatic arthritis patients; furthermore, spinal MRI is used to predict TNFi response or to evaluate treatment effect (16,23–25). Therefore, uniform definitions of SpA-related MRI-detected lesions on the spine and a positive MRI for spondylitis are indispensable. In 2012, the ASAS group proposed the threshold of ≥ 3 corner inflammatory lesions as a positive (for spondylitis) MRI of the spine (16). In addition, the presence of fat metaplasia in several vertebral corners was labeled as suggestive of SpA. Two articles by Bennett et al showed ≥ 3 corner inflammatory lesions and ≥ 6 fat lesions as having 97% and 98% specificity for SpA, respectively (24,26). In 2009, the presence of ≥ 2 corner inflammatory lesions on MRI of the spine was identified as the cutoff with the best combination of sensitivity and specificity for SpA (27). Nonetheless, in a study

by Weber et al, none of the mentioned thresholds was later validated as useful in differentiating nonradiographic axSpA from nonspecific back pain patients (28). Six or more corner inflammatory lesions on spinal MRI yielded a moderate diagnostic value, notwithstanding a decreased sensitivity. In a recent large population-based study of 793 volunteers corner inflammatory lesions on MRI of the spine were seen in 27.2% of the subjects, whereas ≥ 5 lesions were rarely observed (0.8%) (7). Five or more corner inflammatory lesions or ≥ 5 fat lesions on spinal MRI were proposed by de Hooge et al as cutoff values, yielding an acceptable discrimination of axSpA patients and subjects with non-SpA chronic back pain, while assuring a specificity above 95% (13). However, Baraliakos et al described fat metaplasia on spinal MRI in 81.4% of the general population, with one-fourth of subjects having ≥ 5 fat lesions (7). In the present study, only limited spinal involvement was detected on MRI. Although one-third of the subjects ages ≥ 40 years displayed spinal BME, inflammation scores were low, and only 1 of the healthy subjects showed ≥ 3 inflammatory corner lesions. Additionally, the occurrence of relevant structural involvement of the spine was rare. No subjects displayed ≥ 3 fat lesions. This is in contrast to the aforementioned study by Baraliakos and colleagues, which demonstrated a high prevalence of spinal fat metaplasia in the general population (7). However, the high prevalence of recent back pain (41%) in those subjects may explain this discrepancy.

Major strengths of the present study were the acquisition of both STIR/TIRM and T1 MRIs of the SI joints and spine in healthy subjects specifically recruited for a lack of back pain, as this has never been done before. The availability of HLA-B27 status is also an important asset. However, the HLA-B27-positive group was small overall and reflected the ethnicity of the subjects. In conclusion, our study revealed the frequent occurrence of both inflammatory and structural SI joint lesions on MRI in healthy subjects, especially in subjects ≥ 40 years old. This finding has important implications for the interpretation of SI joint MRIs in suspected SpA patients, underscoring the importance of the clinical context. In contrast, SpA-like spinal involvement on MRI was rare.

ACKNOWLEDGMENT

We thank the study subjects for their participation.

AUTHOR CONTRIBUTIONS

All authors were involved in drafting the article or revising it critically for important intellectual content, and all authors approved the final version to be published. Dr. Renson had full access to all of the data in the study and takes responsibility for the integrity of the data and the accuracy of the data analysis.

Study conception and design. Renson, de Hooge, De Craemer, Deroo, Carron, Van den Bosch, Elewaut.

Acquisition of data. Renson, de Hooge, De Craemer, Deroo, Herregods, Jans.

Analysis and interpretation of data. Renson, de Hooge, Lukasik, Carron, Colman, Van den Bosch, Elewaut.

REFERENCES

- Lambert RG, Bakker PA, van der Heijde D, Weber U, Rudwaleit M, Hermann KG, et al. Defining active sacroiliitis on MRI for classification of axial spondyloarthritis: update by the ASAS MRI working group. *Ann Rheum Dis* 2016;75:1958–63.
- Rudwaleit M, Jurik AG, Hermann KG, Landewé R, van der Heijde D, Baraliakos X, et al. Defining active sacroiliitis on magnetic resonance imaging (MRI) for classification of axial spondyloarthritis: a consensual approach by the ASAS/OMERACT MRI group. *Ann Rheum Dis* 2009;68:1520–7.
- Renson T, Depickere A, De Craemer AS, Deroo L, Varkas G, de Hooge M, et al. High prevalence of spondyloarthritis-like MRI lesions in postpartum women: a prospective analysis in relation to maternal, child and birth characteristics. *Ann Rheum Dis* 2020;79:929–34.
- Weber U, Jurik AG, Zeijden A, Larsen E, Jorgensen SH, Rufibach K, et al. Frequency and anatomic distribution of magnetic resonance imaging features in the sacroiliac joints of young athletes: exploring "background noise" toward a data-driven definition of sacroiliitis in early spondyloarthritis. *Arthritis Rheumatol* 2018;70:736–45.
- Varkas G, de Hooge M, Renson T, De Mits S, Carron P, Jacques P, et al. Effect of mechanical stress on magnetic resonance imaging of the sacroiliac joints: assessment of military recruits by magnetic resonance imaging study. *Rheumatology (Oxford)* 2018;57:508–13.
- De Winter J, de Hooge M, van de Sande M, de Jong H, van Hooft L, de Koning A, et al. Magnetic resonance imaging of the sacroiliac joints indicating sacroiliitis according to the Assessment of SpondyloArthritis international Society definition in healthy individuals, runners, and women with postpartum back pain. *Arthritis Rheumatol* 2018;70:1042–48.
- Baraliakos X, Richter A, Feldmann D, Ott A, Buelow R, Schmidt CO, et al. Frequency of MRI changes suggestive of axial spondyloarthritis in the axial skeleton in a large population-based cohort of individuals aged <45 years. *Ann Rheum Dis* 2020;79:186–92.
- Van Praet L, Jans L, Carron P, Jacques P, Glorieux E, Colman R, et al. Degree of bone marrow oedema in sacroiliac joints of patients with axial spondyloarthritis is linked to gut inflammation and male sex: results from the GIANT cohort. *Ann Rheum Dis* 2014;73:1186–9.
- Van Praet L, van den Bosch F, Jacques P, Carron P, Jans L, Colman R, et al. Microscopic gut inflammation in axial spondyloarthritis: a multiparametric predictive model. *Ann Rheum Dis* 2013;72:414–7.
- Varkas G, Vastesaeger N, Cypers H, Colman R, Renson T, Van Praet L, et al. Association of inflammatory bowel disease and acute anterior uveitis, but not psoriasis, with disease duration in patients with axial spondyloarthritis: results from two Belgian nationwide axial spondyloarthritis cohorts. *Arthritis Rheumatol* 2018;70:1588–96.
- Maksymowych WP, Inman RD, Salonen D, Dhillon SS, Williams M, Stone M, et al. Spondyloarthritis research Consortium of Canada magnetic resonance imaging index for assessment of sacroiliac joint inflammation in ankylosing spondylitis. *Arthritis Rheum* 2005;53:703–9.
- Weber U, Lambert RG, Østergaard M, Hodler J, Pedersen SJ, Maksymowych WP et al. The diagnostic utility of magnetic resonance imaging in spondylarthritis: an international multicenter evaluation of one hundred eighty-seven subjects. *Arthritis Rheum* 2010;62:3048–58.
- De Hooge M, van den Berg R, Navarro-Compan V, Reijnen M, van Gaalen F, Fagerli K, et al. Patients with chronic back pain of short duration from the SPACE cohort: which MRI structural lesions in the sacroiliac joints and inflammatory and structural lesions in the spine are most specific for axial spondyloarthritis? *Ann Rheum Dis* 2016;75:1308–14.
- Maksymowych WP, Dhillon SS, Park R, Salonen D, Inman RD, Lambert RG. Validation of the spondyloarthritis research consortium

- of Canada magnetic resonance imaging spinal inflammation index: is it necessary to score the entire spine? *Arthritis Rheum* 2007;57:501–7.
15. Krabbe S, Østergaard M, Pedersen SJ, Weber U, Krober G, Maksymowich W, et al. Canada-Denmark MRI scoring system of the spine in patients with axial spondyloarthritis: updated definitions, scoring rules and inter-reader reliability in a multiple reader setting. *RMD Open* 2019;5:e001057.
 16. Hermann KG, Baraliakos X, van der Heijde D, Jurik AG, Landewé R, Marzo-Ortega H, et al. Descriptions of spinal MRI lesions and definition of a positive MRI of the spine in axial spondyloarthritis: a consensual approach by the ASAS/OMERACT MRI study group. *Ann Rheum Dis* 2012;71:1278–88.
 17. Carron P, Renson T, de Hooge M, Lambert B, De Man K, Jans L, et al. Immunoscintigraphy in axial spondyloarthritis: a new imaging modality for sacroiliac inflammation. *Ann Rheum Dis* 2020;79:844–46.
 18. Bennett AN, McGonagle D, O’Conner P, Hensor EM, Coates LC, Emery P, et al. Severity of baseline magnetic resonance imaging-evident sacroiliitis and HLA-B27 status in early inflammatory back pain predict radiographically evident ankylosing spondylitis at eight years. *Arthritis Rheum* 2008;58:3413–8.
 19. Seven S, Østergaard M, Morsel-Carlsen L, Sorensen IJ, Bonde B, Thamsborg G, et al. Magnetic resonance imaging of lesions in the sacroiliac joints for differentiation of patients with axial spondyloarthritis from control subjects with or without pelvic or buttock pain: a prospective, cross-sectional study of 204 participants. *Arthritis Rheumatol* 2019;71:2034–46.
 20. Oliveira TL, Maksymowich WP, Lambert RG, Muccioli C, Fernandes RA, Pinheiro MM. Sacroiliac joint magnetic resonance imaging in asymptomatic patients with recurrent acute anterior uveitis: a proof-of-concept study. *J Rheumatol* 2017;44:1833–40.
 21. Jacques P, Lambrecht S, Verheugen E, Pauwels E, Kollias G, Armaka M, et al. Proof of concept: enthesitis and new bone formation in spondyloarthritis are driven by mechanical strain and stromal cells. *Ann Rheum Dis* 2014;73:437–45.
 22. Jacques P, McGonagle D. The role of mechanical stress in the pathogenesis of spondyloarthritis and how to combat it. *Best Pract Res Clin Rheumatol* 2014;28:703–10.
 23. Rudwaleit M, Schwarzlose S, Hilgert ES, Listing J, Braun J, Sieper J. MRI in predicting a major clinical response to anti-tumour necrosis factor treatment in ankylosing spondylitis. *Ann Rheum Dis* 2008;67:1276–81.
 24. Bennett AN, Rehman A, Hensor EM, Marzo-Ortega H, Emery P, McGonagle D. Evaluation of the diagnostic utility of spinal magnetic resonance imaging in axial spondylarthritis. *Arthritis Rheum* 2009;60:1331–41.
 25. Baraliakos X, Landewé R, Hermann KG, Listing J, Golder W, Brandt J, et al. Inflammation in ankylosing spondylitis: a systematic description of the extent and frequency of acute spinal changes using magnetic resonance imaging. *Ann Rheum Dis* 2005;64:730–4.
 26. Bennett AN, Rehman A, Hensor EM, Marzo-Ortega H, Emery P, McGonagle D. The fatty Romanus lesion: a non-inflammatory spinal MRI lesion specific for axial spondyloarthropathy. *Ann Rheum Dis* 2010;69:891–4.
 27. Weber U, Hodler J, Kubik RA, Rufibach K, Lambert RG, Kissing RO, et al. Sensitivity and specificity of spinal inflammatory lesions assessed by whole-body magnetic resonance imaging in patients with ankylosing spondylitis or recent-onset inflammatory back pain. *Arthritis Rheum* 2009;61:900–8.
 28. Weber U, Zhao Z, Rufibach K, Zubler V, Lambert RG, Chan SM, et al. Diagnostic utility of candidate definitions for demonstrating axial spondyloarthritis on magnetic resonance imaging of the spine. *Arthritis Rheumatol* 2015;67:924–33.

Treatment With Tumor Necrosis Factor Inhibitors Is Associated With a Time-Shifted Retardation of Radiographic Sacroiliitis Progression in Patients With Axial Spondyloarthritis: 10-Year Results From the German Spondyloarthritis Inception Cohort

Murat Torgutalp,¹ Valeria Rios Rodriguez,¹ Fabian Proft,¹ Mikhail Protopopov,¹ Maryna Verba,¹ Judith Rademacher,¹ Hiltrun Haibel,¹ Joachim Sieper,¹ Martin Rudwaleit,² and Denis Poddubnyy³

Objective. To investigate the longitudinal association between radiographic sacroiliitis progression and treatment with tumor necrosis factor inhibitors (TNFi) in patients with early axial spondyloarthritis (SpA) in a long-term inception cohort.

Methods. We included patients from the German Spondyloarthritis Inception Cohort who underwent radiographic assessment of the sacroiliac joints at baseline and at least once more during the 10-year follow-up. Two central readers scored the radiographs according to the modified New York criteria for ankylosing spondylitis. The sacroiliac sum score was calculated as a mean of the scores determined by both readers. TNFi use was assessed according to exposure in the current and/or previous 2-year radiographic interval. The association between TNFi use and radiographic sacroiliitis progression was examined by longitudinal generalized estimating equation analysis with adjustment for potential confounders.

Results. In this long-term inception cohort, 10-year follow-up data on 737 radiographic intervals assessed in 301 patients with axial SpA (166 patients with nonradiographic axial SpA and 135 patients with radiographic axial SpA) were obtained. Having received ≥ 12 months of treatment with TNFi in the previous 2-year radiographic interval was associated with a significant decrease in the sacroiliitis sum score ($\beta = -0.09$ [95% confidence interval (95% CI) $-0.18, -0.003$]; analyses adjusted for age, sex, symptom duration, HLA-B27 status, Bath Ankylosing Spondylitis Disease Activity Index score, C-reactive protein, and nonsteroidal antiinflammatory drug intake). In contrast, among patients receiving TNFi in the current radiographic interval, there was no significant association with change in the sacroiliitis sum score ($\beta = 0.05$ [95% CI $-0.05, 0.14$]). This effect of having received ≥ 12 months of treatment with TNFi in the previous 2-year radiographic interval was stronger in patients with nonradiographic axial SpA as compared to patients with radiographic axial SpA ($\beta = -0.16$ [95% CI $-0.28, -0.03$] versus $\beta = -0.04$ [95% CI $-0.15, 0.07$]).

Conclusion. Treatment with TNFi was associated with the reduction in radiographic sacroiliitis progression in patients with axial SpA. This effect became evident between 2 and 4 years after treatment was initiated.

INTRODUCTION

Axial spondyloarthritis (SpA) is an inflammatory disease characterized by the primary involvement of the sacroiliac joints and the spine (1). According to the paradigm that emerged with the

development of the new Assessment of SpondyloArthritis international Society (ASAS) axial SpA classification criteria (2), axial SpA is considered to be 1 disease with 2 different stages: nonradiographic and radiographic SpA (or ankylosing spondylitis). Over the years, studies on structural damage in axial SpA have focused

Data from this study were presented in part as an oral presentation at the American College of Rheumatology 2021 Convergence (November 5, 2021) and the European Alliance of Associations for Rheumatology 2021 Virtual Congress (June 2, 2021). This report was previously published in abstract form in *Arthritis & Rheumatology* (Baraliakos X. Structural Damage in Axial Spondyloarthritis: Is There a Preferred Way to Assess Progression over Time? [abstract]. *Arthritis Rheumatol* 2021;73 Supplement 9:0159) and *Annals of Rheumatic Disease* (Ann Rheum Dis 2021;80:155).

The German Spondyloarthropathy Inception Cohort (GESPIC) was supported by Abbott/AbbVie, Amgen, Centocor, Schering-Plough, and Wyeth,

and by the German Federal Ministry of Education and Research (BMBF) projects ANCYLOSS (grant FKZ-01-EC1002D), ArthroMark (grants FKZ-01-EC1009A and FKZ-01-EC1401A), and METARTHROS (grant FKZ-01-EC1407A). Dr. Torgutalp's work was supported by an Assessment of SpondyloArthritis international Society (ASAS) fellowship grant.

¹Murat Torgutalp, MD, Valeria Rios Rodriguez, MD, Fabian Proft, MD, Mikhail Protopopov, MD, Maryna Verba, BSc, Judith Rademacher, MD, Hiltrun Haibel, MD, Joachim Sieper, MD: Charité-Universitätsmedizin Berlin, Freie Universität Berlin, and Humboldt-Universität zu Berlin, Berlin, Germany; ²Martin Rudwaleit, MD: University of Bielefeld and Klinikum Bielefeld,

on assessing radiographic progression in the spine (3) as one of the main factors that determines functional status and spinal mobility (4,5). However, a recent study has shown that sacroiliac radiographic damage could also have an independent impact on these outcomes (6).

The introduction of biologic disease-modifying antirheumatic drugs (bDMARDs), and specifically tumor necrosis factor inhibitors (TNFi), has lead researchers to investigate whether these drugs modify the course of SpA and whether they can reduce the progression of structural damage in the axial skeleton. These effects seem to be possible in the spine if treatment with TNFi is given for at least 4 years (7–10), and the findings of 2 recent studies have indicated that such an effect is also possible in the sacroiliac joints (11,12). However, there is still a lack of data on the long-term effects of TNFi on radiographic sacroiliitis progression in patients with early axial SpA. In the present study, we aimed to investigate the association between TNFi treatment and radiographic sacroiliitis progression in axial SpA patients from a long-term inception cohort with a 10-year follow-up period.

PATIENTS AND METHODS

Patient selection and description of the cohort. The design and a detailed description of the GESPIC (German Spondyloarthritis Inception Cohort) have been reported elsewhere (13–15). Briefly, patients included in the GESPIC were required to have a definite clinical diagnosis of axial SpA according to a local rheumatologist, with a symptom duration of up to 5 years for nonradiographic axial SpA and up to 10 years for radiographic axial SpA. In the present study, we classified patients as having radiographic axial SpA if definite radiographic sacroiliitis was present according to the modified New York classification criteria (16) and as having nonradiographic axial SpA otherwise. If the findings of the radiographic sacroiliitis assessment completed by the central readers (as described below) differed from those of the local rheumatologist, we applied the central reader classification. Of 525 patients with axial SpA included in the GESPIC, we selected 301 based on the availability of sacroiliac joint radiographs at baseline and at least 1 more time point during a 10-year follow-up period (see Supplementary Figure 1, available on the *Arthritis & Rheumatology* website at <http://onlinelibrary.wiley.com/doi/10.1002/art.42144>).

Ethics approval. The study protocol was approved by the ethics committee of the coordinating center (Charité–Universitätsmedizin Berlin, Germany) and by local ethics committees of

participating centers and conducted in accordance with the Declaration of Helsinki and Guidelines for Good Clinical Practice. All patients included in the study provided written consent to participate.

Demographic, clinical, and laboratory data. Clinical and laboratory assessments were performed at baseline and every 6 months until year 2 and annually thereafter. Age, sex, HLA–B27 positivity or negativity, and symptom duration were collected at baseline. Disease activity was assessed using the Bath Ankylosing Spondylitis Disease Activity Index (BASDAI) (17), C-reactive protein (CRP) level, and the Ankylosing Spondylitis Disease Activity Score (ASDAS) (18). Treatment of patients in the GESPIC was conducted at the discretion of the local rheumatologist without any restrictions. Because the start of the cohort coincided with the early phase of the introduction of TNFi treatment for axial SpA, only a small number of patients included in the study received TNFi at baseline. Data related to treatment with nonsteroidal antiinflammatory drugs (NSAIDs) were collected at every visit and the ASAS index of NSAID intake in patients with axial SpA (19) was calculated.

Evaluation of radiographs. All available radiographs of the sacroiliac joints of patients with axial SpA (up to 6 time points per patient: baseline, year 2, year 4, year 6, year 8, and year 10) were independently scored by 2 trained central readers (MT and VRR) who were blinded with regard to all demographic and clinical data, but not to the chronology of the radiographs. Radiographs were scored for disease severity using the radiographic grading system in the modified New York classification criteria. According to this system, each sacroiliac joint was scored as normal (grade 0), exhibiting clinically suspicious changes (grade 1), showing minimal abnormality including subchondral sclerosis or erosions but unaffected joint space (grade 2), having unequivocal abnormality with joint space narrowing, widening, or partial ankylosis (grade 3), or having severe abnormality including total ankylosis (grade 4). Using the same system, patients were classified as having radiographic axial SpA if both readers recorded the presence of definitive radiographic sacroiliitis (at least grade 2 bilaterally or at least grade 3 unilaterally); otherwise, patients were classified as having nonradiographic axial SpA (14).

Statistical analysis. At each time point, 2 readers assessed the sacroiliitis sum score in the right and left sacroiliac joints (score range 0–4 on each side), and added the scores to obtain the final sacroiliitis sum score (ranging 0–8). The mean

Bielefeld, Germany; ³Denis Poddubnyy, MD, MSc: Charité–Universitätsmedizin Berlin, Freie Universität Berlin, Humboldt-Universität zu Berlin, and German Rheumatism Research Center, Berlin, Germany.

Author disclosures are available at <https://onlinelibrary.wiley.com/action/downloadSupplement?doi=10.1002%2Fart.42144&file=art42144-sup-0001-Disclosureform.pdf>.

Address correspondence to Murat Torgutalp, MD, Department of Gastroenterology, Infectiology, and Rheumatology, Charité–Universitätsmedizin Berlin, Campus Benjamin Franklin, Haus II, Hindenburgdamm 30, 12203 Berlin, Germany. Email: murat.torgutalp@charite.de.

Submitted for publication January 1, 2022; accepted in revised form April 12, 2022.

score of the 2 readers was used for each time point (6,14). We evaluated the agreement between readers using the intraclass correlation coefficient (ICC) for sacroiliitis sum score and using Cohen's kappa for classification of axial SpA as nonradiographic or radiographic. With respect to missing radiographic data at a time point, if scores for the previous time point and the following time point were available, and if these time points had the same grade/classification status, we imputed the same grade/classification status for the missing time point (a detailed explanation of the imputations with examples is presented in the Supplementary Methods, available at <http://onlinelibrary.wiley.com/doi/10.1002/art.42144>). No other imputations were performed.

The primary outcome in the present study was radiographic disease progression assessed as change in the sacroiliitis sum score between 2 time points. In addition, we evaluated the following 4 binary endpoints as secondary outcomes in the 2-year intervals: 1) progression by at least 1 grade in at least 1 sacroiliac joint according to the opinion of both readers; 2) progression by at least 1 grade in at least 1 sacroiliac joint according to the opinion of both readers (except progression from 0 to 1); 3) progression by at least 1 grade in the sacroiliitis sum score; 4) progression from nonradiographic axial SpA to radiographic axial SpA according to the opinion of both readers.

Regarding TNFi exposure, we constructed the following 5 variables depending on the duration of TNFi treatment in previous and/or current 2-year radiographic intervals (see Supplementary Figure 2, available at <http://onlinelibrary.wiley.com/doi/10.1002/art.42144>): 1) any TNFi treatment in the current 2-year interval; 2) TNFi treatment for ≥ 12 months in the current 2-year interval; 3) any TNFi treatment in the previous 2-year interval; 4) TNFi treatment for ≥ 12 months in the previous 2-year interval; 5) TNFi treatment for ≥ 12 months in the previous 2-year interval and for ≥ 12 months in the current 2-year interval. The following variables potentially affecting radiographic sacroiliitis progression were identified as potential confounders and were included in the multivariable analysis: age, sex, symptom duration, HLA-B27 status, disease activity (as assessed using the BASDAI and CRP level, or using the ASDAS), TNFi treatment, and NSAID intake, according to the relevant literature (14,20–22). Among these predefined variables, we included age and symptom duration at the beginning of each 2-year radiographic interval and time-averaged values of the BASDAI score, CRP level, ASDAS, and NSAID intake score during the current 2-year radiographic interval in the analyses.

We examined the association between TNFi treatment and radiographic sacroiliitis progression over time by using linear and binomial (depending on the outcome variable) generalized estimating equations (GEE), which consider repeated measures within a patient. An autoregressive correlation structure was used for the models. Parameter estimates (β) or odds ratios, whichever is appropriate, are reported with corresponding 95% confidence intervals (95% CIs).

RESULTS

Patient characteristics. According to their baseline characteristics, 301 patients met the inclusion criteria for the present study: 166 patients with nonradiographic axial SpA and 135 patients with radiographic SpA with at least one 2-year radiographic interval (baseline and at least 1 other time point). Patients from the GESPIC who were included in the study were older and less likely to be male (see Supplementary Table 1, available at <http://onlinelibrary.wiley.com/doi/10.1002/art.42144>) compared to patients who were excluded. Among the patients included in the study, those with radiographic axial SpA were more frequently male, were more frequently HLA-B27-positive, had longer symptom durations, and had higher CRP values compared to patients with nonradiographic axial SpA, but were also younger and had lower BASDAI scores (Table 1).

After sacroiliitis sum scores and classification statuses were imputed for the missing time points, a total of 737 2-year radiographic intervals were assessed for the patients included in the study (see Supplementary Table 2, available at <http://onlinelibrary.wiley.com/doi/10.1002/art.42144>). At baseline, 9 patients (3.0%) had been treated with TNFi, and a total of 87 patients (28.9%) had received treatment with at least 1 TNFi during the entire follow-up period. In total, patients received treatment with TNFi for any duration within 141 radiographic intervals, while in 109 intervals patients received treatment with TNFi for at least 12 months.

Assessment of progression and reliability analyses of sacroiliitis. The mean change in the sacroiliitis sum score for the entire patient population was mean \pm SD 0.25 ± 0.40 per 2-year interval. Table 2 shows the change in sacroiliitis sum score and rate of radiographic progression in binary outcomes (yes versus no) for each of the different definitions of TNFi exposure in the whole axial SpA group and in the radiographic and nonradiographic axial SpA subgroups. There was good agreement between the 2 readers regarding the sacroiliitis sum score, with ICC values ranging from 0.83 to 0.87 and moderate agreement regarding classification status, with Cohen's kappa coefficient values ranging from 0.39 to 0.55 for each time point (see Supplementary Table 3, available at <http://onlinelibrary.wiley.com/doi/10.1002/art.42144>).

Longitudinal analyses of the association between treatment with TNFi and change in sacroiliitis sum score. We excluded a total of 4 patients with a mean sacroiliitis sum score of 8 (complete ankylosis) from the longitudinal GEE analyses. In univariable analyses, definitions including exposure to TNFi in the previous 2-year interval were associated with a significant reduction in radiographic progression based on the sacroiliitis sum score, whereas radiographic sacroiliitis progression in patients receiving TNFi in the current 2-year interval did

Table 1. Demographic and baseline clinical characteristics of axial SpA patients from the German Spondyloarthritis Inception Cohort (GESPIC) included in the present study*

Parameter	All axial SpA patients (n = 301)	Nonradiographic axial SpA patients (n = 166)	Radiographic axial SpA patients (n = 135)
Age, mean \pm SD years	36.7 \pm 10.5	38.0 \pm 10.5	35.1 \pm 10.2
Men	146 (48.5)	59 (35.5)	87 (64.4)
Symptom duration, mean \pm SD years	3.9 \pm 2.6	3.0 \pm 2.1	5.1 \pm 2.7
Current smoker	77 (25.6)	34 (20.5)	43 (31.9)
Clinical characteristics			
HLA-B27 positive	231 (77.8)	116 (70.7)	115 (86.5)
Positive family history for SpA	106 (35.2)	65 (39.2)	41 (30.4)
Peripheral arthritis, current	41 (13.6)	24 (14.5)	17 (12.6)
Enthesitis, current†	62 (20.6)	43 (25.9)	19 (14.1)
Dactylitis, current	19 (6.3)	10 (6.0)	9 (6.7)
Uveitis, ever	52 (17.3)	23 (13.9)	29 (21.5)
Psoriasis, ever	38 (12.6)	24 (14.5)	14 (10.4)
IBD, ever	8 (2.7)	2 (1.2)	6 (4.4)
CRP level, mean \pm SD mg/liter	10.6 \pm 17.3	9.2 \pm 15.5	12.1 \pm 19.2
Elevated CRP level (>6 mg/liter)	111 (38.0)	49 (30.6)	62 (47.0)
Disease activity and function assessment scores, mean \pm SD			
ASDAS-CRP	2.53 \pm 0.97	2.63 \pm 0.94	2.40 \pm 1.00
BASDAI, NRS points	3.9 \pm 2.1	4.4 \pm 2.1	3.3 \pm 2.0
BASFI, NRS points	2.8 \pm 2.3	3.0 \pm 2.4	2.6 \pm 2.2
BASMI, NRS points	1.6 \pm 1.6	1.5 \pm 1.5	1.8 \pm 1.7
Treatment			
NSAIDs	203 (67.4)	119 (71.7)	84 (62.2)
DMARDs	80 (26.6)	44 (26.5)	36 (26.7)
TNFi	9 (3.0)	4 (2.4)	5 (3.7)
Systemic steroids	26 (8.6)	19 (11.4)	7 (5.2)

* Except where indicated otherwise, values are the number (%) of patients. SpA = spondyloarthritis; GESPIC = German Spondyloarthritis Inception Cohort; IBD = inflammatory bowel disease; CRP = C-reactive protein; ASDAS-CRP = Ankylosing Spondylitis Disease Activity Score using CRP level; BASDAI = Bath Ankylosing Spondylitis Disease Activity Index; NRS = numerical rating scale; BASFI = Bath Ankylosing Spondylitis Functional Index; BASMI = Bath Ankylosing Spondylitis Metrology Index; NSAIDs = nonsteroidal antiinflammatory drugs; DMARDs = disease-modifying antirheumatic drugs; TNFi = tumor necrosis factor inhibitor.

† Assessed using the 12-point Berlin Index in the lower legs.

not differ from those who did not receive treatment with TNFi (see Supplementary Table 4, available at <http://onlinelibrary.wiley.com/doi/10.1002/art.42144>). In adjusted multivariable analyses of 603 radiographic intervals, TNFi treatment for ≥ 12 months in the previous 2-year interval was associated with significantly lower radiographic sacroiliitis progression as compared to no TNFi treatment in the previous 2-year interval ($\beta = -0.09$ [95% CI $-0.18, -0.003$]) (Figure 1 and Supplementary Table 4). The given parameter estimate (β) indicates that patients who received treatment with a TNFi for ≥ 12 months in the previous 2-year interval had a 0.09-point lower sacroiliitis progression sum score compared to those not treated with a TNFi for ≥ 12 months.

The decelerating effect of treatment with TNFi on radiographic sacroiliitis progression showed a similar trend in different models, including in the model in which TNFi exposure was defined as treatment with TNFi for ≥ 12 months in the current 2-year interval, and in the models in which exposure to TNFi was defined as any treatment with TNFi in the previous 2-year interval and treatment with TNFi for ≥ 12 months in the previous and the current 2-year intervals (see Supplementary Table 4, available at

<http://onlinelibrary.wiley.com/doi/10.1002/art.42144>). Conversely, any TNFi use in the current 2-year interval was not associated with a reduction in radiographic sacroiliitis progression (see Supplementary Table 4, available at <http://onlinelibrary.wiley.com/doi/10.1002/art.42144>). Figure 2 shows the cumulative probability of radiographic progression of sacroiliitis according to change in sacroiliitis sum score in patients who were exposed to TNFi in the different interval and duration of use categories versus those who were not exposed to TNFi. A significant reduction in progression of radiographic sacroiliitis was seen in patients receiving treatment with TNFi for ≥ 12 months in the previous 2-year interval, whereas treatment with TNFi in the current interval showed no association with a reduction in radiographic sacroiliitis progression. The same associations between treatment with TNFi and radiographic sacroiliitis progression were confirmed when disease activity was assessed using the ASDAS instead of CRP level and BASDAI score (see Supplementary Table 5, available at <http://onlinelibrary.wiley.com/doi/10.1002/art.42144>).

In analyzing the association between TNFi exposure and radiographic sacroiliitis progression stratified by nonradiographic

Table 2. Progression in sacroiliitis sum scores and binary outcomes among all axial SpA patients and within the subsets of radiographic and nonradiographic axial SpA according to different definitions of TNFI exposure*

	Any TNFI use in the current 2-year interval		TNFI use for ≥ 12 months in the current 2-year interval		Any TNFI use in the previous 2-year interval		TNFI use for ≥ 12 months in the previous 2-year interval		TNFI use for ≥ 12 months in the previous 2-year interval and for ≥ 12 months in the current 2-year interval	
	No	Yes	No	Yes	No	Yes	No	Yes	No	Yes
All axial SpA patients										
Progression in sacroiliitis sum score, mean \pm SD; no. of patients	0.24 \pm 0.39; 578	0.29 \pm 0.44; 134	0.26 \pm 0.40; 608	0.23 \pm 0.39; 104	0.27 \pm 0.41; 582	0.19 \pm 0.33; 93	0.27 \pm 0.41; 611	0.15 \pm 0.28; 64	0.26 \pm 0.40; 653	0.15 \pm 0.29; 52
Progression ≥ 1 grade in at least 1 SI joint in the opinion of both readers	28/661 (4.2)	7/166 (4.2)	31/696 (4.5)	4/131 (3.1)	32/658 (4.9)	2/116 (1.7)	34/692 (4.9)	0/82 (0.0)	34/751 (4.5)	0/67 (0.0)
Progression ≥ 1 grade in at least 1 SI joint in the opinion of both readers (except 0 to 1)	20/661 (3.0)	7/166 (4.2)	23/696 (3.3)	4/131 (3.1)	24/658 (3.6)	2/116 (1.7)	26/692 (3.8)	0/82 (0.0)	26/751 (3.5)	0/67 (0.0)
Progression ≥ 1 grade in the sacroiliitis sum score	55/563 (9.8)	17/134 (12.7)	61/593 (10.3)	11/104 (10.6)	62/567 (10.9)	7/93 (7.5)	66/596 (11.1)	3/64 (4.7)	68/638 (10.7)	3/52 (5.8)
Radiographic axial SpA patients										
Progression in the sacroiliitis sum score, mean \pm SD; no. of patients	0.20 \pm 0.37; 261	0.23 \pm 0.39; 70	0.21 \pm 0.38; 274	0.19 \pm 0.32; 57	0.22 \pm 0.39; 269	0.15 \pm 0.29; 47	0.22 \pm 0.39; 283	0.12 \pm 0.28; 33	0.21 \pm 0.38; 301	0.14 \pm 0.30; 28
Progression ≥ 1 grade in at least 1 SI joint in the opinion of both readers	12/277 (4.3)	4/85 (4.7)	13/292 (4.5)	3/70 (4.3)	15/286 (5.2)	1/58 (1.7)	16/303 (5.3)	0/41 (0.0)	16/325 (4.9)	0/34 (0.0)
Progression ≥ 1 grade in at least 1 SI joint in the opinion of both readers (except 0 to 1)	12/277 (4.3)	4/85 (4.7)	13/292 (4.5)	3/70 (4.3)	15/286 (5.2)	1/58 (1.7)	16/303 (5.3)	0/41 (0.0)	16/325 (4.9)	0/34 (0.0)
Progression ≥ 1 grade in the sacroiliitis sum score	23/246 (9.3)	7/70 (10.0)	25/259 (9.7)	5/57 (8.8)	26/254 (10.2)	3/47 (6.4)	27/268 (10.1)	2/33 (6.1)	28/286 (9.8)	2/28 (7.1)
Nonradiographic axial SpA patients										
Progression in the sacroiliitis sum score, mean \pm SD; no. of patients	0.28 \pm 0.40; 317	0.36 \pm 0.49; 64	0.30 \pm 0.41; 334	0.27 \pm 0.45; 47	0.31 \pm 0.42; 313	0.23 \pm 0.36; 46	0.31 \pm 0.42; 328	0.18 \pm 0.28; 31	0.30 \pm 0.42; 352	0.17 \pm 0.28; 24
Progression ≥ 1 grade in at least 1 SI joint in the opinion of both readers	16/384 (4.2)	3/81 (3.7)	18/404 (4.5)	1/61 (1.6)	17/372 (4.6)	1/58 (1.7)	18/389 (4.6)	0/41 (0.0)	18/426 (4.2)	0/33 (0.0)
Progression ≥ 1 grade in at least 1 SI joint in the opinion of both readers (except 0 to 1)	8/384 (2.1)	3/81 (3.7)	10/404 (2.5)	1/61 (1.6)	9/372 (2.4)	1/58 (1.7)	10/389 (2.6)	0/41 (0.0)	10/426 (2.3)	0/33 (0.0)
Progression ≥ 1 grade in sacroiliitis sum score	32/317 (10.1)	10/64 (15.6)	36/334 (10.8)	6/47 (12.8)	36/313 (11.5)	4/46 (8.7)	39/328 (11.9)	1/31 (3.2)	40/352 (11.4)	1/24 (4.2)
Progression from nonradiographic to radiographic axial SpA in the opinion of both readers	38/340 (11.2)	5/37 (13.5)	32/325 (9.8)	11/52 (21.2)	38/322 (11.8)	4/29 (13.8)	41/331 (12.4)	1/20 (5.0)	41/356 (11.5)	1/15 (6.7)

* Except where indicated otherwise, values are the number/total number (%) of patients. For all definitions of progression, available data on TNFI exposure in the corresponding interval were used. Numeric differences regarding TNFI exposure between the current and the previous interval were due to missing information on TNFI exposure in the previous interval. Numeric differences regarding the definitions of progression were due to different imputation methods (for a detailed explanation, see the Patients and Methods section and the Supplementary Methods, available at <http://onlinelibrary.wiley.com/doi/10.1002/art.42144>). SI = sacroiliac (see Table 1 for other definitions).

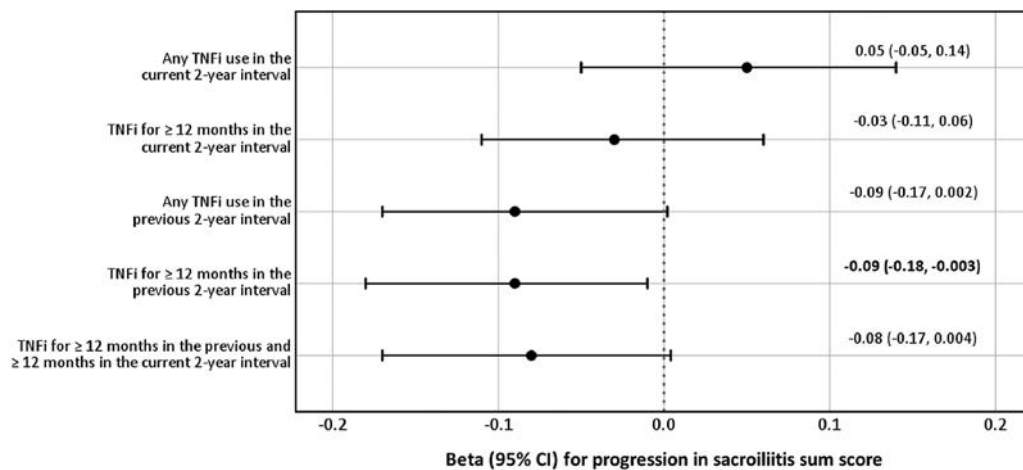


Figure 1. Forest plots indicating associations between treatment with tumor necrosis factor inhibitors (TNFi) according to different definitions of exposure and progression in sacroiliitis sum score in patients with axial spondyloarthritis (SpA), as determined using multivariable longitudinal generalized estimating equations including 603 2-year radiographic intervals from 297 patients. Parameter estimates (closed circles) and accompanying 95% confidence intervals (95% CIs; whiskers) indicate the likelihood of change in sacroiliitis sum score over 2 years in patients who received treatment with TNFi compared to patients who did not receive TNFi. For example, TNFi treatment for ≥ 12 months in the previous interval was associated with a reduction in sacroiliitis sum score compared to no treatment with TNFi for ≥ 12 months in the previous interval ($\beta = -0.09$ [95% CI $-0.18, -0.003$]). Parameter estimates were adjusted for sex, age at the beginning of the current 2-year interval, HLA-B27 status, symptom duration at the beginning of current 2-year interval, time-averaged elevated C-reactive protein level, time-averaged Bath Ankylosing Spondylitis Disease Activity Index score, and time-averaged nonsteroidal antiinflammatory drug intake score in the current 2-year interval.

and radiographic axial SpA, we observed that exposure to TNFi in the previous 2-year interval had a stronger effect on radiographic sacroiliitis progression in both univariable and adjusted multivariable analyses in patients with nonradiographic axial SpA compared to patients with radiographic axial SpA (Table 3). In

patients with nonradiographic axial SpA, TNFi exposure for ≥ 12 months in the previous 2-year interval and exposure for ≥ 12 months in both the previous and the current intervals were associated with a reduction in sacroiliitis sum score of 0.16 and 0.19 points, respectively, compared to TNFi-unexposed patients.

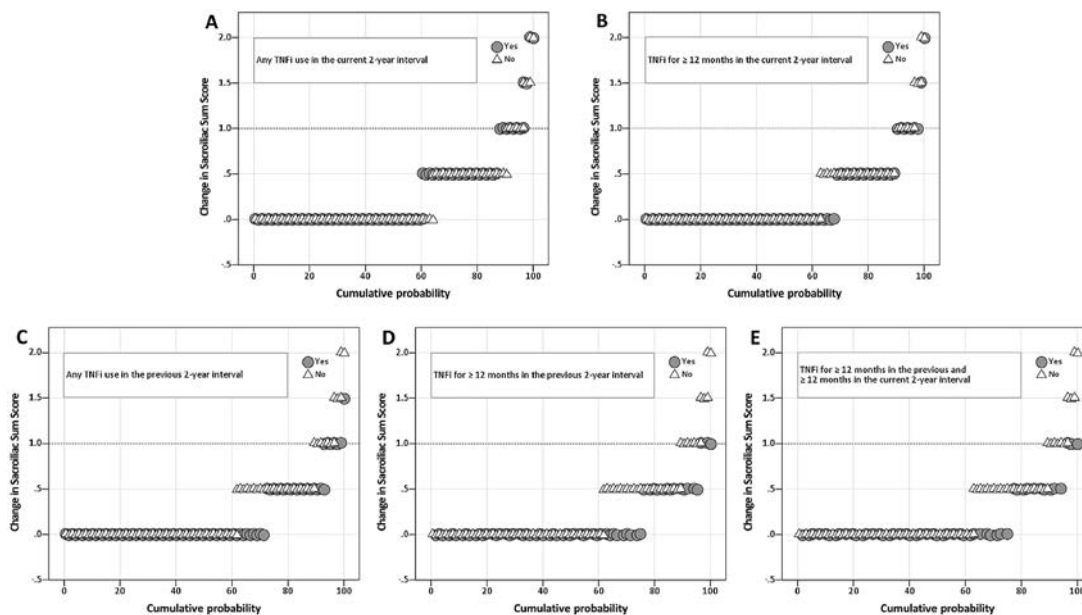


Figure 2. Cumulative probability plots of the 2-year progression in sacroiliitis sum score in patients with axial spondyloarthritis according to exposure to tumor necrosis factor inhibitors (TNFi), including any TNFi use in the current 2-year interval (A), TNFi use for ≥ 12 months in the current 2-year interval (B), any TNFi use in the previous 2-year interval (C), TNFi use for ≥ 12 months in the previous 2-year interval (D), and TNFi use for ≥ 12 months in the previous and current 2-year intervals (E). Symbols represent individual patients.

Table 3. Longitudinal generalized estimating equation analysis of the association between progression in sacroiliitis sum score and TNFi exposure in patients with nonradiographic axial SpA and patients with radiographic axial SpA*

Definition of TNFi exposure	Referent	Nonradiographic axial SpA patients		Radiographic axial SpA patients	
		Univariable β (95% CI)	Multivariable β (95% CI) [†]	Univariable β (95% CI)	Multivariable β (95% CI) [†]
Any use in the current 2-year interval	No use in the current 2-year interval	0.09 (-0.44, 0.22)	0.06 (-0.06, 0.18)	0.03 (-0.08, 0.14)	0.07 (-0.05, 0.19)
Use for ≥ 12 months in the current 2-year interval	No use for ≥ 12 months in the current 2-year interval	-0.04 (-0.18, 0.11)	-0.08 (-0.19, 0.04)	-0.02 (-0.12, 0.09)	0.03 (-0.07, 0.14)
Any use in the previous 2-year interval	No use in the previous 2-year interval	-0.10 (-0.22, 0.02)	-0.13 (-0.25, 0.001)	-0.08 (-0.18, 0.02)	-0.04 (-0.16, 0.08)
Use for ≥ 12 months in the previous 2-year interval	No use for ≥ 12 months in the previous 2-year interval	-0.13 (-0.23, -0.02)	-0.16 (-0.28, -0.03)	-0.10 (-0.19, -0.01)	-0.04 (-0.15, 0.07)
Use for ≥ 12 months in the previous 2-year interval and in the current 2-year interval	No use for ≥ 12 months in the previous 2-year interval and in the current 2-year interval	-0.15 (-0.26, -0.04)	-0.19 (-0.32, -0.07)	-0.07 (-0.17, 0.03)	-0.01 (-0.12, 0.11)

* Values are the parameter estimates (β) with 95% confidence intervals (95% CIs) for the likelihood of change in sacroiliac sum score in each TNFi exposure category relative to the indicated no exposure referent category, as determined in univariable and adjusted multivariable analyses of 318 radiographic intervals assessed in patients with nonradiographic axial SpA and 285 radiographic intervals assessed in patients with radiographic axial SpA.

[†] Parameter estimates from the multivariable models were adjusted for sex, age at the beginning of the current 2-year interval, HLA-B27 status, symptom duration at the beginning of the current 2-year interval, time-averaged elevated CRP level, time-averaged BASDAI score, and time-averaged NSAID intake score in the current 2-year interval. See Table 1 for other definitions.

In patients with radiographic axial SpA, TNFi exposure for ≥ 12 months in the previous 2-year interval and exposure for ≥ 12 months in both the previous and the current intervals were associated with a reduction in sacroiliitis sum score of 0.04 and 0.01 points, respectively.

Analyses of the secondary outcomes. Secondary outcomes included 4 binary definitions of radiographic sacroiliitis progression: 1) progression by at least 1 grade in at least 1 sacroiliac joint according to the opinion of both readers; 2) progression by at least 1 grade in at least 1 sacroiliac joint according to the opinion of both readers (except progression from 0 to 1); 3) progression by at least 1 grade in the sacroiliitis sum score; 4) progression from nonradiographic axial SpA to radiographic axial SpA according to the opinion of both readers. We excluded 9 patients who had a sacroiliitis sum score >7 to analyze radiographic progression for the first 3 secondary outcome variables. There were no intervals with progression according to definitions 1 and 2 in patients who received treatment with TNFi for ≥ 12 months in the previous 2-year radiographic interval or in patients who received treatment with TNFi for ≥ 12 months in both the previous and the current 2-year intervals (see Supplementary Tables 6 and 7, available at <http://onlinelibrary.wiley.com/doi/10.1002/art.42144>). Among all TNFi exposure and interval groups, we observed a trend toward a significant reduction in the odds of radiographic sacroiliitis progression based on a reduction by at least 1 grade in the sacroiliitis sum score (see Supplementary Table 8, available at <http://onlinelibrary.wiley.com/doi/10.1002/art.42144>).

For progression from nonradiographic to radiographic axial SpA, we assessed 311 radiographic intervals from 166 patients with nonradiographic axial SpA and observed that exposure to TNFi in the previous 2-year interval, but not the current interval, was associated with a reduction in radiographic sacroiliitis progression (see Supplementary Table 9, available at <http://onlinelibrary.wiley.com/doi/10.1002/art.42144>).

DISCUSSION

In the present study, we evaluated the association between TNFi therapy and radiographic sacroiliitis progression in patients with axial SpA using long-term follow-up data (up to 10 years) from a large inception cohort. We found that TNFi therapy was associated with a reduction in radiographic sacroiliitis progression in patients with axial SpA; however, a reduction in radiographic progression was only evident 2–4 years after TNFi therapy was initiated. Of note, this effect was present in the setting of both nonradiographic and radiographic axial SpA but was stronger in nonradiographic axial SpA patients. Furthermore, reduction in radiographic progression was consistent across all explored outcome definitions (sacroiliitis sum score and binary progression definitions). Reduction in radiographic sacroiliitis progression was greater in patients who received treatment with TNFi continuously during the 2-year intervals analyzed (i.e., patients received treatment for at least half of the interval). Importantly, we analyzed the long-term results in an inception cohort, meaning that the majority of the patients included in this study were at the early

disease stage in terms of structural damage progression. The GESPIC began before TNFi therapy became widely available for the treatment of axial SpA. This may have reduced the likelihood that channeling bias affected our results, as patients with more active axial SpA are currently more likely to be treated with bDMARDs than patients with milder and potentially less progressive disease.

The results of this study are consistent with those from studies of radiographic progression in the spine. Several studies have demonstrated that the effect of TNFi therapy on radiographic spinal progression becomes evident only after at least 4 years of treatment (7–10). Whether this duration of treatment affect also applies to efforts to modify radiographic progression in the sacroiliac joints has not been clarified previously, although a recent analysis of a TNFi interventional trial of etanercept to treat early axial SpA suggested that 2 years of treatment might be insufficient to allow for a clear reduction in progression of structural damage associated with an effective antiinflammatory treatment (12).

How can the results of this study be explained in the context of the pathophysiology of axial SpA? In the spine, the inflammation process is followed by repair characterized by the transformation of inflamed tissue in the subchondral bone marrow into fibrous repair tissue, which can be detected on magnetic resonance imaging (MRI) as fatty lesions (23,24). New bone formation is subsequently activated (3). The same sequence (inflammation, repair, new bone formation) could be confirmed in axial SpA through the use of longitudinal data from interventional studies comprising both radiography and MRI of the spine (25,26). We expect that the pathophysiologic process leading to structural changes in the sacroiliac joints follows the same pathway as that in the spine. It could also have been expected that osteodestructive components such as erosion resulting from inflammation would have been stopped early by effective antiinflammatory treatment, as suggested by the findings from a recent interventional study of etanercept to treat nonradiographic axial SpA (11). However, we did not observe such an immediate effect of TNFi treatment in terms of early activation of tissue repair after suppression of inflammation in the GESPIC cohort.

Our findings have clinical relevance for the treatment of axial SpA. The relevance of radiographic sacroiliitis progression to the functional status of patients with axial SpA appears to be minor (6); however, inhibition of structural damage progression in the axial skeleton (sacroiliac joints and spine) is conceptually important for any treatment resulting in disease modification.

Our study had some limitations. The first limitation was the risk of selection bias due to the exclusion of patients without at least 2 sets of radiographs. Assuming that it is practically impossible to conduct a randomized controlled trial on radiographic progression, analysis of cohort data is in fact the only way to address the issue of structural damage progression in the sacroiliac joints in axial SpA. In the present work, we attempted to estimate the effects of TNFi exposure on radiographic sacroiliitis progression as precisely as possible using an adjusted longitudinal GEE analysis, which gave us the opportunity to

assess within-patient effects. Compared to the GESPIC patients included in this study, patients who were excluded were younger, more often male, and probably had less severe disease (i.e., less psoriasis, lower BASMI scores, and lower frequency of DMARD use).

The second limitation was the absence of MRI data, which would have been helpful for more precisely addressing the link between inflammation and new bone formation in the sacroiliac joints. Unfortunately, since patient enrollment in the GESPIC cohort began in the early 2000s, MRI was not part of the study protocol. Instead, we used CRP level as a covariate to reflect an objective sign of inflammation.

The third limitation was the reliance on only conventional radiographs of the sacroiliac joints to evaluate the progression of structural damage. It is possible that with low-dose computed tomography or MRI, progression (or retardation) of structural damage could have been detected earlier than 2–4 years after initiation of TNFi therapy, and it could have been detected in a more reliable way. We did not observe any regression of radiographic sacroiliitis according to radiographic progression scores assessed on radiographs in known chronologic order, which could be considered an additional limitation as this could have resulted in the overestimation of progression. However, we chose this approach to increase sensitivity to change (27) and to reduce background noise not related to real structural changes.

Finally, the only bDMARDs administered to patients in the present study were TNFi, and therefore we do not know whether our findings are also applicable to patients receiving treatment with other bDMARDs such as interleukin-17 inhibitors. In summary, this study demonstrated that treatment with TNFi was associated with a deceleration of radiographic sacroiliitis progression in axial SpA patients that became evident between 2 and 4 years after initiation of treatment.

ACKNOWLEDGMENTS

We thank Professor M. Leirisalo-Repo, Professor D. van der Heijde, and Professor M. Dougados for their scientific advice on the design of the cohort. We are grateful to Beate Buss, Petra Tietz, and Annegret Langdon for monitoring the cohort, to Johanna Callhoff, Anja Weiss, Joachim Listing, and Martina Niewerth for data management support and statistical advice, to Torsten Karge for the development of the image scoring interface, and to all the patients who voluntarily participated in the GESPIC. We would also like to thank the following rheumatologists for inclusion of their patients: J. Brandt, H. Brandt, G.-R. Burmester, H. Deister, E. Edelmann, J. Emmerich, M. Enderlein, A. Gauliard, E. Gromnica-Ihle, F. Heldmann, S. Hermann, U. von Hinüber, Ü. Hübner, K. Karberg, H. Nüßlein, R. Pelle-Lohfink, D. Pick, G. Reichmuth, E. Riechers, M. Rühl, R. Schmidt, S. Schnarr, U. Schneider, I.-H. Song, I. Spiller, U. Syrbe, V. Walz, S. Wassenberg, H. M. Wisseler, and S. Zinke. Open Access funding enabled and organized by Projekt DEAL.

AUTHOR CONTRIBUTIONS

All authors were involved in drafting the article or revising it critically for important intellectual content, and all authors approved the final version to be published. Dr. Torgutalp had full access to all of the data in

the study and takes responsibility for the integrity of the data and the accuracy of the data analysis.

Study conception and design. Sieper, Rudwaleit, Poddubnyy.

Acquisition of data. Torgutalp, Rodriguez, Proft, Protopopov, Rademacher, Haibel, Poddubnyy.

Analysis and interpretation of data. Torgutalp, Verba, Poddubnyy.

ROLE OF THE STUDY SPONSOR

Abbott/AbbVie, Amgen, Centocor, Schering-Plough, and Wyeth had no role in the study design or in the collection, analysis, or interpretation of the data, the writing of the manuscript, or the decision to submit the manuscript for publication. Publication of this article was not contingent upon approval by Abbott/AbbVie, Amgen, Centocor, Schering-Plough, or Wyeth.

REFERENCES

- Sieper J, Poddubnyy D. Axial spondyloarthritis. *Lancet* 2017;390:73–84.
- Rudwaleit M, van der Heijde D, Landewe R, Listing J, Akkoc N, Brandt J, et al. The development of Assessment of SpondyloArthritis International Society classification criteria for axial spondyloarthritis (part II): validation and final selection. *Ann Rheum Dis* 2009;68:777–83.
- Poddubnyy D, Sieper J. Mechanism of new bone formation in axial spondyloarthritis. *Curr Rheumatol Rep* 2017;19:55.
- Machado P, Landewé R, Braun J, Hermann KG, Baker D, van der Heijde D. Both structural damage and inflammation of the spine contribute to impairment of spinal mobility in patients with ankylosing spondylitis. *Ann Rheum Dis* 2010;69:1465–70.
- Poddubnyy D, Listing J, Haibel H, Knüppel S, Rudwaleit M, Sieper J. Functional relevance of radiographic spinal progression in axial spondyloarthritis: results from the GERman SPondyloarthritis Inception Cohort. *Rheumatology (Oxford)* 2018;57:703–11.
- Protopopov M, Sieper J, Haibel H, Listing J, Rudwaleit M, Poddubnyy D. Relevance of structural damage in the sacroiliac joints for the functional status and spinal mobility in patients with axial spondyloarthritis: results from the German Spondyloarthritis Inception Cohort. *Arthritis Res Ther* 2017;19:240.
- Haroon N, Inman RD, Learch TJ, Weisman MH, Lee M, Rahbar MH, et al. The impact of tumor necrosis factor α inhibitors on radiographic progression in ankylosing spondylitis. *Arthritis Rheum* 2013;65:2645–54.
- Maas F, Arends S, Brouwer E, Essers I, van der Veer E, Efde M, et al. Reduction in spinal radiographic progression in ankylosing spondylitis patients receiving prolonged treatment with tumor necrosis factor inhibitors. *Arthritis Care Res (Hoboken)* 2017;69:1011–9.
- Sepriano A, Ramiro S, Wichuk S, Chiowchanwisawakit P, Paschke J, van der Heijde D, et al. Tumor necrosis factor inhibitors reduce spinal radiographic progression in patients with radiographic axial spondyloarthritis: a longitudinal analysis from the Alberta Prospective Cohort. *Arthritis Rheumatol* 2021;73:1211–9.
- Baraliakos X, Listing J, Brandt J, Haibel H, Rudwaleit M, Sieper J, et al. Radiographic progression in patients with ankylosing spondylitis after 4 yrs of treatment with the anti-TNF- α antibody infliximab. *Rheumatology (Oxford)* 2007;46:1450–3.
- Dougados M, Maksymowych WP, Landewé RB, Moltó A, Claudepierre P, de Hooge M, et al. Evaluation of the change in structural radiographic sacroiliac joint damage after 2 years of etanercept therapy (EMBARK trial) in comparison to a contemporary control cohort (DESIR cohort) in recent onset axial spondyloarthritis. *Ann Rheum Dis* 2018;77:221–7.
- Rodriguez VR, Hermann KG, Weiß A, Listing J, Haibel H, Althoff C, et al. Progression of structural damage in the sacroiliac joints in patients with early axial spondyloarthritis during long-term anti-tumor necrosis factor treatment: six-year results of continuous treatment with etanercept. *Arthritis Rheumatol* 2019;71:722–8.
- Rudwaleit M, Haibel H, Baraliakos X, Listing J, Märker-Hermann E, Zeidler H, et al. The early disease stage in axial spondylarthritis: results from the German Spondyloarthritis Inception Cohort. *Arthritis Rheum* 2009;60:717–27.
- Poddubnyy D, Rudwaleit M, Haibel H, Listing J, Märker-Hermann E, Zeidler H, et al. Rates and predictors of radiographic sacroiliitis progression over 2 years in patients with axial spondyloarthritis. *Ann Rheum Dis* 2011;70:1369–74.
- Poddubnyy D, Haibel H, Listing J, Märker-Hermann E, Zeidler H, Braun J, et al. Baseline radiographic damage, elevated acute-phase reactant levels, and cigarette smoking status predict spinal radiographic progression in early axial spondylarthritis. *Arthritis Rheum* 2012;64:1388–98.
- Van der Linden S, Valkenburg HA, Cats A. Evaluation of diagnostic criteria for ankylosing spondylitis. a proposal for modification of the New York criteria. *Arthritis Rheum* 1984;27:361–8.
- Garrett S, Jenkinson T, Kennedy LG, Whitelock H, Gaisford P, Calin A. A new approach to defining disease status in ankylosing spondylitis: the Bath Ankylosing Spondylitis Disease Activity Index. *J Rheumatol* 1994;21:2286–91.
- Lukas C, Landewé R, Sieper J, Dougados M, Davis J, Braun J, et al, for the Assessment of SpondyloArthritis international Society. Development of an ASAS-endorsed disease activity score (ASDAS) in patients with ankylosing spondylitis. *Ann Rheum Dis* 2009;68:18–24.
- Dougados M, Simon P, Braun J, Burgos-Vargas R, Maksymowych WP, Sieper J, et al. ASAS recommendations for collecting, analysing and reporting NSAID intake in clinical trials/epidemiological studies in axial spondyloarthritis. *Ann Rheum Dis* 2011;70:249–51.
- Dougados M, Demattei C, van den Berg R, Vo Hoang V, Thevenin F, Reijnierse M, et al. Rate and predisposing factors for sacroiliac joint radiographic progression after a two-year follow-up period in recent-onset spondyloarthritis. *Arthritis Rheumatol* 2016;68:1904–13.
- Dougados M, Sepriano A, Molto A, van Lunteren M, Ramiro S, de Hooge M, et al. Sacroiliac radiographic progression in recent onset axial spondyloarthritis: the 5-year data of the DESIR cohort. *Ann Rheum Dis* 2017;76:1823–8.
- Protopopov M, Proft F, Sepriano A, Landewé R, van der Heijde D, Maksymowych WP, et al. Radiographic sacroiliitis progression in axial spondyloarthritis: central reading of 5 year follow-up data from the Assessment of SpondyloArthritis international Society cohort. *Rheumatology (Oxford)* 2021;60:2478–80.
- Baraliakos X, Boehm H, Bahrami R, Samir A, Schett G, Lubner M, et al. What constitutes the fat signal detected by MRI in the spine of patients with ankylosing spondylitis? A prospective study based on biopsies obtained during planned spinal osteotomy to correct hyperkyphosis or spinal stenosis. *Ann Rheum Dis* 2019;78:1220–5.
- Bleil J, Maier R, Hempfing A, Sieper J, Appel H, Syrbe U. Granulation tissue eroding the subchondral bone also promotes new bone formation in ankylosing spondylitis. *Arthritis Rheumatol* 2016;68:2456–65.
- Baraliakos X, Heldmann F, Callhoff J, Listing J, Appelboom T, Brandt J, et al. Which spinal lesions are associated with new bone formation in patients with ankylosing spondylitis treated with anti-TNF agents? A long-term observational study using MRI and conventional radiography. *Ann Rheum Dis* 2014;73:1819–25.
- Machado PM, Baraliakos X, van der Heijde D, Braun J, Landewé R. MRI vertebral corner inflammation followed by fat deposition is the strongest contributor to the development of new bone at the same vertebral corner: a multilevel longitudinal analysis in patients with ankylosing spondylitis. *Ann Rheum Dis* 2016;75:1486–93.
- Wanders A, Landewe R, Spoorenberg A, de Vlam K, Mielants H, Dougados M, et al. Scoring of radiographic progression in randomised clinical trials in ankylosing spondylitis: a preference for paired reading order. *Ann Rheum Dis* 2004;63:1601–4.

Peripheral $\gamma\delta$ T Cells Regulate Neutrophil Expansion and Recruitment in Experimental Psoriatic Arthritis

Cuong Thach Nguyen,¹ Hiroki Furuya,² Dayasagar Das,¹ Alina I. Marusina,¹ Alexander A. Merleev,¹ Resmi Ravindran,¹ Zahra Jalali,² Imran H. Khan,¹ Emanuel Maverakis,¹ and Iannis E. Adamopoulos³

Objective. This study was undertaken to identify the mechanistic role of $\gamma\delta$ T cells in the pathogenesis of experimental psoriatic arthritis (PsA).

Methods. In this study, we performed interleukin-23 (IL-23) gene transfer in wild-type (WT) and T cell receptor δ -deficient (TCR $\delta^{-/-}$) mice and conducted tissue phenotyping in the joint, skin, and nails to characterize the inflammatory infiltrate. We further performed detailed flow cytometry, immunofluorescence staining, RNA sequencing, T cell repertoire analysis, and in vitro T cell polarization assays to identify regulatory mechanisms of $\gamma\delta$ T cells.

Results. We demonstrated that $\gamma\delta$ T cells support systemic granulopoiesis, which is critical for murine PsA-like pathology. Briefly, $\gamma\delta$ T cell ablation inhibited the expression of neutrophil chemokines CXCL1 and CXCL2 and neutrophil CD11b+Ly6G+ accumulation in the aforementioned PsA-related tissues. Although significantly reduced expression of granulocyte-macrophage colony-stimulating factor (GM-CSF) and IL-17A was detected systemically in TCR $\delta^{-/-}$ mice, no GM-CSF+IL-17A+ $\gamma\delta$ T cells were detected locally in the inflamed skin or bone marrow in WT mice. Our data showed that nonresident $\gamma\delta$ T cells regulate the expansion of an CD11b+Ly6G+ neutrophil population and their recruitment to joint and skin tissues, where they develop hallmark pathologic features of human PsA.

Conclusion. Our findings do not support the notion that tissue-resident $\gamma\delta$ T cells initiate the disease but demonstrate a novel role of $\gamma\delta$ T cells in neutrophil regulation that can be exploited therapeutically in PsA patients.

INTRODUCTION

Psoriatic arthritis (PsA) is a chronic, inflammatory, and heterogeneous disease that affects distinct anatomic sites including peripheral and axial joints, resulting in synovitis, enthesitis, onycholysis, and epidermal hyperplasia (1). The cutaneous features of PsA are characterized by the accumulation of prominent neutrophilic exudates (Munro's microabscesses) and mixed dermal infiltrates including $\alpha\beta$ and $\gamma\delta$ T cells (2). Similarly, nail psoriasis and onycholysis are commonly associated with increased neutrophil populations in the affected nail bed (3), and clinically, the neutrophil-to-lymphocyte ratio is a strong predictor for PsA (4).

Interleukin-23 (IL-23) induces the differentiation, survival, and expansion of Th17 cells, $\gamma\delta$ T cells, and neutrophils (5,6) and is also associated with PsA susceptibility and pathogenesis (7,8).

Although the exact mechanisms are not completely understood, the activation of IL-17A-producing $\gamma\delta$ T cells has been suggested. Activated $\gamma\delta$ T cells regulate multiple immune responses by producing proinflammatory cytokines, including IL-17A, interferon- γ (IFN γ), and tumor necrosis factor (TNF), and chemokines, including CCL5, CXCL10, and lymphotactin (XCL1), which lead to the recruitment of neutrophils and macrophages (9). Additionally, $\gamma\delta$ T cells regulate myelopoiesis and activation of polymorphonuclear neutrophils through granulocyte-macrophage CSF (GM-CSF), G-CSF, and M-CSF (10,11), and an absence of $\gamma\delta$ T cells prevents neutrophil accumulation in cancer (12). The contribution of these pathways in the pathogenesis of spondyloarthritis is of paramount importance as IL-17A+ $\gamma\delta$ T cells and double-producing IL-17A+ GM-CSF+ $\gamma\delta$ T cells have been identified in spondyloarthritis patients (13,14). Despite the high clinical significance and

Supported by the National Institute of Arthritis and Musculoskeletal and Skin Diseases, NIH (grant 2R-01-AR062173). Dr. Adamopoulos's work was supported by a National Psoriasis Foundation Translational Research grant.

¹Cuong Thach Nguyen, PhD, Dayasagar Das, PhD, Alina I. Marusina, PhD, Alexander A. Merleev, PhD, Resmi Ravindran, PhD, Imran H. Khan, PhD, Emanuel Maverakis, MD: University of California, Davis; ²Hiroki Furuya, MD, PhD, Zahra Jalali, MD: Harvard Medical School, Boston, Massachusetts; ³Iannis E. Adamopoulos, DPhil: University of California, Davis, and Harvard Medical School, Boston, Massachusetts.

Author disclosures are available at <https://onlinelibrary.wiley.com/action/downloadSupplement?doi=10.1002%2Fart.42124&file=art42124-sup-0001-Disclosureform.pdf>.

Address correspondence to Iannis E. Adamopoulos, DPhil, Division of Rheumatology and Clinical Immunology, Harvard Medical School, Beth Israel Medical Deaconess Center, Boston, MA. Email: iadamopo@bidmc.harvard.edu.

Submitted for publication December 9, 2021; accepted in revised form March 17, 2022.

the fact that clinical trials of GM-CSF in spondyloarthritis are currently under way, the cellular and molecular mechanisms of pathogenic $\gamma\delta$ T cells remain elusive.

In mice, the importance of $\gamma\delta$ T cells has been widely documented in experimental models of arthritis (15–17) and imiquimod-induced psoriasis (18,19). Additionally, $\gamma\delta$ T cells have been detected in inflamed skin and the entheses, which are commonly observed in PsA patients; however, as enthesitis can occur in the absence of $\gamma\delta$ T cells, the functional evidence is weak (20,21), as was recently reviewed (22). The major discrepancies surrounding $\gamma\delta$ T cell functionality stems from the fact that different $\gamma\delta$ subtypes exist in different tissues and regulate both pro- and anti-inflammatory responses based on the expression of cytokines and activation status. The fundamental subtype differences between human and murine $\gamma\delta$ T cells and the suboptimal tools used in $\gamma\delta$ T cell research further confounded the results (22,23).

In the current study, we performed IL-23 gene transfer in wild-type (WT) mice and T cell receptor δ -deficient ($\text{TCR}\delta^{-/-}$) mice (which lack $\gamma\delta$ T cells) (24), which were purposely backcrossed in the B10.RIII mouse strain (susceptible to autoimmunity), and we report the functional role of $\gamma\delta$ T cells. A systemic rather than a local inflammation is the driver of the disease that is regulated by GM-CSF and IL-17A and by chemotactic factors that are responsible for the accumulation of neutrophil exudates in IL-23-induced synovitis, onycholysis, and epidermal hyperplasia, which are associated with PsA. Our data reconcile previous conflicting observations and demonstrate a novel role of $\gamma\delta$ T cells in neutrophil recruitment and inflammation at anatomic sites critical for the pathogenesis of PsA.

MATERIALS AND METHODS

Animals. B10.RIII and $\text{TCR}\delta^{-/-}$ C57BL/6 mice were purchased from The Jackson Laboratory (Sacramento, CA). In order to generate $\text{TCR}\delta^{-/-}$ B10.RIII mice, $\text{TCR}\delta^{-/-}$ C57BL/6 mice were crossed with inbred B10.RIII mice over >10 generations. Sex- and age-matched mice (8–12 weeks) were used for all experiments under specific pathogen-free conditions. All animal protocols were approved by Institutional Animal Care and Use Committee at Beth Israel Medical Deaconess Center.

Reagents. Monoclonal antibodies of anti-Ly6G (1A8) and anti- $\text{TCR}\gamma\delta$ (GL3) were purchased from R&D Systems, anti-CD11b (M1/70) were purchased from eBioscience, and anti-IL-17A (TC11-18H10.1), anti-GM-CSF (MP1-22E9), and CD3 ϵ (145-2C11) were purchased from BioLegend. IRDye 680CW goat anti-mouse/anti-rabbit secondary antibodies were purchased from Li-Cor Biosciences. IL-23 and IL-27p28 enzyme-linked immunosorbent assay kits were purchased from eBioscience and R&D Systems, respectively. An EndoFree Plasmid Mega Kit was purchased from Qiagen, and Bio-Plex Pro mouse cytokine

23-plex assays were purchased from Bio-Rad. Minicircle-RSV. Flag.mIL23.elasti.bpA or RSV.eGFP.bpA (IL-23 minicircle DNA) was produced as previously described (25) and was injected hydrodynamically via tail vein delivery. Serum evaluation of IL-23 and clinical score was performed as previously described (25).

Flow cytometry. Bone marrow cells were isolated from B10.RIII mice 2 days post-gene transfer of either green fluorescent protein (GFP) or IL-23 minicircle DNA. Bone marrow cells were flushed out using a 27-gauge needle attached to a 1-ml syringe containing phosphate buffered saline (PBS). Red blood cells were lysed with BD Pharm Lyse (BD Biosciences). Nonspecific binding was blocked with TruStain FcX antibody (BioLegend) for 10 minutes at 4°C in fluorescence-activated cell sorting (FACS) buffer (Ca²⁺/Mg²⁺-free PBS with 2% fetal bovine serum and 0.5M EDTA) before staining (30 minutes) with appropriate antibodies. Isotype controls were used at the same protein concentrations as their corresponding markers. AccuCheck counting beads (Life Technologies) or Precision Count Beads (BioLegend) were used to determine absolute cell number/cm² based on the manufacturer's protocol. Flow cytometry was performed on a BD FACSAria flow cytometer (BD Biosciences) or Attune Cytometer (Life Technologies), and the data were analyzed using FlowJo software.

RNA isolation and real-time polymerase chain reaction (PCR). RNA was isolated from mouse tissues using an RNeasy kit (Qiagen) including a DNase I digest step. Quality of RNA was analyzed with a Nanodrop spectrophotometer (ThermoFisher Scientific). Complementary DNA was prepared using iScript cDNA Synthesis Kit (Bio-Rad). Quantitative reverse transcriptase-PCR (qRT-PCR) was performed using iTaq Universal SYBR Green Supermix according to instructions of the manufacturer (Bio-Rad). Relative expression of target genes was performed using the 2^{- $\Delta\Delta C_t$} method and normalized with internal GAPDH control as previously described (25).

Hematoxylin and eosin (H&E) staining and immunohistochemistry. Murine ears, paws, and nails (decalcified in 15% EDTA) were fixed in 10% formalin in PBS and paraffin-embedded for sectioning (6 μ m). Tissue sections were stained with hematoxylin and eosin Y (Sigma). Photos were obtained and analyzed using an Olympus BX61 microscope and BZ-II Analyzer software. Analysis and quantification were performed using ImageJ software. Histology sections (6 μ m) of each paraffin block were stained and used for immunofluorescence microscopy as previously described (26). Sections were deparaffinized and blocked for 1 hour in blocking buffer (1% triton X, 2% bovine serum albumin), then immunostained with appropriate antibodies and DAPI before visualized using a confocal microscope (Nikon C1). Quantification of neutrophils in the nail bed and synovium and bone resorption area was conducted using

the point-counting method, with a counting grid overlaid on an image magnified 400 \times , as previously described (27).

Cultures for expansion of $\gamma\delta$ T cells. For flow cytometry analysis, $\gamma\delta$ T cells were cultured as previously described (28). Briefly, splenocytes were cultured at 1×10^6 cells/ml in RPMI 1640 containing 10% FCS, antibiotics, 1X GlutaMax, 10 mM HEPES, 1 mM sodium pyruvate (Gibco), 55 μ M β -mercaptoethanol and nonessential amino acids (all from Gibco) with 5 ng/ml recombinant IL-23, 5 ng/ml recombinant IL-1 β (both from R&D Systems), and 10 μ g/ml anti-IFN γ (BioLegend) in 96-well, round-bottomed plates coated with 1 μ g/ml anti-TCR $\gamma\delta$ (clone GL3; BioLegend) for 3 days. Cells were washed and reseeded on fresh plastic at 1×10^6 cells/ml for a further 3 days, as described above, without TCR $\gamma\delta$ stimulation. Cells were collected on day 6 for flow cytometry analysis.

RNA sequencing. RNA was isolated from the ears of WT and TCR $\delta^{-/-}$ mice injected with either GFP minicircle DNA or IL-23 minicircle DNA using an RNeasy Plus mini kit and analyzed with a Bioanalyzer. Purified total RNA (RNA integrity number [RIN] >5) was used for library preparation. The 3' Tag RNA-Seq run was performed on an Illumina HiSeq 4000 and generated an average of 600,000 reads per sample. RNA-Seq reads for the 9 individual samples included 3 groups: control (WT mice treated with GFP minicircle DNA), treatment (WT mice treated with IL-23 minicircle DNA), and mutant (TCR $\delta^{-/-}$ mice treated with IL-23 minicircle DNA) (with 3 replicates each, barcoded and run on a single lane). These groups were independently aligned to the mouse genome (ref. ID: GRCh38.p6) using the STAR alignment software, version 2.7.0a, with the corresponding ensembl reference genome. The featureCounts package was used to count the mapped reads, and the edgeR package was used for differential expression analysis. The names of differentially expressed genes (DEGs) that met the criteria of having a fold change of >2 and a false discovery rate (FDR) of <0.05 were collected and used for further gene enrichment analysis. Enrichment analysis was performed using the web-based tool "Enrichr" (29).

T cell repertoire analysis. Mouse ears (9 mice/group) were stabilized by addition of RNAlater (Ambion) and homogenized using TissueLyzer II (Qiagen). Total RNA was extracted using an RNeasy Fibrosis mini kit and quantified using a Qubit Fluorometer. RNA integrity was assessed using the RNA ScreenTape on Agilent TapeStation, with an RIN of ≥ 8 set as an inclusion cutoff. Indexed libraries were constructed from 2,000 ng of total RNA using a TruSeq Stranded mRNA Sample Prep Kit following instructions of the manufacturer (Illumina). The quantity and quality of the libraries were also assessed by Qubit and D1000 ScreenTape on Agilent TapeStation, respectively. To maximize complementarity-determining region 3 (CDR3) reads, the average library size was 400 bp. The libraries' molar concentration was

validated by quantitative PCR for library pooling. Sequencing was performed on the Illumina HiSeq 4000 platform using PE150 chemistry.

Statistical analysis. Statistical differences were analyzed by Mann-Whitney test. All results are representative of ≥ 3 independent experiments, unless otherwise stated. *P* values less than 0.05 were considered statistically significant. Data show the mean \pm SEM.

Data availability. RNA-Seq data were deposited in the NCBI Sequence Read Archive under accession number SUB10952655 (Temporary Submission ID).

RESULTS

IL-23-induced joint inflammation limited by $\gamma\delta$ T cell deficiency. To examine the role of $\gamma\delta$ T cells in joint inflammation, we performed IL-23 gene transfer in WT and TCR $\delta^{-/-}$ mice using hydrodynamic gene delivery of IL-23 minicircle DNA, as previously described (25) (Figures 1A and B). IL-23 gene transfer induced swelling and paw erythema of murine paws, accompanied by synovial inflammation (Figures 1C–E), which was absent in controls. Compared to WT mice, TCR $\delta^{-/-}$ mice showed a significant decrease in disease severity (mean \pm SEM 8.8 \pm 2.9% for WT mice versus mean \pm SEM 2.5 \pm 1.3% for TCR $\delta^{-/-}$ mice; *P* < 0.05) and disease incidence (mean \pm SEM 86.0 \pm 12.8% for WT mice versus mean \pm SEM 43.6 \pm 14.4% for TCR $\delta^{-/-}$ mice; *P* < 0.01) on day 10 post-IL-23 minicircle gene transfer (Figures 1C–E). H&E staining of ankle joints 11 days after IL-23 gene transfer showed that WT mice had a hyperplastic and inflamed synovium with a mixed inflammatory infiltrate of mononuclear cells and numerous polymorphonuclear leukocytes, as well as evidence of bone destruction (Figure 1F and Supplementary Figure 1, available on the *Arthritis & Rheumatology* website at <https://onlinelibrary.wiley.com/doi/10.1002/art.42124>), which is consistent with previous observations (25,30).

The enthesis maintained normal architecture in both the fibrous enthesis and fibrocartilage tissue adjacent to the bone region. The corresponding tendon sheaths revealed slight inflammation accompanied by no or minimal edema, altered vascularity, and disorganized collagen fibers. No collagen hyalinization was found in the extracellular matrix. The bone-tendon borders were minimally blurred, though without any appreciable irregularity or focal defect at the interface of the fibrous attachment to the periosteum. In the absence of extensive infiltration of enthesis, widely dispersed inflammatory infiltrates in the muscle were evident, which is suggestive of mild myositis and tendinitis. Flow cytometric analysis conducted 48 hours post-IL-23 gene transfer confirmed an increase in CD11b+Ly6G+ cells (mean \pm SEM 12.90 \pm 0.74% for GFP minicircle-treated mice versus mean \pm SEM 23.87 \pm 1.87% for IL-23 minicircle-treated mice; *P* < 0.01) in the bone marrow of WT

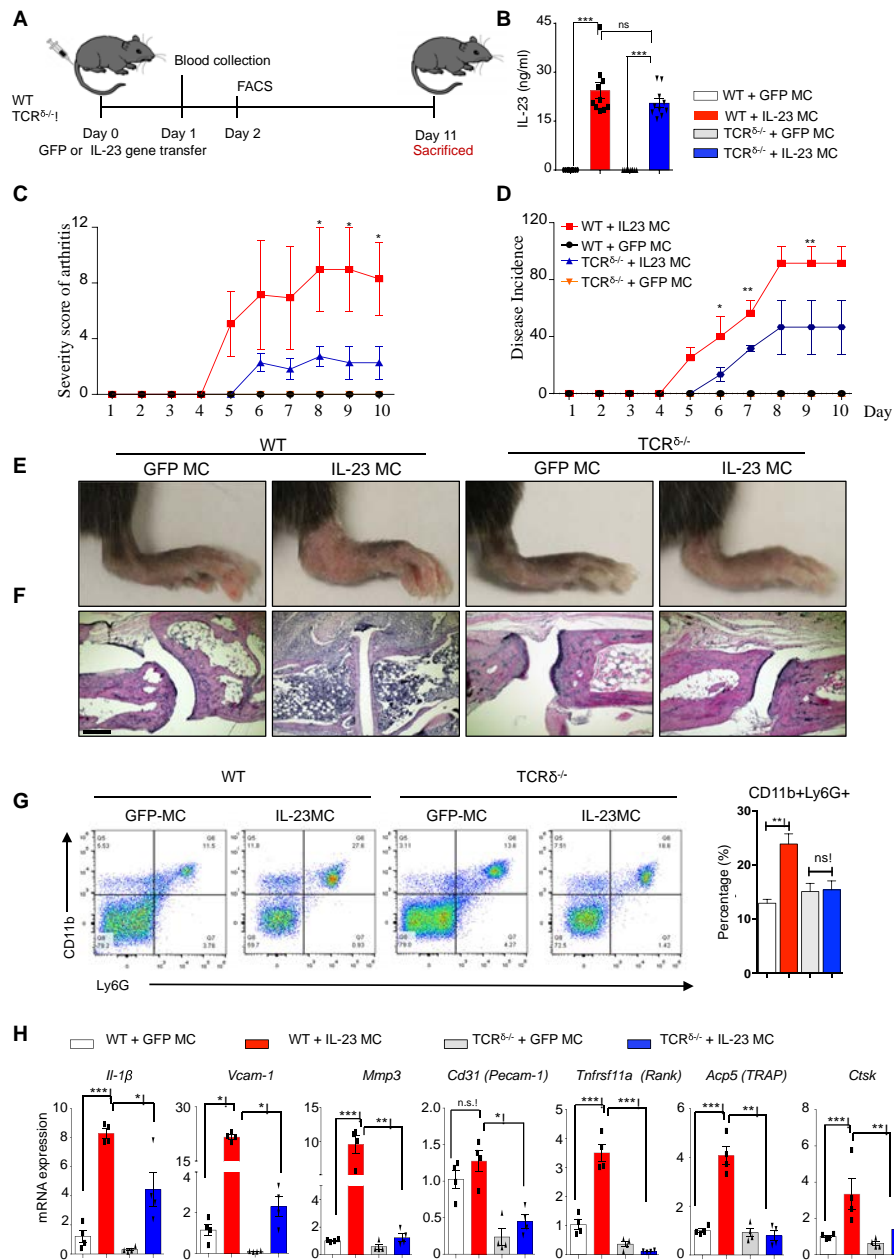


Figure 1. Amelioration of interleukin-23 (IL-23)-induced joint inflammation by $\gamma\delta$ T cell deficiency. **A**, Schematic of IL-23 and green fluorescent protein (GFP; control) minicircle (MC) gene transfer model. **B**, Serum IL-23 concentration 24 hours post-IL-23 minicircle gene transfer. **C** and **D**, Severity score of arthritis (**C**) and disease incidence (**D**) in wild-type (WT) and T cell receptor δ -deficient ($TCR\delta^{-/-}$) mice post-IL-23 minicircle gene transfer. Data are representative of ≥ 3 independent experiments ($n = 10-11$ mice/group). **E**, Photographs of murine ankles 11 days post-IL-23 minicircle gene transfer, showing inflamed mouse paws with extensive erythema and swelling of paws in IL-23 gene transfer mice compared to GFP minicircle-treated mice and $TCR\delta^{-/-}$ mice. **F**, Hematoxylin and eosin staining of murine ankle joints, showing synovial inflammation with infiltrated cells. Bars = 200 μ m. **G**, Representative flow cytometry dot plots gated on live lymphocytes of bone marrow 48 hours post-IL-23 or GFP gene transfer in WT and $TCR\delta^{-/-}$ mice, illustrating an increase in CD11b+Ly6G+ cell populations. **H**, Gene expression analysis of murine paws post-IL-23 minicircle gene transfer, showing an elevation of *Il1 β* , *Vcam1*, *Mmp3*, *Pecam1*, *Tnfrsf11a*, *Acp5*, and *Ctsk*, compared to GFP minicircle-treated mice and $TCR\delta^{-/-}$ mice. Data are representative of 3 independent experiments ($n = 9-11$ mice/group). In **B-D**, **G**, and **H**, symbols represent individual mice; bars show the mean \pm SEM. * = $P < 0.05$; ** = $P < 0.01$; *** = $P < 0.001$, by Mann-Whitney test. FACS = fluorescence-activated cell sorting; NS = not significant. Color figure can be viewed in the online issue, which is available at <http://onlinelibrary.wiley.com/doi/10.1002/art.42124/abstract>.

mice (Figure 1G). This pathology was accompanied by a marked elevation of gene expression of synovial inflammatory markers *Il1 β* , *Vcam1*, *Mmp3*, *Pecam1*, as well as osteoclast related markers

Tnfrsf11a, *Ctsk*, and *Acp5* (Figure 1H). Taken together, our data confirmed that genetic ablation of $\gamma\delta$ T cells reduces joint inflammation and neutrophil expansion.

Prevention of neutrophil accumulation in PsA-related tissues by $\gamma\delta$ T cell deficiency. IL-23 gene transfer also resulted in severe inflammation with psoriatic lesions of the distal nail bed and hyponychium and in severe cases resulted in

onycholysis (Figure 2A), which is commonly observed in PsA patients. The inflammatory infiltrate of the nail bed consisted largely of polymorphonuclear neutrophils similar to the bone marrow. This was confirmed by immunofluorescence staining using

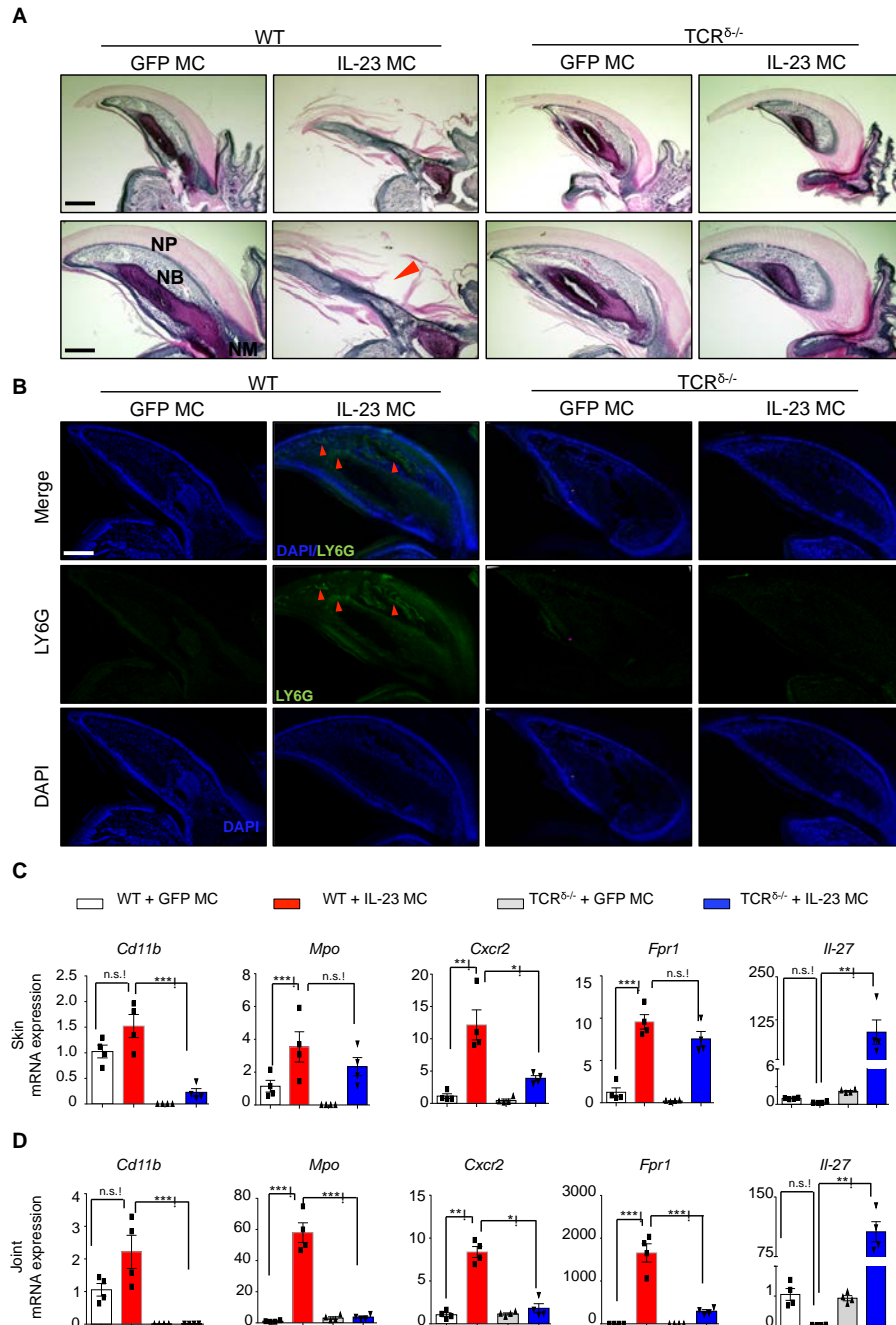


Figure 2. Prevention of nail psoriasis and onycholysis by inhibiting neutrophil accumulation by $\gamma\delta$ T cell deficiency. **A**, Hematoxylin and eosin staining of murine nails, showing nail psoriasis and onycholysis with infiltrated cells in nail bed (NB) (arrowhead). Bars = 300 μ m (upper) and 200 μ m (lower). Arrowhead indicates onycholysis. **B**, Immunofluorescence staining of Ly6G $^{+}$ cells in murine nails post-IL-23 minicircle gene transfer, showing the neutrophil accumulation (arrowheads) in nail beds. Images are representative of 3 independent experiments ($n = 10$ mice/group). Bars = 200 μ m. **C** and **D**, Gene expression analysis of neutrophil markers, showing an elevation of *Cd11b*, *Mpo*, *Cxcr2*, *Fpr1*, and *Il27* in the skin (**C**) and joint tissues (**D**) of IL-23 minicircle-treated WT mice and/or TCR $\delta^{-/-}$ mice compared to GFP minicircle-treated mice (controls). Symbols represent individual mice; bars show the mean \pm SEM ($n = 3$ independent experiments). * = $P < 0.05$; ** = $P < 0.01$; *** = $P < 0.001$, by Mann-Whitney test. NB = nail bed; NP = nail plate (see Figure 1 for other definitions). Color figure can be viewed in the online issue, which is available at <http://onlinelibrary.wiley.com/doi/10.1002/art.42124/abstract>.

neutrophil specific antibodies (anti-Ly6G). $TCR\delta^{-/-}$ mice were protected from IL-23-induced nail psoriasis and onycholysis, and this correlated with a decrease in neutrophil accumulation in the nail bed (Figure 2B and Supplementary Figure 1, <https://onlinelibrary.wiley.com/doi/10.1002/art.42124>). To investigate whether $\gamma\delta$ T cells modulate activation of neutrophils during joint and skin inflammation, neutrophil markers were examined by qRT-PCR in paws and ear tissue, respectively. Our results showed that IL-23 increased expression of neutrophil markers in the joints and skin and that $TCR\delta^{-/-}$ mice differentially regulated the neutrophil marker expression in these tissues. Specifically, IL-23-induced expression of *Cd11b* and *Cxcr2* induction was prevented in the skin (Figure 2C) and *Cd11b*, *Mpo*, *Cxcr2*, and

Frp1 was prevented within the joints (Figure 2D). Collectively, these findings indicate that neutrophilic inflammation in the nails, skin, and joints are down-regulated in $TCR\delta^{-/-}$ mice.

Suppression of IL-23-induced innate skin inflammation by $\gamma\delta$ T cell deficiency.

To investigate whether $\gamma\delta$ T cells are required for IL-23-induced skin inflammation, we examined parameters of skin inflammation between WT and $TCR\delta^{-/-}$ mice. IL-23 induced erythema with silvery white scales at 11 days post-IL-23 gene transfer (Figure 3A) in WT mice but not in $TCR\delta^{-/-}$ mice. The clinical observation was corroborated by histologic analysis, which demonstrated a limited thickening of the epidermis, infiltration by inflammatory cells,

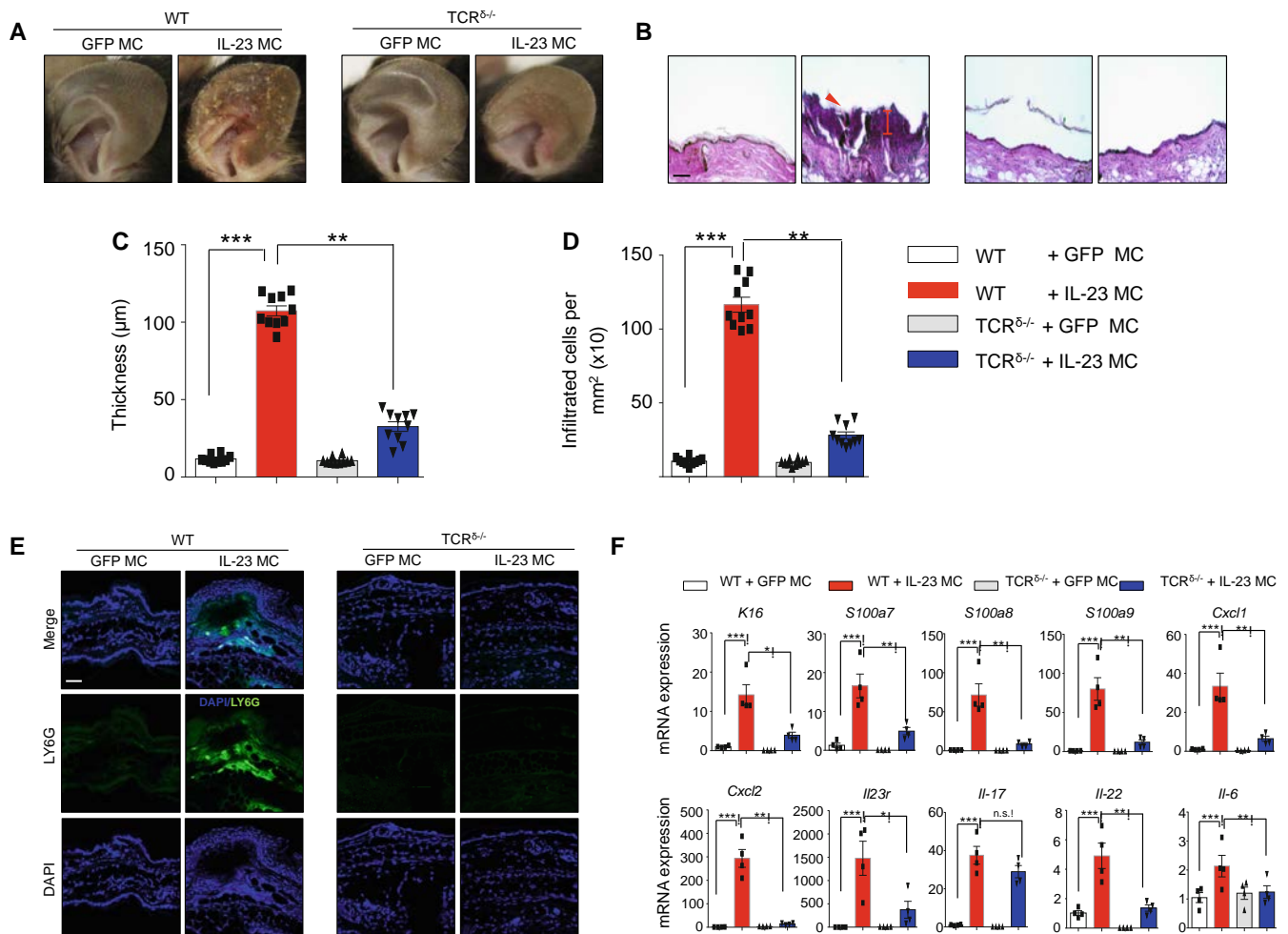


Figure 3. $TCR\delta^{-/-}$ deficiency suppresses IL-23-induced skin inflammation in vivo. **A**, Photographs of ears 11 days post-IL-23 minicircle gene transfer, showing the development of silvery white scales in WT mice compared to GFP minicircle-treated mice and $TCR\delta^{-/-}$ mice. **B**, Hematoxylin and eosin staining of murine ears, showing epidermal hyperplasia and number of infiltrated cells. **Arrowhead** indicates neutrophil exudates (Munro's microabscesses). **Cursor** indicates thickening of the epidermis. Images are representative of 3 independent experiments ($n = 9-11$ mice/group). Bars = 100 μ m. **C** and **D**, Quantification of epidermal thickness (**C**) and infiltrated cell number (**D**). **E**, Immunofluorescence staining of Ly6G+ cells in the ear post-IL-23 minicircle gene transfer, showing the neutrophil accumulation in dermis and epidermis. **F**, Gene expression analysis of inflammation markers, showing an elevation of *K16*, *S100a7*, *S100a8*, *S100a9*, *Cxcl1*, *Cxcl2*, *Il23r*, *Il17a*, *Il22*, and *Il6* in the ears of IL-23 minicircle-treated WT mice compared to GFP minicircle-treated mice (controls) and $TCR\delta^{-/-}$ mice. In **C**, **D**, and **F**, symbols represent individual mice; bars show the mean \pm SEM ($n = 3$ independent experiments). * = $P < 0.05$; ** = $P < 0.01$; *** = $P < 0.001$, by Mann-Whitney test. See Figure 1 for definitions. Color figure can be viewed in the online issue, which is available at <http://onlinelibrary.wiley.com/doi/10.1002/art.42124/abstract>.

and formation of neutrophilic exudates (Munro's microabscesses) in $\text{TCR}\delta^{-/-}$ mice compared to WT mice (Figures 3B–D and Supplementary Figure 1, <https://onlinelibrary.wiley.com/doi/10.1002/art.42124>). Immunofluorescence imaging of ears with neutrophil specific antibodies after IL-23 gene transfer confirmed that neutrophils accumulate in the skin in WT mice

compared to mice injected with control GFP minicircle DNA and $\text{TCR}\delta^{-/-}$ mice (Figure 3E). Furthermore, IL-23 gene transfer in WT mice showed a significant increase in expression of inflammatory gene markers *K16*, *S100a7*, *S100a8*, *S100a9*, *Cxcl1*, *Cxcl2*, *Il23r*, *Il17*, *Il22*, and *Il6*, compared to $\text{TCR}\delta^{-/-}$ mice (Figure 3F). Overall, skin inflammation showed an increase in

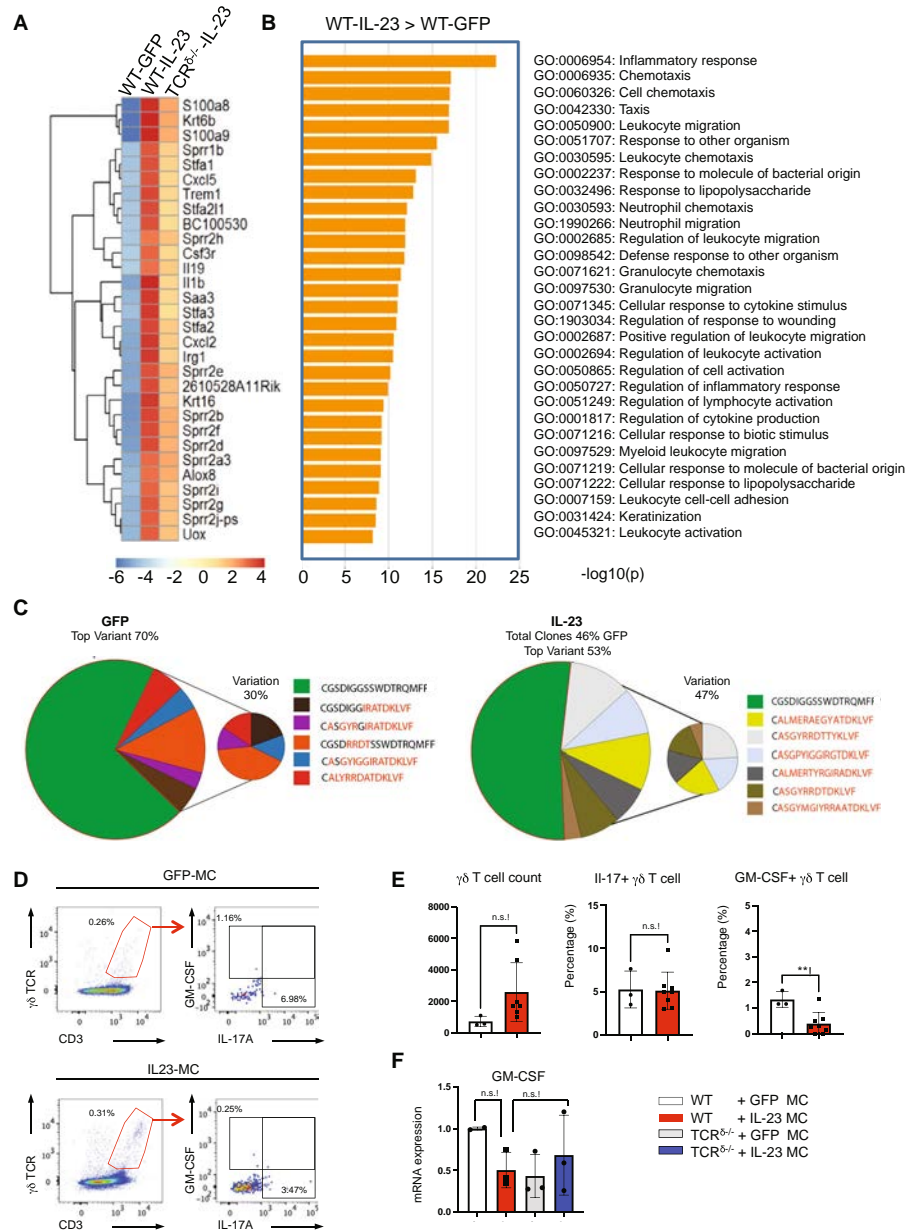


Figure 4. IL-23-induced skin inflammation is not associated with expansion of dermal $\gamma\delta$ T cells. **A** and **B**, Expression profiling of ear tissue collected from WT and $\text{TCR}\delta^{-/-}$ mice post-GFP and/or IL-23 gene transfer, showing a hierarchical clustering heatmap plot of the top 30 differentially expressed genes (**A**) and Gene Ontology (GO) enrichment analysis for the up-regulated genes post-GFP or IL-23 gene transfer (**B**). **C**, TCR repertoire analysis, with pie charts showing the distribution of T cell receptor delta (TRD) complementarity-determining region 3 (CDR3) in each treatment group cluster. Colors represent different TRD CDR3 sequences. The relative abundance of each TRD CDR3 sequence within each group is shown as percentages. **D** and **E**, Representative flow cytometry dot plots pregated on live lymphocytes (**D**) and bar graphs showing the gating strategy and percentages (**E**) of CD3^+ $\gamma\delta\text{TCR}^+$ GM-CSF+IL-17A+ cells in the skin of WT mice at 11 days post-IL-23 or GFP gene transfer. **F**, Granulocyte-macrophage colony-stimulating factor (GM-CSF) mRNA expression in ears isolated from WT and/or $\text{TCR}\delta^{-/-}$ mice 11 days post-GFP or IL-23 minicircle gene transfer. In **E** and **F**, symbols represent individual mice; bars show the mean \pm SEM. ** = $P < 0.01$, by Student's unpaired *t*-test. See Figure 1 for other definitions.

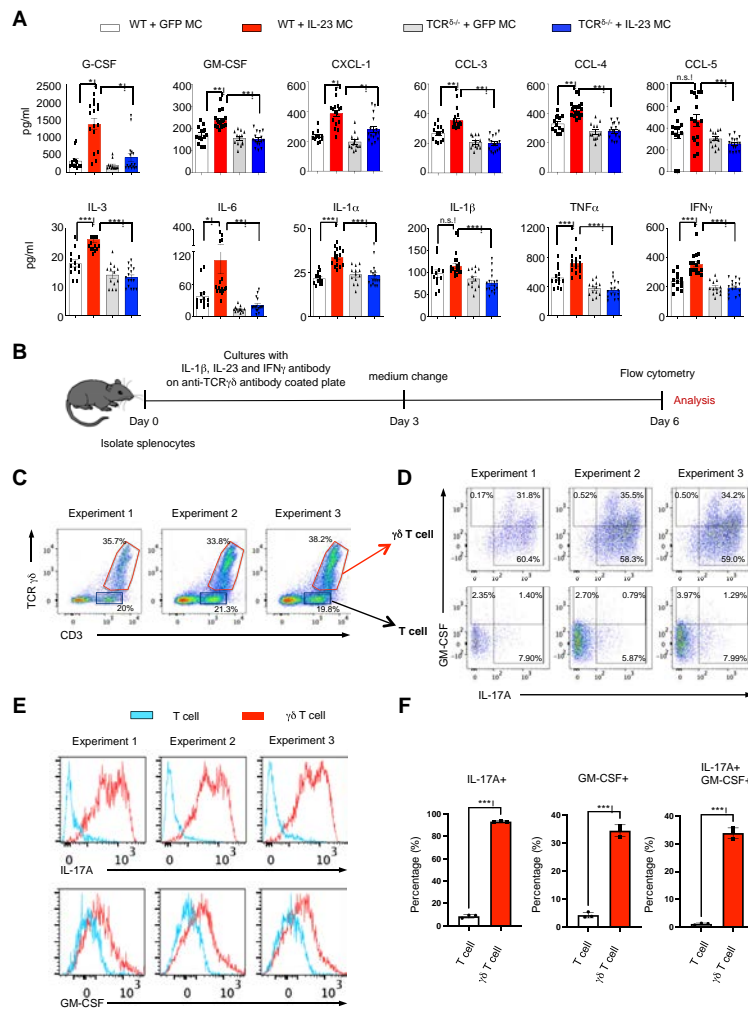


Figure 5. IL-23 induces the development of IL-17A⁺/granulocyte-macrophage colony-stimulating factor-positive (GM-CSF⁺) $\gamma\delta$ T cells in vitro. **A**, Serum cytokine and chemokine profiles of WT mice and TCR $\delta^{-/-}$ mice post-GFP or IL-23 minicircle gene transfer. Dotted line shows sensitivity of each assay. **B**, Schematic diagram of $\gamma\delta$ T cell culture using splenocytes from WT mice. **C** and **D**, Flow cytometry dot plots pregated on live lymphocytes showing the gating strategy. **E**, Histograms of IL-17A and GM-CSF expression on T cells and $\gamma\delta$ T cells. **F**, Bar plots showing percentages of IL-17A⁺ and GM-CSF⁺ cells among cultured T cells and $\gamma\delta$ T cells. In **A** and **F**, symbols represent individual mice; bars show the mean \pm SEM ($n = 3$ independent experiments). * = $P < 0.05$; ** = $P < 0.01$; *** = $P < 0.001$, by Mann-Whitney test in **A** and by Student's unpaired t -test in **F**. See Figure 1 for other definitions. Color figure can be viewed in the online issue, which is available at <http://onlinelibrary.wiley.com/doi/10.1002/art.42124/abstract>.

neutrophil accumulation and neutrophil chemokines that was prevented in TCR $\delta^{-/-}$ mice.

No association of IL-23-induced skin inflammation with expansion of dermal $\gamma\delta$ T cells. To mechanistically investigate the role of $\gamma\delta$ T cells in IL-23-induced skin inflammation, we performed RNA-Seq on ear tissue collected from WT and TCR $\delta^{-/-}$ mice 11 days post-GFP or IL-23 gene transfer. This analysis identified 2,800 genes that were meaningfully (fold change >2) and significantly (FDR >2) differentially expressed in WT animals following IL-23 minicircle-treated mice compared to GFP minicircle-treated controls. Among the 30 most variable genes (Figure 4A), several genes classically associated with psoriasis, including *Krt16*, *S100a8*, *S100a9*, were significantly increased

(fold change = 752 [$P = 2.37 \times 10^{-5}$] for *Krt16*; fold change = 1,562 [$P = 3.85 \times 10^{-6}$] for *S100a8*; fold change = 1,741 [$P = 3.41 \times 10^{-6}$] for *S100a9*). The expression of several neutrophil-attracting chemokines was also up-regulated including *Cxcl2* and *Cxcl5*, as well as the T cell and monocyte-attracting chemokine *Cxcl10* (fold change = 1,415 [$P = 5.73 \times 10^{-4}$] for *Cxcl2*; fold change = 3.96 [$P = 9.89 \times 10^{-4}$] for *Cxcl5*; fold change = 41.74 [$P = 3.79 \times 10^{-2}$] for *Cxcl10*). Other genes of interest included neutrophil proteases and genes associated with neutrophil activation, including innate proinflammatory mediators such as *Il1 β* and *Ptgs2* (fold change = 1,125 [$P = 5.84 \times 10^{-4}$] for *Il1 β* ; fold change = 182 [$P = 2.36 \times 10^{-2}$] for *Ptgs2*) (Figure 4A and Supplementary Figure 2, <https://onlinelibrary.wiley.com/doi/10.1002/art.42124>).

A hierarchical clustering heatmap of DEGs revealed that $\text{TCR}\delta^{-/-}$ mice show greater similarity to GFP minicircle-treated WT mice than to IL-23 minicircle-treated WT mice (Figure 4A). Accordingly, Gene Ontology analyses of the up-regulated genes in IL-23 gene-transferred WT mice showed multiple terms that were compatible with psoriasis, such as “inflammatory response,” “keratinization,” “neutrophil chemotaxis,” and “neutrophil migration” (Figure 4B). To characterize the IL-23-induced alterations in the T cell repertoire, TCR gene segments and the TCR complementarity-determining region 3 (CDR3)-encoding sequences were mined from RNA-Seq data sets of GFP minicircle-treated WT mice and IL-23 minicircle-treated mice. Surprisingly, IL-23 induced a significant decrease in $\gamma\delta$ T cells in the skin (Supplementary Figure 3, <https://onlinelibrary.wiley.com/doi/10.1002/art.42124>). Specifically, the dominant T cell receptor delta (TRD) clone (CGSDIGGSSWDTRQMFF), which normally comprised 70% of the TRD repertoire, declined to 53%, and the second most dominant clone in the TRD repertoire (CALYRRDATDKLVF) dropped to below detection in the skin following IL-23 gene transfer (Figure 4C). Consistent with these findings, results of the flow cytometric analysis after GFP/IL-23 gene transfer revealed no significant increase in absolute number of $\gamma\delta$ T cells or the proportion of GM-CSF/IL-17-producing $\gamma\delta$ T cells among $\gamma\delta$ T cells (Figures 4D and E), not even in messenger RNA (mRNA) levels (Figure 4F). We also performed similar analysis at the bone marrow and again no $\gamma\delta$ T cell expansion was observed (Supplementary 4, <https://onlinelibrary.wiley.com/doi/10.1002/art.42124>).

Development of IL-17A+/GM-CSF+ $\gamma\delta$ T cells induced in vitro by IL-23. Despite the absence of IL-17A/GM-CSF double-positive cells among $\gamma\delta$ T cells in the skin and bone marrow, the levels of proinflammatory cytokines, including GM-CSF and other myeloid supporting factors, were decreased in the circulation in the $\text{TCR}\delta^{-/-}$ mice (Figure 5A and Supplementary Figure 5, <https://onlinelibrary.wiley.com/doi/10.1002/art.42124>). To confirm that $\gamma\delta$ T cells express GM-CSF, we performed experiments to determine the requirements of IL-17A+/GM-CSF+ $\gamma\delta$ T cells differentiation in vitro using cytokines and antigen activation (Figure 5B). Our data showed that IL-23, IL-1 β , anti-IFN γ , and anti-TCR δ antibodies resulted in the differentiation of IL-17A/GM-CSF double-positive cells in splenocyte cultures isolated from WT mice (Figures 5C and D and Supplementary 6, <https://onlinelibrary.wiley.com/doi/10.1002/art.42124>). These experiments also confirmed that the IL-17A/GM-CSF double-positive cells were mainly (95%) $\gamma\delta$ T cells (Figures 5D–F). Taken together, our data demonstrate that although IL-23 can induce the development of IL-17A+/GM-CSF+ $\gamma\delta$ T cells, other factors are also required, and therefore, a systemic elevation of IL-23 is not adequate to induce IL-17A+/GM-CSF+ $\gamma\delta$ T cells.

DISCUSSION

Here, we have demonstrated the importance of $\gamma\delta$ T cells in the development of PsA-like pathology at multiple anatomic sites by applying IL-23 gene transfer technology in mice lacking $\gamma\delta$ T cells. In our model, IL-23 gene transfer in mice elicited skin and joint pathology reminiscent of PsA, which was suppressed in mice lacking $\gamma\delta$ T cells. Other groups have also demonstrated that the absence of $\gamma\delta$ T cells prevented neutrophil accumulation and indicated the importance of the $\gamma\delta$ T cell/IL-17/neutrophil axis in metastatic disease and that $\gamma\delta$ T cells modulate myeloid cell recruitment during peripheral inflammation (12). Myeloid recruitment was also affected by genetic ablation of $\gamma\delta$ T cells in inflammatory pain models (31). However, our findings do not support a local role of resident $\gamma\delta$ T cells but rather a role of $\gamma\delta$ T cells in modulating systemic neutrophil infiltration.

Specifically, we demonstrated that $\gamma\delta$ T cells regulate proinflammatory cytokines, including GM-CSF, IL-6, IFN γ , and TNF and neutrophil specific chemokines CXCL1 and CXCL2 in the circulation, which limits myeloid expansion and neutrophil migration (32). The absence of neutrophil recruitment and the reduction in the inflammatory infiltrate in $\text{TCR}\delta^{-/-}$ mice lead to a reduction of IL-17 (33), TNF (34), and other pro-osteoclastogenic factors (35), thereby reducing bone resorption. Our data are consistent with previous observations in which depletion of neutrophils prevented joint inflammation (36). Similar to synovitis, $\gamma\delta$ T cell deficiency also inhibited IL-23-induced onycholysis, which was again accompanied by a reduced accumulation of Ly6G+ cell neutrophils in the nail bed. These data correlate well with the human disease, in which neutrophilic abscess are commonly observed in nail bed epithelium of patients with nail psoriasis (37).

We focused more on the biology of the skin, because in adult patients psoriasis precedes joint inflammation. Therefore, we reasoned that skin inflammation may provide mechanistic clues of disease initiation and pathogenesis. The neutrophilic inflammation in the upper dermis was reminiscent to the pathologic features of human psoriasis and the formation of Munro’s microabscesses, which is consistent with multiple studies showing the dependence of skin inflammation on neutrophils (26,38). The reduction of neutrophils and inflammation in the skin despite the high levels of IL-17A mRNA locally in the skin suggest that IL-17A pathology is mediated by myelopoiesis and neutrophil migration rather than a local effect of IL-17A. This is consistent with previous observations of IL-17A local injections failing to induce skin inflammation (39) and adoptive transfer of Ly6G+ cells being sufficient to induce skin pathology in the absence of exogenous IL-17A (26). Therefore, it is not surprising that dermal IL-17A+ $\gamma\delta$ T cells did not expand in the skin following IL-23 gene transfer. In fact, these data are in accordance with previous findings in which IL-23 gene transfer in SKG mice only affected the number of $\gamma\delta$ T cells in the lymph nodes (40).

Using an imiquimod animal model, which activates Toll-like receptors, it has previously been shown that IL-17A+ $\gamma\delta$ T cells are commonly observed (18,19), and we confirmed these observations with in vitro stimulations. Our key finding that $\gamma\delta$ T cells did not expand in the skin was corroborated by T cell repertoire analysis. The marked reduction of total clones (by 46%) and of the TRD-dominant clone (by 17%) in the IL-23 gene transfer compared to GFP-treated controls is also consistent with data from other groups demonstrating that the majority of T cells in psoriatic skin express TCR $\alpha\beta$ (41,42). Notably, a systemic elevation of the antiinflammatory cytokine IL-27, which is known to inhibit $\alpha\beta$ T cell development and osteoclastogenesis leading to bone loss, was observed in TCR $\delta^{-/-}$ mice, which suggests that local inflammation may be regulated remotely (30,43,44). This is also corroborated by the fact that IL-17A levels were reduced in the circulation in TCR $\delta^{-/-}$ mice.

One limitation of our study is that we did not detect where the IL-17A+ $\gamma\delta$ T cells were expanded, and more sophisticated experiments in reporter mice will be required to address that. However, we postulate that tissues rich in $\gamma\delta$ T cell polarizing factors such as the peritoneal cavity may be a suitable location for the development of IL-17A+GM-CSF+ $\gamma\delta$ T cells in our model (45,46). An additional point to consider is that $\gamma\delta$ T cells may indirectly regulate other GM-CSF-producing cells such as natural killer cells (47) and collectively regulate myelopoiesis. Whatever the mechanism, we have demonstrated, directly or indirectly, that $\gamma\delta$ T cells are required for IL-23-induced pathology and that they regulate neutrophil accumulation in the skin, spleen, bone marrow, and joints.

Neutrophils are also important effector cells in enthesal inflammation, and the activation of neutrophils is critical in determining the development of enthesitis in humans (48). Previous studies have suggested that, in the IL-23 minicircle model, CD3+CD4-CD8- cells are critical in murine enthesitis (49); however, other groups have demonstrated that enthesitis can occur in the absence of CD3+CD4-CD8- $\alpha\beta$ and $\gamma\delta$ T cells (20,21). Notably, a recent study failed to recapitulate the observations of IL-23-induced enthesitis using the IL-23 minicircle DNA model (50). Consistent with our original findings in our seminal study on IL-23 minicircle DNA (51), we did not detect enthesitis. Our data confirm that the enthesitis is not at all inflamed in this model at the time points tested, and thus it cannot be viewed as responsible for disease pathogenesis (20,21,50).

The identification of double-producing IL-17A+ GM-CSF+ $\gamma\delta$ T cells in the circulation of spondyloarthritis patients (13,14) has already hinted at the importance of granulopoiesis and the systemic nature of SpA. The data presented herein support a model of PsA as a systemic disease and demonstrate a systemic modulatory role of $\gamma\delta$ T cells in IL-23-induced pathogenesis, providing a strong mechanistic rationale to support clinical trials that modulate myelopoiesis in PsA.

AUTHOR CONTRIBUTIONS

All authors were involved in drafting the article or revising it critically for important intellectual content, and all authors approved the final version to be published. Dr. Adamopoulos had full access to all of the data in the study and takes responsibility for the integrity of the data and the accuracy of the data analysis.

Study conception and design. Adamopoulos.

Acquisition of data. Nguyen, Furuya, Das, Marusina, Merleev, Ravindran, Jalali, Adamopoulos.





Analysis and interpretation of data. Nguyen, Furuya, Jalali, Khan, Maverakis, Adamopoulos.

REFERENCES

- Ritchlin CT, Colbert RA, Gladman DD. Psoriatic Arthritis. *N Engl J Med* 2017;376:957–70.
- Nestle FO, Kaplan DH, Barker J. Psoriasis. *N Engl J Med* 2009;361:496–509.
- Werner B, Fonseca GP, Seidel G. Microscopic nail clipping findings in patients with psoriasis. *Am J Dermatopathol* 2015;37:429–39.
- Kim DS, Shin D, Lee MS, Kim HJ, Kim DY, Kim SM, et al. Assessments of neutrophil to lymphocyte ratio and platelet to lymphocyte ratio in Korean patients with psoriasis vulgaris and psoriatic arthritis. *J Dermatol* 2016;43:305–10.
- Sutton CE, Lalor SJ, Sweeney CM, Brereton CF, Lavelle EC, Mills KH. Interleukin-1 and IL-23 induce innate IL-17 production from gamma-delta T cells, amplifying Th17 responses and autoimmunity. *Immunity* 2009;31:331–41.
- Smith E, Zarbock A, Stark MA, Burcin TL, Bruce AC, Foley P, et al. IL-23 is required for neutrophil homeostasis in normal and neutrophilic mice. *J Immunol* 2007;179:8274–9.
- Filer C, Ho P, Smith RL, Griffiths C, Young HS, Worthington J, et al. Investigation of association of the IL12B and IL23R genes with psoriatic arthritis. *Arthritis Rheum* 2008;58:3705–9.
- Bowes J, Orozco G, Flynn E, Ho P, Brier R, Marzo-Ortega H, et al. Confirmation of TNIP1 and IL23A as susceptibility loci for psoriatic arthritis. *Ann Rheum Dis* 2011;70:1641–4.
- Vantourout P, Hayday A. Six-of-the-best: unique contributions of $\gamma\delta$ T cells to immunology [review]. *Nat Rev Immunol* 2013;13:88–100.
- Stark MA, Huo Y, Burcin TL, Morris MA, Olson TS, Ley K. Phagocytosis of apoptotic neutrophils regulates granulopoiesis via IL-23 and IL-17. *Immunity* 2005;22:285–94.
- Mamedov MR, Scholzen A, Nair RV, Cumnock K, Kenkel JA, Oliveira JH, et al. A macrophage colony-stimulating-factor-producing $\gamma\delta$ T cell subset prevents malarial parasitemic recurrence. *Immunity* 2018;48:350–63.
- Coffelt SB, Kersten K, Doornebal CW, Weiden J, Vrijland K, Hau CS, et al. IL-17-producing $\gamma\delta$ T cells and neutrophils conspire to promote breast cancer metastasis. *Nature* 2015;522:345–8.
- Venken K, Jacques P, Mortier C, Labadia ME, Decruy T, Coudenys J, et al. ROR γ t inhibition selectively targets IL-17 producing iNKT and $\gamma\delta$ -T cells enriched in Spondyloarthritis patients. *Nat Commun* 2019; 10:9.
- Al-Mossawi MH, Chen L, Fang H, Ridley A, de Wit J, Yager N, et al. Unique transcriptome signatures and GM-CSF expression in lymphocytes from patients with spondyloarthritis. *Nat Commun* 2017;8: 1510.
- Roark CL, French JD, Taylor MA, Bendele AM, Born WK, O'Brien RL. Exacerbation of collagen-induced arthritis by oligoclonal, IL-17-producing $\gamma\delta$ T cells. *J Immunol* 2007;179:5576–83.
- Ito Y, Usui T, Kobayashi S, Iguchi-Hashimoto M, Ito H, Yoshitomi H, et al. Gamma/delta T cells are the predominant source of

- interleukin-17 in affected joints in collagen-induced arthritis, but not in rheumatoid arthritis. *Arthritis Rheum* 2009;60:2294–303.
17. Akitsu A, Ishigame H, Kakuta S, Chung SH, Ikeda S, Shimizu K, et al. IL-1 receptor antagonist-deficient mice develop autoimmune arthritis due to intrinsic activation of IL-17-producing CCR2(+)/V γ 6(+) γ δ T cells. *Nat Commun* 2015;6:7464.
 18. Pantelyushin S, Haak S, Ingold B, Kulig P, Heppner FL, Navarini AA, et al. Rorgammat+ innate lymphocytes and gammadelta T cells initiate psoriasiform plaque formation in mice. *J Clin Invest* 2012;122:2252–6.
 19. Cai Y, Shen X, Ding C, Qi C, Li K, Li X, et al. Pivotal role of dermal IL-17-producing γ δ T cells in skin inflammation. *Immunity* 2011;35:596–610.
 20. Corthay A, Hansson AS, Holmdahl R. T lymphocytes are not required for the spontaneous development of enthesal ossification leading to marginal ankylosis in the DBA/1 mouse. *Arthritis Rheum* 2000;43:844–51.
 21. Jacques P, Lambrecht S, Verheugen E, Pauwels E, Kollias G, Armaka M, et al. Proof of concept: enthesitis and new bone formation in spondyloarthritis are driven by mechanical strain and stromal cells. *Ann Rheum Dis* 2014;73:437–45.
 22. Nguyen CT, Maverakis E, Eberl M, Adamopoulos IE. γ δ T cells in rheumatic diseases: from fundamental mechanisms to autoimmunity. *Semin Immunopathol* 2019;41:595–605.
 23. Koenecke C, Chennupati V, Schmitz S, Malissen B, Förster R, Prinz I. In vivo application of mAb directed against the γ δ TCR does not deplete but generates “invisible” γ δ T cells. *Eur J Immunol* 2009;39:372–9.
 24. Itohara S, Mombaerts P, Lafaille J, Iacomini J, Nelson A, Clarke AR, et al. T cell receptor δ gene mutant mice: independent generation of α β T cells and programmed rearrangements of γ δ TCR genes. *Cell* 1993;72:337–48.
 25. Adamopoulos IE, Tessmer M, Chao CC, Adda S, Gorman D, Petro M, et al. IL-23 is critical for induction of arthritis, osteoclast formation, and maintenance of bone mass. *J Immunol* 2011;187:951–9.
 26. Suzuki E, Maverakis E, Sarin R, Bouchareychas L, Kuchroo VK, Nestle FO, et al. T cell-independent mechanisms associated with neutrophil extracellular trap formation and selective autophagy in IL-17A-mediated epidermal hyperplasia. *J Immunol* 2016;197:4403–12.
 27. Adamopoulos IE, Sabokbar A, Wordsworth BP, Carr A, Ferguson DJ, Athanasou NA. Synovial fluid macrophages are capable of osteoclast formation and resorption. *J Pathol* 2006;208:35–43.
 28. McKenzie DR, Kara EE, Bastow CR, Tyllis TS, Fenix KA, Gregor CE, et al. IL-17-producing γ δ T cells switch migratory patterns between resting and activated states. *Nat Commun* 2017;8:15632.
 29. Chen EY, Tan CM, Kou Y, Duan Q, Wang Z, Meirelles GV, et al. Enrichr: interactive and collaborative HTML5 gene list enrichment analysis tool. *BMC Bioinformatics* 2013;14:128.
 30. Bouchareychas L, Grossinger EM, Kang M, Adamopoulos IE. γ δ TCR regulates production of interleukin-27 by neutrophils and attenuates inflammatory arthritis. *Sci Rep* 2018;8:7590.
 31. Petrovic J, Silva JR, Bannerman CA, Segal JP, Marshall AS, Haird CM, et al. γ δ T cells modulate myeloid cell recruitment but not pain during peripheral inflammation. *Front Immunol* 2019;10:473.
 32. Griffin GK, Newton G, Tarrío ML, Bu DX, Maganto-Garcia E, Azcutia V, et al. IL-17 and TNF- α sustain neutrophil recruitment during inflammation through synergistic effects on endothelial activation. *J Immunol* 2012;188:6287–99.
 33. Adamopoulos IE, Chao CC, Geissler R, Laface D, Blumenschein W, Iwakura Y, et al. Interleukin-17A upregulates receptor activator of NF- κ B on osteoclast precursors. *Arthritis Res Ther* 2010;12:R29.
 34. Zhang YH, Heulsmann A, Tondravi MM, Mukherjee A, Abu-Amer Y. Tumor necrosis Factor- α (TNF) Stimulates RANKL-induced osteoclastogenesis via coupling of TNF Type 1 receptor and RANK signaling pathways. *J Biol Chem* 2001;276:563–8.
 35. Adamopoulos IE, Mellins ED. Alternative pathways of osteoclastogenesis in inflammatory arthritis. *Nat Rev Rheumatol* 2015;11:189–94.
 36. Wipke BT, Allen PM. Essential role of neutrophils in the initiation and progression of a murine model of rheumatoid arthritis. *J Immunol* 2001;167:1601–8.
 37. Kaul S, Singal A, Grover C, Sharma S. Clinical and histological spectrum of nail psoriasis: a cross-sectional study. *J Cutan Pathol* 2018;45:824–30.
 38. Schon M, Denzer D, Kubitzka RC, Ruzicka T, Schon MP. Critical role of neutrophils for the generation of psoriasiform skin lesions in flaky skin mice. *J Invest Dermatol* 2000;114:976–83.
 39. Chan JR, Blumenschein W, Murphy E, Diveu C, Wiekowski M, Abbondanzo S, et al. IL-23 stimulates epidermal hyperplasia via TNF and IL-20R2-dependent mechanisms with implications for psoriasis pathogenesis. *J Exp Med* 2006;203:2577–87.
 40. Gracey E, Hromadová D, Lim M, Qaiyum Z, Zeng M, Yao Y, et al. TYK2 inhibition reduces type 3 immunity and modifies disease progression in murine spondyloarthritis. *J Clin Invest* 2020;130:1863–78.
 41. Matos TR, O'Malley JT, Lowry EL, Hamm D, Kirsch IR, Robins HS, et al. Clinically resolved psoriatic lesions contain psoriasis-specific IL-17-producing alphabeta T cell clones. *J Clin Invest* 2017;127:4031–41.
 42. Dillen CA, Pinsker BL, Marusina AI, Merleev AA, Farber ON, Liu H, et al. Clonally expanded γ δ T cells protect against *Staphylococcus aureus* skin reinfection. *J Clin Invest* 2018;128:1026–42.
 43. Kallioliadis GD, Zhao B, Triantafyllopoulou A, Park-Min KH, Ivashkiv LB. Interleukin-27 inhibits human osteoclastogenesis by abrogating RANKL-mediated induction of nuclear factor of activated T cells c1 and suppressing proximal RANK signaling. *Arthritis Rheum* 2010;62:402–13.
 44. Stumhofer JS, Laurence A, Wilson EH, Huang E, Tato CM, Johnson LM, et al. Interleukin 27 negatively regulates the development of interleukin 17-producing T helper cells during chronic inflammation of the central nervous system. *Nat Immunol* 2006;7:937–45.
 45. Skeen MJ, Ziegler HK. Induction of murine peritoneal γ δ T cells and their role in resistance to bacterial infection. *J Exp Med* 1993;178:971–84.
 46. Rei M, Goncalves-Sousa N, Lanca T, Thompson RG, Mensurado S, Balkwill FR, et al. Murine CD27(-) V γ 6(+) γ δ T cells producing IL-17A promote ovarian cancer growth via mobilization of protumor small peritoneal macrophages. *Proc Natl Acad Sci U S A* 2014;111:E3562–70.
 47. Louis C, Souza-Fonseca-Guimaraes F, Yang Y, D'Silva D, Kratina T, Dagley L, et al. NK cell-derived GM-CSF potentiates inflammatory arthritis and is negatively regulated by CIS. *J Exp Med* 2020;217:e20191421.
 48. Schett G, Lories RJ, D'Agostino MA, Elewaut D, Kirkham B, Soriano ER, et al. Enthesitis: from pathophysiology to treatment. *Nat Rev Rheumatol* 2017;13:731.
 49. Sherlock JP, Joyce-Shaikh B, Turner SP, Chao CC, Sathe M, Grein J, et al. IL-23 induces spondyloarthritis by acting on ROR- γ t+ CD3+CD4-CD8- enthesal resident T cells. *Nat Med* 2012;18:1069.
 50. Haley EK, Matmusaev M, Hossain IN, Davin S, Martin TM, Ermann J. The impact of genetic background and sex on the phenotype of IL-23 induced murine spondyloarthritis. *PLoS One* 2021;16:e0247149.
 51. Adamopoulos IE, Tessmer M, Chao CC, Adda S, Gorman D, Petro M, et al. IL-23 is critical for induction of arthritis, osteoclast formation, and maintenance of bone mass. *J Immunol* 2011;187:951–9.

Comparative Genetic Analysis of Psoriatic Arthritis and Psoriasis for the Discovery of Genetic Risk Factors and Risk Prediction Modeling

Mehreen Soomro,¹ Michael Stadler,¹  Nick Dand,² James Bluett,³ Deepak Jadon,⁴ Farideh Jalali-najafabadi,¹ Michael Duckworth,⁵ Pauline Ho,³ Helena Marzo-Ortega,⁶ Philip S. Helliwell,⁶  Anthony W. Ryan,⁷ David Kane,⁸ Eleanor Korendowych,⁹ Michael A. Simpson,² Jonathan Packham,¹⁰ Ross McManus,¹¹  Cem Gabay,¹² Céline Lamacchia,¹³  Michael J. Nissen,¹³ Matthew A. Brown,¹⁴ Suzanne M. M. Verstappen,¹⁵ Tjeerd Van Staa,¹⁶ Jonathan N. Barker,⁵ Catherine H. Smith,¹⁷ the BADBIR Study Group, the BSTOP Study Group, Oliver FitzGerald,¹⁸ Neil McHugh,¹⁹ Richard B. Warren,²⁰ John Bowes,³ and Anne Barton³

Objectives. Psoriatic arthritis (PsA) has a strong genetic component, and the identification of genetic risk factors could help identify the ~30% of psoriasis patients at high risk of developing PsA. Our objectives were to identify genetic risk factors and pathways that differentiate PsA from cutaneous-only psoriasis (PsC) and to evaluate the performance of PsA risk prediction models.

Methods. Genome-wide meta-analyses were conducted separately for 5,065 patients with PsA and 21,286 healthy controls and separately for 4,340 patients with PsA and 6,431 patients with PsC. The heritability of PsA was calculated as a single-nucleotide polymorphism (SNP)–based heritability estimate (h^2_{SNP}) and biologic pathways that differentiate PsA from PsC were identified using Priority Index software. The generalizability of previously published PsA risk prediction pipelines was explored, and a risk prediction model was developed with external validation.

Results. We identified a novel genome-wide significant susceptibility locus for the development of PsA on chromosome 22q11 (rs5754467; $P = 1.61 \times 10^{-9}$), and key pathways that differentiate PsA from PsC, including NF- κ B signaling (adjusted $P = 1.4 \times 10^{-45}$) and Wnt signaling (adjusted $P = 9.5 \times 10^{-58}$). The heritability of PsA in this cohort was found to be moderate ($h^2_{\text{SNP}} = 0.63$), which was similar to the heritability of PsC ($h^2_{\text{SNP}} = 0.61$). We observed modest performance of published classification pipelines (maximum area under the curve 0.61), with similar performance of a risk model derived using the current data.

Conclusion. Key biologic pathways associated with the development of PsA were identified, but the investigation of risk classification revealed modest utility in the available data sets, possibly because many of the PsC patients included in the present study were receiving treatments that are also effective in PsA. Future predictive models of PsA should be tested in PsC patients recruited from primary care.

Supported by Versus Arthritis (grants 21173, 21754, and 21755), the NIHR Cambridge Biomedical Research Centre (grant BRC-1215-20014), and Cambridge Arthritis Research Endeavour (CARE). Mr. Stadler's work was supported by an MRC Doctoral Training Partnership (DTP) Studentship (grant MR/N013751/1). Dr. Jalali-najafabadi's work was supported by a Medical Research Council (MRC)/University of Manchester Skills Development Fellowship (grant MR/R016615). Dr. Marzo-Ortega's work was supported by the Leeds NIHR Biomedical Research Centre (LBRC). Dr. Warren's work was supported by the Manchester NIHR Biomedical Research Centre. Dr. Barton's work was supported by the NIHR.

¹Mehreen Soomro MSc, Michael Stadler, MSc, Farideh Jalali-najafabadi, PhD: Centre for Genetics and Genomics Versus Arthritis, Centre for Musculoskeletal Research, Manchester Academic Health Science Centre, The University of Manchester, Manchester, UK; ²Nick Dand, PhD, Michael A. Simpson, PhD: King's College London, London, UK; ³James Bluett, PhD, MBBS, Pauline Ho,

PhD, MBBCh, John Bowes, PhD, Anne Barton, PhD, FRCP: Centre for Genetics and Genomics Versus Arthritis, Centre for Musculoskeletal Research, Manchester Academic Health Science Centre, The University of Manchester, NIHR Manchester Musculoskeletal Biomedical Research Unit, Manchester University NHS Foundation Trust, Manchester, UK; ⁴Deepak Jadon, PhD, MRCP, MBBCh: University of Cambridge, Cambridge, UK; ⁵Michael Duckworth, BSc, Jonathan N. Barker, MD, FRCP, FRCPATH: St John's Institute of Dermatology, King's College London, London, UK; ⁶Helena Marzo-Ortega, PhD, MRCP, Philip S. Helliwell, PhD, FRCP: NIHR Leeds Biomedical Research Centre, Leeds Teaching Hospitals Trust, Leeds Institute of Rheumatic and Musculoskeletal Medicine, University of Leeds, Leeds, UK; ⁷Anthony W. Ryan, PhD: Trinity Translational Medicine Institute, Trinity College Dublin and Genuity Science, Dublin, Ireland; ⁸David Kane, PhD, FRCP: Tallaght University Hospital and Trinity College Dublin, Dublin, Ireland; ⁹Eleanor Korendowych, PhD, BMBCh, MRCP: Royal National Hospital for Rheumatic Diseases and University of Bath, Bath, UK; ¹⁰Jonathan

INTRODUCTION

Psoriatic arthritis (PsA) is a chronic inflammatory condition characterized by the presence of peripheral arthritis, dactylitis, enthesitis, and axial spondyloarthritis (1). PsA affects between 14% and 30% of patients with psoriasis, leading to significant disability and a reduced quality of life (1–3). The ability to identify patients with psoriasis who are at a high risk of developing PsA is an important goal for clinical research, as this would allow early intervention to reduce the impact of PsA and ultimately lead to preventative treatments.

PsA is a typical complex disease in which susceptibility is influenced by a combination of environmental, lifestyle, and genetic risk factors. Previous family pedigree studies have estimated that the heritability of PsA far exceeds that of psoriasis alone, providing evidence of an increased genetic component which, once identified, could help to differentiate those patients at high risk of developing PsA by inclusion of genetic risk factors in clinical prediction models (4–6). However, the results of these family studies have been challenged by data from large-scale case–control studies analyzing variations in single-nucleotide polymorphisms (SNPs), in which only limited differences in heritability estimates have been demonstrated between patients with PsA and patients with psoriasis (7). Several studies have identified genetic risk factors that are specific to PsA, including amino acids within HLA-B and variants at the *IL23R* gene, and the current aim is to translate these genetic discoveries into improved clinical outcomes (8–12). A recent study demonstrated high performance in accurately distinguishing PsA from cutaneous-only psoriasis (PsC) using prediction models based on genetic risk factors. Although this study demonstrated validity by internal cross-validation methods, assessment of these models for generalizability in external data sets is still warranted (13).

To help further our understanding of the genetic basis for PsA, we have constructed a large integrated genetic data set of PsA patients, PsC patients, and population controls imputed to the latest population reference panels. We supplemented this data set by performing a meta-analysis using UK Biobank data, allowing us to contrast PsA patients with population controls and PsC

patients, and to explore differences in the genetic architecture of the 2 traits that could explain the progression to PsA. These data can be used to further our understanding of key genes and biologic pathways important in psoriatic disease using state-of-the-art bioinformatics tools and could be further used to explore the utility of genetic risk prediction models for classifying PsA.

PATIENTS AND METHODS

PsA genome-wide association study (GWAS) cohort.

A total of 4,072 patients with PsA were recruited from rheumatology centers in the UK, Ireland, and Switzerland, from the prospective Swiss Clinical Quality Management (SCQM) registry, and from Australia. Patients recruited in Manchester were diagnosed by a rheumatologist based on the presence of both psoriasis and inflammatory peripheral arthritis, regardless of rheumatoid factor status. While the majority of patients satisfied the CASPAR (Classification of Psoriatic Arthritis) classification system (14), some were recruited prior to the introduction of this classification system. All patients provided written informed consent (UK PsA National Repository Multicentre Research Ethics Committee reference no. 99/8/84). Samples from the Axial Disease in Psoriatic Arthritis Study (ADIPSA) cohort were collected with ethics approval from the French Regional Ethics Committee (reference no. 12/SW/0110). The Leeds cohort comprises adult patients with a clinical diagnosis of PsA fulfilling the CASPAR classification criteria who were recruited as part of an in-house biobank study investigating SNPs of immune response genes in patients with psoriasis, patients with PsA, and patients with ankylosing spondylitis and their relationship to disease susceptibility, articular and extraarticular manifestations, and response to treatment (Research Ethics Committee reference no. 04/Q1205/65, IRAS project no. 232680). All patients provided written informed consent.

A total of 283 patients with PsA were recruited from St. Vincent's University Hospital observational PsA cohort. All patients met the CASPAR criteria. The study protocol received approval from the local ethics committee of St. Vincent's

Packham, BM, DM, FRCP: Haywood Hospital and Midlands Partnership NHS Foundation Trust, Stoke on Trent, UK, and University of Nottingham, Nottingham, UK; ¹¹Ross McManus, PhD, FTCD: Trinity Translational Medicine Institute, Trinity College Dublin, Dublin, Ireland; ¹²Cem Gabay, MD: Geneva University Hospitals, University of Geneva, Geneva, Switzerland; ¹³Céline Lamacchia, PhD, Michael J. Nissen, MBBS, FRACP: Geneva University Hospitals, Geneva, Switzerland; ¹⁴Matthew A. Brown, MBBS, FRACP: King's College London and Genomics England, London, UK; ¹⁵Suzanne M. M. Verstappen, PhD: NIHR Manchester Musculoskeletal Biomedical Research Unit, Manchester University NHS Foundation Trust, Manchester Academic Health Science Centre, Centre for Epidemiology Versus Arthritis, Centre for Musculoskeletal Research, University of Manchester, Manchester, UK; ¹⁶Tjeerd Van Staa, PhD, MD: Health e-Research Centre, Health Data Research UK North, University of Manchester, Manchester, UK; ¹⁷Catherine H. Smith, MD, FRCP: St John's Institute of Dermatology, Guy's and St Thomas' NHS Foundation Trust and King's College London, London, UK; ¹⁸Oliver FitzGerald, MBChB, FRCP: Conway Institute of Biomolecular and Biomedical

Research, University College Dublin, Dublin, Ireland; ¹⁹Neil McHugh, MD: Royal National Hospital for Rheumatic Diseases, University of Bath, Bath, UK; ²⁰Richard B. Warren, PhD, MBChB: Dermatology Centre, Salford Royal NHS Foundation Trust, Manchester NIHR Biomedical Research Centre, University of Manchester, Manchester, UK.

Ms. Soomro and Mr. Stadler contributed equally to this work. Drs. Bowes and Barton jointly supervised this work.

Author disclosures are available at <https://onlinelibrary.wiley.com/action/downloadSupplement?doi=10.1002%2Fart.42154&file=art42154-sup-0001-Disclosureform.pdf>.

Address correspondence to John Bowes, PhD, Centre for Genetics and Genomics Versus Arthritis, Division of Musculoskeletal and Dermatological Sciences, School of Biological Sciences, Faculty of Biology, Medicine and Health, The University of Manchester, AV Hill Building, Oxford Road, Manchester, UK. Email: j.bowes@manchester.ac.uk.

Submitted for publication August 11, 2021; accepted in revised form April 28, 2022.

University Hospital. Written informed consent was obtained from all patients. In addition, a total of 272 patients with PsA were recruited from the prospective SCQM registry in which diagnosis was based on the CASPAR criteria. The study protocol received approval from the local ethics committee of the University Hospital of Geneva (protocol no. 10-089) and the SCQM Biobank Scientific Advisory Board and followed the Guidelines for Good Clinical Practice. Written informed consent was obtained from all patients. A summary of available clinical phenotype data for this cohort is given in Supplementary Table 1 (available on the *Arthritis & Rheumatology* website at <http://onlinelibrary.wiley.com/doi/10.1002/art.42154>).

Psoriasis GWAS cohort. We had access to data from 2,086 psoriasis patient samples obtained through the Biomarkers of Systemic Treatment Outcomes in Psoriasis study (BSTOP) described previously (9). Analysis of patients was restricted to those with no previous diagnosis of PsA, and we refer to this sample group as having cutaneous-only psoriasis (PsC). Patients with psoriasis requiring systemic therapy who also consented to enrolment in the British Association of Dermatologists Biologics Interventions Registry (a UK pharmacovigilance registry) were recruited to BSTOP from over 60 secondary and tertiary care outpatient dermatology departments throughout the UK including centers in London, Manchester, Nottingham, and Liverpool. All patients provided written informed consent (BSTOP Ethics reference no. 11/H0802/7). Classification of PsC in the BSTOP cohort is based on information collected at multiple follow-up consultations (one every 6 months in the first 3 years and then once annually) during which a research nurse or clinician actively investigated the patient's medical records for the presence of a PsA diagnosis made by a rheumatologist. On average, patients in this cohort had a psoriasis disease duration of 27 years without a recorded PsA diagnosis (see Supplementary Figure 1A, available at <http://onlinelibrary.wiley.com/doi/10.1002/art.42154>) and had been participants in the British Association of Dermatologists Biologic and Immunomodulators Register (BADBIR) study for ~7 years (Supplementary Figure 1B) with an average of 8 follow-up consultations.

Control population GWAS cohort. As controls, genotype data were available for 9,965 general population subjects from the UK Household Longitudinal Study (<https://www.understandingsociety.ac.uk/>), accessed through the European Genome-phenome Archive. Samples were genotyped at the Wellcome Trust Sanger Institute using the Illumina Infinium CoreExome genotyping array. The quality control procedures applied to genotyping of control samples were consistent with those described below for patient samples.

Genotyping and statistical quality control. PsA samples were genotyped using the Illumina Infinium CoreExome

genotyping array. This was performed in accordance with the manufacturer's instructions where genotype calling was performed using the GenCall algorithm in the GenomeStudio Data Analysis software platform (Genotyping Module version 1.8.4). Psoriasis samples were genotyped using the Illumina HumanOmniExpressExome-8v1-2_A array performed at King's College London with quality control as previously described (15). The 3 data sets (PsA, PsC, and controls) were combined with the intersection of SNPs being retained; hereafter, this is referred as the PsA-BSTOP GWAS data set. Further details are provided in the Supplementary Materials and Methods and Supplementary Figure 2 (available at <http://onlinelibrary.wiley.com/doi/10.1002/art.42154>).

Imputation. Imputation was performed for the combined data set of PsA, PsC, and control samples described above. Prior to imputation, SNPs with ambiguous alleles (C/G and A/T) were excluded, and remaining SNPs were aligned to the Haplotype Reference Consortium (HRC) panel (version 1.1) using the HRC imputation preparation tool (<https://www.well.ox.ac.uk/~wrayner/tools/>). Imputation was performed using the Michigan Imputation server in which phasing was performed with Shapeit2 and imputation was performed with the HRC panel. Following imputation, SNPs were excluded based on a minor allele frequency (MAF) of <0.01 and imputation accuracy of $r^2 < 0.5$.

UK Biobank. We accessed imputed genotype data from the UK Biobank (application number 799) for self-reported outcomes in 731 PsA patients and 3,197 psoriasis patients (16). Control population data were obtained using random sampling from the remaining cohort at a ratio of 4 controls to 1 patient to minimize inflation of test statistics due to case-control imbalance. All participants were selected from the subset of White patients of British ancestry. In addition, we created a data set based on International Statistical Classification of Diseases and Related Health Problems, Tenth Revision (ICD-10) codes L40 and L405, which yielded a cohort of 795 psoriasis patients and 435 PsA patients.

PsA ImmunoChip data set. Genotype data were available for 1,962 PsA patients and 8,923 controls (controls were recruited from the 1958 Birth Cohort and the National Blood Service) (17). Sample overlap with the GWAS and UK Biobank data sets was determined using identity by descent analysis (Kinship-based Inference for GWAS software) and duplicate samples were excluded from the ImmunoChip data set, leaving a total of 725 PsA patients and 8,897 controls.

Association testing and meta-analysis. Case-control association analyses were performed with the SNPTEST software package (version 2.5.2) using their scoring method to account for imputation uncertainty. Meta-analyses were conducted using an inverse variance meta-analysis assuming fixed effects with version

2.2.2 of the software package Genome-Wide Association Meta-Analysis (GWAMA) (18). Lambda genomic control (λ_{gc}) inflation factor, corrected for sample size (λ_{gc1000}), was calculated to test for inflation of test statistics attributable to population stratification, and potential inflation of test statistics from other sources. An overview of these analyses is available in Supplementary Figure 3 and further details are provided in the Supplementary Materials and Methods (association testing and meta-analysis) (available at <http://onlinelibrary.wiley.com/doi/10.1002/art.42154>).

Heritability estimates. Heritability of PsA and PsC was estimated in the PsA-BSTOP GWAS data set using genome-wide complex trait analysis (GCTA software). SNPs were stratified into quartiles based on levels of linkage disequilibrium, and then further stratified into bins according to MAF values (see Supplementary Materials and Methods). Calculations were performed with no prevalence specified and with a specified disease prevalence of 1% for comparison with previously reported estimates (7). Both calculations were repeated with SNPs excluded from the major histocompatibility complex (MHC).

Gene and pathway prioritization. We prioritized key genes and pathways for psoriatic disease using the priority index (Pi) pipeline (19). Genes were prioritized based on the following criteria: 1) proximity of SNPs to genes and localization to their topologically associated domain (cell line GM12878); 2) physical interaction determined by chromatin conformation (monocytes, macrophages [M0, M1, M2], neutrophils, CD4 T cells [naive and total], CD8 T cells [naive and total], or B cells [naive and total]); 3) correlation with gene expression (monocytes [unstimulated, lipopolysaccharide (LPS)-stimulated for 2 hours and 24 hours, interferon- γ (IFN γ)-stimulated for 24 hours], B cells, peripheral whole blood, CD4 T cells, CD8 T cells, neutrophils, or natural killer cells). Further scoring was based on gene ontologies for immune function, immune phenotype, and rare genetic immune diseases according to the OMIM. Enrichment in pathways was based on Reactome pathways.

Reproducing existing pipelines. A recent publication reported the performance of an analysis pipeline based on multiple machine learning approaches for the classification of PsA in patients with psoriasis, referred to hereafter as the Michigan classification pipeline (13). Based on the author recommendations for reproducing this pipeline, we trained 2 of the reported best performing machine learning algorithms (random forest and conditional inference forest) in the PsA-BSTOP GWAS data set to capture the cohort-specific parameters using the reported model parameters and the sets of genetics features (see Supplementary Table 2, available at <http://onlinelibrary.wiley.com/doi/10.1002/art.42154>). The models were internally validated using k-fold cross-validation and were trained using the Machine Learning in R (MLR) package (see Supplementary Figure 4A for an overview

and the Supplementary Materials and Methods for further details, available at <http://onlinelibrary.wiley.com/doi/10.1002/art.42154>).

Model development and validation. We developed a PsA prediction model using a set of 4,729,872 SNPs with a minimum imputation accuracy score of ≥ 0.9 and call rate of ≥ 0.99 in both the PsA-BSTOP GWAS and the UK Biobank GWAS ICD-10 data sets in which the PsA-BSTOP data set was used as the training data set and the UK Biobank ICD-10 data set was used for external validation (see Supplementary Figure 4B, available at <http://onlinelibrary.wiley.com/doi/10.1002/art.42154>). We utilized a lasso-penalized linear regression model using all post-quality control imputed SNPs where the penalty (L1) was tuned with 10 repetitions of 10-fold cross-validation implemented in the SparSNP software package (20). The best model was selected based on the maximal area under the curve (AUC) and classification and calibration were evaluated in the validation data set.

Data availability. Summary statistics of the GWAS analyzed in the current study are available through the National Human Genome Research Institute-European Bioinformatics Institute GWAS Catalog at <https://www.ebi.ac.uk/gwas/downloads/summary-statistics>. Control population data were obtained from the UK Household Longitudinal Study. Information on how to access the data can be found on the Understanding Society website at <https://www.understandingsociety.ac.uk/>.

RESULTS

Heritability estimates. We calculated the SNP-based heritability (h^2_{SNP}) of PsA in the PsA-BSTOP GWAS data set of 3,609 patients and 9,192 controls. The estimated heritability of PsA in the full data set was $h^2_{SNP} = 0.63$ (SD 0.04), while in analyses using non-MHC SNPs, the estimated heritability was $h^2_{SNP} = 0.61$ (SD 0.04).

In analyses in which the disease prevalence was specified to be 1% (in comparison to previous prevalence estimates [7]), the estimated heritability of PsA was $h^2_{SNP} = 0.43$ (SD 0.03), while the heritability of PsA in analyses using non-MHC SNPs was $h^2_{SNP} = 0.41$ (SD 0.03).

The heritability of PsC in a population of 2,085 patients and 9,192 controls was estimated to be $h^2_{SNP} = 0.61$ (SD 0.05), while in analyses using non-MHC SNPs, the estimated heritability of PsC was $h^2_{SNP} = 0.59$ (SD 0.05). With a disease prevalence of 1%, the estimated heritability of PsC was found to be $h^2_{SNP} = 0.56$ (SD 0.04), while the heritability of PsC in analyses using non-MHC SNPs was $h^2_{SNP} = 0.54$ (SD 0.05).

Association testing and meta-analysis. We performed a meta-analysis of GWAS summary statistics from a total of 5,065 PsA patients and 21,286 controls for a maximum of

Table 1. Non-MHC loci with genome-wide significance in the development of PsA identified through a meta-analysis of GWAS summary statistics from PsA patients and controls*

SNP	Chromosome	Base position	Notable genes	Risk/non-risk allele	RAF	P	OR (95% CI)	P by Cochran's Q test	I ²
rs33980500	6	111913262	<i>TRAF3IP2</i>	T/C	0.07	1.14×10^{-36}	1.66 (1.54–1.8)	0.48	0
rs62377586	5	158766022	<i>IL12B</i>	G/A	0.67	8.17×10^{-35}	1.36 (1.3–1.43)	0.52	0
rs2111485	2	163110536	<i>IFIH1</i>	G/A	0.61	1.24×10^{-20}	1.25 (1.19–1.31)	0.80	0
rs12044149	1	67600686	<i>IL23R</i>	T/G	0.26	3.84×10^{-20}	1.27 (1.2–1.33)	0.27	0.23
rs76956521	5	150464641	<i>TNIP1</i>	C/A	0.05	2.65×10^{-16}	1.49 (1.36–1.64)	0.82	0
rs848	5	131996500	<i>IL13</i>	C/A	0.82	9.49×10^{-16}	1.28 (1.21–1.36)	0.65	0
rs34536443	19	10463118	<i>TYK2</i>	G/C	0.95	1.16×10^{-14}	1.71 (1.49–1.96)	0.70	0
rs17622208	5	131717050	<i>SLC22A5</i>	A/G	0.48	5.73×10^{-14}	1.19 (1.14–1.24)	0.12	0.53
rs2020854	12	56743367	<i>STAT2</i>	T/C	0.93	1.26×10^{-13}	1.43 (1.3–1.57)	0.01	0.78
rs3794767	17	26124605	<i>NOS2</i>	C/T	0.64	4.73×10^{-13}	1.19 (1.14–1.25)	0.83	0
rs13203885	6	111995127	<i>FYN</i>	C/T	0.12	1.55×10^{-11}	1.26 (1.18–1.35)	0.74	0
rs1395621	1	25270572	<i>RUNX3</i>	C/T	0.48	6.48×10^{-11}	1.17 (1.12–1.23)	0.65	0
rs5754467†	22	21985094	<i>CCDC116</i>	G/A	0.19	1.61×10^{-9}	1.19 (1.13–1.27)	0.85	0
rs610604	6	138199417	<i>TNFAIP3</i>	G/T	0.32	7.76×10^{-9}	1.15 (1.1–1.21)	0.14	0.50

* Inconsistency metrics (I²) describing the percentage of variation across studies due to heterogeneity were assessed for significance by Cochran's Q heterogeneity test. The threshold for genome-wide significance was $P = 5 \times 10^{-8}$. MHC = major histocompatibility complex; GWAS = genome-wide association study; SNP = single-nucleotide polymorphism; RAF = risk allele frequency; OR = odds ratio; 95% CI = 95% confidence interval.

† Novel locus not previously identified as significant in the development of psoriatic arthritis (PsA).

8,558,403 SNPs using data from the PsA-BSTOP, the UK Biobank, and the PsA Immuchip data sets (see Supplementary Figure 3A, available at <http://onlinelibrary.wiley.com/doi/10.1002/art.42154>). The genomic control inflation factor λ_{gc} (λ_{gc1000}) for the PsA-BSTOP GWAS data set was estimated to be 1.1 (1.01), indicating minimal residual population stratification based on inflation of test statistics. We identified 16 non-MHC loci with genome-wide significance for the development of PsA ($P = 5 \times 10^{-8}$), 15 of which have previously been reported as significant in PsA and one which is novel (Table 1 and Figure 1). This novel genome-wide association represents an association with the intergenic SNP rs5754467 ($P = 1.61 \times 10^{-9}$) on chromosome

22q11 in close proximity to the gene *UBE2L3*. We also found that the 2 previously reported PsA-specific susceptibility loci *PTPN22* (rs2476601; $P = 6.03 \times 10^{-7}$) and chr5q31 (rs715285; $P = 2.86 \times 10^{-11}$) had genome-wide significance for the development of PsA.

Next, we performed a meta-analysis of summary statistics for the comparison of PsA to PsC (PsA-BSTOP and UK Biobank data) to identify PsA-specific susceptibility loci using a population consisting of 4,340 PsA patients and 6,431 PsC patients (see Supplementary Figure 3B, available at <http://onlinelibrary.wiley.com/doi/10.1002/art.42154>). We identified significant genome-wide association in 2 loci previously reported to be associated

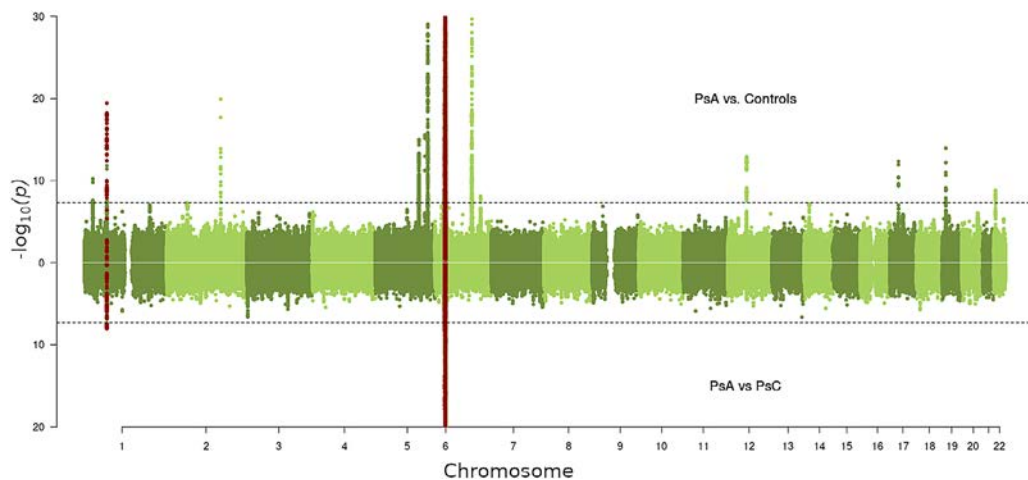


Figure 1. Manhattan plots showing the P values of genome-wide significance from the meta-analysis of summary statistics obtained from psoriatic arthritis (PsA) patients compared to population controls (top), and PsA patients compared to cutaneous-only psoriasis (PsC) patients (bottom). The genome-wide significance threshold was set at $P = 5 \times 10^{-8}$ and is indicated by the dashed lines. Each dot represents a single-nucleotide polymorphism (SNP). Red dots indicate the most significant SNPs in both data sets.

Table 2. Loci showing the most significant association with PsA or PsC from the PsA-STOP, UK Biobank, and meta-analysis data sets*

	SNPs			
	rs17194140	rs11665266	rs76800961	rs306281
Chromosome	3	18	14	7
Base position	2198673	10441470	85656555	154785362
Notable genes	<i>CNTN4</i>	None	None	<i>PAXIP1</i>
Risk/non-risk allele	T/C	A/G	A/C	G/A
<i>P</i> for association, PsA-BSTOP data set	2.75×10^{-5}	0.00304	3.33×10^{-5}	1.81×10^{-4}
<i>P</i> for association, UK Biobank data set	2.62×10^{-3}	6.35×10^{-5}	2.30×10^{-2}	6.92×10^{-3}
<i>P</i> for association, meta-analysis data set	2.51×10^{-7}	1.96×10^{-6}	2.61×10^{-6}	3.97×10^{-6}
OR (95% CI)	1.2 (1.12–1.29)	1.34 (1.19–1.51)	1.39 (1.21–1.59)	1.17 (1.09–1.24)
<i>P</i> by Cochran's Q test	0.97	0.15	0.60	0.95
<i>I</i> ²	0.00	0.53	0.00	0.00

* The overall *P* value for the meta-analysis was $P = 5 \times 10^{-6}$. Inconsistency metrics (*I*²) describing the percentage of variation across studies due to heterogeneity were assessed for significance by Cochran's Q heterogeneity test. See Table 1 for definitions.

with the development of PsA, namely the MHC region (rs1050414; $P = 8.49 \times 10^{-59}$) and the *IL23R* gene (rs72676069; $P = 9.94 \times 10^{-9}$). No other regions reached genome-wide significance. However, 4 loci demonstrated evidence of significant association in both data sets, with an overall *P* value in the meta-analysis of $P < 5 \times 10^{-6}$ (Table 2), giving us confidence in the existence of additional PsA-specific loci.

Gene and pathway prioritization. We utilized the recently described Pi bioinformatics pipeline to identify key genes and pathways in the development of PsA (19). Using summary statistics from the meta-analyses described above for PsA patients versus controls, we found that the most highly ranked gene with regard to PsA susceptibility based on the Pi was *ICAM1*, which has a role in epithelial cell adhesion (see Supplementary Table 3, available at <http://onlinelibrary.wiley.com/doi/10.1002/art.42154>). In addition, several genes involved in IFN regulation were highly ranked (*IRF1*, *IRF5* and *IRF7*). Other highly ranked genes included *UBA52*, *CNPY2*, *STAT2*, and *TYK2*. Using the top 1% of ranked genes, we found significant enrichment in IFN and interleukin signaling pathways (see Supplementary Table 4, available at <http://onlinelibrary.wiley.com/doi/10.1002/art.42154>). These pathways were not found to be enriched when using summary statistics from PsA patients compared to those from PsC patients, suggesting that these pathways are primarily involved in the pathogenesis of psoriasis (see Supplementary Tables 5 and 6, available at <http://onlinelibrary.wiley.com/doi/10.1002/art.42154>). Pathways found to be enriched in the comparison of PsA to PsC included multiple pathways for NF- κ B signaling (adjusted $P = 1.4 \times 10^{-45}$) and Wnt signaling (adjusted $P = 9.5 \times 10^{-58}$), which provides compelling evidence that these pathways are potentially involved in the development of PsA.

Risk prediction. We assessed the ability of the Michigan classification pipeline to discriminate PsA from PsC in our available data sets (see Supplementary Figure 4A). The 2 reported statistical approaches (the random forest model and the conditional inference forest model) performed poorly across both the training

data set (PsA-BSTOP) and the validation data set (UK Biobank ICD-10), with C statistics of <0.6 by external validation (Figure 2). Each model was characterized by high sensitivity but low specificity, indicating a high rate of false positives (see Supplementary Table 7, available at <http://onlinelibrary.wiley.com/doi/10.1002/art.42154>). In addition, calibration and clinical utility were found to be poor for both the random forest model and the conditional inference forest model (see Supplementary Figures 5 and 6). The best performing model based on accuracy of discrimination in the validation data set was the random forest model, where the C statistic was found to be 0.61 (95% confidence interval [95% CI] 0.56–0.76) in internal validation, but which dropped considerably to 0.57 (95% CI 0.54–0.61) in external validation. The overall performance of the random forest model as measured by the Brier score was similar for internal and external validation, with Brier scores of 0.22 and 0.30, respectively, suggesting poor agreement in both data sets. The random forest model was also found to be poorly calibrated, with a calibration-in-the-large (CITL) score of 0.27 (95% CI -0.13 , 0.69) in internal validation and a noticeably worse CITL score of 1.2 (95% CI 0.92–1.51) in external validation.

Finally, we used the PsA-BSTOP GWAS data set to develop a PsA risk prediction model using a set of 4,729,872 SNPs and lasso-penalized linear regression (see Supplementary Figure 4B, available at <http://onlinelibrary.wiley.com/doi/10.1002/art.42154>). The best model achieved an AUC of 0.66 when assessed using 10-fold cross-validation and consisted of 118 SNPs, 34 of which mapped to the MHC (see Supplementary Figure 7). The SNP weights, *P* values, and model intercept are reported in Supplementary Table 8, available at <http://onlinelibrary.wiley.com/doi/10.1002/art.42154>. Independent validation of this model in the UK Biobank GWAS data set demonstrated an AUC of 0.57. The optimal prediction cutoff value to maximize the true-positive rate and minimize the false-positive rate was 0.3, which resulted in a sensitivity of 0.53 and a specificity of 0.58. Calibration of this model was found to be poor, with a CITL score of -2.16 (95% CI -2.31 , -2.01) (see Supplementary Figure 8), suggesting a general overestimation of risk, and a calibration slope of 1.41

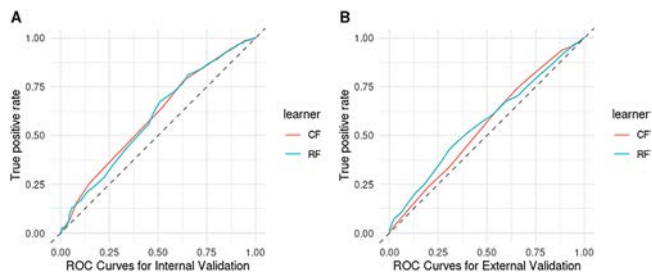


Figure 2. Receiver operating characteristic (ROC) curves showing the sensitivity and specificity of the random forest (RF) and the conditional inference forest (CF) machine learning algorithms in discriminating between psoriatic arthritis (PsA) and cutaneous-only psoriasis (PsC). Both the RF and CF models showed modest performance across the PsA-Biomarkers of Systemic Treatment Outcomes in Psoriasis (PsA-BSTOP) study data set (A) and the UK Biobank International Statistical Classification of Diseases and Related Health Problems, Tenth Revision data set (B). The Concordance statistic for each model was <0.6 by external validation.

(95% CI 0.95–1.86), suggesting that the predictions were too moderate and showing limited variation in the predicted probabilities.

DISCUSSION

Using a large integrated data set of PsA patients, PsC patients, and controls, we have been able to provide accurate heritability estimates, identify a novel susceptibility locus, explore key biologic pathways associated with the development of PsA, and explore the utility of prediction models for classifying PsA risk. While the individual SNP analysis showed large overlap between PsC and PsA, pathway analysis revealed important differences, including enrichment of PsA-significant SNPs found in key pathways such as NF- κ B and Wnt signaling.

The SNP-based heritability estimates reported herein support recent findings by Li et al (7) and show comparable heritability of PsA and PsC. Our results do not support the previous family and population estimates that suggest a substantially larger heritable component for PsA above that of psoriasis alone (4–6). Seventeen genome-wide associations were identified, including rs5754467 ($P = 1.61 \times 10^{-9}$) which maps to chromosome 22q11 and is near the genes *UBE2L3*, *YDJC*, and *CCDC116*. This SNP has not been previously reported in the setting of PsA, but is highly correlated ($r^2 > 0.8$ based on SNP data from a northern European population) with a previously identified psoriasis SNP. This correlation does not represent a PsA-specific genetic effect (12), but further supports the genetic similarity of psoriasis in both patients with PsA and patients with PsC.

We used the Pi pipeline to identify key genes and pathways involved in PsA susceptibility. In analyses of PsA patients compared to controls, we replicated the previously reported findings of prioritized genes (*ICAM1*, *IRF1*, *STAT2*, and *TYK2*) and target pathways (IFN and interleukin signaling) for psoriasis, further

supporting the notion that psoriasis in patients with PsA is genetically and biologically similar to psoriasis in patients with PsC. Interestingly, these pathways for PsA development were reported previously in a study applying the Pi pipeline to a set of 59 SNPs associated with PsA (21). However, of greatest interest is the prioritized target pathways that differ between PsA and PsC, which provide insight into the PsA-specific processes whereby we find enrichment in multiple NF- κ B signaling annotations and the Wnt signaling pathway.

The Wnt signaling pathway plays a key role in bone formation in normal development and in abnormal bone formation in diseases such as axial spondyloarthritis and osteoarthritis. The Wnt signaling pathway may also be of particular interest in the setting of PsA, where bone formation in peripheral joints is included in the CASPAR criteria for the classification of PsA. Blocking of Dkk-1 (an inhibitor of Wnt signaling) in mice has been shown to halt progressive and erosive joint destruction in inflammatory arthritis by encouraging bone formation (22). Interestingly, a previous study on PsA demonstrated that PsA patients had lower levels of Dkk-1 compared to healthy controls, and treatment with secukinumab increased these levels over a period of 6 months to normal Dkk-1 serum levels (23). In contrast, another study reported no significant difference in levels of Dkk-1 in patients with PsA without radiographic axial disease compared to healthy controls (24). Therefore, further work is required to understand the role of Wnt signaling in PsA.

A previous study by Aterido et al investigated pathways associated with PsA susceptibility and reported significant association with the glycosaminoglycan metabolism pathway (Reactome R-HSA-1630316) (25). However, no association between PsA susceptibility and the glycosaminoglycan metabolism pathway was observed in our data, as none of the highly prioritized genes overlapped with genes in this pathway annotation. These differing results could be attributed to differences in the methods used for mapping SNPs to genes, as in the study by Aterido et al SNPs were assigned to genes based solely on proximity. It is now well recognized that causal genes are not always those that are closest to the GWAS hit, and the causal SNP may exert its regulatory effect on distant genes. The Pi pipeline addresses this limitation by including gene expression data and chromatin confirmation data in order to capture evidence for SNP–gene physical interactions in addition to proximity information (19). Aterido et al also reported that the SNP rs10865331 at the *B3GNT2* locus was associated with the risk of developing PsA but not PsC ($P = 0.029$). While we found significant association with this SNP when comparing PsA patients to controls ($P = 2.05 \times 10^{-7}$), we found no evidence that this association is PsA-specific based on our stratified analyses comparing PsA to PsC using PsA-BSTOP data ($P = 0.41$) or on the larger meta-analysis using UK Biobank and ImmunoChip data ($P = 0.31$).

Our prediction models showed only modest ability to discriminate PsA from PsC in the available data sets, which was

consistent with the findings of a recently published study by Smith et al (26). For the first approach, we attempted to reproduce a previously published classification pipeline by following the description and published model parameters, which allowed us to reproduce the workflows (13). Following the author recommendations, we used the 2 sets of genetic features that were selected using a well-phenotyped cohort and estimated the model parameters in our data to capture cohort-specific effects and optimize performance. Second, we attempted to develop a model for our existing data sets through external validation. However, neither of these approaches achieved satisfactory discrimination either with internal or external validation. Given that the predictive performance of a model using the same data on which it was developed (often referred to as apparent performance) will tend to give an optimistic estimate of the model's performance, it is not uncommon for a prediction model to achieve lower performance results when applied to an external population.

The lack of discrimination observed in our data sets could be due to the differences in demographic and clinical characteristics of participants in our data sets compared to those of the participants in the original study. PsA is clinically a heterogeneous disease and differing proportions of patients with oligoarticular or polyarticular arthritis mutilans and axial disease (each with potentially differing genetic risk factors) could have contributed to the decreased performance of the model. This potential issue was recognized by the authors of the original study and, although we followed the author recommendations by modeling the effects of these markers in our data to learn these cohort-specific parameters, the overall classification performance remained low (13).

An important limitation of our study was the potential impact of poor phenotype specificity in the PsC cohorts where the existence of undiagnosed PsA could have confounded the performance of any classification models. Although the participants in the BSTOP study were not screened for the absence of PsA by a rheumatologist, they were routinely followed-up with an average of 8 consultations and had a psoriasis disease duration of 27 years without a recorded diagnosis of PsA. Additionally, restricting analyses to a subgroup of PsC patients with psoriasis for a duration of ≥ 10 (to minimize the risk of undiagnosed PsA) did not improve the performance of the predictive model (data not shown). However, given the extent of undiagnosed PsA in dermatology clinics, we cannot exclude the possibility of undiagnosed PsA in this group, which would have impacted both feature selection and model performance (27). Furthermore, given that patients in the PsC group were treated with biologic drugs that are also effective in the treatment of PsA, it is possible that PsA development was prevented in susceptible individuals, thus limiting the power of the models to discriminate between groups (28).

In conclusion, predicting the risk of PsA development in patients with psoriasis remains an important research question, and external validation in addition to statistical validation is an important step in the clinical translation of PsA prediction models,

as external validation tests the transportability of models to plausibly related populations (29). While polygenic risk scores capture the heritable component of disease susceptibility, they fail to capture the more dynamic risk factors that can modulate susceptibility, such as environmental and lifestyle risk factors. In addition, studies have shown that genetic risk factors can be independent of known clinical risk factors (30). This suggests that future research on PsA susceptibility in patients with psoriasis should move toward combining clinical data and genetics from data collected longitudinally, using a prospective study design in patients with clinically well-defined PsC before treatment with biologic drugs, to create an integrated risk score. Therefore, these future efforts should also investigate the integration of more dynamic biomarkers, such as the host microbiome and immunophenotyping, into the development of PsA risk prediction models.

ACKNOWLEDGMENTS

We are grateful for the assistance given by The University of Manchester IT Services and for the use of the Computational Shared Facility. We thank all of the patient participants and acknowledge the enthusiastic collaboration of all clinicians and research teams in the UK and the Republic of Ireland who recruited for this study. We gratefully acknowledge the substantial contribution to administration of this project by the following members of the Data Monitoring Committee (DMC) of the BADBIR Study Group: Dr. Robert Chalmers, Dr. Carsten Flohr (Chair), Dr. Karen Watson, and David Prieto-Merino. We also thank the following members of the BADBIR Steering Committee: Oras Alabas, Professor Jonathan Barker, Gabrielle Becher, Anthony Bewley, David Burden, Simon Morrison, Professor Phil Laws (Chair), Mr. Ian Evans, Professor Christopher Griffiths, Shehnaz Ahmed, Dr. Brian Kirby, Elise Kleyn, Ms. Linda Lawson, Teena Mackenzie, Tess McPherson, Dr. Kathleen McElhone, Dr. Ruth Murphy, Professor Anthony Ormerod, Dr. Caroline Owen, Professor Nick Reynolds, Amir Rashid, Professor Catherine Smith, and Dr. Richard Warren. We are grateful to the following members of the BSTOP Steering Committee for their valuable role in the oversight of the study delivery: Professor David Burden (Chair), Professor Catherine Smith, Professor Stefan Siebert, Professor Sara Brown, Helen McAteer, Dr. Julia Schofield, and Dr. Nick Dand. Finally, we acknowledge the enthusiastic collaboration of all the dermatologists and specialist nurses in the UK and the Republic of Ireland who provided the BADBIR and BSTOP data. The principal investigators at the participating sites can be found at the following website: <http://www.badbir.org/Clinicians/>. Open access funding was enabled and organized by Projekt DEAL.

AUTHOR CONTRIBUTIONS

All authors were involved in drafting the article or revising it critically for important intellectual content, and all authors approved the final version to be published. Dr. Barton had full access to all of the data in the study and takes responsibility for the integrity of the data and the accuracy of the data analysis.

Study conception and design. Soomro, Stadler, Dand, Barker, Smith, Bowes, Barton.

Acquisition of data. Dand, Jadon, Duckworth, Ho, Marzo-Ortega, Helliwell, Ryan, Kane, Korendowych, Simpson, Packham, McManus, Gabay, Lamacchia, Nissen, Brown, Verstappen, Barker, Smith, Fitzgerald, McHugh, Warren, Bowes, Barton.

Analysis and interpretation of data. Soomro, Stadler, Dand, Bluett, Jalali-najafabadi, Duckworth, Van Staa, Barker, Smith, Bowes, Barton.


ADDITIONAL DISCLOSURES

Author Ryan is an employee of Genuity Science Dublin. Author Brown is an employee of Genomics England.

REFERENCES

1. Ritchlin CT, Colbert RA, Gladman DD. Psoriatic Arthritis. *N Engl J Med* 2017;376:957–70.
2. Ibrahim G, Waxman R, Helliwell PS. The prevalence of psoriatic arthritis in people with psoriasis. *Arthritis Rheum* 2009;61:1373–8.
3. Alinaghi F, Calov M, Kristensen LE, Gladman DD, Coates LC, Jullien D, et al. Prevalence of psoriatic arthritis in patients with psoriasis: a systematic review and meta-analysis of observational and clinical studies. *J Am Acad Dermatol* 2019;80:251–65.
4. Chandran V, Schentag CT, Brockbank JE, Pellett FJ, Shanmugarajah S, Toloza SM, et al. Familial aggregation of psoriatic arthritis. *Ann Rheum Dis* 2009;68:664–7.
5. Moll JM, Wright V. Familial occurrence of psoriatic arthritis. *Ann Rheum Dis* 1973;32:181–201.
6. Brandrup F, Holm N, Grunnet N, Henningsen K, Hansen HE. Psoriasis in monozygotic twins: variations in expression in individuals with identical genetic constitution. *Acta Derm Venereol* 1982;62:229–36.
7. Li Q, Chandran V, Tsoi L, O’Rielly D, Nair RP, Gladman D, et al. Quantifying differences in heritability among psoriatic arthritis (PsA), cutaneous psoriasis (PsC) and psoriasis vulgaris (PsV). *Sci Rep* 2020;10:4925.
8. Bowes J, Budu-Aggrey A, Huffmeier U, Uebe S, Steel K, Hebert HL, et al. Dense genotyping of immune-related susceptibility loci reveals new insights into the genetics of psoriatic arthritis. *Nat Commun* 2015;6:6046.
9. Bowes J, Ashcroft J, Dand N, Jalali-Najafabadi F, Bellou E, Ho P, et al. Cross-phenotype association mapping of the MHC identifies genetic variants that differentiate psoriatic arthritis from psoriasis. *Ann Rheum Dis* 2017;76:1774–9.
10. Budu-Aggrey A, Bowes J, Loehr S, Uebe S, Zervou MI, Helliwell P, et al. Replication of a distinct psoriatic arthritis risk variant at the IL23R locus. *Ann Rheum Dis* 2016;75:1417–8.
11. Okada Y, Han B, Tsoi LC, Stuart PE, Ellinghaus E, Tejasvi T, et al. Fine mapping major histocompatibility complex associations in psoriasis and its clinical subtypes. *Am J Hum Genet* 2014;95:162–72.
12. Tsoi LC, Spain SL, Knight J, Ellinghaus E, Stuart PE, Capon F, et al. Identification of 15 new psoriasis susceptibility loci highlights the role of innate immunity. *Nat Genet* 2012;44:1341–8.
13. Patrick MT, Stuart PE, Raja K, Gudjonsson JE, Tejasvi T, Yang J, et al. Genetic signature to provide robust risk assessment of psoriatic arthritis development in psoriasis patients. *Nat Commun* 2018;9:4178.
14. Taylor W, Gladman D, Helliwell P, Marchesoni A, Mease P, Mielants H, and the CASPAR Study Group. Classification criteria for psoriatic arthritis: development of new criteria from a large international study. *Arthritis Rheum* 2006;54:2665–73.
15. Dand N, Duckworth M, Baudry D, Russell A, Curtis CJ, Lee SH, et al. HLA-C*06:02 genotype is a predictive biomarker of biologic treatment response in psoriasis. *J Allergy Clin Immunol* 2019;143:2120–30.
16. Bycroft C, Freeman C, Petkova D, Band G, Elliott LT, Sharp K, et al. The UK Biobank resource with deep phenotyping and genomic data. *Nature* 2018;562:203–9.
17. Bowes J, Budu-Aggrey A, Huffmeier U, Uebe S, Steel K, Hebert HL, et al. Dense genotyping of immune-related susceptibility loci reveals new insights into the genetics of psoriatic arthritis. *Nat Commun* 2015;6:6046.
18. Magi R, Morris AP. GWAMA: software for genome-wide association meta-analysis. *BMC Bioinformatics* 2010;11:288.
19. Fang H, De Wolf H, Knezevic B, Burnham KL, Osgood J, Sanniti A, et al. A genetics-led approach defines the drug target landscape of 30 immune-related traits. *Nat Genet* 2019;51:1082–91.
20. Abraham G, Kowalczyk A, Zobel J, Inouye M. SparSNP: fast and memory-efficient analysis of all SNPs for phenotype prediction. *BMC Bioinformatics* 2012;13:88.
21. Bui A, Liu J, Hong J, Haderl E, Mosca M, Brownstone N, et al. Identifying novel psoriatic disease drug targets using a genetics-based priority index pipeline. *J Psoriasis Psoriatic Arthritis* 2021;6:185–97.
22. Diarra D, Stolina M, Polzer K, Zwerina J, Ominsky MS, Dwyer D, et al. Dickkopf-1 is a master regulator of joint remodeling. *Nat Med* 2007;13:156–63.
23. Fassio A, Gatti D, Rossini M, Idolazzi L, Giollo A, Adami G, et al. Secukinumab produces a quick increase in WNT signalling antagonists in patients with psoriatic arthritis. *Clin Exp Rheumatol* 2019;37:133–6.
24. Jadon DR, Sengupta R, Nightingale A, Lu H, Dunphy J, Green A, et al. Serum bone-turnover biomarkers are associated with the occurrence of peripheral and axial arthritis in psoriatic disease: a prospective cross-sectional comparative study. *Arthritis Res Ther* 2017;19:210.
25. Aterido A, Cañete JD, Tornero J, Ferrándiz C, Pinto JA, Gratacós J, et al. Genetic variation at the glycosaminoglycan metabolism pathway contributes to the risk of psoriatic arthritis but not psoriasis. *Ann Rheum Dis* 2019;78.
26. Smith MP, Ly K, Thibodeaux Q, Beck K, Yang E, Sanchez I, et al. Evaluation of a genetic risk score for diagnosis of psoriatic arthritis. *J Psoriasis Psoriatic Arthritis* 2020;5:61–7.
27. Mease PJ, Gladman DD, Papp KA, Khraishi MM, Thaçi D, Behrens F, et al. Prevalence of rheumatologist-diagnosed psoriatic arthritis in patients with psoriasis in European/North American dermatology clinics. *J Am Acad Dermatol* 2013;69:729–35.
28. Rosenthal YS, Schwartz N, Sagy I, Pavlovsky L. Incidence of psoriatic arthritis among patients receiving biologic treatments for psoriasis: a nested case-control study. *Arthritis Rheumatol* 2022;74:237–43.
29. Steyerberg EW, Vergouwe Y. Towards better clinical prediction models: seven steps for development and an ABCD for validation. *Eur Heart J* 2014;35:1925–31.
30. Khera A V, Emdin CA, Drake I, Natarajan P, Bick AG, Cook NR, et al. Genetic risk, adherence to a healthy lifestyle, and coronary disease. *New Engl J Med* 2016;375:2349–58.

Interleukin-13 Receptor $\alpha 1$ –Mediated Signaling Regulates Age-Associated/Autoimmune B Cell Expansion and Lupus Pathogenesis

Zhu Chen,¹ Danny Flores Castro,²  Sanjay Gupta,² Swati Phalke,² Michela Manni,² Juan Rivera-Correa,² Rolf Jessberger,³ Habib Zaghouni,⁴ Eugenia Giannopoulou,⁵ Tania Pannellini,² and Alessandra B. Pernis⁶

Objective. Age-associated/autoimmune B cells (ABCs) are an emerging B cell subset with aberrant expansion in systemic lupus erythematosus. ABC generation and differentiation exhibit marked sexual dimorphism, and Toll-like receptor 7 (TLR-7) engagement is a key contributor to these sex differences. ABC generation is also controlled by interleukin-21 (IL-21) and its interplay with interferon- γ and IL-4. This study was undertaken to investigate whether IL-13 receptor $\alpha 1$ (IL-13R $\alpha 1$), an X-linked receptor that transmits IL-4/IL-13 signals, regulates ABCs and lupus pathogenesis.

Methods. Mice lacking DEF-6 and switch-associated protein 70 (double-knockout [DKO]), which preferentially develop lupus in females, were crossed with IL-13R $\alpha 1$ –knockout mice. IL-13R $\alpha 1$ –knockout male mice were also crossed with Y chromosome autoimmune accelerator (Yaa) DKO mice, which overexpress TLR-7 and develop severe disease. ABCs were assessed using flow cytometry and RNA-Seq. Lupus pathogenesis was evaluated using serologic and histologic analyses.

Results. ABCs expressed higher levels of IL-13R $\alpha 1$ than follicular B cells. The absence of IL-13R $\alpha 1$ in either DKO female mice or Yaa DKO male mice decreased the accumulation of ABCs, the differentiation of ABCs into plasma-blasts, and autoantibody production. Lack of IL-13R $\alpha 1$ also prolonged survival and delayed the development of tissue inflammation. IL-13R $\alpha 1$ deficiency diminished in vitro generation of ABCs, an effect that, surprisingly, could be observed in response to IL-21 alone. RNA-Seq revealed that ABCs lacking IL-13R $\alpha 1$ down-regulated some histologic characteristics of B cells but up-regulated myeloid markers and proinflammatory mediators.

Conclusion. Our findings indicate a novel role for IL-13R $\alpha 1$ in controlling ABC generation and differentiation, suggesting that IL-13R $\alpha 1$ contributes to these effects by regulating a subset of IL-21–mediated signaling events. These results also suggest that X-linked genes besides *TLR7* participate in the regulation of ABCs in lupus.

INTRODUCTION

Autoantibody production, up-regulation of interferon-stimulated genes (ISGs), and extensive organ damage are hallmarks of systemic lupus erythematosus (SLE), an autoimmune disease that preferentially affects women (1,2). Aberrant

expansion and dysregulation of T cell and B cell subsets is critical to SLE pathophysiology (3–6). In particular, recent studies have highlighted the importance of a novel B cell subset, age/autoimmune-associated B cells (ABCs), in SLE development (7,8). ABCs prematurely accumulate in murine models of lupus and produce pathogenic autoantibodies (9–11). Furthermore, expansion of

Supported by the NIH, the HSS Research Institute Rheumatology Training Program (awards T32-AR-07-1302 and S10-OD-01-9986), the Rheumatology Research Foundation, the Lupus Research Alliance, the Peter Jay Sharp Foundation, the Tow Foundation, which provided support for the David Z. Rosensweig Genomics Research Center, and Giammaria Giuliani and the Ambrose Monell Foundation. Dr. Manni's work was supported by the Barbara Volcker Center Michael D. Lockshin Fellowship. Dr. Pernis' work was supported by the NIH (awards AR-06-4883 and AR-07-0146).

Drs. Chen and Mr. Flores Castro contributed equally to this work.

¹Zhu Chen, MD, PhD: Hospital for Special Surgery, New York, New York, and University of Science and Technology of China, Hefei, China; ²Danny Flores Castro, MEng, Sanjay Gupta, PhD, Swati Phalke, PhD, Michela Manni, PhD, Juan Rivera-Correa, PhD, Tania Pannellini, PhD: Hospital for Special

Surgery, New York, New York; ³Rolf Jessberger, PhD: Technische Universität Dresden, Dresden, Germany; ⁴Habib Zaghouni, PhD: University of Missouri School of Medicine, Columbia; ⁵Eugenia Giannopoulou, PhD: Hospital for Special Surgery and the City University of New York, New York; ⁶Alessandra B. Pernis, MD: Hospital for Special Surgery and Weill Cornell Medicine, New York, New York.

Author disclosures are available at <https://onlinelibrary.wiley.com/action/downloadSupplement?doi=10.1002%2Fart.42146&file=art42146-sup-0001-Disclosureform.pdf>.

Address correspondence to Alessandra B. Pernis, MD, Autoimmunity and Inflammation Program, Hospital for Special Surgery, 535 East 70th Street, New York, NY 10021. Email: pernis@hss.edu.

Submitted for publication September 2, 2021; accepted in revised form April 12, 2022.

human ABCs (also known as double-negative B cells) has been observed in SLE patients, where ABCs rapidly differentiate into plasmablasts/plasma cells (PCs) and are major producers of autoantibodies (12,13). ABC accumulation occurs to a greater extent in African American patients with SLE, correlates with disease activity and clinical manifestations, and can be detected in SLE kidney biopsy specimens (12–14). ABCs have also been detected in other autoimmune disorders including Sjögren's syndrome, rheumatoid arthritis (RA), and scleroderma (7,15).

ABCs exhibit a unique phenotype and, in addition to classic B cell markers, also express transcription factor T-bet and myeloid markers such as CD11c; hence, these cells are also known as CD11c+ T-bet+ B cells (7). ABC formation is promoted by both innate and adaptive signals, including engagement of Toll-like receptor 7 (TLR-7), an endosomal TLR, which plays a key role in antiviral responses (7). Consistent with ABC regulation by TLR-7, ABCs are an important component of immune responses to viruses like the flu, and ABC expansion is inadequately controlled in patients with severe COVID-19 (16,17). Given the location of TLR-7 on the X chromosome and its ability to partially escape X chromosome inactivation in B cells (18–20); furthermore, TLR-7 engagement is a major contributor to the preferential expansion of ABCs in female mice (9,21).

In addition to TLRs, ABC formation is also regulated by T cell cytokines, with interleukin-21 (IL-21) and interferon- γ (IFN γ) promoting ABC formation and IL-4 normally inhibiting it (22). Similar to IL-21, IL-4 can signal through a receptor complex composed of γ c-chain and a ligand-binding subunit, the IL-4 receptor α (IL-4R α), located immediately adjacent to the IL-21R, with which it shares a high degree of similarity (23,24). IL-4 can also signal through the type II heteroreceptor, which is composed of IL-4R α and IL-13R α 1 and also mediates signaling in response to IL-13 (25,26). In contrast to the ubiquitous expression of IL-4R α in immune cells, IL-13R α 1 is primarily expressed by myeloid cells, and only low levels of IL-13R α 1 expression have been reported in lymphocytes at baseline (26). Genetic ablation of IL-13R α 1 in murine models has revealed the surprising and complex contributions of this receptor not only to classic Th2 diseases like atopic dermatitis, but also to autoimmune pathophysiology. Lack of IL-13R α 1 ameliorates diabetes in NOD mice but increases central nervous system inflammation in experimental autoimmune encephalomyelitis due to distinct effects on Th17, Th1, and regulatory T cell subsets (27,28). Although *IL13R α 1* is located on the X chromosome and, similarly to TLR-7, can also partially escape X chromosome inactivation (20), it is unknown whether signaling mediated by this receptor plays a role in SLE pathogenesis.

The SWEF proteins, switch-associated protein 70 (SWAP-70) and DEF-6, are 2 homologous proteins that control cytoskeletal reorganization and interferon regulatory factor (IRF) activity (29–31). Findings from both human and murine studies support an important immunoregulatory role for these

molecules. *SWAP70* is a susceptibility locus for RA and cardiovascular disease (CVD), while *DEF6* is a risk factor for SLE in multiple ethnic groups (32–34). Moreover, *DEF6* mutations result in early-onset autoimmunity, which includes autoantibody production and up-regulation of an ISG signature, often associated with viral infections (35,36). Consistent with these findings, concomitant lack of *Def6* and *Swap70* in C57BL/6 mice (double-knockout [DKO]) leads to the spontaneous development of SLE, which, similarly to humans, preferentially affects female mice (37). In particular, lupus development in DKO mice is accompanied by marked accumulation and aberrant differentiation of ABCs, occurring in a sex- and TLR-7-dependent manner (11,21).

Given our observation that ABCs can express IL-13R α 1, we investigated its role in ABC formation and SLE pathogenesis by generating IL-13R α 1-deficient DKO mice (IL-13R α 1^{-/-} DKO). Lack of IL-13R α 1 resulted in significantly fewer ABCs and reduced their ability to further differentiate and produce autoantibodies. Surprisingly, IL-13R α 1 deficiency decreased in vitro ABC generation in response to IL-21 alone. RNA sequencing revealed that ABCs lacking IL-13R α 1 down-regulated some of their B cell characteristics but up-regulated myeloid markers and proinflammatory mediators. Taken together, these findings suggest that IL-13R α 1 can help mediate a subset of IL-21-driven signals and impact the ability of ABCs to develop autoimmune or proinflammatory features.

MATERIALS AND METHODS

Data are available from the corresponding author upon request. RNA-Seq data have been deposited in the GEO database.

Mice. DEF-6-deficient (*Def6*^{-/-}) mice (provided by Lexicon Pharmaceuticals) were generated using a gene-trapping strategy as previously described (37). *Swap-70*-deficient mice (*Swap-70*^{-/-}) were also previously described (37). *Def6*^{-/-}*Swap-70*^{-/-} mice were generated by crossing *Def6*^{-/-} mice with *Swap-70*^{-/-} mice and have been backcrossed to a C57BL/6 background for over 10 generations (37). Y chromosome autoimmune accelerator (Yaa) DKO mice have recently been reported (21). IL-13R α 1^{-/-} and IL-13R α 1-green fluorescent protein (GFP) mice were previously generated (38) and were crossed with DKO mice to generate IL-13R α 1^{-/-} DKO mice and IL-13R α 1-GFP DKO mice, respectively. Mice were genotyped using Transnetyx. Mice of the incorrect genotype were excluded. All the mice were bred under specific pathogen-free conditions and standard housing conditions. All experiments were carried out following institutional guidelines, and protocols were approved by the Institutional Animal Care and Use Committee of the Hospital for Special Surgery and Weill Cornell Medicine-Memorial Sloan Kettering Cancer Center.

Flow cytometry, cell sorting, enzyme-linked immunosorbent assay (ELISA), and histologic analysis.

Fluorescence-activated cell sorting (FACS) and flow cytometry analysis of the cells were performed as described previously (21). For cytokine staining, splenocytes were stimulated with phorbol myristate acetate (PMA), ionomycin, and brefeldin A for 5 hours before staining. Monoclonal antibodies used included antibodies to B220 (clone no. RA3-6B2), CD19 (clone no. 6D5), CD11c (clone no. N418), CD11b (clone no. M1/70), T-bet (clone no. 4B10), CD4 (clone no. RM4-5), GL-7 (clone no. GL7), CD21/CD35 (clone no. 7E9), and CD23 (clone no. B3B4) from BioLegend; antibodies to Fas (clone no. Jo2) and CXCR5 (clone no. 2G8) from BD Biosciences; and antibodies to programmed cell death protein 1 (clone no. J43) and Foxp3 (clone no. FJK-16s) from Invitrogen. For apoptotic cell analysis, cells were stained with propidium iodide and annexin V (BD Biosciences) before collection. To exclude dead cells, cells were stained with fixable viability dye (Invitrogen). Efferocytosis assays were performed as recently described (21). Data were collected on a FACSCanto instrument (Becton Dickinson) and analyzed using FlowJo (Tree Star) software. Autoantibody ELISAs were performed as previously described (21,39). CCL22 (product no. DY439; R&D Systems) and IL-1 β ELISAs (product no. 432601; BioLegend) were performed according to the manufacturer's instructions. Histologic analysis of the cells was performed as described previously (11).

B cell differentiation in vitro. CD23+ B cells were purified as described (11) and stimulated with 5 μ g/ml F(ab')₂ anti-mouse IgM (Jackson ImmunoResearch Laboratories), 5 μ g/ml of purified anti-mouse CD40 (Bio X Cell), \pm 50 ng/ml IL-21 (PeproTech), 10 ng/ml IL-4 (PeproTech), or 20 ng/ml IL-13 (PeproTech). For proliferation assays, CD23+ B cells were labeled with 2.5 μ M CellTrace violet dye (Invitrogen) for 2 minutes at room temperature prior to stimulation.

Immunoblot analysis. Extracts were prepared as described (37) and analyzed using immunoblotting with the following antibodies: anti-STAT6 phosphorylated at Tyr⁶⁴¹ (product no. 56554S), anti-Stat3 phosphorylated at Tyr⁷⁰⁵ (product no. 9145S), anti-Stat1 phosphorylated at Tyr⁷⁰¹ (product no. 9167S), anti-Stat5 phosphorylated at Tyr⁶⁹⁴ (product no. 4322S), anti-IRF-4 (product no. 15106), and anti-histone deacetylase 1 (anti-HDAC-1) (product no. 2062) (all from Cell Signaling Technology).

Real-time quantitative polymerase chain reaction (qRT-PCR). We performed qRT-PCR using iTaq Universal SYBR Green Supermix (product no. 1725121; Bio-Rad). Gene expression was calculated using the $\Delta\Delta C_t$ method and were normalized to cyclophilin A (*Ppia*) levels (cyclophilin A *Ppia* forward 5'-TTGCCATTCTGGACCCAAA-3'; *Ppia* reverse 5'-ATGGCACTGGCGGCAGGTCC-3'). IL-21R (product no.

QT00137627; Qiagen) and IL-1 β (mIL-1 β forward 5'-AGCTTCC TTGTGCAAGTGTCT-3'; mIL-1 β reverse GACAGCCCAGGTCA AAGGTT) were the primers used.

RNA-Seq analysis. Total RNA was extracted using RNeasy Plus Mini kit (Qiagen). Illumina-compatible sequencing libraries were constructed at the Epigenomics Core Facility of Weill Cornell Medicine. The quality of all RNA and the library preparations were evaluated using 2100 BioAnalyzer (Agilent) before sequencing. Paired-end sequencing and data evaluation were performed as previously described (11). Heatmaps were made in Morpheus (URL: <https://software.broadinstitute.org/morpheus/>). Gene set enrichment analysis (GSEA) (URL: <http://www.broad.mit.edu/gsea/index.html>) was performed using the difference of log-transformed counts per million between contrasted conditions as a ranking metric. The Molecular Signatures Database (version 7.2) was used as the source of gene sets. Enriched pathway analysis of differentially expressed genes and predicted upstream transcription factor analysis were performed using Ingenuity Pathway Analysis (IPA) (Qiagen).

Statistical analysis. Quantitative data are expressed as the mean \pm SEM. Student's unpaired 2-tailed *t*-test with Welch's correction was performed for comparisons of 2 groups. One-way analysis of variance (ANOVA) with Bonferroni multiple comparisons test was performed for comparisons of multiple groups. Statistical analysis was performed with GraphPad Prism 8 and 9.

RESULTS

Effect of IL-13R α 1 on ABC accumulation and autoantibody production in DKO female mice. DKO female mice exhibit an aberrant accumulation of ABCs in the spleen (11,21). Interestingly, CUT&RUN and RNA-Seq analyses has revealed that, compared to follicular B cells, ABCs exhibit a selective loss of repressive chromatin marks at the *IL13Ra1* locus (21) and can express IL-13R α 1 (Supplementary Figure 1A, available on the Arthritis & Rheumatology website at <http://onlinelibrary.wiley.com/doi/10.1002/art.42146>). This finding was confirmed by crossing DKO female mice with IL-13R α -1GFP reporter mice (Supplementary Figures 1B and C). To investigate whether signals transmitted via IL-13R α 1 contribute to the increased expansion of ABCs observed in DKO female mice, we generated IL-13R α 1^{-/-} DKO mice. Lack of IL-13R α 1 in DKO female mice ameliorated splenomegaly and resulted in significantly fewer ABCs as determined by either CD11c and T-bet or CD11c and CD11b costaining (Figure 1A and Supplementary Figures 1D and E, <http://onlinelibrary.wiley.com/doi/10.1002/art.42146>).

The robust expansion of germinal center (GC) B cells normally observed in DKO female mice also decreased in IL-13R α 1^{-/-} DKO female mice (Figure 1B). DKO female mice also accumulate both B220^{intermediate}CD138+ plasmablasts and

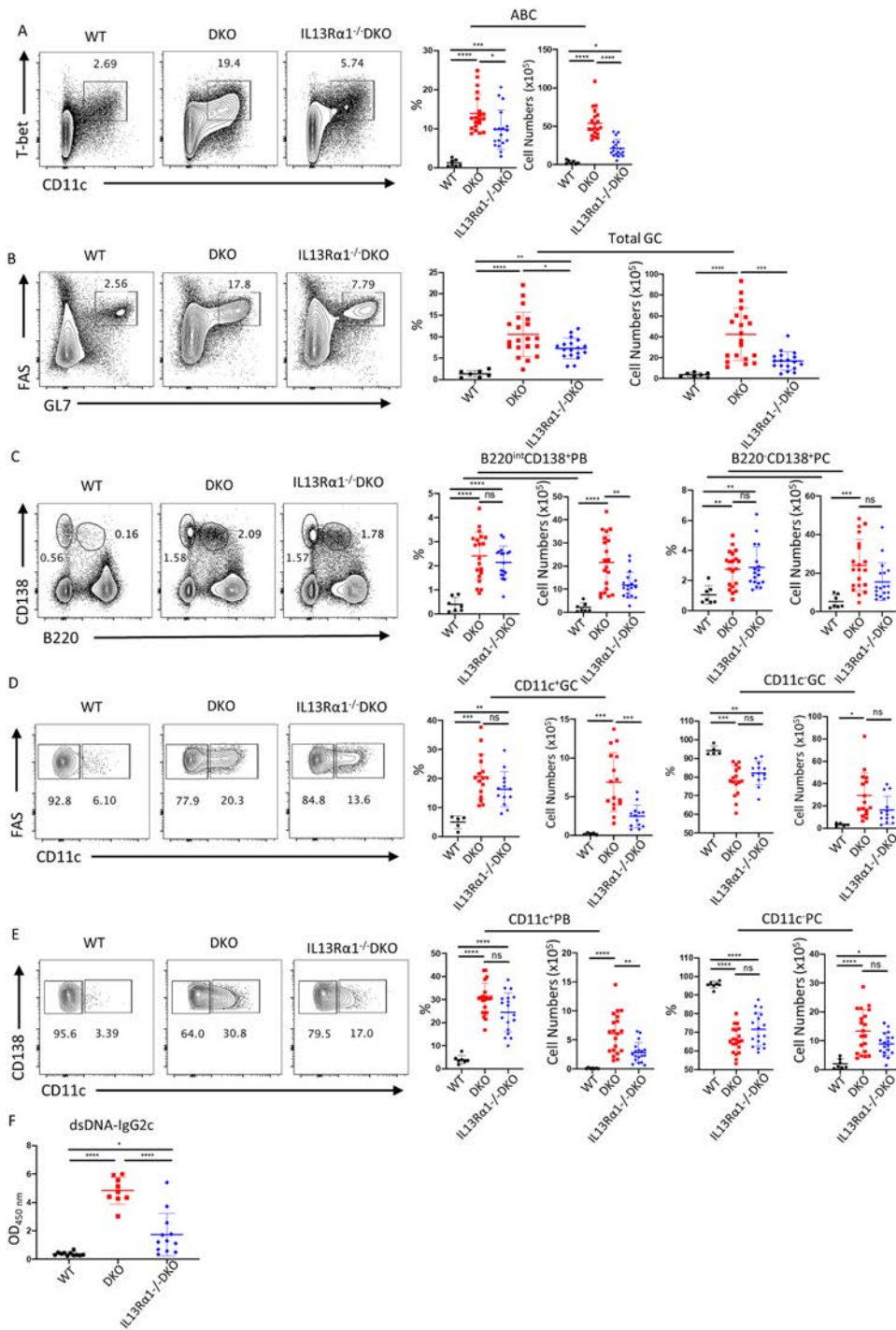


Figure 1. Lack of interleukin-13 receptor α 1 (IL-13R α 1) reduces accumulation of age-associated/autoimmune B cells (ABCs) and autoantibody production in double-knockout (DKO) female mice. **A–E**, Representative flow cytometry plots (left) and percentages of each cell subset (right), showing quantification of splenic CD11c⁺T-bet⁺ ABCs (gated on B220⁺ cells) (**A**), total germinal center (GC) B cells (gated on B220⁺GL7⁺Fas⁺ splenocytes) (**B**), total plasmablasts (PBs)/plasma cells (PCs) (B220^{intermediate/low}CD138⁺) (**C**), CD11c⁺GL7⁺Fas⁺ cells (gated on B220⁺ splenocytes) (**D**), and CD11c⁺ PBs/PCs (B220^{intermediate/low}CD138⁺) (**E**) from 24-week-old wild-type (WT) mice, DKO mice, and IL-13R α 1^{-/-} DKO female mice. **F**, Serum levels of IgG2c anti-double-stranded DNA (anti-dsDNA) assessed using enzyme-linked immunosorbent assay. Bars show the mean \pm SEM; symbols represent individual mice. Data show 7–20 mice per group pooled from 7 independent experiments (sample size derived from previous studies [21]) (**A–C** and **E**), 5–16 mice per group pooled from 5 independent experiments (**D**), and 9–12 mice per group pooled from 3 independent experiments (**F**). * = $P < 0.05$; ** = $P < 0.01$; *** = $P < 0.001$; **** = $P < 0.0001$, by one-way analysis of variance, followed by Bonferroni correction for multiple comparisons. int = intermediate; NS = not significant. Color figure can be viewed in the online issue, which is available at <http://onlinelibrary.wiley.com/doi/10.1002/art.42146/abstract>.

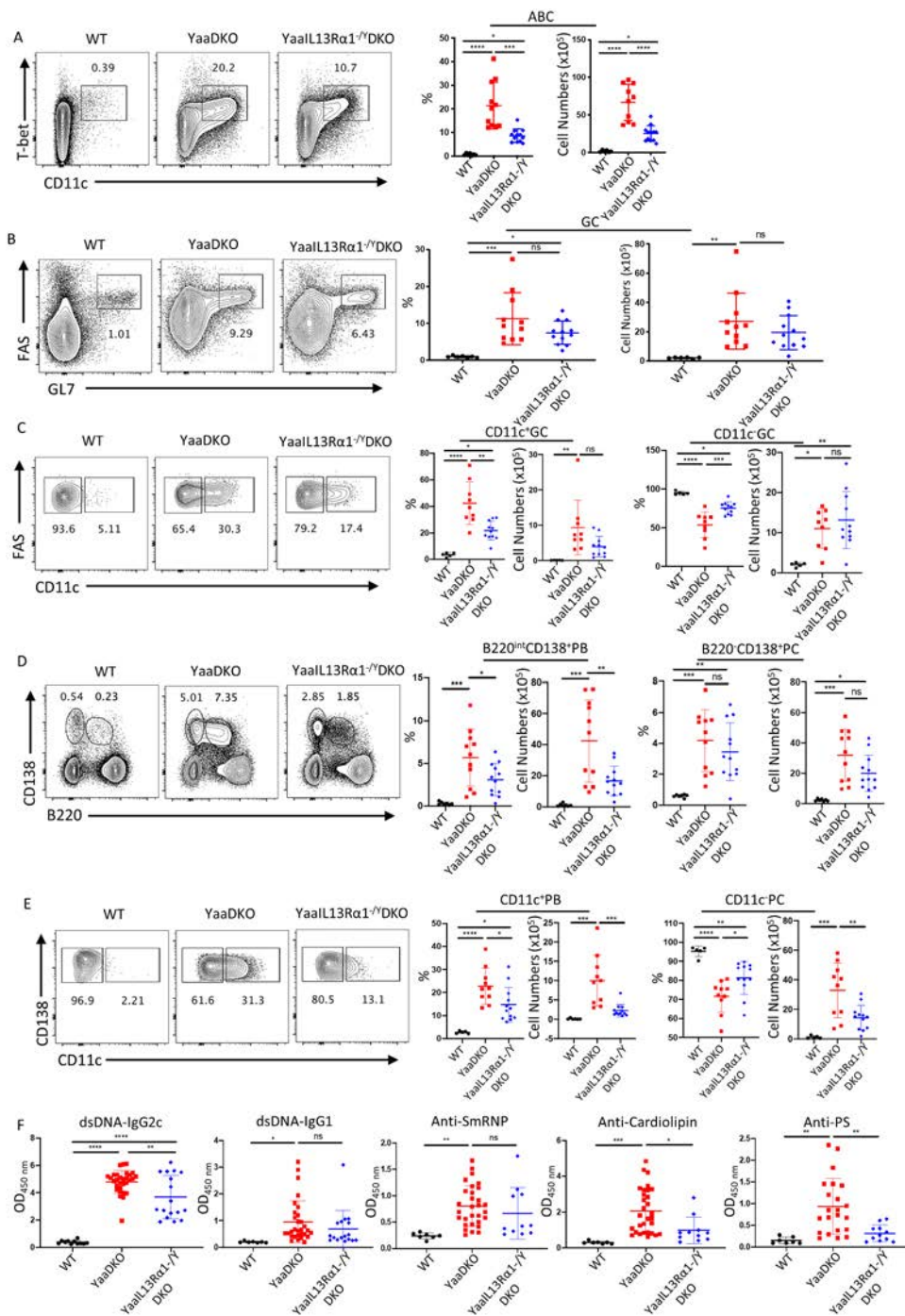


Figure 2. IL-13R α 1 deficiency diminishes Toll-like receptor 7-driven ABC expansion and humoral responses in Y chromosome autoimmune accelerator (Yaa) DKO male mice. **A–E**, Representative flow cytometry plots (left) and percentages of each cell subset (right), showing quantification of splenic CD11c⁺T-bet⁺ ABCs (gated on B220⁺ cells) (**A**), total GC B cells (gated on B220⁺GL-7⁺Fas⁺ splenocytes) (**B**), CD11c⁺GL-7⁺Fas⁺ cells (gated on B220⁺ splenocytes) (**C**), and total splenic (**D**) and CD11c⁺ (**E**) plasmablasts/PCs (B220^{intermediate/low}CD138⁺) from WT mice, Yaa DKO mice, and Yaa IL-13R α 1^{-/-} DKO male mice (age >20 weeks). **F**, Serum levels of IgG2c anti-dsDNA, IgG1 anti-dsDNA, anti-Sm/RNP, IgG anticardiolipin, and IgG antiphosphatidylserine antibody (aPS) assessed using enzyme-linked immunosorbent assay. Bars show the mean \pm SEM; symbols represent individual mice. Data show 7–12 mice per group pooled from 7 independent experiments (**A**, **B**, and **D**), 5–11 mice or 5–12 mice per group pooled from 5 independent experiments (**C** and **E**, respectively), and 7–30 mice per group pooled from 3 independent experiments (**F**). * = $P < 0.05$; ** = $P < 0.01$; *** = $P < 0.001$; **** = $P < 0.0001$, by one-way analysis of variance, followed by Bonferroni correction for multiple comparisons. See Figure 1 for other definitions. Color figure can be viewed in the online issue, which is available at <http://onlinelibrary.wiley.com/doi/10.1002/art.42146/abstract>.

B220^{low}CD138⁺ PCs (21). Absence of IL-13R α 1 reduced the number of plasmablasts but had less of an effect on the numbers of PCs (Figure 1C). GC and plasmablast/PC populations in DKO female mice contain CD11c⁺ populations, which are derived from ABCs and which have transcriptional profiles that are distinct from corresponding CD11c⁻ subsets (21). Lack of IL-13R α 1 had greater effects on CD11c⁺ GC B cell populations than the CD11c⁻ GC populations (Figure 1D). Similarly, when the plasmablast/PC compartment was subdivided according to CD11c expression, lack of IL-13R α 1 preferentially decreased the CD11c-expressing population, which mainly represents plasmablasts (Figure 1E). Lack of IL-13R α 1 also resulted in fewer B220⁺CD11c⁺CD11b⁺ cells (Supplementary Figure 1F, <http://onlinelibrary.wiley.com/doi/10.1002/art.42146>). However, these populations were not expanded in DKO mice, consistent with our previous findings that myeloid cells do not appear to be involved in promoting humoral abnormalities in these mice (40). Consistent with the decrease in ABCs and their effector progeny, the levels of anti-double-stranded DNA (anti-dsDNA) IgG2c were lower in IL-13R α 1^{-/-} DKO mice than in DKO female mice (Figure 1F). Thus, lack of IL-13R α 1 decreased ABC formation and differentiation and ameliorated aberrant humoral responses that characterize the spontaneous autoimmunity that develops in DKO female mice.

Given the ability of ABCs to act as potent antigen-presenting cells and promote aberrant follicular helper T (T_{fh}) cell differentiation (41,42), we also investigated the effects of the lack of IL-13R α 1 in this compartment. Fewer T_{fh} cells, but not T follicular regulatory (T_{fr}) cells, were observed in IL-13R α 1^{-/-} DKO female mice, resulting in a modest decrease in the T_{fh}:T_{fr} cell ratio (Supplementary Figure 1G, <http://onlinelibrary.wiley.com/doi/10.1002/art.42146>). No changes in IL-21 production or IFN γ production were observed (Supplementary Figures 1H and I). An evaluation of Th2 cytokines revealed that IL-13 production was largely unaffected by the absence of IL-13R α 1 and only low levels of IL-4 production were detected (Supplementary Figure 1J, <http://onlinelibrary.wiley.com/doi/10.1002/art.42146>). Thus, absence of IL-13R α 1 in lupus-prone DKO female mice had less marked effects on the T cell compartment than on ABCs and did not significantly affect the production of key cytokines known to regulate ABC differentiation.

Diminished ABC expansion and humoral responses in Yaa DKO male mice lacking IL-13R α 1. The Yaa locus accelerates autoimmunity in lupus models primarily due to the overexpression of TLR-7. While DKO male mice do not normally develop lupus, DKO male mice crossed to Yaa mice display increased accumulation, differentiation, and dissemination of ABCs (21). The profound cellular abnormalities in Yaa DKO male mice were associated with the production of a broader array of autoantibodies and worse immunopathogenesis than that observed not only in DKO male mice, but also in DKO female mice

(21). To investigate whether lack of IL-13R α 1 impacts ABCs and disease in this more severe setting, we generated Yaa DKO IL-13R α 1-deficient male mice. Yaa DKO IL-13R α 1^{-Y} male mice exhibited smaller spleens and decreased numbers of ABCs as compared to age-matched Yaa DKO male mice (Figure 2A and Supplementary Figures 2A and B, <http://onlinelibrary.wiley.com/doi/10.1002/art.42146>). Dissemination of ABCs into the blood was also diminished by the lack of IL-13R α 1 (Supplementary Figure 2C). While lack of IL-13R α 1 in Yaa DKO male mice did not alter the GC B cell compartment, it again resulted in a decrease in CD11c⁺ plasmablasts, which were affected to a greater extent than CD11c⁻ PCs (Figures 2B–E). T_{fh} cell numbers were only modestly affected by the absence of IL-13R α 1, and the T_{fh}:T_{fr} cell ratio remained unchanged (Supplementary Figure 2D, <http://onlinelibrary.wiley.com/doi/10.1002/art.42146>). No differences in IL-21, IFN γ , IL-4, or IL-13 production were observed (Supplementary Figures 2E and F). Thus, even in settings where severe lupus pathogenesis was driven by TLR-7 overexpression, IL-13R α 1-mediated signaling contributed to the aberrant characteristics in the ABC compartment, and, in particular, to their accumulation and further differentiation.

In addition to IgG2c anti-dsDNA, Yaa DKO male mice produced markedly elevated levels of a broad array of autoantibodies, which included anti-Sm/RNP and antiphospholipid antibodies. We previously observed a close correlation between ABC frequencies and production of both anticardiolipin antibodies (aCLs) and antiphosphatidylserine antibodies (APS) (21). In further support of such a connection, the decrease in ABCs in Yaa DKO IL-13R α 1^{-Y} mice was associated with decreased levels of anti-dsDNA IgG2c as well as lower levels of aCLs and APS (Figure 2F). However, production of anti-dsDNA IgG1 and anti-Sm/RNP was not significantly affected (Figure 2F). Although Yaa DKO male mice lacking IL-13R α 1 had greater survival compared to Yaa DKO male mice (Supplementary Figure 2G, <http://onlinelibrary.wiley.com/doi/10.1002/art.42146>), they eventually succumbed to the disease, and histopathologic analysis demonstrated that Yaa-DKO IL-13R α 1^{-Y} male mice develop both renal and pulmonary inflammation although this occurred at an older age than in Yaa DKO male mice (Supplementary Figure 2H–N). Thus, lack of IL-13R α 1 in this model of severe lupus broadly impacted the aberrant autoantibody production that characterizes these mice and delays the development of end-organ damage.

Effect of IL-13R α 1-mediated signaling on ABC formation in vitro. The decrease in ABC accumulation observed in both IL-13R α 1^{-/-} DKO female mice and Yaa DKO IL-13R α 1^{-Y} DKO male mice suggested that IL-13R α 1-mediated signaling directly regulates ABC generation. To further investigate this possibility, we used an established in vitro system whereby purified CD23⁺ B cells from young (6–10-week-old) wild-type (WT) DKO female mice or IL-13R α 1^{-/-} DKO female mice were

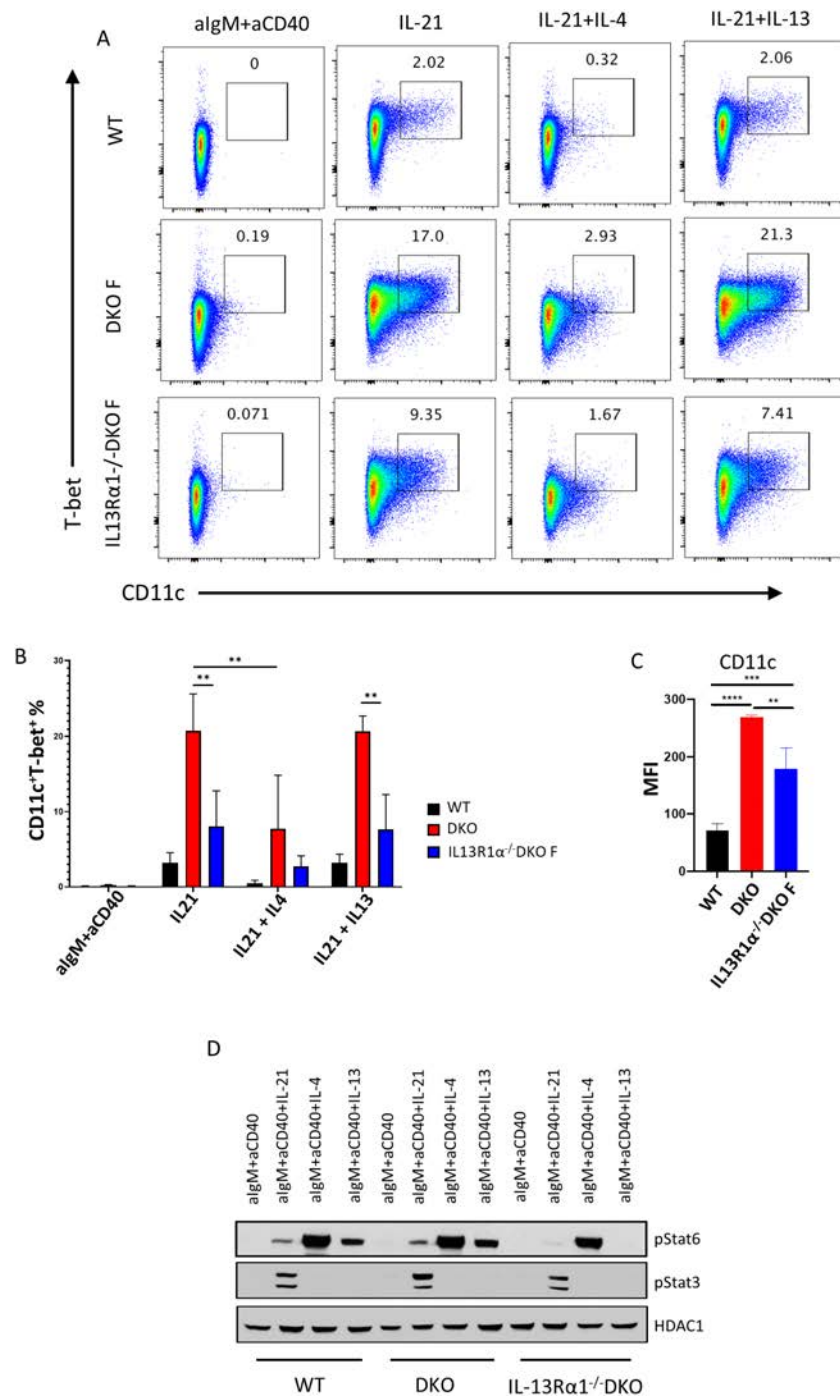


Figure 3. IL-13Rα1-mediated signaling regulates ABC formation in vitro. **A**, Representative flow cytometry plots showing CD11c and T-bet expression by purified CD23+ B cells from WT female mice, DKO female (DKO F) mice, and IL-13Rα1^{-/-} DKO female mice (all ages 6–10 weeks). Cells were stimulated for 3 days with anti-IgM (5 μg/ml) and anti-CD40 (5 μg/ml) or IL-21 (50 ng/ml) alone or together with IL-4 (10 ng/ml) or IL-13 (20 ng/ml). Numbers indicate the percentage of cells in each quadrant. **B**, Quantification of CD11c+T-bet+ ABCs in the same cultures as described in **A**. **C**, Quantification of CD11c expression by CD23+ B cells after stimulation with anti-IgM, anti-CD40, and IL-21. **D**, Western blotting showing pSTAT6 and pSTAT3 expression from nuclear extracts of cells stimulated with anti-IgM (5 μg/ml) and anti-CD40 (5 μg/ml) alone or together with IL-21 (50 ng/ml), IL-4 (10 ng/ml), or IL-13 (20 ng/ml). Reprobing with class I histone deacetylase (HDAC-1) was used as a loading control. Data are representative of 2 independent experiments. In **B** and **C**, bars show the mean ± SEM. Data show 6–8 mice per group pooled from 3 independent experiments (**A–C**). ** = $P < 0.01$; *** = $P < 0.001$; **** = $P < 0.0001$, by one-way analysis of variance, followed by Bonferroni adjustment for multiple comparisons. MFI = mean fluorescence intensity (see Figure 1 for other definitions). Color figure can be viewed in the online issue, which is available at <http://onlinelibrary.wiley.com/doi/10.1002/art.42146/abstract>.

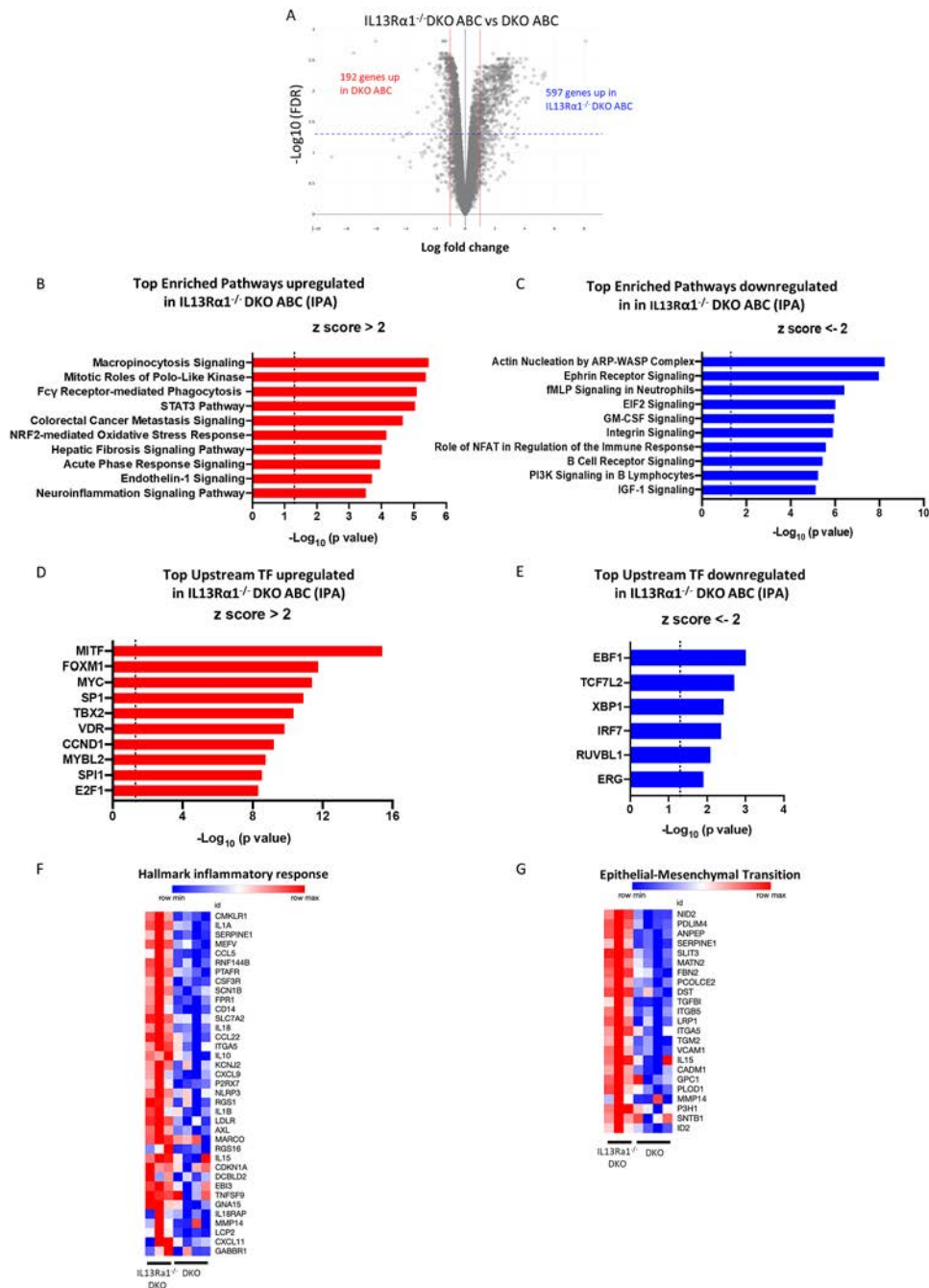


Figure 4. IL-13R α 1-deficient ABCs from DKO mice exhibit enhanced myeloid and proinflammatory features. RNA-Seq analysis was performed using RNA from B220+CD19+CD11c+CD11b+ ABCs sorted using flow cytometry from \geq 24-week-old DKO female mice ($n = 5$) and IL-13R α 1^{-/-} DKO female mice ($n = 3$). **A**, Volcano plot showing differentially expressed genes (i.e., those showing >1 -fold change in gene expression) in cells from DKO female mice relative to gene expression in cells from IL-13R α 1^{-/-} female mice, plotted against the false discovery rate (FDR)-corrected P value ($P < 0.05$; broken horizontal line shows the cutoff $P = 0.05$). **B** and **C**, The top pathways up-regulated (**B**) or down-regulated (**C**) in ABCs from IL-13R α 1^{-/-} DKO mice assessed using Ingenuity Pathway Analysis (IPA). Dotted line shows the significance threshold at FDR $q < 0.25$. Data are presented as Z scores by K-means clustering of log-transformed expression (counts per million) of genes differentially expressed by these cells. **D** and **E**, Top upstream transcription factors (TFs) up-regulated (**D**) or down-regulated (**E**) in ABCs from IL-13R α 1^{-/-} DKO mice as predicted using IPA. **F** and **G**, Heatmaps showing differentially expressed genes in the hallmark inflammatory response pathway (**F**) and hallmark epithelial mesenchymal transition pathway (**G**). ARP = actin-related protein; WASP = Wiskott-Aldrich syndrome protein; EIF2 = eukaryotic initiation factor 2; GM-CSF = granulocyte-macrophage colony-stimulating factor; IGF-1 = insulin-like growth factor 1 (see Figure 1 for other definitions).

cultured with anti-IgM and anti-CD40 in the presence or absence of different combinations of IL-21, IL-4, and IL-13 (Figure 3A). As we previously reported (11), IL-21 led to greater ABC formation in cultures of DKO B cells than WT B cells, as assessed using either CD11c and T-bet or CD11c and CD11b costaining (Figures 3A and B and Supplementary Figures 3A and B, <http://onlinelibrary.wiley.com/doi/10.1002/art.42146>). Surprisingly, IL-13R α 1^{-/-} DKO B cells cultured with IL-21 alone generated significantly fewer ABCs than DKO B cells (Figures 3A and B and Supplementary Figures 3A and B). Lack of IL-13R α 1 also resulted in lower surface-level expression of CD11c in response to IL-21 (Figure 3C).

No differences in terms of the inhibitory effects of IL-4 on IL-21-mediated ABC generation were observed, while IL-13 did not significantly inhibit IL-21-driven ABC formation (Figures 3A and B and Supplementary Figures 3A and B, <http://onlinelibrary.wiley.com/doi/10.1002/art.42146>). Exposure to IL-13 alone, in the absence of IL-21, did not promote ABC generation (Supplementary Figure 3C). IL-13R α 1 deficiency did not affect IL-21R expression or diminish B cell proliferation in vitro or in vivo, suggesting that the inhibitory effects of IL-13R α 1 deficiency on ABC generation did not simply result from alterations to the proliferative capabilities of these B cells (Supplementary Figures 3D–G). Thus, IL-13R α 1 deficiency reduces aberrant ABC formation by DKO B cells upon stimulation with IL-21, an effect that can be observed even in the absence of IL-4 or IL-13.

Given that IL-13R α 1 expression affected B cell responsiveness to IL-21, we examined STAT phosphorylation to gain insights into the mechanisms by which IL-13R α 1 may impact IL-21 signaling in B cells (Figure 3D). Interestingly, low levels of Stat6 phosphorylation were detected upon IL-21 stimulation of WT and DKO B cells but not stimulation of IL-13R α 1^{-/-} DKO B cells. In contrast, IL-21-mediated Stat3 phosphorylation occurred to a similar extent in B cells from all 3 genotypes. IL-4 induced comparable levels of Stat6 phosphorylation in WT, DKO, and IL-13R α 1^{-/-} DKO B cells, while Stat6 phosphorylation triggered by IL-13 was completely dependent on IL-13R α 1 expression (Figure 3D). Absence of IL-13R α 1 did not alter phosphorylation of Stat1 or Stat5 in response to IL-21 stimulation (Supplementary Figure 3H, <http://onlinelibrary.wiley.com/doi/10.1002/art.42146>). Furthermore, IRF-4 was induced at similar levels under all conditions, indicating that the lack of IL-13R α 1 did not affect the activation of the cells (Supplementary Figure 3H). No production of IL-4 or IL-13 was detected in B cell cultures supplemented with IL-21 alone, suggesting that Stat6 phosphorylation in these cultures was not likely due to endogenous production of these cytokines (Supplementary Figures 3I and J, <http://onlinelibrary.wiley.com/doi/10.1002/art.42146>).

Enhanced myeloid and proinflammatory features exhibited by IL-13R α 1-deficient ABCs from DKO mice.

To gain further insight into the mechanisms by which IL-13R α 1

regulates ABCs, we sorted ABCs from the spleens of DKO and IL-13R α 1^{-/-} DKO female mice and performed RNA-based next-generation sequencing (RNA-Seq) to compare the transcriptomes of ABCs from DKO mice and ABCs from IL-13R α 1-deficient DKO mice. A total of 789 genes were differentially expressed in the 2 populations (2-fold change in expression [1-fold log of the value]; false discovery rate <0.05) (Figure 4A). Lack of IL-13R α 1 did not affect expression of γ c chain, IL-21R, or Stat6 and only minimally decreased IL-4R α levels (Supplementary Figure 4A, <http://onlinelibrary.wiley.com/doi/10.1002/art.42146>). On the basis of IPA findings, gene sets with the greatest enrichment in IL-13R α 1^{-/-} ABCs were related to inflammatory responses, cytokine signaling, and phagocytosis, and phagocytic markers such as *Mertk* and *Fcgr1* were up-regulated in ABCs from IL-13R α 1^{-/-} DKO mice compared to ABCs from DKO mice (Figure 4B and Supplementary Figure 4A, <http://onlinelibrary.wiley.com/doi/10.1002/art.42146>).

In contrast, pathways involved in B cell receptor signaling were down-regulated in DKO cells in the absence of IL-13R α 1 (Figure 4C). Consistent with these findings, predicted upstream transcription factors regulating the differentially expressed genes that were up-regulated in ABCs from IL-13R α 1^{-/-} DKO mice (assessed using IPA) included FoxM1 and microphthalmia-associated transcription factor, while the top upstream transcription factor down-regulated in the absence of IL-13R α 1 included early B cell factor 1 and X-box binding protein 1 (Figures 4D and E). We further analyzed enriched pathways, which were either up-regulated or down-regulated in ABCs from IL-13R α 1^{-/-} DKO mice by GSEA, (Supplementary Figures 4B and C, <http://onlinelibrary.wiley.com/doi/10.1002/art.42146>). Lack of IL-13R α 1 in ABCs again resulted in the enrichment of pathways involved in inflammation, cytokine signaling, and cytoskeletal processes. In particular, these cells up-regulated several proinflammatory mediators including IL-1 β , IL-18, CCL22, CCL5, and mediators of cell–cell and cell–matrix interactions (Figures 4F and G). Consistent with the RNA-Seq results, lack of IL-13R α 1 increased expression of IL- β and CCL22 upon in vitro stimulation with IL-21 and resulted in higher serum levels of these mediators (Supplementary Figures 4D–G, <http://onlinelibrary.wiley.com/doi/10.1002/art.42146>). ABCs from DKO mice lacking IL-13R α 1 furthermore exhibited enhanced efferocytic capabilities compared to ABCs from DKO mice (Supplementary Figure 4H). Thus, lack of IL-13R α 1 in ABCs down-regulates some B cell characteristics but enhanced myeloid and proinflammatory features.

DISCUSSION

ABCs are an emerging B cell subset whose aberrant accumulation has increasingly been linked to SLE pathogenesis (7,8). In the current study, we identified a novel role for the X-linked IL-13R α 1 receptor in promoting ABC expansion and differentiation. Indicative of the major contribution of ABCs to autoantibody

production, diminished ABC expansion upon ablation of *IL13R α 1* in this DKO model of lupus was accompanied by decreased autoantibody production and improved survival. Consistent with findings from our recent studies showing that ABCs can give rise to a heterogeneous pool of effector progeny (21), we also observed decreased accumulation of CD11c+ effectors including pre-GC B cells and plasmablasts. While CD11c- GC B cell and CD11c- PC expansion was less affected by the absence of IL-13R α 1, we cannot rule out the possibility that IL-13R α 1 expression may impact the functional capabilities of CD11c- progeny. Thus, decreased autoantibody production observed in the absence of IL-13R α 1 may result from multiple effects on ABC formation and differentiation. Interestingly, the remaining ABCs generated in the absence of IL-13R α 1 up-regulated several myeloid features, including enhanced expression of phagocytic receptors and inflammatory mediators. The shift of ABCs lacking IL-13R α 1 toward a more proinflammatory phenotype likely limited the beneficial effects of the absence of this receptor on humoral immune responses and, albeit with a delay, the mice eventually developed end-organ inflammation. Findings from this study therefore indicate an important role for IL-13R α 1 in modulating the plasticity and functional capabilities of ABCs.

The fact that the *in vivo* effects of the absence of IL-13R α 1 were coupled with diminished ABC formation *in vitro* supports the idea that IL-13R α 1 controls ABC generation in a cell-intrinsic manner. Surprisingly, *in vitro* defects in ABC formation imparted by the lack of IL-13R α 1 were detected upon stimulation of B cells with IL-21 alone, and these defects were associated with differences in the activation of Stat6, but not other STAT proteins, suggesting that IL-13R α 1 helps modulate only a subset of IL-21-mediated signaling events. Given that the *IL21R* and *IL4R α* are neighboring genes and share a high degree of homology (23,24), these findings raise the possibility that, similar to IL-4, IL-21 may signal not only via the IL-21R and γ c chain but also via an alternative receptor complex that involves the IL-21R and IL-13R α 1 chain. Alternatively, the effect may be indirect and the pathways may intersect with each other further downstream of each receptor. Since the IL-13R α 1 receptor is normally expressed by myeloid cells but not by B cells (25,26), up-regulation of this receptor chain by ABCs may thus enable them to respond to IL-21 in a manner distinct from other B cells and represents another example of the unique combination of myeloid cell features and B cell features exhibited by ABCs.

Signaling mediated by the IL-13R α 1 chain in response to IL-4 or IL-13 is known to be controlled by a complex interplay dictated by ligand levels and affinity, its relative abundance compared to the IL-4R α and γ c chains, and actin-dependent recruitment dynamics (25,26). While IL-13R α 1 involvement in IL-21 signaling would add additional complexity, stepwise production of IL-21 and IL-4 that normally accompanies Tfh cell differentiation as GC response evolves (43) could help restrict the contribution of IL-13R α 1 to IL-21 or IL-4 signaling events. This spatial

organization could also help limit the known inhibitory effects of IL-4 on IL-21-driven ABC differentiation. Consistent with this notion, the greater variability in autoantibody production observed upon deleting the IL-13R α 1 chain in Yaa DKO male mice than in DKO female mice could be linked to the greater degree of splenic disorganization observed in these mice as well as their increased ability to produce IL-4 (21). Our finding that, in contrast to IL-4, the addition of IL-13 did not affect IL-21-driven ABC formation *in vitro* suggests that the inhibitory effects of IL-4 on ABCs are mediated by IL-4R α / γ c chain complexes, and binding IL-13 to IL-13R α 2 (the high-affinity receptor that may serve as a decoy receptor and also signals) also has no role, which implies that production of IL-13, for instance by the newly recognized Tfh13 cells (44), may not impact ABC generation.

IL13R α 1 is one of the genes on the X chromosome that can partially escape X chromosome inactivation, together with TLR-7 and the TLR adaptor interacting with endolysosomal SLC15A4/*CXorf21*, an adaptor controlling the TLR-mediated activation of IRF-5 (45–47). Both TLR-7 engagement and IRF-5 play crucial roles in promoting ABC generation (9,11,21), raising the intriguing possibility that ABC formation relies on the coordinated employment of multiple X-linked components, which can then promote the preferential expansion of this compartment in female mice and contribute to the profound sex bias in SLE. Given the emerging evidence that proper regulation of TLR-7 engagement and ABCs may be important for determining the severity of SARS-CoV-2 infections, these pathways may also be relevant to the sex-related differences in responses to this virus that have been observed (48).

While lack of IL-13R α 1 exerted pronounced inhibitory effects on ABC generation and differentiation and a subsequent decrease in autoantibody production, ABCs generated in the absence of IL-13R α 1 expressed a transcriptional profile enriched for inflammatory targets. Furthermore, this phenotype is coupled with up-regulation of several myeloid markers, suggesting that the remaining ABCs, despite down-regulating their humoral features, can acquire more robust myeloid-like proinflammatory effects and potentially mediate a distinct set of pathogenic effects and/or complications. Indeed, lack of IL-13R α 1 resulted in increased expression of IL-1 β and CCL22 *in vitro* as well as *in vivo*. This alternative outcome for IL-13R α 1-deficient ABCs may reduce the beneficial effects that IL-13R α 1-deficiency has on autoantibody responses and may contribute to the eventual development of renal and pulmonary inflammation in these mice. Whether ABCs that express these proinflammatory features can be enriched in subsets of SLE patients is an important question for further investigation.

Although our study primarily focused on the role of IL-13R α 1 in lupus pathogenesis, a study has shown that IL-13R α 1 expression is up-regulated in peripheral blood mononuclear cells from patients with other autoimmune conditions such as scleroderma, where ABC expansion (also known as CD21^{low}) has recently been

recognized (49). Thus, these studies may be relevant to autoimmune disorders in addition to SLE. Furthermore, the ability of IL-13R α 1 to regulate ABCs and lupus pathogenesis may have important therapeutic implications given that IL-13R α 1-neutralizing monoclonal antibodies have recently been developed (50). Although the efficacy of targeting this receptor by itself may be limited by the emergence of proinflammatory effects, combination therapy could potentially eliminate these side effects.

AUTHOR CONTRIBUTIONS

All authors were involved in drafting the article or revising it critically for important intellectual content, and all authors approved the final version to be published. Dr. Pernis had full access to all of the data in the study and takes responsibility for the integrity of the data and the accuracy of the data analysis.

Study conception and design. Chen, Pernis.

Acquisition of data. Chen, Flores Castro, Gupta, Phalke, Manni, Giannopoulou, Pannellini.

Analysis and interpretation of data. Chen, Flores Castro, Gupta, Phalke, Rivera-Correa, Jessberger, Zaghoulani, Giannopoulou, Pannellini, Pernis.

ACKNOWLEDGMENTS

We would like to thank the members of the HSS Research Institute for their thoughtful discussions and for providing the reagents. We also thank the Epigenomics Core Facility, the Microscopy and Imaging Core Facility, and the Flow Cytometry Core Facility of Weill Cornell Medicine; the Laboratory of Comparative Pathology at Memorial Sloan Kettering Cancer Center; and the Office of the Director of the NIH for providing technical support.

REFERENCES

- Liu Z, Davidson A. Taming lupus—a new understanding of pathogenesis is leading to clinical advances [review]. *Nat Med* 2012;18:871–2.
- Tsokos GC. Autoimmunity and organ damage in systemic lupus erythematosus. *Nat Immunol* 2020;21:605–14.
- Seth A, Craft J. Spatial and functional heterogeneity of follicular helper T cells in autoimmunity. *Curr Opin Immunol* 2019;61:1–9.
- Paredes JL, Fernandez-Ruiz R, Niewold TB. T cells in systemic lupus erythematosus. *Rheum Dis Clin North Am* 2021;47:379–93.
- Canny SP, Jackson SW. B cells in systemic lupus erythematosus: from disease mechanisms to targeted therapies. *Rheum Dis Clin North Am* 2021;47:395–413.
- Atisha-Fregoso Y, Toz B, Diamond B. Meant to B: B cells as a therapeutic target in systemic lupus erythematosus. *J Clin Invest* 2021;131.
- Cancro MP. Age-associated B cells. *Annu Rev Immunol* 2020;38:315–40.
- Jenks SA, Cashman KS, Woodruff MC, Lee FE, Sanz I. Extrafollicular responses in humans and SLE. *Immunol Rev* 2019;288:136–48.
- Rubtsov AV, Rubtsova K, Fischer A, Meehan RT, Gillis JZ, Kappler JW, et al. Toll-like receptor 7 (TLR7)-driven accumulation of a novel CD11c(+) B-cell population is important for the development of autoimmunity. *Blood* 2011;118:1305–15.
- Rubtsova K, Rubtsov AV, Thurman JM, Mennona JM, Kappler JW, Marrack P. B cells expressing the transcription factor T-bet drive lupus-like autoimmunity. *J Clin Invest* 2017;127:1392–404.
- Manni M, Gupta S, Ricker E, Chinenov Y, Park SH, Shi M, et al. Regulation of age-associated B cells by IRF5 in systemic autoimmunity. *Nat Immunol* 2018;19:407–19.
- Jenks SA, Cashman KS, Zumaquero E, Marigorta UM, Patel AV, Wang X, et al. Distinct effector B cells induced by unregulated toll-like receptor 7 contribute to pathogenic responses in systemic lupus erythematosus. *Immunity* 2018;49:725–39.
- Wang S, Wang J, Kumar V, Karnell JL, Naiman B, Gross PS, et al. IL-21 drives expansion and plasma cell differentiation of autoreactive CD11c(hi)T-bet(+) B cells in SLE. *Nat Commun* 2018;9:1758.
- Arazi A, Rao DA, Berthier CC, Davidson A, Liu Y, Hoover PJ, et al. The immune cell landscape in kidneys of patients with lupus nephritis. *Nat Immunol* 2019;20:902–14.
- Karnell JL, Kumar V, Wang J, Wang S, Voynova E, Ettinger R. Role of CD11c(+) T-bet(+) B cells in human health and disease. *Cell Immunol* 2017;321:40–5.
- Johnson JL, Rosenthal RL, Know JJ, Myles A, Naradikian MS, Madej J, et al. The transcription factor t-bet resolves memory B cell subsets with distinct tissue distributions and antibody specificities in mice and humans. *Immunity* 2020;52:842–55.
- Woodruff MC, Ramonell RP, Nguyen DC, Cashman KS, Saini AS, Haddad NS, et al. Extrafollicular B cell responses correlate with neutralizing antibodies and morbidity in COVID-19. *Nat Immunol* 2020;21:1506–16.
- Souyris M, Cenac C, Azar P, Daviaud D, Canivet A, Grunenwald S, et al. TLR7 escapes X chromosome inactivation in immune cells. *Sci Immunol* 2018;3:eaap8855.
- Pyfrom S, Paneru B, Knox JJ, Cancro MP, Posso S, Buckner JH, et al. The dynamic epigenetic regulation of the inactive X chromosome in healthy human B cells is dysregulated in lupus patients. *Proc Natl Acad Sci U S A* 2021;118:e2024624118.
- Hagen SH, Henseling F, Hennesen J, Savel H, Delahaye S, Richert L, et al. Heterogeneous escape from X chromosome inactivation results in sex differences in type I IFN responses at the single human pDC level. *Cell Rep* 2020;33:108485.
- Ricker E, Manni M, Flores-Castro D, Jenkins D, Gupta S, Rivera-Correa J, et al. Altered function and differentiation of age-associated B cells contribute to the female bias in lupus mice. *Nat Commun* 2021;12:4813.
- Naradikian MS, Myles A, Beiting DP, Roberts KJ, Dawson L, Herati RS, et al. Cutting edge: IL-4, IL-21, and IFN- γ interact to govern t-bet and CD11c expression in TLR-activated B cells. *J Immunol* 2016;197:1023–8.
- Leonard WJ, Lin JX, O'Shea JJ. The γ c family of cytokines: basic biology to therapeutic ramifications. *Immunity* 2019;50:832–50.
- Parrish-Novak J, Dillon SR, Nelson A, Hammond A, Sprecher V, Gross JA, et al. Interleukin 21 and its receptor are involved in NK cell expansion and regulation of lymphocyte function. *Nature* 2000;408:57–63.
- Karo-Atar D, Bitton A, Benhar I, Munitz A. Therapeutic targeting of the interleukin-4/interleukin-13 signaling pathway: in allergy and beyond [review]. *BioDrugs* 2018;32:201–20.
- Junttila IS. Tuning the cytokine responses: an update on interleukin (IL)-4 and IL-13 receptor complexes. *Front Immunol* 2018;9:888.
- Ukah TK, Cattin-Roy AN, Chen W, Miller MM, Barik S, Zaghoulani H. On the role IL-4/IL-13 heteroreceptor plays in regulation of type 1 diabetes. *J Immunol* 2017;199:894–902.
- Barik S, Ellis JS, Cascio JA, Miller MM, Ukah TK, Cattin-Roy AN, et al. IL-4/IL-13 heteroreceptor influences Th17 cell conversion and sensitivity to regulatory T cell suppression to restrain experimental allergic encephalomyelitis. *J Immunol* 2017;199:2236–48.

29. Becart S, Altman A. SWAP-70-like adapter of T cells: a novel Lck-regulated guanine nucleotide exchange factor coordinating actin cytoskeleton reorganization and Ca²⁺ signaling in T cells. *Immunol Rev* 2009;232:319–33.
30. Shinohara M, Terada Y, Iwamatsu A, Shinohara A, Mochizuki N, Higuchi M, et al. SWAP-70 is a guanine-nucleotide-exchange factor that mediates signalling of membrane ruffling. *Nature* 2002;416:759–63.
31. Phalke S, Rivera-Correa J, Jenkins D, Flores-Castro D, Giannopoulos E, Pernis AB. Molecular mechanisms controlling age-associated B cells in autoimmunity. *Immunol Rev* 2022;307:79–100.
32. Kwon YC, Lim J, Bang SY, Ha E, Hwang MY, Yoon K, et al. Genome-wide association study in a Korean population identifies six novel susceptibility loci for rheumatoid arthritis. *Ann Rheum Dis* 2020;79:1438–45.
33. Sun C, Molineros JE, Looger LL, Zhou X, Kim K, Okada Y, et al. High-density genotyping of immune-related loci identifies new SLE risk variants in individuals with Asian ancestry. *Nat Genet* 2016;48:323–30.
34. Langefeld CD, Ainsworth HC, Graham DS, Kelly JA, Comeau ME, Marion MC, et al. Transancestral mapping and genetic load in systemic lupus erythematosus. *Nat Commun* 2017;8:16021.
35. Serwas NK, Hoeger B, Ardy RC, Stulz SV, Sui Z, Memaran N, et al. Human DEF6 deficiency underlies an immunodeficiency syndrome with systemic autoimmunity and aberrant CTLA-4 homeostasis. *Nat Commun* 2019;10:3106.
36. Fournier B, Tusseau M, Villard M, Malcus C, Chopin E, Martin E, et al. DEF6 deficiency, a mendelian susceptibility to EBV infection, lymphoma, and autoimmunity. *J Allergy Clin Immunol* 2021;147:740–3.
37. Biswas PS, Gupta S, Stirzaker RA, Kumar V, Jessberger R, Lu TT, et al. Dual regulation of IRF4 function in T and B cells is required for the coordination of T–B cell interactions and the prevention of autoimmunity. *J Exp Med* 2012;209:581–96.
38. Haymaker CL, Guloglu FB, Cascio JA, Hardaway JC, Dhakal M, Wan X, et al. Bone marrow-derived IL-13R α 1-positive thymic progenitors are restricted to the myeloid lineage. *J Immunol* 2012;188:3208–16.
39. Jackson SW, Scharping NE, Kolhatkar NS, Khim S, Schwartz MA, Li QZ, et al. Opposing impact of B cell-intrinsic TLR7 and TLR9 signals on autoantibody repertoire and systemic inflammation. *J Immunol* 2014;192:4525–32.
40. Manni M, Gupta S, Nixon BG, Weaver CT, Jessberger R, Pernis AB. IRF4-dependent and IRF4-independent pathways contribute to DC dysfunction in lupus. *PLoS One* 2015;10:e0141927.
41. Rubtsov AV, Rubtsova K, Kappler JW, Jacobelli J, Friedman RS, Marrack P. CD11c-expressing B cells are located at the T cell/B cell border in spleen and are potent APCs. *J Immunol* 2015;195:71–9.
42. Zhang W, Zhang H, Liu S, Xia F, Kang Z, Zhang Y, et al. Excessive CD11c(+)Tbet(+) B cells promote aberrant TFH differentiation and affinity-based germinal center selection in lupus. *Proc Natl Acad Sci U S A* 2019;116:18550–60.
43. Weinstein JS, Herman EI, Lainez B, Licona-Limón P, Esplugues E, Flavell R, et al. TFH cells progressively differentiate to regulate the germinal center response. *Nat Immunol* 2016;17:1197–205.
44. Gowthaman U, Chen JS, Zhang B, Flynn WF, Lu Y, Song W, et al. Identification of a T follicular helper cell subset that drives anaphylactic IgE. *Science* 2019;365:eaaw6433.
45. Heinz LX, Lee J, Kapoor U, Kartnig F, Sedlyarov V, Papakostas K, et al. TASL is the SLC15A4-associated adaptor for IRF5 activation by TLR7-9. *Nature* 2020;581:316–22.
46. Harris VM, Koelsch KA, Kurien BT, Harley IT, Wren JD, Harley JB, et al. Characterization of cxorf21 provides molecular insight into female-bias immune response in SLE pathogenesis. *Front Immunol* 2019;10:2160.
47. Odhams CA, Roberts AL, Vester SK, Duarte CS, Beales CT, Clarke AJ, et al. Interferon inducible X-linked gene CXorf21 may contribute to sexual dimorphism in systemic lupus erythematosus. *Nat Commun* 2019;10:2164.
48. Woodruff MC, Ramonell RP, Cashman KS, Nguyen DC, Ley AM, Kyu S, et al. Critically ill SARS-CoV-2 patients display lupus-like hallmarks of extrafollicular B cell activation [preprint]. *medRxiv* 2020. E-pub ahead of print.
49. Marrapodi R, Pellicano C, Radicchio G, Leodori G, Colantuono S, Iacolare A, et al. CD21(low) B cells in systemic sclerosis: a possible marker of vascular complications. *Clin Immunol* 2020;213:108364.
50. Bitton A, Avlas S, Reichman H, Itan M, Karo-Atar D, Azouz NP, et al. A key role for IL-13 signaling via the type 2 IL-4 receptor in experimental atopic dermatitis. *Sci Immunol* 2020;5:eaaw2938.

Plasmablast-like Phenotype Among Antigen-Experienced CXCR5–CD19^{low} B Cells in Systemic Lupus Erythematosus

Franziska Szelinski,¹ Ana Luisa Stefanski,² Eva Schrezenmeier,¹ Hector Rincon-Arevalo,³ Annika Wiedemann,² Karin Reiter,¹ Jacob Ritter,¹ Marie Lettau,¹ Van Duc Dang,¹ Sebastian Fuchs,⁴ Andreas P. Frei,⁴ Tobias Alexander,¹ Andreia C. Lino,¹ and Thomas Dörner¹

Objective. Altered composition of the B cell compartment in the pathogenesis of systemic lupus erythematosus (SLE) is characterized by expanded plasmablast and IgD–CD27– double-negative B cell populations. Previous studies showed that double-negative B cells represent a heterogeneous subset, and further characterization is needed.

Methods. We analyzed 2 independent cohorts of healthy donors and SLE patients, using a combined approach of flow cytometry (for 16 healthy donors and 28 SLE patients) and mass cytometry (for 18 healthy donors and 24 SLE patients) and targeted RNA-Seq analysis. To compare B cell subset formation during the acute immune response versus that during autoimmune disease, we investigated healthy donors at various time points after receipt of the BNT162b2 messenger RNA COVID-19 vaccine and patients with acute SARS–CoV-2 infection, using flow cytometry.

Results. We found that IgD–CD27+ switched and atypical IgD–CD27– memory B cells, the levels of which were increased in SLE patients, represented heterogeneous populations composed of 3 different subsets each. CXCR5+ CD19^{intermediate}, CXCR5–CD19^{high}, and CXCR5–CD19^{low} populations were found in the switched memory and double-negative compartments, suggesting the relatedness of IgD–CD27+ and IgD–CD27– B cells. We characterized a hitherto unknown and antigen-experienced CXCR5–CD19^{low} subset that was enhanced in SLE patients, had a plasmablast phenotype with diminished B cell receptor responsiveness, and expressed CD38, CD95, CD71, *PRDM1*, *XBP1*, and *IRF4*. Levels of CXCR5–CD19^{low} subsets were increased and correlated with plasmablast frequencies in SLE patients and in healthy donors who received BNT162b2, suggesting their interrelationship and contribution to plasmacytosis. The detection of CXCR5–CD19^{low} B cells among both CD27+ and CD27– populations calls into question the role of CD27 as a reliable marker of B cell differentiation.

Conclusion. Our data suggest that CXCR5–CD19^{low} B cells are precursors of plasmablasts. Thus, cotargeting this subset may have therapeutic value in SLE.

Supported by DFG grants project Do491/7-5, Do491/10-1, Do491/11-1, TR130 project 24, and LI3540/1-1. The Deutsches Rheumaforschungszentrum was supported by the Senate of Berlin. Dr. Stefanski's work was supported by DGRh Research Initiative 2020. Dr. Schrezenmeier's work was supported by a Fellowship of the Berlin Institutes of Health and a grant from the Federal Ministry of Education and Research (BMBF) (BCOVIT, 01KI20161). Mr. Rincon-Arevalo's work was supported by COLCIENCIAS (scholarship 727, 2015). Mr. Ritter's work was supported by a Fellowship of the Berlin Institutes of Health. Prof. Dörner's work was supported by the HTG EdgeSeq 2020 Autoimmune Panel Research Grant Award for transcriptome analysis using the Immune Response Panel.

Dr. Lino and Prof. Dörner contributed equally to this work.

¹Franziska Szelinski, MSc, Eva Schrezenmeier, MD, Karin Reiter, MTA, Jacob Ritter, Marie Lettau, MD (present address: Charité Universitätsmedizin Berlin, Berlin, Germany), Van Duc Dang, Dr rer nat, Tobias Alexander, MD, Andreia C. Lino, PhD, Thomas Dörner, MD: Charité Universitätsmedizin Berlin and Deutsches Rheumaforschungszentrum, Berlin, Germany; ²Ana Luisa Stefanski, MD, Annika Wiedemann, Dr Ing: Charité Universitätsmedizin Berlin, Berlin, Germany; ³Hector Rincon-Arevalo, MSc: Charité Universitätsmedizin Berlin and Deutsches Rheumaforschungszentrum, Berlin, Germany, and

Grupo de Inmunología Celular e Inmunogenética, Facultad de Medicina, Instituto de Investigaciones Médicas, Universidad de Antioquia UdeA, Medellín, Colombia; ⁴Sebastian Fuchs, Dr rer nat, Andreas P. Frei, PhD: Roche Innovation Center Basel, Basel, Switzerland.

The data sets used and analyzed during the current study are available from the corresponding author on reasonable request.

Author disclosures are available at <https://onlinelibrary.wiley.com/action/downloadSupplement?doi=10.1002%2Fart.42157&file=art42157-sup-0001-Disclosureform.pdf>.

[Correction added on 29 August 2022, after first online publication: Franziska Szelinski was designated as corresponding author.]

Address correspondence to Thomas Dörner, MD, Deutsches Rheumaforschungszentrum and Departments of Medicine/Rheumatology and Clinical Immunology, Charité Universitätsmedizin Berlin, Charitéplatz 1, 10117 Berlin, Germany. Email: thomas.doerner@charite.de; or to Franziska Szelinski, Charité - Universitätsmedizin Berlin, Charitépl. 1, 10117 Berlin, Germany.

Submitted for publication July 13, 2021; accepted in revised form April 28, 2022.

INTRODUCTION

Various abnormalities of the B cell lineage have been identified in systemic lupus erythematosus (SLE), a chronic autoimmune disease characterized by autoantibody production and pathogenic immune complex formation. Abnormalities include increased peripheral plasmablasts (PBs) (1), including the expansion of PBs producing IgG and IgA (2), as well as altered composition of the B cell compartment, with increased frequencies of IgD-CD27+ switched and atypical IgD-CD27- memory B cells (3). Greater frequencies of these cells have also been observed in patients with rheumatoid arthritis (RA) (4), as well as in peripheral blood or tissue specimens from patients with various inflammatory diseases, such as chronic inflammatory bowel disease (5) or Alzheimer's disease (6). How these observations are related remains unclear.

In SLE, expansions of switched memory and IgD-CD27- (i.e., double-negative) B cells are not seen in patients with new-onset disease, even though their B cell distribution also differs from that in healthy donors (7). These observations emphasize that enlargement of the switched memory and double-negative B cell compartments is an important characteristic of chronic inflammation (7). In lupus nephritis, a severe complication of SLE, double-negative B cell counts were correlated with the 24-hour urine protein level and inversely correlated with the glomerular filtration rate (8). Interestingly, the double-negative B cell count was diminished in lupus nephritis patients during remission, suggesting a possible role for these cells in pathogenicity and as a prognostic biomarker in lupus nephritis (8).

More recently, it became evident that double-negative B cells represent a heterogeneous subset, including age-/autoimmune-associated B cells (9), Syk++ B cells (10), and double-negative 2 (DN2) cells (IgD-CD27-CXCR5-CD11c+) (11). These subsets have some overlapping characteristics and are linked to disease activity and autoantibody formation. In addition to subset alterations, impaired chemokine receptor expression (12) and reduced B cell receptor responsiveness (13) have been reported for B cells during SLE, suggesting their distinct involvement in autoimmunity.

This study further delineates the heterogeneity of switched memory and double-negative B cells in healthy donors and patients with SLE. Using a combined approach involving flow cytometry and mass cytometry, we identified an enhanced CXCR5-CD19^{low} B cell subset in switched memory and double-negative (mem^{low}/DN^{low}) compartments in SLE patients that has characteristics of antigen-experienced B cells that are distinct from those previously observed in CXCR5+ CD19^{intermediate} (mem^{intermediate}/DN^{intermediate}) and CXCR5- CD19^{high} (mem^{high}/DN^{high}) B cells. The subsets of mem^{low}/DN^{low} B cells were similar to peripheral PBs in terms of their surface marker expression, transcription factor pattern, antibody-secreting

capacity, and reduced B cell receptor responsiveness. Our data provide multiple new insights, including the discovery of B cell-differentiation abnormalities, that may prove to be relevant targets for treatment of SLE.

PATIENTS AND METHODS

Patients. Peripheral blood specimens were obtained from 79 patients with SLE who met the Systemic Lupus International Collaborating Clinics criteria for SLE (14) and from 80 healthy individuals. Additionally, we analyzed 22 patients with primary Sjögren's syndrome, 11 with RA, 15 with mild SARS-CoV-2 infection, and 11 with severe SARS-CoV-2 infection that required intensive care unit admission.

This study was performed in accordance with the recommendations of the ethics committee at Charité University Hospital Berlin. All participants gave written informed consent to participate, in accordance with the Declaration of Helsinki.

Materials and methods. A detailed description of the methods and materials used in the study are provided in the Supplementary Materials, available on the *Arthritis & Rheumatology* website at <http://onlinelibrary.wiley.com/doi/10.1002/art.42157>.

RESULTS

Frequencies of CD19^{low} memory and double-negative B cells in SLE patients. We and others have described several abnormalities within the B cell compartment in SLE, as well as their potential relevance to pathogenicity. Frequencies of IgD-CD27- double-negative B cells, especially those coexpressing CD95 (15), and IgD-CD27+ switched memory B cells are increased in SLE (1). Therefore, we analyzed these B cell subsets in further detail by flow cytometry (for the gating strategy, see Supplementary Figure 1, available on the *Arthritis & Rheumatology* website at <http://onlinelibrary.wiley.com/doi/10.1002/art.42157>) and found that switched memory and double-negative B cells have a similar pattern of CXCR5 and CD19 expression. Notably, expression of these molecules subdivided both compartments into 3 B cell populations (Figure 1A and Supplementary Figure 1A, available at <http://onlinelibrary.wiley.com/doi/10.1002/art.42157>). Two of these populations, CXCR5+ CD19^{intermediate} (mem^{intermediate}/DN^{intermediate}) and CXCR5- CD19^{high} (mem^{high}/DN^{high}), have been previously identified and described in healthy donors and SLE patients, with increased frequencies of the CXCR5-CD19^{high} fraction in patients with SLE (11). Here, we identified a third, novel B cell subset within both switched memory and double-negative B cells that is CXCR5- CD19^{low} (mem^{low}/DN^{low}).

We found that frequencies of DN^{low} B cells among CD19+ B cells were significantly increased in SLE patients as compared

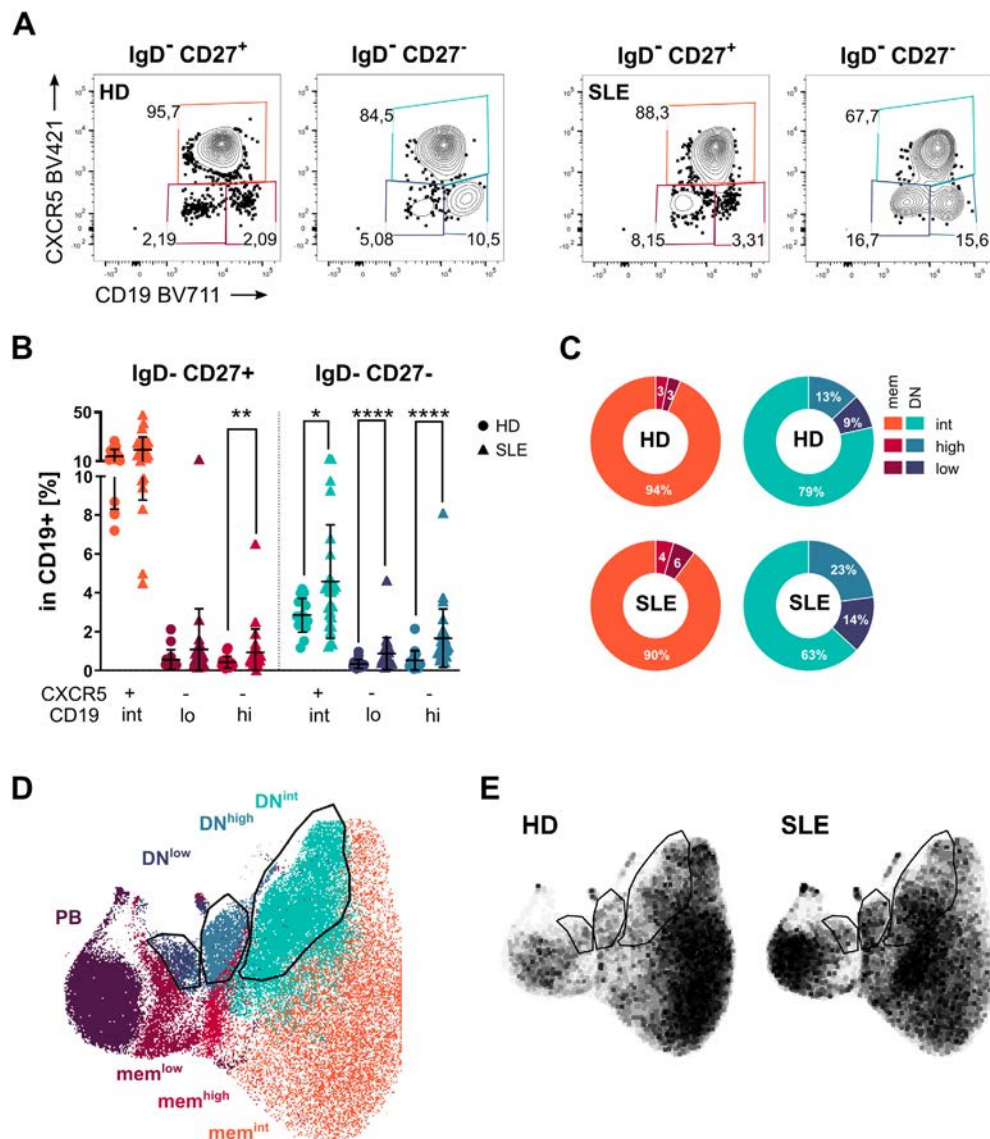


Figure 1. Frequencies of CD19^{low}CXCR5⁻ B cells in patients with systemic lupus erythematosus (SLE). **A**, Representative flow cytometry data for 1 healthy donor (HD) and 1 SLE patient, showing CD19 and CXCR5 expression on IgD-CD27⁺ and IgD-CD27⁻ B cells. **B**, Distribution of CD19⁺ B cell frequencies among the subsets of IgD-CD27⁺ memory (mem) or IgD-CD27⁻ double-negative (DN) B cells (CXCR5⁺CD19^{intermediate} [mem^{intermediate}/DN^{intermediate}], CXCR5-CD19^{low} [mem^{low}/DN^{low}], and CXCR5-CD19^{high} [mem^{high}/DN^{high}]) in healthy donors and SLE patients. **C**, Distribution of subsets within switched memory (IgD-CD27⁺) and double-negative (IgD-CD27⁻) populations in healthy donors and SLE patients. **D**, Overlay of uniform manifold approximation and projections (UMAPs) of clustering of pregated IgD- B cells ($n = 59,000$ events each per cohort of healthy donors and SLE patients) and manually gated IgD-CD27⁻ subsets. Outlined areas indicate gates for DN^{intermediate}, DN^{low}, and DN^{high} populations. **E**, Overlay of UMAPs of B cell subset clustering in healthy donors and SLE patients. Outlined areas indicate gates for DN^{intermediate}, DN^{low}, and DN^{high} populations. Data are for 16 healthy donors and 28 SLE patients unless indicated otherwise. * = $P \leq 0.05$; ** = $P \leq 0.005$; **** = $P \leq 0.0001$, by Mann-Whitney U test.

to healthy donors (Figures 1A and B). Whereas levels of only mem^{high} B cells were increased in the switched memory compartment, levels of all 3 subsets in the double-negative fraction were significantly increased in SLE patients (Figure 1B). Double-negative B cells were enriched for CXCR5-CD19^{low} and CXCR5-CD19^{high} B cell subsets, compared with the CD27⁺ (switched memory) compartment, and in general were remarkably expanded in SLE patients (Figure 1C).

Next, we used the uniform manifold approximation and projections (UMAP) technique, a dimension-reduction algorithm (16), to cluster IgD- B cells. With this approach, we identified mem^{intermediate}/DN^{intermediate}, mem^{high}/DN^{high}, and mem^{low}/DN^{low} cells as distinct populations and found that both CD19^{low} populations clustered together with CD27⁺CD38⁺ PBs (Figure 1D). Comparison of clusters obtained from healthy donors to those from patients with SLE revealed an increased density of the

corresponding subsets in the SLE group (Figure 1E), consistent with their significant expansion during SLE. Similar to our findings in SLE, we found increased frequencies of all 3 double-negative subsets in patients with primary Sjögren's syndrome and those with RA. In patients with primary Sjögren's syndrome, frequencies of both CXCR5- memory subsets (mem^{low} and mem^{high}) were also increased (Supplementary Figures 1C and D, available at <http://onlinelibrary.wiley.com/doi/10.1002/art.42157>).

PB-like phenotype among CD19^{low} B cell subsets.

Next, we investigated DN^{intermediate}, DN^{high}, and DN^{low} B cell subsets for expression of several surface molecules, including lineage, differentiation, and activation markers. The resulting patterns of CD27, CD19, CXCR5, CD24, CD71, CD95, CD38, and CD11c expression were visualized by color code in a dimension-reduced UMAP (Figure 2A). In this analysis, we found that distinctive patterns of CD19 and CXCR5 expression by these subsets allowed further differentiation based on different CD24, CD71, CD95, CD38, and CD11c expression profiles (Figures 2A and B). CD24, a marker that has a dynamic pattern of expression throughout B cell maturation and is absent from antibody-producing cells, was not present in the subsets with low CD19 expression and no CXCR5 expression ($\text{mem}^{\text{low}}/\text{DN}^{\text{low}}$), in contrast to the DN^{intermediate} population.

In addition to CD19 expression, the main factors discriminating between the DN^{low} and DN^{high} populations were CD38 and CD11c expression (Figures 2A and B). As previously described, DN^{high} populations are CD11c^{high} cells but lack CD38 expression (11,17). In contrast, the majority of DN^{low} B cells express CD38 (Figures 2B and C and Supplementary Figure 1E, available at <http://onlinelibrary.wiley.com/doi/10.1002/art.42157>). Expression of CD71, a marker of early B cell activation, was up-regulated on the surface of CXCR5-CD19^{low} B cells at levels comparable to levels on PBs (Figures 2B and C). CD95 was expressed by the majority of DN^{low} and DN^{high} cells but not on DN^{intermediate} cells (Figures 2B and C).

Subsequently, we evaluated the expression of the inhibitory receptor programmed death 1 (PD-1), which is up-regulated on B cells upon activation (18), and its ligand, PD ligand 1 (PD-L1). Surface expression of PD-L1 and PD-1 was only found enhanced in DN^{high} cells (Figure 2D and Supplementary Figure 1F, available at <http://onlinelibrary.wiley.com/doi/10.1002/art.42157>).

Most noteworthy, each of the subsets of double-negative B cells differed from the corresponding subsets in the switched memory compartment mainly with respect to the expression of CD27, whereas frequencies of expression for the other markers were similar (Figure 2F and Supplementary Figure 1). This suggests that memory and double-negative populations consist of complementary subsets.

Because we found differences in the frequencies of these B cell subsets, we also evaluated qualitative differences between healthy donors and SLE patients. Comparison of profiles of the 3 double-negative B cell subsets in healthy donors to those in

patients with SLE showed that, in SLE patients, expression levels of the proliferation marker CD71 and frequencies of the activation markers CD95 and CD38 were increased in the DN^{intermediate} population (Figure 2E) but not in the $\text{mem}^{\text{intermediate}}$ population (Supplementary Figure 1G, available at <http://onlinelibrary.wiley.com/doi/10.1002/art.42157>). Expression of CD71 was enhanced in both DN^{low} and mem^{low} populations in SLE patients (Figure 2E and Supplementary Figure 1E).

Comparison of the newly identified subsets to conventional transitional (CD10+CD24+CD38+), naive (IgD+CD27-), and pre-switched memory (IgD+CD27+) B cells and PBs (CD27++CD38++) demonstrated that switched memory and double-negative subsets expressed levels of CD19, CD24, CD10, CD11c, CD71, PD1, PD-L1, and CD95 that were comparable to those expressed by PBs. The main differences between PBs and $\text{mem}^{\text{low}}/\text{DN}^{\text{low}}$ cells were a diminished level or absence of CD27 expression and a slightly lower level of CD38 expression among both mem^{low} and DN^{low} B cell subsets (Figure 2F). The fact that frequencies of $\text{mem}^{\text{low}}/\text{DN}^{\text{low}}$ B cells strongly correlated with those of PBs (Figure 2G) in SLE patients as well as healthy donors further supports their potential relationship. Additionally, patients with primary Sjögren's syndrome and those with RA showed correlations in frequency between CD19^{low} subsets and PBs. The mem^{low} subset frequency had an especially strong correlation with the frequency of PBs among patients with primary Sjögren's syndrome and those with RA. In RA patients, DN^{low} B cell frequency also correlated with the frequency of PBs (Supplementary Figures 1C and D).

Additionally, we saw a trend of increased cell size (CD19^{low}) and granularity (CD19^{low}/CD19^{high}) for CXCR5- subsets (Supplementary Figures 2A-C, available on the *Arthritis & Rheumatology* website at <http://onlinelibrary.wiley.com/doi/10.1002/art.42157>), potential hints of or consistent with characteristics of antibody-secreting cells. Thus, we next analyzed Ig expression in B cell subsets. Whereas $\text{mem}^{\text{intermediate}}/\text{DN}^{\text{intermediate}}$ and $\text{mem}^{\text{high}}/\text{DN}^{\text{high}}$ cells mainly expressed IgG, $\text{mem}^{\text{low}}/\text{DN}^{\text{low}}$ cells expressed IgG and IgA (Figure 2H).

To test the potential of CD19^{low} populations to secrete Ig, supernatants were harvested after 12 and 24 hours of culture (Figure 2I and Supplementary Figure 2E, available at <http://onlinelibrary.wiley.com/doi/10.1002/art.42157>). Whereas IgD+CD27- conventional naive and IgD-CXCR5+CD27+/-CD19^{intermediate} memory B cells had no evidence of antibody secretion, cultures of IgD-CXCR5-CD27+/-CD19^{low} cells contained notably increased levels of IgA (Figure 2I and Supplementary Figure 2E).

Activation and differentiation profiles and checkpoint molecule expression among CD19^{low} B cells.

Next, we validated our findings in an independent cohort of 27 SLE patients and 18 healthy donors, using mass cytometry to investigate expression of activation markers and checkpoint molecules (Figure 3 and Supplementary Figure 3, available on the *Arthritis & Rheumatology*

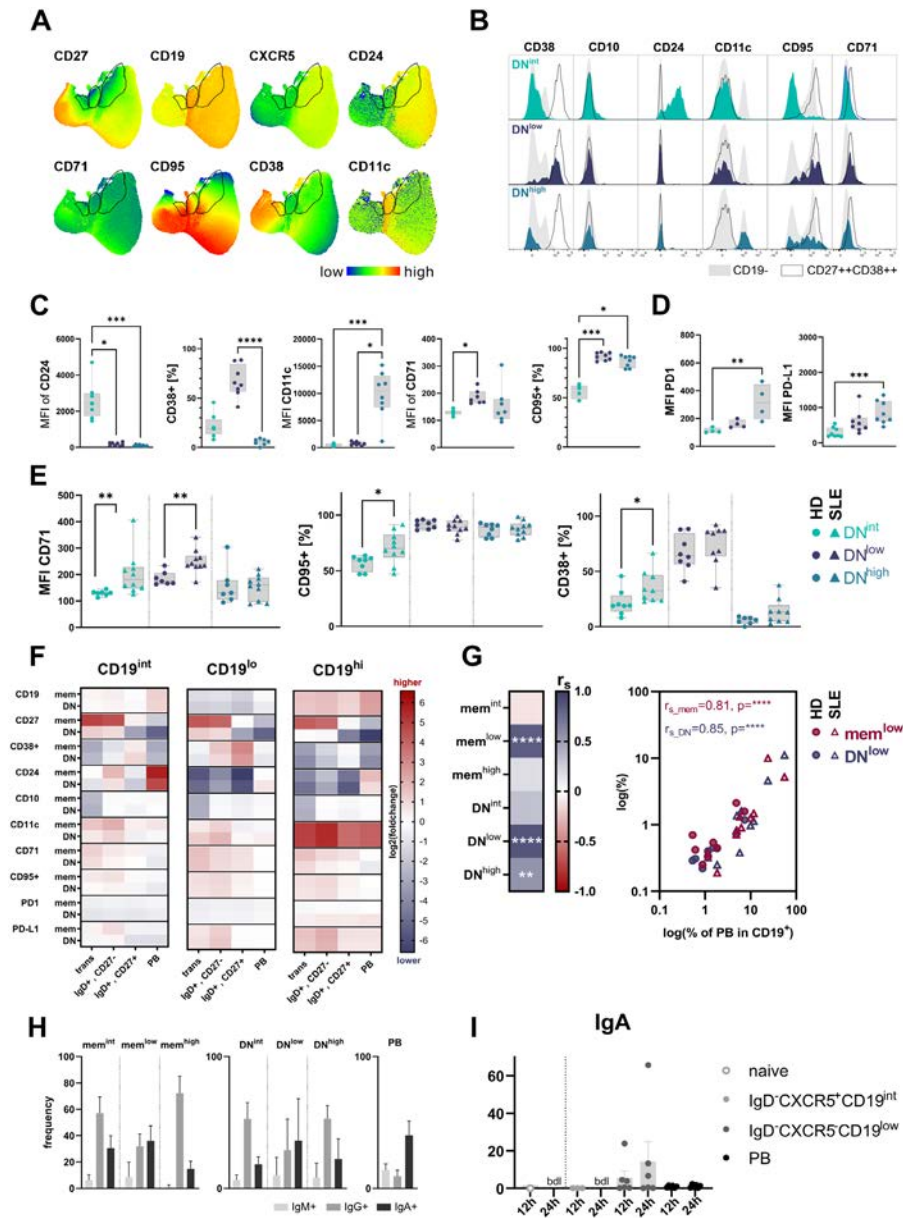


Figure 2. Patterns of surface marker expression among DN^{low} , DN^{high} , and $DN^{intermediate}$ B cell subsets, between double-negative subsets and their corresponding memory subsets, and between double-negative cells and plasmablasts (PBs). **A**, UMAPs of color-coded mean signal intensities for surface marker expression among gated DN^{low} (left), DN^{high} (center), and $DN^{intermediate}$ (right) populations ($n = 59,000$ events each per cohort of healthy donors and SLE patients). **B**, Representative frequencies of double-negative subsets as compared to $CD19^{-}$ cells (gray-shaded areas) and $CD27^{++}CD38^{++}$ PBs (unshaded areas) in 1 healthy donor. **C** and **D**, Median fluorescence intensities (MFIs) of CD24, CD11c, and CD71 expression and frequencies of $CD38^{+}$ or $CD95^{+}$ B cells (**C**) and MFIs of programmed death 1 (PD1) and PD ligand 1 (PD-L1) expression (**D**) in 8 healthy donors for each subset of double-negative cells. * = $P \leq 0.05$; ** = $P \leq 0.005$; *** = $P \leq 0.0005$; **** = $P \leq 0.0001$, by Mann-Whitney U test. **E**, MFI of CD71 surface marker expression and percentages of $CD95^{+}$ and $CD38^{+}$ B cells in 10 SLE patients and 8 healthy donors for each double-negative cell subset. * = $P \leq 0.05$; ** = $P \leq 0.005$, by Kruskal-Wallis test. **F**, Fold changes in MFIs of surface marker expression on $mem^{intermediate}/DN^{intermediate}$, mem^{low}/DN^{low} , and mem^{high}/DN^{high} subsets relative to values for main populations of transitional, $IgD^{+}CD27^{-}$, and $IgD^{+}CD27^{+}$ B cells and PBs. **G**, Spearman's correlation coefficients showing correlations between frequencies of switched memory and double-negative B cell subsets and frequencies of PBs in 8 healthy donors and 10 SLE patients. ** = $P \leq 0.01$; **** = $P \leq 0.0001$. **H** and **I**, Frequencies of Ig isotypes (**H**) and IgA levels (**I**) in the supernatant after culture of $IgD^{+}CD27^{-}$, $IgD^{-}CXCR5^{+}CD19^{intermediate}$, and $IgD^{-}CXCR5^{-}CD19^{low}$ B cells for 12 or 24 hours, using cells from 6 healthy donors. Data in **C–E** are shown as box plots, representing the median, interquartile range, and range. Data in **H** are the mean + SEM. See Figure 1 for other definitions.

website at <http://onlinelibrary.wiley.com/doi/10.1002/art.42157>. Mass cytometry findings with application of a UMAP algorithm indicated an increased frequency of all 3 double-negative subsets

(i.e., $DN^{intermediate}$, DN^{high} , and DN^{low}) in SLE patients (Figure 3A). The frequency of mem^{low} B cells was also substantially increased in SLE patients (Figure 3B), corroborating the flow cytometry findings.

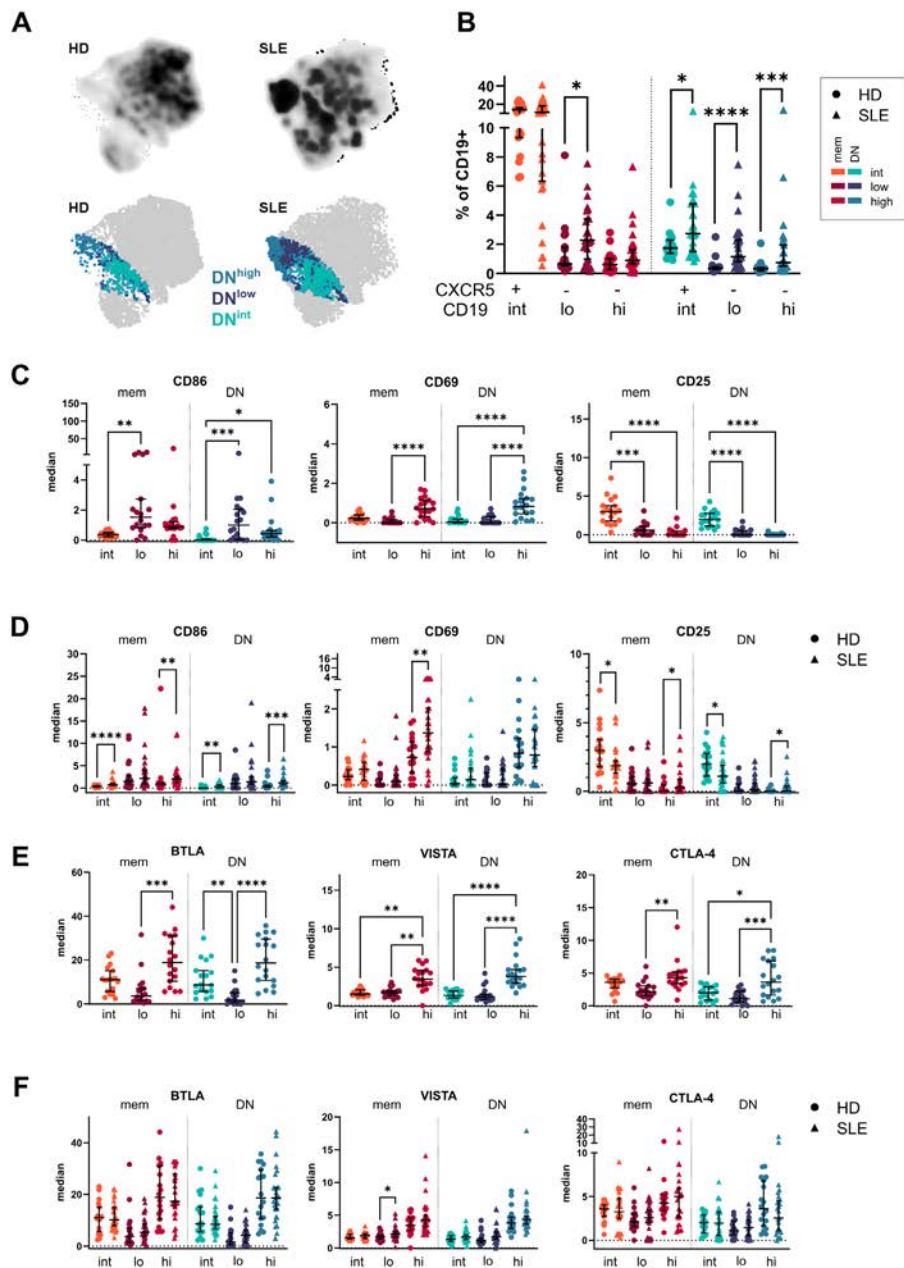


Figure 3. Frequency of an activated phenotype in CXCR5-CD19^{low} B cell populations. **A**, Cytometry analysis by time of flight-derived UMAPs of IgD⁺ B cells (n = 8,841 events per cohort of healthy donors and SLE patients), showing cell densities in healthy donors and SLE patients (top) and the distribution of gated DN^{intermediate}, DN^{low}, and DN^{high} B cells (bottom). **B**, Frequencies of mem^{intermediate}/DN^{intermediate}, mem^{low}/DN^{low}, and mem^{high}/DN^{high} cells in the total CD19⁺ B cell population in 18 healthy donors and 24 SLE patients. **C** and **D**, CD86, CD69, and CD25 activation marker expression among mem^{intermediate}/DN^{intermediate}, mem^{low}/DN^{low}, and mem^{high}/DN^{high} B cell subsets overall (**C**) and in healthy donors and SLE patients (**D**). **E** and **F**, Expression of immune checkpoint molecules among B cell subsets (**E**) and in healthy donors and SLE patients (**F**). Data are for 18 healthy donors and 24 SLE patients. Symbols represent individual subjects; horizontal lines with whiskers represent the median expression with 95% confidence intervals. * = $P \leq 0.05$; ** = $P \leq 0.01$; *** = $P \leq 0.001$; **** = $P \leq 0.0001$ for comparisons between subsets (by Mann-Whitney U test) and between healthy donors and SLE patients (by Kruskal-Wallis test). BTLA = B and T lymphocyte attenuator; VISTA = V-type Ig domain-containing suppressor of T cell activation (see Figure 1 for other definitions).

Characteristics of mem^{low}/DN^{low} and mem^{high}/DN^{high} populations were indicative of an activated phenotype, with increased CD86 expression, and in the case of mem^{high}/DN^{high} cells, increased CD69 expression, compared with mem^{intermediate}/DN^{intermediate} cells. In contrast, mem^{high}/DN^{high}

and mem^{low}/DN^{low} populations expressed less CD25 than did mem^{intermediate}/DN^{intermediate} B cells (Figure 3C). SLE patients expressed more CD86, CD69, and CD25 on the surface of mem^{high} B cells and had elevated CD86 and CD25 expression on DN^{high} cells. In general, mem^{intermediate}/DN^{intermediate} cells in

SLE patients had increased surface expression of CD86 and diminished surface expression of CD25 (Figure 3D), indicating their increased activation status.

Additionally, we evaluated CD45RA and CD45RO, which are known to be differentially expressed throughout B cell differentiation (19). Expression of CD45RA was increased on switched memory B cells, compared with double-negative B cells, but the levels were comparable among the 3 subsets (Supplementary Figure 3D, available at <http://onlinelibrary.wiley.com/doi/10.1002/art.42157>). Comparison of SLE patients and healthy controls revealed that CD45RA expression was reduced on DN^{high} B cells in the SLE group (Supplementary Figure 3D).

Costimulatory and coinhibitory immune checkpoints regulate and modulate immune cells and play an important role in fine-tuning the immune response (17,20,21). Therefore, we analyzed expression profiles of various checkpoint molecules among the cell subsets of interest. Of particular note, mem^{high}/DN^{high} B cells up-regulated immune checkpoint molecules, such as B and T lymphocyte attenuator (BTLA), V-type Ig domain-containing suppressor of T cell activation (VISTA), and CTLA-4 (Figure 3E and Supplementary Figures 3E and F, available at <http://onlinelibrary.wiley.com/doi/10.1002/art.42157>). Whereas levels of VISTA and CTLA-4 expression on mem^{low}/DN^{low} cells were comparable to levels found on mem^{intermediate}/DN^{intermediate} cells, BTLA was down-regulated (Figure 3E). SLE patients expressed higher levels

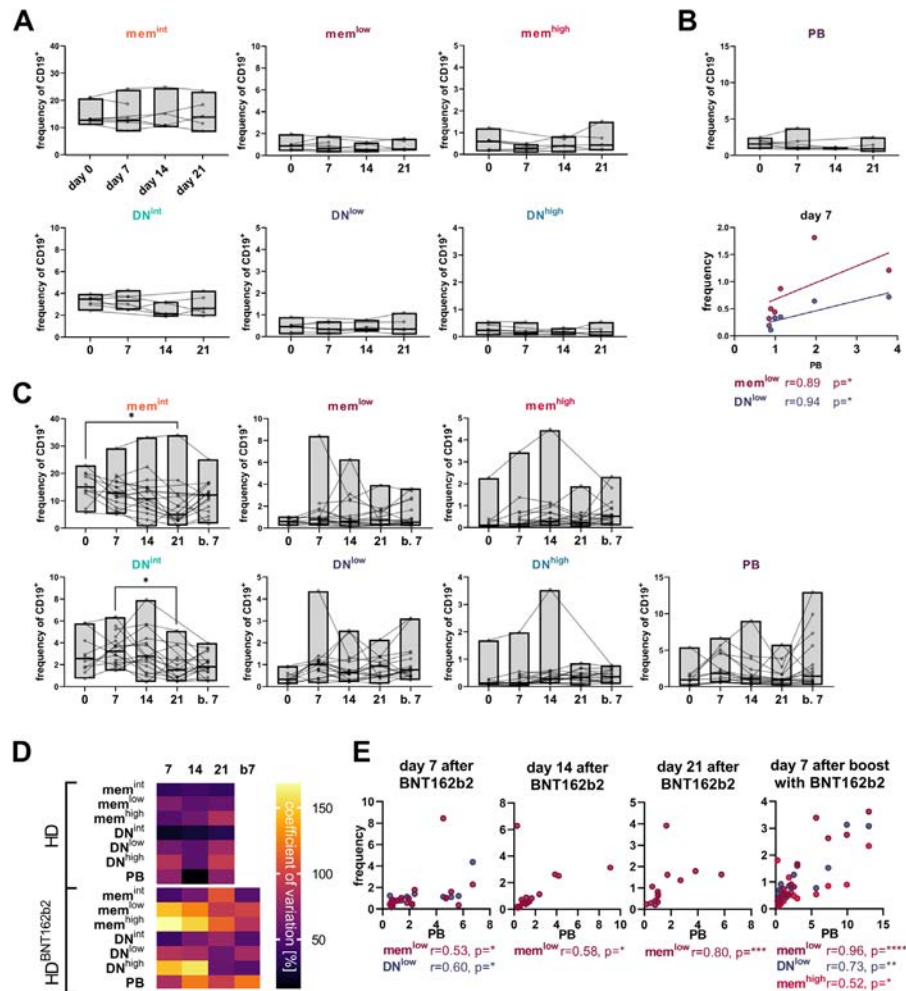


Figure 4. Frequencies of switched memory and double-negative B cell subsets and plasmablasts (PBs) in healthy donors who received BNT162b2 COVID-19 messenger RNA vaccine. **A**, Longitudinal B cell subset frequencies in up to 6 healthy donors before and 7, 14, and 21 days after the first dose, by flow cytometry. **B**, Longitudinal PB frequencies (top) and Spearman's correlations between mem^{low}/DN^{low} subset frequencies and PB frequencies 7 days after vaccine receipt (bottom) in 6 healthy donors. **C**, Kinetics of B cell subset and PB frequencies for up to 17 healthy donors before and 7, 14, and 21 days after the first dose and 7 days after the booster dose (b. 7). * = $P \leq 0.05$, by Kruskal-Wallis test. **D**, Variations in B cell subset frequencies between up to 17 healthy donors 7, 14, and 21 days after the first dose and 7 days after the booster dose (b7) and 6 healthy donors who were not vaccinated. **E**, Select B cell subset and PB frequencies for 17 healthy donors 7, 14, and 21 days after the first dose and 7 days after the booster dose. Values below the graphs are Spearman's correlation coefficients. * = $P \leq 0.05$; ** = $P \leq 0.01$; *** = $P \leq 0.001$; **** = $P \leq 0.0001$. See Figure 1 for other definitions.

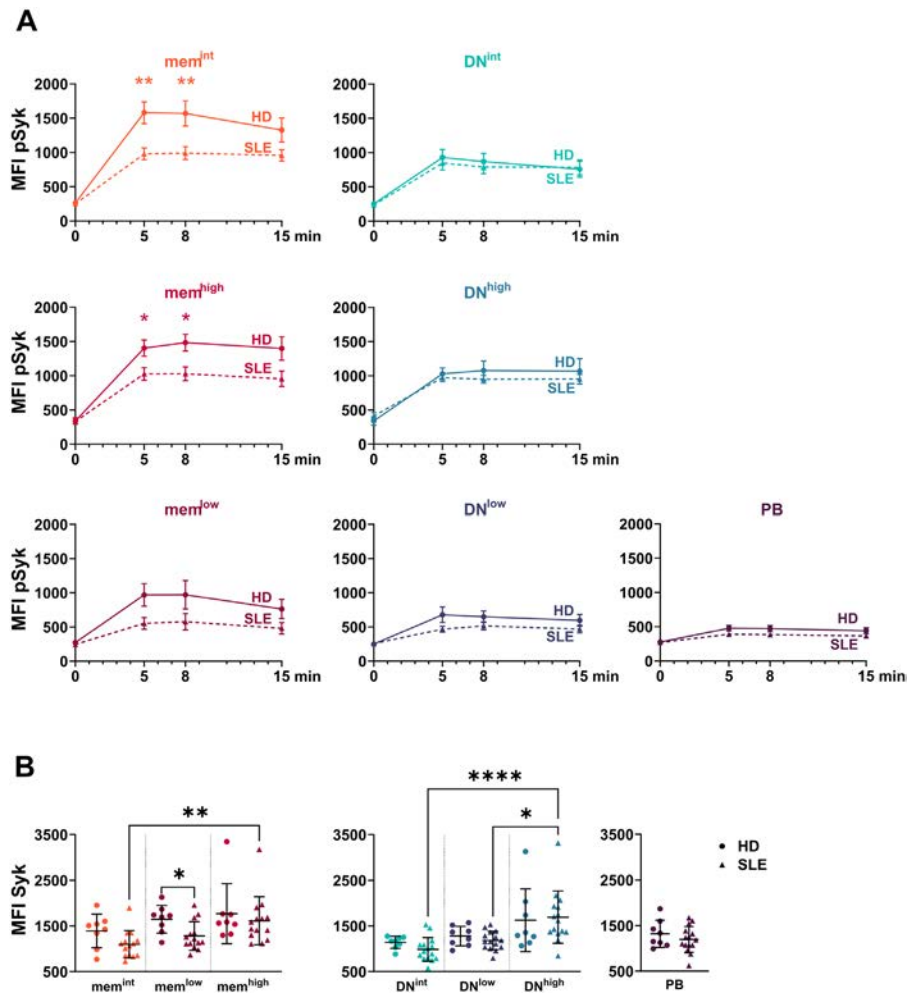


Figure 5. B cell receptor responsiveness in CD19^{low} subsets. **A**, Kinetics of Syk phosphorylation (at Y352) in mem^{intermediate}/DN^{intermediate}, mem^{low}/DN^{low}, and mem^{high}/DN^{high} subsets and plasmablasts (PBs) in 8 healthy donors and 15 SLE patients 0, 5, 8, and 15 minutes after stimulation with antibody to B cell receptor. Data are the mean ± SEM. * = $P \leq 0.05$; ** = $P \leq 0.01$ for comparison between groups at each time point, by Mann-Whitney U test. **B**, Frequencies of Syk expression among mem^{intermediate}/DN^{intermediate}, mem^{low}/DN^{low}, and mem^{high}/DN^{high} subsets for 8 healthy donors and 15 SLE patients. Symbols represent individual subjects; horizontal lines with whiskers represent the mean ± SD. * = $P \leq 0.05$; ** = $P \leq 0.01$; **** = $P \leq 0.0001$, by Kruskal-Wallis test. MFI = median fluorescence intensity; pSyk = phosphorylated Syk (see Figure 1 for other definitions).

of VISTA on mem^{low} B cells (Figure 3F), but findings did not otherwise differ from those for healthy donors. Overall, CD19^{low} B cells showed a strikingly reduced level of checkpoint-molecule expression, which was independent of their level of CD27 expression.

Stability of CD19^{low} subsets in healthy donors over time and correlation with plasmablast frequencies in healthy donors upon vaccination with BNT162b2 or development of acute COVID-19 infection. To investigate the longitudinal stability of these B cell subsets, we used flow cytometry to evaluate them in up to 8 healthy donors over 3 weeks with 6 measurements per time point. No differences in frequencies were detected between different time points (Figure 4A). One donor had slightly increased PB frequencies on day 7 (Figure 4B). This individual was not followed up owing to a

hitherto undiagnosed infection. Because of this single increased value, we saw a correlation between PB and CD19^{low} cell frequencies on day 7, whereas for all other time points no correlation was detected.

To investigate whether an acute immune response resulting in PB formation is accompanied by alteration and expansion of these subsets in individuals without autoimmune disease, we monitored frequencies of these subsets in patients with mild or severe SARS-CoV-2 infection, as well in healthy donors who had received the BNT162b2 messenger RNA (mRNA) COVID-19 vaccine. In patients who had severe COVID-19 and were admitted to the intensive care unit, the mem^{intermediate} cell frequency was less than that in healthy donors and in patients with mild COVID-19, whereas the mem^{low} and PB frequencies were greater. Severe COVID-19 was also associated with a trend

toward increased frequencies of DN^{low} and mem^{high}/DN^{high} B cells, compared with mild COVID-19 and no SARS-CoV-2 infection (Supplementary Figure 4A, available on the *Arthritis & Rheumatology* website at <http://onlinelibrary.wiley.com/doi/10.1002/art.42157>). Only mem^{low}/DN^{low} frequencies correlated with PB frequencies (Supplementary Figure 4B, available at <http://onlinelibrary.wiley.com/doi/10.1002/art.42157>).

Finally, we monitored B cell subsets in healthy donors on days 0, 7, 14, and 21 after receipt of the initial dose of BNT162b2 and 7 days after receipt of the booster dose (Figure 4C). Current studies show that BNT162b2 can generate a strong humoral immune response (22) and specific memory B cells (23) and can also elicit a striking level of T cell-dependent immune activation (24). On day 21 after vaccination, the frequencies of mem^{intermediate} and DN^{intermediate} cells were less than those on day 0 or day 7 (Figure 4C). Follow-up measurements showed that vaccine recipients had more variation in B cell subset frequencies than unvaccinated healthy donors (Figure 4D). A trend toward increased PB formation was detected on day 7 after booster receipt (Figure 4C). Of note, frequencies of mem^{low} B cells correlated with PB frequencies at all time points. DN^{low} B cells also showed a correlation with PBs 7 days after the first dose and especially 7 days after the booster dose (Figures 4D and E). These findings are additional evidence that mem^{low} and DN^{low} expansion follows the kinetics of PB induction and depends on T cell instruction, as was observed in the present study following vaccination with BNT162b2.

B cell receptor responsiveness among CD19^{low} subsets. To evaluate B cell receptor responsiveness among the newly identified subsets as an indication of their functional competence, we studied the phosphorylation kinetics of Syk (Y352) upon stimulation of the subsets with anti-B cell receptor antibody (Figure 5A and Supplementary Figure 5, available on the *Arthritis & Rheumatology* website at <http://onlinelibrary.wiley.com/doi/10.1002/art.42157>). We observed diminished Syk phosphorylation in the double-negative compartment, compared with that in subsets of switched memory B cells. In both switched memory and double-negative B cells, subsets with a low level of CD19 expression showed the lowest kinetics of Syk phosphorylation, whereas CD19^{intermediate} and CD19^{high} subsets responded similarly to B cell receptor stimulation. B cell receptor responsiveness was significantly reduced among mem^{intermediate} and mem^{high} subsets from SLE patients 5–8 minutes after stimulation. While there was an overall lower level of phosphorylation in B cells from SLE patients, the mem^{low} and DN^{low} subsets from SLE patients showed a B cell receptor response similar to that of CD27⁺⁺ CD38⁺⁺ PBs (Figure 5A).

Subsequently, we evaluated whether differences in Syk protein levels at steady state may account for differences among switched memory and double-negative subsets and between SLE patients and healthy donors (Figure 5B). We found that basal Syk levels were highest in mem^{high}/DN^{high} cells for both SLE patients and healthy donors. SLE patients showed significantly

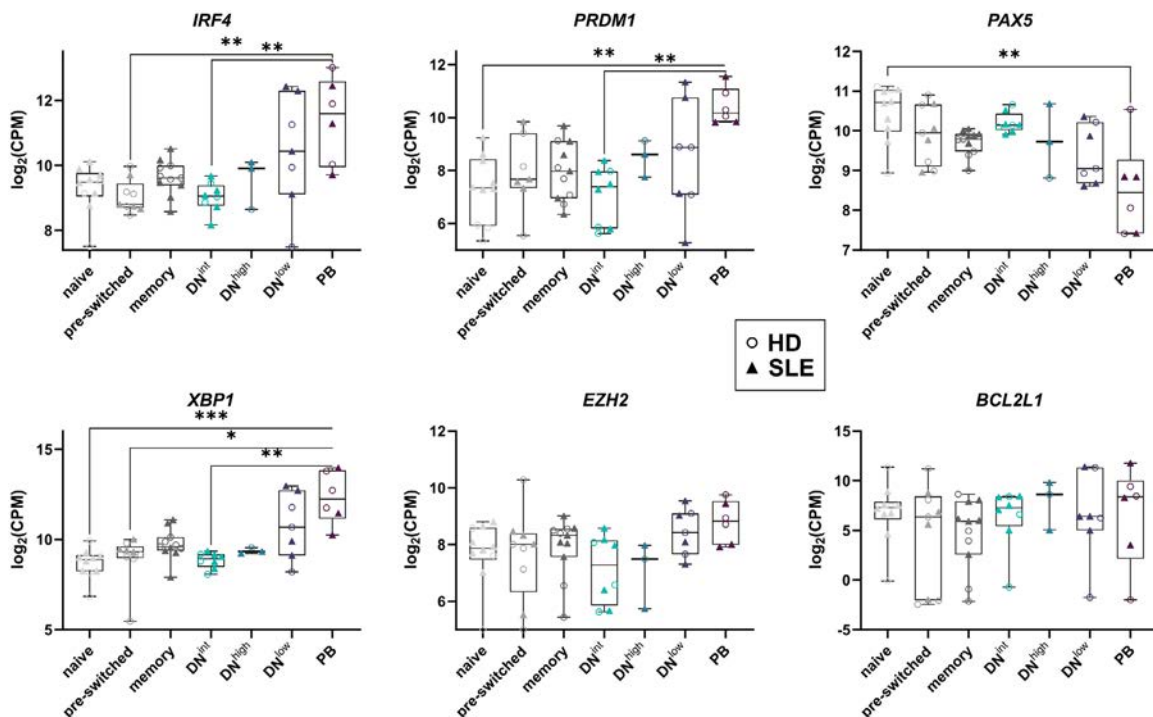


Figure 6. Numbers of *IRF4*, *PRDM1*, *PAX5*, *XBP1*, *EZH2*, and *BCL2L1* transcripts in naive, preswitched, and total memory B cells, plasmablasts (PBs), and double-negative B cell subsets (DN^{intermediate}, DN^{low}, and DN^{high}) in 7 healthy donors (HDs) and 7 patients with systemic lupus erythematosus (SLE). Data are shown as box plots, representing the median, interquartile range, and range. * = $P \leq 0.05$; ** = $P \leq 0.005$; *** = $P \leq 0.0005$, by Kruskal-Wallis test. CPM = counts per million.

decreased Syk levels in mem^{low} B cells, compared with healthy donors. Interestingly, for SLE patients and healthy donors, Syk expression in mem^{low}/DN^{low} subsets was comparable to that in mem^{intermediate}/DN^{intermediate} cells (Figures 5A and B).

PRDM1, XBP1, IRF4, and EZH2 up-regulation in CD19^{low} B cells and PB-like transcription. To further understand the distinct nature of the analyzed B cell subsets, transcriptome analysis was performed on naive, preswitched, total memory (IgD-CD27+), DN^{intermediate}, DN^{high}, and DN^{low} B cells, as well as PBs, in SLE patients and healthy donors (Figure 6). Transcripts of *IRF4*, a transcription factor crucial for differentiation and survival of PBs and plasma cells (25), were up-regulated not only in PBs but also in DN^{low} cells. *IRF4* is known to regulate expression of Blimp-1, a regulator of plasma cell differentiation that is encoded by *PRDM1* (26). Consistent with findings for *IRF4*, the median level of *PRDM1* transcription was increased in DN^{low} cells and PBs. Similarly, the level of *PAX5* mRNA, a transcription factor down-regulated by Blimp-1, was intermediately lower among DN^{low} B cells and PBs, whereas levels of *XBP1* and *EZH2* mRNA were slightly higher. No differences among the B cell subsets and PBs were detected for *BCL2L1* expression, a marker for germinal cell differentiation. Thus, there was an overall trend among key transcription factors in B cells and PBs that indicated that the transcriptional programming in the DN^{low} population is closely related to that of PBs.

DISCUSSION

Here, we identified 2 novel CXCR5-CD19^{low} populations, mem^{low} and DN^{low}, residing among conventional switched and IgD-CD27- atypical memory B cells. Additionally, we found a previously undescribed CXCR5-CD19^{high} population of switched memory B cells that shares characteristics with DN2 B cells, such as CD11c+ expression (11). The DN2 population was found to be increased in patients with autoimmune disease, such as SLE (11), and in individuals with acute SARS-CoV-2 infection (27). It has also been described as giving rise to antibody-secreting PBs upon Toll-like receptor 7 and interleukin-21 extrafollicular activation. We found that this population corresponded to the DN^{high} population, which we further characterized in the present study. The expression profiles of CD19^{high}, CD38-, CD95+, and Ki-67- B cells, together with the high-level response to B cell receptor and increased expression of Syk, also suggest that mem^{high}/DN^{high} cells represent the previously described Syk^{high} population (10).

Overall, CD19^{high} populations seem to have an activated phenotype with a distinct pattern of activation markers and checkpoint molecules. BTLA has an inhibitory effect on the differentiation of naive B cells to PBs in healthy donors, whereas the inhibitory effect is diminished in SLE patients (20). Therefore, it was interesting to find a high level of BTLA expression and a

sufficient level of B cell receptor responsiveness among CD19^{high} cells, although BTLA is known to negatively regulate B cell receptor signaling (28). With regard to VISTA, the general assumption is that it is not expressed on B cells. Therefore, we were surprised to find increased VISTA expression on the CD19^{high} subsets. Its function on B cells remains unknown and, along with confirmation of our findings, needs to be addressed in future studies. The expression and cell-intrinsic function of CTLA-4 on B cells were discussed in a recent review (29). CTLA-4 plays a role in isotype switching (30) and cytokine production (31) in B cells, and its presence reflects an activated state.

While various groups reported an overall reduction of CD19 expression on B cells in SLE, a specific CD19^{low} population has not been characterized so far. In a study of SLE patients by Culton et al (32), the cohort was subdivided into SLE patients with CD19^o cells and those with CD19^{hi} cells, based on global CD19 expression and the presence or lack of a CD19^{hi} B cell population. Autoantibodies were detected in both patient groups. The majority of CD19^o B cells were described as IgD+, CD38+, and CD27-. In other studies, lower CD19 expression levels were observed in CD27- and CD27+ B cells (33,34). These studies did not discriminate populations with respect to IgD expression. Overall, decreased CD19 expression was seen in patients with active SLE (33) and those with quiescent SLE (34) and in patients with antineutrophil cytoplasmic antibody-associated small vessel vasculitis (32), suggesting that variation in CD19 expression is an intrinsic abnormality linked to autoimmunity, rather than an extrinsic abnormality driven by antigen specificity or disease severity.

We found that the CD19^{low} B cell subsets (i.e., mem^{low} and DN^{low}) expressed costimulatory molecule CD86 and proliferation marker CD7, that the majority were CD38+ and CD95+, and that none expressed the early B cell stage markers CD24 and CD10. In combination with surface expression of class-switched IgG and IgA, these findings allowed the conclusion that mem^{low}/DN^{low} B cells were antigen experienced.

Surface expression and secretion of IgA suggest that CD19^{low} subsets might be of mucosal origin. We speculate that CD19^{low} populations with lower or no CD27 expression could be precursors to previously described IgA+ (i.e., CD27^{high}) PBs, which are increased during SLE and enriched for autoreactivity (2). Interestingly, we also found that these cells were enriched during SARS-CoV-2 infection and correlated with PB frequencies in BNT162b2 recipients, which aligns with IgA detection during acute SARS-CoV-2 infection and after vaccination. High anti-SARS-CoV-2 IgA titers were especially common among patients with severe COVID-19 (35), and anti-S2-IgA antibodies were detected in individuals after receipt of their first BNT162b2 dose. In contrast, IgG antibodies were detected after receipt of the second BNT162b2 dose and were generated from the naive B cell pool with specificity for S1 (22).

Although no reductions of baseline Syk levels were observed, phosphorylation kinetics of Syk in DN^{low} cells were

lower than in the other subsets upon anti-B cell receptor stimulation and were similar to the kinetics for PBs. This could have been caused by an anergic postactivation phenotype like the one seen in general naive and memory B cells of patients with autoimmune conditions such as SLE, RA, and primary Sjögren's syndrome (13). An alternative explanation involves down-regulation of the B cell receptor, including B cell receptor-associated surface molecules such as the negative regulator BTLA, which we found to be down-regulated in $\text{mem}^{\text{low}}/\text{DN}^{\text{low}}$ cells. An increased frequency of low BTLA expression among DN^{low} cells during SLE could explain the reduced BTLA expression, as recently reported for the overall double-negative population in SLE patients (20).

Of interest and in alignment with our findings, Ruschil et al (36) recently found that transcripts from the overall double-negative population did not cluster separately from transcripts from other cell populations but instead clustered in a donor-dependent manner with naive B cells, memory B cells, or PBs. Ruschil et al observed a low number of differentially expressed genes in both PBs and the total double-negative B cell population and observed that, upon vaccination against tick-borne encephalitis, the total double-negative population was followed by PBs in contributing to directed maturation trees, based on alignment of clonally related V_H sequences (36). In this context, our study demonstrated that levels of $\text{mem}^{\text{low}}/\text{DN}^{\text{low}}$ populations clearly correlated with levels of PBs in SLE patients and in healthy donors whose immune system was challenged by BNT162b2. In addition, targeted RNA-Seq analysis demonstrated up-regulated PB-like transcriptional programming in DN^{low} cells. Although further studies are needed to evaluate these findings for the mem^{low} population, the current data support that $\text{mem}^{\text{low}}/\text{DN}^{\text{low}}$ cells are a unique subset of B cells with characteristics of PB precursors.

Although it is known that CD27+ memory B cells, as well as certain types of CD27- B cells, have memory B cell characteristics (1,11,15,37), our detection of similar subsets in both the switched memory and double-negative B cell compartments was unexpected. Whereas the double-negative population is known for its heterogeneity and 2 of the 3 subsets shared characteristics with previously described subsets (10,11), not much is known about the diversity of the CD27+ memory compartment beyond its Ig isotype distribution.

The features of the 3 IgD-CD27+ switched memory B cell subsets were comparable to features of the corresponding subsets in the IgD-CD27- atypical memory B cell population. This suggests that the increased level of double-negative B cells during chronic immune disease could also be largely related to the loss of CD27 expression, which is supported by the increased level of soluble CD27 observed in patients with SLE (38). A lack of CXCR5 can result from post-germinal cell, extrafollicular, or activation status, which is also known to be related to CD27 shedding (38).

Until now, it has been assumed that peripheral PBs are marked by a high level of CD27 expression. Here, we showed that a population in which CD27 is present at a low level or even absent not only has a PB-like and antigen-experienced phenotype with regard to surface marker expression but also a transcriptional programming trend toward PBs. We also demonstrated that IgD-CXCR5-CD27+/- cells secreted IgA in vitro. Our data therefore call into question whether CD27 is a reliable marker of memory B cell differentiation and PBs and suggest that these subsets should be evaluated in studies of autoimmunity and infection, to gain a deeper understanding of the B cell response.

B cell-targeted therapeutic interventions for SLE are promising. However, it remains unclear how the heterogeneity of the switched memory and double-negative populations is induced and/or maintained, or how it contributes to the disease course. Using CD19 and CXCR5 clearly not only allows differentiation of switched memory and DN B cells into 3 distinct subsets each, but also suggests that $\text{mem}^{\text{low}}/\text{DN}^{\text{low}}$ are direct precursors of PBs, while $\text{mem}^{\text{intermediate}}$ and $\text{DN}^{\text{intermediate}}$ appear to belong to the classical B memory compartment. With new compounds in the pharmaceutical pipeline that target B cells, it is important to understand the mechanisms that are used by B cell subsets to drive disease and that would require consideration of innovative therapies. Our data suggest that CXCR5- populations might not be targeted by anti-CXCR5 and anti-CD19 strategies but might benefit from anti-CD38 approaches. Belimumab targets early, transitional B cells and partially targets PBs/plasma cells (39), and recent studies demonstrated that use of belimumab to block BAFF/B lymphocyte stimulator had rapid effects on B cell subsets in earlier developmental stages, such as naive B cells. For subsets appearing in the late stage of development, such as memory or plasma cells, levels decreased in a gradual manner later during treatment or did not change. Only early immunologic changes correlated with disease improvement (40). These data, together with those from our study, provide a rationale for strategies that target naive and early B cell stages to prevent not only their differentiation into memory B cells but also their direct differentiation into PBs/plasma cells.

Although not fully understood, it is known that viral infections (such as those due to Epstein-Barr virus and dengue virus) among other factors might trigger autoimmune disease, including SLE (41,42). Recently, investigators found that alterations in the immune response of individuals with severe SARS-CoV-2 infection are similar to those associated with autoimmunity, leading to new insights into immunopathogenesis. For example, COVID-19 and SLE both involve increased induction of extrafollicular $\text{CD19}^{\text{high}}\text{CD11c}^{\text{high}}$ B cells (26,43), as well as changes in the interferon response (44,45) and its regulation (46). Associations between COVID-19 and new-onset autoimmune rheumatic diseases, including SLE, were recently described (47,48). Studying the similar immune phenomena detected in patients

with COVID-19 and those with autoimmune disease can help to improve knowledge about both (49–51). Our finding of increased levels of CD19^{low} subsets and their correlation with PB levels during severe COVID-19 and after receipt of the BNT162b2 vaccine expands our knowledge and is a starting point toward a better understanding of the possible overlap between B cell-dependent immune responses during SARS-CoV-2 infection, after vaccination, and during autoimmune disease. Subsequent investigations should evaluate CD19^{low} B cell subsets during other viral infections, during nonviral infections, and after receipt of other vaccines.

Collectively, the findings presented here, including data on surface marker expression, correlation analysis, Ig secretion, B cell receptor kinetics, and transcription analysis, strongly indicate that mem^{low}/DN^{low} cells are precursors of PBs and directly contribute to plasmacytosis upon immune activation. These mem^{low}/DN^{low} cells reflect a subset of pre-plasma cells that may not need to undergo full or incomplete memory B cell differentiation. Studying the mechanisms by which these cells are selected will be important not only for understanding their immunobiologic features but also for developing potential treatment strategies. In this regard, the current data suggest the potential for selective treatment approaches not only for certain B cell subsets but also for distinct PB/plasma cell compartments, including the possibility of leaving protective PBs/plasma cells untouched.

ACKNOWLEDGMENTS

We thank S. Gaertner, D. Hurd, and M. Rastegar, from HTG Molecular Diagnostics, and J. Kirsch and T. Kaiser, from the Flow Cytometry Core Facility of the Deutsches Rheumaforschungszentrum. Open Access funding enabled and organized by Projekt DEAL.

AUTHOR CONTRIBUTIONS

All authors were involved in drafting the article or revising it critically for important intellectual content, and all authors approved the final version to be published. Dr. Dörner had full access to all of the data in the study and takes responsibility for the integrity of the data and the accuracy of the data analysis.

Study conception and design. Szelinski, Lino, Dörner.

Acquisition of data. Szelinski, Stefanski, Schrezenmeier, Rincon-Arevalo, Wiedemann, Reiter, Ritter, Lettau, Dang, Fuchs, Frei, Alexander, Lino, Dörner.

Analysis and interpretation of data. Szelinski, Lino, Dörner.

ADDITIONAL DISCLOSURES

Authors Fuchs and Frei are employees of F. Hoffmann-La Roche (Roche) AG.

REFERENCES

- Odendahl M, Jacobi A, Hansen A, Feist E, Hiepe F, Burmester GR, et al. Disturbed peripheral B lymphocyte homeostasis in systemic lupus erythematosus. *J Immunol* 2000;165:5970–9.
- Mei HE, Hahne S, Redlin A, Hoyer BF, Wu K, Baganz L, et al. Plasma blasts with a mucosal phenotype contribute to plasmacytosis in systemic lupus erythematosus. *Arthritis Rheumatol* 2017;69:2018–28.
- Wei C, Anolik J, Cappione A, Zheng B, Pugh-Bernard A, Brooks J, et al. A new population of cells lacking expression of CD27 represents a notable component of the B cell memory compartment in systemic lupus erythematosus. *J Immunol* 2007;178:6624–33.
- Souto-Carneiro MM, Mahadevan V, Takada K, Fritsch-Stork R, Nanki T, Brown M, et al. Alterations in peripheral blood memory B cells in patients with active rheumatoid arthritis are dependent on the action of tumour necrosis factor. *Arthritis Res Ther* 2009;11:R84.
- Pararasa C, Zhang N, Tull TJ, Chong MH, Siu JH, Guesdon W, et al. Reduced CD27(-)IgD(-) B cells in blood and raised CD27(-)IgD(-) B cells in gut-associated lymphoid tissue in inflammatory bowel disease. *Front Immunol* 2019;10:361.
- Bulati M, Buffa S, Martorana A, Gervasi F, Camarda C, Azzarello DM, et al. Double negative (IgG+IgD-CD27-) B cells are increased in a cohort of moderate-severe Alzheimer's disease patients and show a pro-inflammatory trafficking receptor phenotype. *J Alzheimers Dis* 2015;44:1241–51.
- Zhu L, Yin Z, Ju B, Zhang J, Wang Y, Lv X, et al. Altered frequencies of memory B cells in new-onset systemic lupus erythematosus patients. *Clin Rheumatol* 2018;37:205–12.
- You X, Zhang R, Shao M, He J, Chen J, Liu J, et al. Double negative B cell is associated with renal impairment in systemic lupus erythematosus and acts as a marker for nephritis remission. *Front Med (Lausanne)* 2020;7:85.
- Rubtsova K, Rubtsov AV, Cancro MP, Marrack P. Age-associated B cells: a T-bet-dependent effector with roles in protective and pathogenic immunity. *J Immunol* 2015;195:1933–7.
- Fleischer SJ, Giesecke C, Mei HE, Lipsky PE, Daridon C, Dörner T. Increased frequency of a unique spleen tyrosine kinase bright memory B cell population in systemic lupus erythematosus. *Arthritis Rheumatol* 2014;66:3424–35.
- Jenks SA, Cashman KS, Zumaquero E, Marigorta UM, Patel AV, Wang X, et al. Distinct effector B cells induced by unregulated toll-like receptor 7 contribute to pathogenic responses in systemic lupus erythematosus. *Immunity* 2018;49:725–39.
- Yoshikawa M, Nakayamada S, Kubo S, Nawata A, Kitanaga Y, Iwata S, et al. Type I and II interferons commit to abnormal expression of chemokine receptor on B cells in patients with systemic lupus erythematosus. *Clin Immunol* 2019;200:1–9.
- Weißenberg SY, Szelinski F, Schrezenmeier E, Stefanski AL, Wiedemann A, Rincon-Arevalo H, et al. Identification and characterization of post-activated B cells in systemic autoimmune diseases. *Front Immunol* 2019;10:2136.
- Petri M, Orbai AM, Alarcon GS, Gordon C, Merrill JT, Fortin PR, et al. Derivation and validation of the Systemic Lupus International Collaborating Clinics classification criteria for systemic lupus erythematosus. *Arthritis Rheum* 2012;64:2677–86.
- Jacobi AM, Reiter K, Mackay M, Aranow C, Hiepe F, Radbruch A, et al. Activated memory B cell subsets correlate with disease activity in systemic lupus erythematosus: delineation by expression of CD27, IgD, and CD95. *Arthritis Rheum* 2008;58:1762–73.
- McInnes L, Healy J, Melville J. UMAP: Uniform Manifold Approximation and Projection for dimension reduction. *arXiv:1802.03426*. 2018. doi: [10.48550/arXiv.1802.03426](https://doi.org/10.48550/arXiv.1802.03426).
- Rincon-Arevalo H, Wiedemann A, Stefanski AL, Lettau M, Szelinski F, Fuchs S, et al. Deep phenotyping of CD11c+ B cells in systemic autoimmunity and controls. *Front Immunol* 2021;12:635615.
- Stefanski AL, Wiedemann A, Reiter K, Hiepe F, Lino AC, Dörner T. Enhanced programmed death 1 and diminished programmed death ligand 1 up-regulation capacity of post-activated lupus B cells. *Arthritis Rheumatol* 2019;71:1539–44.

19. Jackson SM, Harp N, Patel D, Zhang J, Willson S, Kim YJ, et al. CD45RO enriches for activated, highly mutated human germinal center B cells. *Blood* 2007;110:3917–25.
20. Wiedemann A, Lettau M, Weißenberg SY, Stefanski AL, Schrezenmeier EV, Rincon-Arevalo H, et al. BTLA expression and function are impaired on SLE B cells. *Front Immunol* 2021;12:667991.
21. Murphy KA, Bhamidipati K, Rubin SJ, Kipp L, Robinson WH, Lanz TV. Immunomodulatory receptors are differentially expressed in B and T cell subsets relevant to autoimmune disease. *Clin Immunol* 2019;209:108276.
22. Brewer RC, Ramadoss NS, Lahey LJ, Jahanbani S, Robinson WH, Lanz TV. BNT162b2 vaccine induces divergent B cell responses to SARS-CoV-2 S1 and S2. *Nat Immunol* 2022;23:33–9.
23. Turner JS, O'Halloran JA, Kalaidina E, Kim W, Schmitz AJ, Zhou JQ, et al. SARS-CoV-2 mRNA vaccines induce persistent human germinal centre responses. *Nature* 2021;596:109–13.
24. Sahin U, Muik A, Derhovanessian E, Vogler I, Kranz LM, Vormehr M, et al. COVID-19 vaccine BNT162b1 elicits human antibody and TH1 T cell responses. *Nature* 2020;586:594–9.
25. Tellier J, Shi W, Minnich M, Liao Y, Crawford S, Smyth GK, et al. Blimp-1 controls plasma cell function through the regulation of immunoglobulin secretion and the unfolded protein response. *Nat Immunol* 2016;17:323–30.
26. Low MS, Brodie EJ, Fedele PL, Liao Y, Grigoriadis G, Strasser A, et al. IRF4 activity is required in established plasma cells to regulate gene transcription and mitochondrial homeostasis. *Cell Rep* 2019;29:2634–45.
27. Woodruff MC, Ramonell RP, Nguyen DC, Cashman KS, Saini AS, Haddad NS, et al. Extrafollicular B cell responses correlate with neutralizing antibodies and morbidity in COVID-19. *Nat Immunol* 2020;21:1506–16.
28. Vendel AC, Calemine-Fenaux J, Izrael-Tomasevic A, Chauhan V, Arnott D, Eaton DL. B and T lymphocyte attenuator regulates B cell receptor signaling by targeting Syk and BLNK. *J Immunol* 2009;182:1509–17.
29. Oyewole-Said D, Konduri V, Vazquez-Perez J, Weldon SA, Levitt JM, Decker WK. Beyond T-cells: functional characterization of CTLA-4 expression in immune and non-immune cell types. *Front Immunol* 2020;11:608024.
30. Pioli C, Gatta L, Ubaldi V, Doria G. Inhibition of IgG1 and IgE production by stimulation of the B cell CTLA-4 receptor. *J Immunol* 2000;165:5530–6.
31. Merlo A, Tenca C, Fais F, Battini L, Ciccone E, Grossi CE, et al. Inhibitory receptors CD85j, LAIR-1, and CD152 down-regulate immunoglobulin and cytokine production by human B lymphocytes. *Clin Diagn Lab Immunol* 2005;12:705–12.
32. Culton DA, Nicholas MW, Bunch DO, Zhen QL, Kepler TB, Dooley MA, et al. Similar CD19 dysregulation in two autoantibody-associated autoimmune diseases suggests a shared mechanism of B-cell tolerance loss. *J Clin Immunol* 2007;27:53–68.
33. Sato S, Hasegawa M, Fujimoto M, Tedder TF, Takehara K. Quantitative genetic variation in CD19 expression correlates with autoimmunity. *J Immunol* 2000;165:6635–43.
34. Korganow AS, Knapp AM, Nehme-Schuster H, Soulas-Sprauel P, Poindron V, Pasquali JL, et al. Peripheral B cell abnormalities in patients with systemic lupus erythematosus in quiescent phase: decreased memory B cells and membrane CD19 expression. *J Autoimmun* 2010;34:426–34.
35. Cervia C, Nilsson J, Zurbuchen Y, Valaperti A, Schreiner J, Wolfensberger A, et al. Systemic and mucosal antibody responses specific to SARS-CoV-2 during mild versus severe COVID-19. *J Allergy Clin Immunol* 2021;147:545–57.
36. Ruschil C, Gabernet G, Lepennetier G, Heumos S, Kaminski M, Hracsko Z, et al. Specific induction of double negative B cells during protective and pathogenic immune responses. *Front Immunol* 2020;11:606338.
37. Sanz I, Wei C, Jenks SA, Cashman KS, Tipton C, Woodruff MC, et al. Challenges and opportunities for consistent classification of human B cell and plasma cell populations. *Front Immunol* 2019;10:2458.
38. Font J, Pallares L, Martorell J, Martinez E, Gaya A, Vives J, et al. Elevated soluble CD27 levels in serum of patients with systemic lupus erythematosus. *Clin Immunol Immunopathol* 1996;81:239–43.
39. Benitez A, Torralba K, Ngo M, Salto LM, Choi KS, De Vera ME, et al. Belimumab alters transitional B-cell subset proportions in patients with stable systemic lupus erythematosus. *Lupus* 2019;28:1337–43.
40. Ramsköld D, Parodis I, Lakshmikanth T, Sippl N, Khademi M, Chen Y, et al. B cell alterations during BAFF inhibition with belimumab in SLE. *EBioMedicine* 2019;40:517–27.
41. Draborg AH, Jørgensen JM, Müller H, Nielsen CT, Jacobsen S, Iversen LV, et al. Epstein-Barr virus early antigen diffuse (EBV-EA/D)-directed immunoglobulin A antibodies in systemic lupus erythematosus patients. *Scand J Rheumatol* 2012;41:280–9.
42. Chen YW, Hsieh TY, Lin CH, Chen HM, Lin CC, Chen HH. Association between a history of dengue fever and the risk of systemic autoimmune rheumatic diseases: a nationwide, population-based case-control study. *Front Med (Lausanne)* 2021;8:738291.
43. Jenks SA, Wei C, Bugrovsky R, Hill A, Wang X, Rossi FM, et al. B cell subset composition segments clinically and serologically distinct groups in chronic cutaneous lupus erythematosus. *Ann Rheum Dis* 2021;80:1190–200.
44. Rincon-Arevalo H, Aue A, Ritter J, Szelinski F, Khadzhynov D, Zickler D, et al. Altered increase in STAT1 expression and phosphorylation in severe COVID-19. *Eur J Immunol* 2022;52:138–48.
45. Doehn JM, Tabeling C, Biesen R, Saccomanno J, Madlung E, Pape E, et al. CD169/SIGLEC1 is expressed on circulating monocytes in COVID-19 and expression levels are associated with disease severity. *Infection* 2021;49:757–62.
46. Bastard P, Rosen LB, Zhang Q, Michailidis E, Hoffmann HH, Zhang Y, et al. Autoantibodies against type I IFNs in patients with life-threatening COVID-19. *Science* 2020;370:eabd4585.
47. Gracia-Ramos AE, Saavedra-Salinas MÁ. Can the SARS-CoV-2 infection trigger systemic lupus erythematosus? A case-based review. *Rheumatol Int* 2021;41:799–809.
48. Moody R, Wilson K, Flanagan KL, Jaworowski A, Plebanski M. Adaptive immunity and the risk of autoreactivity in COVID-19. *Int J Mol Sci* 2021;22:8965.
49. Schultheiß C, Paschold L, Willscher E, Simnica D, Wöstemeyer A, Muscate F, et al. Maturation trajectories and transcriptional landscape of plasmablasts and autoreactive B cells in COVID-19. *iScience* 2021;24:103325.
50. Buszko M, Nita-Lazar A, Park JH, Schwartzberg PL, Verthelyi D, Young HA, et al. Lessons learned: new insights on the role of cytokines in COVID-19. *Nat Immunol* 2021;22:404–11.
51. Mohkhedkar M, Venigalla SS, Janakiraman V. Untangling COVID-19 and autoimmunity: identification of plausible targets suggests multi organ involvement. *Mol Immunol* 2021;137:105–13.

Symptom-Based Cluster Analysis Categorizes Sjögren's Disease Subtypes: An International Cohort Study Highlighting Disease Severity and Treatment Discordance

Sara S. McCoy,¹ Miguel Woodham,¹ Christie M. Bartels,¹ Ian J. Saldanha,² Vatinee Y. Bunya,³ Noah Maerz,¹ Esen K. Akpek,⁴ Matthew A. Makara,⁵ and Alan N. Baer⁴

Objective. Although symptom relief is a critical aspect for successful drug development in Sjögren's disease, patient experiences with Sjögren's-related symptoms are understudied. Our objective was to determine how pain, dryness, and fatigue, the cardinal symptoms of Sjögren's disease, drive cluster phenotypes.

Methods. We used data from the Sjögren's International Collaborative Clinical Alliance (SICCA) Registry and a Sjögren's Foundation survey. We performed hierarchical clustering of symptoms by levels of dryness, fatigue, and pain. Using international and US cohorts, we performed multiple logistic regression analysis to compare the clusters, which included comparisons of differences in symptoms, quality of life (QoL), medication use, and systemic manifestations.

Results. Four similar clusters were identified among 1,454 SICCA registrants and 2,920 Sjögren's Foundation survey participants: 1) low symptom burden in all categories (LSB); 2) dry with low pain and low fatigue (DLP); 3) dry with high pain and low to moderate fatigue (DHP); and 4) high symptom burden in all categories (HSB). Distribution of SICCA registrants matching the symptom profile for each cluster was 10% in the LSB cluster, 30% in the DLP cluster, 23% in the DHP cluster, and 37% in the HSB cluster. Distribution of survey participants matching the symptom profile for each cluster was 23% in the LSB cluster, 14% in the DLP cluster, 21% in the DHP cluster, and 42% in the HSB cluster. Individuals in the HSB cluster had more total symptoms and lower QoL but lower disease severity than those in the other clusters. Despite having milder disease as measured by laboratory tests and organ involvement, individuals in the HSB cluster received immunomodulatory treatment most often.

Conclusion. We identified 4 symptom-based Sjögren's clusters and showed that symptom burden and immunomodulatory medication use do not correlate with Sjögren's end-organ or laboratory abnormalities. Findings highlight a discordance between objective measures and treatments and offer updates to proposed symptom-based clustering approaches.

INTRODUCTION

Sjögren's disease, a systemic autoimmune disease, is associated with increased health care costs, increased morbidity, and reduced quality of life (QoL) compared with these measures in

people without the disease (1). Sjögren's disease has a heterogeneous phenotype ranging from isolated dryness to life-threatening systemic organ involvement. The heterogeneity of Sjögren's disease creates unique experiences for each patient and complicates the choice of effective treatment. For example, depression

The content is solely the responsibility of the authors and does not necessarily represent the official views of the NIH. The data reported herein have been supplied by the Sjögren's International Collaborative Clinical Alliance (SICCA) Biorepository by the National Institute of Dental and Craniofacial Research (contract HHSN26S201300057C). The interpretation and reporting of these data are the responsibility of the authors and in no way should be seen as an official policy or interpretation of the SICCA investigators or the National Institute of Dental and Craniofacial Research. Dr. McCoy's work was supported by the Clinical and Translational Science Award program and by NIH grants UL1-TR-002373 and KL2-TR-002374 from the National Center for Advancing Translational Sciences and R03DE031340 from the National Institute of Dental and Craniofacial Research. Dr. Bunya's work was supported by NIH grant R01-EY-026972 from the National Eye Institute. Mr. Makara's work was supported by the Sjögren's Foundation. Dr. Baer's work was supported by NIH contract 75N92019P00427 from the National Institute of Dental and Craniofacial Research and the Jerome L. Greene Foundation.

¹Sara S. McCoy, MD, PhD, Miguel Woodham, MD, Christie M. Bartels, MD, MS, Noah Maerz, MD: University of Wisconsin, Madison, Wisconsin; ²Ian J. Saldanha, MBBS, MPH, PhD: Brown University, Providence, Rhode Island; ³Vatinee Y. Bunya, MD, MSCE: University of Pennsylvania, Philadelphia; ⁴Esen K. Akpek, MD, Alan N. Baer, MD: Johns Hopkins University, Baltimore, Maryland; ⁵Matthew A. Makara, MPH: Sjögren's Foundation, Reston, Virginia.

Author disclosures are available at <https://onlinelibrary.wiley.com/action/downloadSupplement?doi=10.1002%2Fart.42238&file=art42238-sup-0001-Disclaimerform.pdf>.

Address correspondence to Sara S. McCoy, MD, PhD, University of Wisconsin, School of Medicine and Public Health, 1685 Highland Avenue, Madison, WI 53705-2281. Email: ssmccoy@medicine.wisc.edu.

Submitted for publication January 19, 2022; accepted in revised form May 12, 2022.

and fatigue are common debilitating symptoms that reduce QoL, yet these symptoms do not respond to traditional immunosuppression (1,2). Additionally, Sjögren's symptoms do not always parallel clinical signs. For example, symptoms of dryness do not necessarily correlate with objective tear or salivary flow measurements (3). In other autoimmune diseases, such as systemic lupus erythematosus, discordance between the severity of symptoms reported by the patient and physician assessment of disease severity has been posited to reduce patient satisfaction (1,4,5). These issues have made the identification of effective therapies in clinical trials challenging. Emphasis has therefore shifted toward Sjögren's treatments that are tailored to specific relevant subsets of patients (6). A critical first step of tailored therapy is to define symptom-based patient clusters.

Recently, a UK-based study used symptoms of pain, dryness, fatigue, anxiety, and depression to generate patient clusters. In their analyses of 608 patients with Sjögren's disease from the UK Primary Sjögren's Syndrome Registry, Tam and colleagues defined 4 symptom-based clusters with unique European League of Associations for Rheumatology (EULAR) Sjögren's Syndrome Disease Activity Index and laboratory profiles (7). Their findings were validated in 2 other European populations: the French Assessment of Systemic Signs and Evolution of Sjögren's Syndrome cohort and the Norwegian Stavanger cohort. Notably, however, 2 of the 5 symptoms included to generate clusters, anxiety and depression, are not cardinal symptoms in Sjögren's disease. In their retrospective analyses of outcomes of the JOQUER trial with hydroxychloroquine and the TRACTISS trial with rituximab, Tam et al found considerably different responses to these therapies by cluster (8,9). The cardinal symptoms caused by Sjögren's disease, however, are dryness, pain, and fatigue, regardless of anxiety and depression presence in a subgroup, which suggests the need for a more disease-focused approach to clustering.

Our objective was to leverage a large international population to determine the clusters of Sjögren's disease based on the cardinal symptoms of dryness, pain, and fatigue. We compared differences in symptoms, QoL, medication use, and disease-specific systemic manifestations between the symptom-based clusters. We aimed to advance the understanding of unique Sjögren's disease phenotypes to 1) enhance mechanistic understanding of the pathogenesis driving distinct Sjögren's disease phenotypes, 2) improve symptom management through tailored therapy, 3) inform the identification of subgroups for clinical trial analyses, and 4) eventually, harmonize patient-provider expectations.

PATIENTS AND METHODS

We obtained data for this analysis from 2 sources: 1) the Sjögren's International Collaborative Clinical Alliance (SICCA) Registry, and 2) a Sjögren's Foundation survey.

SICCA Registry. The SICCA Registry is a National Institutes of Health-funded registry of individuals with suspected or known Sjögren's disease from 9 international research institutions from 2003 to 2012 (10). Participants who were age 21 years or older were enrolled in the registry if they had any of the following: repeated finding of tooth decay or cavities without other risk factors, a known diagnosis of Sjögren's disease, salivary gland enlargement, or abnormal findings on serology (anti-SSA antibody or anti-SSB antibody, antinuclear antibody, or rheumatoid factor [RF]). All registrants completed a standardized visit composed of an interview and questionnaires, physical examination, blood, tear and saliva collections, and labial salivary gland biopsy. Further registry details and enrollment procedures are described on the SICCA web page at <https://sicca-online.ucsf.edu> and in prior publications (11–13). Sjögren's disease was defined by the 2016 American College of Rheumatology (ACR)/EULAR criteria (14).

Data obtained from the SICCA Registry included depression severity, measured with the Patient Health Questionnaire 9 (PHQ-9; scored 0–27, with higher scores indicating greater severity), and health-related QoL, measured with the Short Form 12 (SF-12; with lower scores indicating greater severity) (15). The SF-12 is divided into mental and physical components. The mental component (scored 0–100) focuses on depression, anxiety, accomplishments, socialization, and carelessness. The physical component (scored 0–100) focuses on work limitations due to pain, work limitations due to physical issues, and limitations in climbing stairs. Of the 12 total questions in the SF-12 health survey, 5 relate to mental health, 6 relate to physical health, and 1 relates to both.

Sjögren's Foundation survey. The content of the Sjögren's Foundation survey was developed in 2016 as a collaborative effort with the Harris Poll, a social science market research company, the Sjögren's Foundation, Sjögren's disease providers and experts, and patients with Sjögren's disease (16,17). A total of 2,961 adults who self-reported as having Sjögren's disease based on a physician's diagnosis completed the survey. The survey provided documentation of comprehensive details on the subjective experiences of patients with Sjögren's disease, which enriched our understanding of patient experiences within each cluster.

The survey contained 7 sections: 1) "patient profile" (Sjögren's diagnosis, general health, and past medical histories); 2) "severity" (frequency and impact of symptoms); 3) "emotional and physical well-being" (effects of Sjögren's disease on daily emotional and physical experiences); 4) "effect on quality of life" (the effect of Sjögren's disease on QoL); 5) "treatment" (treatments or medications for Sjögren's disease); 6) "cost of disease" (costs and effects on career as a result of Sjögren's disease); and 7) "background information" (sociodemographic characteristics). Respondents recorded 40 symptoms by frequency of experience

from never to daily. Bivariate comparisons considered each symptom present if the respondent indicated that it occurred at least weekly.

Symptom-based cluster generation and statistical analysis. We generated separate symptom-based clusters for each of the 2 samples. To generate hierarchical clusters in the SICCA Registry sample, we examined self-reported 1) dryness using a weighted composite score of responses to 5 questions, 2) pain on a 5-point Likert scale from “not at all” to “extremely,” and 3) fatigue on a 4-point Likert scale from “not at all” to “nearly every day” (18).

Because we did not have a validated marker for dryness severity, we measured the burden of dryness with a dryness composite score based on 5 questions: 1) “do your eyes feel dry?” (yes or no), 2) “how often do you use artificial tears?” (≤3 times/day or >3 times/day), 3) “during the last week have you experienced any of the following symptoms with your eyes: gritty or scratchy sensation?” (5-point Likert scale from none of the time

to all the time), 4) “does your mouth feel dry?” (yes or no), and 5) “do you need to sip liquids to swallow dry foods?” (yes or no). Questions 2, 3, and 5 had been previously validated in a study that established the ability of these questions to correctly classify patients with Sjögren’s disease versus controls and have been included in the 2002 (subjective components) and 2016 classification criteria for Sjögren’s disease (entry criteria) (14,18,19). The other 2 questions (questions 1 and 4) are similar to other questions in the previously validated criteria but did not include the time elements (e.g., for >3 months). To ensure equal weight for all questions, we multiplied all the binary questions by 100 and the 5-point Likert scale by 20. We then divided the sum by the number of completed questions to yield a final dryness composite score on a scale of 0–100.

Fatigue was evaluated with the following question: “Over the last two weeks how often have you felt bothered by the following problem: feeling tired or having little energy?” Pain was evaluated with the following question: “How much did pain interfere with

Table 1. Baseline demographic characteristics of patients with Sjögren’s disease in the SICCA Registry, in total and according to symptom-based clusters*

	All (n = 1,454)	LSB (n = 146)	DLP (n = 432)	DHP (n = 336)	HSB (n = 540)	Adjusted P†
Age, mean ± SD years	52 (13)	47 (15)	54 (13)	54 (14)	52 (13)	<0.0001
Female patient	1,368 (94)	133 (91)	400 (93)	314 (93)	521 (96)	0.02
Race						<0.0001
White	726 (50)	38 (26)	208 (48)	163 (49)	317 (59)	
Asian	515 (35)	90 (62)	170 (39)	131 (39)	124 (23)	
Other‡	212 (15)	18 (12)	54 (13)	42 (13)	99 (18)	
Hispanic ethnicity	170 (12)	14 (10)	50 (12)	35 (10)	71 (13)	0.51
Education						0.03
Primary	178 (12)	14 (10)	59 (14)	49 (15)	56 (10)	
High school	409 (28)	49 (34)	116 (27)	105 (31)	139 (26)	
College/university	857 (59)	82 (56)	256 (59)	179 (53)	340 (63)	
None	10 (1)	1 (1)	1 (0)	3 (1)	5 (1)	
Employment						<0.0001
Full-time	533 (37)	70 (48)	186 (43)	100 (30)	177 (33)	
Part-time	200 (14)	11 (8)	62 (14)	46 (14)	81 (15)	
Homemaker	193 (13)	21 (14)	50 (12)	49 (15)	73 (14)	
Retired	318 (22)	29 (20)	107 (25)	98 (29)	84 (16)	
Student	23 (2)	4 (3)	7 (2)	3 (1)	9 (2)	
Not working	186 (13)	11 (8)	20 (5)	40 (12)	115 (21)	
Tobacco use						
Current	76 (5)	10 (7)	12 (3)	21 (6)	33 (6)	0.04
Ever	435 (32)	33 (23)	127 (29)	99 (29)	176 (33)	0.1
Recruitment site						<0.0001
JHU	119 (8)	9 (6)	26 (6)	21 (6)	63 (12)	
UPenn	98 (7)	6 (4)	18 (4)	18 (5)	56 (10)	
UCSF	283 (20)	7 (5)	77 (18)	67 (20)	132 (24)	
Argentina	165 (11)	15 (10)	50 (12)	34 (10)	66 (12)	
China	239 (16)	60 (41)	75 (17)	68 (20)	36 (7)	
Denmark	202 (14)	14 (10)	67 (16)	51 (15)	70 (13)	
Japan	205 (14)	22 (15)	77 (18)	46 (14)	60 (11)	
UK	143 (10)	13 (9)	42 (10)	31 (9)	57 (11)	

* Except where indicated otherwise, values are the number (%) of Sjögren’s International Collaborative Clinical Alliance (SICCA) Registry patients. Missing data were as follows: race and ethnicity (n = 1 each), employment (n = 1), and tobacco use ever (n = 76). LSB = low symptom burden; DLP = dry, low pain; DHP = dry, high pain; HSB = high symptom burden; JHU = Johns Hopkins University; UPenn = University of Pennsylvania; UCSF = University of California, San Francisco.

† Adjusted for age, sex, race, and disability.

‡ Other race indicates all non-White and non-Asian races.

your normal work?” We stratified clusters by levels of dryness, pain, and fatigue but not by anxiety and depression as previously reported (7). Dryness, pain, and fatigue are the main symptoms experienced by patients with Sjögren’s disease as identified from patient interviews and the Profile of Fatigue and Discomfort–Sicca Symptoms Inventory (20,21).

Among Sjögren’s Foundation survey participants, we excluded participants for whom age and biologic sex were not reported. We performed unsupervised hierarchical clustering of symptoms with Ward’s minimum variance method (22) to a priori identify 4 clusters to assess phenotypic similarity to the analogous 4 groups studied by Tarn et al based on self-reported severity of pain (visual analog scale [VAS] 0–10), fatigue (VAS 0–10), and dryness (VAS 0–10).

We compared descriptive statistics for demographic features, symptom frequency, QoL, medication use, systemic manifestations, laboratory values, and histopathologic assessment of the labial salivary glands among the 4 symptom-based clusters. We used one-way analysis of variance or chi-square tests to conduct hypothesis testing for differences between clusters. We used multiple logistic regression for analyses of categorical variables and linear regression for analyses of continuous variables,

controlling for age, sex, race, ethnicity, education, and recruitment site for the SICCA Registry sample and age, sex, race, and disability for the Sjögren’s Foundation survey sample. Statistical analyses were performed using JMP Pro statistical software, version 15.

RESULTS

SICCA cluster analysis. We identified 1,541 adults fulfilling the 2016 ACR/EULAR criteria for Sjögren’s disease within the SICCA Registry. Three were excluded for missing data on age or sex, and 84 were excluded for missing data on clustering criteria. We thus included 1,454 adults from the SICCA Registry in the cluster analysis.

The 1,454 individuals in the SICCA Registry sample with complete data on the 3 cardinal symptoms had a mean age of 52 years, were predominantly women (94%), and were mostly White (50%), followed by Asian (35%) and other races (15%) (Table 1). The analysis yielded 4 clusters (Figure 1A). Clusters were characterized by low symptom frequency/severity burden of dryness and fatigue with rare pain (LSB; 10% prevalence), dry with low pain and low fatigue (dry low pain [DLP]; 30%), dry with low pain and low fatigue (dry high pain [DHP]; 30%), dry with

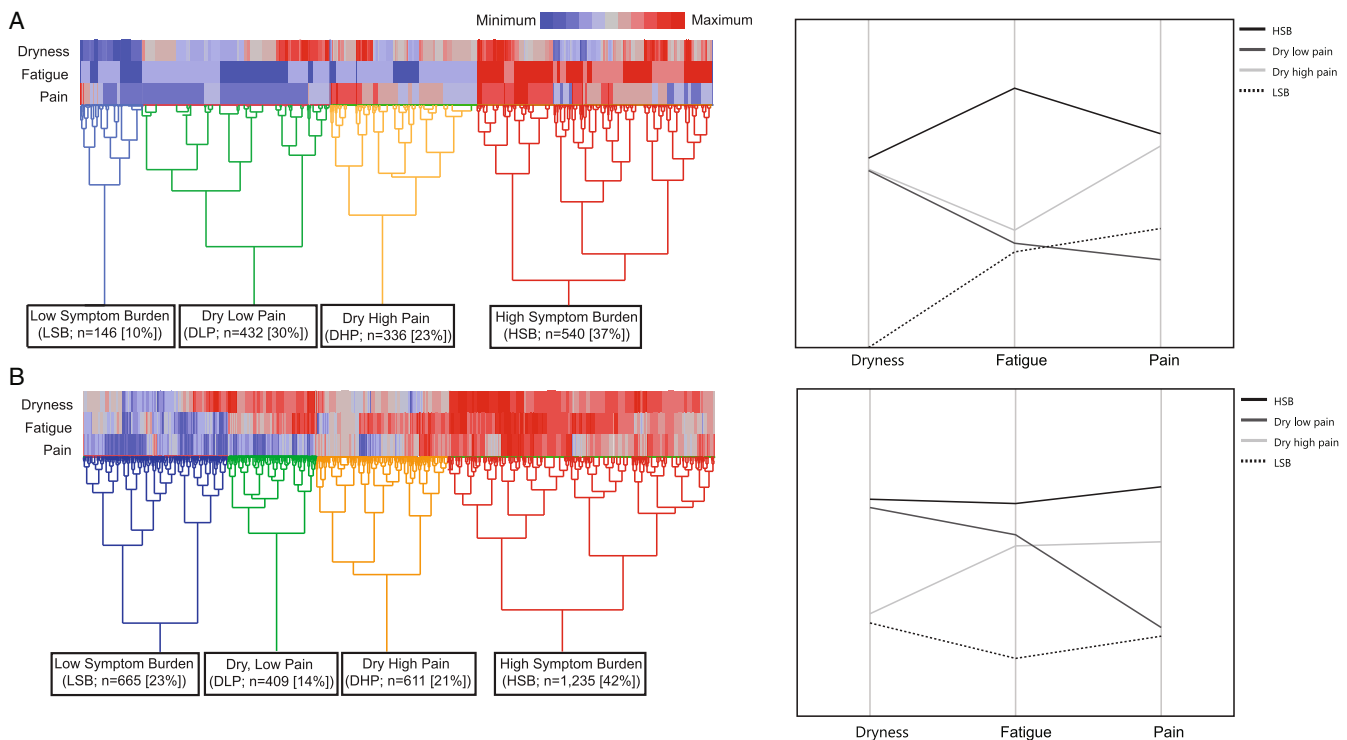


Figure 1. Heatmaps showing hierarchical clustering of Sjögren’s disease symptoms according to severity level. **A**, Sjögren’s International Collaborative Clinical Alliance Registry sample clusters generated by unsupervised hierarchical clustering based on evaluation of the following symptoms: oral and ocular dryness according to a weighted composite score of 5 items (presence of dry mouth, need sips of liquid to swallow food, presence of dry eye, presence of a gritty sensation in the eyes, and use of tear substitutes), fatigue (on a 4-point Likert scale), and pain (on a 5-point Likert scale). **B**, Sjögren’s Foundation sample clusters generated by unsupervised hierarchical clustering based on evaluation of the following symptoms: oral and ocular dryness (on a 0–10-mm visual analog scale [VAS]), fatigue (on a 0–10-mm VAS), and pain (on a 0–10-mm VAS).

high pain and low to moderate fatigue (dry high pain [DHP]; 23%), and high symptom frequency/severity burden in all categories (HSB; 37%).

Symptoms differed significantly among the symptom-based clusters in the SICCA Registry. For example, dry mouth ("does your mouth feel dry?") occurred in 96–99% of patients in the HSB, DLP, and DHP clusters but in only 35% of the patients in the LSB cluster ($P < 0.0001$). A similar pattern was shown for dry eye, which occurred in 87–94% of patients in the DLP, DHP, and HSB clusters but in only 21% of patients in the LSB cluster ($P < 0.0001$). There was an overarching pattern that non-sicca-related symptoms predominated in the HSB cluster, followed by the DHP, DLP, and LSB clusters (Supplementary Table A, available on the *Arthritis & Rheumatology* website at <https://onlinelibrary.wiley.com/doi/10.1002/art.42238>).

The score for depression symptoms, as measured by the PHQ-9, was higher (i.e., worse) in the HSB cluster (mean score 11.3) than in the DHP cluster (mean score 4.5), DLP cluster (mean score 2.9), and LSB cluster (mean score 2.2) (each $P < 0.0001$) (Figure 2A). Health-related QoL, as measured by the SF-12, also differed between the clusters (Figure 2A). The score for the physical components was lower (i.e., worse) in the HSB cluster (mean SF-12 physical component summary score 36) than in the DHP, DLP, and LSB clusters (mean scores of 41, 53, and 51, respectively) ($P < 0.0001$). The score for the mental components was also lower (i.e., worse) in the HSB cluster (mean SF-12 mental component summary score 39) than in the DHP, DLP, and

LSB clusters (mean scores of 44, 44, and 46, respectively) ($P < 0.0001$).

Generally, patients in the HSB cluster more frequently took treatments such as cholinomimetics (14%), nonsteroidal anti-inflammatory drugs (NSAIDs) (28%), and biologics (5%) than patients in the other clusters. When we compared the clusters, steroids (20%) and other disease-modifying antirheumatic drugs (DMARDs) (6%) were the predominant treatment used by patients in the DHP cluster, and antimetabolites were the predominant treatment used by patients in the DHP and LSB clusters (each 10%) (Figure 2B).

Results from objective measurements of sicca symptoms in the mouth and eyes also differed between clusters in the SICCA Registry (Figure 3A). The unstimulated salivary flow was abnormal (≤ 5 ml/5 minutes) in 74% of the DLP cluster, in 70% of the HSB cluster, in 68% of the DHP cluster, and in 37% of the LSB cluster. The ocular surface staining score was abnormal (score ≥ 5) in 88% of the DLP cluster, whereas it was abnormal in only 74% of the HSB, 78% of the DHP, and 69% of the LSB clusters ($P < 0.0001$). Findings from the Schirmer's test (measured in mm/5 minutes) followed a similar pattern, in which patients in the DLP cluster had the greatest degree of sicca on objective ocular testing. Of 13 organ manifestations, 2 differed significantly between clusters, synovitis (which included metacarpophalangeal, wrist, or elbow synovitis) and primary biliary cholangitis (PBC), which were most common in the DHP cluster (11%) and DLP cluster (3%), respectively (Figure 3A).

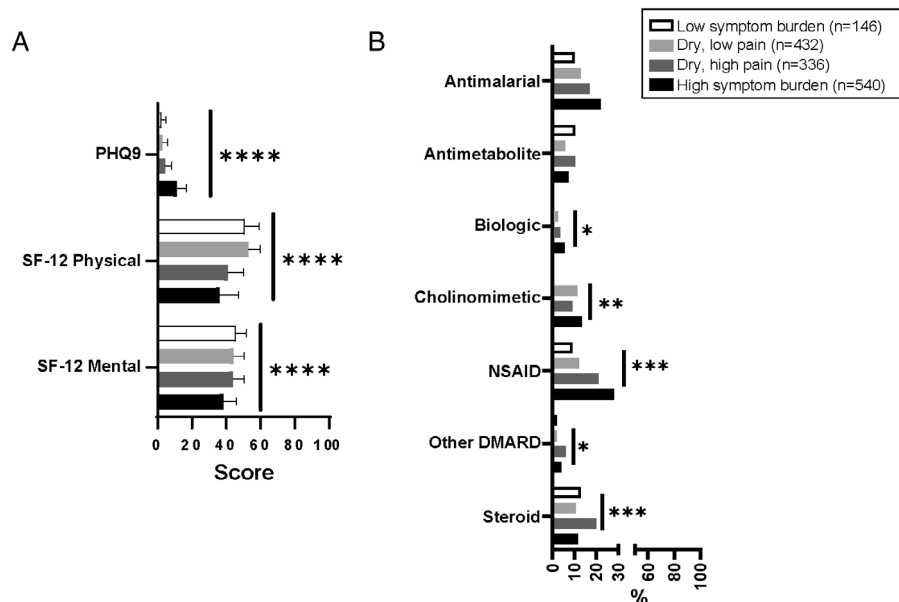


Figure 2. Depression, quality of life, and medication use in patients from the Sjögren's International Collaborative Clinical Alliance Registry ($n = 1,454$) categorized according to Sjögren's disease symptom-based clusters. **A**, Depression, measured by the Patient Health Questionnaire 9 (PHQ-9), and health-related quality of life, measured by the physical and mental components of the Short Form 12 (SF-12). Bars show the mean. **B**, Frequency of medication use. * = $P \leq 0.05$; ** = $P \leq 0.01$; *** = $P \leq 0.001$, by one-way analysis of variance or chi-square test. Biologic = tumor necrosis factor inhibitor or anti-CD20 antibody; NSAID = nonsteroidal antiinflammatory drug; DMARD = disease-modifying antirheumatic drug.

Despite the fact that $\geq 73\%$ of patients were positive for SSA antibodies in all 4 clusters, laboratory evaluations notably showed significantly different frequencies of combined anti-SSA and anti-SSB antibody presence (Figure 3A) and levels of platelets and white blood cells (Figure 3B). The DLP cluster had the lowest level of platelets (mean 227.3×10^3 cells/microliter), and the LSB and DLP clusters had the lowest level of white blood cells (mean 5.1×10^3 cells/microliter in both). The LSB and DLP clusters had higher levels of IgG than the HSB and DHP clusters (Figure 3C). The DLP cluster had the highest predominance of RF positivity (68%) compared with the LSB cluster (55%), the DHP cluster (59%), and the HSB cluster (53%) ($P < 0.0001$) (Supplementary Table B, available at <https://onlinelibrary.wiley.com/doi/10.1002/art.42238>). The DLP cluster had the highest focus score of mononuclear cell infiltrates in the labial salivary glands (mean score 3.4) ($P < 0.0001$) versus the other clusters (Figure 3D). Other laboratory findings, including levels of hemoglobin, lymphocytes, and IgM, did not differ among clusters (Supplementary Table B).

Sjögren's Foundation cluster analysis. Of the 3,072 respondents who completed the Sjögren's Foundation survey, 111 participants were excluded for being younger than age 18 years ($n = 41$), lack of a diagnosis of Sjögren's disease from a health care professional ($n = 68$), or incomplete survey demographics ($n = 2$). A further 41 participants were excluded from hierarchical cluster analysis due to missing item responses needed to generate the clusters (e.g., dryness, pain, or fatigue metrics). We thus included 2,920 participants in the Sjögren's Foundation cohort analysis.

Most of the 2,920 participants were White (93%) and women (96%), and the mean age at the time of the survey was 65 years. Distribution of Sjögren's Foundation survey participants in the 4 identified symptom-based clusters was as follows: 23% in the LSB cluster, 14% in the DLP cluster, 21% in the DHP cluster, and 42% in the HSB cluster. Age at diagnosis, sex, and race were similar among the 4 clusters, but statistically these values differed (Table 2).

In the Sjögren's Foundation sample, members of each cluster experienced their Sjögren's disease differently. As expected, the LSB cluster experienced the lowest frequency of

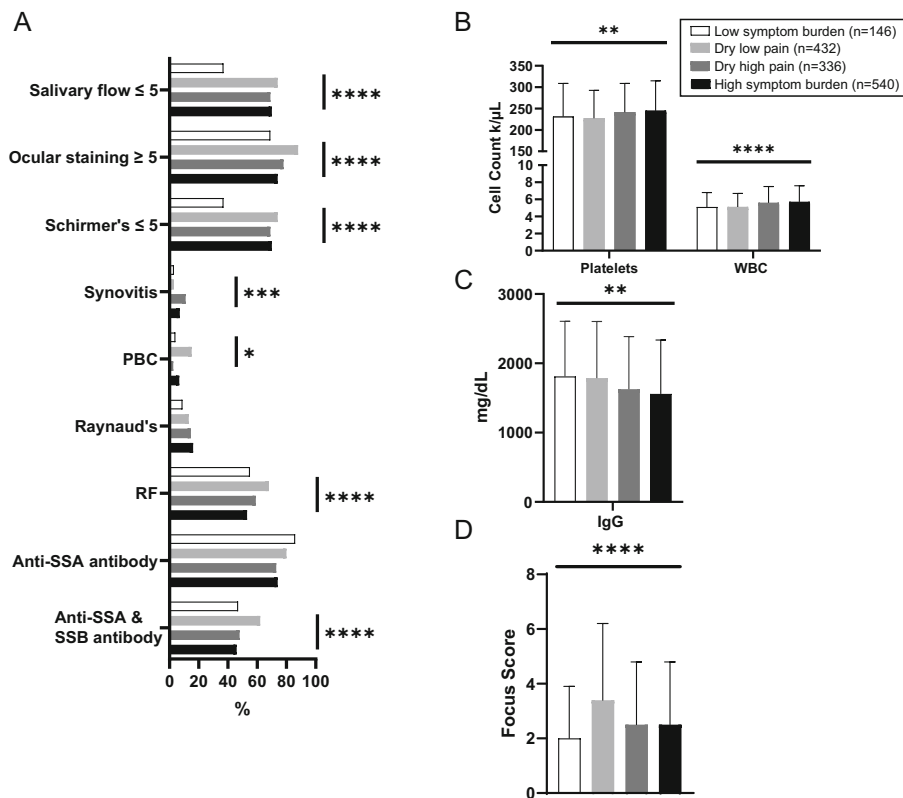


Figure 3. Oral and ocular dryness measurements, organ involvement, and abnormal laboratory and pathology results in patients from the Sjögren's International Collaborative Clinical Alliance Registry according to Sjögren's disease symptom-based clusters ($n = 1,454$). **A**, Frequency of patients with each laboratory or disease-relevant feature according to dryness measurements, organ involvement, and abnormal laboratory results. **B**, Mean platelet and white blood cell (WBC) counts. **C**, Mean IgG levels. **D**, Mean focus score. Bars show the mean. * = $P \leq 0.05$; ** = $P \leq 0.01$, *** = $P \leq 0.001$, by one-way analysis of variance or chi-square test. PBC = primary biliary cholangitis; RF = rheumatoid factor.

Sjögren's disease-related symptoms and the HSB cluster experienced the highest frequency (Supplementary Table C, available at <https://onlinelibrary.wiley.com/doi/10.1002/art.42238>). A fewer number of individuals in the LSB cluster experienced dry mouth and eye (86% and 87%, respectively) compared with the number of individuals in the other clusters. Additionally, only 51% of the individuals in the LSB cluster experienced fatigue compared with 94% in the HSB cluster ($P < 0.0001$). Although fibromyalgia occurred in 31% of the overall cohort, it was most prevalent among members of the HSB cluster (44%) ($P < 0.0001$ versus the other clusters) (Table 2).

Members of the HSB had the highest use of current opioid analgesics (34%) ($P < 0.0001$ versus the other clusters) (Figures 4A and B; Supplementary Table D, available at <https://onlinelibrary.wiley.com/doi/10.1002/art.42238>). More members of the HSB cluster took nonprescription (93%) and prescription eye drops (53%) compared with the other clusters. DMARD use was highest in the DHP and HSB clusters (48% in each). Antidepressant use was high in the HSB cluster; however, current antidepressant use was lower than

“ever” antidepressant use in the HSB cluster (56% compared with 34%). Among the 410 participants with depression in the HSB cluster, 321 participants (78%) had ever taken antidepressants and 241 participants (59%) were currently taking antidepressants.

Members of the HSB cluster had higher mean annual costs of over-the-counter medications (\$785), prescription medications (\$1,595), and health care appointment/copay costs (\$1,052) than members of the other clusters (Figure 4C; Supplementary Table E, available at <https://onlinelibrary.wiley.com/doi/10.1002/art.42238>). Members of the DLP cluster had the lowest health care appointment/copay costs (\$721), whereas members of the LSB cluster had the lowest prescription costs (\$998). Mean dental care cost was lowest in the DHP cluster (\$1,333) and highest in the DLP cluster (\$2,636).

DISCUSSION

Sjögren's disease is a remarkably heterogeneous disease that lacks any US Food and Drug Administration–approved

Table 2. Baseline demographic and clinical characteristics of patients with Sjögren's disease who responded to the Sjögren's Foundation survey, in total and according to symptom-based clusters*

	All (n = 2,920)	LSB (n = 665)	DLP (n = 409)	DHP (n = 611)	HSB (n = 1,235)	Adjusted <i>P</i> †
Age, mean ± SD years						
Age at diagnosis	52 (13)	52 (12)	54 (13)	53 (12)	52 (12)	<0.0001
Age at time of survey	65 (12)	64 (12)	67 (11)	64 (13)	65 (12)	0.01
Female sex	2,791 (96)	624 (94)	392 (96)	581 (95)	1,194 (97)	0.04
Race						0.03
White	2,697 (93)	612 (92)	392 (96)	573 (94)	1,120 (91)	
Other‡	218 (7)	52 (8)	17 (4)	37 (6)	112 (9)	
Employment						<0.0001
Full-time	564 (20)	151 (24)	76 (20)	123 (21)	214 (19)	
Part-time	176 (6)	50 (8)	29 (7)	36 (6)	61 (5)	
Retired	1,379 (50)	321 (50)	225 (58)	284 (46)	549 (48)	
Other§	648 (23)	117 (18)	59 (15)	146 (25)	326 (28)	
Medical comorbidity						
GERD	1,327 (48)	237 (39)	155 (41)	288 (49)	647 (54)	<0.0001
Hypertension	911 (33)	143 (24)	126 (33)	200 (34)	442 (37)	<0.0001
Irritable bowel syndrome	902 (32)	122 (20)	90 (24)	179 (30)	511 (42)	<0.0001
Fibromyalgia	861 (31)	90 (15)	52 (14)	190 (32)	529 (44)	<0.0001
Autoimmune thyroid disease	669 (24)	126 (21)	92 (24)	147 (25)	304 (25)	0.48
Stroke	118 (4)	17 (3)	15 (4)	20 (3)	66 (5)	0.14
Myocardial infarction	59 (2)	7 (1)	6 (2)	14 (2)	32 (3)	0.15
Other rheumatology disease						
Rheumatoid arthritis	597 (21)	92 (15)	52 (14)	109 (19)	344 (28)	<0.0001
Mixed connective tissue disease	374 (13)	38 (6)	43 (11)	80 (14)	213 (18)	<0.0001
SLE	287 (10)	42 (7)	28 (7)	53 (9)	164 (14)	<0.01
Scleroderma	81 (3)	17 (3)	11 (3)	13 (2)	40 (3)	0.77
Sarcoidosis	31 (1)	4 (1)	3 (1)	7 (1)	17 (1)	0.55

* Except where indicated otherwise, values are the number (%) of respondents to the Sjögren's Foundation survey. Missing data were as follows: race and ethnicity (n = 1 each), employment (n = 1), and tobacco use ever (n = 76). GERD = gastroesophageal reflux disease; SLE = systemic lupus erythematosus (see Table 1 for other definitions).

† Adjusted for age, sex, race, and disability.

‡ Other race indicates all non-White races.

§ Other employment indicates self-employed, not employed but looking for work, not employed and not looking for work, not employed and unable to work due to disability or illness, student, or stay-at-home spouse or partner.

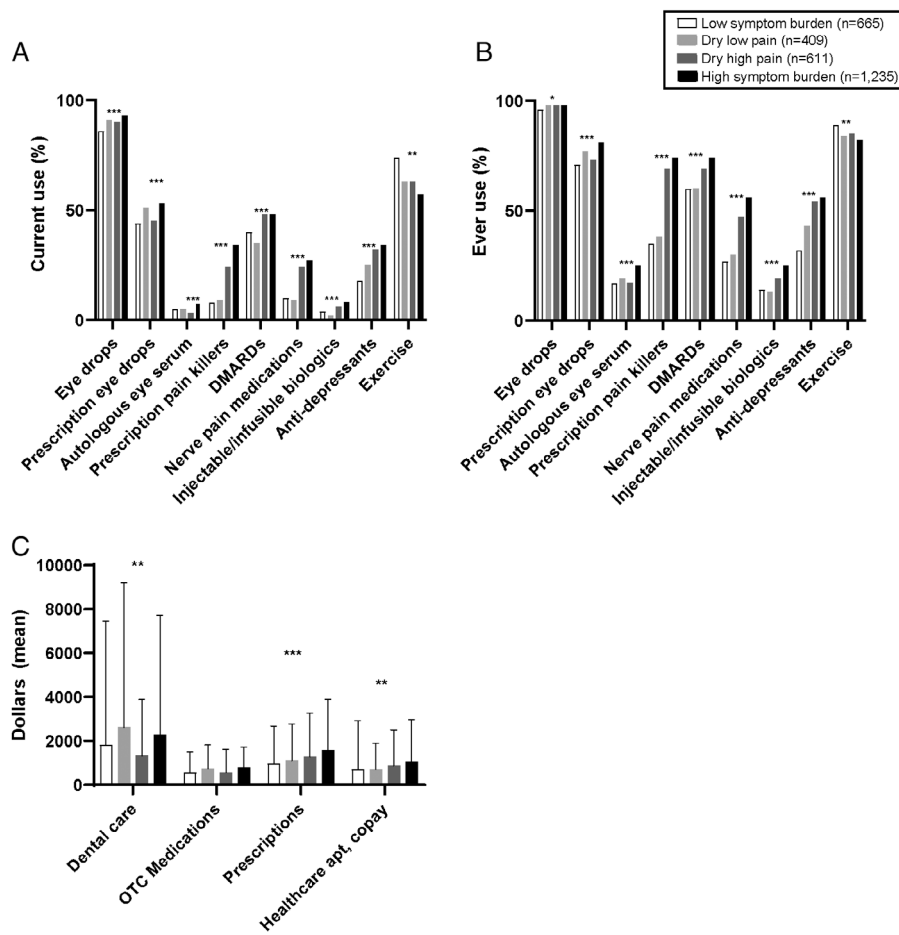


Figure 4. Medication use and cost of health care among participants of the Sjögren's Foundation survey according to Sjögren's disease symptom-based clusters ($n = 2,920$). In the survey, current medication use and exercise (**A**) and ever use of medications and exercise (**B**) were assessed, along with cost (in dollars) of specific aspects of health care for Sjögren's disease (**C**). Bars show the mean. Eye drops include artificial tears or eye ointments (nonprescription); prescription painkillers include, e.g., oxycodone, hydrocodone, tramadol; disease-modifying antirheumatic drugs (DMARDs) include, e.g., hydroxychloroquine, methotrexate, azathioprine, mycophenolate, leflunomide, sulfasalazine; nerve pain medications include, e.g., gabapentin, pregabalin; injectable/infusible biologics include, e.g., rituximab, abatacept, tumor necrosis factor inhibitors. * = $P \leq 0.05$; ** = $P \leq 0.01$, *** = $P \leq 0.001$, by one-way analysis of variance or chi-square test. OTC = over-the-counter; apt. = appointment.

disease-modifying therapy. This lack is partly because of gaps in our understanding of the pathogenesis of Sjögren's disease and because there may be different responses to therapy among the specific disease subgroups. Grouping patients with Sjögren's disease into symptom-based categories has the potential to reduce heterogeneity, inform the understanding of processes driving these various subtypes, and promote tailored therapies to symptom clusters. In contrast to a prior approach that included anxiety and depression (7), we generated clusters that were derived from the cardinal Sjögren's disease symptoms of generalized dryness, pain, and fatigue. When we analyzed the 4 symptom-based clusters that we generated and replicated across 2 large cohorts, we observed a discordance between the experience, disease severity, and treatment of Sjögren's disease, thus framing new opportunities for pathogenic insights, treatment, and approaches to clinical trials.

Our analyses of the SICCA Registry sample resulted in 4 clusters based on symptom severity: 1) a cluster of participants with low dryness and fatigue and rare pain (LSB cluster); 2) a cluster of participants with dryness and low pain and low fatigue (DLP cluster); 3) a cluster of participants with dryness and moderate to high pain and low to moderate fatigue (DHP cluster); and 4) a cluster of participants with high dryness, fatigue, and pain (HSB cluster). Notably, participants in the LSB cluster had infrequent dryness and extraglandular symptoms or organ involvement but had low white blood cell counts, higher levels of IgG, and low focus scores. Participants in the DLP cluster had dryness in the mouth and eyes based on objective measurements, had the highest frequency of PBC, and the most laboratory abnormalities, including anti-SSA and anti-SSB antibody positivity, RF, low blood cell counts, higher levels of IgG, and higher focus scores. However, participants in the DLP cluster took antimalarials,

antimetabolites, biologics, and steroids less often than patients in the DHP and HSB cluster groups. Participants in the DHP cluster had a higher frequency of synovitis (11% frequency) and extraglandular symptoms than other clusters, but the frequency was still less than the frequency for patients in the HSB cluster. Participants in the HSB cluster had the highest overall symptom burden, level of depression, and impaired QoL, although they had less severe dryness, less frequent organ involvement, and fewer laboratory abnormalities. However, participants in the HSB cluster frequently received immune-modulating medications.

We complemented the data generated from the SICCA Registry sample with data from the Sjögren's Foundation survey. We again focused on the same cardinal symptoms of pain, dryness, and fatigue, but data from the survey provided us more granular insight into patient experiences and costs. Although symptom-based clusters between the SICCA Registry sample and the Sjögren's Foundation sample were similar overall, members of the DHP and DLP clusters from the Sjögren's Foundation sample appeared to have more fatigue. In addition, members of the DLP cluster from the Sjögren's Foundation sample reported greater burden of dryness than members of the similar cluster from the SICCA Registry sample. These differences might be attributed to the community-based nature of the Sjögren's Foundation, where people with symptoms seek support for their disease. In contrast, the SICCA Registry may be enriched with patients referred by their physicians for a comprehensive evaluation, including biopsy of the labial salivary gland. Despite the different sources of members in the 2 cohorts, we identified similar clusters in both, strengthening our conclusions.

Symptom burden did not correlate well with traditional disease severity markers, such as abnormalities in laboratory results and extraglandular involvement, which are associated with outcomes like lymphoma and mortality. For example, patients in the DLP cluster had low symptom burden, yet patients in the cluster had the most significant glandular involvement and laboratory and pathology abnormalities. It is possible that the LSB cluster represents an earlier stage of the DLP cluster. This theory is supported by the higher prevalence of positivity for anti-SSA and anti-SSB antibodies in patients in the DLP cluster, potentially indicating epitope spreading. Furthermore, patients in the LSB cluster were younger (mean age 47 years) than patients in the DLP cluster (mean age 54 years). Interestingly, patients in the LSB cluster reported the lowest burden of dryness on objective measurements but had the highest frequency of anti-SSA antibody positivity. This runs counter to prior studies that showed greater dryness in patients with Sjögren's disease who are anti-SSA antibody positive (23). Accordingly, by separating the LSB and the DLP clusters, we revealed distinct subtypes of Sjögren's disease.

We found that treatment type paralleled symptom frequency and severity more than objective measurements of severity in patients with Sjögren's disease. For example, patients in the DHP and HSB clusters took antimalarial drugs, other DMARDs,

NSAIDs, biologics, and steroids more frequently than patients in the DLP and LSB clusters despite an overall lower Sjögren's disease-specific activity metric. Similarly, although patients in the DLP cluster had the greatest level of dryness, patients in the HSB cluster more frequently took cholinomimetic therapy. It is possible that the higher use of cholinomimetics and immune-modulating therapy among patients in the HSB cluster improved their respective measures of dryness and biologic activity. However, clinical practice and clinical trial experiences have demonstrated less response to therapy among those who have the HSB symptom subtype and who have low biologic disease activity (8,24). Together with our results, these findings highlight the discordance between objective disease severity and treatment, with symptoms rather than disease severity measures driving therapies. Thus, the use of immunomodulatory therapy to address symptoms might unnecessarily increase risks for adverse outcomes. Our findings suggest that a more nuanced approach to therapy is needed in patients with Sjögren's disease.

Akin to systemic lupus erythematosus, cluster-based treatment might improve communications between patients and providers as well as patient satisfaction and ultimately reduce costs and unnecessary exposure to high-risk therapy, providing opportunities for improved care (5). Patients in the HSB cluster, characterized by heavy symptom burden, had lower overall end-organ involvement and laboratory abnormalities, yet received more treatment. Patients in the HSB cluster had a high level of fatigue, which is a common and debilitating symptom of Sjögren's disease. Fatigue has been shown to be inversely related to the traditional proinflammatory cytokine profile in Sjögren's disease (25–27), and symptoms of fatigue do not improve with immunomodulation. This discrepancy reveals an opportunity to focus on patient counseling and lifestyle interventions for individuals categorized in the HSB cluster (28).

Furthermore, patients in the HSB cluster had a high use of opioid analgesics (34%), indicating that they may be taking treatments that exacerbate their symptoms of dryness and pain. Opioid analgesics negatively impact individuals with fibromyalgia, which is frequently diagnosed in patients categorized in the HSB cluster (44%), and this treatment can lead to worsening pain, function, and depression (29,30). Opioid analgesics also exacerbate dryness and, particularly in patients with Sjögren's disease, confound disease severity and patient response to therapies. We demonstrated that patients in the HSB cluster had higher medical care costs, which were up to twice the costs reported by the other clusters. By defining and counseling patients on therapies expected to benefit their particular subtype, providers might tailor treatment and control costs. Thus, we can potentially improve the symptom burden and QoL of patients with Sjögren's disease by targeting their particular phenotype with tailored therapy.

We observed interesting results in the DLP cluster because, although patients had lower overall symptom burden, they had

high dryness levels, laboratory abnormalities, focus scores, and frequency of PBC. Akin to the DLP cluster, the LSB cluster also had low blood cell counts but was notable for having the highest levels of IgG. Accordingly, given these objective immunologic markers, members of these clusters might be more responsive to immunosuppressive therapies.

Tarn et al previously described distinct symptom-based clusters generated on the basis of measures of pain, fatigue, and dryness plus anxiety and depression in European samples (7). The 4 main clusters described in their work included LSB, HSB, dryness and fatigue, and pain dominant with fatigue, and they observed different laboratory and transcriptomic profiles among the clusters. The investigators also retrospectively compared responses to treatment with hydroxychloroquine and rituximab from the JOUQER and TRACTISS trials, respectively, among the clusters. Patients in the HSB cluster improved with hydroxychloroquine treatment, and patients in the cluster with dryness dominant with fatigue improved with rituximab treatment (7,24). Cluster membership might remain stable over time (31). Other studies have used latent class analysis to identify symptom-based clusters in patients with Sjögren's disease but did not collect granular data on patient experiences, laboratory test results, or histopathology results (13). In contrast, we performed a simplified cluster analysis that focused on the cardinal symptoms of Sjögren's disease that have been used for validation of multiple patient-reported outcome tools (20,21). We expanded on the findings of Tarn et al by analyzing other clinically important metrics, such as organ involvement and focus score. We also reported whether categorization based on symptoms in patients with Sjögren's disease affected medical care and treatment costs.

Strengths of our study include the use of 2 large Sjögren's disease cohorts. To our knowledge, this is the largest study to report on symptom-based clusters in patients with Sjögren's disease. In addition, the SICCA Registry sample included validated depression (PHQ-9) and health care-related QoL (SF-12) metrics. Registrants were rigorously evaluated by rheumatologists and ophthalmologists with standardized examination, laboratory, and pathology protocols. However, we also acknowledge limitations.

First, registrants were referred to the SICCA Registry sample, so referral bias might have impacted our results. The Sjögren's Foundation survey was created by patients with Sjögren's disease and providers to describe the unique experience of each Sjögren's disease cluster but was not previously validated. The Sjögren's Foundation sample survey carries typical survey-based limitations of response bias, recall bias, and misclassification bias. The Sjögren's Foundation cohort included self-identified cases of Sjögren's disease, potentially allowing for inclusion of patients without a proven diagnosis. Furthermore, respondents to the Sjögren's Foundation survey did not have physical examinations or laboratory testing, so the severity and extent of their Sjögren's disease were unknown.

Another limitation of our analysis was that we did not statistically account for multiple testing. However, most of the *P* values were very small (<0.0001) and would be statistically significant even if we corrected for multiple testing, such as by using the Bonferroni correction method. Both data sources were of cross-sectional design, and changes in clusters over time were not captured.

Extensive medication profiles and sleep habits were also not captured, and so we could not account for medications, such as antihypertensive drugs or sleep agents, that might confound analyses. Future studies should collect and analyze these data. Although our analysis and the other analyses summarized above emphasize the potential promise of targeted therapy for distinct subtypes of Sjögren's disease, further analyses are needed to define the biologic differences among symptom-based clusters of Sjögren's disease for development of therapeutics. More research is also needed to determine the applicability of our findings to more diverse patient populations.

Our findings highlight a discordance in the experiences, disease severity, and treatment approaches among 4 relatively consistent symptom-based clusters from 2 cohorts of patients with Sjögren's disease. We propose that further research into the pathogenesis underpinning these symptom-based clusters could advance our understanding of this heterogeneous disease and move toward cluster-targeted therapies and trials. We believe that clinical trials that account for the heterogeneous experiences of patients with Sjögren's disease might have a higher likelihood of success. In the short term, identification of a symptom-based phenotype for Sjögren's disease could promote appropriate treatment regimens earlier in the disease, thereby improving patient QoL. A refined definition of treatments based on symptom clusters could have the added benefit of harmonizing the expectations and communication between patients and providers.

AUTHOR CONTRIBUTIONS

All authors were involved in drafting the article or revising it critically for important intellectual content, and all authors approved the final version to be published. Dr. McCoy had full access to all of the data in the study and takes responsibility for the integrity of the data and the accuracy of the data analysis.

Study conception and design. McCoy, Woodham, Bunya, Maerz, Akpek.

Acquisition of data. McCoy, Woodham, Maerz, Makara.



Analysis and interpretation of data. McCoy, Woodham, Bartels, Saldanha, Maerz, Baer.

REFERENCES

1. Miyamoto ST, Valim V, Fisher BA. Health-related quality of life and costs in Sjögren's syndrome. *Rheumatology (Oxford)* 2019. doi: [10.1093/rheumatology/key370](https://doi.org/10.1093/rheumatology/key370). E-pub ahead of print.
2. Meijer JM, Meiners PM, Huddlestone Slater JJ, Spijkervet FK, Kallenberg CG, Vissink A, et al. Health-related quality of life, employment and disability in patients with Sjögren's syndrome. *Rheumatology (Oxford)* 2009;48:1077–82.

3. Fox RI, Fox CM. Sjögren syndrome: why do clinical trials fail? *Rheum Dis Clin North Am* 2016;423:519–30.
4. Alarcón GS, McGwin G Jr, Brooks K, Roseman JM, Fessler BJ, Sanchez ML, et al. Systemic lupus erythematosus in three ethnic groups. XI. Sources of discrepancy in perception of disease activity: a comparison of physician and patient visual analog scale scores. *Arthritis Rheum* 2002;474:408–13.
5. Pisetsky DS, Clowse ME, Criscione-Schreiber LG, Rogers JL. A novel system to categorize the symptoms of systemic lupus erythematosus [review]. *Arthritis Care Res (Hoboken)* 2019;716:735–41.
6. Fox RI, Fox CM, Gottenberg JE, Dörner T. Treatment of Sjögren's syndrome: current therapy and future directions [review]. *Rheumatology (Oxford)* 2021;60:2066–74.
7. Tarn JR, Howard-Tripp N, Lendrem DW, Mariette X, Saraux A, Devauchelle-Pensec V, et al. Symptom-based stratification of patients with primary Sjögren's syndrome: multi-dimensional characterisation of international observational cohorts and reanalyses of randomised clinical trials. *Lancet Rheumatol* 2019;12:PE85–E94.
8. Gottenberg JE, Ravaud P, Puéchal X, Le Guern V, Sibilia J, Goeb V, et al. Effects of hydroxychloroquine on symptomatic improvement in primary Sjögren syndrome: the JOQUER randomized clinical trial. *JAMA* 2014;3123:249–58.
9. Fisher BA, Everett CC, Rout J, O'Dwyer JL, Emery P, Pitzalis C, et al. Effect of rituximab on a salivary gland ultrasound score in primary Sjögren's syndrome: results of the TRACTISS randomised double-blind multicentre substudy. *Ann Rheum Dis* 2018;773:412–6.
10. Daniels TE, Cox D, Shiboski CH, Schiødt M, Wu A, Lanfranchi H, et al. Associations between salivary gland histopathologic diagnoses and phenotypic features of Sjögren's syndrome among 1,726 registry participants. *Arthritis Rheum* 2011;637:2021–30.
11. Daniels TE, Criswell LA, Shiboski C, Shiboski S, Lanfranchi H, Dong Y, et al. An early view of the international Sjögren's syndrome registry. *Arthritis Rheum* 2009;615:711–4.
12. Shiboski SC, Shiboski CH, Criswell L, Baer A, Challacombe S, Lanfranchi H, et al. American College of Rheumatology classification criteria for Sjögren's syndrome: a data-driven, expert consensus approach in the Sjögren's International Collaborative Clinical Alliance cohort. *Arthritis Care Res (Hoboken)* 2012;644:475–87.
13. McCoy SS, Sampene E, Baer AN. Association of Sjögren's syndrome with reduced lifetime sex hormone exposure: a case-control study. *Arthritis Care Res (Hoboken)* 2020;729:1315–22.
14. Shiboski CH, Shiboski SC, Seror R, Criswell LA, Labetoulle M, Lietman TM, et al. 2016 American College of Rheumatology/European League Against Rheumatism classification criteria for primary Sjögren's syndrome: a consensus and data-driven methodology involving three international patient cohorts. *Ann Rheum Dis* 2017;761:9–16.
15. Ware J Jr, Kosinski M, Keller SD. A 12-item short-form health survey: construction of scales and preliminary tests of reliability and validity. *Med Care* 1996;343:220–33.
16. Gonzalez-Najera C, Taylor S, Crawford S, Narasimhan P, Shao X, Li J. Characteristics and treatments of patients with Sjögren's syndrome in a real-world setting. Paper presented at: EULAR Annual European Congress of Rheumatology; 2019 June 12–15; Madrid, Spain.
17. McCoy SS, Bartels CM, Saldanha IJ, Bunya VY, Akpek EK, Makara MA, et al. National Sjögren's foundation survey: burden of oral and systemic involvement on quality of life. *J Rheumatol* 2021;48:1029–36.
18. Vitali C, Bombardieri S, Jonsson R, Moutsopoulos HM, Alexander EL, Carsons SE, et al. Classification criteria for Sjögren's syndrome: a revised version of the European criteria proposed by the American-European Consensus Group. *Ann Rheum Dis* 2002;616:554–8.
19. Vitali C, Bombardieri S, Moutsopoulos HM, Balestrieri G, Bencivelli W, Bernstein RM, et al. Preliminary criteria for the classification of Sjögren's syndrome: results of a prospective concerted action supported by the European Community. *Arthritis Rheum* 1993;363:340–7.
20. Bowman SJ, Booth DA, Platts RG. Measurement of fatigue and discomfort in primary Sjögren's syndrome using a new questionnaire tool. *Rheumatology (Oxford)* 2004;436:758–64.
21. Bowman SJ, Booth DA, Platts RG, Field A, Rostron J. Validation of the Sicca Symptoms Inventory for clinical studies of Sjögren's syndrome. *J Rheumatol* 2003;306:1259–66.
22. Milligan GW. An examination of the effect of six types of error perturbation on fifteen clustering algorithms. *Psychometrika* 1980;45:325–42.
23. Kontny E, Lewandowska-Poluch A, Chmielińska M, Olesińska M. Subgroups of Sjögren's syndrome patients categorised by serological profiles: clinical and immunological characteristics. *Reumatologia* 2018;566:346–53.
24. Collins A, Lendrem D, Wason J, Tarn J, Howard-Tripp N, Bodewes I, et al. Revisiting the JOQUER trial: stratification of primary Sjögren's syndrome and the clinical and interferon response to hydroxychloroquine. *Rheumatol Int* 2021;419:1593–600.
25. Bodewes ILA, Al-Ali S, van Helden-Meeuwssen CG, Maria NI, Tarn J, Lendrem DW, et al. Systemic interferon type I and type II signatures in primary Sjögren's syndrome reveal differences in biological disease activity. *Rheumatology (Oxford)* 2018;575:921–30.
26. James K, Al-Ali S, Tarn J, Cockell SJ, Gillespie CS, Hindmarsh V, et al. A transcriptional signature of fatigue derived from patients with primary Sjögren's syndrome. *PLoS One* 2015;1012:e0143970.
27. Tripp NH, Tarn J, Natasari A, Gillespie C, Mitchell S, Hackett KL, et al. Fatigue in primary Sjögren's syndrome is associated with lower levels of proinflammatory cytokines. *RMD Open* 2016;22:e000282.
28. Azizoddin DR, Jolly M, Arora S, Yelin E, Katz P. Longitudinal study of fatigue, stress, and depression: role of reduction in stress toward improvement in fatigue. *Arthritis Care Res (Hoboken)* 2020;7210:1440–8.
29. Fitzcharles MA, Faregh N, Ste-Marie PA, Shir Y. Opioid use in fibromyalgia is associated with negative health related measures in a prospective cohort study. *Pain Res Treat* 2013;2013:898493.
30. Peng X, Robinson RL, Mease P, Kroenke K, Williams DA, Chen Y, et al. Long-term evaluation of opioid treatment in fibromyalgia. *Clin J Pain* 2015;311:7–13.
31. Lee JJ, Park YJ, Park M, Yim HW, Park SH, Kwok SK. Longitudinal analysis of symptom-based clustering in patients with primary Sjögren's syndrome: a prospective cohort study with a 5-year follow-up period. *J Transl Med* 2021;191:394.

Development of Pulmonary Hypertension in Over One-Third of Patients With Th/To Antibody–Positive Scleroderma in Long-Term Follow-Up

Shashank Suresh,¹  Devon Charlton,² Erin K. Snell,³ Maureen Laffoon,² Thomas A. Medsger Jr,² Lei Zhu,² and Robyn T. Domsic² 

Objective. This study was undertaken to describe clinical manifestations in patients with Th/To antibody–positive systemic sclerosis (SSc) during long-term follow-up.

Methods. We performed a case–control study involving anti-Th/To antibody–positive patients with SSc who were newly referred to the University of Pittsburgh Medical Center and the Pittsburgh Scleroderma Center from 1980 to 2015. For every case, 2 anti-Th/To antibody–negative SSc patients (the first 2 consecutively seen after a case) were used as controls. Long-term disease manifestations and survival were then compared between cases and controls.

Results. A total of 204 anti-Th/To antibody–positive SSc patients and 408 controls were identified. The cohort had a mean \pm SD age of 52 ± 12.9 years, and 76% of individuals were women. Anti-Th/To antibody–positive patients more often presented without skin thickening ($P < 0.0001$) and had a higher rate of pulmonary hypertension (PH) ($P < 0.0001$) and interstitial lung disease ($P = 0.05$) compared to anti-Th/To antibody–negative SSc controls. Anti-Th/To antibody–positive SSc patients also had less frequent muscle and joint involvement than anti-Th/To antibody–negative SSc controls ($P < 0.0001$). After a median clinical follow-up period of 6.1 years (interquartile range 2.4–12.7), 38% of anti-Th/To–positive patients had developed PH compared to 15% of anti-Th/To antibody–negative SSc controls ($P < 0.0001$). The rate of PH classified as World Health Organization (WHO) Group 1 pulmonary arterial hypertension [PAH] was 23% in anti-Th/To–positive patients compared to 9% in anti-Th/To antibody–negative SSc controls ($P < 0.0001$). After adjusting for age and sex, anti-Th/To antibody positivity was associated with a hazard ratio (HR) of 3.3 (95% confidence interval 2.3–4.9) for increased risk of developing PH at 10 years of follow-up from the first scleroderma center visit.

Conclusion. This is the largest cohort of patients with anti-Th/To antibody–positive SSc with long-term follow-up data. The very high rate (38%) and associated independent risk of anti-Th/To antibody–positive patients developing PH in follow-up, particularly in WHO Group 1 PAH patients, is striking. Patients presenting with limited skin involvement should be tested for Th/To antibodies, and if present, careful monitoring for PH is warranted.

INTRODUCTION

Patients with systemic sclerosis (SSc) can be classified into 2 primary clinical subsets based on the extent of skin involvement: diffuse cutaneous and limited cutaneous. The spectrum of limited SSc includes patients who have no skin thickening, termed SSc sine scleroderma. There are SSc-specific serum autoantibodies associated with SSc clinical features (i.e., cutaneous subtype,

internal organ involvement) and SSc prognoses (1–5). When both the cutaneous subset and autoantibody status are known, clinical/serologic classification can inform the natural history of disease in SSc patient groups.

Anti-Th/To is an uncommon SSc-associated antinuclear antibody (ANA) in a nucleolar pattern. The Th/To antigen consists of 2 RNA-processing enzymes (RNase mitochondrial RNA and RNase P) plus 10 associated proteins, of which RPP25, RPP38,

Presented in part at the University of Pittsburgh 2021 Department of Medicine Research Day, Pittsburgh, Pennsylvania, April 2021.

Supported by the National Institute of Arthritis and Musculoskeletal and Skin Diseases, NIH (award P50-AR-060780).

¹Shashank Suresh, MD: University of Pittsburgh Medical Center, Pittsburgh, Pennsylvania; ²Devon Charlton, MD, MPH, Maureen Laffoon, BS, Thomas A. Medsger Jr, MD, Lei Zhu, PhD, Robyn T. Domsic, MD, MPH: University of Pittsburgh School of Medicine, Pittsburgh, Pennsylvania; ³Erin K. Snell, MD: Northwest Permanente, Portland, Oregon.

Author disclosures are available at <https://onlinelibrary.wiley.com/action/downloadSupplement?doi=10.1002%2Fart.42152&file=art42152-sup-0001-Disclosureform.pdf>.

Address correspondence to Robyn T. Domsic, MD, MPH, University of Pittsburgh, S724 Biomedical Science Tower, 3500 Terrace Street, Pittsburgh, PA 15261. Email: rtd4@pitt.edu.

Submitted for publication August 12, 2021; accepted in revised form April 19, 2022.

and human POP1 are the main autoantigens (6–9). Recently, anti-Th/To antibody testing, which was historically accessible only to a few research centers, has become available on some commercial platforms, thereby increasing the need for clinical information on this subset of SSc patients.

The first case series of SSc patients with anti-Th/To antibodies was reported by our group in 1990 and included only 15 anti-Th/To antibody-positive patients (4%) of 371 consecutive SSc patients between 1984 and 1988 (10). In 2002, we performed a follow-up study comparing 107 patients with anti-Th/To antibody-positive SSc to 365 SSc patients with anticentromere antibodies (ACAs) seen from 1985 to 2000 (11). Almost all anti-Th/To antibody-positive patients had limited cutaneous SSc, and in this group there was an increased frequency of interstitial lung disease (ILD) and pulmonary arterial hypertension (PAH) (11). Other findings on anti-Th/To-positive SSc patients have been from small cross-sectional studies and are thus limited in their generalizability (6,9,12–23). The long-term frequency of clinical outcomes and prognosis in patients with anti-Th/To antibody-positive SSc are completely unknown.

The World Health Organization (WHO) currently classifies pulmonary hypertension (PH) into 5 groups according to etiology (24). SSc patients can present with PAH (Group 1), PH due to left heart disease (Group 2), or PH due to chronic lung disease such as ILD (Group 3). The relative frequency of these WHO PH classifications in SSc patients and their correlations with SSc-associated serum autoantibodies are topics of current debate. However, SSc patients are widely recognized to be at an increased risk of PH compared to the general population.

The objective of this study was to describe clinical features in patients with anti-Th/To antibody-positive SSc during long-term follow-up, including the development of PH by WHO classification group.

PATIENTS AND METHODS

Patient selection. Informed consent was obtained, and all patients who were anti-Th/To antibody-positive at an initial visit at the University of Pittsburgh Medical Center and the Pittsburgh Scleroderma Center between January 1, 1980 and December 31, 2015 were included in this study. There was no restriction regarding cutaneous subtype. We excluded patients with anti-Th/To antibody positivity who also had another SSc-specific antibody in order to focus on clinical associations with anti-Th/To. All included patients met the updated American College of Rheumatology/European Alliance of Associations for Rheumatology 2013 classification criteria over the course of follow-up (25). This study was reviewed and approved by the University of Pittsburgh institutional review board (approval no. CR19090054-003).

Laboratory methods. ANA testing was performed using indirect immunofluorescence analysis. Anti-Th/To was detected

using RNA immunoprecipitation as previously reported (11). ACA presence was identified by characteristic staining on HEp-2 substrate (1:40 dilution). Ouchterlony immunodiffusion was used to test for anti-topoisomerase I and anti-U1 RNP, as described in previous studies (13). All other SSc autoantibodies (anti-RNA polymerase III, anti-PM/Scl, anti-U3 RNP, anti-U11/U12 RNP, and anti-Ku) were examined using protein immunoprecipitation or a combination of multiple methods as previously reported by Kao et al (26).

Study design. We used a 1:2 case-control design. To control for temporal trends, we matched each case to the next 2 consecutive SSc patients as controls, comprising subjects who had any antibody profile excluding positivity for anti-Th/To. All cases and controls were residents of the US, ensuring that vital status during the follow-up period could be easily determined.

Data collection. All patients had a comprehensive first visit evaluation for symptom data collection, physical examination, laboratory and serologic testing, and objective testing for internal organ dysfunction (pulmonary function tests [PFTs], computed tomography [CT] of the chest, transthoracic echocardiography [TTE], esophagography, etc.). At follow-up, all patients completed an abbreviated 80-variable form. We retrospectively reviewed the electronic medical record system for objective test results and clinical outcomes not previously recorded. We sent a follow-up questionnaire regarding SSc complications and current medications to cases and controls who had not recently been seen, along with a request for outside medical records to supplement data, and we received outside medical records from this inquiry for missing objective testing data (chest imaging, PFTs, TTE). Every effort was made to obtain objective test results to determine the frequency and severity of organ involvement.

Survival. Survival rates as of December 31, 2019 were obtained from the US Social Security Death Index. Cause of death was determined by review of the medical records or discussion with managing physicians. SSc-related causes of death were categorized as PH, pulmonary fibrosis, SSc-related kidney disease, SSc-related heart disease, and combined SSc-related kidney/heart disease. Non-SSc-related causes of death were categorized as cancer, sudden death, atherosclerotic heart disease, other non-SSc-related disease, infection, vasculitis, central nervous system disease, or unknown. If records were incomplete or unavailable, the National Death Index was used to obtain death certificates, which were reviewed in the context of known clinical data. Additional contact with medical personnel or family members, if contact information was available, was made to clarify cause of death.

Definitions of organ manifestations. Organ system manifestations were defined as previously described (27). ILD

was defined as bibasilar fibrosis on chest radiography or high-resolution CT of the lungs. PH was defined as mean pulmonary artery pressure >20 mm Hg on right-sided heart catheterization (24) or TTE showing an estimated peak systolic pulmonary artery pressure >45 mm Hg, with WHO subtype determined in consultation with a PH expert.

Statistical analysis. Baseline characteristics and clinical features at baseline and follow-up were compared between the case and control groups using *t*-tests, chi-square tests, and non-parametric tests (including Fisher's exact test and Mann-Whitney Wilcoxon tests) where appropriate.

The risk of PH and cumulative survival rates were assessed using time-to-event analysis with the Kaplan-Meier method used to generate Kaplan-Meier curves. More specifically, we performed the following survival or time-to-event analyses to compare anti-Th/To-positive cases to controls: 1) 5-year survival from the first visit, 2) 5-year survival from disease onset, 3) time-to-event analysis for all PH types from the first visit over 10 years of follow-up, 4) time-to-event analysis for all PH types from disease onset over 20 years of follow-up, and 5) time-to-event analysis for WHO Group 1 PAH from disease onset over 20 years of follow-up. A Cox proportional hazards model was used to generate unadjusted HRs and age- and sex-adjusted HRs. All statistical analyses were performed using SAS 9.4, and 2-sided *P* values less than or equal to 0.05 were considered statistically significant.

Patient and public involvement. This study followed up a preexisting and longstanding observational cohort over 30 years. Patients and the public were not involved in recruitment for this study or the design and conduct of this study.

RESULTS

In total, we evaluated 3,613 newly diagnosed SSc patients between 1980 and 2015. These patients included 211 SSc patients who were anti-Th/To antibody-positive (5.8%), of which 7 were excluded for having a concomitant second SSc-associated antibody, leaving 204 patients for analysis (Figure 1). We then identified 408 anti-Th/To-negative controls (SSc patients with other SSc-related antibodies). The cohort had a mean \pm SD age of 52 \pm 12.9 years, and 76% of individuals were women.

Baseline demographic characteristics, length of follow-up, and cutaneous subtype of the anti-Th/To antibody-positive cases and anti-Th/To antibody-negative controls are shown in Table 1. There were no significant differences in terms of age, sex, or race between the groups. Anti-Th/To-positive cases were more likely to be prior smokers or current smokers than controls (64% versus 44%; *P* < 0.0001). Nearly all anti-Th/To antibody-positive patients (97%) had limited skin thickening, with 23% presenting with SSc sine scleroderma. Anti-Th/To antibody-positive patients had significantly longer disease duration at presentation than

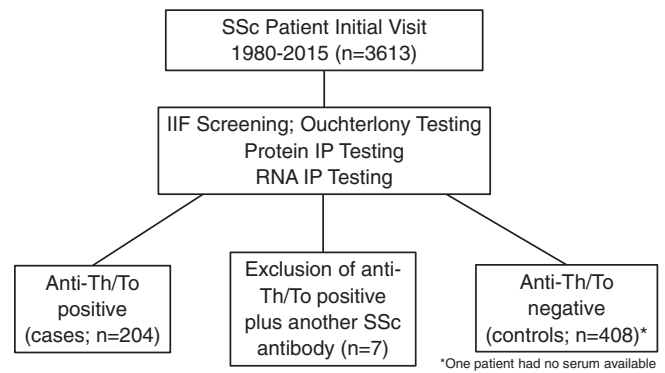


Figure 1. Systemic sclerosis (SSc) patient selection flow chart. IIF = indirect immunofluorescence; IP = immunoprecipitation.

those with other SSc antibodies (median 7.9 years versus 3.3 years; *P* < 0.0001). For the entire cohort, the median duration of follow-up was 6.1 years (interquartile range 2.4–12.7), which did not differ between cases and controls. Raynaud's phenomenon, the most frequently reported first symptom occurring among SSc patients, significantly differed in frequency between anti-Th/To antibody-positive cases and anti-Th/To antibody-negative controls (80% versus 56%; *P* < 0.0001). Differences in frequency of other common first symptoms included puffy fingers/hands in 6% of anti-Th/To-positive cases compared to 16% of controls and joint symptoms in 2% of anti-Th/To-positive patients compared to 11% of controls.

Organ system manifestations. Organ system manifestations at the baseline visit and as of the last follow-up visit are shown in Table 2, with PH shown separately. At baseline, joint and tendon manifestations were less frequently seen in anti-Th/To-positive patients, although ILD was more frequently observed on imaging in anti-Th/To-positive patients than in anti-Th/To antibody-negative SSc controls (45% versus 34%; *P* = 0.05). No other significant differences in baseline organ involvement were observed.

During follow-up, significantly more anti-Th/To-positive patients had ILD on imaging compared to controls (54% versus 39%; *P* = 0.008); of note, 93% of anti-Th/To-positive patients and 87% of controls had chest imaging data available for review. Importantly, there was no difference in terms of ILD severity using Medsger severity scores (28) between anti-Th/To-positive patients and controls (*P* = 0.42). Anti-Th/To-positive patients continued to have significantly lower frequencies of joint and tendon manifestations, and over time had lower frequencies of renal crisis than the SSc control group (3% versus 10%; *P* = 0.003). Very few anti-Th/To-positive patients had muscle involvement at baseline and follow-up (1% and 2%, respectively), compared to controls at baseline and follow-up (5% and 6%, respectively; *P* = 0.04). Given the high rates of ILD on imaging, and the potential theoretical contribution of esophageal reflux to pulmonary radiographic changes, we compared gastrointestinal (GI) tract

Table 1. Demographic and disease features of anti-Th/To antibody-positive SSc cases and anti-Th/To antibody-negative SSc controls at the first clinic visit*

	Cases (n = 204)	Controls (n = 408)	P†
Demographic characteristics			
Age, mean ± SD years	52.6 ± 12.0	51.8 ± 13.4	NS
Sex, % female	79	75	NS
Race, % White	96	91	NS
Tobacco use, %			<0.0001
Lifelong nonsmoker	36	56	
Ex-smoker	37	31	
Current smoker	27	13	
Disease classification, %			
dcSSc	3	44	<0.0001
lcSSc	97	56	<0.0001
SSc sine scleroderma	23	9	<0.0001
Overlap syndrome	5	11	0.02
Clinical follow-up data			
Disease duration from onset to first visit, median (IQR) years	7.9 (2.9–14.9)	3.3 (1.2–10.5)	<0.0001‡
Length of time from first to last visit, median (IQR) years	5.5 (1.8–12.8)	6.3 (2.7–12.7)	0.20‡

* SSc = systemic sclerosis; NS = not significant; dcSSc = diffuse cutaneous SSc; lcSSc = limited cutaneous SSc; IQR = interquartile range.

† By *t*-test.

‡ For this continuous variable, *P* values were obtained by Mann-Whitney Wilcoxon test.

symptom severity between groups using revised Medsger severity scores. Over time, there was a between-group difference in terms of GI tract symptom severity ($P < 0.001$), with only 7% of patients in the anti-Th/To-positive group having moderate GI tract manifestations, 4% having severe GI manifestations, and 2% having end-stage GI tract manifestations, whereas in the control group, 12% had moderate GI manifestations, 3% had severe manifestations, and 5% had end-stage manifestations.

Frequency of PH.

PH frequency data are shown in Table 3. The few patients with PH attributable to non-SSc-related valvular disease ($n = 3$) were not included in this analysis. Overall, SSc-related PH was more frequently detected in anti-Th/To antibody-positive patients than in controls during the first clinic

visit (25% versus 9%, respectively; $P < 0.0001$), with the frequency of PH increasing up to 38% in anti-Th/To antibody-positive patients compared to 15% in controls during follow-up ($P < 0.0001$). Group 1 PAH was the most common WHO classification, with 17% of anti-Th/To-positive patients classified as having Group 1 PAH, which increased up to 23% at the last follow-up visit. In controls, only 5% of patients were classified as having Group 1 PAH at baseline, which increased to 9% as of the last follow-up visit (Table 3).

Risk of PH. Due to the potential of survival bias, given the longer disease duration in anti-Th/To-positive patients at baseline, we evaluated outcomes 10 years from the first visit using Kaplan-Meier analysis. This revealed an increased probability of

Table 2. Joint and organ system manifestations in anti-Th/To antibody-positive SSc cases and anti-Th/To antibody-negative SSc controls at the baseline visit and last follow-up visit*

	Baseline			Last follow-up		
	Cases (n = 204)	Controls (n = 408)	P†	Cases (n = 204)	Controls (n = 408)	P†
Raynaud's phenomenon	95 (n = 192)	91	NS	99	97	NS
Joint/tendon involvement	32 (n = 64)	69 (n = 275)	<0.0001	50	80 (n = 322)	<0.0001
Joint swelling	3 (n = 6)	13 (n = 50)	0.0001	12 (n = 25)	25 (n = 100)	0.0004
Tendon friction rubs	2 (n = 4)	23 (n = 91)	<0.0001‡	3	28 (n = 112)	<0.0001‡
Skeletal myopathy	1 (n = 3)	5 (n = 20)	0.04	2 (n = 5)	6 (n = 26)	0.04
GI tract involvement	38 (n = 77)	46 (n = 185)	NS	109 (n = 54)	60 (n = 246)	NS
Pulmonary fibrosis on imaging	45 (n = 72)	34 (n = 54)	0.05	54 (n = 103)	39 (n = 137)	0.0008
Renal crisis, %	2	4	NS‡	3	10	0.003

* Values are the percentage of subjects (sample size). Some features had missing data. NS = not significant; GI = gastrointestinal.

† By chi-square test.

‡ For this categorical variable, *P* values were obtained by Fisher's exact test.

Table 3. Incidence of PH or WHO Group 1 PAH in anti-Th/To antibody–positive SSc cases and anti-Th/To antibody–negative controls at the first clinic visit and after follow-up*

	Baseline			Follow-up		
	Cases (n = 204)	Controls (n = 407)	P	Cases (n = 204)	Controls (n = 402)	P
No PH	153 (75)	372 (91)	<0.0001	127 (62)	340 (85)	<0.0001
PAH (WHO Group 1)	35 (17)	20 (5)	–	47 (23)	37 (9)	–
Cardiac disease–related PH (WHO Group 2)	1 (<1)	2 (<1)	–	4 (2)	3 (<1)	–
Lung disease–related PH (WHO Group 3)	15 (7)	13 (3)	–	26 (13)	22 (5)	–

* Except where indicated otherwise, values are the number (%) of patients. PH = pulmonary hypertension; PAH = pulmonary arterial hypertension; SSc = systemic sclerosis; WHO = World Health Organization.

developing PH over 10 years of follow-up from the first visit in anti-Th/To–positive patients ($P < 0.0001$) (Figure 2).

In a Cox proportional hazards model, after adjustment for age and sex, anti-Th/To antibody positivity was associated with an HR of 3.3 for the development of any PH (95% confidence interval [95% CI] 2.3–4.9). Upon modeling the development of Group 1 PAH specifically, Th/To antibody positivity was associated with a 4.9 times higher risk of developing Group 1 PAH (95% CI 2.6–9.4) in a model adjusted for age. When additionally adjusted for disease duration, the risk of developing Group 1 PAH 10 years from SSc-associated symptom onset remained similar, at an HR of 5.1 (95% CI 2.7–9.8).

As ACA antibodies have been associated with a significant risk of developing Group 1 PAH, we performed additional Cox proportional hazards modeling for PAH development at 10 years in a model including both anti-Th/To and ACA positivity. After adjusting for age, sex, and disease duration, anti-Th/To positivity was associated with a higher risk of developing PAH (HR 8.5, 95% CI 3.6–20.0; $P < 0.0001$), and presence of ACAs was associated with a lower risk of developing PAH (HR 4.2, 95% CI 1.4–12.6; $P = 0.01$).

Autoantibody profile. Among controls, 27% were ACA-positive ($n = 110$), 26% were anti-Scl-70 positive ($n = 106$), and 25% were RNA polymerase III positive ($n = 101$). Anti-PM/Scl antibody and anti-U1 RNP were both found in 7% of controls ($n = 28$ each). A total of 3% of controls were anti-U3 RNP positive ($n = 12$), 2% were anti-U11 RNP positive ($n = 9$), 1% were anti-RuvBL1/2 positive ($n = 6$), and 1% were anti-Ku positive ($n = 5$). A total of 25 patients had other antibodies (none were anti-Th/To antibody positive, so they were not excluded from analysis), and 1 patient did not have an available serum sample.

Survival. As of the last follow-up visit, 56% of anti-Th/To–positive patients and 55% of controls had died. Despite higher rates of PH at presentation, the 5-year cumulative survival rate from the first University of Pittsburgh Medical Center and Pittsburgh Scleroderma Center visit was 68% in anti-Th/To antibody–positive cases, significantly lower than controls (76%; $P = 0.02$) (Figure 3).

Cause of death. We were able to ascertain the cause of death in 101 of 113 anti-Th/To antibody–positive cases (89%)

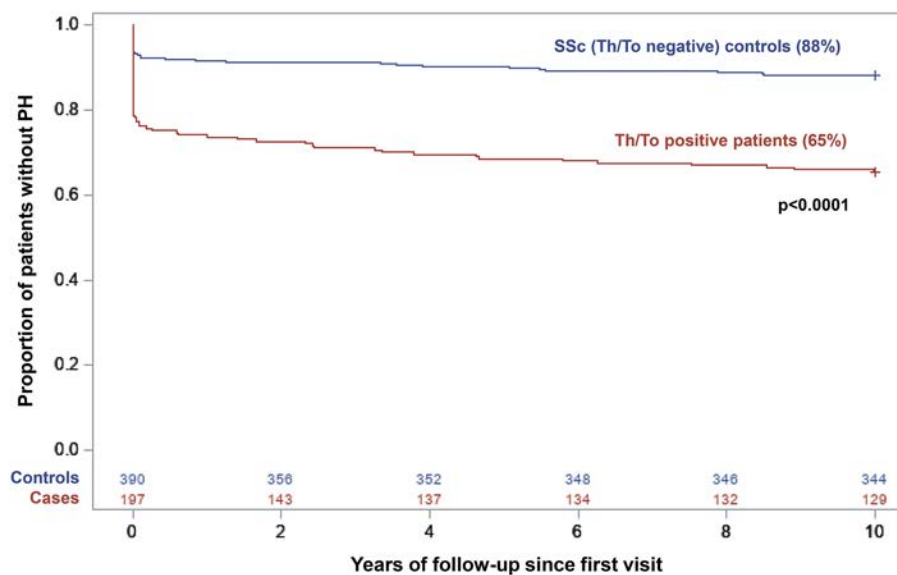


Figure 2. Development of pulmonary hypertension (PH) over a 10-year follow-up period from the first scleroderma center visit. The number of patients with systemic sclerosis (SSc) at risk of developing PH is indicated at the bottom according to antibody status.

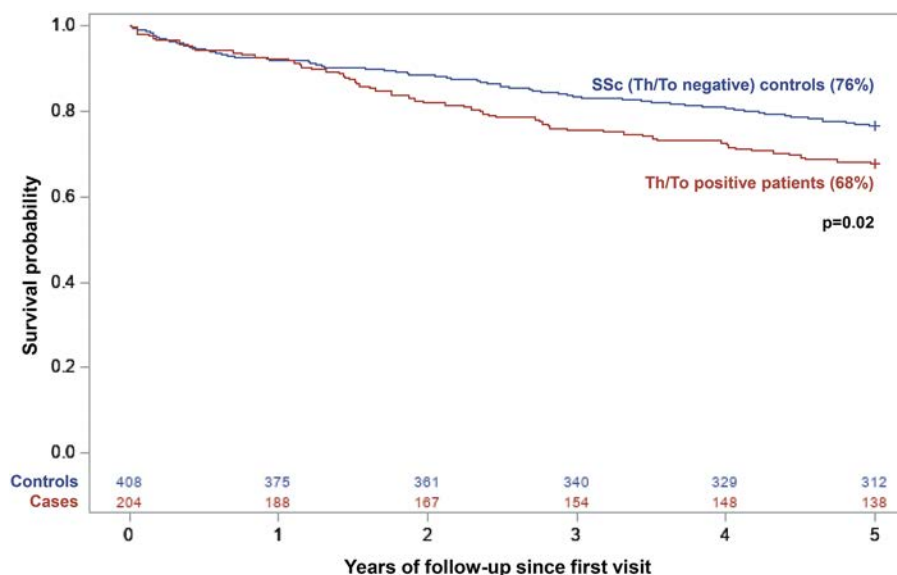


Figure 3. Lower five-year cumulative survival from the first scleroderma center visit in anti-Th/To antibody-positive systemic sclerosis (SSc) patients compared to anti-Th/To antibody-negative SSc patients as controls. The number of patients at risk of death is indicated at the bottom according to antibody status.

and 164 of 224 controls (73%) (Table 4). In both groups, most deaths were related to SSc: 61% of deaths among cases and 55% among controls were related to SSc. Overall, there was no difference in terms of the proportion of deaths attributed to SSc-related and non-SSc-related causes between the groups ($P = 0.3$). The most frequent cause of death in anti-Th/To antibody-positive patients was PH (28%), and the most frequent cause of death in controls was pulmonary fibrosis (18%).

DISCUSSION

In the current study, we report the clinical characteristics of 204 SSc patients with anti-Th/To antibody positivity, compared to 408 temporally matched SSc patients without this antibody, in long-term follow-up. We showed that, as compared to SSc patients with other antibodies, patients with anti-Th/To antibody-positive disease have a significantly higher risk of developing PH of any WHO group PH classification in long-term follow-up. This is

of seminal importance, as over one-third of all anti-Th/To-positive patients developed PH in long-term follow-up. These findings are relevant, as Th/To antibody testing using immunoprecipitation, as we have done here, is now commercially available.

Recently, several SSc studies have described anti-Th/To antibody frequency in various populations. The incidence of anti-Th/To antibody positivity ranged from 2% to 8% in studies in SSc patients who were American, Algerian, or Han Chinese (29-31). A study comparing a total of 260 SSc patients who were African Brazilian or White Brazilian showed a higher proportion of anti-Th/To positivity among White Brazilian patients (5% compared to 2% of African Brazilian patients) that was not statistically significant (32). Thus, anti-Th/To antibody positivity occurs in a small proportion of SSc patients worldwide, except for its potential rarity or absence in Subsaharan Africa (33) and the Hispanic populations of Central and South America (not yet studied). Overall, in 35 years of new patient visits in Pittsburgh, 5% of SSc patients were identified as having anti-Th/To antibody positivity.

Higher frequencies of ILD have been observed in anti-Th/To antibody-positive patients compared to controls in prior studies (11,12). In these studies, the controls used for comparison were ACA-positive patients, and the frequencies of ILD were 48% in anti-Th/To antibody-positive patients and 13% in ACA-positive patients, compared to 38% and 5% of controls, respectively. These results were expected, as multiple studies have shown lower rates of ILD in ACA-positive SSc patients (34,35). We confirmed this finding in long-term follow-up, since the cumulative frequency of ILD (on imaging) in our population was 54% in anti-Th/To antibody-positive patients and 39% in controls. However, there was no difference in terms of ILD severity as assessed by Medsger severity scores between groups.

Table 4. Incidence and causes of death in anti-Th/To antibody-positive SSc cases compared to anti-Th/To antibody-negative SSc controls*

Cause of death	Cases (n = 101)	Controls (n = 164)
SSc-related	62 (61)	90 (55)
Non-SSc-related	39 (39)	74 (45)

* Systemic sclerosis (SSc)-related causes of death included pulmonary hypertension, fibrosis, SSc-related kidney disease, heart disease, kidney/heart disease combined, SSc-related gastrointestinal disease, and other SSc-related causes of death. Non-SSc-related causes of death included cancer, sudden death, atherosclerotic heart disease, infection, vasculitis, central nervous system disease, other non-SSc-related causes of death, and unknown.

The finding of an ~5-fold increased risk of anti-Th/To-positive patients developing PAH within 10 years of their first SSc symptom is noteworthy. The increased risk is consistent with our previous shorter-term follow-up of anti-Th/To-positive patients (11), which demonstrated higher frequencies of PAH in anti-Th/To antibody-positive patients. In that study, the comparator group was ACA-positive patients, although ACA positivity has been associated with PAH risk in the literature (36). Higher frequencies of PAH or PH have not been reported in other case series of anti-Th/To antibody-positive patients, although the numbers of patients included in these studies were small (12,37). Thus, our finding indicating an ~3-fold increased risk of Th/To-positive patients developing PH of any WHO classification (groups 1, 2, or 3) at 10 years of follow-up compared to other SSc patients is a new observation. What is of highest clinical relevance is the high rate of over one-third of anti-Th/To-positive patients (37%) developing some type of PH over the long-term follow-up. As our mean clinical follow-up period was only 6 years, it is likely that a longer-term follow-up period would reveal an even higher rate of PH among these patients.

We also found lower rates of skeletal muscle and joint/tendon involvement in anti-Th/To antibody-positive SSc patients compared to other SSc patients. Lower rates of esophageal involvement were also described in earlier studies (11,37). In this study, we found similar rates of GI involvement in both groups, although higher GI severity scores were less frequently observed in anti-Th/To-positive patients. Renal crisis occurred in 3% of anti-Th/To-positive patients, but this was less frequent than that observed in controls in long-term follow-up (10%). This differs from the prior Pittsburgh case series (11), perhaps related to the ACA-positive control group, whose risk of scleroderma renal crisis is well known to be very low. Other small case series have not demonstrated increased frequencies of renal crisis.

Of note, only 5 of 204 anti-Th/To-positive patients (2.5%) developed diffuse skin involvement. Thus, the overwhelming majority of anti-Th/To antibody-positive patients have limited or no skin involvement, consistent with other case series (12,37).

Finally, we reported lower 5-year cumulative survival from the first SSc visit in anti-Th/To antibody-positive patients compared to controls, which persisted after adjusting for age and sex. Due to a significant difference in disease duration at first visit, survival from first SSc visit was analyzed from the first visit rather than from symptom onset. This is consistent with prior research suggesting reduced survival rates in anti-Th/To antibody-positive patients (11). The most frequent SSc-associated causes of death in anti-Th/To antibody-positive patients and control patients were PH and ILD, which is consistent with recent studies of causes of death in SSc (14,15). Although not statistically significant, there were more PH-related causes of death in the anti-Th/To group compared to controls, as would be expected given the higher frequency of PH, regardless of WHO grouping.

The primary strength of this study is the large number of anti-Th/To antibody-positive SSc patients with detailed long-term

follow-up data, by far the largest case series reported to date. Another strength is the use of RNA immunoprecipitation, the gold standard method to detect anti-Th/To antibodies. One limitation is that the cases were from a single tertiary care referral center, which may limit the generalizability of the results. Second, not all patients before 1995 had a diagnosis of PH identified by right-sided heart catheterization available for review. However, in all these cases, the diagnosis and WHO classification were confirmed by a physician at the University of Pittsburgh Medical Center Pulmonary Hypertension Center, and all patients had an estimated pulmonary arterial systolic pressure >45mm Hg at that time. Third, it is possible that patients with mild PH and PH secondary to ILD may have been overlooked in the first 15 years in which patients were included in this study, as both high-resolution CT and echocardiograms were not routinely available for screening during that time. However, these omissions should have occurred at similar rates in the case and control populations, given that cases were temporally matched to the next 2 consecutive SSc patients seen at the clinic. Finally, as we did not have CT scans or imaging dating back to 1980 for quantification, we relied on the Medsger severity scores to determine the severity of ILD rather than formal CT quantification scores.

In long-term follow-up, anti-Th/To-positive SSc patients have extremely high rates of developing PH, with an overall frequency of 37%, of which WHO Group 1 PAH occurred most frequently (23%). Anti-Th/To antibody-positive patients typically present with limited or no skin thickening and a nucleolar ANA pattern. Such patients should be tested for anti-Th/To antibodies and be vigilantly monitored for the development of PH and ILD.

AUTHOR CONTRIBUTIONS

All authors were involved in drafting the article or revising it critically for important intellectual content, and all authors approved the final version to be published. Dr. Domsic had full access to all of the data in the study and takes responsibility for the integrity of the data and the accuracy of the data analysis.

Study conception and design. Charlton, Snell, Medsger Jr, Domsic.

Acquisition of data. Suresh, Charlton, Snell, Laffoon, Medsger Jr, Domsic.

Analysis and interpretation of data. Suresh, Charlton, Medsger Jr, Zhu, Domsic.

ADDITIONAL DISCLOSURE

Author Snell is an employee of Northwest Permanente.




REFERENCES

1. Silver RM, Medsger TA Jr, Bolster MB. "Systemic sclerosis and scleroderma variants: clinical aspects." In: Koopman WJ, Moreland LW, editors. *Arthritis and allied conditions: a textbook of rheumatology*. 15th ed. Philadelphia: Lippincott Williams & Wilkins; 2005. p. 1633–80.

2. Domsic RT. Scleroderma: the role of serum autoantibodies in defining specific clinical phenotypes and organ system involvement. *Curr Opin Rheumatol* 2014;26:646–52.
3. Cepeda EJ, Reveille JD. Autoantibodies in systemic sclerosis and fibrosing syndromes: clinical indications and relevance. *Curr Opin Rheumatol* 2004;16:723–32.
4. Mehra S, Walker J, Patterson K, Fritzler MJ. Autoantibodies in systemic sclerosis. *Autoimmun Rev* 2013;12:340–54.
5. Kuwana M, Medsger TA Jr. “The clinical aspects of autoantibodies.” In: Varga J, Denton CP, Wigley FM, Allanore Y, Kuwana M, editors. *Scleroderma: from pathogenesis to comprehensive management*. 2nd ed. New York: Springer, 2017. p. 207–20.
6. Kuwana M, Kimura K, Hirakata M, Kawakami Y, Ikeda Y. Differences in autoantibody response to Th/To between systemic sclerosis and other autoimmune diseases. *Ann Rheum Dis* 2002;61:842–6.
7. Van Eenennaam H, Vogelzangs JH, Lugtenberg D, Van Den Hoogen FH, Van Venrooij WJ, Pruijn GJ. Identity of the RNase MRP- and RNase P-associated Th/To autoantigen. *Arthritis Rheum* 2002;46:3266–72.
8. Mahler M, Gascon C, Patel S, Ceribelli A, Fritzler MJ, Swart A, et al. Rpp25 is a major target of autoantibodies to the Th/To complex as measured by a novel chemiluminescent assay. *Arthritis Res Ther* 2013;15:R50.
9. Mahler M, Satoh M, Hudson M, Baron M, Chan JY, Chan EK, et al. Autoantibodies to the Rpp25 component of the Th/To complex are the most common antibodies in patients with systemic sclerosis without antibodies detectable by widely available commercial tests. *J Rheumatol* 2014;41:1334–43.
10. Okano Y, Medsger TA Jr. Autoantibody to Th ribonucleoprotein (nucleolar 7–2 RNA protein particle) in patients with systemic sclerosis. *Arthritis Rheum* 1990;33:1822–8.
11. Mitri GM, Lucas M, Fertig N, Steen VD, Medsger TA Jr. A comparison between anti-Th/To- and anticentromere antibody-positive systemic sclerosis patients with limited cutaneous involvement. *Arthritis Rheum* 2003;48:203–9.
12. Ceribelli A, Cavazzana I, Franceschini F, Airò P, Tincani A, Cattaneo R, et al. Anti-Th/To are common antinucleolar autoantibodies in Italian patients with scleroderma. *J Rheumatol* 2010;37:2071–5.
13. Poormoghim H, Lucas M, Fertig N, Medsger TA Jr. Systemic sclerosis sine scleroderma: demographic, clinical, and serologic features and survival in forty-eight patients. *Arthritis Rheum* 2000;43:444–51.
14. Nihtyanova SI, Tang EC, Coghlan JG, Wells AU, Black CM, Denton CP. Improved survival in systemic sclerosis is associated with better ascertainment of internal organ disease: a retrospective cohort study. *QJM* 2010;103:109–15.
15. Steen VD, Medsger TA. Changes in causes of death in systemic sclerosis, 1972–2002. *Ann Rheum Dis* 2007;66:940–4.
16. Graf SW, Hakendorf P, Lester S, Patterson K, Walker JG, Smith MD, et al. South Australian Scleroderma Register: autoantibodies as predictive biomarkers of phenotype and outcome. *Int J Rheum Dis* 2012;15:102–9.
17. Cabrera CM, Fernández-Grande E, Urra JM. Serological profile and clinical features of nucleolar antinuclear pattern in patients with systemic lupus erythematosus from southwestern Spain. *Lupus* 2016;25:980–7.
18. Hudson M, Satoh M, Chan JY, Tatibouet S, Mehra S, Baron M, et al. Prevalence and clinical profiles of ‘autoantibody-negative’ systemic sclerosis subjects. *Clin Exp Rheumatol* 2014;32 Suppl:S127–32.
19. Mierau R, Moinzadeh P, Riemekasten G, Melchers I, Meurer M, Reichenberger F, et al. Frequency of disease-associated and other nuclear autoantibodies in patients of the German Network for Systemic Scleroderma: correlation with characteristic clinical features. *Arthritis Res Ther* 2011;13:R172.
20. Van Praet JT, Van Steendam K, Smith V, De Bruyne G, Mimori T, Bonroy C, et al. Specific anti-nuclear antibodies in systemic sclerosis patients with and without skin involvement: an extended methodological approach. *Rheumatology (Oxford)* 2011;50:1302–9.
21. Rodriguez-Reyna TS, Hinojosa-Azaola A, Martinez-Reyes C, Nuñez-Alvarez CA, Torrico-Lavayen R, García-Hernández JL, et al. Distinctive autoantibody profile in Mexican Mestizo systemic sclerosis patients. *Autoimmunity* 2011;44:576–84.
22. Villalta D, Imbastaro T, Di Giovanni S, Lauriti C, Gabini M, Turi MC, et al. Diagnostic accuracy and predictive value of extended autoantibody profile in systemic sclerosis. *Autoimmun Rev* 2012;12:114–20.
23. Wielosz E, Dryglewska M, Majdan M. Serological profile of patients with systemic sclerosis. *Postepy Hig Med Dosw (Online)* 2014;68:987–91.
24. Simonneau G, Montani D, Celermajer DS, Denton CP, Gatzoulis MA, Krowka M, et al. Haemodynamic definitions and updated clinical classification of pulmonary hypertension [review]. *Eur Respir J*. 2019;53:1801913.
25. Van den Hoogen F, Khanna D, Fransen J, Johnson SR, Baron M, Tyndall A, et al. 2013 classification criteria for systemic sclerosis: an American College of Rheumatology/European League Against Rheumatism collaborative initiative. *Arthritis Rheum* 2013;65:2737–47.
26. Kao AH, Lacomis D, Lucas M, Fertig N, Oddis CV. Anti-signal recognition particle autoantibody in patients with and patients without idiopathic inflammatory myopathy. *Arthritis Rheum* 2004;50:209–15.
27. Doré A, Lucas M, Ivanco D, Medsger TA Jr, Domsic RT. Significance of palpable tendon friction rubs in early diffuse cutaneous systemic sclerosis. *Arthritis Care Res (Hoboken)* 2013;65:1385–9.
28. Medsger TA Jr, Bombardieri S, Czirjak L, Scorza R, Della Rossa A, Bencivelli W. Assessment of disease severity and prognosis. *Clin Exp Rheumatol* 2003;21 Suppl:S42–6.
29. Mecoli CA, Adler BL, Yang Q, Hummers LK, Rosen A, Casciola-Rosen L, et al. Cancer in systemic sclerosis: analysis of antibodies against components of the Th/To complex. *Arthritis Rheumatol* 2021;73:315–23.
30. Tahiat A, Allam I, Abdessamed A, Mellal Y, Nebbab R, Ladjouze-Rezig A, et al. Autoantibody profile in a cohort of Algerian patients with systemic sclerosis. *Ann Biol Clin (Paris)* 2020;78:126–33.
31. Liu C, Hou Y, Yang Y, Xu D, Li L, Li J, et al. Evaluation of a commercial immunoassay for autoantibodies in Chinese Han systemic sclerosis population. *Clin Chim Acta* 2019;491:121–5.
32. Mendes C, Viana VS, Pasoto SG, Leon EP, Bonfa E, Sampaio-Barros PD. Clinical and laboratory features of African-Brazilian patients with systemic sclerosis. *Clin Rheumatol* 2020;39:9–17.
33. Erzer JN, Jaeger VK, Tikly M, Walker UA. Systemic sclerosis in sub-Saharan Africa: a systematic review. *Pan Afr Med J* 2020;37:176.
34. Nihtyanova SI, Schreiber BE, Ong VH, Rosenberg D, Moinzadeh P, Coghlan JG, et al. Prediction of pulmonary complications and long-term survival in systemic sclerosis. *Arthritis Rheumatol* 2014;66:1625–35.
35. Cottin V, Brown KK. Interstitial lung disease associated with systemic sclerosis (SSc-ILD). *Respir Res* 2019;20:13.
36. Nunes JPL, Cunha AC, Meirinhos T, Nunes A, Araújo PM, Godinho AR, et al. Prevalence of auto-antibodies associated to pulmonary arterial hypertension in scleroderma – a review. *Autoimmun Rev* 2018;17:1186–201.
37. Hamaguchi Y, Hasegawa M, Fujimoto M, Matsushita T, Komura K, Kaji K, et al. The clinical relevance of serum antinuclear antibodies in Japanese patients with systemic sclerosis. *Br J Dermatol* 2008;158:487–95.

BRIEF REPORT

Performance of the 2017 European Alliance of Associations for Rheumatology/American College of Rheumatology Classification Criteria in Patients With Idiopathic Inflammatory Myopathy and Anti-Melanoma Differentiation-Associated Protein 5 Positivity

Ho So,¹  Jacqueline So,² Tommy Tsz-On Lam,² Victor Tak-Lung Wong,³ Roy Ho,⁴ Wai Ling Li,⁵ Chi Chiu Mok,⁶  Chak Sing Lau,⁷ and Lai-Shan Tam¹ 

Objective. This study aimed to evaluate whether the 2017 European Alliance of Associations for Rheumatology (EULAR)/American College of Rheumatology (ACR) classification criteria for adult and juvenile idiopathic inflammatory myopathies (IIMs) could appropriately classify the diagnosis in adult patients with anti-melanoma differentiation-associated protein 5 (anti-MDA-5)-positive IIM. In addition, this study sought to determine whether a status of anti-MDA-5 positivity could be incorporated into the EULAR/ACR IIM classification criteria set and whether the recently modified criteria based on the presence of myositis-specific autoantibodies (MSAs) could be used to appropriately classify the diagnosis in patients with anti-MDA-5-positive IIM.

Methods. Consecutive adult patients clinically diagnosed as having anti-MDA-5-positive IIM from 10 hospitals in Hong Kong were retrospectively recruited; patient characteristics were obtained from electronic medical records. We used a commercial line blot immunoassay to detect MSAs. We also determined a proposed set of phenotypic-serologic classification criteria specific for anti-MDA-5.

Results. In the patient cohort ($n = 120$; 31.7% with dermatomyositis, 68.3% with clinically amyopathic dermatomyositis [CADM]), the diagnosis could be classified with the EULAR/ACR criteria in 86 patients (71.7%) and with the Bohan and Peter criteria in 49 patients (40.8%). However, when combined with criteria specifically modified for CADM, the diagnosis could be classified by the Bohan and Peter criteria in 76.7% of patients. We observed that the sensitivity of the EULAR/ACR criteria could be improved to 98.3% if anti-MDA-5 antibody-positive status was considered as one of the criteria. The MSA-based criteria had 100% sensitivity. When we applied our proposed specific phenotypic-serologic criteria for the classification of patients with anti-MDA-5 antibodies, 97.5% of patients were able to be classified as having IIM.

Conclusion. In this cohort of patients with anti-MDA-5-positive IIM, the diagnosis could not be classified by the EULAR/ACR criteria in almost 30% of patients. We suggest incorporating anti-MDA-5 antibody positivity as a criterion into existing criteria sets or developing specific criteria for patients with anti-MDA-5-positive IIM.

INTRODUCTION

Since Bohan and Peter first described their criteria for idiopathic inflammatory myopathy (IIM) in 1975, the field has

evolved tremendously (1). In addition to typical dermatomyositis (DM) and polymyositis (PM), a subset of patients with the hallmark skin manifestations but no clinically significant muscle involvement has been recognized; this type of presentation has been named

Supported by the Hong Kong Society of Rheumatology Project Fund 2019.
¹Ho So, MBBS, FRCP, FHKAM, MSc, Lai-Shan Tam, MBChB, FRCP, FHKAM, MD: The Chinese University of Hong Kong, Hong Kong; ²Jacqueline So, MBChB, MRCP, Tommy Tsz-On Lam, MBBS, MRCP: The Prince of Wales Hospital, Hong Kong; ³Victor Tak-Lung Wong, MBChB, FHKAM: Kwong Wah Hospital, Hong Kong; ⁴Roy Ho, MBBS, FHKAM: Queen Elizabeth Hospital, Hong Kong; ⁵Wai Ling Li, MBBS, FHKAM: Queen Mary Hospital, Hong Kong; ⁶Chi Chiu Mok, MBBS, FRCP, FHKAM, MD: Tuen Mun Hospital, Hong Kong; ⁷Chak Sing Lau, MBChB, FRCP, FHKAM: The University of Hong Kong, Hong Kong.

Author disclosures are available at <https://onlinelibrary.wiley.com/action/downloadSupplement?doi=10.1002%2Fart.42150&file=art42150-sup-0001-Disclosureform.pdf>.

Address correspondence to Chak Sing Lau, MBChB, FRCP, FHKAM, Department of Medicine, The University of Hong Kong, Hong Kong (email: cslau@hku.hk); or to Lai-Shan Tam, MBChB, FRCP, FHKAM, MD, Department of Medicine and Therapeutics, The Chinese University of Hong Kong, Hong Kong (email: lstam@cuhk.edu.hk).

Submitted for publication November 15, 2021; accepted in revised form April 19, 2022.

as “clinically amyopathic dermatomyositis” (CADM) (2). Over 10 myositis-specific autoantibodies (MSAs) have so far been identified; these MSAs can be specific, mutually exclusive, and associated with distinct clinical features. The use of MSAs can potentially allow the categorization of patients into homogeneous subgroups and thus better inform prognosis (3).

The long-awaited European Alliance of Associations for Rheumatology (EULAR)/American College of Rheumatology (ACR) classification criteria for adult and juvenile idiopathic inflammatory myopathies (IIMs) were published in 2017 (4). The internal cross-validation showed that the 2017 EULAR/ACR classification criteria had better sensitivity and specificity than the Bohan and Peter criteria. Because external validation in other populations was advised by the authors of the EULAR/ACR criteria, Casal-Dominguez et al recently devised a set of MSA-based classification criteria that demonstrated perfect sensitivity and specificity in the internal validation cohorts (5).

Patients with IIM and positive for anti-melanoma differentiation-associated protein 5 (anti-MDA-5) can have rapidly progressive interstitial lung disease (RP-ILD) and high rates of mortality (6). Ulceration at sites of Gottron’s papules, digital pulps, and elbows together with palmar papules are the cardinal cutaneous features of anti-MDA-5-positive IIM (7). In this study, we aimed to examine the performance of the 2017 EULAR/ACR IIM classification criteria in a cohort of adult patients with anti-MDA-5-positive IIM, which is typically clinically amyopathic and more prevalent in East Asia (8). Various modifications of the existing criteria and the recently developed MSA-based criteria from Casal-Dominguez et al were also evaluated. In view of the unique phenotypic presentation of patients with anti-MDA-5-positive IIM, we also proposed and evaluated a specific set of phenotypic-serologic criteria for “anti-MDA-5 syndrome.”

METHODS

Study design and patients. This was a multicenter, retrospective cohort study conducted in Hong Kong. Ten regional hospitals participated in this study. Consecutive adult patients with anti-MDA-5-positive IIM were identified from the Hong Kong Myositis Registry and the Clinical Data Analysis and Reporting System (CDARS) from January 2015 to December 2020. The Hong Kong Myositis Registry is a territory-wide registry that was set up in 2019 to systematically collect clinical information on patients with IIM in Hong Kong. The CDARS is an electronic database created by the Hong Kong Hospital Authority and has been in operation since 1991 mainly for audit and research purpose. The CDARS has been extensively used in large-scale epidemiologic studies (9,10).

The diagnosis of anti-MDA-5-positive IIM had been based on the decision of the treating rheumatologists. Patients with juvenile-onset (age <18 years) myositis or with <50% of the required data available were excluded. We classified patients into subgroups of DM, PM, and CADM. As recently defined by

Table 1. Demographic and clinical characteristics of 120 patients with anti-MDA-5-associated IIM*

Female sex	66 (55.0)
Age at disease onset, mean ± SD years	52.7 ± 12.6
Smoker	10 (8.6) [†]
Ethnicity	
Chinese	117 (97.5)
Indonesian	2 (1.7)
Malaysian	1 (0.83)
Myositis subtype	
DM	38 (31.7)
CADM	82 (68.3)
PM	0 (0)
Time to diagnosis, mean ± SD days	85.9 ± 75.1
ILD	104 (86.7)
RP-ILD	49 (40.8)
Arthritis	73 (60.8)
Fever at presentation	58 (48.7) [‡]
Weight loss	43 (38.4) [§]
Hoarseness of voice	16 (13.3)
Leukoplakia	10 (8.3)
Infection at presentation, culture positive	28 (23.3)
Cutaneous features	
Gottron’s sign/papules	76 (63.3)
Cutaneous vasculitic rash/ulcers	57 (47.5)
Heliotrope rash	54 (45.0)
Periungual erythema	39 (32.5)
Periorbital edema	21 (17.5)
Mechanic’s hands	20 (16.7)
V sign	18 (15.0)
Shawl sign	16 (13.3)
Palmar papules	6 (5.0)
Raynaud’s phenomenon	2 (1.7)
Calcinosis	0 (0)
Dysphagia	16 (13.3)
Cardiac involvement	5 (4.2)
Malignancy	5 (4.2)

* Except where indicated otherwise, values are the number (%) of patients. Anti-MDA-5 = anti-melanoma differentiation-associated protein 5; IIM = idiopathic inflammatory myopathy; DM = dermatomyositis; CADM = clinically amyopathic dermatomyositis; PM = polymyositis; ILD = interstitial lung disease; RP-ILD = rapidly progressive interstitial lung disease.

[†] n = 116 patients.

[‡] n = 119 patients.

[§] n = 112 patients.

Sontheimer, patients could be classified as having CADM if they had the typical Gottron’s papules/signs or heliotrope rash (as determined by rheumatologists or dermatologists) but minimal or no clinical features of myositis (2). We used a commercial line blot immunoassay kit (EuroLine Autoimmune Inflammatory Myopathies 15 Ag; Euroimmun) to detect the MSAs.

We proposed a new set of phenotypic-serologic criteria specific for patients with anti-MDA-5-positive IIM (“anti-MDA-5 syndrome”), which included a positive serologic test for an anti-MDA-5 antibody plus one of the following conditions: IIM by the 2017 EULAR/ACR criteria, ILD, or typical rash (skin vasculitic rash/ulceration, palmar papules) determined by rheumatologists or dermatologists. We selected these characteristic features based on the pivotal studies by Fiorentino et al (7) and Sato et al (11).

Table 2. Agreement between the 2017 EULAR/ACR and Bohan and Peter classification criteria for IIMs*

	Bohan and Peter		Total
	No	Yes	
EULAR/ACR			
No	30	4	34
Yes	41	45	86
Total	71	49	120

* Results show number of patients with anti-melanoma differentiation-associated protein 5 antibodies who could be classified (yes) or not (no) as having idiopathic inflammatory myopathy (IIM) by the 2017 European Alliance of Associations for Rheumatology (EULAR)/American College of Rheumatology (ACR) classification criteria and by the Bohan and Peter criteria. Percent agreement between criteria was 62.5% (Cohen's kappa 0.31).

The strong associations between these characteristics and anti-MDA-5-positive IIM were later confirmed by meta-analyses (12,13).

Disease variables. All 10 participating hospitals used the same electronic patient record system for clinical information documentation, and all clinical data for our analyses were stored in this system. Clinical parameters required by the different criteria, as well as other clinical and demographic characteristics, were collected from the electronic patient record system by the investigators (HS, JS). ILD was diagnosed according to the presence of typical lung radiologic features of ILD on computed tomography or high-resolution computed tomography. RP-ILD was defined as evidence of worsening of ILD on imaging, progressive dyspnea, and hypoxemia within 1 month of onset of respiratory symptoms (14).

Statistical analysis. Descriptive statistics are presented as frequencies, mean \pm SD, or median with ranges as appropriate. Patients were dichotomized into none/possible and probable/definite IIM according to different criteria. We calculated the sensitivity of the criteria using the clinical judgment of the physician as the standard diagnosis. We measured correlations between the new and the old criteria by the percent agreement and Cohen's kappa. We used the Statistical Package for Social Sciences software, version 24.0 (SPSS), for statistical analysis.

RESULTS

Our cohort included 120 patients with anti-MDA-5-positive IIM who had a mean follow-up duration of 19.4 ± 21.6 months. Review of demographic and clinical characteristics showed a slight predominance of women in the cohort (55.0%) (Table 1). The mean \pm SD age at diagnosis was 52.7 ± 12.6 years, ranging from 21 to 88 years. Most patients (117 [97.5%] of 120 patients) were Chinese. Among patients in the cohort, 38 (31.7%) had

Table 3. Agreement between the 2017 EULAR/ACR classification criteria for IIMs and Bohan and Peter criteria for IIMs combined with Sontheimer's criteria for clinically amyopathic dermatomyositis*

	Bohan and Peter + Sontheimer		Total
	No	Yes	
EULAR/ACR			
No	25	9	34
Yes	3	83	86
Total	28	92	120

* Results show number of patients with anti-melanoma differentiation-associated protein 5 antibodies who could be classified (yes) or not (no) as having idiopathic inflammatory myopathy (IIM) by the 2017 European Alliance of Associations for Rheumatology (EULAR)/American College of Rheumatology (ACR) classification criteria and by the Bohan and Peter criteria with addition of the criteria for clinically amyopathic dermatomyositis (Sontheimer's criteria). Percent agreement between criteria was 90.0% (Cohen's kappa 0.74).

DM, 82 (68.3%) had CADM, and none had PM. The mean \pm SD time from onset of symptoms to diagnosis by physician was 85.9 ± 75.1 days. In addition to Gottron's sign/papules (63.3%) and heliotrope rash (45.0%), common cutaneous features in patients included vasculitic rash/ulceration (47.5%), periungual erythema (32.5%), periorbital edema (17.5%), and mechanic's hands (16.7%). Among patients in the cohort, 104 (86.7%) had ILD and 49 (40.8%) developed RP-ILD. Other common clinical manifestations in the patients included arthritis (60.8%), fever at presentation (48.7%), weight loss (38.4%), hoarseness of voice (13.3%), and leukoplakia (8.3%). Other complications included dysphagia (16 [13.3%] of 120 patients), cardiac involvement (5 [4.2%] of 120 patients), and malignancy (5 [4.2%] of 120 patients).

The 2017 EULAR/ACR classification criteria could classify 86 (71.7%) of 120 patients with definite/probable anti-MDA-5-positive IIM. The mean \pm SD summed performance score was 7.6 ± 3.3 , and median probability was 80% (range 3–100%). Of the 86 patients with definite/probable anti-MDA-5-positive IIM, 55 (64.0%) belonged to the CADM subtype, 27 (31.4%) belonged to the DM subtype, and 1 (1.2%) belonged to the PM subtype; subtypes of the remaining patients could not be determined. The Bohan and Peter criteria could only classify 40.8% of the patients as having definite/probable anti-MDA-5-positive IIM. However, when we combined the Bohan and Peter criteria with the criteria for CADM from Sontheimer, 76.7% of the patients were classified as having anti-MDA-5-positive IIM. In addition, with supplementation of the Bohan and Peter criteria with the Sontheimer criteria for CADM, the percent agreement between the EULAR/ACR and the Bohan and Peter criteria increased from 62.5% to 90.0%, with Cohen's kappa increasing from 0.31 to 0.74 (Table 2 and Table 3). Nevertheless, 25 (20.8%) of 120 patients remained unclassified by these established criteria. The common clinical features of these unclassified patients were ILD (88.0%), arthritis (56.0%), and ulcerative vasculitic rash or palmar papules

(24.0%). Some patients (6/25 unclassified patients; 24%) had elevated creatine kinase, but only 1 patient (4%) had clinical weakness.

After we substituted the criterion of anti-Jo-1 positivity in the 2017 EULAR/ACR classification criteria with the criterion of anti-MDA-5 positivity, the sensitivity of the 2017 EULAR/ACR classification criteria improved to 98.3%. The mean \pm SD performance score increased to 11.4 ± 3.3 and median probability to 99% (range 47–100%). The recently modified criteria from Casal-Dominguez et al, which includes an MSA-positive status, could identify all the patients in this cohort as having anti-MDA-5-positive IIM. However, our proposed phenotypic-serologic criteria could also classify 117 (97.5%) of the 120 patients as having anti-MDA-5 syndrome.

DISCUSSION

Classification criteria are designed mainly to group uniform and comparable subjects together for research. IIM is increasingly regarded as a group of very heterogeneous disorders and can be associated with severe extra-musculocutaneous complications. Patients with IIM and anti-MDA-5 antibody positivity present with characteristic clinical features. Anti-MDA-5 antibody is one of the most common MSAs identified in East Asian populations, with a study showing 14.9% of a cohort of 201 Hong Kong Chinese IIM patients having this MSA (15). Importantly, RP-ILD is a complication that often presents early in patients with anti-MDA-5-positive IIM and is associated with a high mortality rate. In a Japanese cohort of DM patients who had positive serologic findings for anti-MDA-5, 46% died within 6 months from disease onset due to respiratory failure (16). The early identification of anti-MDA-5-positive IIM is crucial so that timely treatment can be implemented in these patients. Accurate classification is also important for mechanistic, prognostic, and therapeutic research.

The 2017 EULAR/ACR IIM classification criteria for adult and juvenile idiopathic IIMs were data driven and developed in an international multidisciplinary collaboration. However, most patients in the development cohort were White, and patients without muscle involvement were underrepresented. Therefore, because of the typical clinically amyopathic phenotype in patients who are anti-MDA-5 antibody positive, we believe that the 2017 EULAR/ACR classification criteria required further evaluation, particularly in patients from East Asia. In our evaluation of the performance of the classification criteria in a cohort of adult patients with anti-MDA-5-positive IIM from Hong Kong, only 71.7% could be classified by the 2017 EULAR/ACR criteria and less than half of patients could be classified by the Bohan and Peter criteria. The poor results that we obtained with the Bohan and Peter criteria were likely because of its heavy reliance on muscle involvement, and we found that performance of the Bohan and Peter criteria improved after addition of the criteria for CADM. Nevertheless, with the existing 2017 EULAR/ACR IIM criteria, around 30% of

the patients with anti-MDA-5-positive IIM remained unclassified. Similarly, in a US cohort of 211 adult patients who had been diagnosed as having CADM by dermatologists, 26.3% did not meet the EULAR/ACR criteria (17). Unfortunately, the MSA status of the recruited patients in the US cohort was not available.

Because of its high specificity, we tested the effect of replacing anti-Jo-1 antibody with anti-MDA-5 while keeping the same score for the criterion (8). With this change, we found that the performance of the 2017 EULAR/ACR criteria greatly improved in classifying our study patients with anti-MDA-5-positive IIM, and only 2 patients (2.5%) could not be classified. We also tested the modified classification based on MSAs that was recently devised by Casal-Dominguez et al using data from 524 patients (5% anti-MDA-5 positive) (5). The modified criteria to classify patients with IIM, which includes presence of MSAs plus muscle weakness, elevated creatine kinase, ILD, arthritis, or Gottron's/heliotrope rash, were highly sensitive in our patient cohort, although the specificity remains to be examined as the modified criteria do not account for the hallmark cutaneous features.

Using a diagnostic criterion similar to that used by Connor et al (18) or Solomon et al (19) for antisynthetase syndrome, we proposed a specific set of phenotypic-serologic criteria for anti-MDA-5 syndrome in which a patient must have a serologic test indicating positivity for anti-MDA-5 antibody, plus one of the following conditions: IIM by the 2017 EULAR/ACR criteria, ILD, or typical rash (skin vasculitic rash/ulceration, palmar papules), as determined by rheumatologists or dermatologists. We found that the criteria had an excellent inclusion performance. However, external validation is required. Further studies could determine whether the proposed criteria could hasten the diagnosis and subsequent management of this potentially life-threatening disease.

This study has some limitations. First, despite the increasing popularity, the line blot immunoassay has not been fully validated. Two studies comparing the line blot immunoassay technique to immunoprecipitation for the detection of anti-MDA-5 showed good agreement between the 2 methods (20,21). Second, selection bias may have occurred. Patients with DM who were solely followed up by dermatologists or who had significant disability prohibiting their clinical visits were underrepresented. Third, because of our study's retrospective design, incomplete data collection was inevitable. Finally, the newly proposed criteria are not strictly data-driven, and the specificity of the criteria could not be assessed due to the lack of a control group.

In conclusion, in a cohort of patients with anti-MDA-5-positive IIM, although the recent 2017 EULAR/ACR classification criteria apparently outperformed the traditional Bohan and Peter criteria, it did not classify the diagnosis in almost 30% of the patients. Incorporating a status of anti-MDA-5 antibody positivity into the 2017 EULAR/ACR classification criteria, using a generic MSA-based classification method, or adopting a specific phenotypic-serologic approach to diagnosing anti-MDA-5

syndrome greatly improved our ability to classify patients as having anti-MDA-5-positive IIM.

AUTHOR CONTRIBUTIONS

All authors were involved in drafting the article or revising it critically for important intellectual content, and all authors approved the final version to be published. Dr. H. So had full access to all of the data in the study and takes responsibility for the integrity of the data and the accuracy of the data analysis.

Study conception and design. H. So, Lam, Mok, Tam.



Acquisition of data. H. So, J. So, Lam, Wong, Ho, Li, Lau, Mok, Tam.

Analysis and interpretation of data. H. So.

REFERENCES

- Bohan A, Peter JB. Polymyositis and dermatomyositis (first of two parts). *N Engl J Med* 1975;292:344–7.
- Sontheimer RD. Clinically amyopathic dermatomyositis: what can we now tell our patients? *Arch Dermatol* 2010;146:76–80.
- Betteridge Z, McHugh N. Myositis-specific autoantibodies: an important tool to support diagnosis of myositis. *J Intern Med* 2016;280:8–23.
- Lundberg IE, Tjærnlund A, Bottai M, Werth VP, Pilkington C, de Visser M, et al. 2017 European League Against Rheumatism/American College of Rheumatology classification criteria for adult and juvenile idiopathic inflammatory myopathies and their major subgroups. *Arthritis Rheumatol* 2017;69:2271–82.
- Casal-Dominguez M, Pinal-Fernandez I, Pak K, Huang W, Selva-O'Callaghan A, Albayda J, et al. Performance of the 2017 European Alliance of Associations for Rheumatology/American College of Rheumatology classification criteria for idiopathic inflammatory myopathies in patients with myositis-specific autoantibodies. *Arthritis Rheumatol* 2022;74:508–17.
- Gono T, Sato S, Kawaguchi Y, Kuwana M, Hanaoka M, Katsumata Y, et al. Anti-MDA5 antibody, ferritin and IL-18 are useful for the evaluation of response to treatment in interstitial lung disease with anti-MDA5 antibody-positive dermatomyositis. *Rheumatology (Oxford)* 2012;51:1563–70.
- Fiorentino D, Chung L, Zwerner J, Rosen A, Casciola-Rosen L. The mucocutaneous and systemic phenotype of dermatomyositis patients with antibodies to MDA5 (CADM-140): a retrospective study. *J Am Acad Dermatol* 2011;65:25–34.
- So H, Ip RW, Wong VT, Yip RM. Analysis of anti-melanoma differentiation-associated gene 5 antibody in Hong Kong Chinese patients with idiopathic inflammatory myopathies: diagnostic utility and clinical correlations. *Int J Rheum Dis* 2018;21:1076–81.
- Chiu SS, Lau YL, Chan KH, Wong WH, Peiris JS. Influenza-related hospitalizations among children in Hong Kong. *N Engl J Med* 2002;347:2097–103.
- So H, Mak JW, So J, Lui G, Lun F, Lee J, et al. Incidence and clinical course of COVID-19 in patients with rheumatologic diseases: a population-based study. *Sem Arthritis Rheum* 2020;50:885–9.
- Sato S, Hoshino K, Satoh T, Fujita T, Kawakami Y, Fujita T, et al. RNA helicase encoded by melanoma differentiation-associated gene 5 is a major autoantigen in patients with clinically amyopathic dermatomyositis: association with rapidly progressive interstitial lung disease. *Arthritis Rheum* 2009;60:2193–200.
- Li J, Liu Y, Li Y, Li F, Wang K, Pan W, et al. Associations between anti-melanoma differentiation-associated gene 5 antibody and demographics, clinical characteristics and laboratory results of patients with dermatomyositis: a systematic meta-analysis. *J Dermatol* 2018;45:46–52.
- Chen Z, Cao M, Plana MN, Liang J, Cai H, Kuwana M, et al. Utility of anti-melanoma differentiation-associated gene 5 antibody measurement in identifying patients with dermatomyositis and a high risk for developing rapidly progressive interstitial lung disease: a review of the literature and a meta-analysis. *Arthritis Care Res (Hoboken)* 2013;65:1316–24.
- Sato S, Hoshino K, Satoh T, Fujita T, Kawakami Y, Fujita T, et al. RNA helicase encoded by melanoma differentiation-associated gene 5 is a major autoantigen in patients with clinically amyopathic dermatomyositis: association with rapidly progressive interstitial lung disease. *Arthritis Rheum* 2009;60:2193–200.
- Wong VT, So H, Lam TT, Yip RM. Myositis-specific autoantibodies and their clinical associations in idiopathic inflammatory myopathies. *Acta Neurol Scand* 2021;143:131–9.
- Nakashima R, Imura Y, Kobayashi S, Yukawa N, Yoshifuji H, Nojima T, et al. The RIG-I-like receptor IFIH1/MDA5 is a dermatomyositis-specific autoantigen identified by the anti-CADM-140 antibody. *Rheumatology (Oxford)* 2010;49:433–40.
- Patel B, Khan N, Werth VP. Applicability of EULAR/ACR classification criteria for dermatomyositis to amyopathic disease. *J Am Acad Dermatol* 2018;79:77–83.
- Connors GR, Christopher-Stine L, Oddis CV, Danoff SK. Interstitial lung disease associated with the idiopathic inflammatory myopathies: what progress has been made in the past 35 years? *Chest* 2010;138:1464–74.
- Solomon J, Swigris JJ, Brown KK. Myositis-related interstitial lung disease and antisynthetase syndrome. *J Bras Pneumol* 2011;37:100–9.
- Cavazzana I, Fredi M, Ceribelli A, Mordenti C, Ferrari F, Carabellese N, et al. Testing for myositis specific autoantibodies: comparison between line blot and immunoprecipitation assays in 57 myositis sera. *J Immunol Methods* 2016;433:1–5.
- Tansley SL, Li D, Betteridge ZE, McHugh NJ. The reliability of immunoassays to detect autoantibodies in patients with myositis is dependent on autoantibody specificity. *Rheumatology* 2020;59:2109–14.

Evaluation of the Relationship Between Serum Urate Levels, Clinical Manifestations of Gout, and Death From Cardiovascular Causes in Patients Receiving Febuxostat or Allopurinol in an Outcomes Trial

Kenneth G. Saag,¹  Michael A. Becker,² William B. White,³ Andrew Whelton,⁴ Jeffrey S. Borer,⁵ Philip B. Gorelick,⁶ Barbara Hunt,⁷ Majin Castillo,⁷ and Lhanoo Gunawardhana,⁷  on behalf of the CARES Investigators

Objective. To investigate whether serum urate levels, number of gout flares, and tophi burden are related to death from cardiovascular (CV) causes after treatment with febuxostat or allopurinol in patients with gout from the Cardiovascular Safety of Febuxostat or Allopurinol in Patients With Gout and Cardiovascular Comorbidities (CARES) trial.

Methods. Patients were randomly assigned to receive febuxostat (40 mg or 80 mg once daily, according to serum urate levels at week 2) or allopurinol titrated in 100-mg increments from 200–400 mg or 300–600 mg (with dose determined according to kidney function). Changes from baseline in serum urate level, gout flares, and tophus resolution were key exploratory efficacy parameters in the overall population and in subgroups of patients who died and those who did not die from a CV-related cause. The latter subgroup included patients who died due to non-CV causes and those who did not die due to any cause.

Results. Patients received treatment with febuxostat (n = 3,098) or allopurinol (n = 3,092) for a median follow-up period of 32 months (for a maximum of 85 months). In the overall population, mean serum urate levels were lower in those receiving febuxostat compared with those receiving allopurinol at most study visits. There were no associations between serum urate levels and death from CV causes with febuxostat. The number of gout flares requiring treatment was higher within 1 year of treatment with febuxostat compared with allopurinol (mean incidence of gout flares per patient-years of exposure 1.33 versus 1.20), but was comparable thereafter and decreased overall throughout the study period (mean incidence of gout flares per patient-years of exposure 0.35 versus 0.34 after 1 year of treatment; overall mean incidence 0.68 versus 0.63) irrespective of whether the patient died from a CV-related cause. Overall, 20.8% of patients had ≥ 1 tophus at baseline; tophus resolution rates were similar between treatment groups, with cumulative resolution rates of $>50\%$.

Conclusion. In the CARES trial, febuxostat and allopurinol (≤ 600 mg doses) had comparable efficacy in patients with gout and CV disease, and there was no evidence of a relationship between death from CV causes and serum urate levels, number of gout flares, or tophus resolution among the patients receiving febuxostat.

INTRODUCTION

Gout is the most common form of inflammatory arthritis, affecting an estimated 9.2 million adults in the US (1). Development of hyperuricemia, defined as elevated serum urate levels above the limit of urate solubility (~ 6.8 mg/dl), is an important prerequisite for the development of gout (2,3).

There is a high incidence of comorbidities, especially cardiovascular disease (CVD) and chronic kidney disease, associated with both hyperuricemia and gout (4,5). Several recent studies demonstrated an increased risk of CV events (including those leading to death) in patients with gout compared with those without (6–8). There is some evidence to suggest that high serum urate levels may be an independent predictive factor for CVD (8,9). Indeed, after

[ClinicalTrials.gov](https://clinicaltrials.gov/ct2/show/study/NCT01101035): NCT01101035.

Supported by Takeda Development Center Americas, Inc.

¹Kenneth G. Saag, MD, MSc: University of Alabama at Birmingham; ²Michael A. Becker, MD: University of Chicago Pritzker School of Medicine, Chicago, Illinois; ³William B. White, MD: Cardiology Center, University of Connecticut School of Medicine, Farmington; ⁴Andrew Whelton, MD, FACP: Johns Hopkins University, Baltimore, Maryland; ⁵Jeffrey S. Borer, MD: State University of New York Downstate University of the Health Sciences, Brooklyn, New York; ⁶Philip B. Gorelick, MD, MPH, FACP: Davee Department of Neurology, Northwestern University Feinberg School of Medicine, Chicago, Illinois;

⁷Barbara Hunt, MS, Majin Castillo, MD, Lhanoo Gunawardhana, MD, PhD: Takeda Development Center Americas, Inc., Lexington, Massachusetts.

Author disclosures are available at <https://onlinelibrary.wiley.com/action/downloadSupplement?doi=10.1002%2Fart.42160&file=art42160-sup-0001-Disclosureform.pdf>.

Address correspondence to Kenneth G. Saag, MD, MSc, University of Alabama at Birmingham, Birmingham, AL 35233. Email: ksaag@uabmc.edu.

Submitted for publication May 17, 2021; accepted in revised form May 4, 2022.

adjusting for other risk factors (including age, sex, smoking status, alcohol consumption, body weight, blood pressure, history of CVD, kidney function, and plasma glucose levels), serum urate levels were still strongly associated with death from all causes, including CVD (9). However, contrary to findings from these epidemiologic studies, data from Mendelian randomization studies do not support a consistent causal role of serum urate in CVD (10,11). Therefore, the relationship between serum urate levels and death from CV causes remains to be determined (12,13).

The mainstay of chronic gout management is reduction of serum urate levels and maintenance of these levels at <6.0 mg/dl (14–16). The urate-lowering xanthine oxidase inhibitors are considered first-line pharmacologic therapy for hyperuricemia in patients with gout (13–16). Currently, allopurinol and febuxostat are the only available xanthine oxidase inhibitors.

The Cardiovascular Safety of Febuxostat or Allopurinol in Patients With Gout and Cardiovascular Comorbidities (CARES) trial (ClinicalTrials.gov identifier: NCT01101035) examined rates of major CV events in patients with gout and CVD who received treatment with febuxostat or allopurinol (17). The CARES trial has the longest study duration (median follow-up period of 32 months), and largest data set ($n = 6,190$) of any randomized controlled trial comparing febuxostat with allopurinol. In this study, the proportion of patients with the primary end point (a composite of cardiovascular death, nonfatal myocardial infarction, nonfatal stroke, and unstable angina with urgent revascularization) was noninferior between febuxostat and allopurinol. However, in the secondary end point analysis, the rate of death from CV causes was greater in patients who received treatment with febuxostat compared with patients who received treatment with allopurinol (4.3% and 3.2%, respectively; hazard ratio [HR] 1.34) (17). In addition, prespecified subgroup analyses were performed in order to investigate the potential effects of non-steroidal antiinflammatory drug (NSAID) use, since NSAIDs are known to be associated with CVD (18). These analyses found that both the use of NSAIDs and absence of low-dose aspirin at baseline were associated with death from CV causes (unadjusted $P < 0.05$ for both comparisons) (17). With the exception of NSAID use for gout flare prophylaxis and/or treatment, use of NSAIDs and low-dose aspirin were not systematically monitored during the study. In an additional analysis, all-cause mortality was higher with febuxostat treatment compared with allopurinol treatment (HR 1.22) as a result of an imbalance in the rates of death from CV causes (17).

The objective of this exploratory analysis was to evaluate data from the CARES trial to investigate if serum urate levels, gout flares, and tophi burden were associated with death from CV causes after febuxostat or allopurinol treatment.

PATIENTS AND METHODS

The CARES trial has been described previously (17,19). In brief, the CARES trial was a multicenter, randomized, double-blind trial designed to evaluate the CV safety and efficacy of

febuxostat compared with allopurinol in patients with gout and significant CV comorbidities.

Patients. Patients were men aged ≥ 50 years and women aged ≥ 55 years who had been postmenopausal for ≥ 2 years. Eligibility criteria included a history or presence of gout according to the American College of Rheumatology criteria (20), as well as a history of major CVD or cerebrovascular disease, including ≥ 1 of the following: myocardial infarction, cardiac or cerebrovascular revascularization, stroke, hospitalization for unstable angina or transient ischemic attack, peripheral vascular disease, or history of diabetes mellitus with evidence of microvascular disease or macrovascular disease. Patients had serum urate levels ≥ 7.0 mg/dl at screening, or ≥ 6.0 mg/dl at screening and inadequately controlled gout (i.e., the presence of flares and/or the presence of tophi in the 12 months prior to screening). Written informed consent was obtained from each patient in accordance with the Declaration of Helsinki and the International Council for Harmonisation Guidelines for Good Clinical Practice, and the study was conducted in accordance with all applicable laws and regulations. The appropriate national and institutional regulatory authorities and ethics committees approved the trial design.

Key exclusion criteria included myocardial infarction within 60 days prior to screening, secondary hyperuricemia, history of xanthinuria, known hypersensitivity to febuxostat or allopurinol, or an estimated creatinine clearance (CrCl) of <30 ml/minute using the Cockcroft-Gault formula.

Treatments and procedures. Eligible patients were randomly assigned in a 1:1 ratio to receive once-daily febuxostat or allopurinol. Patients randomized to receive febuxostat initially received 40 mg every day; patients with serum urate levels <6.0 mg/dl at the week 2 visit continued to receive the 40-mg dose for the remainder of the study. Patients with serum urate levels ≥ 6.0 mg/dl at week 2 received once-daily febuxostat (80 mg) at week 4 and continued to receive this dose for the remainder of the study. Patients who were randomized to receive allopurinol and who had normal renal function or mild renal impairment (estimated CrCl ≥ 60 ml/minute) initially received 300 mg of allopurinol daily, with the dose increased in 100-mg increments monthly until either the serum urate level was <6.0 mg/dl or a daily allopurinol dosage of 600 mg was achieved. Patients who had moderate renal impairment (estimated CrCl ≥ 30 but <60 ml/minute) initially received once-daily allopurinol (200 mg), with the dose increased in 100-mg increments monthly until either the serum urate level was <6.0 mg/dl or a daily allopurinol dosage of 400 mg was achieved.

For the first 6 months of the study, all patients received once-daily colchicine (0.6 mg) as gout flare prophylaxis. Alternatively, if once-daily 0.6 mg of colchicine was not tolerated by the patient, 0.6 mg every other day was permitted. If colchicine was not tolerated and the estimated CrCl was ≥ 50 ml/minute, naproxen was

Table 1. Baseline demographic and clinical characteristics of patients with gout in the modified intent-to-treat population*

	Overall		Patients who died from a CV-related cause		Patients who did not die from a CV-related cause†	
	Febuxostat (n = 3,098)	Allopurinol (n = 3,092)	Febuxostat (n = 134)	Allopurinol (n = 100)	Febuxostat (n = 2,964)	Allopurinol (n = 2,992)
Years since gout diagnosis, mean ± SD‡	11.8 ± 11.4	11.9 ± 11.2	11.5 ± 12.2	10.3 ± 11.5	11.8 ± 11.4	11.9 ± 11.2
Baseline serum urate level, mean ± SD mg/dl	8.7 ± 1.7	8.7 ± 1.7	9.3 ± 1.8	9.8 ± 1.9	8.7 ± 1.7	8.7 ± 1.7
Baseline serum urate category						
<7 mg/dl	412 (13.3)	436 (14.1)	8 (6.0)	5 (5.0)	404 (13.6)	431 (14.4)
7–<8 mg/dl	631 (20.4)	620 (20.1)	26 (19.4)	11 (11.0)	605 (20.4)	609 (20.4)
8–<9 mg/dl	735 (23.7)	759 (24.5)	26 (19.4)	19 (19.0)	709 (23.9)	740 (24.7)
9–<10 mg/dl	666 (21.5)	646 (20.9)	28 (20.9)	26 (26.0)	638 (21.5)	620 (20.7)
≥10 mg/dl	654 (21.1)	631 (20.4)	46 (34.3)	39 (39.0)	608 (20.5)	592 (19.8)
Months since last gout flare						
<1	1,017 (32.8)	978 (31.6)	47 (35.1)	42 (42.0)	970 (32.7)	936 (31.3)
1–<4	981 (31.7)	1,009 (32.6)	39 (29.1)	29 (29.0)	942 (31.8)	980 (32.8)
4–<6	311 (10.0)	353 (11.4)	14 (10.4)	9 (9.0)	297 (10.0)	344 (11.5)
6–<12	471 (15.2)	455 (14.7)	20 (14.9)	10 (10.0)	451 (15.2)	445 (14.9)
≥12	317 (10.2)	296 (9.6)	14 (10.4)	10 (10.0)	303 (10.2)	286 (9.6)
No. of gout flares in the past year						
1–3	1,880 (60.7)	1,842 (59.6)	77 (57.5)	56 (56.0)	1,803 (60.8)	1,786 (59.7)
4–6	544 (17.6)	544 (17.6)	25 (18.7)	17 (17.0)	519 (17.5)	527 (17.6)
>6	356 (11.5)	409 (13.2)	18 (13.4)	17 (17.0)	338 (11.4)	392 (13.1)
Presence of tophi	668 (21.6)	650 (21.0)	28 (20.9)	30 (30.0)	640 (21.6)	620 (20.7)
No. of tophi, mean ± SD	4.1 ± 10.2	4.2 ± 7.0	12.3 ± 39.6	5.3 ± 6.2	3.8 ± 6.3	4.1 ± 7.0
Renal function at baseline§						
Moderately impaired	1,636 (52.8)	1,631 (52.7)	93 (69.4)	78 (78.0)	1,543 (52.1)	1,553 (51.9)
Mildly impaired	1,217 (39.3)	1,231 (39.8)	34 (25.4)	19 (19.0)	1,183 (39.9)	1,212 (40.5)
Normal	239 (7.7)	228 (7.4)	6 (4.5)	3 (3.0)	233 (7.9)	225 (7.5)
Patients who received prior urate-lowering therapy	1,914 (61.8)	1,914 (61.9)	88 (65.7)	68 (68.0)	1,826 (61.6)	1,846 (61.7)

* Except where indicated otherwise, values are the number (%) of patients. CV = cardiovascular.

† Included patients who died due to non-CV causes and those who did not die due to any cause.

‡ Years are calculated according to the first double-blind dose of study drug.

§ Moderately impaired indicates an estimated creatinine clearance (CrCl) 30–59 ml/minute, mildly impaired indicates an estimated CrCl 60–89 ml/minute, and normal indicates an estimated CrCl ≥90 ml/minute. Seven patients had baseline estimated CrCl <30 ml/minute. One patient was missing baseline estimated CrCl measurements.

administered at a dose of 250 mg twice daily with 15 mg of once-daily lansoprazole. In instances when patients could not receive colchicine or naproxen, other NSAIDs or prednisone were provided at the investigator's discretion. In the event that colchicine, naproxen, other NSAIDs, proton-pump inhibitors, or prednisone were not tolerated or were contraindicated, the investigator could choose not to use prophylaxis but rather to manage gout flares as they occurred.

End points and assessments. In this analysis, key exploratory efficacy end points included changes from baseline in serum urate levels, gout flares, and tophus assessment. Effects on the efficacy end points were explored in post hoc analyses in patients who died from a CV-related cause and patients who did not die from a CV-related cause (i.e., the remainder of the study population, which included those who died due to non-CV causes and those who did not die due to any cause).

Clinic visits occurred on weeks 2, 4, 6, 8, and 10; months 3 and 6; and every 6 months thereafter. If a patient's serum urate

level was <6.0 mg/ml at week 4 or 8, then that patient would not be required to return to the study clinic until month 3. Clinical assessments, including those regarding gout flare assessment, serum urate measurements, tophus physical examination, vital signs, treatment compliance, and concomitant medication usage were performed at each visit.

Statistical analysis. Efficacy end points were assessed in the modified intent-to-treat (ITT) population, which included all randomized patients who received ≥ 1 dose of study medication. Demographic and baseline clinical characteristics and changes in efficacy parameters in the subgroup of patients who died from a CV-related cause and those who did not die from a CV-related cause are summarized.

Gout flare rate was stratified by post-baseline serum urate levels and was calculated as the number of flares from the end of the first year of treatment to the end of the study divided by the length of time on treatment during the period after the first year of treatment until the end of the study.

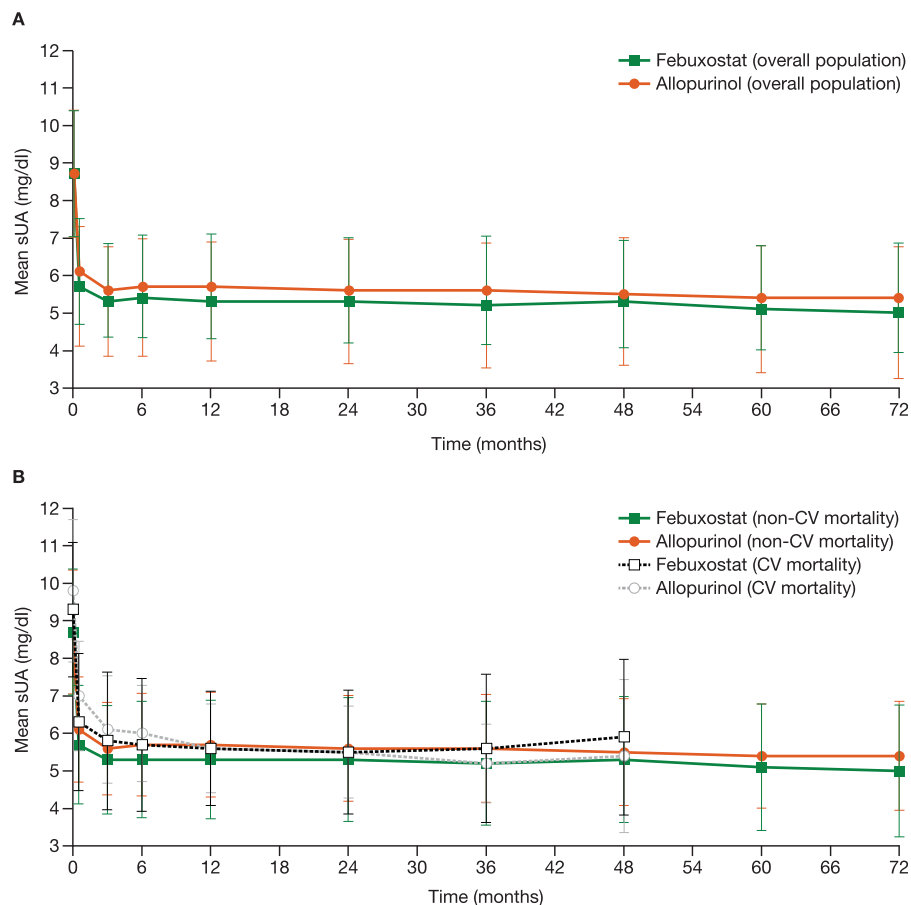


Figure 1. Change in mean serum urate (sUA) levels in patients receiving febxostat and those receiving allopurinol in the overall modified intent-to-treat (ITT) population (A) and in the subgroup of patients who died from a cardiovascular (CV)-related cause compared with patients who did not die from a CV-related cause (B). The modified ITT population comprised patients randomized to a treatment group who received ≥ 1 dose of study drug. Bars show the mean \pm SD. Patient numbers are summarized in Supplementary Table 2 (available on the *Arthritis & Rheumatology* website at <http://onlinelibrary.wiley.com/doi/10.1002/art.42160>). The number of patients in each subgroup who had serum urate (sUA) data at months 60 and 72 was too low ($n \leq 5$) to allow for meaningful interpretation of serum urate levels at these time points.

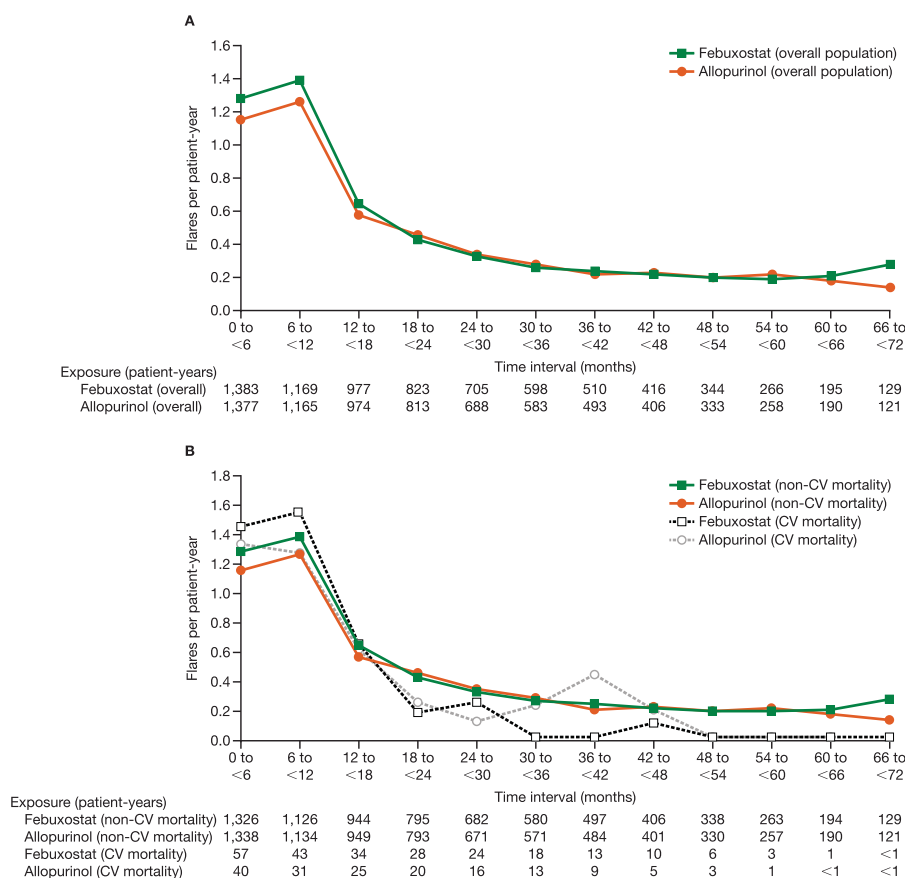


Figure 2. Gout flares requiring treatment among patients receiving febuxostat or allopurinol in the overall modified ITT population (A) and in the subgroup of patients who died from a CV-related cause compared with patients who did not die from a CV-related cause (B). The modified ITT population comprised patients who were randomized to a treatment group and received ≥ 1 dose of study drug. Symbols represent the mean number of gout flares per patient-years of exposure, with numbers of patient-years shown in the tables below the graphs. See Figure 1 for definitions.

Post hoc analyses for the relationship between treatment, death from CV causes, and on-treatment serum urate levels were performed using Cochran-Armitage test for trend. Reported *P* values are nominal and are not provided as indicators of statistical significance.

RESULTS

A total of 6,198 patients were enrolled and were randomized to receive either febuxostat or allopurinol in the CARES trial; of these, 8 patients did not receive treatment; therefore, 6,190 patients were included in the modified ITT population. Patients were randomized to receive treatment with febuxostat ($n = 3,098$) or allopurinol ($n = 3,092$). The median follow-up period was 32 months (maximum 85 months).

Baseline demographic and clinical characteristics have been described previously and were comparable between treatment arms (17). The study population was predominantly male (83.9%) and White (69.5%), the median (range) age was 65.0 (44–93) years, and the mean \pm SD body mass index was 33.5 ± 6.92 kg/m². The overall mean \pm SD serum urate level at

baseline was 8.7 ± 1.7 mg/dl; 20.8% of patients had a baseline serum urate level ≥ 10.0 mg/dl. Approximately 90% of patients in the CARES trial had experienced a gout flare within the year prior to study entry, and most patients (61.8%) previously received a urate-lowering therapy. In total, 21.3% of patients had a tophus or tophi at baseline (Table 1). Data regarding the disposition of patients have been previously reported (Supplementary Table 1, available on the *Arthritis & Rheumatology* website at <http://onlinelibrary.wiley.com/doi/10.1002/art.42160>) (17).

Death from CV causes subgroups were composed of patients in the CARES trial who died from a CV-related cause (febuxostat $n = 134$; allopurinol $n = 100$) and those who did not die from a CV-related cause (febuxostat $n = 2,964$; allopurinol $n = 2,992$) (see Table 1 for baseline demographic and clinical characteristics).

Relationship between serum urate levels and death from a CV-related cause. In the overall modified ITT population, baseline serum urate levels were comparable between the febuxostat treatment group (8.7 mg/dl, $n = 3,098$) and

Table 2. Incidence of gout flares among patients receiving febuxostat or allopurinol, by treatment duration and severity of flare*

	Febuxostat (n = 3,098)†			Allopurinol (n = 3,092)‡		
	Overall	≤1 year of treatment	>1 year of treatment	Overall	≤1 year of treatment	>1 year of treatment
All flares	0.68	1.33	0.35	0.63	1.20	0.34
Severe	0.20	0.40	0.09	0.17	0.32	0.09
Moderate	0.33	0.63	0.17	0.30	0.56	0.16
Mild	0.14	0.27	0.08	0.15	0.29	0.08

* The highest level of severity reported for the 4 symptoms collected for each flare (swelling, redness, tenderness, and joint warmth) was used to categorize the flare as mild, moderate, or severe. Values are the mean incidence of flares per patient-years of exposure. The total number of patients for each treatment group refers to the number at baseline.

† Per 7,574 patient-years of exposure.

‡ Per 7,455 patient-years of exposure.

allopurinol treatment group (8.7 mg/dl, n = 3,092) (Figure 1 and Supplementary Table 2, <http://onlinelibrary.wiley.com/doi/10.1002/art.42160>). However, after the first dose of study medication, serum urate levels in patients receiving febuxostat were nominally lower than in those receiving allopurinol at most study visits (week 2 and months 3, 6, 12, 24, 36, 48, 60, and 72). Baseline serum urate levels were higher in patients who died from a CV-related cause (febuxostat 9.3 mg/dl, n = 134; allopurinol 9.8 mg/dl, n = 100) than in those who did not die from a CV-related cause (8.7 mg/dl in both the febuxostat treatment group [n = 2,964] and allopurinol treatment group [n = 2,992]). In patients who did not die from a CV-related cause, serum urate levels with febuxostat treatment were nominally lower than with treatment with allopurinol at week 2 and months 3, 6, 12, 24, 36, 48, 60, and 72. By contrast, in the subgroup of patients who died from a CV-related cause, serum urate levels varied throughout the study period and were comparable between the febuxostat and allopurinol treatment group (Figure 1 and Supplementary Table 2, <http://onlinelibrary.wiley.com/doi/10.1002/art.42160>).

Gout flares. *Relationship between gout flares requiring treatment and death from CV causes.* The incidence rates of gout flares requiring treatment (per patient-year) were similar between the febuxostat and allopurinol treatment groups over the entire study period (overall modified ITT population, febuxostat 0.68 versus allopurinol 0.63) (Figure 2 and Supplementary Table 3,

<http://onlinelibrary.wiley.com/doi/10.1002/art.42160>). In the overall modified ITT population, gout flare rates (per patient-year) had a trend of being higher with febuxostat than with allopurinol during the first year of treatment (overall modified ITT population, 1.33 versus 1.20, respectively) but were comparable thereafter (overall modified ITT population >1 year, febuxostat 0.35 versus allopurinol 0.34) and decreased over the study period in both treatment groups (Figure 2 and Supplementary Table 3, <http://onlinelibrary.wiley.com/doi/10.1002/art.42160>). The incidence rates of gout flares within the first year of study treatment were slightly higher in the subgroup of patients who died from a CV-related cause compared with the subgroup of patients who did not die from a CV-related cause, but was generally lower for the remainder of the study period (Figure 2 and Supplementary Table 3). Throughout the duration of the study, gout flare severity was similar between the febuxostat and allopurinol treatment groups, with most flares classified as moderate in intensity (febuxostat 0.33 versus allopurinol 0.30) (Table 2), although the number and severity of gout flares were slightly higher within the first year of treatment in the febuxostat group (overall 1.33 flares versus moderate-to-severe flares 1.03) compared with the allopurinol group (overall flares 1.20 versus moderate-to-severe flares 0.88) (Table 2).

In the overall modified ITT population, gout flare rates within the 3-month period over which data were available closest to death from a CV-related cause were low. The number of gout flares was higher with febuxostat treatment (6% [8 of 134])

Table 3. Gout flare rates among patients receiving febuxostat or allopurinol according to post-baseline mean serum urate levels, overall and by treatment group*

Post-baseline mean serum urate level	Mean flare rates per patient-years of exposure (95% CI)		
	Febuxostat	Allopurinol	Total
<4.0 mg/dl	0.27 (0.24–0.31)	0.25 (0.19–0.33)	0.27 (0.24–0.30)
4.0–5.0 mg/dl	0.27 (0.25–0.30)	0.20 (0.18–0.23)	0.24 (0.23–0.26)
5.0–6.0 mg/dl	0.35 (0.32–0.39)	0.31 (0.29–0.34)	0.33 (0.31–0.35)
≥6.0 mg/dl	0.49 (0.45–0.53)	0.52 (0.48–0.55)	0.50 (0.48–0.53)

* Post-baseline serum urate level measurements were collected from the end of the first year of treatment until the end of the study. The mean flare rates per patient-years of exposure (with 95% confidence intervals [95% CIs]) include occurrence of gout flares from the end of the first year of treatment until the end of the study.

Table 4. Numbers of patients who died from a CV-related cause by average post-baseline mean serum urate level and treatment group*

	Post-baseline mean serum urate level				<i>P</i> for trend, death from CV-related cause and mean serum urate level†
	<4.0 mg/dl	4.0–<5.0 mg/dl	5.0–<6.0 mg/dl	≥6.0 mg/dl	
Overall					0.034
Total no. of patients	383	1,353	2,345	2,109	
Patients who died from a CV-related cause	6 (1.6)	16 (1.2)	34 (1.4)	47 (2.2)	
Patients who did not die from a CV-related cause	377 (98.4)	1,337 (98.8)	2,311 (98.6)	2,062 (97.8)	
Febuxostat					0.199
Total no. of patients	298	838	1,012	950	
Patients who died from a CV-related cause	6 (2.0)	13 (1.6)	18 (1.8)	25 (2.6)	
Patients who did not die from a CV-related cause	292 (98.0)	825 (98.4)	994 (98.2)	925 (97.4)	
Allopurinol					0.012
Total no. of patients	85	515	1,333	1,159	
Patients who died from a CV-related cause	0 (0)	3 (0.6)	16 (1.2)	22 (1.9)	
Patients who did not die from a CV-related cause	85 (100.0)	512 (99.4)	1,317 (98.8)	1,137 (98.1)	

* The mean serum urate level was calculated using all post-baseline serum urate values collected after the first dose of study drug and >1 day after a patient's final dose of study drug. Death from a cardiovascular (CV)-related cause includes deaths up to 30 days after a patient's final dose of study drug. Except where indicated otherwise, values are the number (%) of patients.

† Other associations evaluated included the overall relationship between treatment and death from a CV-related cause ($P = 0.038$) and between treatment and mean serum urate level ($P \leq 0.001$). *P* values were determined by Cochran–Armitage test for trend.

compared with allopurinol (2% [2 of 100]) (Supplementary Table 4, <http://onlinelibrary.wiley.com/doi/10.1002/art.42160>).

Relationship between post-baseline serum urate levels, gout flares, and death from CV causes. In a post hoc analysis, we identified a trend toward a reduction in gout flare rates with lower serum urate levels in both the febuxostat and allopurinol treatment groups (Table 3). There was a positive association between serum urate levels and death from CV causes in the overall population ($P = 0.034$) and in the allopurinol treatment group ($P = 0.012$), but not in the febuxostat treatment group ($P = 0.199$). The total number of deaths from CV causes that occurred during treatment and up to 30 days after the final dose of study medication was lower ($P = 0.038$) in those who received allopurinol (1.3% [41 of 3,092]) compared with those who received febuxostat (2.0% [62 of 3,098]) (17), but the number of deaths was lower in patients with serum urate levels <5 mg/dl compared with those who had levels ≥5 mg/dl in both treatment groups (febuxostat $n = 19$ [1.7%] versus $n = 43$ [2.2%]; allopurinol $n = 3$ [0.5%] versus $n = 38$ [1.5%]) (Table 4).

Relationship between tophus resolution and death from CV causes. The overall proportion of patients with ≥1 tophus at baseline was 20.8% (1,287 of 6,190), with similar proportions in the febuxostat group (21.0% [650 of 3,098]) and allopurinol group (20.6% [637 of 3,092]). Tophus resolution rates were similar between treatment groups in year 1 and remained similar throughout the study period. By the end of the treatment period, cumulative tophus resolution rates in both treatment groups were >50% (Supplementary Figure 1A, <http://onlinelibrary.wiley.com/doi/10.1002/art.42160>). Tophus resolution rates within the first 2 years of treatment in the study were also comparable between treatment groups irrespective of whether the patient died from a CV-related cause or not (Supplementary Figure 1B, <http://onlinelibrary.wiley.com/doi/10.1002/art.42160>).

DISCUSSION

The CARES trial has the longest study duration of any trial investigating patients with gout and CVD. In this analysis, we evaluated the relationships between serum urate levels, gout flares, tophus resolution, and deaths from CV causes. In the CARES trial, the incidence rates of the nonfatal components of the composite primary end point were similar between febuxostat and allopurinol treatment groups (17). However, in the secondary end point analysis, the rate of death from CV causes was higher in patients who received treatment febuxostat compared with those who received allopurinol. All-cause mortality was higher in patients who received febuxostat compared with allopurinol as a result of the imbalance in the rates of deaths from CV causes (17). Further analyses of data from the CARES trial demonstrated that both febuxostat and allopurinol were associated with comparable, clinically relevant improvements in efficacy. We did not observe a relationship between gout flares and deaths from CV causes; however, there was a positive association between greater serum urate levels and deaths from CV causes in the overall population and in the allopurinol treatment group, while the rates of death from CV causes in the febuxostat treatment group were similar across serum urate levels. Additionally, data from the Febuxostat versus Allopurinol Streamlined Trial demonstrated that febuxostat was noninferior to allopurinol with regard to the occurrence of major CV outcomes with no indication of increased all-cause mortality or deaths from CV causes with febuxostat treatment (21). Therefore, the underlying mechanisms of the increase in deaths from CV causes observed in patients who received febuxostat compared with those who received allopurinol in the CARES trial remain unclear.

The primary goal of urate-lowering therapy in gout is to lower and maintain serum urate levels at subsaturating levels in

order to prevent progressive joint damage resulting from flare recurrence and reduce deformity caused by tophus formation. Achievement of long-term serum urate levels at a minimum of <6.0 mg/dl or even lower at <5.0 mg/dl to durably improve the signs and symptoms of gout, including palpable and visible tophi detected on physical examination (16,22), is essential to preventing these pathologic processes. In the overall modified ITT population in the CARES trial, febuxostat was associated with lower serum urate levels than allopurinol at most study visits. To further investigate a potential association between febuxostat and increased deaths from CV causes, we analyzed participants from the CARES trial organized into subgroups of either patients who died from a CV-related cause or those who did not die from a CV-related cause. Baseline serum urate levels in the CARES trial patient population were higher in those who died from a CV-related cause than in those who did not. In the subgroup of patients who did not die from a CV-related cause, at most study visits those who received treatment with febuxostat had lower serum urate levels than those who received allopurinol. In the subgroup of patients who died from a CV-related cause there were no clear relationships between serum urate levels and treatment groups; however, interpretation of these findings is limited by the small number of patients (febuxostat $n = 134$ versus allopurinol $n = 100$).

In the overall modified ITT population, gout flare rates were similar in patients who received febuxostat and those who received allopurinol and decreased during the study period regardless of whether the patient died from a CV-related cause or not. Moreover, in patients who died of a CV-related cause, 94% and 98% of those who received febuxostat and those who received allopurinol, respectively, did not have a reported gout flare within 3 months of death. Across different post-baseline serum urate categories, regardless of treatment group, there was a trend toward a reduction in the rate of gout flare at lower serum urate levels.

The overall proportion of patients with ≥ 1 tophus at baseline was 20.8%, with similar proportions of patients in the febuxostat and allopurinol treatment groups. Tophus resolution rates were similar between treatment groups throughout the study period. Within the first 2 years, tophus resolution rates remained comparable between treatment groups, regardless of whether the patient died from a CV-related cause or not.

The links between serum urate levels, hyperuricemia, gout flares, and CVD are unclear. Some studies suggest that there is no link between increased serum urate levels and coronary heart disease (10). However, other studies indicate that increased serum urate levels may be associated with worse outcomes in patients with CVD and renal disease (6,7,9). One potential mechanism by which serum urate levels could lead to increased CV events is by impairing nitric oxide synthesis, resulting in vascular endothelial dysfunction that may lead to inflammation and prothrombosis (23). It is important to note the relatively high CV

risk in patients from the CARES trial, which included patients with CV event rates of >10%, which is higher compared with other gout studies (17,24,25). The CARES trial previously demonstrated that the rates of predefined major adverse CV events with febuxostat treatment were noninferior to allopurinol (17). Findings from the present analyses show that very few patients experienced a gout flare within the 3-month period over which data were available closest to a cardiac event. Furthermore, there were no imbalances in nonfatal CV events, including acute coronary syndrome, ischemic stroke, or revascularization rates in the CARES trial (17). These findings suggest a lack of an association between an off-target effect of febuxostat on mechanisms such as inflammation and prothrombosis.

Our study had several strengths. First, it is the largest and longest clinical trial in the gout population. Second, it is the only trial enriched for CVD. Finally, there were frequent measurements of serum urate levels and clinical assessments for gout flares and tophi status during the trial. This allowed for examination of the relationships between serum urate levels and gout flares with CV outcomes in the entire cohort as well as each treatment assignment.

Limitations of this study have been discussed previously (17). First, there was no placebo arm in the trial, which could have characterized the incidence rates of CV events in the high-risk gout population; use of a placebo group was not feasible considering the planned length of the trial. Second, a large proportion of participants either discontinued participation in the study, did not complete follow-up, or discontinued treatment, making the complete analysis of all patients difficult. However, baseline demographic and clinical characteristics were comparable between treatment groups and between patients who either continued or discontinued treatment (17). Third, we cannot draw any conclusions between levels of inflammation markers in serum and death from CV causes in this study, as the former was not collected as part of the CARES study design. Additionally, it is important to note that the positive association between serum urate levels and death from CV causes seen in the overall population and in allopurinol treatment group, but not in the febuxostat treatment group, was based on post hoc analyses and should be considered exploratory. Further studies with large sample sizes are necessary to confirm these trends. Finally, rates of gout flares in clinical trials are difficult to capture accurately, despite the best efforts by site personnel (study coordinator, study nurse, or the investigator). Misclassification of gout flares may complicate the interpretation of data and potentially bias findings toward the null hypothesis.

In conclusion, in this new analysis of patients from the CARES trial, we found no relationships between death from CV causes and gout flares or tophus resolution in patients who received treatment with febuxostat or allopurinol. There were also no clear associations between serum urate levels and death from CV causes in patients who received treatment with febuxostat.

ACKNOWLEDGMENTS

We would like to thank all of the investigators and patients who participated in this study, and we would also like to thank Eric Lloyd from Takeda Development Center Americas, Inc. for his contributions and advice on our statistical analyses and Eileen Hartman from Takeda Development Center Americas, Inc. for her review of the manuscript for scientific accuracy. Medical writing assistance was provided by Simon Wigfield (Caudex, Oxford, UK) and Lauren Gwynne (Caudex, Oxford, UK), and editorial assistance was provided by Danielle Johnson (Caudex, Oxford, UK) (all supported by Takeda Development Center Americas, Inc.).

AUTHOR CONTRIBUTIONS

All authors were involved in drafting the article or revising it critically for important intellectual content, and all authors approved the final version to be published. Dr. Saag had full access to all of the data in the study and takes responsibility for the integrity of the data and the accuracy of the data analysis.

Study conception and design. Becker, White, Whelton, Hunt, Gunawardhana.

Acquisition of data. Saag, Becker, White, Whelton, Borer, Gorelick, Hunt, Castillo, Gunawardhana.

Analysis and interpretation of data. Saag, Becker, White, Whelton, Borer, Gorelick, Hunt, Castillo, Gunawardhana.

ROLE OF THE STUDY SPONSOR

Takeda Development Center Americas, Inc. funded this study and contributed to the collection, analysis, and interpretation of the data. Takeda reviewed the manuscript for scientific accuracy/data integrity prior to submission. All authors, including those employed by Takeda, approved the content of the submitted manuscript and the decision to publish the manuscript was wholly that of the authors.

REFERENCES

- Chen-Xu M, Yokose C, Rai SK, Pillinger MH, Choi HK. Contemporary prevalence of gout and hyperuricemia in the United States and decadal trends: the National Health and Nutrition Examination Survey 2007–2016. *Arthritis Rheumatol* 2019;71:991–9.
- Roddy E, Doherty M. Epidemiology of gout. *Arthritis Res Ther* 2010; 12:223.
- Guthrie RM. New perspectives on the management of gout, a common primary care disorder. *Postgrad Med* 2012;124:151–3.
- Krishnan E. Reduced glomerular function and prevalence of gout: NHANES 2009–10. *PLoS One* 2012;7:e50046.
- Zhu Y, Pandya BJ, Choi HK. Comorbidities of gout and hyperuricemia in the US general population: NHANES 2007–2008. *Am J Med* 2012; 125:679–87.
- Choi HK, Curhan G. Independent impact of gout on mortality and risk for coronary heart disease. *Circulation* 2007;116:894–900.
- Krishnan E, Svendsen K, Neaton JD, Grandits G, Kuller LH, Group MR. Long-term cardiovascular mortality among middle-aged men with gout. *Arch Intern Med* 2008;168:1104–10.
- Stack AG, Hanley A, Casserly LF, Cronin CJ, Abdalla AA, Kiernan TJ, et al. Independent and conjoint associations of gout and hyperuricemia with total and cardiovascular mortality. *QJM* 2013;106:647–58.
- Ioachimescu AG, Brennan DM, Hoar BM, Hazen SL, Hoogwerf BJ. Serum uric acid is an independent predictor of all-cause mortality in patients at high risk of cardiovascular disease: a preventive cardiology information system (PreCIS) database cohort study. *Arthritis Rheum* 2008;58:623–30.
- Keenan T, Zhao W, Rasheed A, Ho WK, Malik R, Felix JF, et al. Causal assessment of serum urate levels in cardiometabolic diseases through a Mendelian randomization study. *J Am Coll Cardiol* 2016; 67:407–16.
- Kleber ME, Delgado G, Grammer TB, Silbernagel G, Huang J, Kramer BK, et al. Uric acid and cardiovascular events: a Mendelian randomization study. *J Am Soc Nephrol* 2015;26:2831–8.
- Richette P, Latourte A, Bardin T. Cardiac and renal protective effects of urate-lowering therapy. *Rheumatology (Oxford)* 2018;57:i47–50.
- Drug and Therapeutics Bulletin. Latest guidance on the management of gout. *BMJ* 2018;362:k2893.
- Borghesi C, Perez-Ruiz F. Urate lowering therapies in the treatment of gout: a systematic review and meta-analysis. *Eur Rev Med Pharmacol Sci* 2016;20:983–92.
- Robinson PC, Dalbeth N. Advances in pharmacotherapy for the treatment of gout. *Expert Opin Pharmacother* 2015;16:533–46.
- Khanna D, Fitzgerald JD, Khanna PP, Bae S, Singh MK, Neogi T, et al. 2012 American College of Rheumatology guidelines for management of gout. Part 1: Systematic nonpharmacologic and pharmacologic therapeutic approaches to hyperuricemia. *Arthritis Care Res (Hoboken)* 2012;64:1431–46.
- White WB, Saag KG, Becker MA, Borer JS, Gorelick PB, Whelton A, et al. Cardiovascular safety of febuxostat or allopurinol in patients with gout. *N Engl J Med* 2018;378:1200–10.
- Varga Z, Sabzwari SR, Vargova V. Cardiovascular risk of nonsteroidal anti-inflammatory drugs: an under-recognized public health issue [review]. *Cureus* 2017;9:e1144.
- White WB, Chohan S, Dabholkar A, Hunt B, Jackson R. Cardiovascular safety of febuxostat and allopurinol in patients with gout and cardiovascular comorbidities. *Am Heart J* 2012;164:14–20.
- Wallace SL, Robinson H, Masi AT, Decker JL, McCarty DJ, Yü TF. Preliminary criteria for the classification of the acute arthritis of primary gout. *Arthritis Rheum* 1977;20:895–900.
- Mackenzie IS, Ford I, Nuki G, Hallas J, Hawkey CJ, Webster J, et al. Long-term cardiovascular safety of febuxostat compared with allopurinol in patients with gout (FAST): a multicentre, prospective, randomised, open-label, non-inferiority trial. *Lancet* 2020;396:1745–57.
- Khanna D, Khanna PP, Fitzgerald JD, Singh MK, Bae S, Neogi T, et al. 2012 American College of Rheumatology guidelines for management of gout. Part 2: Therapy and antiinflammatory prophylaxis of acute gouty arthritis. *Arthritis Care Res (Hoboken)* 2012;64:1447–61.
- Choi YJ, Yoon Y, Lee KY, Hien TT, Kang KW, Kim KC, et al. Uric acid induces endothelial dysfunction by vascular insulin resistance associated with the impairment of nitric oxide synthesis. *FASEB J* 2014;28: 3197–204.
- Wei L, Mackenzie IS, Chen Y, Struthers AD, MacDonald TM. Impact of allopurinol use on urate concentration and cardiovascular outcome. *Br J Clin Pharmacol* 2011;71:600–7.
- Bardin T, Keenan RT, Khanna PP, Kopicko J, Fung M, Bhakta N, et al. Lesinurad in combination with allopurinol: a randomised, double-blind, placebo-controlled study in patients with gout with inadequate response to standard of care (the multinational CLEAR 2 study). *Ann Rheum Dis* 2017;76:811–20.

LETTERS

DOI 10.1002/art.42126

Increased risk of statin-associated autoimmune myopathy among American Indians

To the Editor:

Statins reduce the risk of cardiovascular disease and have an acceptable side-effect profile. However, autoimmune muscle disease can develop, although rarely, in patients taking statins. Statin-associated autoimmune myopathy is characterized by symmetric proximal muscle weakness, appearance of myofiber necrosis on muscle biopsy, elevated muscle enzyme levels, and presence of autoantibodies against 3-hydroxy-3-methylglutaryl-coenzyme A (HMG-CoA) reductase (1). Patients with statin-associated autoimmune myopathy do not usually improve with statin discontinuation alone and typically require treatment with immunomodulatory medications.

Statin-associated autoimmune myopathy is thought to occur in as few as 0.002% of patients taking statins (1). However, in a recent study of 1,800 American Indians from rural Arizona who were taking statins, 6 patients (0.3%) developed statin-associated autoimmune myopathy (2). Here, we report an unexpectedly high rate of this disease among a separate cohort of American Indians who were seen at the Gallup Indian Medical Center, which is located on the Navajo Reservation. Indeed, from among ~5,000 patients seen at the Gallup Indian Medical Center who were receiving treatment with statins over a 2-year period (from September 2017 through September 2019), we identified 14 patients (0.3%) who presented with the typical clinical manifestations of this disease. These clinical manifestations included

proximal muscle weakness, elevated muscle enzyme levels, and the presence of anti-HMG-CoA reductase autoantibodies after patients received atorvastatin (3) (Table 1). The incidence among American Indians at the Gallup Indian Medical Center represents an ~150-fold increase in the risk of statin-associated autoimmune myopathy compared with that seen in the general population taking statins (1). Of note, American Indian patients treated with statin at the Gallup Indian Medical Center were not systematically screened for weakness and muscle enzyme elevations. Consequently, some patients with statin-associated autoimmune myopathy, especially those with mild cases, could have been missed and not included in our estimate of the incidence of this disease.

The presence of HLA class II DR11 is strongly associated with the development of statin-associated autoimmune myopathy in other ethnic groups. DR11 was present in 70% of White patients with anti-HMG-CoA reductase myopathy but in only 18% of a healthy control group of White and Black subjects (4). HLA typing was not available for the Navajo patients described here, and, as far as we know, the frequencies of DR11 and other HLA types have not been reported among the Navajo population as a whole. Nonetheless, we suspect that genetic and/or environmental factors common among the American Indian population may predispose them to developing statin-associated autoimmune myopathy. Defining risk factor(s) in this population would be of interest and might allow screening to identify those at the greatest risk for developing autoimmune myopathy after taking statins. These patients could be offered proprotein convertase subtilisin/kexin type 9 inhibitors, which, unlike statins, do not

Table 1. Clinical characteristics of 14 American Indian patients with statin-associated autoimmune myopathy who were seen at the Gallup Indian Medical Center (Navajo Reservation, Arizona)*

No./total no. (%) of men	4/14 (28.6)
Age at symptom onset, mean (range) years	62.7 (51–78)
Age at diagnosis, mean (range) years	62.9 (52–78)
Peak creatine kinase, mean (range) IU/liter	9,791.3 (1,422–23,077)
No./total no. (%) of patients with myofiber necrosis on muscle biopsy†	6/6 (100)
Anti-HMG-CoA reductase, mean (range) titers in AU‡	154.4 (41 to >200)
Duration of statin therapy before onset of muscle weakness, mean (range) months	39.6 (9–76)
Outcomes	11/14 patients improved; 2 patients started immunomodulatory treatment; 1 patient died of an unrelated cause before treatment could be started

* All patients were taking atorvastatin at the time of symptom onset and diagnosis of autoimmune myopathy. Anti-HMG-CoA reductase = anti-3-hydroxy-3-methylglutaryl-coenzyme A reductase.

† Seven patients did not undergo muscle biopsy and were diagnosed as having anti-HMG-CoA–positive myopathy based on the following clinical features: proximal muscle weakness, elevated creatine kinase levels, and presence of anti-HMG-CoA reductase autoantibodies (3).


‡ Eight patients had titers of >200 arbitrary units (AU) (the highest value); thus, a cutoff value of 200 AU was used to calculate the mean.

appear to trigger or exacerbate myositis with anti-HMG-CoA reductase autoantibodies (5).

Taken together with the prior report (2), the clinical findings among subjects in the Gallup Indian Medical Center indicate that physicians should have a high index of suspicion for the development of autoimmune myopathy when prescribing statins to American Indian patients. Patients who develop muscle weakness and elevated creatinine kinase levels should be tested for anti-HMG-CoA reductase autoantibodies. In those who test positive, statins should be stopped and treatment initiated to improve muscle strength and prevent permanent muscle damage.

Supported in part by the Intramural Program of the National Institute of Arthritis and Musculoskeletal and Skin Diseases of the National Institutes of Health. Dr. Mammen is coinventor of a commercially available assay for anti-HMG-CoA reductase autoantibodies but receives no royalties or other compensation for this. The opinions expressed in this manuscript are those of the author(s) and do not necessarily reflect the views of the Indian Health Service.

Author disclosures are available at <https://onlinelibrary.wiley.com/action/downloadSupplement?doi=10.1002%2Fart.42126&file=art42126-sup-0001-Disclosureform.pdf>.

Jennie Wei, MD, MPH
Elizabeth Ketner, MD
Gallup Indian Medical Center
Gallup, NM
Andrew L. Mammen, MD, PhD 
andrew.mammen@nih.gov
National Institutes of Health
Bethesda, MD

- Mammen AL. Statin-associated autoimmune myopathy. *N Engl J Med* 2016;374:664–9.
- Close RM, Close LM, Galdun P, Gerstberger S, Rydberg M, Christopher-Stine L. Potential implications of six American Indian patients with myopathy, statin exposure and anti-HMGCR antibodies. *Rheumatology (Oxford)* 2021;60:692–8.
- Allenbach Y, Mammen AL, Benveniste O, Stenzel W, Immune-Mediated Necrotizing Myopathies Working Group. 224th ENMC International Workshop: clinico-sero-pathological classification of immune-mediated necrotizing myopathies Zandvoort, The Netherlands, 14–16 October 2016. *Neuromuscul Disord* 2018;28:87–99.
- Mammen AL, Gaudet D, Brisson D, Christopher-Stine L, Lloyd TE, Leffell MS, et al. Increased frequency of DRB1*11:01 in anti-HMG-CoA reductase-associated autoimmune myopathy. *Arthritis Care Res (Hoboken)* 2012;64:1233–7.
- Tiniakou E, Rivera E, Mammen AL, Christopher-Stine L. Use of proprotein convertase subtilisin/kexin type 9 (PCSK9) inhibitors in statin-associated immune-mediated necrotizing myopathy: a case series. *Arthritis Rheumatol* 2019;71:1723–6.

DOI 10.1002/art.42142



von Willebrand factor as an indicator of endothelial injury in COVID-19: comment on the article by Shi et al

To the Editor:

We read with great interest the article by Dr. Shi et al (1) on their efforts to “identify circulating factors contributing to endothelial cell activation and dysfunction in COVID-19.” Conspicuous by its

absence in this otherwise thorough investigation was any mention of von Willebrand factor (vWF), a coagulation factor and early indicator of endothelial injury (2). Increases in circulating vWF antigen precede and directly promote thrombosis by mediating platelet adhesion and preventing clearance of coagulation factor VIII (3). Shi and colleagues postulated that antiphospholipid antibodies may activate endothelial cells in COVID-19, which others have shown to be mediated by vWF (4). Patients with COVID-19 commonly have increased levels of vWF antigen, and its presence is a marker that could be used to predict the risk of death and increased length of hospitalization in patients with COVID-19 (5–9).

Author disclosures are available at <https://onlinelibrary.wiley.com/action/downloadSupplement?doi=10.1002%2Fart.42142&file=art42142-sup-0001-Disclosureform.pdf>.

Darryl E. Palmer-Toy, MD, PhD 
darryl.e.palmer-toy@kp.org
Timothy M. Cotter, MD
Hedyeh Shafi, MD
Su-Jau T. Yang, PhD
Alexander H. Cotter, BS 
Southern California Permanente Medical Group
North Hollywood, CA

- Shi H, Zuo Y, Navaz S, Harbaugh A, Hoy CK, Gandhi AA, et al. Endothelial cell-activating antibodies in COVID-19. *Arthritis Rheumatol* 2022;74:1132–8.
- Brogan P, Eleftheriou D. Vasculitis update: pathogenesis and biomarkers. *Pediatr Nephrol* 2018;33:187–98.
- Ruggeri ZM. Von Willebrand factor, platelets and endothelial cell interactions. *J Thromb Haemost* 2003;1:1335–42.
- Huang S, Ninivaggi M, Chayoua W, de Laat B. WVF, Platelets and the antiphospholipid syndrome. *Int J Mol Sci* 2021;22:4200.
- Cotter AH, Yang ST, Shafi H, Cotter TM, Palmer-Toy DE. Elevated von Willebrand factor antigen is an early predictor of mortality and prolonged length of stay for coronavirus disease 2019 (COVID-19) inpatients. *Arch Pathol Lab Med* 2022;146:34–7.
- Escher R, Breakey N, Lämmle B. ADAMTS13 activity, von Willebrand factor, factor VIII and D-dimers in COVID-19 inpatients. *Thromb Res* 2020;192:174–5.
- Helms J, Tacquard C, Severac F, Leonard-Lorant I, Ohana M, Delabranche X, et al. High risk of thrombosis in patients with severe SARS-CoV-2 infection: a multicenter prospective cohort study. *Intensive Care Med* 2020;46:1089–98.
- Philippe A, Chocron R, Gendron N, Bory O, Beauvais A, Peron N, et al. Circulating Von Willebrand factor and high molecular weight multimers as markers of endothelial injury predict COVID-19 in-hospital mortality. *Angiogenesis* 2021;24:505–17.
- Marco A, Marco P. Von Willebrand factor and ADAMTS13 activity as clinical severity markers in patients with COVID-19. *J Thromb Thrombolysis* 2021;52:497–503.

DOI 10.1002/art.42141

Reply

To the Editor:

We appreciate Dr. Palmer-Toy et al's interest in our article. We agree that vWF is an important mediator of


thromboinflammation. After activation of endothelial cells and platelets, vWF is released from Weibel-Palade bodies and platelet alpha granules, respectively, leading to a cascade of heterotypic cellular interactions that support a procoagulant and proinflammatory milieu (1). Correlations between increases in the circulating pool of vWF and severity of COVID-19 or death resulting from complications of COVID-19 have been reported by many investigators (2–7), including Palmer-Toy and colleagues.

Because polyclonal COVID-19 antibody fractions have been shown to activate neutrophils and platelets, as well as to suppress physiologic antiviral responses, we focused on autoantibodies in our study's exploration of endothelial dysfunction in COVID-19. Of note, we reported that purified IgG fractions from patient COVID-19 serum samples, especially from patients with elevated circulating antiphospholipid antibodies, recapitulated activation of endothelial cells by intact COVID-19 serum, suggesting that the circulating antibody milieu in COVID-19 bears a foudroyant capacity to transform the endothelial surface and facilitate leukocyte adhesion. The specific targets of these antibodies and whether they ligate receptors or recognize antigens at the endothelial surface remain unknown and are worthy of investigation. Additional mechanisms of endothelial activation in COVID-19 include denudation of the protective glycocalyx, mobilization of Weibel-Palade bodies, and sex-specific steroid effects. In our opinion, defining these upstream stimuli that trigger the shift away from a quiescent state likely supersedes understanding the kinetics by which the endothelium acquires a thromboinflammatory phenotype.

Although we did not examine platelet–endothelial interactions in our study, these have been described in COVID-19 and have been shown to be, at least in part, attributable to the actions of vWF (8). Polyclonal COVID-19 IgG pools enriched in antiphospholipid antibodies may facilitate platelet–endothelial interactions through vWF string formation, as previously reported in antiphospholipid syndrome (9,10). We certainly support the intent of Palmer-Toy and colleagues to promote the exploration of endothelial and hematopoietic cell interactions in pursuit of understanding the mechanisms that differentiate normal physiologic responses from their maladaptive counterparts that result in tissue injury.

Dr. Kanthi is an inventor on an unrelated pending patent to the University of Michigan (US20180369278A1). The remaining authors have no competing interests.

Hui Shi, MD, PhD
University of Michigan
Ann Arbor, MI
and Shanghai Jiao Tong University
School of Medicine
Shanghai, China

Jason S. Knight, MD, PhD 
jsknight@umich.edu
University of Michigan
Ann Arbor, MI
Yogendra Kanthi, MD
yogen.kanthi@nih.gov

National Heart, Lung, and Blood Institute
Bethesda, MD
and University of Michigan
Ann Arbor, MI

1. Colling ME, Tourdot BE, Kanthi Y. Inflammation, infection and venous thromboembolism. *Circ Res* 2021;128:2017–36.
2. Goshua G, Pine AB, Meizlish ML, Chang CH, Zhang H, Bahel P, et al. Endotheliopathy in COVID-19-associated coagulopathy: evidence from a single-centre, cross-sectional study. *Lancet Haematol* 2020;7:e575–82.
3. Cotter AH, Yang ST, Shafi H, Cotter TM, Palmer-Toy DE. Elevated von Willebrand factor antigen is an early predictor of mortality and prolonged length of stay for coronavirus disease 2019 (COVID-19) inpatients. *Arch Pathol Lab Med* 2022;146:34–7.
4. Schmaier AA, Pajares Hurtado GM, Manickas-Hill ZJ, Sack KD, Chen SM, Bhamhani V, et al. Tie2 activation protects against prothrombotic endothelial dysfunction in COVID-19. *JCI Insight* 2021;6:e151527.
5. Mancini I, Baronciani L, Artoni A, Colpani P, Biganzoli M, Cozzi G, et al. The ADAMTS13-von Willebrand factor axis in COVID-19 patients. *J Thromb Haemost* 2021;19:513–21.
6. Fernandez S, Moreno-Castano AB, Palomo M, Martinez-Sanchez J, Torramade-Moix S, Tellez A, et al. Distinctive biomarker features in the endotheliopathy of COVID-19 and septic syndromes. *Shock* 2022;57:95–105.
7. Taus F, Salvagno G, Cane S, Fava C, Mazzaferri F, Carrara E, et al. Platelets promote thromboinflammation in SARS-CoV-2 pneumonia. *Arterioscler Thromb Vasc Biol* 2020;40:2975–89.
8. Barrett TJ, Cornwell M, Myndzar K, Rolling CC, Xia Y, Drenkova K, et al. Platelets amplify endotheliopathy in COVID-19. *Sci Adv* 2021;7:eabh2434.
9. Hulstein JJ, Lenting PJ, de Laat B, Derksen RH, Fijnheer R, de Groot PG. beta2-Glycoprotein I inhibits von Willebrand factor dependent platelet adhesion and aggregation. *Blood* 2007;110:1483–91.
10. Ng CJ, McCrae KR, Ashworth K, Sosa LJ, Betapudi V, Manco-Johnson MJ, et al. Effects of anti-beta2GPI antibodies on VWF release from human umbilical vein endothelial cells and ADAMTS13 activity. *Res Pract Thromb Haemost* 2018;2:380–9.

DOI 10.1002/art.42148

Addressing readability of online patient materials: comment on the American College of Rheumatology online information pages for patients and caregivers

To the Editor:

Health literacy is the ability to acquire, process, and comprehend health information to make informed health decisions (1). Health literacy rates, among adults in the US and worldwide, vary considerably, and lower health literacy has been understandably correlated with worse health outcomes (2). Therefore, the current recommendation by the American Medical Association is that health care information should be written at or below a sixth-grade reading level, corresponding to 6 years of education, to meet the needs of the general population (3).

The website of the American College of Rheumatology (ACR) features a valuable patient/caregiver-directed section, where online educational content is organized and presented for 47 conditions on separate web pages (4). I calculated the grade-level readability of the educational content for each condition using formulas from the following established readability indices: Gunning Fog, Coleman–Liau, Flesch–Kincaid, Automated Readability, and Simple Measure of Gobbledygook (5). These indices are used to determine average grade-level readability scores by analyzing the length and complexity of sentences and the use of polysyllabic words.

The mean readability grade levels for all patient/caregiver-directed educational content were as follows: mean 13.1 (range 9.9–17.3) on the Gunning Fog index, mean 12.8 (range 10–15.7) on the Coleman–Liau index, mean 11.5 (range 8.6–15.2) on the Flesch–Kincaid index, mean 11.2 (range 7.7–15.3) on the Automated Readability index, and mean 12.8 (range 10.4–16) on the Simple Measure of Gobbledygook index. As such, none of the educational web pages, for any condition and assessed by any of the 5 readability formulas, was written at the recommended reading level of sixth grade or below.

The accessibility of health information is inherently linked to its readability. Across the 5 different validated readability indices, the calculated mean readability level exceeded an eleventh-grade reading level, which is noticeably higher than the recommended level. This, combined with variable health literacy rates, may exacerbate existing barriers between health care providers and patients/caregivers. These gaps in communication not only risk the dissemination of misinformation and confusion but also may reinforce already profound health inequities, disproportionately affecting people who are medically underserved. Addressing readability issues therefore offers a viable starting point to bridge such gaps.

Author disclosures are available at <https://onlinelibrary.wiley.com/action/downloadSupplement?doi=10.1002%2Fart.42148&file=art42148-sup-0001-Disclosureform.pdf>.

Ahmad AlAbdulkareem, MB, BCh, BAO, LRCPI,
LRCSI (Hons), MSc 
ahmadalabdulkareem@hotmail.com
Kuwait Ministry of Health,
The Capital, Kuwait

1. US Department of Health and Human Services. Health literacy online. URL: <https://www.health.gov/communication/>.
2. Weiss BD. How to bridge the health literacy gap. *Fam Pract Manag* 2014;21:14–8.
3. Weiss BD. Health literacy and patient safety: help patients understand. 2nd ed. Chicago (IL): American Medical Association Foundation and American Medical Association; 2007.

4. American College of Rheumatology. URL: <https://www.rheumatology.org/I-Am-A/Patient-Caregiver>.
5. Hutchinson N, Baird GL, Garg M. Examining the reading level of internet medical information for common internal medicine diagnoses. *Am J Med* 2016;129:637–9.

DOI 10.1002/art.42147

Reply

To the Editor:

We thank Dr. AlAbdulkareem for his insightful letter and the concern raised about the reading level of the educational content in the patient/caregiver section of the American College of Rheumatology (ACR) website (<https://www.rheumatology.org/I-Am-A/Patient-Caregiver>). We agree that there are numerous barriers to health care and that having gaps in literacy and education is a challenge that can affect health outcomes. The field of rheumatology, including the disease processes, their immunologic etiologies, symptoms, and management techniques, are complex by nature, and this has been reflected in the online patient/caregiver web pages.

In 2018, we revamped our educational materials and tried to maintain as close to the sixth-grade reading level as was possible. This included efforts to simplify the content by replacing medical jargon with more common terms (e.g., “in the vein” instead of “intravenous”). However, we came across some limitations. For example, terms required to help define the conditions or their symptoms such as “antibody,” “platelet,” “autoimmunity,” “vasculitis,” and others could not always be replaced with simpler terms given the complexity of their definition. In addition, the names of the medications used to treat these conditions likely raised the average grade-level readability scores in the mentioned indices. If we are correct in our assumptions, we believe it is these terms that are raising the scores of the indices.

The ACR is always looking for ways to improve content and generalize it to reach a broader audience in hopes of improving awareness and expanding the knowledge of rheumatic conditions to patients, caregivers, and the larger community. We are open to specific suggestions regarding replacing complex words and getting closer to the desired sixth-grade reading level. Furthermore, we would welcome more details on the efforts made by other societies in improving the reading level of their patient educational content.

Author disclosures are available at <https://onlinelibrary.wiley.com/action/downloadSupplement?doi=10.1002%2Fart.42147&file=art42147-sup-0001-Disclosureform.pdf>.

Mohammad A. Ursani, MD 
mohammad.ursani@gmail.com
On behalf of the American College of Rheumatology
Chair, Committee on Communications and Marketing
Atlanta, GA

DOI 10.1002/art.42159

Criteria for the pathogenicity of anticentromere (anti-CENP-B) autoantibodies in systemic sclerosis: comment on the article by van Leeuwen et al

To the Editor:

We read with interest the article by Dr. van Leeuwen et al whose recent study showed that serum levels of anticentromere autoantibodies (ACAs) of IgG isotype, primarily anti-CENP-B, were significantly higher in patients with definite systemic sclerosis (SSc) than in patients with very early SSc (1). Moreover, the authors reported that progression to definite SSc in patients with very early SSc was associated with significantly higher levels of IgG ACAs at baseline. The authors concluded that increased levels of IgG-specific anti-CENP-B antibodies may serve as a biomarker to identify patients with very early SSc at risk for progression to definite SSc.

Specifically, anti-CENP-B antibodies in SSc are strongly associated with the limited cutaneous SSc subset (2,3). However, given that polyclonal B cell activation and hypergammaglobulinemia are common in SSc (4), we wondered whether these features may have contributed in part to the higher levels of IgG ACAs noted by van Leeuwen et al in some of their patients and therefore whether total serum IgG levels were measured. We pose this question because, in the definite SSc group, although van Leeuwen et al reported numerically higher IgG ACA levels in patients with organ involvement compared with those without, the difference was not significant. If total serum IgG levels had been measured, would these levels be higher in the group of patients with higher IgG ACA levels? Would a linear correlation be shown between total serum IgG levels and IgG ACA levels? Lastly, would higher IgG ACA levels still be observed after adjusting for the raised total serum IgG levels?

In addition, in their study, van Leeuwen et al concluded that IgG-specific anti-CENP-B antibodies may potentially contribute to the pathogenesis of SSc. Indeed, a pathogenic role for ACAs has been previously suggested. For example, nuclear autoantigen CENP-B was demonstrated to be a bifunctional molecule that, when released from apoptotic endothelial cells, bound to the surface of human pulmonary artery smooth muscle cells and stimulated their migration and the secretion of interleukin-6 and interleukin-8 (5). Moreover, CENP-B transactivated the epidermal growth factor receptor via chemokine receptor 3 in smooth muscle cells, with anti-CENP-B from SSc patients abolishing this signaling pathway (6). Therefore, it was hypothesized that the sustained high titers of ACAs that are typically observed in SSc patients who are followed up longitudinally may be a factor contributing to arterial damage via the promotion of unremitting vascular repair (6).

Finally, the potential pathogenic role of ACAs evoked by the authors raises the necessity for robust criteria to demonstrate the pathogenicity of autoantibodies. Such criteria, originally proposed

Table 1. Seven proposed pathogenicity criteria for definition of pathogenic autoantibodies in systemic sclerosis (scleroderma) and other systemic autoimmune rheumatic diseases*

Clinical pathogenicity criteria	
Criterion 1	The autoantibody should be specific to the disease. An even greater pathogenic value is suggested when the autoantibody is phenotype specific; i. e., within the disease spectrum, it is associated with a particular set of clinical and laboratory manifestations.
Criterion 2	The autoantibody is serologically present before the onset of clinical manifestations.
Criterion 3	Autoantibody levels and disease activity/severity should, in general, be correlated with one another.
Criterion 4	Removal of the autoantibody, or blocking its functional effects, should ameliorate the disease process (e.g., by immunosuppression, plasma exchange, biologic agent, immunotherapy, or other means).
Experimental pathogenicity criteria	
Criterion 5	The autoantibody should be capable of causing the lesions attributed to the disease in experimental systems (e.g., in living cells or in experimental animal models).
Criterion 6	A suitable immunization that leads to the production of similar autoantibodies should lead to a similar disease process.
Criterion 7	The autoantibody should be found along with a plausible target antigen at the site of tissue damage.

* Modified from refs. 7 and 8.

by Naparstek and Plotz (7), were recently updated for the definition of pathogenic autoantibodies in SSc (Table 1) (8). Of the 7 proposed criteria defining autoantibody pathogenicity in SSc, anti-CENP-B fulfill the first and second criteria and, in part, the fifth criterion (8,9). Interestingly, if ACA-specific IgG levels are significantly associated with progression to definite SSc and progression of organ system manifestations (1), as well as being associated with the severity of microangiopathy (10), as was suggested in the study by van Leeuwen et al, this may support the idea that anti-CENP-B also fulfill the third SSc pathogenicity criterion. Taken together, these data do support, although they do not prove, a contributory role of anti-CENP-B to the pathogenesis of SSc.

Author disclosures are available at <https://onlinelibrary.wiley.com/action/downloadSupplement?doi=10.1002%2Fart.42159&file=art42159-sup-0001-Disclosureform.pdf>.

Jean-Luc Senécal, MD, FRCPC, MCRA 
dr.j.l.senecal.md@gmail.com
 Martial Koenig, MD, MSc
 Gabriel Archambault, MD
 Sabrina Hoa, MD, MSc, FRCPC 
 Centre Hospitalier de l'Université de Montréal
 Montréal/Québec, Canada

1. Van Leeuwen NM, Boonstra M, Bakker JA, Grumeels A, Jordan S, Liem S, et al. Anticentromere antibody levels and isotypes and the development of systemic sclerosis. *Arthritis Rheumatol* 2021;73: 2338–47.

2. Van den Hoogen F, Khanna D, Fransen J, Johnson SR, Baron M, Tyndall A, et al. 2013 classification criteria for systemic sclerosis: an American College of Rheumatology/European League Against Rheumatism collaborative initiative. *Arthritis Rheum* 2013;65:2737–47.
3. Koenig M, Dieudé M, Sénécal JL. Predictive value of antinuclear autoantibodies: the lessons of the systemic sclerosis autoantibodies. *Autoimmun Rev* 2008;7:588–93.
4. White B. Immunopathogenesis of systemic sclerosis. *Rheum Dis Clin North Am* 1996;22:695–708.
5. Robitaille G, Hénault J, Christin MS, Sénécal JL, Raymond Y. The nuclear autoantigen CENP-B displays cytokine-like activities toward vascular smooth muscle cells. *Arthritis Rheum* 2007;56:3814–26.
6. Robitaille G, Christin MS, Clément I, Sénécal JL, Raymond Y. Nuclear autoantigen CENP-B transactivation of the epidermal growth factor receptor via chemokine receptor 3 in vascular smooth muscle cells. *Arthritis Rheum* 2009;60:2805–16.
7. Naparstek Y, Plotz PH. The role of autoantibodies in autoimmune disease. *Annu Rev Immunol* 1993;11:79–104.
8. Sénécal JL, Hoa S, Yang R, Koenig M. Pathogenic roles of autoantibodies in systemic sclerosis: current understandings in pathogenesis. *J Scleroderma Relat Disord* 2020;5:103–29.
9. Doering Maurer K, Rosen A. Autoantibodies as markers and possible mediators of scleroderma pathogenesis. In: Varga J, Denton CP, Wigley FM, Allanore Y, Kuwana M, editors. *Scleroderma. From pathogenesis to comprehensive management*. New York (NY): Springer; 2017. p. 197–204.
10. Van Leeuwen NM, Wortel CM, Fehres CM, Bakker JA, Scherer HU, Toes RE, et al. Association between centromere- and topoisomerase-specific immune responses and the degree of microangiopathy in systemic sclerosis. *J Rheumatol* 2021;48:402–9.

DOI 10.1002/art.42161

Reply

To the Editor:

We read with great interest the letter from Dr. Sénécal et al in which they refer to our recent findings on the presence of IgG ACAs in serum of patients with SSc. In our study, we reported higher serum levels of IgG ACAs in patients with definite SSc compared with patients with very early SSc. Among patients with very early SSc, disease progressed to definite SSc in 39% of patients, and these patients had higher levels of IgG ACAs at baseline. Although these findings suggested a possible role for IgG ACAs as biomarkers for disease development, they also indicated that an active ACA B cell response may be implicated in SSc development. In this context, Sénécal and colleagues correctly questioned whether a general increase in polyclonal serum IgG levels might have confounded the observed associations.

To address this question, we evaluated levels of total IgG and IgG ACAs in serum samples from 167 patients in the Leiden cohort who were included in our original study. The mean \pm SD levels of total IgG were comparable ($P = 0.83$) among patients with very early SSc (10.3 ± 3.0 gm/liter), definite SSc without organ involvement (10.5 ± 2.9 gm/liter), and SSc with organ

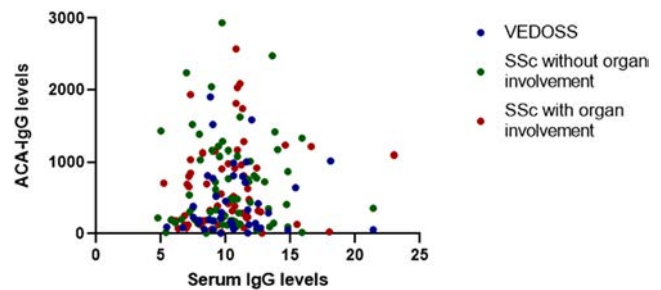


Figure 1. Comparison of serum levels of IgG anticentromere antibodies (ACAs) and total IgG in patients with very early systemic sclerosis (VEDOSS), those with definite systemic sclerosis (SSc) without organ involvement, and those with definite SSc with organ involvement. No linear relationship was found as demonstrated in the regression model ($\beta \pm$ SE 9.5 ± 15.2 ; $P = 0.54$).

involvement (10.2 ± 3.1 gm/liter). In contrast, IgG ACA levels varied significantly ($P < 0.05$) among the patient groups (445 arbitrary units [AU]/ml, 651 AU/ml, and 697 AU/ml, respectively).

Next, we analyzed linearity (scatterplots and linear regression) between serum levels of total IgG and IgG ACAs in the total patient group and in predefined groups. No associations were observed between total serum IgG and IgG ACA levels (Figure 1). Using multivariate linear regression, we observed that IgG ACAs were associated with progression from very early to definite SSc after correcting for total serum IgG levels (odds ratio 3.42, 95% confidence interval 1.3–11.69).

From these analyses, we considered it unlikely that polyclonal B cell activation and/or hypergammaglobulinemia confounded our observations. Our data and the additional analyses presented here support a possible role of ACAs in SSc pathogenesis by providing evidence for criterion 2 and criterion 3 according to Naparstek and Plotz (1,2).

Questions remain with regard to if and how the SSc-specific autoimmune response might contribute to tissue damage (3). The clear and strong associations between SSc-specific antibodies and distinct clinical phenotypes indicate different pathophysiologic cascades of events in patient subsets characterized by autoantibody subtype (4). In a recent study that evaluated predictors of SSc development in 553 patients with very early SSc, SSc-specific autoantibodies (ACAs, anti-RNA polymerase III, and antitopoisomerase antibodies [ATAs]) were present before onset of definite SSc, and their presence was reported as the strongest single predictor of SSc development in the near future (5). Interestingly, in our study, 31.6% of patients were ACA positive and only 7.4% were ATA positive, which contrasts with the prevalence shown in patients with established disease and indicates that, already from the earliest disease phases, trajectories of tissue damage differ between ACA-positive and ATA-positive patients (4,6). Considering the few studies addressing the targets of ACAs and ATAs (7,8),

we hypothesize that, in SSc, disease-specific autoreactive B cell responses, and/or its underlying T cell response, contribute to tissue damage in diverging directions.

Acknowledgement of these distinct pathways, both in time and in “quality,” combined with ongoing research on how they are involved in tissue damage, is warranted and will further elucidate SSc pathophysiology.

Author disclosures are available at <https://onlinelibrary.wiley.com/action/downloadSupplement?doi=10.1002%2Fart.42161&file=art42161-sup-0001-Disclosureform.pdf>.

Nina M. van Leeuwen, MD, PhD 
n.m.van_leeuwen@lumc.nl
Sophie I. E. Liem, MD 
Hans U. Scherer, MD PhD 
Jeska K. de Vries-Bouwstra, MD, PhD
On behalf of all coauthors
*Leiden University Medical Center
Leiden, The Netherlands*

1. Naparstek Y, Plotz PH. The role of autoantibodies in autoimmune disease. *Annu Rev Immunol* 1993;11:79–104.
2. Senécal JL, Hoa S, Yang R, Koenig M. Pathogenic roles of autoantibodies in systemic sclerosis: current understandings in pathogenesis. *J Scleroderma Relat Disord* 2020;5:103–29.
3. White B. Immunopathogenesis of systemic sclerosis. *Rheum Dis Clin North Am* 1996;22:695–708.
4. Steen VD. Autoantibodies in systemic sclerosis. *Semin Arthritis Rheum* 2005;35:35–42.
5. Bellando-Randone S, Del Galdo F, Lepri G, Minier T, Huscher D, Furst DE, et al. Progression of patients with Raynaud’s phenomenon to systemic sclerosis: a five-year analysis of the European Scleroderma Trial and Research group multicentre, longitudinal registry study for Very Early Diagnosis of Systemic Sclerosis (VEDOSS). *Lancet Rheumatol* 2021;3:e834–43.
6. van Leeuwen NM, Liem SI, Maurits MP, Ninaber M, Marsan NA, Allaart CF, et al. Disease progression in systemic sclerosis. *Rheumatology (Oxford)* 2021;60:1565–7.
7. Robitaille G, Hénault J, Christin MS, Senécal JL, Raymond Y. The nuclear autoantigen CENP-B displays cytokine-like activities toward vascular smooth muscle cells. *Arthritis Rheum* 2007;56:3814–26.
8. Hénault J, Tremblay M, Clément I, Raymond Y, Senécal JL. Direct binding of anti-DNA topoisomerase I autoantibodies to the cell surface of fibroblasts in patients with systemic sclerosis. *Arthritis Rheum* 2004;50:3265–74.

Arthritis & Rheumatology

An Official Journal of the American College of Rheumatology
www.arthritisrheum.org and wileyonlinelibrary.com

GENERAL INFORMATION

TO SUBSCRIBE

Institutions and Non-Members

Email: wileyonlinelibrary.com
Phone: (201) 748-6645
Write: Wiley Periodicals LLC
Attn: Journals Admin Dept
UK
111 River Street
Hoboken, NJ 07030

Volumes 74, 2022:
Institutional Print Only:

Institutional Online Only:
Institutional Print and
Online Only:

Arthritis & Rheumatology and Arthritis Care & Research:

\$2,603 in US, Canada, and Mexico
\$2,603 outside North America

\$2,495 in US, Canada, Mexico, and outside North America
\$2,802 in US, Canada, and Mexico; \$2,802 outside
North America

For submission instructions, subscription, and all other information visit: wileyonlinelibrary.com.

Arthritis & Rheumatology accepts articles for Open Access publication. Please visit <https://authorservices.wiley.com/author-resources/Journal-Authors/open-access/hybrid-open-access.html> for further information about OnlineOpen.

Wiley's Corporate Citizenship initiative seeks to address the environmental, social, economic, and ethical challenges faced in our business and which are important to our diverse stakeholder groups. Since launching the initiative, we have focused on sharing our content with those in need, enhancing community philanthropy, reducing our carbon impact, creating global guidelines and best practices for paper use, establishing a vendor code of ethics, and engaging our colleagues and other stakeholders in our efforts.

Follow our progress at www.wiley.com/go/citizenship.

Access to this journal is available free online within institutions in the developing world through the HINARI initiative with the WHO. For information, visit www.healthinternetwork.org.

Disclaimer

The Publisher, the American College of Rheumatology, and Editors cannot be held responsible for errors or any consequences arising from the use of information contained in this journal; the views and opinions expressed do not necessarily reflect those of the Publisher, the American College of Rheumatology and Editors, neither does the publication of advertisements constitute any endorsement by the Publisher, the American College of Rheumatology and Editors of the products advertised.

Members:

American College of Rheumatology/Association of Rheumatology Professionals

For membership rates, journal subscription information, and change of address, please write:

American College of Rheumatology
2200 Lake Boulevard
Atlanta, GA 30319-5312
(404) 633-3777

ADVERTISING SALES AND COMMERCIAL REPRINTS

Sales: Kathleen Malseed, National Account Manager
E-mail: kmalseed@pminy.com
Phone: (215) 852-9824
Pharmaceutical Media, Inc.
30 East 33rd Street, New York, NY 10016

Production: Patti McCormack
E-mail: pmccormack@pminy.com
Phone: (212) 904-0376
Pharmaceutical Media, Inc.
30 East 33rd Street, New York, NY 10016

Publisher: Arthritis & Rheumatology is published by Wiley Periodicals LLC, 101 Station Landing, Suite 300, Medford, MA 02155

Production Editor: Ramona Talantor, artprod@wiley.com

ARTHRITIS & RHEUMATOLOGY (Print ISSN 2326-5191; Online ISSN 2326-5205 at Wiley Online Library, wileyonlinelibrary.com) is published monthly on behalf of the American College of Rheumatology by Wiley Periodicals LLC, a Wiley Company, 111 River Street, Hoboken, NJ 07030-5774. Periodicals postage paid at Hoboken, NJ and additional offices. POSTMASTER: Send all address changes to Arthritis & Rheumatology, Wiley Periodicals LLC, c/o The Sheridan Press, PO Box 465, Hanover, PA 17331. **Send subscription inquiries care of** Wiley Periodicals LLC, Attn: Journals Admin Dept UK, 111 River Street, Hoboken, NJ 07030, (201) 748-6645 (nonmember subscribers only; American College of Rheumatology/Association of Rheumatology Health Professionals members should contact the American College of Rheumatology). **Subscription Price:** (Volumes 74, 2022: Arthritis & Rheumatology and Arthritis Care & Research) Print only: \$2,603.00 in U.S., Canada and Mexico, \$2,603.00 rest of world. For all other prices please consult the journal's website at wileyonlinelibrary.com. All subscriptions containing a print element, shipped outside U.S., will be sent by air. Payment must be made in U.S. dollars drawn on U.S. bank. Prices are exclusive of tax. Asia-Pacific GST, Canadian GST and European VAT will be applied at the appropriate rates. For more information on current tax rates, please go to www.wileyonlinelibrary.com/tax-vat. The price includes online access to the current and all online backfiles to January 1st 2018, where available. For other pricing options including access information and terms and conditions, please visit <https://onlinelibrary.wiley.com/library-info/products/price-lists>. Terms of use can be found here: <https://onlinelibrary.wiley.com/terms-and-conditions>. **Delivery Terms and Legal Title:** Where the subscription price includes print issues and delivery is to the recipient's address, delivery terms are Delivered at Place (DAP); the recipient is responsible for paying any import duty or taxes. Title to all issues transfers Free of Board (FOB) our shipping point, freight prepaid. We will endeavor to fulfill claims for missing or damaged copies within six months of publication, within our reasonable discretion and subject to availability. **Change of Address:** Please forward to the subscriptions address listed above 6 weeks prior to move; enclose present mailing label with change of address. **Claims** for undelivered copies will be accepted only after the following issue has been received. Please enclose a copy of the mailing label or cite your subscriber reference number in order to expedite handling. Missing copies will be supplied when losses have been sustained in transit and where reserve stock permits. Send claims care of Wiley Periodicals LLC, Attn: Journals Admin Dept UK, 111 River Street, Hoboken, NJ 07030. If claims are not resolved satisfactorily, please write to Subscription Distribution c/o Wiley Periodicals LLC, 111 River Street, Hoboken, NJ 07030. **Cancellations:** Subscription cancellations will not be accepted after the first issue has been mailed. **Journal Customer Services:** For ordering information, claims and any enquiry concerning your journal subscription please go to <https://wolsupport.wiley.com/s/contactsupport?tabset-a7d10=2> or contact your nearest office. **Americas:** Email: cs-journals@wiley.com; Tel: +1 877 762 2974. **Europe, Middle East and Africa:** Email: cs-journals@wiley.com; Tel: +44 (0) 1865 778315; 0800 1800 536 (Germany). **Asia Pacific:** Email: cs-journals@wiley.com; Tel: +65 6511 8000. **Japan:** For Japanese speaking support, Email: cs-japan@wiley.com. **Visit our Online Customer Help** at <https://wolsupport.wiley.com/s/contactsupport?tabset-a7d10=2>. **Back Issues:** Single issues from current and prior year volumes are available at the current single issue price from csjournals@wiley.com. Earlier issues may be obtained from Periodicals Service Company, 351 Fairview Avenue-Ste 300, Hudson, NY 12534, USA. Tel: +1 518 822-9300, Fax: +1 518 822-9305, Email: psc@periodicals.com. Printed in the USA by The Sheridan Group.